ANNUAL REVIEW OF NUCLEAR SCIENCE

EMILIO SEGRÈ, *Editor*
University of California

GERHART FRIEDLANDER, *Associate Editor*
Brookhaven National Laboratory

WALTER E. MEYERHOF, *Associate Editor*
Stanford University

VOLUME 8

ANNUAL REVIEWS, INC
PALO ALTO, CALIFORNIA, U.S.A.

FOREIGN AGENCY

Maruzen Company, Limited
6 Tori-Nichome Nihonbashi
Tokyo

PREFACE

During the last year there have been changes in the Editorial Committee of the Annual Review of Nuclear Science; in particular, Dr. James G. Beckerley, the Editor for the past six years, has been forced by other commitments to relinquish the editorship. During the previous eight years the general pattern and policies of this Review have been established; and although we must naturally expect that they will evolve as time goes on in order to keep abreast of scientific developments, no sudden drastic change is to be expected.

The responsibility for the choice of authors and subjects for this volume rests with the previous Editorial Committee: J. G. Beckerley, C. L. Critchfield, L. F. Curtiss, T. P. Kohman, E. Segrè, and R. E. Zirkle. An endeavor has been made to give a balanced view of the ever-widening field of nuclear science, ranging from rather abstract theoretical ideas on the symmetries of nature to the practical considerations resulting from the effects of radiation on man and the associated safety precautions.

The Annual Review of Nuclear Science again takes pleasure in thanking the authors of the various articles for their unselfish cooperation. It is hoped that the feeling of having made a useful contribution to the very serious problem of the dissemination of information in an assimilable form might in part compensate for the labors of writing the articles.

We must register regretfully several severe blows suffered by nuclear science during the last year through the loss of men who have opened entire new provinces of its domain. Frederic Joliot Curie died on August 14, at the early age of 58. The discovery of artificial radioactivity will make his name remembered forever. On August 27, Ernest O. Lawrence died at 57. The invention of the cyclotron was the pioneering step in the accelerator field and transformed in many ways the experimental art of nuclear physics. Death also took Friedrich A. Paneth on September 17, shortly after his seventy-first birthday. He pioneered in the use of isotopes as indicators in chemistry and in the nuclear aspects of geochemistry and cosmochemistry. Each of these men will also be remembered for his contributions to science as teacher, administrator, and public servant, and will be sorely missed by the wide circle of colleagues who have known him personally.

<div style="text-align:right">

C.L.C.   E.S.
T.P.K.   L.I.S.
D.J.H.   R.E.Z.

</div>

TOPICS AND AUTHORS
ANNUAL REVIEW OF NUCLEAR SCIENCE
VOLUME 9

CONTENTS

INVARIANCE PRINCIPLES OF NUCLEAR PHYSICS[1]

By G. C. Wick

Brookhaven National Laboratory, Upton, L. I., New York

1. INTRODUCTION

The study of nuclear energy-levels and reactions, and of high-energy processes between elementary particles, offers a wide and fruitful field to the application of invariance principles and symmetry considerations. The classical symmetry groups (rotations, etc.), that played so large a role in the applications of quantum mechanics to optical spectroscopy, have a completely analogous role here. Unlike spectroscopy, however, nuclear physics does not borrow entirely its symmetry principles from classical physics, but has to invent new invariance principles, to fit the new regularities and hidden symmetries that apparently exist, but do not show up at the usual macroscopic scale of things. Such symmetries are, for example, charge conjugation (or the symmetry between matter and antimatter) and isotopic-spin invariance. At the same time some of the older and most respected principles, such as the symmetry between left and right, are found to fail under certain circumstances.

This article is an attempt to summarize the present status of those principles, about which nuclear physics has had something new to say. The rotation group and proper Lorentz group, therefore, are barely mentioned in passing. Of the "classical" groups only space inversion or "P" and time reversal or "T" are discussed (see Sect. 2 and 3). Charge-conjugation (C) is discussed in Section 4; and some mixed operations obtained by combining P, T, and C are discussed in Section 5.

The emphasis throughout is on the general ideas, rather than on special applications; the latter are mentioned insofar as they illustrate the former. One cannot really present ideas of such a fundamentally mathematical nature without a certain amount of formal developments. The reviewer has made rather systematic use of the idea of quantized field, but has otherwise managed to avoid complicated calculations.

A discussion of isotopic spin-invariance or charge-independence and other related operations follows in Section 6. Finally in Section 7 the extension of these ideas to the heavy unstable particles, and the related notion of "strangeness" are mentioned. In the whole article, however, the reviewer assumes that the reader is already familiar with certain recent ideas, such as the distinction between "strong," "electromagnetic," and "weak" interactions. Explanations about notations will be found in Appendix A.

2. PARITY

2.1. *Space inversion and parity operator.*—The first subjects to be discussed are invariance against "space-inversion" and the associated concept

[1] The survey of literature pertaining to this review was concluded in April, 1958.

1

of parity, which plays a fundamental role in atomic and nuclear spectroscopy, as well as in the theory of collisions, nuclear reactions, etc. These classical applications of the parity concept, as will be seen, are not seriously invalidated by the recent discovery of violations of space-inversion invariance in β-decay and other weak interactions.

Parity is a rather subtle concept and it cannot be fully appreciated without paying attention to certain unfamiliar features of the general quantum mechanics of particles and fields. Let us begin, however, with the more elementary aspects of the parity concept. In the familiar discussion of the energy states of an electron in a central field, one finds that the levels can be classified into even and odd, i.e., levels with a Schrödinger function which is either an even or an odd function of the coordinate vector $x = (x_1 x_2 x_3)$. The same distinction can also be made in an elementary way for the levels of n electrons in a fixed central field, or for a free atom or molecule consisting of an arbitrary number of electrons and nuclei. In the latter case one must consider only that part of the wave function which describes the "relative" motion.

Another familiar point in spectroscopy is the statement (Laporte's rule) that allowed optical transitions only occur between states of opposite parity. This may be called the "law of parity change."

Attractive as these simple formulations are, they are unsuitable to deal with the more complex situations encountered in nuclear and high-energy physics. The key to a more general formulation is offered by the remark that all the above-mentioned propositions are a consequence of the invariance of the Schrödinger equation with respect to the coordinate transformation

$$x' = -x \qquad\qquad 1.$$

or $x_i' = -x_i$ ($i = 1, 2, 3$), i.e., the simultaneous inversion or reflection of all three coordinate axes, which is the simplest possible transformation from a right-handed to a left-handed coordinate system. The particular simplicity of it lies in the fact that it commutes with all the rotations. In the case of an external central field, the center must, of course, be chosen as the origin, but in the case of a free atom or molecule any point in space may act as center of inversion. The principle involved is, then, the symmetry of the Laws of Nature between right-handed and left-handed coordinate systems. The nature of the argument will be outlined before going into any formal details.

The assumed symmetry between right and left allows us to postulate that for every state of a free system one can define a "mirror-state," which is related to it in the same way as an object is related to its image after a reflection in the origin, as in Eq. 1.

One argues, then, that there must be a transformation, called the "parity operator" P, connecting a state-vector ψ and its mirror-image ψ'

$$\psi' = P\psi. \qquad\qquad 2.$$

One argues further, that this operator is linear-unitary[2] and satisfies the condition

$$P = P^{-1} \text{ i.e. } P^2 = 1 \qquad \qquad 3.$$

which expresses mathematically the reciprocal nature of the connection between a state and its mirror-image.

In the elementary case of the nonrelativistic Schrödinger equation of a system of interacting particles, the state-vector is simply a function $\psi(q)$ of the coordinates of all the particles, symbolized by a single letter q; and it is quite easy to see that the operator P can be defined by the equation

$$\psi'(q) = \psi(-q) \qquad \qquad 2'.$$

where, of course, the minus sign is applied simultaneously to all the coordinates. In the state ψ' the positions of all the particles and their momenta are inverted with respect to the state ψ, in the sense that the "probability" to find a certain particle at position x (or with momentum p) in the state ψ' is the same as the probability to find it at position $-x$ (with momentum $-p$) in the state ψ. All this can be easily demonstrated explicitly for Eq. 2', but must be a quite general property of the operator P, from the very definition of it.

The argument goes on further to state that if ψ is an eigenstate, of the energy operator H, then so is $P\psi$, and with the same eigenvalue (which again can be easily verified in the elementary case, but is a quite general consequence of the assumed invariance principle). A familiar argument shows, then, that P and H commute

$$PH = HP. \qquad \qquad 4.$$

According to well known theorems, the hermitian operator H and the unitary operator P can, therefore, be reduced simultaneously to diagonal form, i.e., it is possible to set up a complete set of energy states which are also eigenstates of P. If one also wants to diagonalize the total linear momentum p, he must limit himself to the case $p = 0$ (rest system) since otherwise ψ and $P\psi$ must have different values of p. Going back to Eq. 3 one sees that all eigenvalues of P are either $+1$ or -1, which concludes the argument leading to a classification into even and odd states, i.e., states for which

$$P\psi = \pm\psi. \qquad \qquad 5.$$

One realizes, now, that the argument is of an extremely general nature and should be applicable to all systems for which the left-right symmetry is valid.

Laporte's rule can be similarly generalized, but, interestingly enough, it now appears as a special case of a "law of parity conservation." This is immediately apparent if one enlarges the Hamiltonian in Eq. 4 to include the energy of the radiation field and its interaction with the atom, in which

[2] See the remarks in Section 2.3. For a deeper discussion of this point see Wigner's book (1), especially the Appendix to Chap. XX.

case one must similarly enlarge the operator P to include the effect of the space inversion on the state of the radiation field; and the equation then expresses the fact that P is a constant of the motion. Now the wavefunction ψ of the "whole system" will be a function of the coordinates q_A of the particles of the atom and of an infinite number of coordinates q_R pertaining to the various oscillator modes of the radiation field. In order to "reflect" the state ψ, one must operate on the particle coordinates q in the manner specified by Eq. 2′ and also operate in some suitable manner on the coordinates q_R. The global operator P is, therefore, the "product" of two operators

$$P = P_A P_R \qquad\qquad 6.$$

one of which affects the state of the atom (P_A) and the other one that of the radiation field (P_R). In the process of light emission or absorption, it will turn out that under the circumstances normally obtaining for spectroscopic lines (i.e., when the radiation emitted or absorbed is of the electric dipole type), the value of P_R changes sign in the transition. In order to conserve P, therefore, the parity of the atomic level P_A must also change, which is the rule of Laporte.

In a similar way, the parity selection rules for electric-quadrupole, magnetic-dipole, etc. radiation can all be obtained as special cases of the general parity conservation law.[3]

2.2. *Applications and Limits of Validity of Parity in Low Energy Nuclear Physics.*—In low energy nuclear reactions, excluding β-decay, no particles are created or destroyed, except photons. Therefore, the elementary discussion based on Eq. 2′ plus an assignment of parity to the multipole states of a photon covers most cases of interest. The shell-model, when it is valid, allows one to assign a priori a parity eigenvalue to the ground state of a nucleus. The parity of the low excited states may often be predicted by the shell-model or in other cases by the Bohr-Mottelson theory, etc. The parity of the initial state (in a center of mass reference system, as usual) in a reaction, such as

$$n + Be^7 \rightarrow He^4 + He^4 \qquad\qquad 7.$$

may be computed by noticing that an inversion of the coordinates of all protons and neutrons may be performed in two steps, i.e., (a) an inversion of the nucleons in Be^7 with respect to the center of mass of Be^7 (plus a similar inversion in the other colliding nucleus, if it is complex), and (b) an inversion

---

[3] It is appropriate to point out here, that although a parity quantum number $+1$ or -1 is assigned to each individual state of a system, the only question that ever really counts is the parity of a state relative to that of another state, i.e., whether they have the same or opposite parities. This is not surprising, since P and $-P$ satisfy the same defining equations (compare Section 2.3), and, therefore, either of them may be used as the "correct" parity operator. The unambiguous choice of P is, therefore, always based on some (tacit or explicit) convention, such as $P = +1$ for the "vacuum state" (compare end of Section 2.4 or Eq. B.9 in the Appendix).

of the relative coordinates of the two centers of mass of the two colliding nuclei. The parity is, therefore, in general

$$P = p_1 p_2 (-1)^l \qquad 8.$$

where p_1 and p_2 are the parities of the ground states of the two colliding nuclei and l is the orbital momentum of the collision. A similar expression holds for the final state. Case 7 is especially interesting because in the final state the parity is simply $(-1)^{l'}$, where the relative angular momentum l' of the He-nuclei can only take the values $l' = 0, 2, 4, \cdots$, (Bose-Einstein statistics). Hence the selection rule: reaction 7 can only occur if the initial value of P, Eq. 8, is $+1$. As an example: slow-neutron-induced reactions have $l = 0$; thus in Eq. 7 the initial parity is -1 [^{7}Be contains two ($1s$) neutrons and protons, two ($2p$) protons, and one ($2p$) neutron] and the reaction is forbidden for slow neutrons.

Recently, examples of such parity-forbidden reactions have been looked for with care, with negative results (2, 2a, b). The idea is that if small deviations from the right-left symmetry were present in the law of nuclear force, the wave function of a nuclear level would contain in general a small admixture F of a component of the "wrong parity" and thus forbidden reactions might occur. The experiments to date set upper limits to F of the order

$$F^2 \leq 10^{-7}. \qquad 9.$$

This limit is comparable to the limits that can be set to possible parity violations in the interactions of the electrons in the external structure of atoms, from the study of "forbidden" spectral lines.

Another argument, which has often been quoted in support of P-conservation, is the absence of static dipole moments in the stationary states of atoms or molecules. This follows from P-conservation, provided one assumes that there is no "accidental" degeneracy of states, i.e., no degeneracy besides that due to the $2J+1$ possible orientations of the angular momentum J. A well known theorem states, then, that the dipole moment D must be parallel to J

$$D = kJ \qquad 10.$$

where k is independent of the direction of J. Under a P-transformation, however, D, as a polar vector, changes sign while J does not, showing that k in Eq. 10 must be zero.

It was pointed out years ago (3, 3a) that the neutron would be an especially suitable object for the detection of a small electric dipole moment. The experiment has in fact set an upper limit (4)

$$|D/e| \leq 10^{-20} \text{ cm.}$$

which is quite low. It has been pointed out more recently, however, that the conclusions to be drawn from this result with regard to parity conservation are limited by the fact that a vanishing dipole moment is also required by invariance under time reversal (T). In fact, under the latter transformation J changes sign, while D does not. The roles of J and D are now interchanged,

but the conclusion $k = 0$ is obviously the same as before. Thus, only a theory which violates simultaneously P- and T-invariance could yield a non-vanishing static dipole moment.

2.3. *The parity operator, formal theory.*—The existence of a linear unitary P-operator can be demonstrated rather easily in any specific case of interest. In the case on nonrelativistic particle dynamics, the assertion follows immediately from the explicit form of the operator, Eq. 2′. In other cases, it is somewhat easier and more elegant to infer the existence and properties of P indirectly from the transformation properties of the quantum mechanical operators or matrices.

If the quantum-mechanical laws of a system are assumed to be invariant against the transformation from a right-handed to a left-handed coordinate system, Eq. 1, it must be possible to establish connections between the operators representing the physical variables in the two coordinate systems, in such a way, that the commutation laws and equations of motion have exactly the same form in the two systems.

In order to explain the method, let us re-examine from this angle the case of a nonrelativistic electron with spin, in a central field. Suppose the Hamiltonian operator has the form

$$H = (1/2m)p^2 + V(r) + s \cdot x \times p V_1(r) \qquad \qquad 11.$$

where $s = (s_1 s_2 s_3)$ is the vector operator representing the spin. The commutation laws are

$$[x_j, x_k] = [p_j, p_k] = [x_j, s_k] = [p_j, s_k] = 0.$$
$$[x_j, p_k] = i\delta_{jk}; \qquad [s_j, s_k] = is_l \qquad \qquad 12.$$

where j, $k = 1, 2, 3$ and $jkl = 123, 231$, or 312. The equations of motion follow from the general law

$$\frac{dQ}{dt} = i[H, Q] \qquad \qquad 13.$$

and from the commutation relations.

Now it is easy to see that the dependence of H on the canonical variables x, p, and s remains unchanged under the transformation

$$x = -x', \qquad p = -p', \qquad s = +s' \qquad \qquad 14.$$

The transformation is "canonical," i.e., it leaves the commutation laws Eq. 12 unchanged, whereby the "plus" sign in the transformation equation for the spin vector is essential. Now the quite essential assumption is made that Eq. 14 also represents the connection between the operators representing variables in the two systems. Notice in particular that the spin vector behaves as an "axial" vector, as indeed it should.

From the general theorems of transformation theory one can then infer the existence of a unitary operator P which transforms the matrices x', p', s' into the matrices x, p, s, or vice versa;

$$P^{-1}xP = x' = -x \qquad\qquad \text{15a.}$$
$$P^{-1}pP = p' = -p \qquad\qquad \text{15b.}$$
$$P^{-1}sP = s' = +s \qquad\qquad \text{15c.}$$

and it is quite easy to see that this is precisely the operator defined by Eq. 2 and 2'. To be sure, these equations were written for spinless particles, and we must now consider a "two-component" ψ. The last Eq. 15c shows, however, that P does not affect the spin state, so that Eq. 2' may be assumed for each of the two components independently. What Equations 15a and 15b assert, then, is that the matrices x and p calculated with respect to any complete orthonormal set of functions $u_1(x)$, $u_2(x)$, $u_3(x)$, $\cdots$, will simply change their sign if we transform to another orthonormal set $v_1(x)$, $\cdots$, where $v_n = Pu_n$; the verification of which may be left to the reader.

2.4. *Parity operator in electrodynamics.*—We are now ready to examine more complicated systems. Consider for example, the electromagnetic field: we may ask, what is the analogue of the canonical transformation 14? The dynamical variables are now the electric and magnetic field components $E_k(x)$ and $H_k(x)$, $(k = 1, 2, 3)$. The x coordinates are no longer dynamical variables, but merely "labels" for the field components! We know already from classical electrodynamics, that, in order to leave Maxwell's equations invariant under the coordinate transformation 1 we must assume the transformation law

$$E_k'(x') = -E_k(x); \qquad H_k'(x') = +H_k(x) \qquad\qquad \text{16.}$$

where $x'(=-x)$ on the left represents the "same point in space" as x does on the right. Since the equations must hold for any value of x we may also write them in the equivalent form

$$E_k'(x) = -E_k(-x); \qquad H_k'(x) = +H_k(-x). \qquad\qquad \text{17.}$$

One says that E transforms like a "polar" and H like an "axial" vector. In order to make this identification, one has assumed that the charges of the particles which produce the electromagnetic field are treated as scalar quantities, i.e., have the same value in the two systems. This is equivalent to saying that the current four-vector ρ, j_k $(k = 1, 2, 3)$ transforms according to

$$\rho'(x') = +\rho(x)$$
$$j_k'(x') = -j_k(x). \qquad\qquad \text{18.}$$

The current, of course, depends on the product of the charges by their velocities and, therefore, changes sign.

In quantum theory $E_k(x)$ and $H_k(x)$ are represented by "operators" obeying certain commutation relations:

$$[\mathcal{E}_j(x), \mathcal{E}_k(y)] = [\mathcal{H}_j(x), \mathcal{H}_k(y)] = 0$$
$$[\mathcal{E}_i(x), \mathcal{H}_j(y)] = -i\frac{\partial}{\partial x_k}\delta(x - y) \qquad\qquad \text{19.}$$

where we have used script characters to distinguish the operators from the corresponding classical quantities, and i, j, k is a cylical permutation of 1, 2, 3. It is natural to ask whether, in analogy to what we have done before, we are allowed to interpret 16 and 17 as equations between the "operators" which represent the fields in the two reference systems. One can indeed verify that the transformation is again canonical, i.e., $\mathcal{E}_j'(x)$ and $\mathcal{K}_k'(x)$ are operator functions of x which obey the same commutation relations as the unprimed operator functions, and there must be, therefore, a unitary linear transformation

$$P^{-1}\mathcal{E}_i(x)P = \mathcal{E}_i'(x) \equiv -\mathcal{E}_i(-x)$$
$$P^{-1}\mathcal{K}_j(x)P = \mathcal{K}_j'(x) \equiv \mathcal{K}_j(-x) \qquad\qquad 20.$$

where P will be called the parity operator for the electromagnetic field. If ψ is a state of the field, then the value of the magnetic field H in the state ψ and at the point x is equal to the value of H in the "mirror state" $P\psi$ and at the point $-x$; the corresponding values of the electric field E are equal and opposite.[4]

The Hamiltonian operator for the free Maxwell-field is, of course,

$$H = 1/2 \int [\mathcal{E}^2(x) + \mathcal{K}^2(x)]d^3x \qquad\qquad 21.$$

and remains unchanged under the substitutions $\mathcal{E}(x) \rightarrow -\mathcal{E}(-x)$, $\mathcal{K}(x) \rightarrow +\mathcal{K}(-x)$; therefore

$$PHP^{-1} = H \qquad\qquad 4.$$

as in the previous elementary cases, Eq. 4.

It is not difficult to exhibit an explicit form for the operator P. Let us consider for simplicity only the transverse part of the field, which is adequate to describe free photons. Let us expand the field, as usual, in normal modes, using the well known TM and TE spherical waves as modes. The expansion takes the form (5)

$$\mathcal{E}(x) = -\Sigma_n p_n E_n(x)$$
$$\mathcal{K}(x) = \Sigma_n q_n H_n(x) \qquad\qquad 22.$$

where n is the index of the n-th mode and q_n, p_n are the corresponding canonical variables; Maxwell's equation reduce to the oscillator form $p_n = \dot{q}_n$, $\dot{p}_n = -\omega_n^2 q_n$. The modes subdivide naturally into electric and magnetic 2^l-multipole waves. The components of $H_n(x)$ are even functions of x for the electric 2^l-poles of "even" l (quadrupole, sixteenpole, etc.) and for the magnetic 2^l-poles of "odd" l (dipole, octupole, etc.). These shall be called the "even" modes. For these modes the components of $E_n(x)$ are odd functions of x. Thus, the oscillator variables q_1, p_1, q_2, p_2, $\cdots$ naturally subdivide into two groups, the "even" variables symbolized by $q_e p_e$ and the odd vari-

---

[4] These statements should be understood, in general, in the same probabilistic sense as similar statements in Section 2.1.

ables by $p_o p_o$. The state-vector of the system may be taken to be a function $\psi(q_e q_o)$ of the positional variables. It is now immediately obvious that the canonical transformation of the fields, Eq. 17 or 20, corresponds to a reversal of the "odd" dynamical variables $q_o p_o$. The "even" variables remain unchanged. The behavior of the odd variables is completely analogous to Eq. 15a and 15b and, therefore, one is led to the definition for the parity operator $\psi' = P\psi$

$$\psi'(q_e, q_o) = \psi(q_e, -q_o). \qquad 23.$$

Of course, $\psi' = -\psi(q_e, -q_o)$ would be an equally valid definition. It is now easy to derive the selection rules for multipole emission. When an atom (which for simplicity is assumed to have an infinitely heavy nucleus at the origin) emits or absorbs a light-quantum, one of the modes of the field changes its quantum number from N to $N \pm 1$. The wavefunction of the field may be assumed to be a product of oscillator wavefunctions corresponding to the various modes. The oscillator wave functions for $N = 0, 1, 2, \cdots$ are known to be alternatively even and odd in the oscillator coordinate q. Eq. 23 shows that the parity of the state of the field is $(-1)^{\Sigma N}$, where the sum extends "over the odd modes only." Hence, emission to (or absorption from) an odd mode (such as electric dipole) changes the parity of the field. Emission into an even mode does not affect the parity. This result will be seen to confirm all parity selection rules for emission or absorption of light. The result is true also for emission by a free atom, molecule, or nucleus. although the proof given here does not apply strictly to that case.

It is noticed that the wavefunction of the "vacuum" state (the state in which there are no photons in the field) is a product of ground state wavefunctions for all oscillators, which is "even" in all the coordinates. Hence, the parity of the vacuum state is $+1$. This is, of course, the result of the arbitrary choice that was made between 23 and the other possible sign for the P operator. It shows why that particular choice was preferable!

Actually, one could in practice always assume that there are no other photons present except the photon which is emitted or absorbed. All that one needs to know is the parity of the one-photon states (that of the vacuum being set $= +1$). This could also be studied by means of a "wave equation" for the photon, and a corresponding parity operator for the photon wavefunction. The reader may try his hand at applying the method of Appendix B to the present case.

2.5. *The parity of spinless particles.*—In π-meson physics the question arises whether the parity of a system of colliding nucleons should change when a π-meson is emitted (or absorbed). Clearly this is analogous to the problem discussed in the preceding section, the main difference being that a π-meson has zero spin. The possible states of the emitted meson can now be classified as $s, p, d, \cdots$, i.e., states with orbital momentum $l = 0, 1, 2, \cdots$. A slight complication is that this should really be discussed as a problem in relative motion, but for the moment the reviewer will proceed as if he were

allowed to compound angular momenta with respect to a fixed center in the usual way.

The parity of the meson states with $l=0$, 2, 4, $\cdots$ is obviously the opposite of that of the states with $l=1$, 3, 5, $\cdots$, but, just as in the case of photon emission, the problem involves a comparison between the parity of a state with one meson with that of a state with no mesons. One may, of course, adopt the usual convention that the one-meson states have parity $+(-1)^l$, but then one is still left with the alternative possibilities to assign parity $+1$ or -1 to the no-meson state. Conversely, and this is perhaps more natural, one may assign parity $+1$ to the no-meson state and then consider two alternative assignments

$$+(-1)^l \quad \text{or} \quad -(-1)^l \qquad\qquad 24.$$

to the one-meson states.

In a field theoretic treatment the question appears as follows: A system of identical spinless bosons is described in the second quantization method by a field operator with a single component $\phi(x)$ which behaves as a scalar under a rotation of the coordinate axes. With regard to the inversion Eq. 1, however, ϕ may behave as a true scalar

$$\phi'(-x) = + \phi(x) \qquad\qquad 25.$$

or as a pseudoscalar

$$\phi'(-x) = - \phi(x). \qquad\qquad 25'.$$

It is absolutely essential to realize that, unlike the $\pm$ ambiguity of the P-operator, the difference between Eq. 25 and 25′ is very real. $\phi(x)$ is an "operator" (not a "state-vector!") which may appear in an interaction term in the Hamiltonian. As an example, the field representing the π°-meson might interact with the electromagnetic field through a term of the form

$$g \int \phi(x)\{E^2(x) - H^2(x)\}d^3x \qquad\qquad 26.$$

or of the form

$$g \int \phi(x)E(x)\cdot H(x)d^3x \qquad\qquad 26'.$$

where g is a proportionality constant. In view of the transformation law for the electromagnetic field, one sees that 26 is invariant under the assumption 25 and 26′ under the assumption 25′, but not vice versa. Thus, if parity is conserved, the two assumptions have different physical consequences; for example, both 26 and 26′ have matrix elements corresponding to a decay of the π° into two photons, but the mode of decay is different and can eventually be distinguished by experiment.

When 25 or 25′ is interpreted as an operator equation,[5] one can again

---

[5] A technical point is that one must also write an analogous equation for the canonically conjugate field representing the time derivative of ϕ. Another point is

infer the existence of a linear unitary operator P such that

$$P^{-1}\phi(x)P = \phi(-x) \qquad\qquad 27.$$

or respectively,

$$P^{-1}\phi(x)P = -\phi(-x). \qquad\qquad 27'.$$

The method described in the last section for light-quanta can obviously be extended. The operator $\phi(x)$ can be expanded in "normal modes" characterized by orbital and magnetic quantum numbers l, m, and by a third quantum number specifying the wavelength. Omitting m and the wavelength for simplicity, one may write

$$\phi(x) = \sum_l q_l Y_l(x) f_l(r) \qquad\qquad 28.$$

where Y_l is a spherical harmonic and f_l is the radial function of the l-th mode. Then, just as in the previous section, one sees that there are "even" modes and "odd" modes for which $q'_l = \pm q_l$ respectively, and precisely with 25 the even modes are those with even l, while with 25' the even modes are those with odd l. The reader will recognize immediately that this leads to the parity assignments of Eq. 24.

All evidence to date points to a pseudoscalar nature of the π-meson field, i.e., to the correctness of Eq. 25' and 27' and of the second assignment in Eq. 24. Strongest evidence is afforded by the selection rules in π^--capture by deuterium. Here there is good evidence (6) that the mesons cascade down to the K-orbit before being captured. The transition which is experimentally found to be allowed is one in which the π-meson in the K-orbit ($l=0$) is absorbed, while the deuterium nucleus decays into two neutrons (and nothing else). Because of conservation of angular momentum and the Pauli principle, the two neutrons can only be in the state $^3P_1$. Thus the nucleon system makes a transition from an "even" (^3S) to an odd ^3P state[6] which is compatible with parity conservation only if the π-meson is pseudoscalar.

2.6. *The parity of Dirac particles.*—The parity operator for a spin $1/2$ particle in the nonrelativistic theory has already been examined briefly. If one now investigates which transformation of the Dirac wave function is necessary in order to preserve the form of the Dirac Equation under the coordinate transformation 1, one finds immediately the rule

$$\psi'(x) = \epsilon\beta\psi(-x) \qquad\qquad 29.$$

where ϵ is an arbitrary complex constant, and β is the fourth Dirac matrix ($=\gamma_4$) (for notations used see Appendix A). In the ordinary scheme, multi-

---

that the operators P defined by 27 and 27' are quite different, which again emphasizes the difference between the $\pm$ sign in these equations, and the overall $\pm$ ambiguity of P!

[6] It is true, though, that the transition also involves the transformation of a proton into a neutron. One assumes that this does not affect the parity. About this point, see also the paragraph following Eq. 35' in Section 2.6.

plication of ψ by β means multiplication of the large (small) components of ψ by $+1$ (-1). The behavior of the "large" components (i.e., the components that are large in a nonrelativistic, positive-energy, state) corresponds exactly to what was said about the Pauli "two component" ψ (see lines following Eq. 15).

The 4×4 matrix β is unitary ($\beta = \beta^{\dagger}$ and $\beta^2 = 1$) and one sees easily that Eq. 29 in the one-particle or c-number interpretation of the Dirac equation defines a unitary P operator provided $|\epsilon| = 1$. If in addition we request $P^2 = 1$ (see Eq. 3), we must have

$$\epsilon = \pm 1 \qquad\qquad\qquad 29'.$$

which, of course, is the customary $\pm$ ambiguity of the P-operator. The choice $\epsilon = +1$ leads to the usual identification of s, d, g, $\cdots$, states as $P = +1$ states, and p, f, $\cdots$, states as $P = -1$ states. In fact, for example, in an s, d, $\cdots$, state the "large" components, for which $\beta = +1$, are even functions of x, while the "small" components, for which $\beta = -1$, are odd functions of x. As a result $\psi' = +\psi$ (and vice-versa for the other states).

In order to discuss the many problems in which Dirac particles are created or destroyed we go over to the second-quantized or q-number theory. The 4-components of the spinor ψ are then regarded as field operators obeying anticommutation relations

$$\{\psi_\rho(x), \psi_\sigma(y)\} = 0; \qquad \{\psi_\rho(x), \psi_\sigma{}^{\dagger}(y)\} = \delta_{\rho\sigma}\delta(x - y) \qquad 30.$$

where ρ, $\sigma (= 1, \cdots, 4)$ are spinor indices. Here, the theory is considered in the form applicable to particles which are different from their anti-particles (see Sect. 4), so that ψ and $\psi^{\dagger}$ are independent.

In the second quantized theory, Equation 29 defines the transformation of the field operator,[7] whereby one must point out that, provided $|\epsilon| = 1$, 29 preserves not only the form of the Dirac equation under 1, but also the anti-commutation laws of 30. Hence, in the usual manner the existence of a unitary P is inferred, such that

$$P^{-1}\psi(x)P = \psi'(x) = \epsilon\beta\psi(-x). \qquad 31.$$

The hermitean-conjugate of this equation reads (since $P^{-1} = P^{\dagger}$)

$$P^{-1}\psi^{\dagger}(x)P = -\epsilon^*\beta\psi^{\dagger}(-x) = \epsilon^*\psi^{\dagger}(-x)\beta \qquad 32.$$

(since $\beta^* = -\beta$; we use here the Majorana representation, see App. A). The "big" P-operator, defined by Eq. 31 and 32, is equivalent (as explained in App. B), when it acts on one-particle states, to the "small" P-operator defined directly by Eq. 29 in the c-number theory; that is to say, the two operators make the same relative parity assignments to the one-particle states.[8]

---

[7] The more detailed explanations of Section 2.3 and 2.4 as to the meaning of such statements need not be repeated here.

[8] A trivial but necessary remark is that the ϵ in Eq. 31 must not be confused with an overall phase factor for the P-operator. It is easy to see that the effect of ϵ is to multiply the parities of the one-particle states (relative to the vacuum) by ϵ, those of the two-particle states by ϵ^2, and more generally those of the states with n particles and m antiparticles by ϵ^{n-m}.

Obviously, however, "big" P covers an enormously wider range of states and contains more information. Let us consider, for example, following the method of Appendix B, the parity of positronium states, which are typical examples of states containing a particle and an antiparticle. A simple product wavefunction $u_r(x)u_s(y)$ for an electron in state r and a positron in state s (notice that both u_r and u_s must be positive energy states) corresponds to the ket $|r, \bar{s}\rangle = a_r{}^\dagger \bar{a}_s{}^\dagger | \rangle$. A more general state ζ may be described by a wavefunction $f_\zeta(x, y)$ which is a superposition of product wavefunctions. Since the corresponding ket is also given similarly by superposition, one has, in analogy to B.6, B.6′, and B.8, B.8′

$$| \zeta \rangle = \int \psi^\dagger(x)\psi(y)f(x, y)dxdy | \rangle \qquad\qquad 33.$$

$$f_\zeta(x, y) = \langle | \psi^\dagger(y)\psi(x) | \zeta \rangle \qquad\qquad 34.$$

where it should be understood that f has two spinor indices, equal to the spinor indices of $\psi(x)$ and $\psi'(y)$ in the above equations. If the state has zero total momentum, f_ζ is a function of $x-y$ only. If P is applied and Eqs. 31, 32, and B.9 are used, one finds that the wavefunction of the state $P|\zeta\rangle$ is

$$f_\zeta'(x, y) = \langle | \psi^\dagger(y)\psi(x)P | \zeta \rangle = \langle | P^{-1}\psi^\dagger(y)PP^{-1}\psi(x)P | \zeta \rangle$$
$$= - \epsilon\epsilon^*\langle | \beta_y\psi^\dagger(-y)\beta_x\psi(-x) | \zeta \rangle = - \beta_y\beta_xf_\zeta(-x, -y) \qquad 35.$$

where the subscripts x and y are appended to indicate that the β matrices operate on two different spinor indices, which go with x and y, respectively. Eq. 35 may now be regarded as the defining equation of P in the subspace of the positronium states. Remember that, as usual, the parity of these states has been anchored to $P=1$ for the vacuum state, Eq. B.9.

One may transform Eq. 35 back to a representation in which $\beta_x = 1$ and $\beta_y = 1$ for the "large" components. Hence, for these components the parity is defined by

$$f_\zeta'(x - y) = - f_\zeta(-x + y) \qquad\qquad 35'.$$

which means that $s, d, g, \cdots$, states are odd! Thus, for example, there is the selection rule, that when positronium in the ground (^1S or ^3S) state decays (into two or three photons) it can only decay into an odd state. [(For the parity of two-photon states see (7, 7a).] The -1 factor in front of Eq. 35′ is an "intrinsic" parity factor which, as the calculation shows (see also Footnote 8), is completely independent of the value of ϵ in Eq. 31. This remark is important, because in the case of the electron-positron field (or other charged fields), the general requirement of gauge invariance of the electrodynamic interactions implies in particular that multiplication of ψ by a phase-factor ϵ is devoid of any physical significance; hence, an unambiguous determination of ϵ in Eq. 31 is certainly impossible. This does not mean, however, that each Dirac field ψ_n has a completely arbitrary constant ϵ_n independent of the behavior of the other fields. But it is clear that a discussion of possible ties between ϵ_n's of different fields must depend on the structure of the existing interactions between the fields (see also next section).

Attempts to restrict the possible values of ϵ by more formal devices are necessarily somewhat arbitrary. For example, Eq. 3, or more generally the requirement that P^2, an unobservable transformation, be represented by a multiple of the unit matrix, which commutes with every operator, leads to

$$\psi(x) = P^{-2}\psi(x)P^2 = \epsilon^2\psi(x) \qquad 36.$$

and hence to $\epsilon = \pm 1$. What this argument ignores, however, is that the Dirac theory already has other unobservable transformations which are not represented by operators commuting with ψ, namely, any rotation through 360° about an arbitrary direction in space, and time-reversal repeated twice (see Sect. 3). This situation has been elucidated by Wigner, by means of the concept of "superselection rule" [see Wick, Wightman & Wigner (8)]. The basic point is that the measurability of the operators of quantum field theory is, in general, subject to limitations of a kind which is not usually anticipated in the usual treatments of the general principles of quantum mechanics. In case of Dirac's ψ, limitations exist a priori because physically measurable quantities can be scalars, vectors, etc., but never spinors. Further limitations may exist, however, as we shall see, because of other restrictions on the possible types of interactions existing in Nature.

2.7. *The parity operator for interacting fields.*—Let us first consider the interaction between charged particles and electromagnetic field, which is expressed in a well known way by the introduction of suitable interaction terms in the combined Lagrangean or Hamiltonian function for the electromagnetic field and the field or fields describing the charged particles. The effect of these extra terms is to produce the appearance of interaction terms in the field equations, e.g., of a charge and current-density term in Maxwell's equations. The essential point is now that the well known form of the interaction Hamiltonian, as obtained from other consideration, automatically satisfies the invariance law, Eq. 4, whereby the transformation properties of the various fields are simply taken over from the Equations 20, 27, or 27', 31, and 32 for noninteracting fields. A P-operator of this kind for the combined system of interacting fields may be obtained, of course, by multiplication of the previously defined P-operators, each of which acts only on the variables of a specific field. Only an example of such invariance considerations will be given here, by showing that the customary expressions for the charge- and current-density in the Dirac theory

$$\rho(x) = e\psi^\dagger(x)\psi(x); \qquad j_k(x) = e\psi^\dagger(x)\alpha_k\psi(x) \qquad 37.$$

do indeed transform according to Eq. 18. In fact, beginning with ρ one finds by definition

$$\rho'(x) \equiv P^{-1}\rho(x)P = eP^{-1}\psi^\dagger(x)PP^{-1}\psi(x)P = e\epsilon\epsilon^*\psi^\dagger(-x)\beta\beta\psi(-x) = \rho(-x)$$

where a harmless $PP^{-1} = 1$ has been inserted, and the Dirac relation $\beta^2 = 1$ has been used. Similarly $j'(x)$ is found to agree with Eq. 18 by using the Dirac relation $\beta\alpha_k\beta = -\alpha_k$. Since the transformation laws for the electromagnetic field, Eq. 16 and 20, were chosen precisely so as to accommodate

the invariance of Maxwell's equation with the transformation 18, it will be apparent that the essential step in the invariance proof has thus been achieved. The proof in the case of the current four-vector for spinless particles (scalar or pseudoscalar fields) proceeds along exactly similar lines and will not be repeated here.

As another example, let us consider the interaction between nucleon and meson fields. Following Yukawa's general ideas, one describes this interaction in the closest possible analogy with the interaction between electron and Maxwell fields, the mesons playing a corresponding role to that of photons. Thus, if ψ is the Dirac field which describes the nucleons, one describes the interaction by introducing on the "right hand side" of the free meson field equation a source function, which like the electrodynamic current four-vector Eq. 37 is bilinear in $\psi^\dagger$ and ψ. The essential differences between the two cases arise from (a) the finite mass μ of the mesons, (b) the pseudoscalar nature of the meson field as against the vector nature of the Maxwellian field, and (c) the existence of two kinds of nucleons (n and p) and three kinds of mesons ($\pi^\pm$ and π^0). Let us for the moment neglect the latter circumstance; that is, let us describe, for example, only the interaction of π^0 mesons with protons. There is then a single pseudoscalar meson field ϕ and a single Dirac field ψ. The source function j in the meson field-equation

$$(\Box - \mu^2)\phi = j \qquad\qquad 38.$$

must be a pseudoscalar bilinear form in $\psi^\dagger$ and ψ, and if one assumes, for simplicity, that no derivatives are involved the only possible choice is

$$j = ig\psi^\dagger \gamma_4 \gamma_5 \psi \equiv g\psi^\dagger \rho_2 \psi \qquad\qquad 39.$$

where g is a proportionality constant. That 39 is invariant against ordinary rotations and proper Lorentz transformations may be easily proved. Only the behavior under a P transformation will be considered here. Using Equations 31 and 32 one sees that

$$P^{-1}j(x)P = g\psi^\dagger(-x)\beta\rho_2\beta\psi(-x) = -j(-x) \qquad\qquad 40.$$

i.e., $j(x)$ is pseudoscalar. Accordingly, Eq. 38 remains invariant if ϕ obeys 27'. The interaction term in the Hamiltonian which gives rise to the source term j in Eq. 38 is of the form

$$H' = \int j(x)\phi(x)d^3x \qquad\qquad 41.$$

and commutes, therefore, with P.

The situation is essentially the same in the complete treatment (see Sect. 6.4) provided one assumes that proton and neutron field both transform in exactly the same way, Eq. 31, or, in other words, if one assigns the same parity to neutron and proton.[9]

---

[9] Compare Footnote 5. The statement means, of course, that if one assigns the same ϵ to ψ_p and ψ_n, then the similar constant for the meson field can be set equal to -1. This is an example of the tying together of different ϵ-constants for various fields (Sect. 2.6).

2.8. *Violations of parity in β-decay and similar processes.*—The tests of P conservation, that have been mentioned before are fairly sensitive, but β-decay and similar phenomena provide an enormously more sensitive test, because the coupling constant involved is about 10^{-7} in natural units ($\hbar$, c, and the π-meson mass, say). It is now well known that many experiments on β-decay, $\pi - \mu - e$ decay, and Λ-decay exhibit asymmetries which allow one in an obvious manner to draw a distinction between a left-hand and a right-hand. The distinction only becomes ambiguous when one draws the notion of antimatter into the picture (see Sect. 5). The operation P, however, by definition does not interchange matter and antimatter, and the experiments, therefore, represent a clear violation of P-invariance.

In view of this, a legitimate question may be asked, as to whether it makes any sense at all to talk about parity. A symmetry operator is, in fact, definable on the assumption that the symmetry exists. Strictly speaking, therefore, one ought to say now that the mirror image of a μ^- meson does not exist, because according to our definition it would be again a μ^- meson, but its decay probability in the various directions, relative to its spin-direction, would not be compatible with the observed law.

One does not need take this extreme point of view, however. Since the β-decay interaction is so extraordinarily weak, one may assume for a moment, that it just does not exist. Parity then becomes an approximate concept that is valid to an extraordinarily high degree of accuracy. Formally, this means that the P operators for the various fields must be defined so as to satisfy invariance for the "strong" and electromagnetic interactions. Experimentally, it means that only "strong" reactions or electromagnetic processes can be used in determining the intrinsic parity of particles.

It is obvious that these limitations imply corresponding limitations in our ability to define P. That is to say, they increase the number of possible ambiguities, that have been already found to exist. Let us examine, for example, β-decay in more detail. It has been known for a long time that it is possible to write formally parity-violating interactions within the customary scheme. Let us now designate by p, n, e, and ν the Dirac fields describing protons, neutrons, electrons, and neutrinos, respectively. Let us write, for example, the so-called vector interaction

$$V = C_v \int (p^\dagger \beta \gamma_\mu n)(e^\dagger \beta \gamma_\mu \nu) d^3x \qquad\qquad 42.$$

where p, n, e, and ν are all functions of the same field-point x, and C_v is a coupling constant. This is not only invariant against proper Lorentz transformations, which will not be discussed, but also against P, provided one defines the P transformation of all four fields by means of Eq. 31 and 32 with the same ϵ, say $\epsilon = 1$, for all four fields. This is easy to verify, using $\beta(\beta \gamma_\mu)\beta = \pm \beta \gamma_\mu$ (+ for $\mu = 4$, − for $\mu = 1, 2, 3$).

This is, however, by no means necessary. One could assume, for example,

that the neutrino field has $\epsilon = -1$, i.e., the opposite parity. In this case, Equation 42 is not invariant, but the following interaction is

$$V' = C_{v}' \int (p^{\dagger}\beta\gamma_{\mu}n)(e^{\dagger}\beta\gamma_{\mu}\gamma_{5}\nu)d^{3}x. \qquad 43.$$

If, however, one assumes a combination of both: $H = V + V'$ there is no assumption about the P transformation of the four fields which will preserve the invariance of H. It is just by assuming combinations such as these, that Lee & Yang (9) first predicted the asymmetries that were later observed in Co^{60}, etc.

This being the case, there clearly is no criterion to decide which is the correct P for the neutrino field, since the neutrino only appears in weak interactions. Comparable ambiguities appear in the parity of the strange particles, owing to nonconservation of parity in their decay processes.

3. Time Reversal

3.1. *Time Reversal.*—The classical equations of motion of a dynamical system possess the property of time reversibility, which has played, in the past, a considerable role in discussions about fundamental principles in statistical mechanics and thermodynamics.

That the laws of quantum mechanics possess a similar property can be seen most simply in the case of the nonrelativistic time-dependent Schrödinger equation where one verifies easily that, if $\psi(x, t)$ is a solution, then $\psi'(x, t) = \psi^{*}(x, -t)$ is also a solution representing, in general, a wave packet whose density distribution performs the time reversed motion by comparison with the density distribution of the wave packet ψ.

Considering the transformation "at a given time," say $t = 0$, one will say that

$$\psi'(x) = \psi^{*}(x), \qquad 44.$$

represents the time reversed state with regard to ψ.

In analogy with Equation 2' one anticipates that, quite in general, it will be possible to define some operator T which transforms a state ψ into the "time reversed state"

$$\psi' = T\psi. \qquad 45.$$

This time reversed state must have the property that, in it, momenta and angular momenta have the opposite sign, while positions remain unchanged; all of which must be understood in the same sense as similar statements made for P.

It is now important to notice, that, even in the elementary case above, T is obtained so simply by complex conjugation only because of the particular representation used. If, for example, one considers the Fourier transforms (wavefunctions in momentum space) $\phi(p)$ and $\phi'(p)$ corresponding to ψ and ψ' one has

$$\phi'(p) = \phi^{*}(-p) \qquad 46.$$

where, in addition to complex conjugation, one has the transformation $\phi(p) \to \phi(-p)$.

The generalization which is necessary to cover all cases has been indicated by Wigner (1). One may notice that, unlike the other transformation operators one usually meets in quantum mechanics, the T-transformations, Eq. 44 and 46, are nonlinear. They possess, however, a property very similar to linearity; namely, when T is applied to a linear combination of two state vectors ψ_1 and ψ_2 with coefficients c_1 and c_2 one has

$$T(c_1\psi_1 + c_2\psi_2) = c_1^*T\psi_1 + c_2^*T\psi_2. \qquad 47.$$

One says that T is "antilinear." For comparison, the equation for a linear operator U is

$$U(c_1\psi_1 + c_2\psi_2) = c_1U\psi_1 + c_2U\psi_2. \qquad 48.$$

At the same time Eq. 44 or 46 preserves the norm of ψ, i.e.,

$$(T\psi, T\psi) = (\psi, \psi). \qquad 49.$$

Later it will be seen, that for all time-reversible systems a T-operator with the properties 47 and 49 exists. Such an operator is called antilinear-unitary or, more briefly, antiunitary. It is easy to see that such an operator transforms the scalar product of two state-vectors as follows:[10]

$$(T\psi_1, T\psi_2) = (\psi_2, \psi_1) \equiv (\psi_1, \psi_2)^*. \qquad 50.$$

From Eq. 48, 49, and 50 one can easily infer that T must be of the form

$$T = UK \qquad 51.$$

where U and K are defined as follows. Expanding ψ in a complete set of orthonormal states, $\psi = \sum_n c_n\psi_n$, one may say, as usual, that ψ is a vector with components $c_1, c_2, \cdots$, and write symbolically

$$\psi = (c_1, c_2, c_3, \cdots). \qquad 52.$$

We may then define a complex-conjugate vector $K\psi$ as the vector with the complex conjugate components

$$K\psi = (c_1^*, c_2^*, c_3^*, \cdots). \qquad 53.$$

We further have, because of Eq. 47,

$$T\psi = \sum_n c_n^*T\psi_n \qquad 54.$$

where the states $T\psi_1, T\psi_2, \cdots$ also form, as a consequence of 49 and 50, an orthonormal set. One can also argue that the T-transformation must possess an inverse T^{-1} (which is essentially T itself, see later), so that the set $T\psi_1, T\psi_2, \cdots$, must also be complete and, hence, is connected to the original set $\psi_1, \psi_2, \cdots$, by a transformation

[10] To prove Eq. 50 apply the unitarity conditions successively to $\psi = \psi_1 + \psi_2$ and $\psi = \psi_1 + i\psi_2$ remembering Eq. 47. A more general and rigorous proof of the antilinear-unitary nature of the T-operator will be found in Wigner's work (1).

$$T\psi_n = U\psi_n \equiv \sum_m \psi_m U_{mn}$$ 55.

where the matrix U is unitary

$$UU^\dagger = U^\dagger U = 1.$$ 56.

This completes the definition of U and K. Eq. 54 may now be written

$$T\psi = \sum_n c_n{}^* U\psi_n = U\left(\sum_n c_n{}^*\psi_n\right) = UK\psi,$$

which constitutes the proof of 51.

The reader should notice that the definition 53 of the complex conjugate of ψ is tied to the particular representation used. This is, however, unavoidable. A more natural definition might seem to be $\psi^* = \sum c_n{}^*\psi_n{}^*$, but this leads to a vicious circle, since one must say what $\psi_n{}^*$ means. If one changes representation, i.e., uses a new orthonormal set ψ_1', ψ_2', $\cdots$, the rule 53 defines a new operation K' which is in general different from K; one has $K' = VK$, where V is a unitary transformation; this need not affect T, as V can be "absorbed" into the factor U.

3.2. *Applications and validity of T-invariance.*—Time-reversal considerations have numerous applications in nuclear physics, which space does not allow us to discuss. An example is the theorem on static dipole moments, mentioned at the end of Section 2.2. The consequences of T-invariance generally appear in the form of connections between inverse processes and phase-relations between matrix-elements or emission amplitudes.

Suppose one has a matrix element $\langle A|\Omega|B\rangle$ of a certain operator Ω, which may be, for example, a small perturbation Hamiltonian producing a transition from B to A. Very often the time reversed operator $\Omega' = T^{-1}\Omega T$ will be related to Ω in some simple way, such as $\Omega' = \pm\Omega$. Similarly, the time reversed states $|A'\rangle = T|A\rangle$ and $|B'\rangle = T|B\rangle$ will be related to the original states in some simple manner; for example, if A belongs to a set of states describing free particles with variable momenta, A' will be a state of the same set, with reversed momenta. A slightly more complicated example will be considered below.

Now consider the matrix element of Ω between the time reversed states $\langle A'|\Omega|B'\rangle$; one sees, by applying theorem 50 to the states $\psi_1 = |A\rangle$ and $\psi_2 = T^{-1}\Omega|B'\rangle$, that

$$\langle A'|\Omega|B'\rangle^* \equiv \langle A'|TT^{-1}\Omega|B'\rangle^* = \langle A|T^{-1}\Omega|B'\rangle$$
$$= \langle A|T^{-1}\Omega T|B\rangle = \langle A|\Omega'|B\rangle.$$ 57.

This connects, then, the complex conjugate of a matrix element of Ω to a matrix element of Ω'. In certain cases $|A\rangle$ and $|B\rangle$ may be eigenstates of T (e.g., discrete stationary states with $J_z = 0$ belong to this category); for example, $|A'\rangle = |A\rangle$, $|B'\rangle = |B\rangle$. Then according as $\Omega' = \pm\Omega$, one has proved by means of Eq. 57 that $\langle A|\Omega|B\rangle$ is real or alternatively pure imaginary.

Such reality conditions occur, for example, in mixed electromagnetic transitions (10).

In other cases Eq. 57 is used to prove equalities between the probabilities of inverse processes. A particularly simple formulation is obtained by means of the scattering matrix S. One finds then that

$$S' = T^{-1}ST = S^{-1} = S^{\dagger}. \qquad 57'.$$

This gives rise to various theorems on scattering (11, 11a, b, c).

These numerous consequences depend, of course, on the assumption that T-invariance is valid. The evidence with regard to strong interactions has been re-examined by Henley & Jacobsohn (12). Various tests of T-invariance in weak interactions have been suggested (13, 13a, b, c), but no violation of T has been observed to date (14, 14a, b).

3.3. *The time reversal operator, formal theory.*—The discussion here can be carried on in complete analogy to our earlier discussion of P, if time-reversibility is defined as invariance of the laws of a system against the transformation from the four-dimensional coordinate system x, t to the system x', t' defined by

$$x' = x, \qquad t' = -t. \qquad 58.$$

In this case the observer O' uses the same space axes, but a clock running backwards! One may then define the time-reversed state as the state which is described by O' in the same way as the original state is described by O.

Let us now examine again as an example the Hamiltonian Eq. 11. The classical connection between variables in the two systems is obviously

$$x = x', \qquad p = -p', \qquad s = -s' \qquad 59.$$

where the variables x, p, s are regarded as functions of t, and x', p', s' as functions of $t' = -t$. One now notices that the substitution 59 leaves the form of the Hamiltonian 11 unchanged, as desired; one also notices that, together with the time transformation 58, it leaves the form of the equations of motion unchanged, as desired; for example,

$$\frac{dx'}{dt'} = -\frac{dx'}{dt} = -\frac{dx}{dt} = -\frac{p}{m} = \frac{p'}{m} \text{ etc.}$$

One notices, however, that 59 is "anticanonical," i.e., if it is regarded as a connection between the operators or matrices representing $x, \cdots, s'$, the commutation laws, 12, for the primed variables come out with the wrong sign!

At first sight this might seem to wreck our invariance proof, but it is really only another facet of the odd nature (i.e., antilinearity!) of the time-reversal operation. Usually, two sets of matrices are defined as "equivalent" if they are obtained from one another by the scheme

$$x \to U^{-1}xU \qquad 60.$$

where U is a unitary matrix. Let us, however, introduce the idea of "anti-unitary transformation"

$$x \to T^{-1}xT \qquad 61.$$

where T is an operator of the form 51. The reader may convince himself easily that it is perfectly legitimate to treat the symbol K as an ordinary operator acting on state vectors and write, for example, $T^{-1} = K^{-1} U^{-1}$. The inverse of the operation 53 is, however, identical with K itself, i.e.,

$$K = K^{-1} \quad \text{or} \quad K^2 = 1. \qquad\qquad 62.$$

If the reader has any difficulty with this symbolism, he may think of an n-dimensional complex vector $\psi = (c_1 c_2 \cdots, c_n)$ as a $2n$-dimensional real vector $\psi = (a_1 a_2 \cdots, a_n; b_1 b_2 \cdots, b_n)$, where each component $c_n = a_n + i b_n$ is replaced by its real and imaginary parts. The whole matrix scheme can, of course, be transcribed in this real $2n$-dimensional notation. K is now a linear orthogonal transformation $\psi \rightarrow (a_1 a_2 \cdots a_n; -b_1, -b_2, \cdots, -b_n)$ and notations such as 62, etc. become perfectly normal.

Now transformation 61 may be decomposed into two steps; the first is

$$x \rightarrow K x K^{-1} \qquad\qquad 63.$$

and the second step is of the "ordinary" type 60. One may, therefore, limit himself to examining what happens to the ordinary matrix scheme of quantum mechanics when the transformation 63 is applied. Actually, all that 63 means is that every matrix element is changed to its complex conjugate value. Obviously all the commutators, Eq. 12, change sign. When 63 is applied to the basic time-differentiation law, Eq. 13, it becomes

$$\frac{dQ}{dt} = -i[H, Q]. \qquad\qquad 64.$$

This change, together with the sign reversal of the commutators, means that the Hamiltonian equations of motion remain unchanged! All this boils down to the rather trivial remark that if in all the fundamental equations of quantum mechanics the imaginary unit i is changed to $-i$, none of the physical results are altered.

This is, however, precisely all that is needed, in order to assert that the transformation Eq. 59, regarded as operator equalities, define two equivalent schemes in the two systems of reference! Analogously to our procedure in the case of P, one may argue that, since 63 transforms x, p, and s into matrices obeying the same commutation laws as x', p', s', there must be a unitary matrix U which, combined together with K as in 51, effects the transformation

$$
\begin{aligned}
T^{-1} x T &= x' = x \\
T^{-1} p T &= p' = -p \\
T^{-1} s T &= s' = -s.
\end{aligned}
\qquad\qquad 65.
$$

Now, let us assume that we work in the customary Pauli representation, i.e., that ψ is a two-component wavefunction in configuration space. Then K alone already satisfies the first two Eq. 65. Therefore, the matrix U need

only operate on the spin index, i.e., it is a 2 by 2 matrix satisfying

$$U^{-1}sU = -s^*$$ 66.

where the components $s_k = (1/2)\sigma_k$ are the customary Pauli matrices. One easily sees that the matrix

$$U = \begin{pmatrix} 0 & 1 \\ -1 & 0 \end{pmatrix} = i\sigma_y$$ 67.

and only this matrix (apart from an arbitrary multiplicative constant) satisfies Eq. 66. The connection with the y-axis is, of course, purely accidental; it is easy to see that U does not depend on the particular representation used for the Pauli spin matrices.

In conclusion the time-reversal operation of the Pauli 2-component wavefunction is

$$T \begin{pmatrix} \psi_1 \\ \psi_2 \end{pmatrix} = \begin{pmatrix} \psi_2^* \\ -\psi_1^* \end{pmatrix}.$$ 68.

The meaning of 68 may become more clear as follows: first, the complex-conjugation sign reverses the sign of the linear momentum; then since $|\psi_1|^2$ and $|\psi_2|^2$ are the probabilities for spin up and down respectively, and since time reversal interchanges the two situations, T must also involve an interchange of ψ_1 and ψ_2. Finally, one of the two components must change sign, because T must also interchange the probabilities for spin parallel and antiparallel to the x-direction, which are given by $(1/2)|\psi_1 \pm \psi_2|^2$, or in the y direction, which are given by $(1/2)|\psi_1 \mp i\psi_2|^2$.

Before proceeding to other examples one notices an important property of the T-operator. Repeating time-reversal twice must lead back to the original state. Therefore, $T^2\psi = c\psi$ where c is a multiplicative constant. If this constant were different for two different states ψ_1 and ψ_2, then $T^2(\psi_1 + \psi_2) = c_1\psi_1 + c_2\psi_2$ would not be a multiple of $\psi_1 + \psi_2$; therefore, c must be independent of ψ, i.e., $T^2 = c1$, a multiple of the unit matrix. Now, from Eq. 51, $T^2 \equiv UKUK \equiv UU^* = c1$ or $U = cU^{*-1}$. Now U is unitary, hence $U^{*-1} = U^T$, the transpose of U. So finally, $U = cU^T$ and transposing both sides $U^T = cU = c^2U^T$ from which $c^2 = 1$. Thus the only two possible values for T^2 are

$$T^2 = 1$$ 69.

which is satisfied by Eq. 44 for a spinless particle, and

$$T^2 = -1$$ 70.

which is satisfied by 68 for a spin 1/2 particle, and more generally, as Wigner pointed out, by a system with an odd number of spin 1/2 particles, e.g., a nucleus with odd A. The reader should take careful note of the fact that multiplication of the matrix U by a phase factor $e^{i\delta}$ will not alter the value of $UU^* = T^2$. The difference between 69 and 70 is an intrinsic one.

3.4. *T for the electromagnetic field.*—One may proceed as in Section 2.4. In order to preserve Maxwell's equations under time-reversal, without

changing the sign of electric charges, one must leave $\mathcal{E}$ unchanged and reverse the sign of $\mathcal{K}$; hence

$$T^{-1}\mathcal{E}_i(x)T = \mathcal{E}_i{}'(x) = \mathcal{E}_i(x)$$

$$T^{-1}\mathcal{K}_i(x)T = \mathcal{K}_i{}'(x) = -\mathcal{K}_i(x)$$

71.

which, of course, leaves the Hamiltonian invariant. It is easy to see, by methods similar to those of Appendix B, that T transforms a one-photon state into a one-photon state of opposite linear momentum, without interchanging right-circular with left-circular polarization.

3.5. *T for Dirac particles.*—This case will be examined starting right away from the q-number theory. There are several new features of interest in this case. First of all, the anticommutation laws, 30, do not contain the imaginary unit i; hence, they will not tell us whether T is linear or antilinear. For the reasons already mentioned (see footnote 10) we shall proceed, however, on the assumption that it is antilinear as in the other cases.

Dirac's equation for electrons in the presence of an electromagnetic field is written

$$\left(\frac{\partial}{\partial t} + \boldsymbol{\alpha}\cdot\boldsymbol{\nabla} + im\beta\right)\psi = ie(\boldsymbol{\alpha}\cdot\boldsymbol{A} - V)\psi$$

72.

where V is the scalar and $\boldsymbol{A}$ is the vector-potential of the field. The assumption is that the Dirac field ψ' in the time-reversed coordinate system is connected to ψ by a "suitable" linear relation $\psi' = u\psi$, which is chosen in such a way that the Dirac wave equation and the corresponding equation satisfied by ψ' have an "equivalent" form. Here, we must say equivalent and not the "same form" because the equations contain the imaginary unit, which must change sign from one system to the other! Hence

$$\left(\frac{\partial}{\partial t'} + \boldsymbol{\alpha}^*\cdot\boldsymbol{\nabla}' - im\beta^*\right)\psi' = ie(\boldsymbol{\alpha}^*\cdot\boldsymbol{A}' - V')\psi'.$$

However, in view of the Equations 71 one must write $V' = V$, and $\boldsymbol{A}' = -\boldsymbol{A}$ (for $t' = -t$, of course). Furthermore matters are simplified by using the Majorana representation $\alpha^* = \alpha$, $\beta^* = -\beta$. Finally, since $t' = -t$, $\boldsymbol{x}' = \boldsymbol{x}$

$$\left(-\frac{\partial}{\partial t} + \boldsymbol{\alpha}\cdot\boldsymbol{\nabla} + im\beta\right)\psi' = ie(\boldsymbol{\alpha}\cdot\boldsymbol{A} + V)\psi'$$

73.

which differs from 72 only in the sign of the terms not containing α or β. One infers that the matrix u must anticommute with α and β. The only such matrix (apart from a factor) is $\rho_2 = i\gamma_4\gamma_5$ (see App. A). Therefore, we shall write (for $t = 0$)

$$T^{-1}\psi(x)T = \psi'(x) = \rho_2\psi(x)$$

74.

The hermitean conjugate of this equation (compare Eq. 32) is

$$T^{-1}\psi^\dagger(x)T = \rho_2{}^*\psi^\dagger(x) = \psi^\dagger(x)\rho_2.$$

75.

Using $\rho_2{}^2 = 1$ one sees that the anticommutation laws 30 are indeed left unchanged. From Eq. 37 one sees that

$$T^{-1}\rho T \equiv \rho' = e\psi^\dagger \rho_2 \psi = \rho \qquad\qquad 76.$$

$$Tj_k T^{-1} \equiv j_k' = e\psi^\dagger \rho_2 \alpha_k{}^* \rho_2 \psi = -j_k \qquad\qquad 77.$$

($\alpha_k{}^* = \alpha_k$ was used) which is as it should be and fits in nicely with (71).

The really interesting point is the Hamiltonian. For simplicity only the part relating to the free field will be written

$$H = -i \int \psi^\dagger (\boldsymbol{\alpha} \cdot \boldsymbol{\nabla} + im\beta) \psi d^3x. \qquad\qquad 78.$$

Notice the i in front! Therefore, the "equivalent" Hamiltonian

$$T^{-1}HT = +i \int \psi'^\dagger (\boldsymbol{\alpha} \cdot \boldsymbol{\nabla} + im\beta) \psi' d^3x \qquad\qquad 79.$$

has the opposite sign. However, with 74 and 75, and using $\rho_2 \alpha \rho_2 = -\alpha$ $\rho_2 \beta \rho_2 = -\beta$ one has

$$THT^{-1} = H \qquad\qquad 80.$$

which proves the invariance of the Hamiltonian.

Finally let us examine, as in the case of parity, the connection between "big" T, the operator for the full-scale q-number Dirac theory, and "small" T the time reversal operator which connects the ordinary ("c-number") wavefunctions of a state and of the time-reversed state. Let $|\alpha\rangle$ be a one-particle state, as in Appendix B. The corresponding Dirac wavefunction is, at time 0

$$f_\alpha(x, 0) = \langle | \psi(x) | \alpha \rangle. \qquad\qquad 81.$$

The wavefunction of the time-reversed state may be written in the same way as a matrix element of $\psi(x)$ between the time reversed states $T|\alpha\rangle$ and $T| \rangle = | \rangle$, the latter being the usual convention (compare Eq. B.9, etc.). Hence, from the theorem Eq. 57

$$f_{\alpha}'(x) = \langle | \psi'(x) | \alpha \rangle^* = [\rho_2 f_\alpha(x)]^* = -\rho_2 f_\alpha{}^*(x). \qquad\qquad 82.$$

The reason why in the case of time-reversal, contrary to the theorem of Appendix B, the transformation law for the c-number wavefunction is slightly different from the transformation 74 of the q-number wave function lies, of course, in the complex conjugation sign in 82, which is required by the antilinear nature of T, when the Dirac wavefunction is regarded as a state vector!

The reader should carefully remember that many of the equations written are valid (without modification) only in the Majorana representation. Eq. 82 is an example; this explains the lack of any apparent connection between it and the transformation law for the Pauli 2-component wavefunction, Eq. 68. In Appendix A it is shown, however, that 82 implies pre-

cisely the transformation 68 for the "large" components. Thus, one may say that 82 reverses the linear momentum and the spin direction of the particle, as of course it must. Another way of verifying this, is to consider a state of definite "helicity," i.e., an f_α such that

$$p \cdot \delta f_\alpha \equiv -i\delta \cdot \nabla f_\alpha = \epsilon f_\alpha$$

where $\epsilon = \pm |p|$. Then, since δ and ρ_2 commute and $i\delta$ is a real matrix:

$$p \cdot \delta f_\alpha' = -\rho_2(-i\delta \cdot \nabla f_\alpha)^* = \epsilon f_\alpha'.$$

The time reversed state has the same helicity, as expected!

3.6. *Interacting fields.*—The invariance of other schemes involving interacting fields can be discussed by means of the transformation laws 71, 74, etc. in a manner analogous to Section 2.7. The only point to remember is that the complex conjugation implied by T also changes every coefficient into its complex conjugate, whereby the reality properties of the Dirac matrices in the Table of Appendix A will have to be used. In this way it may be seen, for example, that the β-decay interactions, Eq. 42 and 43, are T-invariant provided C_v and C_v' (and more generally the customary 10 constants) are real. If, as is rather likely, the neutrino has strictly zero mass, a further invariance property of the theory (15, 15a, b, c) which shall not be discussed here, allows one to show that the invariance of the β-decay theory under time-reversal may be formulated in a somewhat less restrictive form (16).

4. Charge Conjugation

4.1. *History.*—In earlier days a fundamental difference or asymmetry was thought to exist between the two kinds of electricity, positive and negative, an asymmetry which, to be sure, does not show up in the known laws of electromagnetism, and was assumed, therefore, to lie deeper, in the as yet unknown laws which determine the structure and properties of the elementary particles.

This belief was struck at the core by the discovery of the positron. Not only did the positron appear as the exact counterpart to the negative electron; it also fulfilled one of the boldest predictions of the Dirac theory of the electron, and thus considerably enhanced the weight of the argument on which the prediction had been based. That argument was the charge conjugation symmetry of Dirac's theory, which was later formulated more precisely by Majorana, Heisenberg, and Kramers. When shortly afterward the same symmetry was found to be a feature of other field theories, such as the Pauli-Weisskopf Scalar theory and was confirmed by the discovery of the $\mu^\pm$ and $\pi^\pm$ charge-conjugate pairs, and more recently by the discovery of the antiproton, it became one of the fixed canons of elementary particle theory. We shall see, however, that even more recent developments indicate a more complex situation.

4.2. *Charge conjugation in Dirac's theory of the electron.*—Let us consider for a moment the Dirac equation 72 as the c-number theory for an electron

in an external field. The charge-symmetry of the equation can be exhibited most simply (but not necessarily) by using a Majorana representation of the matrices α and β (see App. A). By paying attention to the reality of α and $i\beta$, one then finds that the complex-conjugate $\psi' = \psi^*$ of the wave-function ψ obeys the equation

$$\left(\frac{\partial}{\partial t} + \alpha \cdot \nabla + im\beta\right)\psi' = -ie(\alpha \cdot A - V)\psi' \qquad\qquad 83.$$

which is identical with 72 except for a reversal of the sign of e. Solutions of Eq. 72 and 83 associated by the rule $\psi' = \psi^*$ are called "charge conjugate solutions," and it is important to notice that if ψ is a positive energy solution $(\psi \sim e^{-iEt}, E > 0)$, then ψ' is a negative energy solution, and vice versa.

These remarks, as is well known, play a vital role in Dirac's hole-theory, where they are used to show that a "hole" in the "sea" of normally occupied negative energy states will behave like a particle of charge $-e$ in a positive energy state. The theory definitely predicts that such "holes" will be produced under suitable circumstances, but it is not immediately apparent that holes must have the same mass as electrons.[11] Dirac's hole theory is, in fact, at first sight quite unsymmetrical in the two particles, and one may wonder whether effects due to the interaction of the electron with the infinite "sea" of electrons in negative energy states, and of the latter amongst themselves, could not affect the masses of electron and hole so as to make them quite different.

We shall prove now that the theory is actually quite symmetrical, so that, for example, the same results would be obtained if the positron were regarded as the basic particle, and the electron as a hole in an infinite sea of negative energy positrons.

In order to do this, let us go back to the method of second quantization. Let us now assume that there is no external field, but take into account the electromagnetic field generated by the charge- and current-density of the Dirac field Eq. 37 by the assumption that, in Eq. 72, V and A are operator solutions of Maxwell's equations representing this field. Eq. 83 is still a consequence of 72, but since ψ is an operator we shall write $\psi' = \psi^\dagger$.

Before writing the expressions 37 on the "right-hand side" of Maxwell's equation, one must, however, according to Dirac's well known prescription, subtract from $\rho(x)$ an infinite negative constant ρ_0, representing the physically meaningless infinite charge density of the negative sea. By counting the number of negative energy states per unit volume one gets easily an expression for ρ_0 as an integral in momentum space

$$\rho_0 = (e/4\pi^3) \int d^3p.$$

One easily sees that essentially the same integral is involved in the value of

---

[11] At one time Dirac even thought that they might be identified with protons!

the second anticommutator, 30, for $x=y$, which is also obtained by counting states in momentum space; in fact one can show that

$$e^{-1}\rho_0 = \tfrac{1}{2} \sum_\rho \lim_{z \to y} \{\psi_\rho(x)\psi_\rho{}^\dagger(y) + \psi_\rho{}^\dagger(y)\psi_\rho(x)\} = \tfrac{1}{2}\{\psi(x)\psi^\dagger(x) + \psi^\dagger(x)\psi(x)\}.$$

Therefore, after subtracting ρ_0, the expression for the charge density becomes

$$\rho(x) = \tfrac{1}{2}e[\psi^\dagger(x)\psi(x) - \psi(x)\psi^\dagger(x)] \qquad \qquad 84.$$

In the case of the current-density one could argue that the corresponding infinite constant vanishes for symmetry reasons (all directions in space being equivalent), but it is nevertheless desirable to perform an "anti-symmetrization" as in 84 by subtracting from j_k the quantity

$$(1/2) \sum_{\rho\sigma} (\alpha_k)_{\rho\sigma}(\psi_\rho\psi_\sigma{}^\dagger + \psi_\sigma{}^\dagger\psi_\rho) \equiv (1/2)\delta(0) \sum_\rho (\alpha_k)_{\rho\rho} \equiv 0$$

(remember $Tr\ \alpha_k = 0$). One finds

$$j_k(x) = \tfrac{1}{2}e[\psi^\dagger(x)\alpha_k\psi(x) - \psi(x)\alpha_k\psi^\dagger(x)] \qquad \qquad 85.$$

where use has been made of the fact that α_n is symmetric (see Appendix 1).

Now it can be seen that the theory has become quite symmetric in field ψ and "antifield" $\psi' \equiv \psi^\dagger$. One could start equally well from 83 regarded as an equation for a particle of charge $-e$, and write the corresponding expression for the charge density $-e\psi'^\dagger\psi'$, adding, instead of subtracting, the infinite constant ρ_0. The result would be equivalent to 84. The same symmetry may be shown to exist in the Hamiltonian, the total momentum, etc. (all of which will not be discussed in detail here), so that the complete symmetry of the theory with respect to particles (electrons) and antiparticles (positrons) is apparent.

This further suggests that it must be possible to define an operator C which transforms any state containing m electrons and n positrons, in the sense that every electron (positron) is changed into a positron (electron) without changing its position, momentum, or spin, and without affecting the total energy, momentum, etc., of the whole system. A similar operator should exist for other Dirac fields, proton-antiproton field, μ-meson field, etc.

That this is indeed the case follows from the fact that ψ and ψ' obey the same anticommutation rules. From this one infers the existence of a linear unitary operator C such that (in the Majorana representation)

$$C^{-1}\psi(x)C = \psi'(x) \equiv \psi^\dagger(x) \qquad \qquad 86.$$

which equation is meant to hold for each component of ψ separately. The hermitean conjugate of Eq. 86 is

$$C^{-1}\psi^\dagger(x)C = \psi(x). \qquad \qquad 87.$$

One now sees immediately, by means of the customary sequence $C^{-1}\psi^\dagger\psi C = C^{-1}\psi^\dagger CC^{-1}\psi C$ etc., that C reverses the sign of the charge and current density, 84, 85

$$C^{-1}\rho(x)C = -\rho(x)$$
$$C^{-1}j_k(x)C = -j_k(x). \qquad \qquad 88.$$

In proving the latter equation one has to use the fact that the matrix a_k is "symmetric." Because of the change in sign of charge and current, also the sign of the electromagnetic field must change

$$C^{-1}V(x)C = -V(x); \qquad C^{-1}A_k(x)C = -A_k(x).$$
89.

One can show, then, that the total energy is invariant

$$C^{-1}HC \equiv H$$
90.

so that C is a constant of the motion!

4.3. *Charge conjugation in other theories.*—These ideas can be extended to other theories. For example, for a spinless charged particle, described by a scalar or pseudoscalar complex field $\phi = \phi_1 + i\phi_2$, one finds that C must transform ϕ into $\phi^\dagger = \phi_1 - i\phi_2$; that is

$$C^{-1}\phi_1 C = \phi_1; \qquad C^{-1}\phi_2 C = -\phi_2.$$
91.

One can show that this reverses the sign of the current four-vector, as in Eq. 88. These equations will apply, for example, to the charged π-meson field.

It is now very important to realize that a charge-conjugation operator may be considered also for neutral particles. If C exists in general, one may ask, for example, what happens if C is applied to a one-neutron state. The result ought to be a particle of the same mass, momentum, spin, etc. For consistency with Eq. 88 and 89 one must assume, however, that the magnetic moment is reversed. The particle, therefore, must be different from a neutron; the field describing this "antineutron" will be related to the neutron field by formulae exactly similar to 86.

On the other hand, a neutral spinless particle such as the π^0 need not have an antiparticle. There is at present no evidence contrary to the assumption that the π^0 is the charge conjugate of itself. One may assume that the corresponding field ϕ_0 is hermitean and transforms according to

$$C\phi_0 C^{-1} = \phi_0$$
92.

i.e., like ϕ_1. An alternative possibility would be to assume that ϕ_0 transforms like ϕ_2; the reason why 92 is chosen is that the transformation laws 91 and 92 leave the "charge-independent" interaction Hamiltonian of Section 6.4 invariant.

4.4. *Eigenstates of C.*—It is possible to show, by the same arguments used for P, that one can assume

$$C^2 = 1.$$
93.

Hence, if a state $|\alpha\rangle$ is an eigenstate of C, the corresponding eigenvalue must be ± 1.

$$C|\alpha\rangle = \pm |\alpha\rangle.$$
94.

It is clear, however, that a system can be in such a state only if it is neutral. More than that, a state which is transformed into itself by C must contain

equal numbers of electrons and positrons, of protons and antiprotons, etc. Such systems are not very common, but interesting examples are positronium and the similar system consisting of a proton and antiproton, and finally systems consisting only of photons and π^0's, which are self-conjugate particles. When such systems having a definite value ± 1 for C make transitions, C cannot vary (see Eq. 90). Selection rules arising from conservation of C have been studied by various authors (17, 17a, b).

The method by which one can decide which value of C belongs to a specified state of such a system, for example, a state $|\zeta\rangle$ of positronium, will be sketched by examining the symmetry properties of the wavefunction $f_\zeta(x, y)$ Eq. 34. The state may, of course, be classified as ^1S, ^3S, ^1P, ^3P, $\cdots$ etc., i.e., by means of an orbital quantum number $l = 0, 1, 2, \cdots$ and a total spin $S = 0, 1$. The symmetry or antisymmetry of $f_\zeta(x, y)$ with respect to an interchange of spin and space coordinates is then determined by the factor $(-1)^{l+S+1}$. Now consider the state $|\zeta'\rangle = C|\zeta\rangle$; the corresponding wavefunction is, writing spin indices explicitly

$$f_{\zeta'}(x\rho; y\sigma) = \langle | \psi_\sigma^\dagger(y)\psi_\rho(x)C | \zeta \rangle$$

where one can, as usual, replace $\langle |$ by $\langle | C^{-1}$ and insert CC^{-1} between $\psi^\dagger$ and ψ, so that[12]

$$f'_\zeta(x\rho, y\sigma) = \langle | \psi_\sigma(y)\psi_\rho^\dagger(x) | \zeta \rangle = \delta_{\rho\sigma}\delta(x - y) < |\zeta\rangle$$
$$- \langle | \psi_\rho^\dagger(x)\psi_\sigma(y) | \rangle = - f_\zeta(y\sigma, x\rho) = (-1)^{l+S}f_\zeta(x\rho, y\sigma).$$

One may conclude, therefore, that

$$C = (-1)^{l+S}. \qquad\qquad 95.$$

The result is the same that one would obtain if one were to consider electron and positron as two states of the same particle to be distinguished from one another by an additional two-valued index (a "charge" variable $\kappa = \pm 1$) similar to a spin index. In fact, formally one could consider ψ and $\psi^\dagger$ as the two components of a field ψ_κ, and could extend the definition 34 to give a wavefunction of the system antisymmetric with respect to simultaneous interchange of space, spin, and charge variables of the two particles. One could then say that the wavefunction must either be the product of a symmetric function of the space and spin variables by an antisymmetric function of the charge variables or vice versa. The argument is a familiar one. C interchanges the values of the charge coordinates of the two particles, and clearly $C = +1$ for a "charge symmetric" and $C = -1$ for a "charge-antisymmetric" state. The argument leads, of course, again to Eq. 95.

The value of C for one, two, $\cdots$ photon states is easily obtained by similar methods. A one-photon state, for example, may be generated by applying an electric or magnetic field operator to the vacuum state, e.g., $\mathcal{E}_k(x)|\rangle$. In a very loose sense, this may be said to be a photon at position x

---

[12] The term $\langle |\zeta\rangle$ in the equation can be set equal to "zero," since positronium and the vacuum are mutually orthogonal states.

and polarization k. One can further superpose such states with a weight function $f_\alpha(x, k)$ where α is an index designating the one-photon state

$$| \alpha \rangle = \sum_k \int f_\alpha(x, k) d^3x \mathcal{E}_k(x) |\rangle. \qquad 96.$$

Now by means of 89 one sees at once that

$$C| \alpha \rangle = - \sum_k \int f_\alpha(x, k) d^3x \mathcal{E}_k(x) |\rangle = - | \alpha \rangle.$$

More generally a state of n photons will require n field-factors in front of the vacuum state. Each of these changes sign when C is applied, so that

$$C = (-1)^n \qquad 97.$$

for such a state. From such considerations one deduces, for example, that the ^1S state of positronium has $C = +1$ from Eq. 95, and can decay into two but not three photons, while the ^3S state can decay into three but not into two photons.[13] Many selection rules of this kind have been derived.

4.5. *Violations of C-invariance.*—As is well known, the experiments on β-decay indicate that not only P-, but also C-invariance is violated. A direct indication of this is, for example, the fact that the positive and negative electrons emitted in μ^+-resp. μ^--decay have opposite longitudinal polarization. The evidence from ordinary β-decay is based on easier and more accurate experiments, but is somewhat less direct. The charge-conjugate picture of an ordinary nucleus undergoing β^--decay would be an antinucleus undergoing β^+-decay, which is not easily come by.

One can, however, take the reasonable view, that if C were strictly valid, then also TP would be conserved (see later, CPT theorem) (this is, of course, automatically true if one assumes that β-decay is correctly described by a linear combination of the customary ten invariant interactions $S, P, \cdots$; $S', P', \cdots$ of which 42 and 43 are two examples). Since TP does not involve a change from nucleons to antinucleons, it is immediately plausible, that it can be tested on β-decay of ordinary nuclei. A theorem by Lee, Yang & Oehme (18) shows that if one neglects the effect of the Coulomb field on the outgoing electron waves, then TP conservation would be sufficient to prevent us from detecting parity-violation in experiments like the β-decay of polarized nuclei or the longitudinal polarization of β-rays. A more direct calculation (9) shows that the observed effects are too large to be accounted for by Coulomb effects, and thus clearly indicate violations of C-invariance.

5. The CPT-Theorem. CP-Invariance

By combining together the operators C, T, and P one obtains an operation which reverses simultaneously the sign of all four space-time coordinates and changes each particle into its antiparticle. Such an operation has a

---

[13] Decay of ^3S into two photons is also forbidden by conservation of angular momentum [see Yang or Landau (7, 7a)].

particular simplicity, in that it commutes with every proper homogeneous Lorentz transformation.

It was first recognized by Lüders (19, 19a, b, c), that while it is easily possible in the ordinary schemes of relativistic field-theories to write interactions which violate either C- or P- or T-invariance, or a combination of two of these such as CP, it is not possible to do so for the product of all three, or CPT. The theorem does not state that a relativistically invariant theory which violates CPT is strictly impossible; but it would have to be a theory very different indeed from any of the present schemes (20). If CPT-invariance is granted, which at present seems a very reasonable assumption to make, it becomes a very useful tool in analyzing processes, such as K-, Λ- or Σ-decay, about which little is known a priori (18, 18a, b; 22). For all questions concerning strange particles consult (21, 21a). An immediate consequence of the theorem is that many of the statements one makes about particles and antiparticles do not really depend on the exact validity of C-invariance. For example, applying CPT to a state of a particle with an exactly defined four-momentum p, one gets a state of the antiparticle with exactly the same four-momentum p. Hence, the particle and antiparticle have exactly the same mass; there is, of course, in this argument a qualifying assumption, namely, that the "particle" has an exactly defined mass to begin with. Another similar property which is also subject to some qualifications is that an unstable particle has the same half life as its antiparticle (18, 21).

Another consequence of the CPT theorem is that invariance under any of the three operations implies invariance with respect to the product of the other two. This has already been mentioned in the discussion on C-violations. As another example, T-invariance should have the same consequences as CP-invariance, which has been studied in detail by Feinberg (23).

6. Isotopic Spin

6.1. *Charge symmetry and charge independence.*—Already a cursory examination of the systematics of isotopes suggests strongly the existence of a basic symmetry between neutrons and protons, which is quite prominent in the early part of the periodic system, and becomes less and less manifest, as the atomic number increases. From a quantitative point of view, the study of light "mirror nuclei," such as H^3 and He^3, or Li^7 and Be^7, etc., is particularly significant. It appears that the difference in binding energy between the ground states of two mirror nuclei is entirely accounted for by the presence, in the Hamiltonian, of the "Coulomb energy term," which differentiates neutrons from protons. The most natural interpretation of these facts is the assumption that the short-range interaction between two nucleons, which is left after the Coulomb force and other smaller electromagnetic effects are omitted, is completely invariant against an interchange between neutrons and protons. This means not only that the n-n force is equal to the p-p force, but also that the n-p force is symmetric with respect to a simultaneous interchange of the position- spin- and velocity-variables

of the two particles. The most sensitive tests of this "charge-symmetry" hypothesis are perhaps given not so much by the comparison of levels in mirror nuclei as by experiments that look for reactions which violate a selection rule which follows from the hypothesis (24, 24a).

A more far-reaching symmetry hypothesis is known as "charge-independence." It has its origin in the early observation of a nuclear phase-shift in the ^1S-state in p-p scattering at energies of the order of 0.1 Mev to a few Mev. Remarkably, this phase-shift, after allowance is made for minor effects due to the Coulomb interaction, turns out to be quite accurately equal to the ^1S phase-shift in n-p scattering.

When this fact became known, the existence of a more general law was suspected (25, 25a, b), which can be stated most simply, but somewhat ambiguously, by saying that the short-range interaction between two nucleons is "independent of their charge." To appreciate fully the meaning of this statement, one must recall that in order to represent all the known experimental facts one has been led to consider interaction potentials of a rather wide class, involving a dependence not only on the distance r_{12} between the two nucleons but also on their spin matrices σ_1 and σ_2, and involving furthermore exchange operators (i.e., exchange of space- or spin-coordinates, or of both) and velocity-dependent terms ($l \cdot s$ terms, for example). The charge independence assumption may now be formulated more precisely by saying that if an interaction Hamiltonian of the above specified type for two particles 1 and 2 is found which represents correctly the n-p force in all possible states (^1S, ^1P, ^1D, $\cdots$; ^3S, ^3P, ^3D, $\cdots$), then this same Hamiltonian represents correctly the p-p and n-n force in the states ^1S, ^3P, ^1D, $\cdots$ which are allowed by the exclusion principle.[14]

It is rather obvious that charge independence implies equalities between levels of isobars (not merely of mirror nuclei!). Very roughly speaking one may say that if the nucleus A_Z (with Z protons and A-Z neutrons) has a state of a certain energy, and if the configuration of this state (more precisely, the symmetry of the wavefunction) is such that one is able to replace one of the neutrons by a proton, without violating the Pauli exclusion principle, one must then obtain a state of the same energy, for the isobaric nucleus $A_{(Z+1)}$. If the operation can be repeated one obtains a state for the nucleus $A_{(Z+2)}$ and so on. In this way states of isobaric nuclei associate themselves into multiplets. (For example: the ground states of C^{14} and O^{14} and the excited state of N^{14} at 2.3 Mev excitation constitute an "isotope triplet.")

These considerations must now be formulated more precisely. Let particles 1 and 2 be a proton and neutron respectively and $V(1, 2)$ their interaction. Let us consider an orthonormal set

$$u_1, u_2, u_3, \cdots \qquad\qquad 98.$$

of individual particle states, and product states $f = (nm)$, $i = (rs)$ for the n-p

---

[14] This implies in particular that the Hamiltonian is symmetric in the two particles, as already required by the weaker assumption of charge symmetry.

system. The interaction Hamiltonian has matrix elements

$$\langle f \mid H \mid i \rangle = V_{nm;rs} = \int u_n{}^*(1)u_m{}^*(2)V(1, 2)u_r(1)u_s(2) \qquad 99.$$

where the integral means integration over the space and summation over the spin variables of particles 1 and 2. One notices that, since $V(1, 2)$ is symmetric in 1 and 2, one has

$$V_{mn;sr} = V_{nm;rs}. \qquad 100.$$

Now let 1 and 2 be two protons (or two neutrons). The charge-independent interaction may be represented by the same function $V(1, 2)$. The wave-function for the state $i = (rs)$ may now be written[15]

$$(1/\sqrt{2})\{u_r(1)u_s(2) - u_s(1)u_r(2)\} \qquad 101.$$

and similarly for $f = (n, m)$. Then

$$\langle f \mid H \mid i \rangle = V_{nm;rs} - V_{nm;sr} \qquad 102.$$

where the result has been simplified by means of Eq. 100.

Let us describe protons and neutrons, respectively, by two fields $\psi_p(x)$ and $\psi_n(x)$. Each of these fields by itself must obey the customary anti-commutation rules (see Eq. 30); furthermore, one may assume that they anti-commute with each other

$$\psi_p(x)\psi_n(y) + \psi_n(y)\psi_p(x) = 0$$
$$\psi_p(x)\psi_n{}^\dagger(y) + \psi_n{}^\dagger(y)\psi_p(x) = 0 \qquad 103.$$

etc. The positive energy part of ψ_p (or alternatively ψ_n) may be expanded with respect to the set 98, the coefficients being proton-(neutron) destruction operators $a_r(b_r)$. One need not be concerned for the moment with the nega-tive-energy part of the field, which contains antinucleon-creation operators. Then the Hamiltonian, having matrix elements 99 for the n-p system, may be written

$$H_{np} = \sum V_{nm;rs}a_n{}^\dagger a_r b_m{}^\dagger b_s = -\Sigma V_{nm;rs}a_n{}^\dagger b_m{}^\dagger a_r b_s \qquad 104.$$

where the summation extends over all values of the indices n, m, r, and s.

One notices that 104 is a quadrilinear form in the two fields $\psi_p\psi_n$ and their hermitean conjugates, which may be indicated symbolically by

$$H_{np} = \{\psi_p{}^\dagger \psi_n{}^\dagger \psi_p \psi_n\}.$$

Remembering 100 and the identity $a_n{}^\dagger b_m{}^\dagger a_r b_s = b_m{}^\dagger a_n{}^\dagger b_s a_r$ one notices that the quadrilinear form is symmetric with respect to a simultaneous inter-change of the first two and the last two fields

$$\{\psi_p{}^\dagger \psi_n{}^\dagger \psi_p \psi_n\} = \{\psi_n{}^\dagger \psi_p{}^\dagger \psi_n \psi_p\} \equiv -\sum V_{nm;rs}b_n{}^\dagger a_m{}^\dagger b_r a_s. \qquad 105.$$

---

[15] A sign convention is necessary, for example, that 101 holds with $r < s$. Eq. 102 holds them if $n < m$, $r < s$.

As is well known (29), the interaction of identical particles, with the matrix elements 100 may be written[16]

$$H_{pp} = - (1/2) \sum V_{nm;ys} a_n{}^\dagger a_m{}^\dagger a_r a_s = (1/2) \{\psi_p{}^\dagger \psi_p{}^\dagger \psi_p \psi_p\} \qquad 106.$$

and similarly for H_{nn}. Collecting together the H_{np}, H_{pp}, and H_{nn} interactions one sees now that the Hamiltonian has the quadrilinear form

$$H = (1/2) \sum_{i,j} \{\psi_i{}^\dagger \psi_j{}^\dagger \psi_i \psi_j\} \qquad 107.$$

where i and j are two-valued indices ($i, j = p$ or n).

6.2. *Isotopic spin.*—The above expression exhibits quite openly a remarkable invariance property. Just as the expressions $\sum_i a_i{}^* b_i$, $\sum_{ij} a_i{}^* b_j{}^* c_i d_j$ are invariant against a simultaneous linear unitary transformation of the vectors a, b, c, d, it is easy to see that in 107 one may regard ψ_i ($i = p$ or n) as a two-component vector, and that H is invariant against a linear-unitary transformation u of the two components. It is easy to see that such a transformation leaves the anticommutation relations 30 and 103 unchanged, and, therefore, it must be possible to generate the linear transformation by means of an operator U, according to the usual $U^{-1} \psi U$ scheme. The most general 2×2 unitary matrix may be written in the form

$$u = e^{i\delta} \begin{pmatrix} \alpha & \beta \\ -\beta^* & \alpha^* \end{pmatrix}. \qquad 108.$$

The factor $e^{i\delta}$ in front simply corresponds to the fact that 107 contains the same number of ψ-fields and $\psi^\dagger$-fields and, therefore, does not change if all ψ's are multiplied by the same $e^{i\delta}$. This invariance may be regarded as a formal expression of the principle of the "conservation of nucleons," which does not throw any particular light on the principle itself. We shall, from now on, specialize 108 to the case $\delta = 0$. The transformation, then, also has unit determinant. In conclusion, the inference is that for any two complex constants α and β such that

$$|\alpha|^2 + |\beta|^2 = 1 \qquad 109.$$

there is a unitary operator U, acting on the state of the two coupled fields ψ_p and ψ_n, such that

$$U^{-1} \psi_p U = \alpha \psi_p + \beta \psi_n$$
$$U^{-1} \psi_n U = - \beta^* \psi_p + \alpha^* \psi_n. \qquad 110.$$

This transformation leaves not only 107 but also the "free" part of the Hamiltonian of the two fields invariant, provided the small neutron-proton mass-difference is neglected. Thus U commutes with the whole Hamiltonian. Conversely one can easily see that if the quadrilinear forms describing H_{np}, H_{pp}, and H_{nn} are such that their sum is invariant against 110, then they satisfy charge-independence. Therefore, the principle of charge-independence is equivalent to invariance under the two-dimensional unitary group 110.

---

[16] If $n < m$, $r < s$, for example, one verifies easily that
$$\langle f | a_n{}^\dagger a_m{}^\dagger a_r a_s | i \rangle = - \langle f | a_n{}^\dagger a_m{}^\dagger a_s a_r | i \rangle = -1 \text{ etc.}$$

As is well known from the theory of the electron spin, the two-dimensional unitary unimodular matrices form a group which is strictly related to the three-dimensional real rotations. The connection is most simply exhibited by means of the three components of the "isotopic spin density" $Q_i(i=1, 2, 3)$. If τ_1, τ_2, τ_3 are three matrices similar to the Pauli matrices $\sigma_x, \sigma_y, \sigma_z$ and operating on the two component vector (ψ_p, ψ_n), one defines $Q_i = (1/2)\psi^\dagger \tau_i \psi$, i.e.,

$$Q_1 = (1/2)(\psi_p^\dagger \psi_n + \psi_n^\dagger \psi_p)$$
$$Q_2 = (1/2i)(\psi_p^\dagger \psi_n - \psi_n^\dagger \psi_p)$$
$$Q_3 = (1/2)(\psi_p^\dagger \psi_p - \psi_n^\dagger \psi_n).$$ 111.

One then sees that the transformation 110 induces an orthogonal transformation (a rotation)

$$U^{-1}Q_iU = \sum_{j=1}^{3} a_{ij}Q_j$$ 112.

of the three-dimensional vector $(Q_1Q_2Q_3)$. The coefficients a_{ij} are real and easily calculable.

Alternatively, one considers the infinitesimal transformations

$$U_k = 1 - i\theta T_k \qquad (k = 1, 2, 3)$$ 113.

of the group 110, defined as follows. If U defined by 110 is designated by $U(\alpha, \beta)$ and θ is an infinitesimal parameter, one sets

$$U_1 = U\left(1, -\frac{i}{2}\theta\right); \qquad U_2 = U\left(1, -\frac{1}{2}\theta\right); \qquad U_3\left(1 - \frac{i}{2}\theta, 0\right).$$ 114.

Furthermore, neglecting terms of order θ^2 one sees from 113 that

$$U_k^{-1}\psi U_k = \psi + i\theta[T_k, \psi]$$ 115.

so that, after an easy calculation

$$[\psi, T_k] = \tau_k\psi.$$ 116.

Equations 116 must hold for $\psi=\psi(x)$ where x is any point in space. By means of 30 and 103 one verifies that T_k defined by

$$T_k = \int Q_k(x)d^3x$$ 117.

satisfies 116. One then sees easily that

$$[T_j, T_k] = iT_l$$ 118.

where (j, k, l) is a cyclical permutation of 1, 2, 3.

These are the same commutation relations, as are obeyed by the components of angular momentum, which again establishes the connection with the ordinary rotation group.

All the essential formulae pertaining to the isotopic spin group have now been given. In particular from $U^{-1}HU=H$ it follows

$$[T_k, H] = 0;$$ 119.

the three hermitean operators T_k are constants of the motion, and so is the "square of the total isotopic spin vector"

$$T_1{}^2 + T_2{}^2 + T_3{}^2 = T(T + 1).$$ 120.

From the analogous proof for angular momentum it follows that the possible values of the quantum number T are integers or half-integers. For a given value of T, the possible values of T_3 are the $(2T+1)$ eigenvalues

$$T_3 = T, T - 1, \cdots, -T.$$ 121.

6.3. *Applications and validity of charge independence.*—The Equations 119, 120, and 121 constitute the starting point for the familiar discussion of the multiplet structure of nuclear levels. In light nuclei, where the distortion of the nuclear wave function by the Coulomb interactions is small, one can, in general, assign unambiguously a T-value to each level. In a collision between nuclei the T-vectors of the colliding particles can be added according to the usual rules, and conservation of the total T-vector gives rise to selection rules.

Charge independence can be tested either by comparing the energies of states belonging to the same T-multiplet, or by looking for violations of the selection rules. The most recent work on this subject is contained in a series of 12 papers by Wilkinson *et al.* (26). See also the end of the next section.

6.4. *Extension of isotopic spin to antinucleons and π-mesons.*—If nuclear forces are due to the exchange of mesons, the symmetry that manifests itself in the charge independence of the nucleon-nucleon interaction must have its deeper origin in a corresponding symmetry of the interaction between nucleon and meson-fields. This is the same as saying that it is hard to see how a quantity such as T_1 can be conserved in a nucleon-nucleon collision, unless the virtual meson-emission and reabsorption processes which form the invisible substratum of the collision also obey a corresponding conservation law.

In a similar way one may argue that, since formation of nucleon-antinucleon pairs probably plays a role in nuclear forces at short distances, the symmetry expressed by the group 110 must also extend to antinucleons. In fact, although antinucleons have been barely mentioned in the previous discussion, such an assumption was already implicit in writing Equation 110, because a minimum of mathematical consistency requests us to assume that the equations hold for the whole operator ψ, i.e., for the antinucleon-creation part as well as for the nucleon-destruction part of ψ! Thus, the formulae written already automatically imply certain isotopic spin assignments for antinucleons.

In order to see this more clearly, let us introduce, together with a_r and b_r, the corresponding operators $\bar{a}_r$ and $\bar{b}_r$ which destroy antiprotons and antineutrons (the bar does not mean complex conjugation!). Using a Majorana representation, as in Appendix A, one may expand ψ_p and ψ_n as in Equation A.10. One finds, then, by means of the orthogonality relations A.8 and A.9.

$$\int \psi_p{}^\dagger(x)\psi_p(x)d^3x = \sum_r (a_r{}^\dagger a_r + \bar{a}_r\bar{a}_r{}^\dagger) = \sum_r (a_r{}^\dagger a_r - \bar{a}_r{}^\dagger \bar{a}_r + 1)$$

which, apart from an infinite additive constant, is equal to the total charge

$$Q = N(p) - N(\bar{p}), \qquad\qquad 122.$$

$N(p)$ and $N(\bar{p})$ being the total numbers of protons and antiprotons, respectively. Let us similarly designate by N the number of nucleons minus antinucleons

$$N = N(p) + N(n) - N(\bar{p}) - N(\bar{n}) \qquad\qquad 123.$$

also called the "nucleon number." In calculating T_3 a cancellation of infinite constants occurs and one finds

$$T_3 = \tfrac{1}{2}\{N(p) - N(n) - N(\bar{p}) + N(\bar{n})\} = Q - \tfrac{1}{2}N \qquad 124.$$

in particular for an ordinary nucleus $T_3 = Z - 1/2A$ showing that T_3 is integer (half-integer) for nuclei with even (odd) A.

The equation also shows that antiproton and antineutron have the opposite T_3 assignments to proton and neutron. More precisely let us consider two one-nucleon states $|p\rangle$ and $|n\rangle$ or two one-antinucleon states $|\bar{p}\rangle$ and $|\bar{n}\rangle$, the two particles being (in either case) in the same state of orbital motion and ordinary spin (i.e., one assumes they have the same wavefunction as defined in Appendix B). The two states then form an isotopic spin doublet in the sense that they transform linearly into one another under U. Moreover, the transformation law is the same for the two doublets, provided one chooses corresponding states as follows

TABLE I

T_3	Nucleon State	Corresponding Antinucleon State
+1/2	$|p\rangle$	$|\bar{n}\rangle$
-1/2	$|n\rangle$	$-|\bar{p}\rangle$

This may be seen, by noticing that the relation of $|\bar{p}\rangle$ and $|\bar{n}\rangle$ to the operators $\psi_p{}^\dagger$ and $\psi_n{}^\dagger$ is precisely the same as that of $|p\rangle$ and $|n\rangle$ to the operators ψ_p and ψ_n and that, furthermore,

$$U^{-1}\psi_n{}^\dagger U = \alpha\psi_n{}^\dagger + \beta(-\psi_p{}^\dagger)$$
$$U^{-1}(-\psi_p{}^\dagger)U = -\beta^*\psi_n{}^\dagger + \alpha^*(-\psi_p{}^\dagger) \qquad 125.$$

so that $\psi_n{}^\dagger$ and $-\psi_p{}^\dagger$ transform like ψ_p and ψ_n.

To put it another way, if by means of Eq. 116 one calculates the matrix elements of the infinitesimal operators $T_1 T_2 T_3$ for the two nucleon states, one finds the matrices $(1/2)\tau_k$. One also finds precisely the same matrices for the two antinucleon states, as chosen in Table I. In this calculation one uses the customary fact that the vacuum state is invariant under the transformation, or, in other words

$$T_k|\,\rangle = 0. \qquad\qquad 126.$$

Turning now to the interaction between nucleon field and π-meson field, let us examine more closely the meson field equation 38. The structure of the bilinear form $j(x)$ is already known with regard to the Dirac spinor indices of the nucleon fields $\psi^\dagger$ and ψ; one must now take into account the two-component nature of $\psi = (\psi_p, \psi_n)$. By inserting a matrix $\rho_2 = i\beta\gamma_5$ into the forms of Eq. 111, one obtains the three analogous quantities

$$j_\alpha(x) = g\psi^\dagger\rho_2\tau_\alpha\psi \qquad (\alpha = 1, 2, 3) \qquad\qquad 127.$$

which under the effect of U undergo the same transformation, Eq. 112, as $Q_1Q_2Q_3$.

In addition there is a fourth bilinear form $j_0 = \psi^\dagger\rho_2\psi$ or explicitly

$$j_0 = \psi_p{}^\dagger\rho_2\psi_p + \psi_n{}^\dagger\rho_2\psi_n \qquad\qquad 128.$$

which is invariant under U. There are no further independent pseudoscalar bilinear forms. There are, therefore, two possibilities. Either one considers an "isotopic singlet" meson described by a single field ϕ_0, invariant under U, and having j_0 as a source function, or one considers an "isotopic triplet" described by three fields $\phi_1\phi_2\phi_3$ and writes field equations

$$(\Box - \mu^2)\phi_\alpha = j_\alpha \qquad (\alpha = 1, 2, 3). \qquad\qquad 129.$$

The invariance of this scheme under the group of transformations U is quaranteed if (a) the same mass μ appears for $\alpha = 1, 2, 3$ and (b) the fields ϕ_α transform according to

$$U^{-1}\phi_\alpha U = \sum_{\beta=1} a_{\alpha\beta}\phi_\beta. \qquad\qquad 130.$$

In particular, by considering the infinitesimal transformations, one finds easily

$$[\phi_\alpha, T_k] = \sum_{\beta=1}^{3} (t_k)_{\alpha\beta}\phi_\beta \qquad\qquad 131.$$

where the matrices t_k have elements $(t_1)_{23} = -(t_1)_{32} = -i$, etc. (with all cyclical permutations) and all the other elements are zero. These matrices give a well known representation of the spin matrices for a spin-one particle.

So far no experimental evidence of the existence of an isotopic-singlet meson has been found, while the three mesons $\pi^\pm$ and π^0 (apart from a small difference in mass) fit in beautifully with the scheme Eq. 130 and 131.

By a procedure completely analogous to Eq. 124 one can show that ϕ_3 creates and destroys particles having $T_3 = 0$, while the complex field $\phi = (\phi_1 + i\phi_2)/\sqrt{2}$ creates particles with $T_3 = -1$ and destroys particles having $T_3 = +1$. The interaction Hamiltonian which gives the field Eq. 129 may be written in the alternative forms

$$H = \sum_{\alpha=1}^{3} j_\alpha\phi_\alpha = g\{\sqrt{2}\psi_p{}^\dagger\rho_2\psi_n\phi + \sqrt{2}\psi_n{}^\dagger\rho_2\psi_p\phi^\dagger + (\psi_p{}^\dagger\psi_p - \psi_n{}^\dagger\psi_n)\phi_3\}. \qquad 132.$$

Here one verifies again immediately that T_3 is conserved, for example, the first term causes a nucleon to make a transition from $T_3 = -1/2$ to $T_3 = +1/2$ while a meson with $T_3 = +1$ (-1) is destroyed (created).

Invariance under the isotopic spin group has many important consequences. For instance, as was first pointed out by Heitler, in meson-nucleon scattering the initial and final states may be classified into eigenstates of T^2 and T_3. A very considerable simplification is then achieved in the analysis of the scattering, because of the fact that the three components of T are conserved (27). The experiments to date have not revealed any serious discrepancy between π-meson phenomena and charge-independence.

6.5. *Isotopic parity* (G).—Isotopic spin and charge conjugation do not commute, for example, the charge conjugate of a proton $(T_3 = 1/2)$ is an antiproton $(T_3 = -1/2)$. Therefore, a combined discussion of the two assumptions has a certain interest. Various authors (28, 28a, b) have derived selection rules for proton-antiproton annihilation and other processes following from the simultaneous validity of the two assumptions.

For the purposes of such a discussion one can replace C by an operation G which is obtained by a successive application of C and an isotopic spin rotation. Consider Eq. 110 with parameters $\alpha = 0$; $\beta = 1$; the corresponding transformation of the Q-quantities in Eq. 111 or, what is the same, of the meson fields ϕ_α is $(\phi_1 \phi_2 \phi_3) \rightarrow (-\phi_1, \phi_2, -\phi_3)$. This is, therefore, a rotation of $180°$ around the "2" axis: $U = e^{i\pi T_2}$. Writing

$$G = C e^{i\pi T_2} \qquad\qquad 133.$$

one finds, from Eq. 86, 91 and 92

$$G\psi_p G^{-1} = \psi_n{}^\dagger; \qquad G\psi_n G^{-1} = -\psi_p{}^\dagger; \qquad G\phi_\alpha G^{-1} = -\phi_\alpha. \qquad 134.$$

The first two equations show the interchange $p \rightarrow \bar{n}$, $n \rightarrow -\bar{p}$ which was found in the comparison of the nucleon with the antinucleon doublet, Eq. 125. The third equation shows that, in the three-dimensional space of the meson-field components, G acts in a manner similar to P in ordinary space (hence, the name "isotopic parity"). The three equations show that G commutes with all three isotopic spin components, which is the main advantage of G as compared to C.

7. Baryon- and Lepton-Conservation Laws. Strangeness

For the sake of completeness we mention here some other empirically observed conservation laws, which may be a manifestation of some deeper and as yet little understood symmetries (21, 21a).

The most fundamental of these laws is probably conservation of baryons. This is a generalization of the law of conservation of nucleons, which has long been recognized as one of the most striking features in the stability of ordinary matter. The quantity conserved is, the number of nucleons minus antinucleons, or more generally of baryons minus antibaryons. All elementary particles heavier than nucleons (i.e., all hyperons) observed so far are

baryons, i.e., must be counted as such in applying the conservation law. Antinucleons, but no heavier antibaryons, have been directly observed. The existence of the latter is, however, hardly in doubt. In a sense one can conceive the "baryon-number" as a kind of "charge" (analogous to the electric charge) attached to each particle. Baryons have charge $+1$, antibaryons charge -1, and all particles lighter than nucleons have charge 0. As far as is known, all baryons are "fermions," i.e., particles of half-integer spin.

Below the nucleons, one finds massive bosons, i.e., the K-mesons, with ordinary spin almost certainly zero, and the π-mesons, with spin zero. There is no apparent conservation law applying to the number of these bosons; they can be freely created and destroyed.

Leptons are by definition the μ-mesons, electrons, and neutrinos, all spin $1/2$ particles. A lepton-conservation law has been suspected earlier, and has now a fair amount of experimental support. Again one can define a kind of "lepton-charge" which is $+1$, say, for e^-, μ^-, and ν (ν being by definition the particle emitted in β^+ emission) and -1 for e^+, μ^+ and $\bar{\nu}$ (the latter being the particle emitted in β^- emission). These assignments are justified by a detailed discussion (21a) of the consequences of the assumption that the total lepton-charge is conserved in all processes involving creation or destruction of leptons (β-decay, $\pi-\mu$ decay, etc.). So far as is known, baryon- and lepton-conservation may be exact laws of Nature.

A third conservation law, which is not exact, but, like parity, is violated in the "weak" interactions, emerges from the Gell-Mann-Nishijima systematics of strange particles, which is a successful attempt to understand the associated-production rule of Pais and other selection rules operating in strange particle production and decay, in terms of an extension of the isotopic-spin invariance principle. The basic assumption is that the ideas of isotopic spin quantum numbers T and T_3, isotopic-spin multiplets, etc. are applicable to all strongly interacting particles (i.e., so far as is known to all particles except photons and leptons), and that T_1, T_2, T_3 are constants of the motion quite generally, as long as one neglects electromagnetic and "weak" interactions. It is easy to verify that, in the case of nucleons and π-mesons, which have been examined in some detail, T_3 is strictly conserved also by the electromagnetic interactions;[17] in fact one has in that case

$$T_3 = Q - \tfrac{1}{2}N \qquad\qquad 135.$$

where N is the nucleon-number ond Q is the total electric charge (divided by e), so that conservation of T_3 follows from the "exact" laws of conservation for Q and N.

The essential remark is now, that one can order the "strange" particles into isotopic spin multiplets and assign isotopic spins in such a way that the "strong" production reactions such as

$$\pi^- + p \to \Lambda^0 + K^0, \Sigma^0 + K^0, \Sigma^- + K^+ \qquad\qquad 136.$$

[17] This puts T_3 in a very different category from T_1 and T_2, since electromagnetic interactions are many orders of magnitude stronger than the "weak" interactions.

are "allowed" by isotopic spin invariance, while the "weak" decay processes such as

$$\Lambda^0 \to p + \pi^-, \quad \text{or} \quad K^0 \to \pi^+ + \pi^- \qquad\qquad 137.$$

etc. are "forbidden." This is achieved by assigning integer isotopic spin to the hyperons Λ^0, Σ^0, $\Sigma^\pm$ (which have half-integer ordinary spin!) and half-integer isotopic spin to the K-mesons (which have integer spin). The reader can easily verify that in Eq. 137 T or T_3 is necessarily an integer on the left side and a half-integer on the right hand side, or vice versa. In fact the more specific assignments (21) give

$$\Delta T_3 = \pm 1/2 \qquad\qquad 138.$$

for these decays. This is, of course, not an "explanation" but it brings considerable order into the subject and has led to several strikingly successful predictions.

Gell-Mann assumes that, in a multiplet, Q varies linearly with T_3 as in Eq. 135, but the above-mentioned assignments do not allow one to generalize Eq. 135 by saying that N is the baryon-number. Incidentally, this would tie T_3 to two exactly conserved quantities, and the very key to the success of the Gell-Mann-Nishijima scheme is the idea that T_3 is only "almost exactly" conserved and provides a distinction between T_3 conserving (or allowed) and T_3 violating (or very weak) processes.

In generalizing Eq. 135, one may remark that for the (n, p) and $(\bar{p}, \bar{n})$ doublets and the $(\pi^\pm, \pi^0)$ triplets, for which 135 is valid, the term $1/2N$ represents a variable shift ($N = +1$, -1 and 0 in the three above-mentioned multiplets) of Q relative to T_3. In a general multiplet one will write (borrowing a notation from Schwinger)

$$T_3 = Q - Y/2 \qquad\qquad 139.$$

where Y is a shift characteristic of the multiplet. In a system of particles, the sum of the individual Y values will give a total Y (the "hypercharge"), which like T_3 is an approximate constant of the motion. As was said Y is distinct from N. In Gell-Mann's notation

$$Y = N + S \qquad\qquad 140.$$

where S is the "strangeness" quantum number. For example, the Λ-singlet and the Σ-hyperon triplet have $Y = 0$, hence $S = -1$; the (K^+, K^0) doublet has $Y = 1$, $N = 0$ and hence $S = +1$. S is so defined that "ordinary" particles have zero strangeness (and by this is meant π-mesons and nucleons). No useful isotopic spin assignment has been devised so far for leptons, and the notion of "strangeness" does not, therefore, apply to them.

APPENDIX A: NOTATIONS; DIRAC EQUATION; MAJORANA REPRESENTATION

A summary is presented here of some of the notations employed. The dagger, †, is used throughout to denote the Hermitean conjugate (of a matrix or of an operator), while the asterisk, *, denotes simply complex con-

jugation (i.e., in the case of a matrix, the * means c.c. without transposition of rows and columns).

The four components $\psi_\rho(\rho=1, \cdots, 4)$ of a Dirac spinor are multiplied by 4×4 Dirac matrices in symbolic notation (as usual); for example, $\beta\psi$ means the spinor with components $(\beta\psi)_\rho = \sum_\sigma \beta_{\rho\sigma}\psi_\sigma$. The summation convention over equal indices is used often, thus: $\beta_{\rho\sigma}\psi_\sigma$ omitting the summation sign. It is convenient to allow multiplication of ψ (or ψ^*) by a matrix on the right hand side. Summation over adjacent indices is then understood, thus $\psi^*\beta$ means $(\psi^*\beta)_\rho = \psi_\sigma^*\beta_{\sigma\rho}$. If a matrix is hermitean $(\beta=\beta\dagger)$ multiplication by β on the right is equivalent to multiplication by β^* on the left $\beta^*\psi^* = \psi^*\beta$.

Commutators are denoted by: $[A, B] = AB - BA$, and anticommutators by: $\{A, B\} = AB + BA$. All the commutation or anticommutation relations written in this article are for operators "at equal times" or for "Schrödinger operators."

The free Dirac equation is written

$$\left(\frac{\partial}{\partial t} + \boldsymbol{\alpha}\cdot\boldsymbol{\nabla} + im\beta\right)\psi = 0 \qquad\qquad \text{A.1.}$$

and the three σ matrices are defined by

$$\sigma_x = -i\alpha_2\alpha_3, \qquad \sigma_y = -i\alpha_3\alpha_1, \qquad \sigma_z = -i\alpha_1\alpha_2 \qquad \text{A.2.}$$

and the three ρ matrices by

$$\rho_1 = -i\alpha_1\alpha_2\alpha_3, \qquad \rho_3 = \beta, \qquad \rho_2 = -i\rho_3\rho_1. \qquad \text{A.3.}$$

Other symbols are defined in Table II below.

In this article the reviewer sometimes uses the ordinary (Dirac) representation in which β is diagonal, sometimes a "Majorana" representation, in which the α matrices are hermitean and symmetric (and therefore real) and β is hermitean and antisymmetric (and therefore purely imaginary). This makes all the coefficients in Eq. A.1 real.

A Majorana representation may be obtained, starting from the usual representation in which α_1, α_3, and β are real and α_2 is imaginary, by applying to each Dirac matrix Γ the unitary transformation

$$\Gamma' = u\Gamma u^{-1} \qquad\qquad \text{A.4.}$$

where

$$u = (1 - \beta\alpha_2)/\sqrt{2}; \qquad u^{-1} = (1 + \beta\alpha_2)/\sqrt{2}. \qquad \text{A.5.}$$

This leaves α_1 and α_3 unchanged, while replacing α_2 and β with $-\beta$ and α_2, respectively. The corresponding transformation from the Dirac wavefunction ψ to the Majorana ϕ is $\phi = u\psi$, $\psi = u^{-1}\phi$ or explicitly

$$\psi_1 = (\phi_1 - i\phi_4)/\sqrt{2}, \qquad \psi_2 = (\phi_2 + i\phi_3)/\sqrt{2},$$
$$\psi_3 = (i\phi_2 + \phi_3)/\sqrt{2}, \qquad \psi_4 = (-i\phi_1 + \phi_4)/\sqrt{2}. \qquad \text{A.6.}$$

This is useful, for example, in calculating the effect of time reversal, Eq. 82, on the "large" components ψ_1 and ψ_2. One easily sees that A.5 leaves the

form of ρ_2 unchanged. Therefore, the transformation $\phi' = -\rho_2\phi^*$ of the Majorana wavefunction means $\phi' = i(+\phi_3{}^*, +\phi_4{}^*, -\phi_1{}^*, -\phi_2{}^*)$. One sees that the large components $\psi_1 \psi_2$ transform (apart from an irrelevant sign) according to the scheme 68. In a Majorana representation the ρ and σ matrices are all imaginary and antisymmetric (as one easily sees by means of the anticommutation relations). The ρ matrices commute with the σ matrices; hence the nine products $\rho_i\sigma_j$ are real and hermitean, and, therefore, symmetric. These conclusions are summarized, together with some customary designations, in the following table.

TABLE II

SYMMETRY OF DIRAC MATRICES IN A MAJORANA REPRESENTATION

Imaginary-antisymmetric	σ_k, ρ_k $(k = 1, 2, 3)$
Also:	$\beta = \gamma_4 = \rho_3$, $\quad \gamma_5 = -\rho_1$, $\quad -i\gamma_5\gamma_4 = \rho_2$
Real—symmetric	$\alpha_k = \rho_1\sigma_k$, $\quad \gamma_k = -i\beta\alpha_k = \rho_2\sigma_k - i\gamma_5\gamma_k = -\rho_3\sigma_k$

Let us discuss briefly Eq. A.1 in the Majorana representation. Owing to the "real" form of the equation, one knows that if ψ is a solution, ψ^* is also a solution. It is often called the "charge-conjugate" solution. If ψ is a stationary solution

$$\psi = e^{-iEt}u(x)$$

with a positive energy $E > 0$, then ψ^* is a negative energy solution. More generally, a superposition of positive energy solutions of the above form is called also a positive energy solution. The equation obviously possesses "real" solutions, of the form $\psi + \psi^*$ where ψ is a positive energy solution, and hence ψ^* is a negative energy solution.

One often has to do with complete orthonormal sets of positive energy solutions $u_1, u_2, \cdots$ and negative energy solutions $v_1, v_2, \cdots$. One can assume that the negative energy solutions of the set are the charge conjugates of the positive energy solutions: Then the whole set is

$$\cdots, u_r{}^*, \cdots, u_2{}^*, u_1{}^*; \quad u_1, u_2, \cdots, u_r, \cdots. \tag{A.7.}$$

The orthogonality relations are

$$\int u_r{}^* u_s d^3x = \delta_{rs} \tag{A.8.}$$

$$\int u_r u_s d^3x = 0. \tag{A.9.}$$

In the q-number theory ψ and $\psi^\dagger$ are operators, which may be expanded

$$\psi(x) = \sum_r \{a_r u_r(x) + \bar{a}_r{}^\dagger u_r{}^*(x)\} \tag{A.10.}$$

$$\psi^\dagger(x) = \sum_r \{a_r{}^\dagger u_r{}^*(x) + \bar{a}_r u_r(x)\} \tag{A.11.}$$

where a_r and $\bar{a}_r$ are destruction operators for particles and antiparticles, respectively. From A.8 and A.9 one has

$$a_r = \int u_r^*(x)\psi(x)d^3x, \qquad a_r{}^\dagger = \int \psi^\dagger(x)u_r(x)d^3x \qquad \text{A.12.}$$

and similarly for $\bar{a}_r$, $\bar{a}_r{}^\dagger$.

APPENDIX B. TRANSFORMATION OF STATES IN THE DIRAC THEORY

The following section contains a discussion of the connection between the transformation of the Dirac wavefunction (corresponding to a given coordinate transformation) when ψ is regarded as a Schrödinger function for a particle, and the corresponding transformation of the Dirac state-vector $|\alpha\rangle$ for a one-particle state in the second quantized theory. Since the two formalisms describe the same thing, it is desirable to verify the theorem which states that the two transformations are equivalent.

Consider a Lorentz transformation

$$x_i = \sum_{k=1}^{4} a_{ik}x_k' \qquad \text{B.1.}$$

which one can write $x = ax'$ or $x' = a^{-1}x$. In the text one needs only special cases of this, but it costs no extra effort to prove the theorem in general.

If $\psi(x)$ is a solution of the free Dirac Equation A.1, then $\psi(x') \equiv \psi(a^{-1}x)$ is not in general a solution, but can be transformed into one (29) by multiplication with a suitable matrix u, which is a function of the parameters defining the Lorentz transformation. Thus one writes

$$\psi'(x) = u\psi(a^{-1}x). \qquad \text{B.2.}$$

In "c-number theory" ψ is an ordinary complex function of x and is regarded as the state-vector for a particle. B.2 is then the transformation of the state associated to or "induced by" the Lorentz transformation B.1. One can show that the matrix u can be normalized in such a way that the transformation B.2 of the state vector thus defined is unitary. This may be called the "small" operator U; it is defined only for one particle states.

In "q-number theory" ψ is a field operator, and ψ' is another field operator which "obeys the same field equations" and (as one could show) "the same anticommutation rules" (in the text this is proved for the special case at hand). Hence, one can argue, as usual, that there must be a "big" linear-unitary operator U such that

$$U^{-1}\psi(x)U = \psi'(x) \equiv u\psi(a^{-1}x). \qquad \text{B.3.}$$

(It is desirable to point out that in this formula u is not an operator, but simply a linear transformation of the components of the operator ψ; it can, therefore, be freely commuted with "big" U.) One also notices that if in B.3, a, u, U are replaced by a^{-1}, u^{-1}, U^{-1}, respectively, one gets the analogous formula

$$U\psi(x)U^{-1} = u^{-1}\psi(ax) \qquad \text{B.4.}$$

which can, in fact, be obtained directly from B.3 by a juggling of factors from one side to the other.

If $|\,\rangle$ is the normalized ket representing the vacuum, a one-particle state may be obtained by applying the creation operator $a_r{}^\dagger$ to $|\,\rangle$. The connection between $a_r{}^\dagger$ and the c-number wavefunction u_r is given by A.12. More generally, one may consider any positive energy solution $f(x)$ of A.1 (we now use f to avoid confusion with the second-quantized ψ) and defines the corresponding creation operator $a_f{}^\dagger$ by

$$a_f{}^\dagger = \int \psi^\dagger(x)f(x)d^3x. \qquad \text{B.5.}$$

The corresponding one-particle ket $|\alpha\rangle$ is then

$$|\alpha\rangle = a_f{}^\dagger|\,\rangle = \int \psi^\dagger(x)f(x)d^3x|\,\rangle \qquad \text{B.6.}$$

where the time t in $x = (x,\, t)$ may be chosen arbitrarily since the integral does not depend on t. Alternatively when the ket $|\alpha\rangle$ is given, one may construct the corresponding $f(x)$ as follows. First it is noticed that for any state $|\xi\rangle$ one has identically

$$\langle\,|\, a_f{}^\dagger\,|\, \xi\rangle = 0. \qquad \text{B.7.}$$

In fact the state $a_r{}^\dagger|\xi\rangle$ must at least contain one particle, and is, therefore, orthogonal to the vacuum state. Now applying $\psi(y)$ to B.6 where y is simultaneous with x, and using Eq. 30 and the normalization of the vacuum one finds

$$\langle\,|\,\psi(y)\,|\,\alpha\rangle = \langle\,|\,\psi(y)a_f{}^\dagger\,|\,\rangle = \langle\,|\,\int \delta(x-y)f(x)d_3x - a_f{}^\dagger\psi(y)\,|\,\rangle$$

where the last term vanishes because of B.7. Finally,

$$f(x) = \langle\,|\,\psi(x)\,|\,\alpha\rangle. \qquad \text{B.8.}$$

The corresponding equations for an antiparticle state $|\bar\alpha\rangle$ are (in the Majorana representation)

$$|\bar\alpha\rangle = \int \psi(x)d^3xf(x)|\,\rangle \qquad \text{B.6'.}$$

and

$$f(x) = \langle\,|\,\psi^\dagger(x)\,|\,\bar\alpha\rangle. \qquad \text{B.8'.}$$

Now U is an operator transforming all states of the field, and in particular it must transform the vacuum state into itself (since the vacuum is the only state with four-momentum equal to zero). With a suitable normalization of U one may always assume

$$U|\,\rangle = |\,\rangle; \qquad \langle\,|\,U^{-1} = \langle\,|. \qquad \text{B.9.}$$

This equation will apply to the operators representing parity, time reversal, etc. The transformation of one-particle states may now be examined im-

mediately by applying U to $|\alpha\rangle$ and seeing what happens in either Eq. B.6 or B.8. For example, using B.8 one finds that the wavefunction $f'(x)$ of the transformed state is

$$f'(x) = \langle | \psi(x)U | \alpha\rangle = \langle | U^{-1}\psi(x)U | \alpha\rangle = u\langle | \psi(a^{-1}x) | \alpha\rangle = uf(a^{-1}x) \qquad \text{B.10.}$$

where the Eq. B.3 and B.9 have been used; this is precisely of the same form as B.2: hence the theorem: the transformation B.2 in c-number theory and the operator U of Eq. B.3 are equivalent, when U is applied to one-particle states.[18]

[18] For the slightly different result in the case of time-reversal see Section 3.5.

LITERATURE CITED

1. Wigner, E., *Gruppentheorie und ihre Anwendung auf die Quantenmechanik der Atomspektren* (Edwards Brothers, Transl., Ann Arbor, Mich., 332 pp., 1944; English translation with additions, including a discussion of time reversal, in press) (Wigner's original paper on time reversal is in *Göttinger Nachr.*, 546–59, 1932)
2. Tanner, N., *Phys. Rev.*, **107**, 1203–4 (1957)
2a. Segel, R. E., Kane, J. V., and Wilkinson, D. H., *Phil. Mag.*, **3**, 204–7 (1958)
2b. Wilkinson, D. H., *Phys. Rev.*, **109**, 1603–9, 1610–13, 1614–19 (1958)
3. Purcell, E. M., and Ramsay, N. F., *Phys. Rev.*, **78**, 807 (1950)
3a. Ramsay, N. F., *Phys. Rev.*, **109**, 225–26 (1958)
4. Smith, J. H., Purcell, E. M., and Ramsay, N. F., *Phys. Rev.*, **108**, 120–22 (1957)
5. Blatt, J. M., and Weisskopf, V. F., *Theoretical Nuclear Physics* (John Wiley & Sons, Inc., New York, N. Y. 864 pp., 1952) (The expressions for E_n and H_n may be found on p. 801.)
6. Brueckner, K., Serber, R., and Watson, K., *Phys. Rev.*, **81**, 575–78 (1951)
7. Landau, L., *Doklady Akad. Nauk S.S.S.R.*, **60**, 207–9 (1948)
7a. Yang, C. N., *Phys. Rev.*, **77**, 242–45 (1950)
8. Wick, G. C., Wightman, A. S., and Wigner, E. P., *Phys. Rev.*, **88**, 101–5 (1952)
9. Lee, T. D., and Yang, C. N., *Phys. Rev.*, **104**, 254 (1956); **105**, 1671–75 (1957)
10. Lloyd, S. P., *Phys. Rev.*, **81**, 161–62 (1951)
11. Wolfenstein, L., and Ashkin, J., *Phys. Rev.*, **85**, 947–49 (1952)
11a. Dalitz, R. H., *Proc. Phys. Soc. (London)*, [*A*]**65**, 175–78 (1952)
11b. Wigner, E. P., and Eisenbud, L. *Phys. Rev.*, **72**, 29–41 (1947)
11c. Coester, F., *Phys. Rev.*, **84**, 1259 (1951); **89**, 619–20 (1953)
12. Henley, E. M., and Jacobsohn, B. A., *Phys. Rev.*, **108**, 502–3 (1957)
13. Jackson, J. D., Treiman, S. B., and Wyld, H. W., *Phys. Rev.*, **106**, 517–21 (1957)
13a. Curtis, R. B., and Lewis, R. R., *Phys. Rev.*, **107**, 1381–82 (1957)
13b. Morita, M., and Morita, R. S., *Phys. Rev.*, **107**, 1316–21 (1957)
13c. Wyld, H. W., and Treiman, S. B., *Phys. Rev.*, **106**, 169–70 (1957)
14. Ambler, E., Hayward, R. W., Hoppes, D. D., and Hudson, R. P., *Phys. Rev.*, **108**, 503–5 (1957); **110**, 787 (1958)
14a. Burgy, M. T., Krohn, V. E., Novey, T. B., Ringo, G. R., and Telegdi, V. L., *Phys. Rev.*, **110**, 1214 (1958)
14b. Boehm, F., and Wapstra, A. H., *Phys. Rev.*, **109**, 456 (1958)
15. Landau, L., *Nuclear Phys.*, **3**, 127–31 (1957)
15a. Salam, A., *Nuovo cimento*, **5**, 299–301 (1957)
15b. Touschek, B. F., *Nuovo cimento*, **5**, 1281–91 (1957)
15c. Sudarshan, E. C. G., and Marshak, R. E., *Phys. Rev.* (In press)
16. Pursey, D. L., *Nuovo cimento*, **6**, 266–77 (1957)
17. Pais, A., and Jost, R., *Phys. Rev.*, **87**, 871–75 (1952)
17a. Wolfenstein, L., and Ravenhall, D. G., *Phys. Rev.*, **88**, 279–82 (1952)
17b. Michel, L., *Nuovo cimento*, **10**, 319–39 (1953) (see also Reference 28)
18. Lee, T. D., Yang, C. N., and Oehme, R., *Phys. Rev.*, **106**, 340–45 (1957)
18a. Lee, T. D., Steinberger, J., Feinberg, G., Kabir, P. K., and Yang, C. N., *Phys. Rev.*, **106**, 1367–69 (1957)
18b. Gatto, R., *Phys. Rev.*, **108**, 1103–4 (1957)
19. Lüders, G., *Kgl. Danske Videnskab. Selskab, Mat. fys. Medd.*, **28**, 5 (1954)
19a. Lüders, G. and Zumino, B. *Phys. Rev.*, **106**, 385–86 (1957), Footnote 2.

19b. Schwinger, J., *Phys. Rev.*, **82**, 914–27 (1951); **91**, 713–40 (1953)

19c. Pauli, W., in *Niels Bohr and the Development of Physics*, 30 (Pergamon Press, Ltd., London, Engl., 195 pp., 1955)

20. Jost, R., *Helv. Phys. Acta*, **30**, 409–16 (1957)

21. Gell-Mann, M., and Rosenfeld, A. H., *Ann. Rev. Nuclear Sci.*, **7**, 407–78 (1957)

21a. Dalitz, R. H., *Repts. Progr. in Phys.*, **20**, 163–303 (1957)

22. Gatto, R., *Phys. Rev.*, **106**, 168–69 (1957)

23. Feinberg, G., *Phys. Rev.*, **108**, 878–81 (1957)

24. Kroll, N. M., and Foldy, L. L., *Phys. Rev.*, **88**, 1177–79 (1952)

24a. Adair, R. K., *Phys. Rev.*, **87**, 1044–47 (1952)

25. Breit, G., Condon, E. U., and Present, R. D., *Phys. Rev.*, **50**, 825–45 (1956)

25a. Cassen, B., and Condon, E. U., *Phys. Rev.*, **50**, 846–49 (1956)

25b. Breit, G., and Feenberg, E., *Phys. Rev.*, **50**, 850–56 (1956)

26. Wilkinson, D. H., *Phil. Mag.*, **44**, 1019 (1953), **1**, 379, 1031 (1956), **2**, 83 (1957); Clegg, A. B., and Wilkinson, D. H., *Phil. Mag.*, **44**, 1269, 1322 (1953), **1**, 291 (1956); Jones, G. A., and Wilkinson, D. H., *Phil. Mag.*, **44**, 542 (1953), **45**, 703 (1954); Bloom, S. D., Toppel, B. J., and Wilkinson, D. H., *Phil. Mag.*, **2**, 57, 61 (1957); Bloom, S. D., and Wilkinson, D. H., *Phil. Mag.* **2**, 63 (1957)

27. Fermi, E., *Nuovo cimento* **2**, Suppl. 1, 17–95 (1955)

28. Lee, T. D., and Yang, C. N., *Nuovo cimento*, **3**, 749–53 (1956)

28a. Bethe, H. A., and Hamilton, J., *Nuovo cimento*, **4**, 1–22 (1956)

28b. Goebel, C., *Phys. Rev.*, **103**, 258–61 (1956) (see also Reference 17, 17a, b)

29. Dirac, P. A. M., *The Principles of Quantum Mechanics* (Oxford University Press. London, Engl., 311 pp., 1947)

THE OPTICAL MODEL AND ITS JUSTIFICATION[1,2]

By Herman Feshbach

Department of Physics and Laboratory for Nuclear Science, Massachusetts Institute of Technology, Cambridge, Massachusetts

1. Introduction

This article will deal with the optical model description of the scattering of a nuclear particle by a nucleus. In this model the many-body problem arising from the interactions of the nucleons in the target nucleus with the incident particle is approximated by a two-body problem. The various interactions are replaced by a potential V between the incident particle and the nucleus. In other words, in the center-of-mass system the motion of the particle is given by the Schroedinger equation:

$$\nabla^2 \psi + \frac{2\mu}{\hbar^2}(E - V)\psi = 0 \qquad\qquad 1.$$

where μ is the reduced mass. This approximation is referred to as the "optical model," because it is in many ways analogous to the index of refraction approximation which is employed to describe the propagation of light in a medium. There the many-body problem, the interaction of light with each particle in the medium, is approximated by a propagation problem in which the effect of the medium is represented by an index of refraction. Of course, this analogy should not be taken too literally, as will be seen in Section 4.

The replacement of the target nucleus by a potential well was first suggested in 1935 by Bethe (1) and many others (2, 3, 4). They hoped to understand nuclear reactions and, in particular, the slow neutron resonances which had been discovered by Bjerge & Westcott (5) and Moon & Tillman (6). This effort was unsuccessful. The resonances obtained by Bethe (1) are now referred to as single-particle resonances. The Bohr-Breit-Wigner (7, 7a) theory of nuclear reactions successfully demonstrated that the slow neutron resonances were a many-body effect. Nuclear reactions were considered to occur in two steps. In the first, there was an amalgamation of the incident nucleon and the target nucleus to form a compound nuclear state which lived a relatively long time. The compound state was thought to be a complex many-body state in which the identity of the incident nucleon was completely lost. In the second step the compound nucleus decayed. The particle (or particles) emitted bore essentially no genetic relation to the incident particle except as demanded by the various conservation laws. Such a description seemed to have little relation to an optical model description and

49

was certainly incompatible with the first attempts to use the optical model as described above.

There was one single-particle aspect of this description which was pointed out by Ostrofsky, Breit & Johnson (8). In calculating the penetrabilities required to describe the amalgamation step, these authors suggested that one should include in the calculation of the incident particle wavefunction an average potential well describing the average interaction of the incident nucleon with the nucleus. They indicated that the well needed to be complex in order to take into account the absorption of the incident particle when it is inside the nucleus. They, of course, automatically found that single-particle resonances would enhance the penetrabilities and, therefore, the cross section for nuclear reactions.

Bethe (9) was the first to point to a single-particle approximation to the Bohr theory which corresponds quite closely to the present day point of view. When the incident nucleon energy is high, the resonances broaden, and the cross sections vary smoothly with the energy. Bethe surmised that here an optical model description would be valid. Because it was thought that nuclear matter was very absorptive, Bethe assumed that the principal effects in nuclear reactions came from the imaginary part of the potential V, and that the corresponding mean free path would be much smaller than a nuclear radius. He was then able to show that such a theory predicted the energy average of the nuclear reaction cross sections given by resonance theory.

After World War II, several developments led to the revival of the optical model. Primarily there were the first high-energy experiments. These were initially examined by Serber (10) and Goldberger (11) using essentially a kinetic theory approach. The nucleus was represented by a Fermi gas. One of the principal things learned from these investigations was that the Pauli exclusion principle, which reduces the number of possible final states in the individual nucleon-nucleon scattering, caused a considerable increase in the mean free path of the incident nucleon. The first use of the optical model was made by Fernbach, Serber & Taylor (12). These authors described the nucleus in terms of a complex index of refraction, the imaginary part of which was directly related to the mean free path. This enabled them to include in the calculation the diffraction small-angle scattering. In the calculations, the WKBJ approximation was used, rather than purely classical approach.

The use of the optical model for high-energy phenomena was not restricted to nucleon-nucleus scattering. For example, it was used by Bethe & Wilson (13) and by Byfield, Kessler & Lederman (14) to describe π-meson absorption and scattering by the carbon nucleus.

In the low-energy domain the optical model cannot attempt to describe the fine structure resonances exhibited, for example, by slow neutrons. It is concerned, as will be seen (Section 4), with the energy average of the cross sections. For this reason, the term optical potential is a misnomer. Energy

averages of resonance theory had been discussed by Bethe (15) in 1937. However, the connection with an optical potential was not made except at the higher energies where the widths of the resonances become comparable with or larger than the spacing between levels (9). That this latter theory, which assumed that nuclear matter was strongly absorptive, was not correct was indicated by the success of the shell theory. In fact, as Goldberger (11) had already observed, the mean free path is of the order of nuclear dimensions. These arguments were very much reinforced by the experimental results. Ford & Bohm (16), in 1950, had discovered that the low-energy neutron-nucleus scattering length showed a resonance structure (these resonances have since been dubbed "giant resonances") as a function of mass number. They interpreted this in terms of the optical model, employing a real, attractive square well. Assuming a range $R = 1.4 \ A^{1/3}$ fermis, the depth of the well was found to be 45 Mev. All of this indicated that the mean free path of the incident nucleon in the nucleus must be of the order of the nuclear radius, for only then would it be possible for the constructive interference required for the resonance to occur.

At higher energies, a boundary condition model for neutron scattering and absorption (17) was proposed. It was presumed to be valid when the resonance widths became of the order of the spacing between levels. This model, which antedated Ford & Bohm (16), assumed, as did Bethe's (9) earlier version, that nuclear matter was strongly absorbent. It was essentially equivalent to an optical model, as was pointed out by LeLevier & Saxon (18). These authors, encouraged by the success of the optical model at high energies, applied it to the elastic proton scattering (18 Mev) by Al, employing a complex square well for the potential V. The results did not differ strikingly from the strong interaction model.

It was not until the decisive experiments of Barschall and his co-workers (19, 19a), that the optical model was seriously considered as applying to low-energy phenomena. The average total cross section for neutrons, whose energy spread is sufficiently large so as to include many fine structure resonances (or if the energy average is performed directly), is found to depend in a markedly regular fashion on the energy E and on the mass number A. For example, peaks (giant resonances) in the cross section move in a regular way on changing E or A. This phenomenon suggests a potential well model since, roughly speaking, it becomes possible for the amplitude of the wave inside the nucleus to become very large for particular values of the parameter KR, where K is the neutron wave number inside the nucleus and R is the nuclear radius. Again, for such constructive interference to occur, the mean free path of the nucleon inside the nucleus must be at least of the order of the nuclear radius. This qualitative description of the Barschall experiments was verified by calculation (20, 20a) using a complex square well as the optical model potential. A further triumph of the model was the prediction, for low neutron energies, of a giant resonance structure for $(v\sigma_r)$, where v is the neutron velocity and σ_r is the reaction cross section. The model

also gave a reasonable fit to the angular distribution of the elastically scat-
tered neutrons. This should be compared with the strong absorption theories
(9, 17) in which the giant resonances are completely damped out so that, for
example, there are no oscillations in the total cross section as a function of
the energy.

There were, of course, many points in which the fit of the square well to
the data was unsatisfactory. The most serious of these was that the reaction
cross sections predicted seemed to be too small. This was shown in detail by
several authors (20 to 24). When the square well was employed by Chase &
Rohrlich (25) to fit the elastic proton scattering observed by Burkig &
Wright (26), Gugelot (27), and Cohen & Neidigh (28), it was found that the
square well gave much too much scattering. Both of these difficulties (20,
21, 25) could be removed when the square well was replaced by a well with
a tail. This was demonstrated for 20 Mev protons by Woods & Saxon (29),
who replaced the square well by the potential

$$V = -(V_0 + iW_0)[1 + \exp{(r - R)/a}]^{-1} \qquad\qquad 2.$$

where V_0, W_0, R, and a are parameters. So far as the neutron reaction cross
sections were concerned, it had already been noted by Bethe (9) that round-
ing the well would increase the reaction cross section relative to elastic scat-
tering cross section. Walt & Beyster (21), using the Wood-Saxon potential,
found that a considerably improved fit to the reaction cross sections could
be obtained as well as to the total cross section and angular distribution.

In the meantime, theory which was required to justify the use of the
optical model was developed. Naturally, there were different attacks for the
high-energy Serber optical model and for the optical model as applied to
relatively low-energy phenomena, since different physical situations and,
therefore, different approximations were involved. At the high-energy limit,
a multiple scattering theory was developed by Watson and his collaborators
(30 to 34). For low energies, Feshbach, Porter & Weisskopf (20) related the
total cross section of the optical potential with the energy average of the
cross sections as calculated from Wigner R-matrix theory. Thomas (35)
carried this process further, showing how with a suitable *Ansatz* one can, in
fact, obtain the optical potential (as opposed to the average total cross sec-
tion which is only indirectly related to the optical potential) directly from
resonance theory. The meaning of the averaging process was elucidated by
Friedman & Weisskopf (36).

The historical introduction will stop at this point. More recent work will
be discussed in the other sections of this review. Section 2 will contain a
proof of the physical existence of an optical potential together with a discus-
sion of its relation to the index of refraction of nuclear matter. Section 3 will
review the justification of the optical potential for high energies. This dis-
cussion will be based primarily on Watson's work (30 to 34). Section 4 will
concern itself with the low-energy domain. Section 5 will contain a summary
of the various optical potentials which have been considered together with
the empirical values of the optical potential parameters.

In Sections 2 to 4 our primary interest is in the justification of the optical model. Except for the high-energy limit no attempt will be made to discuss the calculation of the parameters of the optical model from nucleon-nucleon forces. This, of course, should receive a separate review. For this reason, the present review will not include the work of Brueckner, Eden & Francis (37), of the so-called "frivolous models" (38 to 44), of Lane, Thomas, & Wigner, (77) and of Vogt & Lascoux (80, 81).

Finally, it should be emphasized that in Sections 2 and 4, particularly, the effect of the identity of the incident nucleon and the nucleons in target nucleus is not considered. This is a serious defect. There are two connected effects of the identity of the particles. One is the requirement of antisymmetrization. The second is the so-called exchange scattering (45), in which the incident nucleon and one of the target nucleons exchange. The second of these difficulties is the more serious. For high energies (Section 3), the exchange scattering can be neglected (32), and then it is not difficult to manage the antisymmetrization. Low has given an argument (46) to show that the optical potential can include exchange scattering.

2. THE GENERALIZED OPTICAL POTENTIAL (47)

In this section, the main interest will be in showing that, except for the neglect of effects of the identity of particles (see Section 1), there is an optical potential. This will then be related with the index of refraction. Let the coordinates (including spin and isotopic spin) of the incident nucleon be r_0 and the coordinates of the target nucleus of mass number, A, be $r_1, r_2, \cdots,$ r_A. Let the Hamiltonian for the target nucleus be H_A, the kinetic energy operator for the incident nucleon be K_0 and the potential energy of the incident nucleon in the field of the target nucleon be V. V is the sum

$$V = \sum_{\alpha} V(r_0, r_a) = \sum V_{\alpha}. \qquad 3.$$

The unperturbed Hamiltonian is H_0:

$$H_0 = H_A + K_0.$$

The eigen functions of H_0 are $\Phi_{n,k}(r_0 \cdots r_A)$, where

$$\Phi_{n,k} = \phi_n(r_1, \cdots r_A) \left(\frac{1}{2\pi}\right)^{3/2} \exp{(ik \cdot r_0)}. \qquad 4.$$

The ϕ_n are the normalized states of the target nucleus. ϕ_0 is the ground state. The eigenstate of H, which in the absence of the perturbing potential V would be $\Phi_{0,k}$, is Ψ_k. (The index k will be suppressed often in the following.) Then the wave matrix operator is defined by the equation

$$\Psi_k = \Omega\Phi_{0,k}; \qquad 5.$$

Ω satisfies the equation

$$\Omega = 1 + \frac{1}{E^+ - H_0} V\Omega. \qquad 6.$$

Here

$$E^+ = E + i\eta, \qquad \eta \to 0^+ \tag{7.}$$

in accordance with the usual scattering boundary conditions. The transition matrix T is

$$T = V\Omega \tag{8.}$$

and

$$T(nk' \leftarrow 0k) = (\Phi_{nk'}, V\Omega\Phi_{0k}). \tag{9.}$$

For elastic scattering which leaves the target nucleus in the ground state, we need

$$T(0k' \leftarrow 0k) = (\Phi_{0k'}, V\Omega\Phi_{0k}). \tag{10.}$$

The single-particle transition matrix operator $\Im$ which will give the same scattering is

$$\Im \equiv \langle \phi_0, V\Omega\phi_0 \rangle \tag{11.}$$

where round parentheses are used here to indicate integration over all the coordinates r_0 to r_A, while the angular brackets in Equation 11 indicate integration only over the variables r_1 to r_A, excluding r_0. The generalized optical potential $\mathcal{V}_0$ is defined by the equation

$$\Im = \mathcal{V}_0 \langle \phi_0, \Omega\phi_0 \rangle \tag{12.}$$

where it will be shown that $\mathcal{V}_0$ and $\langle \phi_0, \Omega\phi_0 \rangle$ are related by the appropriate form of Equation 6.

It is convenient to introduce the projection operator P_0 on the ground state, ϕ_0, of the target nucleus, and

$$Q_0 = 1 - P_0. \tag{13.}$$

Then we are interested in the relation between $P_0 V\Omega P_0$ and $P_0 \Omega P_0$. Note that

$$P_0 V\Omega P_0 = P_0 V P_0 \Omega P_0 + P_0 V Q_0 \Omega P_0. \tag{14.}$$

It is clearly necessary to eliminate the excited states of the target nucleus, i.e., express $Q_0 \Omega P_0$ in terms of $P_0 \Omega P_0$. This is readily obtained from Equation 6, since

$$Q_0 \Omega = Q_0 + \frac{1}{E^+ - H_0} Q_0 V P_0 \Omega + \frac{1}{E^+ - H_0} Q_0 V Q_0 \Omega$$

or

$$Q_0 \Omega = \frac{1}{E^+ - H_0 - Q_0 V}(E^+ - H_0)Q_0 + \frac{1}{E^+ - H_0 - Q_0 V} Q_0 V P_0 \Omega.$$

Inserting this result for $Q_0 \Omega$ in Equation 14 yields

$$P_0 V\Omega P_0 = P_0 \left[V + V \frac{1}{E^+ - H_0 - Q_0 V} Q_0 V \right] P_0 \Omega P_0. \tag{15.}$$

The second term inside the square brackets comes from the elimination of the excited states of the target nucleus. Comparing with Equation 12, we see that

$$\mathcal{V}_0 = \left\langle \phi_0, \left[V + V \frac{1}{E^+ - H_0 - Q_0 V} Q_0 V \right] \phi_0 \right\rangle \qquad 16.$$

or

$$\mathcal{V}_0 = \left\langle \phi_0, V \frac{1}{E^+ - H_0 - Q_0 V} (E^+ - H_0) \phi_0 \right\rangle . \qquad 17.$$

Now one needs only to verify that $\mathcal{V}_0$ and $\langle \phi_0, \Omega \phi_0 \rangle$ satisfy the appropriate form of Equation 6: This is trivial. Taking the diagonal matrix element of Equation 6 with respect to ϕ_0, one obtains

$$\langle \phi_0, \Omega \phi_0 \rangle = 1 + \frac{1}{E^+ - K_0} \langle \phi_0, V \Omega \phi_0 \rangle = 1 + \frac{1}{E^+ - K_0} \mathcal{V}_0 \langle \phi_0, \Omega \phi_0 \rangle.$$

Here the energy of the ground state of the target nucleus has been put equal to zero.

$\mathcal{V}_0$ is then the generalized optical potential (without the effects of the identity of particles included). It should not be confused with the low-energy optical potential, since the latter involves an energy average. However, at sufficiently high energy, where the cross sections are smooth functions of the energy, $\mathcal{V}_0$ should become identical with the optical potential. Note that $\mathcal{V}_0$ is complex:

$$\operatorname{Im} \mathcal{V}_0 = - \pi \langle \phi_0, V \delta(E - H_0 - Q_0 V) Q_0 V \phi_0 \rangle. \qquad 18.$$

As can be seen directly from this expression, $\operatorname{Im} \mathcal{V}_0$ differs from zero only when inelastic processes are possible.

It can also be seen that $\mathcal{V}_0$ is a nonlocal potential. The optical model usually employs a local potential which it interprets as being the deviation of the square of the index of refraction, n, for a homogeneous nuclear medium from unity. However, in order to make up for the nonlocal nature of $\mathcal{V}_0$, the empirical optical potential is taken to be energy-dependent. As can be seen from Equation 16, $\mathcal{V}_0$ is itself energy-dependent so that the energy-dependence of the empirical potential is the consequence of two effects: the intrinsic energy-dependence of $\mathcal{V}_0$ and the energy-dependence arising from the replacement of a nonlocal by a local potential. Let us discuss this point in somewhat more detail (48, 49).

Let us consider the case of the infinite target nucleus and let us suppress spin effects. (The inclusion of the latter only complicates and, thereby, beclouds the fundamental points.) The infinite target nucleus is a homogeneous, isotropic medium so that there must be an invariance against translations of the origin. There is no preferred direction or origin. Then the most general nonlocal potential $\mathcal{V}_0$ is given by

$$\mathcal{V}_0 \psi = \int dr' \psi(r') K(E, r' - r). \qquad 19.$$

Let

$$\varrho = r' - r \qquad\qquad 20.$$

then

$$\mathcal{U}_0\psi = \int d\varrho K(E, \varrho)\psi(r + \varrho) = \left(\int d\varrho K(E, \varrho) \exp(\varrho \cdot \nabla) \right) \psi(r). \qquad 21.$$

It is obviously convenient to introduce the three-dimensional Fourier transform of K:

$$K(E,\varrho) = \left(\frac{1}{2\pi}\right)^{3/2} \int dq k(E, q) \exp(-iq \cdot \varrho)$$

$$\qquad\qquad\qquad\qquad\qquad\qquad\qquad 22.$$

$$k(E,q) = \left(\frac{1}{2\pi}\right)^{3/2} \int d\varrho K(E, \varrho) \exp(iq \cdot \varrho).$$

Then

$$\mathcal{U}_0\psi = (2\pi)^{3/2} k \left(E, \frac{1}{i}\, \nabla \right) \psi(r). \qquad 23.$$

The Schroedinger equation for ψ

$$\left\{ \frac{\hbar^2}{2m} \nabla^2 + \left[E - (2\pi)^{3/2} k \left(E, \frac{1}{i}\, \nabla \right) \right] \right\} \psi = 0 \qquad 24.$$

should be compared with the optical model equation

$$\left\{ \frac{\hbar^2}{2m} \nabla^2 + [E - V^{(0)}(E)] \right\} \psi = 0. \qquad 25.$$

One can relate $V^{(0)}$ and k if one now makes use of the assumption of the isotropy of nuclear matter in the infinite nucleus. Then k is a function only of ∇^2 or explicitly

$$(2\pi)^{3/2} k \left(E, \frac{1}{i}\, \nabla \right) \equiv \kappa \left(E, \frac{\hbar^2}{2m}\, \nabla^2 \right).$$

Then

$$V^{(0)}(E) = \kappa(E,(V^{(0)} - E)) \qquad 26.$$

is an equation determining $V^{(0)}$. It can be seen, as stated above, that the energy-dependence of $V^{(0)}$ comes from two sources, the intrinsic energy-dependence of $\mathcal{U}_0$ (nuclear matter is dispersive) and the nonlocality of $\mathcal{U}_0$.

Another way of describing this situation has been used by Brueckner et al. (50, 51, 52). These authors introduce the concept of the effective mass m^* of a nucleon in nuclear matter. In the present context, this is an expression of the nonlocality of the potential $\mathcal{U}_0$. To see this, expand k in a power series in $(1/i)\nabla$:

$$k[E,(1/i)\nabla] \simeq k(E, 0) + (1/i)\nabla \cdot \nabla_q [k(E, q)] - \tfrac{1}{2}(\nabla \cdot \nabla_q)^2 [k(E, q)] \qquad 27.$$

where q is to be put equal to zero after the differentiation is performed.

From Equation 22

$$k(E, 0) = (1/2\pi)^{3/2} \int d\varrho K(E, \varrho) \qquad \text{28a.}$$

$$\left\{ \frac{1}{i} \, \mathbf{\nabla}_q [k(E, q)] \right\}_{q=0} = [1/(2\pi)]^{3/2} \int d\varrho \varrho K(E, \varrho) \qquad \text{28b.}$$

$$-\{ (\mathbf{\nabla} \cdot \mathbf{\nabla}_q)^2 [k(E, q)] \}_{q=0} = [1/(2\pi)]^{3/2} \int d\varrho K(E, \varrho)(\varrho \cdot \mathbf{\nabla})^2. \qquad \text{28c.}$$

Assuming isotropy of the infinite nuclear medium, the integral in Equation 28b vanishes so that

$$(2\pi)^{3/2} k[E, (1/i)\mathbf{\nabla}] \simeq K_0(E) + (1/6) K_2(E) \nabla^2 \qquad \text{29.}$$

where

$$K_0 = \int d\varrho K(E, \varrho), \qquad K_2 = \int d\varrho \rho^2 K(E, \varrho). \qquad \text{30.}$$

Insert this result in Equation 24 to obtain:

$$\left[\left(\frac{\hbar^2}{2m} - \frac{1}{6} K_2 \right) \nabla^2 + E - K_0 \right] \psi = 0.$$

One can obtain the effective mass from[3]

$$\frac{\hbar^2}{2m} - \frac{1}{6} K_2 = \frac{\hbar^2}{2m^*}$$

or

$$\frac{m^*}{m} = \frac{1}{1 - \frac{m}{3\hbar^2} K_2}. \qquad \text{31.}$$

For attractive potentials, K_2 is negative so that $m^*/m < 1$. As was asserted, the effect of the nonlocality of $\mathcal{U}_0$ is reflected by deviation of m^* from m since, if $\mathcal{U}_0$ were local, K_2 would equal zero. One could, of course, solve Equation 26 to the same approximation as Equation 31:

$$V^{(0)} \simeq \frac{K_0(E) - \frac{m}{3\hbar^2} E K_2(E)}{1 - \frac{m}{3\hbar^2} K_2(E)} \qquad \text{32.}$$

[3] This definition of m^* differs from Brueckner's which, near zero wave number, is

$$m \left[1 - \left(\frac{\partial K_0}{\partial E} \right)_{E=0} \right] \bigg/ \left[1 - \frac{m}{3\hbar^2} K_2(0) \right],$$

so that

$$E = \frac{\hbar^2}{2m^*} \, (\text{wave no.})^2$$

showing the equivalence of the two points of view, the effective mass, and the energy-dependent potential for describing a nonlocal potential.

In summary, we have shown that one can obtain a generalized optical potential by projecting out the ground state of the target nucleus. This optical potential is energy-dependent, nonlocal, and, finally, complex if there is inelastic scattering. In the empirical optical potential, the nonlocalizability is reflected by an additional energy-dependence of the potential. These remarks do not apply to the low-energy optical model as yet because the latter is obtained only after averaging over resonances. However, as will be seen in Section 4, the above discussion is, in fact, valid for low energies as well as high.

3. Optical Model at High Energies; Multiple Scattering Approximation

Serber (10) first pointed out that at high energies the motion of the incident nucleon within the target nculeus could be treated classically as a series of successive two-body collisions of the incident nucleon with the individual nucleons of the target nucleus. In addition, at sufficiently high energies, these collisions could be treated as collisions between free nucleons, employing, of course, an appropriate momentum distribution for the target nucleons. This kinetic theory approach was employed by Goldberger (11), who replaced the target nucleus by a Fermi gas. One can then obtain the inelastic cross section and mean free path of the incident nucleon. The imaginary part of the optical potential is thereby obtained, but no information is obtained on the real part and, therefore, on the elastic scattering.

To obtain the elastic scattering, it is obviously necessary to consider the incident nucleon as a wave and to generalize the Serber-Goldberger multiple scattering of a particle to the multiple scattering of a wave. The assumptions about the nuclear medium remain essentially the same as in Serber's model. However, the motion of the incident nucleon is treated quantum mechanically.

The multiple scattering of waves is actually a relatively ancient subject since it was employed in discussing the index of refraction of a medium for waves of light or sound. The history of this subject is reviewed by Lax (53). Lax also generalized the earlier work of Foldy (54), employing the T-matrix formalism of Lippman & Schwinger (55). In this treatment, the medium is considered to be a fixed (albeit possibly random) system of scatterers. The wave incident on a particular scatterer consists of the incident wave plus the scattered waves emanating from all the other scatterers. It is assumed that the distance between the scatterers is (a) many wavelengths and (b) much larger than the range of the potential energy between the incident and target particle. Then the wave from one scatterer at another scatterer is just the asymptotic form, an outgoing wave times a scattering amplitude. The total wave then consists of all the scattered waves plus the incident wave. The wave scattered from a particular scatterer is the result of the

scattering of the incident wave plus the scattered waves from all other par-
ticles. These two statements lead to the two fundamental equations of
multiple scattering theory. The final step for a random set of scatterers is
to average these equations over the distribution functions describing the
probabilities for the positions and states of the scatterers. As a final approxi-
mation, one assumes that the average incident wave at a scatterer is just
proportional to the average total wave. Then the average total wave satisfies
a modified wave equation. If in vacuo

$$(E - H_0)\psi = 0$$

then in a medium

$$\left[E - H_0 - \int \rho(r_s)t(r_s)dr_s \right] \langle \psi \rangle = 0 \qquad 33.$$

where ρ is the density of scatterers and where $\langle \psi \rangle$ signifies average total
wave. (The local field correction has been dropped.) Here t is the T matrix
for two-particle scattering of the incident particle by a particle in the medium
for a scatterer located at r_s. The meaning of this term becomes clearer if its
matrix elements are evaluated with respect to plane waves, i.e., if one goes
over into momentum space. Then

$$\int dr \exp(-ik_b \cdot r) \int \rho(r_s)t(r_s)dr_s \exp(ik_a \cdot r) = t_{ba} \int \rho(r_s) \exp(i(k_a - k_b) \cdot r_s)dr_s. \quad 34.$$

Here t_{ba} is the T-matrix element which gives the scattering, by a scatterer
located at the origin, of a plane wave (wave number k_a) into a plane wave,
wave number k_b, where these are evaluated inside the medium. It will be
seen that in the nuclear case an essentially identical formula is obtained.

Let us summarize the approximations involved. If r_0 is the distance
between the scatterers, ρ_0 the range of the potential, and k the wave number
inside the medium, then the following is required:

$$k\rho_0 \gg 1, \qquad kr_0 \gg 1. \qquad 35.$$

These inequalities are required in order that the scattering from one of the
scatterers can be treated as a two-body rather than a many-body problem.
For nuclei, this assumption is part of the impulse approximation (56 to 58).
Two assumptions are made with regard to the medium. First, it is treated
as a system of scatterers, each of whose position is known; i.e., the adiabatic
approximation has been used for the motion of the scatterers. This approxi-
mation is certainly correct if the incident particle's energy is high. However,
in addition, it is necessary that forward scattering be dominant. From Equa-
tion 34, one can see that this means that

$$|k_a - k_b| r_0 \gg 1 \qquad 36.$$

where one has assumed that $\hbar/r_0$ is the maximum momentum in the density
function ρ, which in turn is just the square of the wavefunction for the scat-
terer. Inequalities 35 and 36 require that the energy of the incident particle

be high. Finally, one must assume a large number of scatterers in the medium. This is necessary for the replacement of the average wave incident on a scatterer by the average total wave.

The classical multiple scattering of waves has been discussed in detail because it motivates the analysis for the high-energy optical model approximation. Moreover, the results of the latter are identical with Equation 34, and the very same conditions of Equations 35 and 36 enter.

It should be clear from this discussion that the goal of multiple scattering theory is the expression of the optical potential in terms of the two-body scattering amplitudes. Actually, this replacement had been employed by several authors (59 to 63) for reactions such as meson production in nuclei by photons. The authors essentially used physical arguments whose justification was later considered by Chew, Goldberger, Ashkin & Wick (56, 57, 58) and dubbed by them the impulse approximation. (This term will be used later in this paper, but in a narrower sense.) Lax discusses these problems also, and he points out that they can be considered as examples of the multiple scattering of waves.

The adaptation of the multiple scattering formalism of Foldy and Lax to describe the scattering of a nucleon by a nucleus has been given by Watson and his collaborators (30 to 34). This work is completely general, describing the multiple scattering of any particle by any quantum-mechanical system. It has been recently discovered by Kerman, McManus & Thaler (64) that considerable simplification is obtained if immediate use is made of the antisymmetry of the wave function for the ground and excited states of the target nucleus. We start with the integral equation for the transition matrix T:

$$T = V\left[1 + \frac{1}{E^+ - H_0}T\right].$$
37.

Kerman *et al.* point out that one is interested only in matrix elements of T between antisymmetrized states of the target nucleus. Since both V and H_0 are symmetric in the coordinates of the target nucleons, the target nucleus wavefunctions which can appear as intermediate states must all be antisymmetric. Therefore, the definition of the operators in Equation 37 can be restricted to the subspace of antisymmetrized wavefunctions. Now it is assumed that V is a sum of two-body potentials:

$$V = \sum_1^A V_\alpha = \sum V(r_0, r_\alpha).$$
38.

Then the matrix element of V between any two antisymmetrized states ϕ_n and ϕ_m is

$$\langle \phi_n, V\phi_m \rangle = A \langle \phi_n, V(r_0, r_1)\phi_m \rangle$$
39.

where r_1 is any one of the target nucleon coordinates. One may, therefore, replace V in Equation 37 by

$$V = Av; \qquad v = V(r_0, r_1)$$
40.

so that

$$T = Av\left[1 + \frac{1}{E^+ - H_0}T\right].$$ 41.

Since v is a two-body operator, a correspondence can now be established between the two-body and many-body problem. In the two-body case the T matrix, t, is

$$t = v\left[1 + \frac{1}{E^+ - K_0}t\right].$$ 42.

One is, therefore, led to consider the many-body operator

$$\tau = v\left[1 + \frac{1}{E^+ - H_0}\tau\right].$$ 43.

The relation between t and τ will be discussed later. Let us now eliminate v from Equation 41 in favor of τ. The formal solution of Equation 43 for v is

$$v = \tau\left[1 + \frac{1}{E^+ - H_0}\tau\right]^{-1} = \left[1 + \tau\frac{1}{E^+ - H_0}\right]^{-1}\tau.$$ 44.

Similarly, the formal solution of Equation 41 is

$$T = \left[1 - Av\frac{1}{E^+ - H_0}\right]^{-1}Av.$$ 45.

Substituting the second form of Equation 44 in Equation 45 yields

$$T = \left[1 - (A - 1)\tau\frac{1}{E^+ - H_0}\right]^{-1}A\tau$$ 46.

or

$$T = A\tau + (A - 1)\tau\frac{1}{E^+ - H_0}T.$$ 47.

The form of Equation 47 suggests the definition of a new T operator

$$T' = [(A - 1)/A)]T$$ 48.

so that T' satisfies

$$T' = (A - 1)\tau\left[1 + \frac{1}{E^+ - H_0}T'\right].$$ 49.

If we find T' we can obtain the actual scattering by multiplying by $A(A-1)$. Equation 49 is identical in form with Equation 37. The effective many-body potential is $(A-1)\tau$. One can, therefore, take over the analysis in Section 2, which led to the generalized optical potential. One obtains (see Equation 16)

$$\mathcal{V}_0' = \langle\phi_0, \mathcal{V}'\phi_0\rangle$$ 50.

$$\mathcal{V}' = (A - 1)\tau\left[1 + \frac{1}{E^+ - H_0 - Q_0(A - 1)\tau}Q_0(A - 1)\tau\right].$$ 51.

The scattering amplitude computed from the optical potential $\mathcal{V}_0'$ must be multiplied by $A/(A-1)$ to obtain the true scattering amplitude. Equation 51 is identical with Watson's result to order $1/A$.

Up to this point the analysis is exact. The high-energy approximation involves two steps. First, there is the "multiple scattering approximation":

$$\mathcal{V}' \simeq (A-1)\tau. \qquad 52.$$

Second, there is the impulse approximation

$$\langle \phi_0, \tau\phi_0 \rangle \simeq \langle \phi_0, t\phi_0 \rangle. \qquad 53.$$

From these one obtains the approximate result for the optical potential:

$$\mathcal{V}_0' \simeq (A-1)\langle \phi_0, t\phi_0 \rangle. \qquad 54.$$

It is most convenient to obtain the components of $\mathcal{V}_0'$ in momentum space. The following notation is used:

$$\mathcal{V}_0'(q'\,|\,q) \equiv \left(\frac{1}{2\pi}\right)^3 \int \exp\left(-iq'\cdot r\right)\mathcal{V}_0' \exp\left(iq\cdot r\right)dr. \qquad 55.$$

Inserting this into Equation 54 one obtains

$$\mathcal{V}_0'(q'\,|\,q) = (A-1)\left\langle \phi_0, \left[\left(\frac{1}{2\pi}\right)^3 \int \exp\left(-iq'\cdot r\right)t \exp\left(iq\cdot r\right)dr\right]\phi_0 \right\rangle. \qquad 56.$$

Recall that t is (except for trivial proportionality factors) the scattering amplitude evaluated at r for a scatterer located at r_1. It is, therefore, a function $r-r_1$ with the consequence that

$$\left(\frac{1}{2\pi}\right)^3 \int \exp\left(-iq'\cdot r\right)t(r-r_1) \exp\left(iq\cdot r\right)dr = \exp\left(i(q-q')\cdot r_1\right)t(q'\,|\,q) \qquad 57.$$

where $t(q'\,|\,q)$ is just the ordinary T matrix for the scatterer placed at the origin, as is customary:

$$t(q'\,|\,q) = \left(\frac{1}{2\pi}\right)^3 \int \exp\left(-iq'\cdot r\right)t(r) \exp\left(iq\cdot r\right)dr. \qquad 58.$$

The components of $\mathcal{V}_0'$ in momentum space become finally

$$\mathcal{V}_0'(q'\,|\,q) = (A-1)t(q'\,|\,q)\int \rho(r_1) \exp\left(i(q-q')\cdot r_1\right)dr_1. \qquad 59.$$

where $\rho\,dr_1$ is just the probability of finding a target nucleon in volume element dr_1:

$$\rho = \int dr_2 \cdots dr_A \,|\, \phi_0(r_1 \cdots r_A)\,|^2. \qquad 60.$$

Equation 59 is essentially identical with the expression of Lax, Equation 34. We have succeeded using the approximations of Equations 52 and 53 in expressing the optical potential in terms of two-body scattering amplitudes. This result will be developed later, but let us now consider the region of validity of the approximations. In general, they will be found to be valid in the high-energy domain.

Let us first consider the multiple scattering approximation in which the second term in Equation 51 is dropped. Calling this term $\Delta \mathcal{V}'$ and rewriting it slightly, one obtains:

$$\Delta \mathcal{V}_0' \equiv \langle \phi_0, \Delta \mathcal{V}' \phi_0 \rangle = \left\langle \phi_0, (A-1)\tau Q_0 \frac{1}{E^+ - H_0 - (A-1)\tau} Q_0(A-1)\tau \phi_0 \right\rangle. \quad 61.$$

The matrix element has been written in this form in order to emphasize that this correction term involves only transitions of the target nucleus from the ground state ϕ_0 to excited states and then back again to the ground state. In terms of the impulse approximation, this is an inelastic scattering via $(A-1)\tau$ by one nucleon of the target nucleus followed by a second inelastic scattering which brings the target nucleus back to its original state. This implies a strong correlation between the nucleons of the target nucleus, as well as the requirement that the distance over which the corrleation exists is smaller than a wavelength of the incident nucleon. Correction term 61 is expected, therefore, not to be important when

$$qr_0 \gg 1. \quad 62.$$

Here it is assumed that the correlation distance is of the order of magnitude of the distance between particles. Condition 62 is also obtained by Lax (see Equation 35).

Using the methods of Francis & Watson (31), it is possible to be more specific. We first shall replace $(A-1)\tau$ in the denominator of 61 by an average value for all excited states of the target nucleus. If we make the shell model assumption that the effective potential is about the same for all states, then the average value of $(A-1)\tau$ is the same as it is in the ground state and, therefore, according to Equation 54 is approximately $\mathcal{V}_0'$. Therefore,

$$\Delta \mathcal{V}_0' \simeq (A-1)^2 \left\langle \phi_0, \tau Q_0 \frac{1}{E^+ - H_0 - \mathcal{V}_0'} \tau \phi_0 \right\rangle \quad 63.$$

$$\simeq (A-1)^2 \left[\left\langle \phi_0, \tau \frac{1}{E^+ - H_0 - \mathcal{V}_0'} \tau \phi_0 \right\rangle \\ - \langle \phi_0, \tau \phi_0 \rangle \left\langle \phi_0, \frac{1}{E^+ - H_0 - \mathcal{V}_0'} \phi_0 \right\rangle \langle \phi_0, \tau \phi_0 \rangle \right]. \quad 64.$$

The second form makes it clear that one is dealing with a fluctuation type term. Replacing τ by t one finds $\Delta \mathcal{V}_0'$ in momentum space:

$$\Delta \mathcal{V}_0'(q' \mid q) \simeq \left(\frac{1}{2\pi}\right)^3 (A-1)^2 \int dr_1 dr_2 dq'' [\rho(r_1, r_2) - \rho(r_1)\rho(r_2)]$$

$$\cdot \exp \left(i[(q'' - q') \cdot r_1 + (q - q'') \cdot r_2]\right) \frac{t(q' \mid q'') t(q'' \mid q')}{E^+ - K_0(q'') - (2\pi)^3 \frac{(A-1)}{V_A} t(q'' \mid q'')} \quad 65.$$

where V_A is the nuclear volume. Here it has been assumed that $\mathcal{V}_0'(q \mid q') \sim \delta(q-q')$ as is evident from Equation 59 if $\rho(r_1)$ is essentially uniform and

if the target nucleus is very large. Here condition 36 is used. The function $\rho(r_1, r_2)$ is

$$\rho(r_1, r_2) = \int \left| \phi_0(r_1, r_2, \cdots r_A) \right|^2 dr_4 \cdots dr_A. \qquad 66.$$

If, for example, ϕ_0 were the product of single-particle wavefunctions (no correlation between particles), $\rho(r_1, r_2) - \rho(r_1)\rho(r_2)$ is zero. Actually, there is at least the correlation enforced by the exclusion principle as well as that required by the nucleon-nucleon forces. Since the correlation range is of the order of the internucleon distance, it is clear that one of the $(A-1)$ factors will be cancelled. The coefficient of the remaining term has been evaluated very roughly by Watson (31, 65), and the indications are that it is small, decreasing inversely with qr_0. The evaluation of Equation 65 is then in part still an open problem. In any event, it is clear so far that conditions, Equations 35 and 36, are certainly necessary. Watson's calculation indicates that they are also sufficient. Empirically, as will be seen, the potential of Equation 59 does predict the small-angle scattering at high-energy nucleon-nucleus scattering and polarization (64, 66).

Let us turn now to the impulse approximation, Equation 53, in which we wish to compare $\langle \phi_0, \tau\phi_0 \rangle \simeq \langle \phi_0, t\phi_0 \rangle$. From Equation 43 one finds immediately that

$$\langle \phi_0, \tau\phi_0 \rangle = \langle \phi_0, v\phi_0 \rangle \left[1 + \frac{1}{E^+ - K_0} \langle \phi_0, \tau\phi_0 \rangle \right] + \left\langle \phi_0, v \frac{1}{E^+ - H_0} Q_0\tau\phi_0 \right\rangle. \qquad 67.$$

If the last term in the above could be dropped, $\langle \phi_0, \tau\phi_0 \rangle$ would satisfy the same equation as t, Equation 42. It is of some interest that $\langle \phi_0, \tau\phi_0 \rangle$ does exactly satisfy an equation of the form of Equation 42, except that v must be replaced by v', where

$$v' = \left\langle \phi_0, \left[v + v \frac{1}{E^+ - H_0 - Q_0v} Q_0v \right] \phi_0 \right\rangle.$$

A condition for the validity of the impulse approximation is then that

$$\left\langle \phi_0, v \frac{1}{E^+ - H_0} Q_0\tau\phi_0 \right\rangle \ll t. \qquad 68.$$

Replacing v by τ, Equation 44, this condition becomes

$$\left\langle \phi_0, \tau \frac{1}{E^+ - H_0 + \tau} Q_0\tau\phi_0 \right\rangle \simeq \left\langle \phi_0, \tau \frac{1}{E^+ - H_0} Q_0\tau\phi_0 \right\rangle \ll t. \qquad 69.$$

This term is quite similar to $\Delta\mathcal{U}_0'$ except for the $(A-1)^2$ term and a somewhat different energy denominator. From the discussion there one can expect that the correlation will again be important and that the left-hand side of Equation 69 will be of the order of $(1/A)t$, so that inequality 69 should be satisfied very well for large nuclei. Another effect arises from the energy denominator in Equation 69 (which has been approximated) in that we are considering the scattering from a bound nucleon rather than from a free one.

This effect has been evaluated by Chew, Goldberger, Ashkin & Wick (56, 57, 58), who have found that the relevant parameter is $(V_{av}^2/E^2)(q)$ (free scattering amplitude), where V_{av} is the average potential energy of the bound nucleon. This parameter decreases with increasing E, indicating that at sufficiently high energies the approximation is very good.

We shall now return to Equation 59 for the optical potential $\mathcal{V}'_0(q'|q)$. As Bethe (66) points out, this is the optical potential in momentum space, and there is no need to transform to ordinary space. Actually, one requires $t(q'|q)$ both on and off the energy shell ($q = q'$). These values can be obtained from the wavefunctions describing the nucleon-nucleon system, which, for example, are contained in Gammel & Thaler's analysis (67). However, the integral over ρ in Equation 59 shows that for sufficiently high energy and uniform ρ and large A that $q \simeq q'$. In the discussion below, we shall follow Riesenfeld & Watson (33) and Clementel (68). Related discussions are given by Fernbach, Heckrotte & Lepore (69) and Tamor (70).

It is now customary to express t as an operator in spin space; that is, as a function of σ_0 and σ_1. Then $t(q'|q)$ is the expectation value of this operator with respect to the ground state of the target nucleus. Assuming the latter to be of spin zero, the expectation value of σ_1 is zero. When the spin is not zero, there are effects which depend on the total spin J of the nucleus which, as Takeda & Watson (32) point out, are of the order of J/A. Therefore, $t(q'|q)$ is a linear function of σ_0. A second point is that t is generally given in the center-of-mass system of the two nucleons. If we let p and p' be the center of mass system momenta, then the average scattering amplitude $\bar{f}(p'|p)$ must be of the form

$$\bar{f}(p'\,|\,p) = F_0(p, p', p \cdot p') + i\sigma_0 \cdot \frac{(p' \times p)}{pp'} F_1(p, p', p \cdot p'). \qquad 70.$$

Now, since $q \simeq q'$, we shall place $p = p'$ and evaluate Equation 70 to first order in the angle between q and q':

$$\bar{f}(p'\,|\,p) \simeq M_0(p) + i\sigma_0 \cdot \frac{p' \times p}{p^2} M_1(p) \qquad 71.$$

where the functions M_0 and M_1 are obviously evaluated on the energy shell. The next task is to transform from the center-of-mass system to the laboratory system. Including relativistic effects, it is found that

$$t(q'\,|\,q) = -\frac{4\pi}{(2\pi)^3} \frac{E_c}{E_L} \frac{\hbar^2}{m} \bar{f} \qquad 72.$$

$$\frac{p \times p'}{p^2} = \frac{2E_c}{mc^2} \frac{q \times q'}{q^2} \qquad 73.$$

where E_c and E_L are the energies in the center of mass and laboratory systems, respectively. The optical potential becomes

$$\mathcal{U}_0'(q' \mid q) \simeq - 4\pi \frac{E_0}{E_L} \frac{\hbar^2}{2m} (A - 1) \left[M_0 + \frac{2iE_0}{mc^2q^2} \mathfrak{d}_0 \cdot (q' \times q) M_1 \right]$$

$$\cdot \left(\frac{1}{2\pi} \right)^3 \int \rho(r_1) \exp \left(i(q - q') \cdot r_1 \right) dr_1. \qquad 74.$$

Riesenfeld & Watson (33) give M_0 and M_1 in terms of the nucleon-nucleon phase shifts and mixing parameters.

To obtain the optical potential $V^{(0)}$ in ordinary space, one proceeds as follows (33, 68). The wavefunction in momentum space $\psi(q)$ is related to the wavefunction in ordinary space $\Psi(r)$ by the Fourier transform

$$\psi(q) = \int dr \exp (-iq \cdot r) \Psi(r). \qquad 75.$$

Therefore,

$$\int dq' \psi(q') \mathcal{U}_0'(q' \mid q) = \int dr \Psi(r) \exp (-iq \cdot r) \int \exp (i(q - q') \cdot r) \mathcal{U}_0'(q' \mid q) dq'$$

$$= \int dr \Psi(r) \exp (-iq \cdot r) V^{(0)}(q, r)$$

where

$$V^{(0)}(q, r) = \int \exp (iQ \cdot r) \mathcal{U}_0' dQ, \qquad Q = q - q'. \qquad 76.$$

The potential operator is then

$$V^{(0)} \left(\frac{1}{i} \nabla, r \right).$$

Inserting $\mathcal{U}_0'$, from Equation 74 and evaluating Equation 76, one readily obtains for a large nucleus

$$V^{(0)} \left(\frac{1}{i} \nabla, r \right) = - 4\pi \frac{E_0}{E_L} \frac{\hbar^2}{m} (A - 1) \left[M_0(q)\rho(r) + \frac{2E_0}{mc^2q^2} M_1(q) \mathfrak{d}_0 \cdot L \frac{1}{r} \frac{d\rho}{dr} \right] \qquad 77.$$

where, in accordance with the discussion in Section 2, all functions of ∇^2 have approximately been replaced by q^2, where $E_L = \hbar^2 q^2 / 2m$. One notes the appearance of the spin-orbit force. It is characteristically a surface effect. Of course, the simple relation between the central and spin-orbit potentials given in Equation 77 is not exact. The nonlocal nature of the potential has been converted into the energy-dependence of M_0 and M_1. M_0 and M_1 are complex. As can be seen from Equation 59, the imaginary part of M_0 for spherically symmetric ρ is directly connected with the total nucleon-nucleon cross section and, therefore, with the mean free path of a nucleon in nuclear matter. One, therefore, finds

$$\text{Im } 4\pi \frac{E_0}{E_L} \frac{\hbar^2}{m} (A - 1)\rho M_0 = \hbar v_L (A - 1)\rho \bar{\sigma}. \qquad 78.$$

Here v_L is the incident nucleon velocity in the laboratory system and $\bar{\sigma}$ is the average nucleon-nucleon total scattering cross section.

This concludes our discussion of the high-energy approximation. We have found that an optical potential exists (Equation 59) under the multiple scattering and impulse approximations. These should be valid at sufficiently high energies. At sufficiently high energies and small angle scattering, it is possible to relate the optical potential directly with nucleon-nucleon scattering amplitudes on the energy shell (Equations 74 and 77). The range of validity of the high-energy approximation, particularly with respect to the scattering angle, is not clear. Certainly it would be dangerous to use these results near and beyond the first diffraction minimum since large cancellations occur there.

Finally, the effects of the identity of particles should be mentioned. These have been considered by Takeda & Watson (32). These authors show that the above formalism can be kept as long as the exchange scattering in which the incident nucleon exchanges with a nucleon in the nucleus is small. They estimate that the exchange scattering decreases with energy and is unimportant above 100 Mev.

4. The Optical Model at Low Energies

4.1. *Energy averages.*—The optical model at low energies is concerned with energy averages of the cross sections. The energy average is required in order to smooth out the cross sections which, because of resonances, fluctuate wildly with even minute changes in the energy. The predictions of the optical model are compared with the average cross sections which vary smoothly with energy. In the discussion below of these energy averages, reference (20, 20a) will be followed, where the spin of the incident nucleon is neglected.

The energy average $\bar{\eta}$ of a quantity, η, is defined as follows

$$\bar{\eta}(E) = \frac{1}{\Delta} \int_{E-\Delta/2}^{E+\Delta/2} \eta(E')dE' = \int_{\Delta} \eta(E')dE'. \qquad 79.$$

The width of the energy interval, Δ, must be large compared to the distance D between the levels so that a sufficiently large number of levels is included in the average. Then $\bar{\eta}(E)$ will be insensitive to the exact size of Δ. The two cross sections of interest are the total σ_t and the reaction cross section σ_r. The total elastic scattering cross section σ_{el} is

$$\sigma_{el} = \sigma_t - \sigma_r. \qquad 80.$$

The scattering amplitude for spinless particles is written

$$f = \frac{i}{2k} \sum (2l+1)(1-\eta_l)P_l(\cos\theta); \qquad \eta_l = e^{2i\delta_l} \qquad 81.$$

where δ_l is the phase shift. Then

$$\sigma_t = \frac{\pi}{k^2} \sum (2l+1)[2 \operatorname{Re}(1-\eta_l)] \equiv \sum \sigma_t^{(l)} \qquad 82.$$

$$\sigma_{el} = \frac{\pi}{k^2} \sum (2l+1 \mid 1 - \eta_{\cdot} \mid^2 \equiv \sum \sigma_{el}^{(l)} \qquad 83.$$

and

$$\sigma_r = \frac{\pi}{k^2} \sum (2l + 1)[1 - |\eta_l|^2] \equiv \sum \sigma_r^{(l)}. \qquad 84.$$

The average of $\sigma_t^{(l)}$ can be directly expressed in terms of the average of η_l:

$$\bar{\sigma}_t^{(l)} = \frac{\pi}{k^2} (2l + 1)[2 \, \mathrm{Re} \, (1 - \bar{\eta}_l)] \qquad 85.$$

while

$$\sigma_r^{(l)} = \frac{\pi}{k^2} (2l + 1)[1 - |\bar{\eta}_l|^2 - (\overline{|\bar{\eta}_l|^2} - |\bar{\eta}_l|^2)] \qquad 86.$$

$$\bar{\sigma}_{el}^{(l)} = \frac{\pi}{k^2} (2l + 1)[|1 - \bar{\eta}_l|^2 + \overline{|\bar{\eta}_l|^2} - |\bar{\eta}_l|^2]. \qquad 87.$$

These equations suggest an "average" problem in which the η_l in Equation 81 is replaced by $\bar{\eta}_l$. For this "average" problem whose cross sections will be indicated by the symbol $\langle \ \rangle$,

$$\bar{\sigma}_t^{(l)} = \langle \sigma_t^{(l)} \rangle \qquad 88.$$

$$\bar{\sigma}_r^{(l)} = \langle \sigma_r^{(l)} \rangle - \sigma_{fl}^{(l)} \qquad 89.$$

$$\sigma_{el}^{(l)} = \langle \sigma_{el}^{(l)} \rangle + \sigma_{fl}^{(l)} \qquad 90.$$

where $\sigma_{fl}^{(l)}$ is the fluctuation cross section (36)

$$\sigma_{fl}^{(l)} = \frac{\pi}{k^2} (2l + 1)[\overline{|\eta_l|^2} - |\bar{\eta}_l|^2]. \qquad 91.$$

It can also be written

$$\sigma_{fl}^{(l)} = \frac{\pi}{k^2} (2l + 1)\overline{|\eta_l - \bar{\eta}_l|^2}. \qquad 92.$$

The optical model potential is defined as that potential which will produce the average reflection coefficient $\bar{\eta}_l$. Such a potential must be complex since even when there is no inelastic processes present (δ_l real, $\sigma_r = 0$), the magnitude of $\bar{\eta}_l$ cannot be unity unless there are no fluctuations present in the cross section. The absorption cross section arising from the complex potential, $\langle \sigma_r^{(l)} \rangle$, consists of two parts

$$\langle \sigma_r^{(l)} \rangle = \bar{\sigma}_r^{(l)} + \sigma_{fl}^{(l)}$$

of which the first represents real inelastic processes, the second $\sigma_{fl}^{(l)}$ contributes to elastic scattering as can be seen from Equation 89. Since $\langle \sigma_r^{(l)} \rangle$ measures the probability of the removal of a particle from the beam, $\sigma_{fl}^{(l)}$ must represent a process in which a particle is absorbed and subsequently re-emitted, i.e., elastically scattered. This suggests that $\sigma_{fl}^{(l)}$ equals $\sigma_{ce}^{(l)}$ the cross section for elastic scattering via the formation of the compound nucleus. Then $\langle \sigma_r^{(l)} \rangle$ must be the cross section for the formation of the compound nucleus $\sigma_o^{(l)}$:

$$\sigma_{fl}^{(l)} = \sigma_{ce}^{(l)} \qquad \qquad 93.$$

$$\langle \sigma_r^{(l)} \rangle = \sigma_o^{(l)}. \qquad \qquad 94.$$

Equations 93 and, therefore, 94 are, however, not universally valid (36), being correct at low energies only. As the energy increases, the width becomes of the same order as the distance between levels, and $\sigma_{fl}^{(l)}$ tends toward zero so that

$$\sigma_r^{(l)} \rightarrow \langle \sigma_r^{(l)} \rangle \qquad \qquad 95.$$

$$\bar{\sigma}_{el}^{(l)} \rightarrow \langle \sigma_{el}^{(l)} \rangle. \qquad \qquad 96.$$

In this limit the absorption cross section, as obtained from the optical potential, equals the average reaction cross section, etc. However, there is no need for σ_{ce} to go to zero as the energy increases at the same rate as σ_{fl}. In fact one can show (47) that, even when σ_{fl} is essentially zero, σ_{ce} still exists. However, σ_{ce} now contributes to the real part of the optical potential.

An understanding of this is provided by Friedman & Weisskopf's (36) interpretation of the energy averaging and of σ_{ce}. The evergy averaging is equivalent to the formation of a wave packet. When the incident wave packet is scattered by the target nucleus, it separates into two parts. One leaves the nucleus at once and is responsible for cross sections $\langle \sigma_t \rangle$, $\langle \sigma_r \rangle$ and $\langle \sigma_{el} \rangle$. The other is delayed inside the nucleus because of the formation of compound nuclear states, the delay being of the order of the lifetime of these states. From the point of view of the incident wave packet, this delayed portion constitutes an absorption from the incident beam in spite of the fact that some, σ_{ce}, of the delayed wave packet will contribute to elastic scattering. However, as the energy increases, the nuclear widths increase and, therefore, the lifetimes decrease. Hence, as energy increases, the delays due to compound nuclear formation can become of the order of the transit time of the undelayed wave packet. At these energies, the compound elastic scattering would need to be included in the calculation of $\langle \sigma_t \rangle$, etc. From the point of view of the undelayed wave packet, no absorption is involved.

In summary, it can be seen that at low energies, where $\Gamma/D \ll 1$ (Γ = level width, D = level spacing) $\langle \sigma_r \rangle$ equals $\bar{\sigma}_r + \sigma_{ce}$, while at high energies $\Gamma/D \gtrsim 1$, $\langle \sigma_r \rangle$ equals $\bar{\sigma}_r$. The compound elastic scattering is now automatically included in the shape elastic scattering cross section $\langle \sigma_{el} \rangle$. However, in the intermediate energy range between these two limits, σ_{fl} cannot be equated to σ_{ce}. Further information is necessary (47).

4.2. *Kapur-Peierls formalism.*—In order to obtain an optical potential which will reproduce $\bar{\eta}_l$, it is essential to have a convenient form of resonance theory. The Kapur-Peierls formalism (71) seems to fill the bill. This writer has developed another formalism (47) based on Equation 17, but it is as yet unpublished. The Kapur-Peierls formalism breaks configuration space up into two regions $r_0 > R$ and $r_0 < R$, where R is roughly the nuclear radius and r_0 is the coordinate of the incident nucleon. For r_0 greater than R, the incident (or emergent) nucleon no longer interacts so that it is possible to write the wavefunction for the system as

$$\Psi = \sum \phi_n (r_1 \cdots r_A) u_n(r_0)/r_0, \qquad 97.$$

where u_n are free field wavefunctions. ϕ_n are the various possible states for the target nucleus, $n = 0$ being the ground state. For spinless neutral particles and $l = 0$ (see Equation 81)

$$u_0 \rightarrow e^{-ikr_0} - \eta_0 e^{ikr_0}. \qquad 98.$$

Inside the nucleus, Ψ is expanded in a complete set, Ψ_c, of wavefunctions which are solutions of the full problem

$$(H_0 + V)\Psi_c = W_c\Psi_c. \qquad 99.$$

These wavefunctions satisfy outgoing boundary conditions at $r_0 = R$. More specifically,

$$\text{at } r_0 = R: \frac{\partial}{\partial r_0} \int \phi_n^*(r_1 \cdots r_A)\Psi_c dr_1 \cdots dr_A = ik_n \int \phi_n^*(r_1 \cdots r_A)\Psi_c dr_1 \cdots dr_A \quad 100.$$

where k_n is the wave number for u_n. For the entrance channel, $n = 0$, $k_0 = k$. The energies W_c are complex with negative imaginary part. The problem of nuclear reaction theory is to join a linear combination of Ψ_c and the Ψ of Equation 97. To accomplish this, the Green's function method is employed (72). The Green's function for Equation 99, i.e., inside the nucleus is written as

$$G = \frac{1}{E - H} \qquad 101.$$

where in a space representation $G = G(r_0 \cdots r_A | r_0' \cdots r_A')$. G satisfies the same boundary conditions as Ψ_c (see Equation 100). Using the Green's function, Ψ can be expressed in terms of its values on the surface $r_0 = R$ as follows:

$$\Psi = \frac{\hbar^2}{2m} \int \left[G(r_0 \cdots r_A | r_0' \cdots r_A') \right] \frac{\partial \Psi}{\partial r_0'}$$
$$- \Psi \frac{\partial G}{\partial r_0'} (r_0 \cdots r_A | r_0' \cdots r_A') \Big]_{r_0' = R} R^2 d\Omega_0' dr_1' \cdots dr_A'. \qquad 102.$$

Evaluate both sides of this equation at $r_0 = R$ and take the scalar product with ϕ_0. Then, using Equation 97, one has

$$u_0(R) = \frac{\hbar^2}{2m} \langle \phi_0 G \phi_0 \rangle \left[\frac{\partial u_0}{\partial r_0} - iku_0 \right]_{r_0 = R} \qquad 103.$$

where one has specialized (again to keep the discussion simple) to $l = 0$ spinless particles. G, as far as its dependence on r_0 and r_0' is concerned, is now a radial Green's function, permitting the absorption of the 4π and R^2 factors in Equation 102. The symbol $\langle \phi_0 G \phi_0 \rangle$ is

$$\langle \phi_0 G \phi_0 \rangle$$

$$= \int dr_1 \cdots dr_A dr_1' \cdots dr_A' \phi_0^*(r_1 \cdots r_A) G(R, r_1 \cdots r_A | R, r_1' \cdots r_A')\phi_0(r_1' \cdots r_A')$$

so that

$$\langle\phi_0 G\phi_0\rangle = \sum_c \frac{\int \phi_0^* \Psi_c d\tau_1 \cdots d\tau_A \int \tilde{\Psi}_c \phi_0 d\tau_1' \cdots d\tau_A'}{E - W_c} \text{ at } r_0 = R. \qquad 104.$$

We shall be more specific about $\tilde{\Psi}_c$ in a moment (see Equation 108). For the present, it is sufficient to say that

$$\int \tilde{\Psi}_c \Psi_d d\tau_0 \cdots d\tau_A = \delta_{cd}$$

the integration between taken over the region in configuration space $r_0 < R$. Substituting expression 98 for u_0, Equation 103 can be solved for η_0:

$$\eta_0 = e^{-2ix}\left[1 + ik\frac{\hbar^2}{m}\langle\phi_0 G\phi_0\rangle\right]; \ x = kr_0. \qquad 105.$$

The first term is just the repulsive potential scattering, while the second term gives the resonance scattering, as can be seen from Equation 104. The imaginary part of W_c measures the width of the level.

The important point to be learned from this calculation is that the resonance terms in η_0 depend on the structure of the compound system only via the Green's function that is only on

$$\left\langle \phi_0, \frac{1}{E - H_0 - V}\phi_0 \right\rangle$$

evaluated at r_0 and $r_0' = R$.

If one had gone through the very same process replacing the nucleus by a complex potential well, the final expression for $\bar{\eta}_0$ would be identical with Equation 105, except that $\langle\phi_0 G\phi_0\rangle$ would be replaced by the single particle Green's function g

$$g = \frac{1}{E - K_0 - \mathcal{U}_0} \qquad 106.$$

with both variables of g, r_0 and r_0' evaluated at R, where $\mathcal{U}_0$ is the complex optical potential. The problem then of the optical potential now becomes that of finding a g which will reproduce the average behavior of $\langle\phi_0 G\phi_0\rangle$. The formulation of the problem in these terms is essentially that of Bowcock (73) and Brown & Dominicis (74).

4.3. *Intermediate coupling model.*—Barschall's data (19) with its giant resonances suggested immediately that the shell model was a good zero approximation to the wavefunctions of the compound nucleus (75, 76). The deviation from the average potential of the shell model is then responsible for the fine structure and the narrow resonances of nuclear cross sections. But the average behavior of nuclear cross sections was expected to be a reflection of the shell model. This concept suggests the following expansion of the compound nuclear wavefunction Ψ_c:

$$\Psi_c = \sum_{np} (c \mid np) \phi_n(r_1 \cdots r_A) \chi_p(r_0) \qquad\qquad 107.$$

where χ_p are wavefunctions of a single particle moving in a complex potential well $\mathcal{V}_0$, subject to outgoing wave boundary conditions.

The intermediate coupling assumption reveals itself in the properties of the coefficients $(c \mid np)$. We shall assume a coefficient $(c \mid np)$ to be small when the energy $\mathrm{Re}\, W_c$ differs markedly from the shell model energy $\epsilon_n + \mathcal{E}_p$, where ϵ_n is the energy of the nth excited state of the target nucleus, while $\mathcal{E}_p$ is the real part of the energy for χ_p. We can now be more explicit about $\tilde{\Psi}_c$:

$$\tilde{\Psi}_c = \sum_{np} (c \mid np)^* \phi_n{}^*(r_1 \cdots r_A) \chi_p(r_0). \qquad\qquad 108.$$

The functions χ_p satisfy the orthogonality relation

$$\int \chi_p \chi_q dr_0 = \delta_{pq} \qquad r_0 < R. \qquad\qquad 109.$$

Inserting these expansions into Equation 104, one obtains

$$\langle \phi_0 G \phi_0 \rangle = \sum_{cpq} \frac{(c \mid 0p)^*(c \mid 0q) \chi_p(R) \chi_q(R)}{E - W_c}. \qquad\qquad 110.$$

To make contact with experiment, one must average this expression over many resonances c contained within an energy interval Δ. We take Δ to be much larger than the width of any of the resonances and, of course, large enough to contain many resonances. One also makes the "statistical approximation," in which one asserts that the coefficients in the expansion 107 have a random phase. One, therefore, obtains for the average:

$$\overline{\langle \phi_0 G \phi_0 \rangle} = -\frac{i\pi}{\Delta} \sum_{pc} \mid (c \mid 0p) \mid^2 \chi_p{}^2(R) + \text{terms from distant levels.} \qquad 111.$$

The sum is, of course, taken over the levels contained in interval Δ. The terms from the distant levels contribute to the potential scattering so that the net potential scattering includes these terms as well as the first term in Equation 105. The first group of terms is just the compound elastic scattering terms and is solely responsible for the complex nature of the optical potential, if, for the present, one assumes that the energy of the incident nucleon is below the threshold for inelastic scattering. The intermediate coupling model asserts that $\mid (c \mid 0p) \mid^2$ has a maximum near $\mathrm{Re}\, W_c = \mathcal{E}_p$ and that only this term is needed in the sum over p.

Consider now the scattering from the optical potential model. One finds that $g(R \mid R)$ is

$$g(R \mid R) = \sum_p \frac{\chi_p{}^2(R)}{E - \mathcal{E}_p + iV_p}. \qquad\qquad 112.$$

One now asks what properties the optical potential is required to have in order that expressions 112 reproduce Equation 111. It is clearly required that

V_p, the width of single-particle level, p, must be small compared with the distance between single-particle levels $\mathfrak{D}$

$$\text{Im } W_o \ll V_p \ll \mathfrak{D}. \qquad 113.$$

In that event one can rewrite Equation 112 as follows:

$$g(R \mid R) = \frac{-i V_p \chi_p{}^2(R)}{(E - \mathcal{E}_p)^2 + V_p{}^2} + \text{terms which do not resonate at } E = \mathcal{E}_p. \qquad 114.$$

Comparing Equations 114 and 111, one sees that the optical model must satisfy the following equality:

$$\frac{|(c \mid 0p)|^2}{D} \sim \frac{1}{\pi} \frac{V_p}{(E - \mathcal{E}_p)^2 + V_p{}^2}. \qquad 115.$$

This equality holds for E near $\mathcal{E}_p$. One sees that $|(c \mid 0p)|^2$ does, in fact, start to fall off as E differs from $\mathcal{E}_p$. The equality does not hold when E differs considerably from $\mathcal{E}_p$, for then the nonresonating terms must be included.

If the optical potential is a square well, then V_p is equal to the imaginary part of the potential (35). One can then determine from the empirical analysis of scattering, which yields V_p, that inequality 113 is satisfied. The left-hand side of Equation 115 is directly proportional to the strength function (35), which, in turn, at low energy is proportional to the reduced widths/D. Equation 115 is the giant resonance interpretation of this quantity.

This discussion, which is for the most part a composite of the work of Thomas (35); Lane, Thomas & Wigner (77, 78b); and Bloch (78) is not complete. [See also Agronovich & Davydov (79).] One needs to know the range of validity of Equation 115. One needs to discuss the real as well as the imaginary part of the potential. In this connection, the work of Bloch (78a), Bowcock (73), and Brown & Dominicis (74) will be reviewed. In all three of these papers, the main effort is directed toward obtaining an approximation for the average value of $[1/(E-H)]$.

We shall discuss first the work of Bloch (78a), whose attention is directed toward Equation 115. As it stands, Equation 115 was derived presuming the existence of the optical potential. Bloch is interested in deriving Equation 115 and, therefore, in effect proving the existence of the optical potential. His starting point is the equation

$$\frac{1}{D} \mid (c \mid 0p) \mid^2 = \frac{1}{2\pi i} \lim_{\delta \to 0^+} [G_p(W_c - i\delta) - G_p(W_c + i\delta)] \qquad 116.$$

where G_p is defined by

$$G_p(E) = \left(\chi_p \phi_0, \frac{1}{E - H} \chi_p \phi_0 \right). \qquad 117.$$

In taking this matrix element, note that because of the orthogonality condition 109, the complex conjugate of χ_p is not taken to the left of the comma. Equation 116 may be verified by direct substitution of series 107 and 108

in the expansion of the Green's function $[1/(E-H)]$. The interest then lies in the average value of $G_p(E)$.

The function $\phi_n \chi_p$ are solutions of the Schroedinger equation

$$(H_0 - E_\sigma)\phi_n \chi_p = 0 \qquad\qquad 118.$$

where H_0 contains the Hamiltonian for the target nucleus and the Hamiltonian for the coordinate r_0 in which the incident nucleon is presumed to move in some average, possibly complex, potential. The difference between H_0 and H is introduced as:

$$U = H - H_0. \qquad\qquad 119.$$

Then, in terms of U, one has

$$\frac{1}{E-H} = \frac{1}{E-H_0-U}$$

$$= \frac{1}{E-H_0} + \frac{1}{E-H_0} U \frac{1}{E-H_0} + \frac{1}{E-H_0} U \frac{1}{E-H_0} U \frac{1}{E-H_0} \cdots . \quad 120.$$

Forming G_p, one has

$$G_p(E) = \sum \frac{1}{E-E_p} U_{p\sigma} \frac{1}{E-E_\sigma} U_{\sigma\tau} \frac{1}{E-E_\tau} \cdots U_{\zeta p} \frac{1}{E-E_p} . \qquad 121.$$

where $U_{\sigma\tau}$ are matrices of the operator U with respect to the solutions of Equation 118. The next step is to average $G_p(E)$ over the various possible values of E_σ, etc., and over the possible values of the matrix elements. Bloch makes the following assumptions. First, the values of $U_{\sigma\tau}$ are chosen at random from a distribution. It is assumed that the distribution has such properties (e.g., $U_{\sigma\tau}$ has a random phase) that

$$\overline{(U_{\sigma\tau})^{(2q+1)}} = 0, \qquad q \text{ integer.} \qquad\qquad 122.$$

The average value of an odd power of $U_{\sigma\tau}$ is zero. Secondly, it is assumed that the average value of the even powers of $U_{\sigma\tau}$ is a function only of E_σ and E_τ. This function is presumed to differ from zero only when E_σ and E_τ are within a range $\mathcal{W}$ of each other:

$$|E_\sigma - E_\tau| \leq \mathcal{W}. \qquad\qquad 123.$$

In addition it is assumed that

$$\overline{(U_{\sigma\tau})^{2q}} = U^{(2q)}(E_\sigma, E_\tau) = U_0{}^{2q} u_{2q} \left(\frac{E_\sigma - E_\tau}{\mathcal{W}} \right) \qquad 124.$$

where

$$u_{2q}(0) = 1$$

and

$$u_{2q}(\zeta) \to 0 \qquad \text{for } |\zeta| > 1. \qquad\qquad 125.$$

Under these assumptions the average value of a term in the sum in Equation 121 takes on the following form

$$\int \frac{dE_1 \cdots dE_q}{D(E_1) \cdots D(E_q)} \frac{U_{p1}U_{12} \cdots U_{qp}}{(E - E_p)^{\nu_p+1}(E - E_1)^{\nu_1}(E - E_2)^{\nu_2} \cdots (E - E_q)^{\nu_q}};$$

where ν_i gives the number of pairs of matrix elements in which the subscript i occurs. Introducing assumption 124 and the new variables

$$E_i = \mathfrak{W}x_i; \qquad E = \mathfrak{W}x,$$

this integral becomes

$$\frac{U_0{}^k}{\mathfrak{W}^{-q+\nu_1+\nu_2\cdots+\nu_q}D^q(E - E_p)^{2p+1}} \int dx_1 \cdots dx_q \frac{\Pi u_{2j}}{(x - x_1)^{\nu_1} \cdots (x - x_q)^{\nu_q}}$$

where k is just equal to the number of matrix elements $U_{\sigma\tau}$ present,

$$k = \nu_p + \nu_1 + \cdots \nu_q.$$

For sufficiently large $\mathfrak{W}$, the dominant terms in the series for $\overline{G}_p$ are those for which

$$q = \nu_1 + \nu_2 + \cdots \nu_q.$$

This corresponds to each energy denominator (1 to q) occurring just once. Because of Equation 122 the matrix elements must describe transitions from p to 1 and then 1 back to p, from p to 2 and then back to p, etc. Keeping only these terms, one finds

$$\overline{G}_p \simeq \sum_{q=0}^{\infty} \int \frac{dE_1 \cdots dE_q}{D(E_1) \cdots D(E_q)} \frac{U^{(2)}(E_p, E_1)U^{(2)}(E_p, E_2) \cdots}{(E - E_p)^{q+1}(E - E_1)(E - E_2) \cdots}.$$

Finally

$$\overline{G}_p \simeq \frac{1}{E - E_p - \varphi(E)}$$

$$\varphi(E) = \int \frac{d\mathcal{E}}{D(\mathcal{E})} \frac{U^{(2)}(E_p, \mathcal{E})}{E - \mathcal{E}}. \qquad \qquad 126.$$

In order to evaluate Equation 116 one requires

$$\varphi(E + i\delta) = \lim_{\delta \to 0^+} \int \frac{d\mathcal{E}}{D(\mathcal{E})} \frac{U^{(2)}(E_p, \mathcal{E})}{E + i\delta - \mathcal{E}}$$

$$= \Delta - i\pi \frac{U^{(2)}(E_p, E)}{D(E)} \qquad \qquad 127.$$

where we employed the usual separation of the integral into a principal value integral and a residue at $\mathcal{E} = E$. If this result is inserted for φ in Equation 116, the desired form (Equation 115) is obtained and V_p can be identified as follows:

$$V_p = \frac{\pi U^{(2)}(E_p, \mathfrak{W}_c)}{D(\mathfrak{W}_c)}. \qquad \qquad 128.$$

Bloch has thus obtained an expression for the width of the giant resonances in terms of the matrix element of the perturbing Hamiltonian $U = H - H_0$. He has, moreover, shown that the giant resonance form (Eq. 115) is correct,

from which it follows that the optical potential exists. The statistical model he uses (Eq. 122 to 124) is quite realistic. The parameters of the approximation are $D/\mathcal{W}$ and $V_p/\mathcal{W}$. He requires that the distance over which u_{2q} differs appreciably from zero be much larger than the distance between the levels or the width of the giant resonance. If this is the case, it is shown to be plausible that Equation 126 is the first term in an asymptotic expansion in $D/\mathcal{W}$ and $V_p/\mathcal{W}$. The only issue which remains then is the estimate of $\mathcal{W}$. Bloch shows that

$$\frac{V_p^2\mathcal{W}}{M_2} = \frac{\pi}{2} \qquad\qquad 129.$$

where

$$M_2 = \sum (W_c - E_p)^2 |\, (c\,|\,0p) \,|^2. \qquad\qquad 130.$$

This second moment has been estimated by several authors, notably by Lane, Thomas & Wigner (77) and more recently by Vogt (80) and Vogt & Lascoux (81). These last authors obtain the result that M_2 is less than $(10 \text{ Mev})^2$. Using empirical values of V_p, one finds that the ratio $V_p/\mathcal{W}$ is indeed small.

Bowcock's (73) main results are concerned with the real part of the optical potential. It is this potential which is responsible for the scattering between resonances. We had already mentioned Bowcock's starting point in the discussion following Equation 105. In order that the optical potential $\mathcal{U}_0$ approximates the actual scattering, the single-particle Green's function $1/(E-K_0-\mathcal{U}_0)$ should equal the expectation value in the ground state of the target nucleus of $1/(E-H)$, i.e.

$$\left\langle \phi_0, \frac{1}{E-H}\,\phi_0 \right\rangle.$$

In both quantities the coordinates r_0 and r_0' in the incident channel are evaluated at the surface of the nucleus. It is now noted that

$$\left\langle \phi_0, \frac{1}{E-H}\,\phi_0 \right\rangle$$

$$= \left\{ \frac{1}{E-K_0-\mathcal{U}_0} \right\} + \left\{ \frac{1}{E-K_0-\mathcal{U}_0}\, \langle\phi_0, (V-\mathcal{U}_0)\phi_0\rangle\, \frac{1}{E-K_0-\mathcal{U}_0} \right\}$$

$$+ \left\{ \frac{1}{E-K_0-\mathcal{U}_0} \left\langle \phi_0, (V-\mathcal{U}_0)\, \frac{1}{E-K_0-\mathcal{U}_0}\, (V-\mathcal{U}_0)\phi_0 \right\rangle \frac{1}{E-K_0-\mathcal{U}_0} \right\} \qquad 131.$$

$$+ \left\{ \left\langle \phi_0, \frac{1}{E-H}\, (V-\mathcal{U}_0)\, \frac{1}{E-K_0-\mathcal{U}_0}\, (V-\mathcal{U}_0)\, \frac{1}{E-K_0-\mathcal{U}_0}\, (V-\mathcal{U}_0)\phi_0 \right\rangle \right.$$

$$\left. \cdot \frac{1}{E-K_0-\mathcal{U}_0} \right\}$$

where the braces indicate that the coordinates r_0 and r_0' are to be evaluated at R. The assumption of intermediate coupling enters in the approximation

$$\left\langle \phi_0, (V - \mathcal{V}_0) \frac{1}{E - K_0 - \mathcal{V}_0} (V - \mathcal{V}_0)\phi_0 \right\rangle \simeq \langle \phi_0, (V - \mathcal{V}_0)^2\phi_0 \rangle \frac{1}{E - K_0 - \mathcal{V}_0} \cdot \qquad 132.$$

This approximation is valid if, as the intermediate coupling theory proposes to first order, the only intermediate state of importance in the evaluation of $1/(E - K_0 - \mathcal{V}_0)$ is just the single-particle state responsible for the giant resonance near the energy E. This essentially assumes that the width of the giant resonance is very much less than the energy spacing between single-particle levels of the same character. The intermediate coupling approximation also permits the reduction of the last term in Equation 131 to a finite number of terms coming from the fine structure resonances contained in the giant resonance near E. Therefore, according to Bowcock, the first three terms in Equation 131 may be interpreted as describing the potential scattering. A potential $\mathcal{V}_0$ which does describe the potential scattering must satisfy the equation

$$\left\{ \frac{1}{E - K_0 - \mathcal{V}_0} (\overline{V} - \mathcal{V}_0) \frac{1}{E - K_0 - \mathcal{V}_0} \right\}$$

$$+ \left\{ \frac{1}{E - K_0 - \mathcal{V}_0} [\overline{V^2} - (\overline{V})^2 + (\overline{V} - \mathcal{V}_0)^2] \left[\frac{1}{E - K_0 - \mathcal{V}_0} \right]^2 \right\} = 0 \qquad 133.$$

where

$$\overline{V} = \langle \phi_0, V\phi_0 \rangle \quad \text{and} \quad \overline{V^2} = \langle \phi_0, V^2\phi_0 \rangle. \qquad 134.$$

For the $l = 0$ spinless particle case, the single-particle Green's function $g(r_0, r_0')$ [the representation of $1(E - K_0 - \mathcal{V}_0)$ in space] can be represented for $r_0' < r_0$ as a product of factors which individually depend upon r_0 and r_0'. Therefore

$$g(R, r_0') = f(r_0')d(R)$$

Equation 133 becomes

$$(f, [\overline{V} - \mathcal{V}_0]f) + \left(f, [\overline{V^2} - (\overline{V})^2 + (\overline{V} - \mathcal{V}_0)^2] \frac{1}{E - K_0 - \mathcal{V}_0} f \right) = 0.$$

or defining $h(r)$ by

$$\frac{1}{E - K_0 - \mathcal{V}_0} f = h \qquad 135.$$

one finally obtains

$$(f, [\overline{V} - \mathcal{V}_0]f) + (f, [\overline{V^2} - (\overline{V})^2 + (\overline{V} - \mathcal{V}_0)^2]h) = 0. \qquad 136.$$

Since f and h are known functions, this equation relates $\mathcal{V}_0$, $\overline{V}$ and $\overline{V^2}$. By assuming simple forms (e.g., square well inside nucleus), the real and imaginary depths of $\mathcal{V}_0$ can be determined if $\overline{V}$ and $\overline{V^2}$ were known. Note these last two quantities are real. Actually, Bowcock works this in inverse order. By assuming a form independent of energy for $\mathcal{V}_0$ from empirical data, he evaluates $[\overline{V}]$ and $\overline{V^2} - (\overline{V})^2$.

Brown & Dominicis' paper (74) is a continuation of Bowcock's attack. They stop the expansion Equation 131 one term earlier, viz:

$$
\left\langle \phi_0, \frac{1}{E-H}\phi_0 \right\rangle
$$

$$
= \left\{ \frac{1}{E-K_0-\mathcal{U}_0} \right\} + \left\{ \frac{1}{E-K_0-\mathcal{U}_0} \quad \langle \phi_0, (V-\mathcal{U}_0)\phi_0 \rangle \quad \frac{1}{E-K_0-\mathcal{U}_0} \right\}
$$

$$
+ \left\{ \left\langle \phi_0, \frac{1}{E-H}(V-\mathcal{U}_0)\frac{1}{E-K_0-\mathcal{U}_0}(V-\mathcal{U}_0)\phi_0 \right\rangle \frac{1}{E-K_0-\mathcal{U}_0} \right\}. \qquad 137.
$$

Brown and Dominicis are able to show, using the intermediate coupling approximation, that when E is between two giant resonances the last term in the above equation is of the order of width of a resonance divided by the single particle level spacing. The main device employed is the replacement of $1/(E-H)$ by $1/(E-\overline{E})$, where $\overline{E}$ is the average energy between two giant resonances. They then replace the last term by its average over the resonances and obtain the following equation for the $\mathcal{U}_0$, which will reproduce the elastic scattering:

$$
0 = (u_p, (\overline{V}-\mathcal{U}_0)u_p) - \frac{i\pi}{\Delta}\sum_c (u_p\phi_0, (V-\mathcal{U}_0)\Psi_c)^2 \qquad 138.
$$

where Ψ_c are the various compound nuclear states and u_p is the single-particle wavefunction corresponding to the giant resonance. The quantity Δ is the energy region over which the average of Equation 137 was performed.

This concludes our review of the justification of the optical potential for low-energy phenomena. One serious omission has been made in that the work of Brueckner et al. (50, 51, 52) has not been discussed because this would necessitate a review of the Brueckner method which more properly should be reviewed in a separate article. In summary on the work reported here, it seems fair to say that one has reasonably good arguments for the existence of an optical potential, but that the general character of the potential such as its nonlocalizability as well as its radial, spin, and velocity dependence is not at all clear. These treatments, moreover, do not discuss the effect of exchange scattering, which certainly must be important at low energies.

5. THE PHENOMENOLOGICAL OPTICAL MODEL

5.1. *Forms for the optical potential.*—In this section, the attempts at the determination of the optical potential from experimental data will be summarized. The procedure involves first the assumption of a form for the optical potential, which contains a number of parameters. Best values of these parameters are then determined by comparing the predictions of such a potential with experiment. The most general form which has been employed for spherical nuclei is a combination of central and spin-orbit potentials:

$$V = - \left[V_c \rho_c(r) + i W_c \rho_c'(r) \right] + \left(\frac{\hbar}{\mu c} \right)^2 \left[V_{so} \frac{1}{r} \frac{d\rho_{so}}{dr} + i W_{so} \frac{1}{r} \frac{d\rho_{so}'}{dr} \right] \mathbf{\sigma} \cdot \mathbf{L} \qquad 139.$$

where V_c etc. are constants, ρ_c etc. are functions of r, which are unity at the origin; σ and L are the Pauli spin and angular momentum operators for the incident particle. The constant $(\hbar/\mu c)$ is the π-meson Compton wavelength so that $(\hbar/\mu c)^2$ is 2×10^{-26} cm.^{2} (Additional terms come in if the target nucleus is deformed. This will be considered later in a separate subsection. Outside of the latter section, we shall always have spherical nuclei in mind.) Expression 139 already assumes that the potential is local. From the analysis of the previous two sections we can see that this is not generally the case. For infinite nuclei (see Sect. 2) the nonlocality can be simulated by velocity-dependent potentials. A similar discussion can be carried through for finite nuclei. However, the results are considerably more complicated. The co-efficient of each power of the energy in the potential could very easily have a different space-dependence. In Equation 139, this would mean that not only the parameters in ρ_c etc. change with energy, but also the form itself. This is, in fact, indicated by the calculations of McManus & Thaler (82) employing high-energy multiple scattering approximation. They find the following inequalities in the mean square radius at 310 Mev.

$$\bar{R}^2(\rho_c) > \bar{R}^2(\rho_{so}) > \bar{R}^2(\rho_{so}') > \bar{R}^2(\rho_c')$$

while at 156 Mev

$$\bar{R}^2(\rho_{so}) > \bar{R}^2(\rho_c) > \bar{R}^2(\rho_{so}') > \bar{R}^2(\rho_c').$$

In other words, one must use forms for ρ_c which contain many energy-dependent parameters. One may expect that these effects are not serious, i.e., one needs only a few parameters as long as $\hbar$/(change in wave number of the nucleon inside the nucleus) upon scattering is large compared to the range of the nonlocality. For this reason, the scattering in the forward direction at high energies can be represented by the potential of Equation 139.

Expression 139 also assumes that the spin I of the target nucleus is zero. If it is not, a whole host of additional interactions are possible. A few of these are:

$$\begin{aligned} &\mathbf{\sigma} \cdot \mathbf{I} \\ &\mathbf{L} \cdot \mathbf{I} \\ &(\mathbf{\sigma} \cdot \mathbf{I})(\mathbf{L} \cdot \mathbf{I}) \qquad\qquad 140. \\ &(\mathbf{\sigma} \cdot \mathbf{p})(\mathbf{I} \cdot \mathbf{p}) \\ &(\mathbf{\sigma} \cdot \mathbf{r})(\mathbf{I} \cdot \mathbf{r}). \end{aligned}$$

In the high-energy limit (Sect. 3) one can show that these terms are $1/A$ times the major terms in Equation 139 and hence for heavy nuclei are not important. They should show themselves in the comparison of scattering from an even-even nucleus with the scattering from an odd nucleus and also in scattering of polarized beams from odd nuclei. A wide variety of forms have been used in Equation 139. These are listed in Table IA and Table IB below.

TABLE IA*

TABLE OF POTENTIAL FORMS USED: NO SPIN-ORBIT COUPLING

Type	Designation	ρ_o	$\rho_e{'}$	References
Square	V_{sq}	$\begin{cases} 1 & r \le R \\ 0 & r > R \end{cases}$	ρ_e	(12, 16, 18, 20 to 25, (69, 83 to 97)
Woods-Saxon	V_{WS}	$\left[1+\exp\left(\dfrac{r-R}{a}\right)\right]^{-1}$	ρ_e	(29, 76, 93, 98 to 106)
Gaussian taper	V_G	$\left[1+\exp\left(\dfrac{r^2-R^2}{a^2}\right)\right]^{-1}$	ρ_e	(101)
Wine bottle	V_{WB}	$\dfrac{1+b(r/R)^2}{1+b\beta}\left[1+\exp\left(\dfrac{r-R}{a}\right)\right]^{-1}$	ρ_e	(101)
Hill-Ford	V_{HF}	$\left[1-\dfrac{1}{2}\exp\left(-\dfrac{R}{a}\right)\right]^{-1}\begin{cases}1-\dfrac{1}{2}\exp\dfrac{r-R}{a}; & r \le R \\ \dfrac{1}{2}\exp\left[-\left(\dfrac{r-R}{a}\right)\right]; & r \ge R\end{cases}$	ρ_e	(101, 102)
Trapezoidal	V_t	$\begin{cases} 1; & r \le (R-a) \\ \dfrac{1}{2}-\dfrac{r-R}{2a}; & R-a \le r \le R+a \\ 0; & r \ge R+a \end{cases}$	ρ_e	(107, 108, 109)

Type	Designation	ρ_e	ρ_e'	References
Exponential taper	V_E	$\begin{cases}1; & r \leq R \\ \exp (R-r)/a; & r \geq R\end{cases}$	ρ_e	(110, 111, 139, 140)
Step	V_{st}	$\begin{cases}1; & r \leq R-d \\ \beta; & R-d < r \leq R \\ 0; & r > R\end{cases}$	$\begin{cases}1; & r \leq R-d \\ \gamma; & R-d < r \leq R \\ 0; & r > R\end{cases}$	(112, 113)
Gaussian surface absorption	V_{GS}	$[1+\exp (r-R)/a]^{-1}$	$\exp\left[-\left(\frac{r-R}{b}\right)^2\right]$	(114)
Derivative surface absorption	V_{DS}	$\begin{cases}1; & r \leq R \\ \{[(\exp x)-x]^{-1}; & r \geq R\end{cases}$	$-\dfrac{d}{dx}\rho_{ei}; \quad x=\dfrac{r-R}{a}$	(115, 116, 117)
"Parabolic" taper	V_{PT}	$\begin{cases}1; & r \leq R \\ \dfrac{E}{V_0}\left[1-\left\{\left[\sqrt{1-\dfrac{V_0}{E}}-1\right]\left[\dfrac{(R+a)^2-r^2}{4aR}\right]+1\right\}^2\right]; & R-a < r < R+a \\ 0; & r > (R+a)\end{cases}$	ρ_e	(97)

* See also D. C. Peaslee (130).

TABLE IB

TABLE OF POTENTIAL FORMS: WITH SPIN-ORBIT COUPLING*

Type	Designation		ρ_c	ρ_c'	ρ_{so}	ρ_{so}'	References
Square	$V_{sq}{}^{(so)}$		$1 \quad r \leq R$ $0 \quad r > R$	ρ_c	ρ_c	ρ_c	(66, 69, 118 to 121)
Bjorklund-Fernbach	$V_{BF}{}^{(so)}$		$\left[1+\exp\left(\dfrac{r-R}{a}\right)\right]^{-1}$	$\exp-\left[\dfrac{r-R}{b}\right]^2$	ρ_c	ρ_c	(122, 123)
Woods-Saxon	$V_{WS}{}^{(so)}$		$\left[1+\exp\left(\dfrac{r-R}{a}\right)\right]^{-1}$	ρ_c	ρ_c	ρ_c	(124, 125)
Step	$V_{st}{}^{(so)}$	$r \leq R-d \quad :$ $R-d < r \leq R:$ $r > R \qquad :$	1 β 0	1 γ 0	1 $\dfrac{R-r}{d}$ 0	ρ_{so}	(69, 112, 126, 127, 128)

* See also N. A. Gulia (129).

Only the specifically nuclear interactions have, of course, been listed, to which one must add the electromagnetic interactions. For the most part, only the static Coulomb interaction has been considered. It was shown by Woods & Saxon (29) and later by Glassgold & Kellogg (101) that the predicted scattering of protons by nuclei was insensitive to various possible forms for the charge distribution. Glassgold and Kellogg varied the diffusivity (parameter a for the charge distribution), and the radius of the charge distribution was made 10 per cent smaller than the nuclear "radius" without finding any appreciable consequences over the range of proton energies 10 Mev to 100 Mev. Schwinger (131) calculated the effect of the interaction of the Coulomb field of the nucleus on the neutron polarization in small angles of scattering. Some improvements have been made by Sample (135) and by several Russian authors (132, 133), while Eriksson (134) has investigated the corresponding effect in proton scattering.

The square well potential is principally of historical interest now. The parameter $V_c = 42$ Mev, $R = 1.45\ A^{1/3}$ f. (fermi) and $W_c/V_c = 0.03$ gave a reasonably good fit to the total cross section and to the angular distribution (20, 21, 24, 90, 95). However, even in the first papers on neutron scattering it was recognized that the cross section for the formation of the compound nucleus, σ_c, was much too small. A number of papers on neutron scattering verified and reinforced this conclusion (20, 21, 22, 24). The cure was fairly obvious (20, 21, 112). The reflectivity of the square well was too large. The potential should not plunge to zero abruptly at $r = R$, but should become zero more gradually. Such wells have been referred to as rounded or tapered wells. The principal point here is that the reaction cross section is sensitive to the nature of the surface of the nucleus.

The need for tapering the potential was first noticed (18, 25, 96) for proton scattering. As one might suspect for large Z, where the Coulomb repulsion is most effective, the details of the nuclear surface would play an important role. This is indeed the case, the square well giving much too much scattering for large scattering angles.

The remaining potentials in Table IA are all tapered. V_{WS}, introduced by Woods & Saxon (29), has been most frequently used. It is relatively constant for $r < R - a$ and then drops rapidly to zero for larger r. At $r = R$, $V = V_0/2$, V_E and V_t are quite similar to V_{WS} except for a discontinuity in slope as the potential starts to fall off. They have been used because of the analytic simplicity of the corresponding Schroedinger equation for $l = 0$. V_{st} is even more discontinuous, but is quite easy to handle for all l. V_G, V_{WB} and V_{HF} were employed by Glassgold & Kellogg (101) in order to see how sensitive the consequent cross sections are to particular forms of the potential. V_{WB} permitted a rise in the potential as the surface of the nucleus is approached.

In all of these potentials, the imaginary part of the potential is simply proportional to the real part. It has, however, been suggested by Emmerich & Amster (113, 115, 116) and by Bjorkland, Fernbach & Sherman (114) that the absorption should be concentrated near the surface. This is suggested by

the argument that the interaction of an incident nucleon and a nucleon in the nucleus is most vigorous near the surface where the inhibiting effects of factors, which lead to saturation, such as the exclusion principle, are smallest. This contention cannot be completely correct since even infinite nuclear matter would be expected to be absorbing. However, it may very well be the case that the mean free path inside the nucleus is much larger than the mean free path in the surface region (136). On the other hand, McManus & Thaler (82), using the high-energy multiple scattering approximation, find that the mean square radius for ρ_c is much larger than ρ_c', the difference decreasing as A increases.

But none of these potentials can explain the polarization of nucleons upon scattering by nuclei. A spin-orbit force must be invoked when the target nucleus has zero total angular momentum. Most authors employ a Thomas spin-orbit force, for which spin-orbit term is proportional to $1/r d\rho_c/dr$. This form, first used by Fermi (137) and Malenka (138), is also suggested by the results of Riesenfeld & Watson (33) and Fernbach, Heckrotte & Lepore (69). In the latter's analysis, it is a consequence of the assumption that infinite nuclear matter is isotropic.

5.2. *Numerical values of potential parameters.*—The qualitative dependence of these potentials on their parameters is listed below as far as it is known. These results have been obtained for the most part by direct numerical computation so that their region of validity may be limited.

(*a*) The cross sections at low energy depend on the parameters V and R through the combination $V_0 R^2$ (20, 99 to 104, 106, 107, 116, 122). This remark applies to the angular distribution and to the total cross section σ_t, as functions of energy or mass number. This result is not surprising and may, in fact, be qualitatively explained using the WKB approximation. For greater energies the combination involved is $V_0 R^n$, where n varies from two toward three, as the energy increases. The criterion of energy independence of the parameters can be used to determine V_0 and R separately. However, the positions of the minima and maxima depend only on $V_0 R^n$.

(*b*) As the imaginary part of the potential W_c is increased, the oscillations in the angular distribution or in σ_t or in the cross section for the formation of the compound nucleus, σ_c, as functions of E or A damp out, each peak broadening. The positions of the minima and maxima do not change (99, 100).

(*c*) The angular distribution is sensitive to the surface parameter a. (99, 100, 102). The positions of the minima and maxima do not change. Increasing a lowers the cross section for elastic scattering, but raises the cross section σ_c. Small a means a more rapid change in the potential near the surface which in turn leads to greater reflectivity and smaller absorption, since fewer nucleons can enter the target.

(*d*) Potentials of similar shape, e.g. V_{WS}, V_{HF}, will give nearly identical results if the parameter a is adjusted in each case so as to give identical values to the thickness, t, of the surface region. The parameter t is defined to

be the distance over which the central potential drops from 9/10 of its value at the center to 1/10 of the same. For example, if V_{HF} is to be equivalent to V_{WS}, the parameter a_{HF} (a for the Hill-Ford potential) should be $1.367 \times a_{WS}$ (a for the Saxon potential), while the values of R, V_c and W_o should be the same for both potentials. Table II gives a detailed comparison (102).

TABLE II

COMPARISON OF HILL-FORD AND WOOD-SAXON
TYPE POTENTIALS (102)

E (Mev)*	Element	V_{HF}/V_{WS}	W_{HF}/W_{WS}	R_{HF}/R_{WS}	a_{HF}/a_{WS}
14	C	1.03	1.02	1.01	1.32
17	Au	0.99	1.05	1.00	1.28
40	C	0.96	0.99	1.01	1.48
40	Pb	1.04	0.91	1.00	1.27
95	Al	1.00	1.04	1.00	1.43

* Energy of incident proton.

(e) Concentrating the imaginary part of the potential in the surface instead of spreading it through the volume reduces the average slope of σ_t and σ_c as a function of mass number A. Qualitatively, this follows from the fact that the surface area is proportional to $A^{2/3}$, while the volume is proportional to A (116).

(f) Including a spin-orbit term dampens the oscillations in the angular distribution of elastically scattered neutrons or protons (69, 77, 112, 120, 121, 122). This comes from the splitting of resonance for a given l, for a purely central potential into two for $j = l \pm \frac{1}{2}$, when spin-orbit potentials are present. This splitting also shows up in the total cross section whose oscillations as a function of E or A are correspondingly reduced.

(g) At high energies, the Born approximation may be used to obtain the polarization in small angle scattering (66, 118, 141). The polarization depends only upon the magnitudes of the potentials and not on their radial shapes. Similarly, the forward scattering peak is insensitive to the form of the potential once the potentials have been adjusted to give the same scattering at a particular angle (97, 142). In other words, model dependent features appear only at large angles of scattering. These remarks have been demonstrated for Thomas type spin-orbit potentials.

(h) At high energies and when the spin-orbit potential is effective only in the surface region, as it is for the Thomas type potential, the polarization at larger angles is sensitive to the width of the surface region (124, 127).

Let us consider next the evaluation of the phenomenological parameters, V_c, W_o, etc., from experiment. A few words of caution are in order. First, as has been mentioned earlier, the potentials listed in Table I are local potentials. From the discussion of Riesenfeld & Watson (33), it seems plausible

to expect this approximation to break down for large angles of scattering and at low energies. For these angles and energy, deviations of the scattering, as predicted by the potentials in Table I, from experiment should be expected. A rough guess indicates that inclusion of the nonlocality of the potential would reduce the amplitude of oscillation of the computed cross sections. Second, for odd A nuclei the potential of Equation 139 is not the most general. There are, in addition, the possibilities listed in Equation 140. Including these in the potential would also damp the oscillations in the theoretical cross sections. Third, the potentials in Table I predict only the shape elastic angular distribution to which one must add the compound elastic scattering in order to complete the theoretical computation of the angular distribution. This effect is not important at sufficiently high energies. At low energies, where it is significant, it is difficult to make a theoretical evaluation of σ_{ce}, since it depends sensitively on the energy level structure of the target nucleus which is not always known. A semiempirical procedure has been adopted by Beyster, Walt & Salmi (103) and others (90, 104, 116). One can obtain the total compound elastic cross section by equating it to the difference between the computed cross section for the formation of the compound nucleus, σ_c, and the measured total reaction cross section. This total compound elastic cross section must then be distributed over all the scattering angles. Beyster, Walt, and Salmi distribute it isotropically; this method should be quite good if the target nucleus has a large spin (20), but should in any event give a rough estimate of the effect of the compound elastic scattering on the angular distribution. It might be added parenthetically that Beyster, Walt & Salmi and Emmerich & Sinclair (143) find that compound elastic scattering is of some importance at nuclear energies as high as 4 to 6 Mev. This is also indicated by Wall & Waldorf (144).

There are also a number of experimental difficulties. Corrections to the data must be made for finite angular and energy resolution of the detection apparatus for multiple scattering and for the energy spread of the incident beam. Finite energy resolution can result in the inclusion of some inelastically scattered particles in the elastically scattered group. Finite angular resolution will reduce the amplitude of oscillations in the angular distribution.

5.3. *The function* $\overline{\Gamma_n/D}$.—One of the more dramatic accomplishments of the optical model at low energies has been the prediction of the dependence of the average ratio of neutron width to level spacing, $\overline{\Gamma_n/D}$, on the mass number. The direct energy average of a sum of Breit-Wigner terms gives for $l=0$ and nearly zero energy neutrons incident on a nucleus the cross sections $\bar{\sigma}_t$ and σ_c as follows:

$$\bar{\sigma}_t = 4\pi \sum g_J (R_J')^2 + 2\pi^2 \lambdabar^2 g_J \left(\overline{\frac{\Gamma_n^{(J)}}{D}} \right)$$

$$\sigma_c = 2\pi^2 \lambdabar^2 \sum g_J \left(\overline{\frac{\Gamma_n^{(J)}}{D}} \right) \left[1 - \frac{\pi}{2} \left(\overline{\frac{\Gamma_n^{(J)}}{D}} \right) \right]$$

141.

where the sum extends over to two possible values of $J = I + \frac{1}{2}$ (I = spin of the target nucleus) and g_J are the corresponding statistical weights $\frac{1}{2}[1 \pm 1/(2I+1)]$. R_J' is the scattering length to a first order in $\overline{\Gamma_n/D}$.

Equations 141 are to be compared with the calculations of the optical model. The potentials listed in Table I do not depend upon I, which is to be expected only if $I = 0$. For other target spins these potentials implicitly assume that Γ_n/D and R' are independent of J (and I). A term in the potential proportional to $I \cdot \mathbf{\sigma}$ (see Equation 140) would, for example, differentiate between the two values of J. The validity of this assumption is by no means obvious, and it should be studied experimentally. For the present, it is assumed to be true so that Equation 141 becomes

$$\sigma_t = 4\pi R'^2 + 2\pi^2 \mathchar'26\mkern-10mu\lambda^2 \left(\frac{\overline{\Gamma_n}}{D} \right) \qquad 142a.$$

$$\sigma_0 = 2\pi^2 \mathchar'26\mkern-10mu\lambda^2 \left(\frac{\overline{\Gamma_n}}{D} \right) \left(1 - \frac{\pi}{2} \left(\frac{\overline{\Gamma_n}}{D} \right) \right). \qquad 142b.$$

The cross sections σ_0 and $\bar{\sigma}_t$ can be evaluated directly from the optical model by solving the corresponding Schroedinger equation. Then $\overline{\Gamma_n/D}$ can be evaluated from Equation 142b and R' from Equation 142a. Putting

$$|\bar{\eta}_0| = \exp[-\operatorname{Im}\delta_0] \qquad 143.$$

where δ_0 is the phase shift, it is found to second order from Equation 142b that

$$\left(\frac{\overline{\Gamma_n}}{D} \right) = \frac{2}{\pi} \operatorname{Im}\delta_0 - \frac{4}{\pi} (\operatorname{Im}\delta_0)^2 + \frac{\pi}{2} \left(\frac{\overline{\Gamma_n}}{D} \right)^2$$

$$\simeq \frac{2}{\pi} \operatorname{Im}\delta_0 (1 - \operatorname{Im}\delta_0) \qquad 144.$$

so that

$$\sigma_t \simeq \left[4\pi R'^2 - \pi^3 \mathchar'26\mkern-10mu\lambda^2 \left(\frac{2}{\pi} \operatorname{Im}\delta_0 \right)^2 \right] + 2\pi^2 \mathchar'26\mkern-10mu\lambda^2 \left(\frac{2}{\pi} \operatorname{Im}\delta_0 \right) \qquad 145.$$

which is the form proposed by Lane & Lynn (145). At very low energies the last term is proportional to $\mathchar'26\mkern-10mu\lambda$, while the other terms are independent of $\mathchar'26\mkern-10mu\lambda$. Feshbach et al. (20), in their final evaluation of $\bar{\sigma}_t$ for the square well, did not include the second term in Equation 145. As a final remark, we note an evaluation of $\operatorname{Im}\delta_0$ obtained by Porter (146) from the continuity equation:

$$\operatorname{Im}\delta_0 \simeq \frac{1}{2i} \sin(\delta_0 - \delta_0^*) = \frac{2mk}{\hbar^2} \int \operatorname{Im} V |u|^2 dr \qquad 146.$$

where $u = r\psi$ for $l = 0$ and u approaches $(1/k) \sin(kr + \delta_0)$ for large values of r.

It is convenient to extract the $1/k$ energy-dependence of $\overline{\Gamma_n/D}$ by introducing the quantity

FESHBACH

$$\Gamma_n^{(0)}/D = \sqrt{E_0/E}(\overline{\Gamma_n/D}) \qquad\qquad 147.$$

where E_0 is a fixed energy, say 1 e.v., and E is the energy at which $\overline{\Gamma_n/D}$ is measured. The quantities $\Gamma_n^{(0)}/D$ and R'/R have a dependence on mass number which is reminiscent of the optical absorption and dispersion curves. This is illustrated (105) in Figures 1 and 2, in which $\Gamma_n^{(0)}/D$ and R'/R have been plotted for the case of a Saxon well with the parameters:

$$V_0 = 52 \text{ Mev}, \quad W_0/V_0 = 0.06, \quad R = [1.15A^{1/3} + 0.4]\text{f.(fermis)}, \quad a = 0.57\text{f}. \quad 148.$$

The position of the peaks depends for a fixed value of a on the quantity V_cR^2 and is roughly independent of W_c/V_c. The effect of increasing W_0/V_0 is to broaden and lower the peaks in Figure 1 and the corresponding structure
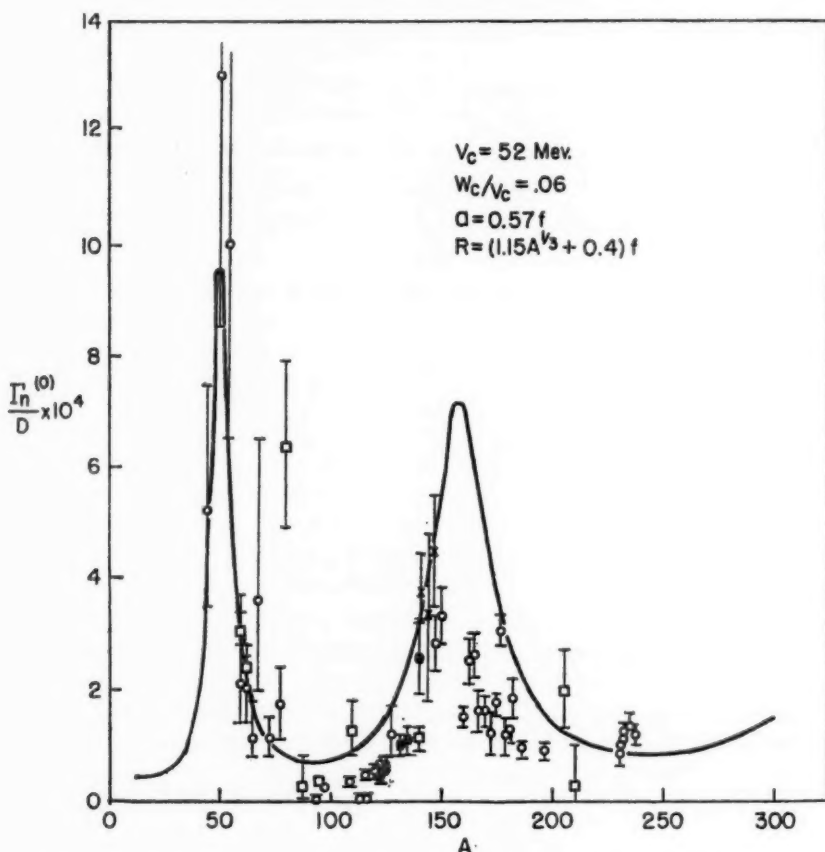
Fig. 1. Ratio $\Gamma_n^{(0)}/D$ of neutron width to level spacing. Here $\Gamma_n^{(0)}/D = (E_0/E)^{1/2}$ (Γ_n/D). The solid curve is taken from Feshbach et al. (105), who employ a potential well V_{WS} with parameters given in the figure.
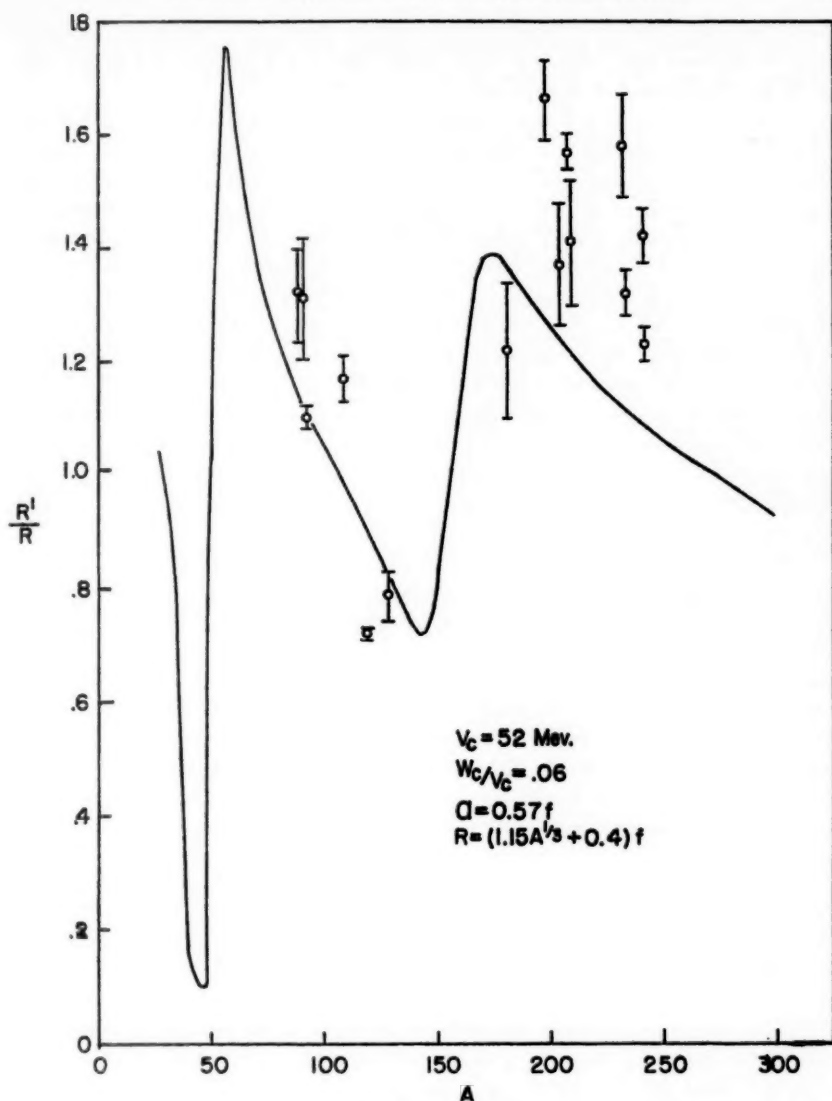
FIG. 2. Ratio of potential scattering length R' to nuclear radius R. The solid curve is taken from Feshbach *et al.* (105), who employ potential well V_{WS} with the parameters given in the figure.

in Figure 2. Increasing a, or equivalently the skin depth, raises the curves. In particular, the valleys between the peaks in Figure 1 do not fall to such small values as a is increased, as is apparent in comparing Figure 1 with the corresponding figure for the square well in (20). It is also clear that in going

from the square well to a tapered well such as the Saxon well it will be neces-
sary to increase the ratio W_0/V_0 in order that the height of the peaks may
be of the right order of magnitude.

In Figures 1 and 2, we compare the calculated $\Gamma_n^{(0)}/D$ and R'/R em-
ploying the parameters in Equation 148 with the experimental values.
(References to experimental work will generally not be given. The appropri-
ate references will be found in the papers under review.) It is apparent that
a qualitative description of these data is provided by the optical potential
but that a quantitative description is still to be achieved. On the positive side,
note that the general description of the $\Gamma_n^{(0)}/D$ curve, a giant resonance
around $A = 55$ and another broader and lower one at $A = 155$ are given cor-
rectly. Moreover, the experimental points around $A = 55$, as well as those
points near $A = 155$, which belong to nuclei near a closed shell (147), fall
fairly close to the predicted values, although it should be mentioned that
the experimental errors for all these points are large. The major discrepancies
are twofold. First, the valley between the two giant resonances is much
deeper than theory predicts. Second, the peak at $A = 155$ is much broader,
lower and generally more irregular than the calculated curve.

Bohr & Mottelson (148) suggested that the asphericity of the target nu-
clei in the region around $A \sim 155$ might be responsible for the second dif-
ficulty. This has since been verified by Margolis & Troubetzkoy (147) by
Drozdov (149) and by Inopin (150) and Vladimirsky & Ilyina (139), who
replaced the spherical square well by a spheroidal square well. More re-
cently, Chase, Wilets & Edmonds (151) employed a spheroidal trapezoidal
well. The general effect of the asphericity is to break the giant resonance up
into a number of resonances, the number increasing with increasing deforma-
tion. It is clear that this, together with the variations in deformation from
nucleus to nucleus, will account for the qualitative features of $\Gamma_n^{(0)}/D$ near
$A = 155$.

No simple explanation for the deep minimum in $\Gamma_n^{(0)}/D$ between $A = 55$
and 155 is as yet available. Note that no such deep minimum exists beyond
the $A = 155$ resonance. McVoy (152) has pointed out that this occurs in part
because these nuclei are still quite aspherical. It might, therefore, be per-
missible to reduce the value of a considerably, improving the fit in the deep
minimum without affecting the fit beyond the $A = 155$ resonance. However,
as will be seen, the value of a in Equation 148 is quite close to the values
obtained from proton-nucleus scattering. The R'/R prediction agrees quite
well with experiment except for the heavier nuclei with $A > 200$. Closer
agreement might be obtained here if the effect of the deformation of these
nuclei were evaluated.

Giant resonance phenomena should also make their appearance when the
incident particle is a proton. This has been, in fact, observed by Schiffer
et al. (153, 154) in (p, n) reactions. The values of A at which the maxima
occur have been calculated by Margolis & Weisskopf (155), who obtain ex-
cellent agreement with experiment once the difference between the neutron-

nucleus and proton-nucleus interaction arising from the Coulomb forces and the difference in neutron and proton Fermi energies are included. It would be interesting to see whether similar effects exist for other charged incident particles.

5.4. *Optical potential parameters from neutron scattering.*—Let us turn next to neutron scattering experiments for energies less than 14 Mev. Feshbach, Porter & Weisskopf (105), employing the Saxon well, have fitted the total cross section and angular distribution data, as well as the zero energy data discussed above, with the Saxon well employing the parameters of Equation 148. They considered data for which the neutron energy was less than 4 Mev. It was, of course, not possible to obtain a detailed fit. A compromise fit was obtained in which the principal emphasis was put on medium and heavy elements. The fit for light elements was not as good. However, keeping in mind the possible fluctuations of the nuclear parameters away from the best values (Equation 148), a reasonably good fit is obtained except for the behavior of the angular distribution in the D-wave resonance region. This, however, occurs for nuclei which are strongly deformed. Taking the deformation into account may be enough to remove the discrepancy. Finally it should be remembered that compound elastic scattering is at a maximum in this energy region.

Schrandt, Beyster, Walt & Salmi (103, 104) have looked at the data up to 14 Mev and have fitted it for each element (26 in all) and at each energy with a Saxon well. They find the following average values:

$$\text{nuclear radius} = (1.17\ A^{1/3} + 0.79)\ \text{f. all elements}$$
$$= (1.21\ A^{1/3} + 0.56)\ \text{f. elements heavier than Zr}$$

$a = 0.36$ f.		light elements
$= 0.50$ f.		heavy elements
$V_0 = 47$ Mev		low energy
$= 44$ Mev		14 Mev

These authors find that the ratio W_c/V_c for $E > 4$ Mev is not a constant over the periodic system, but that it decreases linearly with nuclear radius. For example, at 14 Mev and Fe this ratio is 0.20, while for Bi it is (0.075). This result suggests that the absorption should be limited to the surface region. That is, if it were so limited, the strength of the complex potential would be more independent of nuclear radius. The ratio W_c/V_c is also energy-dependent increasing by a factor of from two to three in going from 0 and 14 Mev. The principal failure of the above fit is in the angular distribution at the back angles. The calculations fitted the experimental first and second maxima and minima in the forward direction. But the calculated curves have much too much structure in the back angles.

Let us turn next to potentials which put the absorption on the surface. Such potentials have been employed by Bjorklund, Fernbach & Sherman (114) and Emmerich & Amster (115, 116), who used V_{GS} and V_{DS} (see Table IA), respectively. Emmerich and Amster obtain the results shown in Table

III. The other authors find $V_c = 40.3$ Mev, $a = 0.6$ f., $R = 1.2A^{1/3} + 0.64$ f., $W_0 = 8$ Mev, $b = 0.98$ f. Both sets of authors obtain poor agreement at back angles.

TABLE III

PARAMETERS FOR DERIVATIVE SURFACE ABSORPTION (116)

$V_c = 43$ Mev independent of A
$\bar{R} = R + 1.36a = (1.25A^{1/3} + 0.5)$ f.
$a = 0.84$ f.; $A < 150$
$a = 0.90$ f.; $A > 150$

	Values of W_c/V_c		
a		Energy	
	0	4	14 Mev
0.84 f.	0.35	0.40	0.45
0.90 f.	0.30	0.35	0.40

None of these potentials so far involve spin-orbit forces. To some extent, this might be considered permissible since the spin-orbit potentials are not large as will be seen. However, neutron polarization in scattering by nuclei can only be explained by spin-orbit potentials. Use of the latter is also suggested by the failure of the simpler potentials to predict back-angle scattering. With spin-orbit forces, the diffraction oscillations in the angular distribution have smaller amplitudes.

The simplest type of spin-orbit force $V_{\text{sq}}^{(\text{so})}$ was used by Thomas, who added on to the square well central force of (156) a surface spin-orbit force proportional to $\delta(r - R)$. These calculations of Thomas are reported by Zucker (120) and by Clement et al. (121). Polarization is found at the appropriate energy and mass number. In this case, the giant P-wave resonance is involved. Qualitative agreement is obtained with a $W_c/V_c = 0.03$ and $V_{\text{so}} = 5$ Mev. Tapered wells have been considered by Gulia (129) and by Culler, Fernbach & Sherman (112).

The most elaborate and most successful calculation so far has been that of Bjorklund & Fernbach (122), who employ $V_{\text{BF}}^{(\text{so})}$ which contains both surface absorption and the (L.H.) Thomas type of spin-orbit term. Their surface parameters are obtained from the data at 14 Mev; the remaining parameters vary with energy. Their results are given in Table IV. These potentials give a good fit to nearly all the data for 4.1, 7, and 14 Mev neutrons. Note the energy variation of the parameters, both V_c and V_{so} decreasing with increasing energy, W_c increasing. It is also noteworthy that Bjorklund and Fernbach's result at 4.1 Mev seems to be in rough agreement with that of (105) quoted in Equation 148. The polarizations predicted by

TABLE IV

PARAMETERS FOR BJORKLUND-FERNBACH POTENTIAL (122)

$$R = 1.25A^{1/3} \text{ f.}$$
$$b = 0.98 \text{ f.}$$
$$a = 0.65 \text{ f.}$$

E (Mev)	V_c (Mev)	W_e (Mev)	V_{so} (Mev)
4.1	50	7	9.5
7	45.5	9.5	8.6
14	44	11	8.3

these potentials are large. A severe test of their validity will be possible when more polarization data in this energy range becomes available.

5.5. *Optical potential parameters from proton scattering.*—Let us turn now to the optical model analysis as it has been applied to elastic proton scattering at proton energies of approximately 10, 17, 30, 40, and 90 Mev. Exact phase shift calculations employing the Saxon well or the essentially equivalent Hill and Ford potential (no spin-orbit term) have been performed by Saxon and co-workers in a series of papers and by Glassgold and co-workers. Their summaries of the average values of the parameters are given in the Tables V and VI. For the parameters for specific elements and energies, the reader is referred to the original papers. The average deviation is given when

TABLE V

PARAMETERS FOR SAXON POTENTIAL ACCORDING TO SAXON *et al.* (99)

$$R = 1.33A^{1/3} \text{ f.}$$

E (Mev)	V_c (Mev)	W_e (Mev)	a (fermi)
17	47	8.5	0.49
31.5	35.5	15.5	0.53

TABLE VI

PARAMETERS FOR SAXON POTENTIAL ACCORDING TO GLASSGOLD *et al.* (102, 106)

$$R = 1.3A^{1/3} \text{ f.}$$

E (Mev)	V_c (Mev)	W_e (Mev)	a (fermi)
10	53	7	0.50
17	50	8	0.50
40	36	15 ± 5	0.66 ± 0.1
95	26	10 ± 5	0.66 ± 0.1

this is large. The fits to the angular distribution were made without adding
the correction coming from compound elastic scattering. Presumably, it is
small at energies greater than 10 Mev. At lower energies, 5.25 and 7.5 Mev,
important effects of compound elastic scattering seem to be noticeable at
back angles according to Wall & Waldorf (144). In general, although not for
all elements, the theoretical curves for the angular distribution oscillate too
rapidly in the back direction. This effect is most serious for the lighter ele-
ments. However, this discrepancy may be removed once spin-orbit forces
are added to the optical potential. At 10 Mev, compound elastic effects may
be important. Some tests were made by Glassgold & Kellogg (101) on the
form of the potential by employing the wine bottle potential, V_{WB}. They
found that the best agreement for the scattering of 14 Mev protons from
carbon is obtained if no significant central elevation or depression in the
potential is allowed. The differences between Table V and Table VI indicate
the latitude in choosing best parameters. It is very significant that here, as
in the neutron case, the value of V_c is roughly independent of A.

5.6. *Optical potential parameters from high-energy experiments.*—Finally,
let us turn to the high-energy data, i.e., to data for which the incident
neutron or proton has an energy greater than about 100 Mev. In this energy
range, it may be expected that the Watson-Riesenfeld (33) multiple scatter-
ing analysis will hold for sufficiently small angles of scattering. Here, as
Bethe (66) points out, the multiple scattering theory gives the matrix ele-
ments of the effective potential in momentum space, so that for the under-
standing of high-energy nucleon-nucleus elastic scattering it is not necessary
to construct the potential in ordinary space. For the purpose of this review,
it is, however, important to discuss the implication of the Watson-Riesenfeld
analysis for the optical potential. These results have already been stated
in Equation 79. But now let us remark with McManus & Thaler (82) that,
if the use of these formulae is limited to small-angle scattering, $q \simeq q'$, then,
according to Equation 74, the potential integrated over the volume is de-
termined if only $q = q'$ terms are kept; if terms up to second order in $q - q'$
are retained, then $\overline{R^2}$ is determined. Higher moments are determined if
higher powers of $q - q'$ enter. But this implies both validity of the multiple
scattering analysis for larger angles of scattering as well as accurate measure-
ments at these angles. Neither of these requirements is generally met. From
the point of view of the optical model, it seems appropriate in this energy
range to consider only the integrated potential and the mean of the square
of the radius. More specifically, if V is given by Equation 139, one is inter-
ested in the parameters

$$I(V^{(o)}) \equiv \int [V_o\rho_o + iW_o\rho_o']d\mathbf{r} \text{ etc.} \qquad \qquad \text{149a.}$$

and

$$I(V^{(o)})\overline{R^2}(V^{(o)}) \equiv \int r^2[V_o\rho_o + iW_o\rho_o']d\mathbf{r} \text{ etc.} \qquad \qquad \text{149b.}$$

These parameters can be related to the parameters describing the phenomenological optical potentials. For example, using a Saxon well V_{WS} for $V^{(c)}$ it is found

$$I(V^{(c)}) \simeq \frac{4\pi}{3} R^3 [V_0 + iW_0] \left[1 + \left(\frac{\pi a}{R}\right)^2 \right] \qquad 150.$$

and

$$\overline{R^2}(V^{(c)}) \simeq \frac{3}{5} R^2 \left[1 + \frac{10\pi^2}{3} \left(\frac{a}{R}\right) + \frac{7\pi^4}{3} \left(\frac{a}{R}\right)^4 \right] \Big/ \left[1 + \left(\frac{\pi a}{R}\right)^2 \right]. \qquad 151.$$

If the spin-orbit term is in the Thomas form

$$-V_{so} \left(\frac{\hbar}{\mu c}\right)^2 \frac{1}{r} \frac{d\rho}{dr} \boldsymbol{\sigma} \cdot \boldsymbol{L}$$

then

$$-4\pi V_{so} \left(\frac{\hbar}{\mu c}\right)^2 \int \frac{1}{r} \frac{d\rho}{dr} r^2 dr \equiv I(V^{(so)}) \simeq 4\pi \left(\frac{\hbar}{\mu c}\right)^2 R V_{so} \qquad 152.$$

and

$$\overline{R^2}(V^{(so)}) \simeq R^2 \left[1 + \left(\frac{\pi a}{R}\right)^2 \right]. \qquad 153.$$

The square well limit is obtained by placing a equal to zero.

Let us turn now to the optical model analyses which have been made. For additional remarks, see the review paper on polarization by Wolfenstein (157) and the papers by Bethe (66) and Peaslee (158). The data usually considered are the total cross section, the angular distribution reaction cross section and polarization data, if available. Experiments with protons as the incident particles are more revealing because of interference with the Coulomb field. For example, Wilson (127) and Fernbach, Heckrotte & Lepore (69) show that the polarization produced by nuclear scattering is opposite to that produced by the Coulomb field interaction with magnetic moment of the nucleon. Except for one case (125), all of the realistic optical model calculations employ some generalization of the WKB method. These approximations should be valid for small angles of scattering.

The first analysis of high-energy neutron data, 50–300 Mev, was performed by Taylor (84), who employed a square well. Since he had only total cross sections available, he assumed that the potentials were the same for all nuclei, permitting a determination of both the nuclear radius and the potential. Mandl & Skyrme (85) performed an analysis of the data up to 160 Mev, employing a variational technique. Wilson (93) combined total cross sections and angular distribution data, using a trapezoidal well except for carbon, where he employed a Saxon well. These calculations have been recently redone by Riese (97) using a more accurate version of the WKB method and the potential V_{PT} (see Table IA). His results are given in Table VII. Riese uses a surface thickness which corresponds to a Saxon parameter

TABLE VII

PARAMETERS FOR PARABOLIC TAPERED WELL (NEUTRONS) (97)*

Element	Energy: 84 Mev				Energy: 136 Mev				Energy: 290 Mev			
	V_e (Mev)	W_e (Mev)	R_M (f.)	$\langle R \rangle$ (f.)	V_e (Mev)	W_e (Mev)	R_M (f.)	$\langle R \rangle$ (f.)	V_e (Mev)	W_e (Mev)	R_M (f.)	$\langle R \rangle$ (f.)
Li					20.3	9.6	2.27	3.4				
Be					21.8	11.6	2.38	3.53				
C					21.6	11.2	2.7	3.77	16.2	17.6	2.54	3.65
N					22.2	9.41	2.89	3.92				
O					21	8	3.15	4.1				
Al	28.8	12.5	3.75	4.65	17.7	10.4	3.8	4.68	13.1	11.0	3.91	4.78
Cu	36	13.9	4.83	5.6	14.0	9.6	5.39	6.1	12.1	16.4	4.81	5.61
Cd					16.7	9.8	6.18	6.85				
Pb					14.4	10.5	7.69	8.2	9.46	7.7	8.19	8.75

* The author has been informed by R. Wilson that the data on which the 290 Mev analysis is based may have a considerably larger error than was originally suspected.

a of 0.68. His average results are given in Table VII. The parameter R_M is the value of the radius at which the potential falls to half of its value at the origin. $\langle R \rangle$ equals $5/3 \ \overline{R}^2$. This parameter and the volume integral of the potential are the only significant parameters which can be determined from experiment (97). The error in these determinations because of experimental error is of the order of 10 per cent at 136 Mev and of 20 per cent at 84 and 290 Mev.

Table VII agrees quite well with those of Wilson, if one takes into account his value of $a = 0.39$ f. There is a reasonably good join with Glassgold and Kellogg's proton scattering values. The value of the nuclear radius is reasonably independent of the energy. For the light elements, $R = 1.2 \ A^{1/3}$ f. while for the heavy ones $R = 1.3 \ A^{1/3}$ f.

An analysis of the proton data including polarization for C and Al has been made at 130 and 310 Mev by Sternheimer (124) using the Saxon well plus the WKB method. Bjorklund, Blandford & Fernbach (125) working at 310 Mev with a variety of target elements varying in mass number from C to Pb, and using a Saxon well, have made an exact phase shift analysis. [See also Fernbach, Heckrotte & Lepore (69).] Bethe (66) considers the 310 Mev protons on Co, using a small angle approximation as well as the approximation that the spin-orbit potential can be treated as a perturbation. Bethe uses both the square and Gaussian well shapes. The results are given in Table VIII. Nedzel (88), considering 410 Mev protons, finds that roughly $V_e = 0$.

Let us compare these results with those obtained by the multiple scattering results of Riesenfeld & Watson (33). The approximations made are described in Section 2. These calculations have been recently carried out by Bethe (66), Kerman, McManus & Thaler (64) and Ohnuma (159). The nucleon-nucleon data employed include the Gammel-Thaler phase shifts, which provide a description of nucleon-nucleon scattering at 300 Mev and below. Ohnuma (159) also calculates the optical potential using the Sig-

TABLE VIII

PARAMETERS FOR OPTICAL POTENTIAL FOR PROTON SCATTERING

Energy (Mev)	Element	Potential	r_0^*	a (f.)	V_e (Mev)	W_e (Mev)	V_{so} (Mev)	W_{so} (Mev)	Ref.
130	C	$V_{WS}^{(so)}$	1.23	0.49	15	18	1.38	—	(124)
130	Al	$V_{WS}^{(so)}$	1.23	0.49	15	18	1.05	—	(124)
310	Al	$V_{WS}^{(so)}$	1.07	0.49	16.5	16.5	1.93	—	(124)
310	C to Pb	$V_{WS}^{(so)}$	1.25	0.65	0	16	1.08	−1.3	(125)
310	C	$V_{WS}^{(so)}$	1.20	—	5.7	22	1.76	−0.55	(66)
310	C	$V_{WS}^{(so)}$	1.4	—	0	18	2.50	—	(69)
160	Na to Bi	V_{WS}	1.2	0.57	16	15	—	—	(161)

* $R = r_0 \ A^{1/3}$ f.

nell-Marshak phase shifts which are possible phase shifts below 150 Mev. All these calculations assume $Z = A/2$ which leads to an additional error of order $(1/A)$. (It is, however, a simple matter to take the actual number of neutron and protons into account. This is under calculation by Kerman, McManus, and Thaler.) In Table IX, we list the results of Kerman *et al.*, using the Gammel-Thaler phase shifts. Between 100 and 150 Mev, the Signell-Marshak phase shifts give about the same results except for V_c, which is smaller (20 per cent at 100 Mev) than the values listed in Table IX.

The empirical values obtained from the data in Tables VI and VII are given in Table X.

Before comparing Tables IX and X, the uncertainties in each should be mentioned. In Table IX, beside the $(1/A)$ approximation mentioned earlier, there is also the error arising from the neglect of the Pauli exclusion principle which would act to reduce the imaginary part of $I(V^{(c)})$. The

TABLE IX

INTEGRATED OPTICAL POTENTIAL IN MULTIPLE
SCATTERING APPROXIMATION (64)

Energy (Mev)	$I(V^{(c)})$ (Mev-f.^{3})	$V_{so} + i\,W_{so}$ (Mev)
90	$291 + 213i$	$4.55 - 1.45i$
156	$220 + 175i$	$3.62 - 0.83i$
310	$83 + 202i$	$2.25 - 0.41i$

"frivolous" models indicate that this could be as large as 10 per cent at 300 Mev and 25 per cent at 100 Mev. Glauber (160) has, however, pointed to a compensating effect which tends to reduce these errors. The real part also has other uncertainties in that the expansion of $\mathrm{Re}F_0$ about $|p - p'|$ in Equation 70 has a larger error (i.e., the term in $(p - p')^2$ has a large coefficient) than the error in the expansion of the other terms in Equation 70. To this must be added the uncertainties arising from the impulse and multiple scattering approximations.

On the other hand, the extraction of optical potentials from the data also involves uncertainties coming from the experimental uncertainties. There is, in other words, considerable flexibility in fitting the data, as may be seen directly from the table, in that different authors fit the same data with considerably different potential parameters. Actually, it would be more appropriate to take the optical potentials of Table IX and compute the experimental results directly. This has been done by McManus & Thaler (82) for σ_e (0°), P(polarization)$/\theta$ at small angles, σ_t, and σ_{in} for the three energies of Table IX with carbon as the target nucleus. The fit is excellent. Ohnuma (159) has also looked at the polarization and found that with the Gammel-Thaler phase shifts excellent agreement is obtained out to 10° at 300 Mev, at 95 Mev and fair agreement at 135 and 155 Mev.

TABLE X

EMPIRICAL VALUES OF THE INTEGRATED OPTICAL POTENTIALS

Energy (Mev)	Element	$I(V^{(c)})$ (Mev-f.^{3})	$V_0^{(so)}+iW_0^{(so)}$ (Mev)
84	Al	$295+128i$	—
	Cu	$308+120i$	—
95	C	$356+137i$	—
	Cu	$280+107i$	—
	Ag	$262+101i$	—
130	C	$152+184i$	1.38
	Al	$137+165i$	1.05
136	Li	$240+114i$	—
	Be	$220+118i$	—
	C	$220+119i$	—
	N	$229+97i$	—
	O	$231+90i$	—
	Cu	$162+110i$	—
	Cd	$159+93i$	—
	Pb	$137+102i$	—
160	Pb	$118+111i$	—
290	C	$144+156i$	—
	Al	$153+125i$	—
	Cu	$103+139i$	—
	Pb	$106+87.5i$	—
310	C	$42+163i$	$1.76-.55i$
	C	$203i$	$1.08-1.3i$
	Al	$170i$	$1.08-1.3i$
	Pb	$141i$	$1.08-1.3i$
	Al	$103+103i$	1.93
	C	$208i$	2.50

With these comments in mind, let us compare Table IX and Table X. It can be seen that there is agreement as to order of magnitude and in the qualitative behavior with energy. The errors in both tables are so large that quantitative agreement is as good as could be expected. The empirical imaginary central potential is, however, consistently lower than the theoretical value.

5.7 *Summary*.—This section is concluded with a summary of the qualitative results indicated by the empirical determinations of the optical potential.

(a) Within the errors implicit in the concept of the optical potential, it is possible to describe the interaction of a nucleon with a nucleus in terms of a potential which is insensitive to the mass number. In other words, the concept of an index of refraction for nuclear matter seems to be approximately valid.

(b) The "nuclear radius" (the parameter R in the Saxon well) is about $1.2A^{1/3}$ f. for small A and about $1.3A^{1/3}$ f. for large A.

(c) The real part of the central potential decreases as the energy of the incident nucleon increases. It is about 52 Mev at zero and about 10 Mev or possibly less at 300 Mev.

(d) The imaginary part of the central potential increases as the nucleon energy increases, being about 3 Mev at zero energy and between 10 and 20 Mev at 300 Mev.

(e) The spin-orbit term is confined to the surface of the nucleus.

(f) The magnitude of the spin-orbit term decreases as the energy increases. At 4 Mev (see Table IV) it is 9.5 Mev while at 300 Mev it is of the order of 2 Mev.

(g) At low energies, a difference between the potential seen by an incident neutron and an incident proton has been detected by the difference in the position of the giant resonances for protons and neutrons. The proton potential is, according to Margolis & Weisskopf (155), nine-tenths of the neutron potential. The empirical fits at high energies are not sufficiently accurate to demonstrate any difference.

The author is very much indebted to Thaler, McManus, and Kerman for making their results available before publication and for many enlightening discussions on the high-energy data and theory. He is also indebted to G. E. Brown for some critical comments.

LITERATURE CITED

1. Bethe, H. A., *Phys. Rev.*, **47**, 747 (1935)
2. Beck, G., and Horsely, L. H., *Phys. Rev.*, **47**, 510 (1935)
3. Perrin, F., and Elsasser, W. M., *J. phys radium*, **6**, 195 (1935)
4. Amaldi, E., D'Agostino, O., Fermi, E., Pontecorvo, B., Rasetti, F., and Segrè, E., *Proc. Roy. Soc. (London)*, A149, 522 (1935)
5. Bjerge, T., and Westcott, C. H., *Proc. Roy. Soc. (London)*, A150, 709 (1935)
6. Moon, P. B., and Tillman, J. R., *Nature*, **135**, 904 (1935); **136**, 66 (1935); *Proc. Roy. Soc. (London)*, A153, 476 (1936)
7. Bohr, N., *Nature* **137**, 344 (1936)
7a. Breit, G., and Wigner, E., *Phys. Rev.*, **49**, 519 (1936)
8. Ostrofsky, Breit, and Johnson, *Phys. Rev.*, **49**, 22 (1936)
9. Bethe, H. A., *Phys. Rev.*, **57**, 1125 (1940)
10. Serber, R., *Phys. Rev.*, **72**, 1114 (1947)
11. Goldberger, M. L., *Phys. Rev.*, **74**, 1269 (1948)
12. Fernbach, S., Serber, R., and Taylor, T. B., *Phys. Rev.*, **75**, 1352 (1949)
13. Bethe, H. A., and Wilson, R. R., *Phys. Rev.*, **83**, 690 (1951)
14. Byfield, H., Kessler, J., and Lederman, L. M., *Phys. Rev.*, **86**, 17 (1952)

15. Bethe, H. A., *Revs. Modern Phys.*, **9,** 69 (1937)
16. Ford, K. W., and Bohm, D., *Phys. Rev.*, **79,** 745 (1950)
17. Feshbach, H., and Weisskopf, V. F., *Phys. Rev.*, **76,** 1550 (1949)
18. LeLevier, R. E., and Saxon, D. S., *Phys. Rev.*, **87,** 40 (1952)
19. Barschall, H. H., *Phys. Rev.*, **86,** 431 (1952)
19a. Walt, M., and Barschall, H. H., *Phys. Rev.*, **93,** 1062 (1954)
20. Feshbach, H., Porter, C., and Weisskopf, V. F., *Phys. Rev.*, **96,** 448 (1954)
20a. Adair, R. K., *Phys. Rev.*, **94,** 737 (1954)
21. Walt, M., and Beyster, J. R., *Phys. Rev.*, **98,** 677 (1955)
22. Kawai, M., and Ui, H., *Progr. Theoret. Phys. (Kyoto)*, **14,** 263 (1955)
23. Burge, E. J., Fujimoto, Y., and Hossain, A., *Phil. Mag.*, **1,** 19 (1956)
24. Kawai, M., Nagasaki, M., Soga, M., Terasawa, T., Ui, H., Wada, Y., *Progr. Theoret. Phys. (Kyoto)*, **18,** 66 (1957)
25. Chase, D. M., and Rohrlich, F., *Phys. Rev.*, **94,** 81 (1954)
26. Burkig, J. W., and Wright, B. T., *Phys. Rev.*, **82,** 451 (1951)
27. Gugelot, P. C., *Phys. Rev.*, **87,** 525 (1952)
28. Cohen, B. L., and Neidigh, R. V., *Phys. Rev.*, **93,** 282 (1954)
29. Woods, R. D., and Saxon, D. S., *Phys. Rev.*, **95,** 577 (1954)
30. Watson, K. M., *Phys. Rev.*, **89,** 575 (1953)
31. Francis, N. C., and Watson, K. M., *Phys. Rev.*, **92,** 291 (1953)
32. Takeda, G., and Watson, K. M., *Phys. Rev.*, **94,** 1087 (1954); **97,** 1336 (1955)
33. Riesenfeld, W. B., and Watson, K. M., *Phys. Rev.*, **102,** 1157 (1956)
34. Watson, K. M., *Phys. Rev.*, **105,** 1388 (1957)
35. Thomas, R. G., *Phys. Rev.*, **97,** 224 (1955)
36. Friedman, F. L., and Weisskopf, V. F., *Niels Bohr and the Development of Physics*, 134 (Pergamon Press, London, Engl., 195 pp., 1955)
37. Brueckner, K. A., Eden, R. J., and Francis, N. C., *Phys. Rev.*, **100,** 891 (1955)
38. Kind, A., and Patergnani, G., *Nuovo cimento*, **10,** 1375 (1953)
39. Lane, A. M., and Wandel, C. F., *Phys. Rev.*, **98,** 1524 (1955)
40, Kind, A., and Villi, C., *Nuovo cimento*, **1,** 749 (1955)
41. Clementel, E., and Villi, C., *Nuovo cimento*, **2,** 176 (1956)
42. Kind, A., and Jess, L., *Nuovo cimento*, **4,** 595 (1956)
43. Kind, A., *Nuovo cimento*, **5,** 318 (1957)
44. Kind, A., and Jess, L., *Nuovo cimento*, **5,** 1020 (1957)
45. Mott, N. F., and Massey, H. S. W., *The Theory of Atomic Collisions*, 2nd ed. (Oxford University Press, New York, N.Y., 388 pp., 1949)
46. Low, F., in Feshbach, H., *Ann. Phys. (N.Y.)* (To be published)
47. Feshbach, H., *Ann. Phys. (N.Y.)* (To be published)
48. Frahn, W. E., *Nuovo cimento*, **4,** 313 (1956); **5,** 393 (1957)
49. Frahn, W. E., and Lemmer, R. H., *Nuovo cimento*, **5,** 523, 1564 (1957)
50. Brueckner, K. A., Levinson, C. A., and Mahmoud, H. M., *Phys. Rev.*, **95,** 217 (1954)
51. Brueckner, K. A., *Phys. Rev.*, **96,** 508 (1954)
52. Brueckner, K. A., *Phys. Rev.*, **98,** 769 (1955)
53. Lax, M., *Rev., Modern Phys.*, **23,** 287 (1951)
54. Foldy, L. L., *Phys. Rev.*, **67,** 107 (1945)
55. Lippman, B., and Schwinger, J., *Phys. Rev.*, **79,** 469 (1950)
56. Chew, G. F., and Wick, G. C., *Phys. Rev.*, **85,** 636 (1952)
57. Ashkin, J., and Wick, G. C., *Phys. Rev.*, **85,** 686 (1952)

58. Chew, G. F., and Goldberger, M. L., *Phys. Rev.*, **87,** 778 (1952)
59. Chew, G. F., *Phys. Rev.*, **80,** 196 (1950)
60. Lax, M., and Feshbach, H., *Phys. Rev.*, **81,** 189 (1951); **88,** 509 (1952)
61. Fernbach, S., Green, T. A., and Watson, K. M., *Phys. Rev.*, **82,** 980 (1951)
62. Chew, G. F., and Lewis, H., *Phys. Rev.*, **84,** 779 (1951)
63. Fujimoto, Y., and Yamaguchi, Y., *Progr. Theoret. Phys. (Kyoto),* **6,** 166 (1957)
64. Kerman, A., McManus, R. M., and Thaler, H., *Ann. Phys. (N. Y.)* (To be published)
65. Watson, K., *Stanford Univ. Conf. on Nuclear Sizes* (Stanford, California, 1957)
66. Bethe, H. A., *Ann. Phys. (N. Y.),* **3,** 190 (1958)
67. Gammel, J. L., and Thaler, R. M., *Phys. Rev.*, **107,** 291, 1337 (1957)
68. Clementel, E., *Nuovo cimento,* **1,** 509 (1955)
69. Fernrotte, S., Heckrotte, W., and Lepore, J. V., *Phys. Rev.*, **97,** 1059 (1955)
70. Tamor, S., *Phys. Rev.*, **97,** 1077 (1955)
71. Kapur, P. I., and Peierls, R., *Proc. Roy. Soc. (London),* A**166,** 277 (1937)
72. Morse, P. M., and Feshbach, H., *Methods of Theoretical Physics,* Chap. 7 (McGraw-Hill Book Co., New York, N.Y., **1978** pp., 1953)
73. Bowcock, J., *Proc. Phys. Soc. (London),* A**70,** 515 (1957)
74. Brown, G. E., and Dominicis, C. T., *Proc. Phys. Soc. (London),* A**70,** 668 (1957)
75. Wigner, E. P., *Science,* **120,** 790 (1954)
76. Scott, J. M. C., *Phil. Mag.*, **45,** 441, 751, 1322 (1954)
77. Lane, A. M., Thomas, R. G., and Wigner, E. P., *Phys. Rev.*, **98,** 18 (1955)
78. Bloch, C., *J. phys. radium,* **17,** 510 (1956)
78a. Bloch, C., *Nuclear Phys.,* **3,** 137 (1957)
78b. Wigner, E. P., *Ann. Math.*, **62,** 548 (1955)
79. Agronovich, V. M., and Davydov, A. S., *Zhur. Eksptl. i teoret. Fiz.*, **32,** 1249 (1957)
80. Vogt, E., *Phys. Rev.*, **101,** 1792 (1956)
81. Vogt, E., and Lascoux, J., *Phys. Rev.*, **107,** 1028 (1957)
82. McManus, H., and Thaler, R. M., *Phys. Rev.* (In press)
83. Bratenahl, A., Fernbach, S., Hildebrand, R. H., Leith, C. E., Moyer, B. J., *Phys. Rev.*, **77,** 597 (1950)
84. Taylor, T. B., *Phys. Rev.*, **92,** 831 (1953)
85. Mandl, F., and Skyrme, T. H., *Phil. Mag.*, **44,** 1028 (1954)
86. Gomes, L. C., and Lopes, J. L., *Nuovo cimento,* **1,** 792 (1955)
87. Heckrotte, W., *Phys. Rev.*, **94,** 1797 (1954)
88. Nedzel, V. A., *Phys. Rev.*, **94,** 174 (1954)
89. Cassels, J. M., and Lawson, J. D., *Proc. Phys. Soc. (London),* A**67,** 135 (1954)
90. Darden, S. E., Perkins, R. B., and Walton, R. B., *Phys. Rev.*, **100,** 1315 (1955)
91. Fujimoto, Y., and Hossain, A., *Phil. Mag.*, **46,** 542 (1955)
92. Culler, V., and Waniek, R. W., *Phys. Rev.*, **99,** 740 (1955)
93. Wilson, R., *Phil. Mag.*, **1,** 1013 (1956)
94. Voss, R. G., and Wilson, R., *Proc. Roy. Soc. (London),* A**236,** 52 (1956)
95. Elliot, J. O., *Phys. Rev.*, **101,** 684 (1956)
96. Ghoshal, S. N., and Baliza, B. B., *Progr. Theoret. Phys. (Kyoto),* **17,** 556 (1957)
97. Riese, J., *Optical Model Analysis of Neutron-Nucleus Scattering* (Doctoral thesis, Massachusetts Institute of Technology, Cambridge, Mass., 1958)
98. Melkanoff, M. A., Moszkowski, S. A., Nodvik, J., and Saxon, D. S., *Phys. Rev.*, **101,** 507 (1956)

99. Melkanoff, M. A., Nodvik, J., Saxon, D. S., and Woods, R. D., *Phys. Rev.*, **106**, 793 (1957)

100. Glassgold, A. E., Cheston, W. B., Stein, M. L., Schuldt, S. B., and Erickson, G. W., *Phys. Rev.*, **106**, 1207 (1957)

101. Glassgold, A. E., and Kellogg, P. J., *Phys. Rev.*, **107**, 1372 (1957)

102. Glassgold, A. E., and Kellogg, P. J., *Phys. Rev.*, **109**, 1291 (1958)

103. Beyster, J. R., Walt, M., and Salmi, E. W., *Phys. Rev.*, **104**, 1319 (1956)

104. Schrandt, Beyster, J. R., Walt, M., and Salmi, E. W. (Unpublished L.A. report 2099, 1957)

105. Feshbach, H., Porter, C., and Weisskopf, V. F. (Unpublished)

106. Glassgold, A. E., *Revs. Modern Phys.*, **30**, 419 (1958)

107. Jankovic, Z., *Phil. Mag.*, **46**, 376 (1955)

108. Mohr, C. B. O., *Proc. Phys. Soc. (London)*, **A68**, 340 (1955)

109. Mohr, C. B. O., and Robson, B. A., *Proc. Phys. Soc. (London)*, **A69**, 365 (1956)

110. Nemirovskii, P. E., *Proc. Intern. Conf. Peaceful Uses Atomic Energy, United Nations, August, 1955*, **2**, 86 (1956); *Zhur. Eksptl. i Teoret, Fiz.*, **30**, 551 (1956); **32**, 1143 (1957)

111. Kikuchi, K., *Progr. Theoret. Phys. (Kyoto)*, **17**, 643 (1957)

112. Culler, G., Fernbach, S., and Sherman, N., *Phys. Rev.*, **101**, 1047 (1956)

113. Amster, H. J., *Phys. Rev.*, **104**, 1606 (1956)

114. Bjorklund, F. E., Fernbach, S., and Sherman, N., *Phys. Rev.*, **101**, 1832 (1956)

115. Emmerich, W. S., and Amster, H. J., *Physica*, **22**, 1163 (1956)

116. Emmerich, W. S., *Westinghouse Research Laboratory Report, 60-94511-6-R17* (Unpublished data)

117. Emmerich, W. S., in *Fast Neutron Physics* (Interscience Publishers, New York, N. Y., in press, 1959)

118. Kohler, H. S., *Nuovo cimento*, **2**, 911 (1955); *Nuclear Phys.*, **1**, 433 (1956)

119. Ozaki, A., *Phys. Rev.*, **99**, 55 (1955)

120. Zucker, M. S., *Phys. Rev.*, **104**, 1025 (1956)

121. Clement, J. D., Boreli, F., Darden, S. E., Haberli, W., and Striebel, H. R., *Nuclear Phys.*, **6**, 177 (1958)

122. Bjorklund, F. E., and Fernbach, S., *Phys. Rev.*, **109**, 1295 (1958)

123. Bjorklund, F. E., in McCormac, B. M., Steuer, M. F., Bond, C. D., and Hereford, F. L., *Phys. Rev.*, **108**, 116 (1957)

124. Sternheimer, R. M., *Phys. Rev.*, **97**, 1319 (1955); **100**, 886 (1955)

125. Bjorklund, F. E., Blandford, I., and Fernbach, S., *Phys. Rev.*, **108**, 795 (1957)

126. Adair, R. K., Darden, S. E., Fields, R. E., *Phys. Rev.*, **96**, 503 (1954)

127. Wilson, R., *Phil. Mag.*, **46**, 769 (1955)

128. Remund, A., *Helv. Phys. Acta*, **29**, 545 (1956)

129. Gulia, N. A., *Zhur. Eksptl. i. Teoret. Fiz.*, **31**, 144 (1956)

130. Peaslee, D. C., *Nuclear Phys.*, **3**, 255 (1957)

131. Schwinger, J., *Phys. Rev.*, **73**, 407 (1948)

132. Baz, A. F., *Zhur. Eksptl. i Tearet. Fiz.*, **31**, 159 (1957)

133. Barashenkov, V. S., Stakhanov, I. P., and Alekandrov, yu. A., *Zhur. Eksptl. i Teoret. Fiz.*, **32**, 154 (1957)

134. Eriksson, T., *Nuclear Phys.*, **2**, 91 (1956)

135. Sample, J. T., *Can. J. Phys.*, **34**, 36 (1956)

136. Bethe, H. A. (Private communication)

137. Fermi, E., *Nuovo cimento*, **11**, 407 (1954)

138. Malenka, B. J., *Phys. Rev.*, **95**, 522 (1954)
139. Vladimirsky, V. V., and Ilyina, I. I., *Nuclear Phys.*, **6**, 295 (1958)
140. Gribov, V. N., *Zhur. Eksptl. i. Teoret. Fiz.*, **32**, 647 (1957)
141. Levintov, I. I., *Doklady Akad. Nauk* S.S.S.R., **98**, 373 (1955); **107**, 240 (1952)
142. Kohler, H. S., *Nuclear Phys.*, **6**, 161 (1958)
143. Emmerich, W. S., and Sinclair, R. M., *Phys. Rev.*, **104**, 1399 (1956)
144. Wall, N. S., and Waldorf, W. F., *Phys. Rev.*, **107**, 1602 (1957)
145. Lane, A. M., and Lynn, J. E., *Atomic Energy Research Establ. (Gt. Brit.) Rept. T/R 2210* (Unpublished data, 1957)
146. Porter, C. E., *Phys. Rev.*, **100**, 935 (1955)
147. Margolis, B., and Troubetzkoy, E. S., *Phys. Rev.*, **106**, 105 (1957)
148. Barschall, H. H., in *Phys. Rev.*, **96**, 448 (1954)
149. Drozdov, S. I., *Zhur. Eksptl. i Teoret. Fiz.*, **28**, 734 (1955); *Physica*, **22**, 1165 (1956)
150. Inopin, E. V., *Zhur. Eksptl. i Teoret. Fiz.*, **28**, 210 (1955)
151. Chase, D., Wilets, L., and Edmonds, A. (To be published)
152. McVoy, K. (Private communication)
153. Schiffer, J. P., and Lee, L. L., Jr., *Phys. Rev.*, **107**, 640 (1957)
154. Schiffer, J. P., Lee, L. L., Jr., Davis, R. H., and Prosser, F. W., Jr., *Phys. Rev.*, **107**, 547 (1957)
155. Margolis, B., and Weisskopf, V. F., *Phys. Rev.*, **107**, 641 (1957)
156. Thomas, R. G., quoted in Zucker, M. S., *Phys. Rev.*, **99**, 55 (1955) and Clement, J. D., Boreli, F., Darden, S. E., Haberli, W., Striebel, H. R., *Nuclear Phys.*, **6**, 177 (1958)
157. Wolfenstein, L., *Ann. Rev. Nuclear Sci.*, **6**, 43 (1956)
158. Peaslee, D. C., *Ann. Rev. Nuclear Sci.*, **5**, 99 (1955)
159. Ohnuma, S. (To be published)
160. Glauber, R. J., *Physica*, **22**, 1185 (1956)
161. Gerstein, G., and Strauch, K., *Bull. Am. Phys. Soc.*, [II] **3**, 205 (1958)

HYPERFRAGMENTS[1]

By W. F. Fry

Department of Physics, University of Wisconsin, Madison, Wisconsin

INTRODUCTION

The first example of the disintegration of a nuclear fragment containing a bound hyperon, a so-called hyperfragment, was found by Danysz & Pniewski (26) in a plate exposed to cosmic rays. The event, shown in Figure 1, consisted of a nuclear disintegration of 18 shower particles, 21 gray and black prongs, and the track of a nuclear fragment which caused a secondary star. From the thin-down of the nuclear fragment track, it was deduced that the fragment had stopped before producing the secondary star. The kinetic energy of charged particles from the secondary disintegration was found to be 99 Mev. This high-energy release along with the estimate of the moderation time led the authors to postulate that the fragment probably contained a bound Λ hyperon. Shortly after this discovery, many additional examples of hyperfragments were found (1 to 6, 8 to 13, 15, 16, 18, 20, 25, 26, 31, 33, 33a, 35 to 48, 51 to 58, 60, 61a, 62, 63, 65, 66a to 71, 73 to 81, 83). The most conclusive events were the mesonic decays, namely those where a π meson was emitted. In these cases, the total energy release could be measured with considerable precision and was found to be close to the Q-value of the free Λ hyperon decay. Furthermore, the nuclear charge and mass of the fragment could be determined in favorable cases. A typical example is shown in Figures 2 and 3.

IDENTIFICATION OF HYPERFRAGMENTS

Most of the information on hyperfragments has come from studies in nuclear emulsions. Several of the properties of photographic plates are well suited to this study. The two most important are that they permit accurate determinations of energy and charge on particles of low velocity. The relatively high stopping power of emulsion makes it possible to study hyperfragment decays at rest, which is essential for accurate measurements of the binding energy of the hyperon; however, this very characteristic also makes it difficult to determine the lifetime of hyperfragments, a very interesting parameter. Photographic emulsions contain both light and heavy elements in proportions which are essentially fixed. Hyperfragments of a wide variety of elements are formed from the break-up of the heavy elements. On the other hand, studies of particular reactions involving light hyperfragments will in the near future be more conveniently studied in bubble chambers. A program to study hyperfragments, produced in a helium bubble chamber by

[1] The survey of the literature pertaining to this review was concluded in April, 1958.
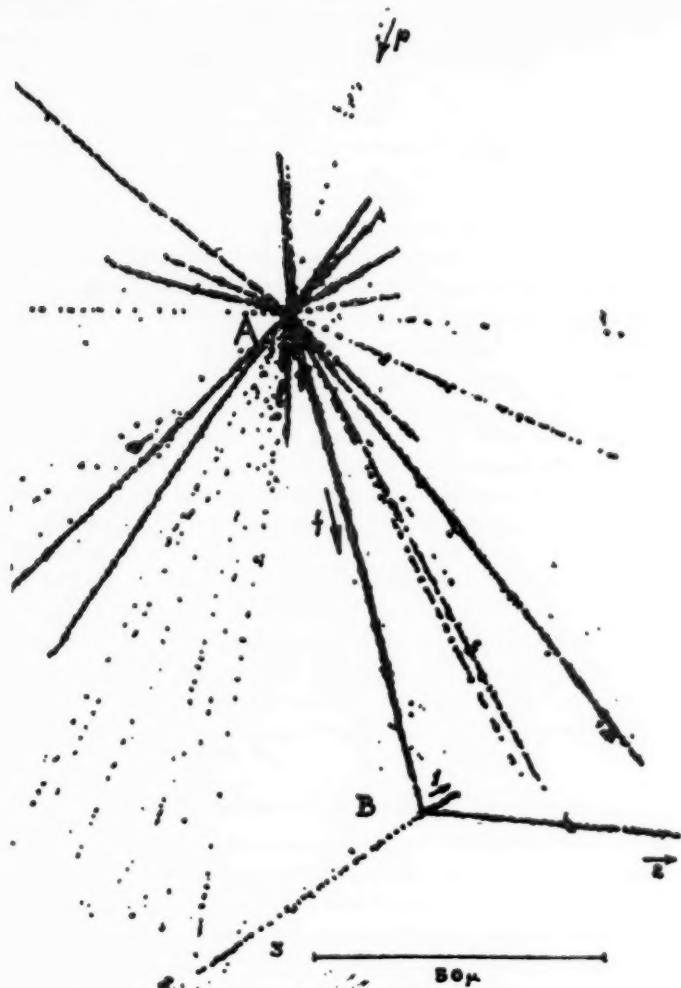
FIG. 1. A photograph of the first hyperfragment found by Danysz & Pniewski (26). The fragment f was produced in star A and decayed nonmesonically at point B into three particles, tracks 1, 2, and 3.

the Duke University, Johns Hopkins University, and Los Alamos Scientific Laboratory groups, is in progress.

A study of the production of hyperfragments can be separated into two basic processes that involve difficulties of recognition and identification which are somewhat different. These are the production by high-energy particles and by the nuclear capture of K^- mesons and Σ^- hyperons. The production by high-energy particles is characterized by a somewhat higher
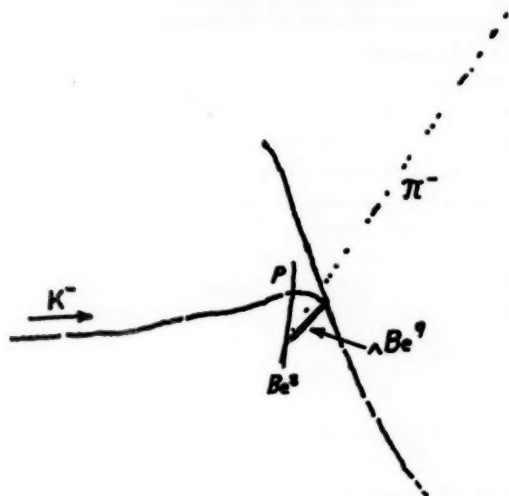
FIG. 2. A tracing of an event which is interpreted as the mesonic decay of $_\Lambda Be^9$ into two α-particles, a proton and a π^- meson (39).

kinetic energy of the fragment and, therefore, more information can be derived from the fragment track. This is especially important in the study of moderately heavy elements $3 \leq Z \leq 8$, where, at best, the range of the fragments is very short. However, the number of events of various types which can be mistaken as hyperfragments is much higher in the case of
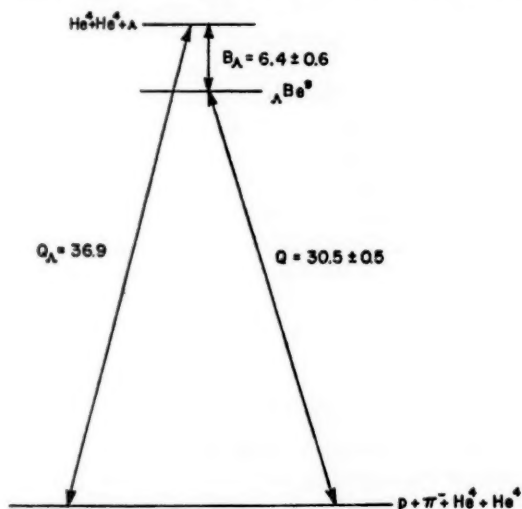
FIG. 3. An energy-level diagram for calculating the binding energy of the Λ hyperon in $_\Lambda Be^9$ (see Fig. 2). Energies are given in Mev.

production by energetic particles as compared to the production by K^- mesons and Σ^- hyperons.

The usual method of scanning for hyperfragments, produced by high-energy particles, is to search for the interaction of the high-energy primary particle and then follow out the secondaries to see if there is a secondary star. In following this procedure, there will be many events which will have the appearance of a hyperfragment decay. In this category are: (a) The production of a very slow negative pion which then produces a secondary star upon absorption in the emulsion; (b) The production of a very slow K^- meson or Σ^- hyperon; (c) Collisions in flight of stable nuclear fragments which lead to break-up of only the fragments; (d) Collisions in flight of stable fragments with subsequent break-up of target nucleus as well as the fragment. The inclusion of negative pions of very low energy is probably the largest contaminant.

The recognition of hyperfragments of charge one and of charge greater than one will be considered separately. For those of charge one, it is necessary to determine the mass by scattering; this demands a minimum track length of about 1 mm. For hyperfragments of charge two or greater, profile measurements permit discrimination against particles of type (a) and (b) for lengths greater than about 20μ in G-5 emulsions. Further, for lengths greater than about 50μ it is possible to detect the existence of a thin-down and, therefore, to verify that the fragment stopped. Sometimes it is possible to show that the fragment stopped by a large amount of scattering very near the end of the track, even though it is shorter than 50μ. Further, it is possible, in some cases, to use the visible energy and charge balance to discriminate against contaminants for processes (c) and (d). Unfortunately, profile measurements have not been used for all hyperfragment studies.

The largest percentage of contaminants arises from double starts with connecting tracks shorter than about 20μ, which are principally caused by very slow negative pions. Recently, a very fine-grade emulsion has been developed by Ilford which permits better discrimination of ionization by width measurements near the end of tracks. To the author's knowledge there are no published results on this emulsion, but a preliminary study by the University of Wisconsin group of double stars in plates exposed to 4 Bev pions has been made. Among double stars with connecting tracks longer than 2μ and shorter than 20μ, ~ 80 per cent were the result of charge greater than one.

PRODUCTION

A systematic study of the general aspects of production of hyperfragments by high-energy particles has been made by the University of Wisconsin group (39, 67), by Castagnoli et al. (15), and by Blau (10). A study of the production by cosmic rays, 3 Bev protons, 6 Bev protons, and 3 Bev pions has been made. The production frequency is tabulated in Table I. The

TABLE I

FREQUENCY OF PRODUCTION OF HYPERFRAGMENTS

Nature of Experiment	Hyperfragments	Hyperfragments $R \geq 15\mu$	Ref.
	Total Stars	Total Stars	
3 Bev π mesons	$72/80,000 = 9 \times 10^{-4}$	$19/80,000 = 2.4 \times 10^{-4}$	39, 67
3 Bev protons	$19/20,000 = 9.5 \times 10^{-4}$ $14/14,480 = 9.7 \times 10^{-4}$	$3/20,000 = 1.5 \times 10^{-4}$ $11/14,480 = 7.6 \times 10^{-4}$	39, 67 10
6 Bev protons	$7/10,000 = 7 \times 10^{-4}$	$3/10,000 = 3 \times 10^{-4}$	39, 67
Cosmic rays	$61/119,000 = 5.1 \times 10^{-4}$	$19/119,000 = 1.6 \times 10^{-4}$ $6/\ 24,000 = 2.5 \times 10^{-4}$	39, 67 15
K^- stars	$46/1,001 = 4.6 \times 10^{-2}$	$9/1,001 = 9 \times 10^{-3}$	39, 67

angle between the hyperfragment and the charged incoming particle is shown in Figure 4. A range distribution of the connecting track of the events which were classified as hyperfragments is shown in Figure 5. About 74 per cent of all the double stars have connecting tracks less than 15 μ (67).
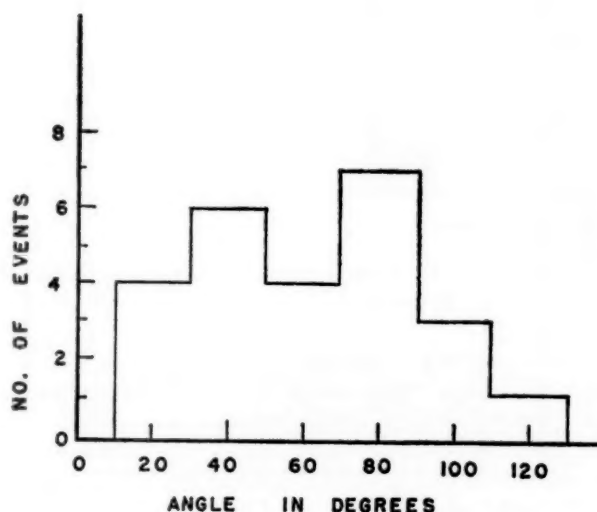
FIG. 4. The angular distribution of the direction of motion of hyperfragments with respect to the direction of the incoming high-energy primary particle (39).
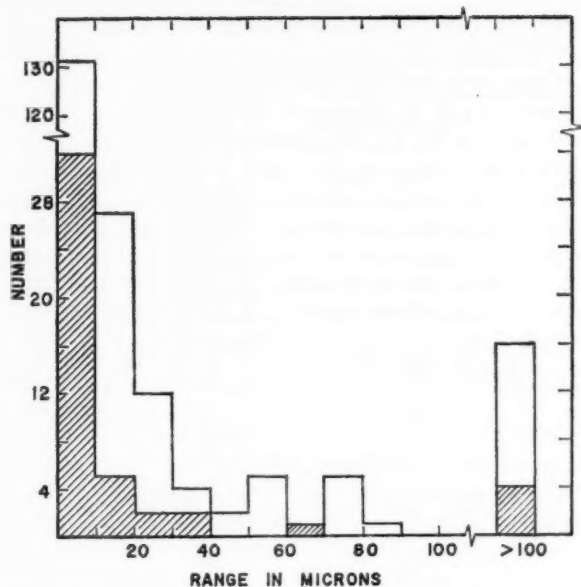
FIG. 5. The distribution in range of hyperfragments. The shaded portion is for hyperfragments produced by K^- absorption at rest (67).
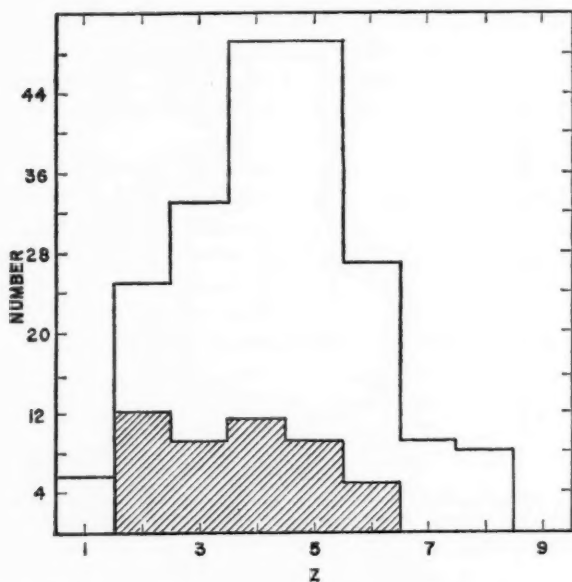
FIG. 6. The charge distribution of hyperfragments. The shaded area represents hyperfragments from K^- stars (67).

An estimate of the charge distribution of the hyperfragments produced
by high energy particles is shown in Figures 6 and 7. In most cases, the
charge of the fragment cannot be determined directly but is taken to be
equal to the total visible charge from the secondary star. In many cases, this
is only the lower limit, as the charge of short tracks from the fragment dis-
integration could not be determined and was assumed to be one. There is a
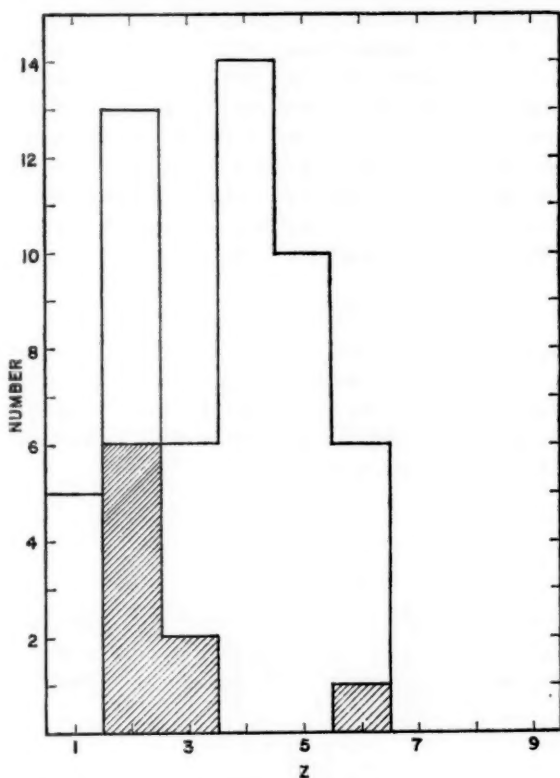
FIG. 7. The charge distribution of hyperfragments whose range is greater than 15 μ.
The shaded area represents hyperfragments from K^- stars (67).

bias against high Z, because many fragment tracks may have been too short
to be recognized. There is also a bias against finding all the hydrogen and
helium hyperfragments caused by the escape of the fragment from the plate
containing the parent star. Only when the two connecting tracks were in
the same plate would the hyperfragment disintegration be recognized as
such. However, the range distribution as shown in Figure 5 would suggest
that this bias is probably not too important. It can be seen that the Λ hyperon
is captured preferentially in moderately heavy fragments even though the

frequency of production of stable light fragments is considerably greater than that of heavy fragments. The energy distribution of Λ hyperons produced by pions of 1.9 Bev has been studied by Slaughter *et al.* (72). These authors find that $\sim$20 per cent of the Λ hyperons which were produced in Fe have an energy below 50 Mev. Using a cross section of 1 mb/nucleon in hydrogen for the production of Λ hyperons by pions of 1.9 Bev, one finds that $\sim$2 per cent of the total inelastic pion interactions lead to a Λ hyperon formation and $\sim$0.4 per cent to Λ hyperons of energy below about 50 Mev. The fraction of pion interactions which produce slow Λ hyperons ($E < 50$ Mev) is comparable with the fraction leading to hyperfragment production, suggesting that the Λ hyperon trapping probability is not very small. The percentage of Λ hyperons, from K^- absorptions in emulsion, which become trapped in hyperfragments of range greater than about 2 μ is 6.6 per cent (40). It is possible that comparable numbers of Λ hyperons from K^- absorptions in emulsion also become trapped in shorter fragments or in the residual nucleus and are not observed.

DECAY MODES

It is found that hyperfragments can decay with the emission of a pion and nucleons, the so-called mesonic decay, or with the emission of only nucleons, the nonmesonic mode. The mesonic decay mode can be thought of as the normal decay of the Λ inside the nucleus without subsequent absorption of the pion (p = proton, n = neutron).

$$\Lambda \rightarrow p + \pi^- + Q_1 \hspace{3cm} 1.$$

or

$$\Lambda \rightarrow n + \pi^0 + Q_2 \hspace{3cm} 2.$$

where $Q_1 = 37.45 \pm 0.17$ Mev (7) and $Q_2 = 40.7$ Mev. Alternatively, hyperfragments can decay without the emission of a pion, which probably corresponds to the interaction with a single nucleon according to the following reactions:

$$\Lambda + p \rightarrow p + n + Q_3 \hspace{3cm} 3.$$
$$\Lambda + n \rightarrow n + n + Q_4. \hspace{3cm} 4.$$

Reaction 3 will be called a proton stimulated decay and reaction 4 a neutron stimulated decay. The ratio R of nonmesonic to mesonic decays was shown to increase rapidly with Z, as was predicted by Cheston & Primakoff (17). In reality, a direct measurement of R is not possible because of the inability to detect the neutral pion mode of decay. Experimentally, one determines

$$R^{(-)} = \text{Nonmesonic decays}/\pi^- \text{ mesonic decays.}$$

It is to be expected that the ratio of charged pion mode to the neutral pion mode of hyperfragments differs by a small amount from that for the free Λ decays, because of the effect of the Pauli principle on the nucleons from the decay in the fragment. The ratio for the free Λ decay is two. Furthermore,

very few decays of the neutral pion mode will be included as nonmesonic decays, since the visible energy in the secondary star is expected to be small and in most cases the event would not have been recognized as a hyper-fragment decay. (A few cases have been reported which can be interpreted as neutral pion decays.) One conclusive event has been reported by Levi-Setti & Slater (56) in which an electron pair was observed (see Fig. 8). Under
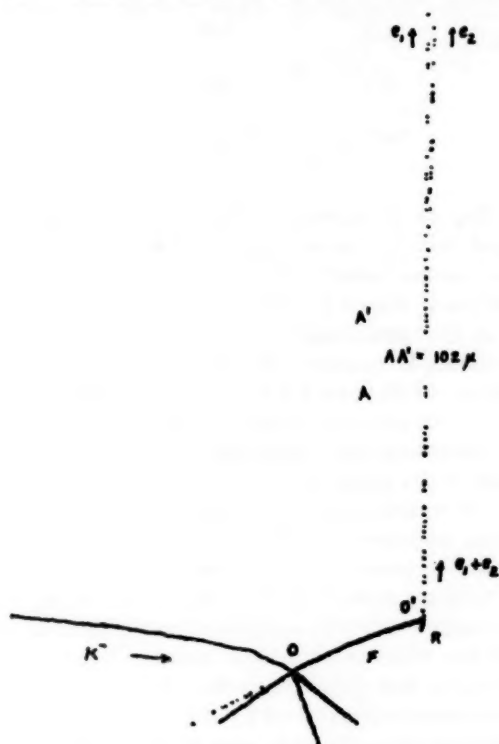
Fig. 8. A tracing of a decay of a $_\Lambda$He fragment into an electron pair, a recoil and one or more neutral particles. The electron pair presumably originated from the alternative decay of a π^0 meson (56).

the assumption above, the ratio R of the nonmesonic to mesonic decays is then $(2/3) R^{(-)}$. Data on the ratio $R^{(-)}$ have been reported by Blau (10), by Castagnoli et al. (15), and by the University of Wisconsin group (67). The data of Blau come from a systematic study of 3 Bev proton interactions and that of Castagnoli et al. from similar studies in plates exposed to cosmic rays. These data are included in Table II.

It is difficult to add the data of the three groups in a simple way because of the difference that may exist in the criteria for selection. In spite of the possible differences that may exist among the data, several important con-

TABLE II

The Ratio $R^{(-)} =$ Non π^- Mesonic Decays/π^- Mesonic Decays

Reference	$Z=1$	$Z=2$	$Z=3$	$Z=3$
Wisconsin (39, 67)	0/6	18/7	31/2	140/2
Blau (10)	1/0	2/0	4/0	6/1
Rome (15)	0/1	0/1		4/0
Average	$1/7=0.14$	$20/8=2.5$	$185/5=37$	

clusions can be derived. It seems clear that the mesonic decay predominates for hydrogen and that the nonmesonic and mesonic rates for helium are comparable. The predominance of the nonmesonic decay mode in fragments heavier than helium is shown by the data. Fowler (30) has shown that the rapid increase in the percentage of nonmesonic decays with increase in atomic number cannot be explained by the absorption of a real pion, emitted in the mesonic decay of the bound Λ hyperon. This agrees with the argument previously made by Cheston & Primakoff (17) that the nonmesonic decays result from the absorption of a virtual pion in the decay process.

From elementary considerations, it is to be expected that the nonmesonic to mesonic ratio R would rapidly increase with increasing atomic number. The overlap of the wavefunction of the Λ hyperon with that of the nucleons would be expected to increase rapidly with mass number because of the increase in the binding energy of the Λ hyperon and correspondingly decreased volume occupied by the Λ hyperon wavefunction and also because of the increase in the number of nucleons and the volume occupied by them. Ruderman & Karplus (66) pointed out that the ratio R depends sensitively on the angular momentum carried off by the final decay products, and hence the value of R should depend on the spin of the Λ hyperon, as is evidenced in Tables III and IV. If the Λ hyperon has a high spin, this will favor the nonmesonic decay mode because of the ability of the two heavy nucleons

TABLE III

Revised Estimate* for $R^{(-)}$ as a Function of Pion Angular Momentum for He⁴

l	0	1	2	3
$R^{(-)}$ for $B=2.0$ Mev	1.1	20	340	5600

* Private communication from Ruderman & Karplus (66); the correction for the Pauli principle (64), and position correlations from Λ-n attraction have been included.

to carry away a large value of angular momentum. Primakoff (64) calculated the influence of the Pauli exclusion principle on the mesonic decays. Since the nucleon from the mesonic decay of the Λ has on the average a low kinetic energy, the mesonic decay of heavy hyperfragments is inhibited by the restrictions of the Pauli principle on the possible states of the final nucleon. Primakoff (64) found that the inhibition factor is about $1/10$ for $Z > 3$, $A > 7$. The correction for the Pauli principle has been included in Tables III and IV. In spite of the possible biases that may be involved in the experimental data, the agreement of $R^{(-)}$ for $_\Lambda$He with the predictions for low spin values of the Λ hyperon is quite remarkable. It is clear that the experimental results rule out the possibility that the Λ hyperon has a large spin.

TABLE IV

REVISED ESTIMATE $R^{(-)}$ AS A FUNCTION OF PION ANGULAR MOMENTUM
FOR HYPERFRAGMENTS OF $Z \geqq 3$

l	0	1	2	3
$R^{(-)}$	50	800	14,000	240,000

Nonmesonic decays.—Several examples of nonmesonic decays have been observed in which the total energy of the nucleons could be determined and the binding energy of the Λ hyperon could be calculated. An example of one such event is shown in Figures 9 and 10. In general, it is more difficult to obtain binding energies from the nonmesonic decays which are as accurate as from the mesonic decays because of the higher kinetic energy release in the former decays. For this reason, there has been less interest in work on the nonmesonic decays. It has recently been shown by Baldo-Ceolin *et al.* (5) that it is possible to distinguish reaction 3 from 4 in the nonmesonic decays of the light hyperfragments, in particular those of helium, lithium, and beryllium. The energy distribution of the charged particles from the events was measured. The authors argued that it is possible to separate events where the Λ interacted with a proton from those where the interaction was with a neutron, by the presence of a fast proton from the decay. The mean energy of the high-energy protons ($E_p > 30$ Mev) was found to be about 73 Mev, which is in agreement with the expected value ($1/2$ of the Λ-nucleon mass difference minus the binding energy of the nucleons in the fragment). Also, the spread in energy of the fast protons is consistent with the Fermi momentum of 200 Mev/c for the nucleon. In this way, it was found that the ratio of neutron to proton stimulated decays in helium, lithium, and beryllium is 1.2. This result is from a total of 79 events, which includes 48 additional events not included in the publication. It was pointed out by Ferrari & Fonda (29) that the ratio of proton to neutron stimulations depends upon the nature of interaction leading to Λ hyperon decay as well
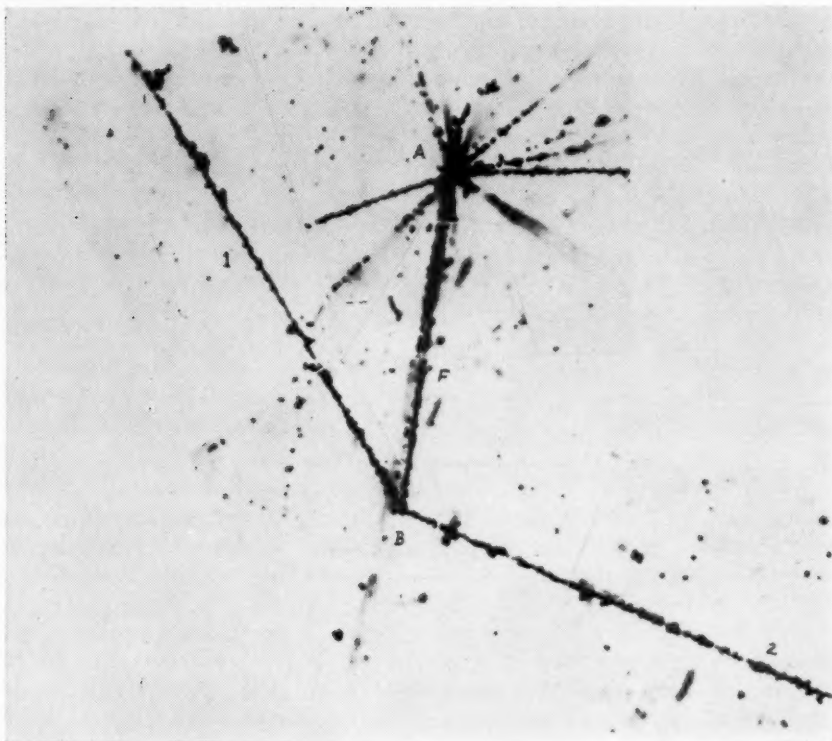
FIG. 9. The nonmesonic decay of a $_\Lambda Be^8$ hyperfragment into two helium nuclei and a neutron. The energy release is 170 ± 3Mev (57).

as the overlap of the Λ hyperon wavefunction with protons and with neutrons.

If it is assumed that the nonmesonic decay occurs through a process of the type suggested by Ruderman & Karplus (66) and that the stimulated bound Λ hyperons decay with the same branching ratio as the free Λ hyperons, then the expected value for the ratio

$$\alpha = \text{stimulation by neutrons/stimulation by protons}$$

is unity or 1/9, depending upon the relative parity of the hyperons and nucleons. If parity is not conserved, this ratio will lie between 0.1 and 1.0.

It has, however, been suggested by Ferrari and Fonda that the stimulation may occur by a virtual process involving a Σ hyperon and a pion with subsequent emission and absorption of a second pion. Such a process would lead to a neutron to proton ratio greater than or equal to unity. It might be expected that the process involving the Σ hyperon may be as important as,

or perhaps more important than the single virtual pion reaction because the binding of a Λ hyperon in a hyperfragment can only result from virtual processes involving more than one pion, or from processes such as the virtual Σ hyperon, as has been calculated by Lichtenberg & Ross (59) and by Dallaporta & Ferrari (24).

Dalitz & Downs (23) pointed out that the value $R^{(-)}$ can yield information on the fraction of Λ hyperon decays which occur through the S and P channels. The calculated value of $R^{(-)}$ for S-wave decay is $R_0^{(-)}=1.1$ and for P-wave $R_1^{(-)}=20$. Using the experimental value $R^{(-)}$, the fraction X of decays that occur through the P state can be calculated, and is found to be about 0.1. This is to be compared with the limit 0.18 to 0.82 set by the up-down asymmetry for free Λ decays by Eisler *et al.* (27) and by Crawford *et al.* (19). Data on the value of $R^{(-)}$ on fragments of $Z > 2$ have little statistical significance although they are not inconsistent with the value of X found from other data. A value of $X = 1/3$ has been assumed by Dalitz & Downs (23). From this value of $X = 1/3$, Dalitz and Downs estimate that about 5 per cent of the H^4 would decay by the two-bodied reaction

$$\Lambda H^4 \rightarrow He^4 + \pi^- \qquad\qquad 5.$$

if the spin of $_\Lambda H^4$ is $J = 1$. The value 0.05 is to be compared with the experimental value 12/(21 to 27). If $J = 0$ for $_\Lambda H^4$, the two-bodied decay can also occur through the S channel. They estimate that if $J = 0$ for $_\Lambda H^4$ the proportion of $(He^4 + \pi^-)$ decays of $_\Lambda H^4$ will be about 1/3, which is consistent with
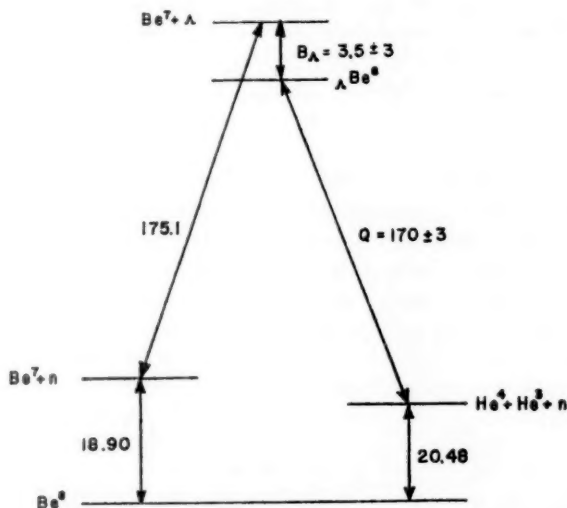
FIG. 10. An energy-level diagram for calculating the binding energy of the Λ hyperon in $_\Lambda Be^8$ (see Fig. 9). Energies are given in Mev.

observations. The authors interpret this result to mean that the spin of $_\Lambda H^4$ is zero, and hence the Λ-nucleon interaction in the singlet state is stronger than in the triplet state. It should be remarked, however, that this result also depends upon an estimate of the probability that the proton from the decay will be captured to form He^4.

In favorable cases, there may be an angular correlation between the decayed products of hyperfragments and the direction of motion of initial fragment. If such correlations are found to exist, they will yield interesting information on the spin of the hyperfragment which in turn will shed light on the Λ-nucleon interaction. To date, there is no information on this interesting problem.

LIFETIME

The first hyperfragment found by Danysz & Pniewski (26), alone, proved that the process which stabilizes the Λ hyperon is essentially unaffected by the presence of nuclear matter, because the moderation time of this fragment was about 3×10^{-12} sec. which is to be compared to about 10^{-23} sec. for a normal nuclear process involving this amount of energy.

Hyperfragments yield not only information on the relatively strong Λ-nucleon interactions but also on the weak process which leads to violation of "strangeness." Aside from the normal process of free decays of the strange particles, the hyperfragments alone can give information on reactions which do not conserve strangeness.[2] It is difficult to determine the lifetime dependence on Z and A from published data of hyperfragments for several reasons: (a) Difficulties of distinguishing decays in flight of nonmesonic decays from break-up of normal fragments; (b) The short moderation time of most fragments relative to their lifetime, leading to very few decays in flight; (c) Nonmesonic fragment decays have not been systematically studied by many groups, since their interest lies in the properties of the mesonic decays.

It is comparatively easy to recognize a charged pion decay in flight from other events. Likewise, a nonmesonic decay in flight can, in general, be distinguished from a fragment break-up, if a fast proton is produced in the decay. From the work of Baldo-Ceolin, which gives the energy distribution of fast protons from nonmesonic decays at rest, it can be estimated that 25 per cent of hyperfragments that decay in flight will give rise to a proton of energy greater than 50 Mev, and hence they can be readily recognized as hyperfragment decays rather than normal fragment break-ups. (In general, the velocity of the hyperfragment will not appreciably affect the energy distribution of protons faster than 50 Mev.) The characteristics of the decays in flight of hyperfragments are given in Table V.

Friedlander (36) has estimated the lifetime of $_\Lambda H^3$ to be 3.7×10^{-10} sec., based upon two decays in flight and 12 decays at rest. The moderation time

---

[2] If the Σ compound exists, this also can yield similar information.

in non-mesonic decays has not been given in most studies. Schneps *et al.* (67) give a value comparable to the free lifetime of the Λ hyperon. No decays in flight were observed. About 66 per cent of all the hyperfragments (36 out of 64) with a range greater than 15 μ have a Z greater than two. An appreciable fraction of the moderation time comes from heavy hyperfragments which predominantly decay nonmesonically. These data show that the lifetime of heavy fragments is not greatly different from that of the free Λ

TABLE V

CHARACTERISTICS OF DECAYS IN FLIGHT

Observers	Technique	Hyperfragment	Range	Decay Mode	Time (sec.)
Alexander *et al.* (1)	Cloud chamber	$_\Lambda H^3$ or $_\Lambda H^4$	2.5 cm.	Mesonic	3.3×10^{-10}
Sorrels *et al.* (74)	Cloud chamber	$_\Lambda He^4$		Mesonic	5.4×10^{-10}
Skjeggested *et al.* (70)	Emulsion	$_\Lambda H^3$	44 μ	Mesonic	10^{-12}
Skjeggested *et al.* (71)	Emulsion	$_\Lambda H^3$ or $_\Lambda H^4$	31 μ	Mesonic	10^{-12}
Brisbout *et al.* (12)	Emulsion	$_\Lambda H^3$	8340 μ	Mesonic	1.3×10^{-10}
Baldo-Ceolin *et al.* (6)	Emulsion	$_\Lambda He^4$	477 μ	Nonmesonic	1.1×10^{-11}
Fowler *et al.* (31)	Emulsion	$_\Lambda He^4$	5180 μ	Mesonic	7.7×10^{-11}

hyperon. Superficially, one might think that this is in disagreement with the rapid increase of the nonmesonic decay mode with Z. However, Primakoff (64) and Rudermann & Karplus (66) have shown that the rapid increase in the nonmesonic decay mode does not imply that the lifetime need be greatly different in heavier hyperfragments because the mesonic decay mode is inhibited by the effect of the Pauli exclusion principle. The inhibition factor can be as large as 10 for hyperfragments of Z greater than three.

BINDING ENERGY

Levi-Setti *et al.* (51, 55) have made a "world survey" of binding energies of hyperfragments. The results are tabulated in Table VI. The absence of $_\Lambda H^1$ and $_\Lambda H^3$ (in spite of the ease of their detection) is noteworthy, for it indicates that the interaction with one and two protons is not strong enough to cause binding and, therefore, the Λ nucleon interaction must be weaker than the nucleon-nucleon interaction. Also, the binding of the Λ hyperon in

TABLE VI

Summary of Binding Energies of Mesonic Decays, May, 1958

Identity	As reported at Rochester, April, 1957[*]				May, 1958[†]				Total
	B_Λ (Mev)	σ_{av} (Mev)	δ_{RE} (Mev)	No. of events averaged	B_Λ (Mev)	σ_{av} (Mev)	δ_{RE} (Mev)	No. of events averaged‖	
Uniquely identified events									
$_\Lambda H^3$	0.25	0.31	0.2	9	0.20	0.50†	0.2	7	9
$_\Lambda H^4$	1.44	0.20	0.25	21	1.81	0.20†	0.25	21	26
$_\Lambda He^4$	1.70	0.24	0.2	9	1.99	0.20†	0.2	9	9
$_\Lambda He^5$	2.56	0.17	0.2	15	2.82	0.20‡	0.2	17	19
$_\Lambda Li^7$	4.17	0.62	0.2	2	4.80	0.50§	0.2	3	2
$_\Lambda Li^8$	5.2	1.0	0.3	1	5.60	0.40§	0.25	3	3
$_\Lambda Li^9$	—	—	—	—	6.7	0.70	0.3	1	1
$_\Lambda Be^8$	5.9	0.5	0.2	1	6.25	0.60	0.2	1	1
$_\Lambda Be^9$	6.13	0.33	0.2	3	6.43	0.40§	0.35	3	3
Non-uniquely identified events									
$_\Lambda H^{2,3,4}$	−0.31	0.36	0.2	5	0.0	0.7‡	0.2	5	7
$_\Lambda H^{4,5}$	—	—	—	—	—	—	—	12	14
$Z>2$	—	—	—	—	—	—	—	19	22

$B_\Lambda = \Lambda$ binding energy

δ_{RE} = random error

δE = error in binding energy of individual event

[*] Based on $Q_\Lambda = (36.9 \pm 0.2)$ Mev (34).

[†] The value of Q_Λ used in the present computation is (37.22 ± 0.2) Mev, weighted average of the previous value (a) and the value (37.45 ± 0.17) (7).

[‡] σ_{av} obtained from the distribution of B_Λ.

$$\sigma_{av} = \left(\frac{\sum \omega_i (B_{\Lambda i} - B_\Lambda)^2}{(n-1) \sum \omega_i} \right)^{1/2}, \qquad \omega_i = (\delta E)^{-2}.$$

[§] $\sigma_{av} = (\Sigma \, \omega_i)^{-1/2}$.

‖ Only events in which the π^- stops in the emulsion have been included in the average.

$_\Lambda$H^2, $_\Lambda$He^4, and $_\Lambda$Li^7 is weaker than the binding of a neutron to a H^3, H^3, and Li^6. However, the binding of the Λ in $_\Lambda$H^4, $_\Lambda$H^5, and $_\Lambda$Be^9 is larger than that of a neutron to a similar core nuclei.

The binding energy of the Λ hyperon increases almost linearly with increasing atomic number, while there are large fluctuations in the binding of the most loosely bound neutrons to similar nuclei. These facts can be readily understood in terms of the effects of the Pauli exclusion principle on the neutron and the absence of any such effect on the Λ hyperon. The Λ hyperon can always occupy the lowest state in the potential well. As a result, B_Λ would be expected to increase monotonically with increasing atomic number to some limiting value for every large hypernuclei. In light nuclei, departures would be expected as a result of variations in the nuclear density of the core with different nuclei and possible spin dependence of the Λ-nucleon interaction. For these reasons, the light hypernuclei are of great interest.

Charged independence asserts that the Λ-neutron interactions should be equal to the Λ-proton interaction. Experimental values for B_Λ of $_\Lambda$H^4 and $_\Lambda$He^4 are in agreement with the assumption of charge independence (B_Λ for $_\Lambda$H$^4 = 1.81$ Mev, B_Λ for $_\Lambda$He$^4 = 1.99$ Mev). The possible difference, if any, in the binding energies of $_\Lambda$H^4 and $_\Lambda$He^4 becomes insignificant when one considers that a difference of 0.4 Mev in the binding energy reflects only a difference of 5 per cent in the well depth. The importance of isotopic spin in hyperfragment multiplets was clearly stated by Dalitz (21) and by Jones & Knipp (50).

If the isotopic spin of the hyperon is taken to be zero, charge independence forbids the reaction

$$\Lambda \rightarrow \Lambda + \pi^0 \qquad\qquad 6.$$

and, therefore, it is not too surprising that the Λ-nucleon interaction is weaker than the nucleon-nucleon interaction for which the single pion exchange is not forbidden. Several schemes for the Λ-nucleon interaction have been proposed:

(a) The process involving two pions

$$\Lambda + p \rightarrow \Sigma^+ + \pi^- + p \rightarrow \Lambda + (\pi^+ + \pi^- + p) \rightarrow \Lambda + p,$$
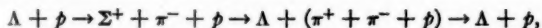
which would give rise to a nonexchange force with a range of the order of $h/(2m_\pi c)$. The details of this interaction have been discussed by Lichtenberg & Ross (59) and by Dallaporta & Ferrari (24);

(b) A process where a virtual K-meson is emitted such as the following reaction

$$\Lambda + p \rightarrow p + K^- + p \rightarrow p + \Lambda,$$
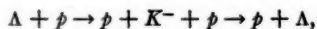
which gives rise to an exchange force with a range of the order of $h/m_K c$. This reaction has been discussed by Wentzel (82);

(c) Reactions involving more than two pions with a corresponding range shorter than the above two reactions.

An estimate of the strength of the Λ-nucleon interaction can be obtained from the B_Λ in $_\Lambda$He^5 using data from electron scattering experiments of McAllister & Hofstadter (61). These authors evaluated the nucleon density of He^4 nucleus. The core of $_\Lambda$He^5 is assumed to be an undistorted He^4 nucleus, and the potential well is taken to be of the size of the nuclear core, since the Λ-nucleon range is probably short. In this way, Dalitz (22) finds

$$U_4{}^- = 1.71/m_\pi c^2$$

where $U_4{}^-$ is the volume integral of the Λ-nucleon interaction for the four nucleons.

The volume integral of the interaction for $_\Lambda$He^4 $U_3{}^- = 1.91/m_\pi c^2$ can be compared with $U_4{}^-$, by noting that for a spin-independent force

$$U_3{}^- = (3/4)U_4{}^- = 1.28/m_\pi c^2.$$

This value is to be compared with $1.91/m_\pi c^2$ obtained from $_\Lambda$He^4. From this inequality, Dalitz (22) concluded that the Λ-nucleon interaction is spin-dependent. It should be noted that small errors in the binding energy of $_\Lambda$He^4 and $_\Lambda$He^5 do not materially affect the argument, since the volume integrals depend primarily on the depth of the well and not directly on the binding energy.

A measure of the degree of the spin-dependence was found by the following argument. In $_\Lambda$He^5, the spins of the nucleons in the α-particle core couple to give a total spin of zero as dictated by the exclusion principle, so the potential for the Λ hyperon is the sum of both spin orientations for both neutrons and protons. For a spin S of the Λ hyperon

$$U_4{}^- = 4[SU_a{}^- + (S + 1)U_p{}^-](2S + 1),$$

where $U^-{}_a$ and $U^-{}_p$ are the volume integrals for the Λ-nucleon interaction in the antiparallel and parallel spin orientations respectively. In $_\Lambda$He^4, the Λ hyperon is free to couple in the most advantages way to the neutron and, since the coupling to the protons is $U^-{}_4/2$, then

$$U^-{}_{max} = U_3{}^- - (1/2)U_4{}^- = 1.05/m_\pi c^2,$$

which is to be compared to $U_4{}^-/4 = 0.43/m_\pi c^2$. The difference between $U_{max}{}^-$ and $U_4{}^-/4$ is the difference between the volume integral for the most favorable Λ-nucleon spin orientation and the average volume integral for both spin orientations. Perhaps the weak point in the argument comes from the assumptions regarding the shape and size of the He^3 core of $_\Lambda$He^4. Electron scattering measurements are not available on He^3.

Brown & Peshkin (14), on the other hand, find that all of the data for various fragments can be explained without introducing a spin-dependent interaction, and attribute the $_\Lambda$He^4, $_\Lambda$He^5 difference to distortions of the nuclear core.

HYPERNUCLEI

Charged hyperons are not expected to be stable in nuclear fragments containing both protons and neutrons because of the fast reactions

$$\Sigma^- + p \rightarrow \Lambda + n \qquad\qquad 7.$$

$$\Sigma^+ + n \rightarrow \Lambda + p. \qquad\qquad 8.$$

However, the compounds $(\Sigma^+ + p)$ and $(\Sigma^- + n)$ would be stable against Λ formation as emphasized by Holladay (49). The emission of a single virtual pion which could lead to binding comparable to those of nucleons (which is forbidden for the Λ hyperon) suggests that such compounds might exist. One event has been reported by Baldo-Ceolin *et al.* (4) which was interpreted as a $(\Sigma^+ + p)$ compound. The decay star consisted of a pion of 85 ± 11 Mev and a proton of 15.5 Mev. These two tracks were not colinear. Assuming a neutron balanced momentum, the total energy release was 106 ± 14 Mev, which gives a binding energy of 6 ± 14 Mev. The only alternative interpretation is that the secondary star was produced by the absorption from rest of a K^- meson. The connecting track is 22 μ long and profile measurements give a charge of two. From the same measurements, the probability that the charge is one is estimated to be 5 per cent.

Judging from the absence of compounds from the large number of K^- capture stars that have been studied by many groups, the probability of compound formation must be quite small ($< 1/500\ \Sigma$'s form a fragment).

LITERATURE CITED

1. Alexander, G., Astbury, J. P., Ballario, C., Bizzarri, R., Brunelli, B., De Marco, A., Michelini, A., Moneti, G. C., Zavattini, E., and Zichichi, A., *Nuovo cimento*, **2**, 365 (1955)
2. Anderson, F., Lawlor, G., and Nevin, T. E., *Nuovo cimento*, **2**, 605 (1955)
3. Baldo-Ceolin, M., Belliboni, G. Ceccarelli, M., Grilli, M., Sechi, B., Vitale, B., and Zorn, G. T., *Nuovo cimento*, **1**, 1180 (1955)
4. Baldo-Ceolin, M., Fry, W. F., Greening, W. D. B., Huzita, H., and Limentani, S., *Nuovo cimento*, **6**, 144 (1957)
5. Baldo-Ceolin, M., Dilworth, C., Fry, W. F., Greening, W. D. B., Huzita, H., Limentani, S., and Sichirollo, A. E., *Nuovo cimento*, **7**, 328 (1958)
6. Baldo-Ceolin, M., Fry, W. F., and Huzita, H., *Nuovo cimento*, **9**, 551 (1958)
7. Barkas, W. H., Giles, P. C., Heckman, H. H., Inman, F. W., Mason, C. J., and Smith, F. M., *Intern. Conf. on Mesons and Recently Discovered Particles*, Padova-Venezia Conference (1957)
8. Barkow, A. G., and Chamany, B., *Phys. Rev.*, **105**, 692 (1957)
9. Barrett, P. H., *Phys. Rev.*, **94**, 1328 (1954)
10. Blau, M., *Phys. Rev.*, **102**, 495 (1956)
11. Bonetti, A., Levi-Setti, R., Panetti, M., Scarsi, L., and Tommasini, G., *Nuovo cimento*, **11**, 210 (1954) and **11**, 330 (1954)
12. Brisbout, F., Friedlander, M. W., and Iredale, P., *Nuovo cimento*, **4**, 948 (1956)
13. Brisbout, B. A., and Hopper, V. D., *Australian Phys.*, **7**, 352 (1954)
14. Brown, L. M., and Peshkin, M., *Phys. Rev.*, **107**, 272 (1957)
15. Castagnoli, C., Cortini, G., and Franzinetti, C., *Nuovo cimento*, **12**, 550 (1955)
16. Ceccarelli, M., Dallaporta, N., Grilli, M., Merlin, M., Salandin, G., Sechi, B., and Ladu, M., *Nuovo cimento*, **2**, 542 (1955)
17. Cheston, W. B., and Primakoff, H., *Phys. Rev.*, **92**, 1537 (1953)
18. Ciok, P., Danysz, M., and Gierula, J., *Nuovo cimento*, **11**, 436 (1954)
19. Crawford, F. S., Crest, M., Good, H. L., Gottstein, K., Lyman, E. M., Solmitz, F. T., Stevenson, M. L., and Ticho, H. K., *Phys. Rev.*, **108**, 1102 (1957)
20. Crussard, J., and Morellet, D., *Compt. rend.* **236**, 64 (1955)
21. Dalitz, R. H., *Phys. Rev.*, **99**, 1475 (1955)
22. Dalitz, R. H., *Repts. on Progr. in Phys.*, **XX**, 163 (1957)
23. Dalitz, R. H., and Downs, B. W. (To be published, 1958)
24. Dallaporta, N., and Ferrari, F., *Nuovo cimento*, **5**, 111 (1957)
25. De Benedetti, A., Garelli, C. M., Tallone, L., and Visone, M., *Nuovo cimento*, **2**, Suppl., 249 (1955); *Nuovo cimento*, **12**, 466 (1954); *Nuovo cimento*, **12**, 952 (1954)
26. Danysz, M., and Pniewski, J., *Phil. Mag.*, **44**, 1, 348 (1953)
27. Eisler, F., Llano, R., Prodell, A., Samuels, N., Schwartz, M., Steinberger, J., Bassi, T., Boreli, V., Puppi, G., Tanaka, G., Waloschek, P., Conversi, M., Franzini, P., Manelli, I., Santangelo, R., Silverstrini, V., Glaser, D. A., Graves, C., and Perl, M. L., *Phys. Rev.*, **108**, 1353 (1957)
28. Ferrari, F., and Fonda, L., *Nuovo cimento*, **6**, 1027 (1957)
29. Ferrari, F., and Fonda, L., *Nuovo cimento*, **7**, 320 (1958)
30. Fowler, T. K., *Phys. Rev.*, **102**, 844 (1956)
31. Fowler, P. H., and Hansen, K. H., *Nuovo cimento*, **4**, 158 (1956)
33. Freier, P. S., Anderson, G. W., and Naugle, J. E., *Phys. Rev.*, **94**, 677 (1954)
33a. Fridlender, E., and Bercha, S., *Doklady Akad. Nauk. S.S.S.R.*, **107**, 51 (1956)

34. Friedlander, M. W., Keefe, D., Menon, M. G. K., and Merlin, M., *Phil. Mag.*, **45**, 533 (1954)
35. Friedlander, M. W., Keefe, D., and Menon, M. G. K., *Nuovo cimento*, **2**, 663 (1955)
36. Friedlander, M. W., *Nuovo cimento*, **5**, 283 (1956)
37. Fry, W. F., and White, G. R., *Nuovo cimento*, **11**, 555 (1954)
39. Fry, W. F., Schneps, J., and Swami, M., *Phys. Rev.*, **99**, 1561 (1955); *Phys. Rev.*, **101**, 1526 (1956)
40. Fry, W. F., Schneps, J., Snow, G. A., Swami, M. S., and Wold, D. C., *Phys. Rev.*, **107**, 257 (1957)
41. Gilbert, F. C., Violet, C. E., and White, R. S., *Phys. Rev.*, **103**, 298 (1956)
42. Gottstein, K., *Nuovo cimento*, **12**, Suppl., 306 (1954)
43. Grilli, M. G., and Levi-Setti, R., *Nuovo cimento*, **12**, Suppl. 466 (1954)
44. Grilli, M., Sechi, B., and Zorn, G. T., *Nuovo cimento*, **12**, Suppl. 310 (1954)
45. Gurevich, I. I., and Mishakova, A. P., *Doklady Akad. Nauk S.S.S.R.*, **108**, 207 (1956)
46. Haskin, D. M., Bowen, T., and Glasser, R. G., *Phys. Rev.*, **102**, 244 (1956)
47. Haugerud, O., and Sorensen, S. O., *Phys. Rev.*, **99**, 1946 (1955)
48. Hill, R., Salant, E., Wigdoff, M., Osborne, L. S., Pevsner, A., Ritson, D. M., Crussard, J., and Walker, W. D., *Phys. Rev.*, **94**, 797 (1954)
49. Holladay, W. (Private communication, 1954)
50. Johnes, J. T., and Knipp, J. K., *Nuovo cimento*, **2**, 857 (1955)
51. Lal, D., Pal. Y., and Peters, B., *Phys. Rev.*, **92**, 438 (1953)
52. Leenov, D., Haskin, D. M., and Schein, M., *Phys. Rev.*, **100**, 1263 (1955)
53. Leprince-Ringuet, L., Crussard, J., Fouche, V., Hennessy, J., Kayas, G., Morellet, D., and Renard, F., *Compt. rend.*, **242**, 1554 (1956)
54. Levi-Setti, R., and Slater, W. E., *Nuovo cimento*, **6**, 51 (1957)
55. Levi-Setti, R., Slater, W. E., and Telegdi, V. L., *Proc. 7th Annual Rochester Conf.* (April, 1957)
56. Levi-Setti, R., and Slater, W. E. (To be published, *Phys. Rev.*)
57. Levi-Setti, R., Slater, W. E., and Telegdi, V. L., *Proc. 7th Annual Rochester Conf.*, (April, 1957) recomputation and addition of date (Private communication, May, 1958)
58. Levi-Setti, R., Ammar, R. G., Slater, W. E., Limentani, S., Roberts, J. H., Schlein, P. E., and Steinberg, P. H., *Bull. Am. Phys. Soc.*, [II]**3**, 175 (1958)
59. Lichtenberg, D. B., and Ross, M., *Phys. Rev.*, **103**, 1131 (1956)
60. Lovera, G., Barabanti-Silva, L., Bonacini, C., DePietri, C., Perilli-Fedeli, R., and Roveri, A., *Nuovo cimento*, **10**, 986 (1953)
61. McAllister, R. W., and Hofstadter, R., *Phys. Rev.*, **102**, 851 (1956)
61a. Matsumoto, S., (Preprint, 1958)
62. Naugle, J. E., Ney, E. P., Freier, P. S., and Cheston, W. B., *Phys. Rev.*, **96**, 1383 (1954)
63. Naugle, J. E., Freier, P. S., and Ney, E. P., *Phys. Rev.*, **96**, 829 (1954)
64. Primakoff, H., *Nuovo cimento*, **3**, 1394 (1956)
65. Rosselet, P., Weil, R., and Gailloud, M., *Nuovo cimento*, **3**, 505 (1956)
66. Ruderman, M., and Karplus, R., *Phys. Rev.*, **102**, 247 (1956)
66a. Schlein, P. E., Limentani, S., Roberts, J. H., and Steinberg, P. H., *Bull. Am. Phys. Soc.*, [II] **3**, 175 (1958)
67. Schneps, J., Fry, W. F., and Swami, M., *Phys. Rev.*, **106**, 1062 (1957)

68. Seeman, N., Shapiro, M. M., and Stiller, B., *Phys. Rev.*, **100,** 1480 (1955)
69. Skjeggested, O., and Sorensen, S. O., *Phys. Rev.*, **104,** 511 (1956)
70. Skjeggested, O., and Sorensen, S. O., *Nuovo cimento*, **3,** 652 (1956)
71. Skjeggested, O., Sorensen, S. O., and Solheim, A., *Phys. Rev.*, **106,** 1280 (1957)
72. Slaughter, G. G., Harth, E. M., and Block, M. M., *Phys. Rev.*, **109,** 2111 (1958)
73. Solheim, A., and Sorensen, S. O., *Phil. Mag.*, **45,** 1284 (1954)
74. Sorrels, J. D., Thrilling, G. H., and Leighton, R. B., *Phys. Rev.*, **100,** 5, 1484 (1955)
75. Schein, M., Haskin, D. M., and Leenov, D., *Phys. Rev.*, **100,** 1455 (1955)
77. Stiller, B., Seeman, N., and Shapiro, M. M., *Phys. Rev.*, **100,** 959 (1955)
78. Steinberg, P. H., Limentani, S., Roberts, J. H., Schlein, P. E., Ammar, R. G., Levi-Setti, R., and Slater, W. E., *Bull. Am. Phys. Soc.*, [II]3, 175 (1958)
79. Tidman, D. A., Davis, G., Herz, A. J., and Tennent, R. M., *Phil. Mag.*, **44,** 348 (1953)
80. Varfolomeev, A. A., Gerasimova, R. I., and Karpova, L. A., *Doklady Akad. Nauk S.S.S.R.*, **110,** 758 (1956)
81. Waldeskog, B., *Arkiv Fysik*, **8,** 369 (1954)
82. Wentzel, G., *Phys. Rev.*, **101,** 835 (1956)
83. Yagoda, H., *Phys. Rev.*, **98,** 153 (1955); *Phys. Rev.*, **99,** 651 (1955)

ANTINUCLEONS[1]

By Emilio Segrè[2]

Physics Department, University of California, Berkeley, California

Introduction

The idea of "antiparticles," as is well known, originated with Dirac, who in establishing the relativistic equations for the electron noted that besides the solutions corresponding to ordinary electrons there were also "unwanted solutions" corresponding to particles of electronic mass but of charge $+e$ instead of the electronic charge $-e$. (45). The discovery of the positron by Anderson (10) offered a brilliant experimental confirmation of Dirac's prediction and gave the first example of an "antiparticle."

One could think of applying Dirac's theory of the electron without changes, except in the mass of the particle, to the proton; however, this view is obviously untenable because the magnetic moment of the proton is not one nuclear magneton, nor would it account for the neutron which is clearly related to the proton. Even if such a literal extension of Dirac's theory is impossible, the feature of giving sets of solutions which represent "charge-conjugate" particles is preserved in all theories of elementary particles. In particular the appearance of the anomalous moment of the proton is no obstacle because it is ascribed to the pion cloud surrounding it, and the interaction between pions and nucleons is of the "strong" type for which invariance on charge conjugation is valid (105). We shall consider here only fermions of spin $\frac{1}{2}$. For them a particle and its "charge conjugate" are related by the set of properties given in Table I.

Properties 1 to 5, inclusive, are established by very general arguments and require only invariance under the product of charge conjugation C, space reflection P, and time reversal $T(CPT$ theorem); they are rigorously true even if invariance under charge conjugation alone is not valid [see (105)].

Originally, properties 1 to 4 were derived from the principle of invariance under charge conjugation, which can be formulated by saying that a possible physical situation is transformed into another possible physical situation by changing the sign of all electric charges. Since this principle is violated in weak interactions, it is important to point out that it is not necessary to establish the properties listed above, but that the weaker requirement expressed by the invariance under the CPT transformation is sufficient (76, 77).

TABLE I

Particle-Antiparticle Relations

	Particle		Antiparticle
1) Charge	q		$-q$
2) Mass	m		m
3) Spin		same	
4) Magnetic moment	μ		$-\mu$
5) Mean life		same	
6) Creation		in pairs	
7) Annihilation		in pairs	

Properties 6 and 7 in the nuclear case are a consequence of the conservation of nucleons; the number of antinucleons must be subtracted from the number of nucleons in establishing the nucleon number of a system.

Verification of Dirac's Attributes of the Antiproton

After the discovery of the positron in cosmic rays it was natural to expect that antinucleons also might be found there; indeed, prior to 1955, processes in which the energies available were sufficient to produce nucleon-antinucleon pairs occurred only in cosmic rays. Several cosmic-ray events (5, 24, 25, 98) have been observed in cloud chambers and in photographic emulsions which are attributable to antiprotons. In none of them, however, is the evidence obtained sufficient to establish with certainty the identity of the particle involved.

With the advent of accelerators powerful enough to produce antinucleons in the laboratory, it became possible to investigate systematically antiprotons and antineutrons, and to identify them beyond any doubt. The first successful investigation was carried on by Chamberlain, Segrè, Wiegand & Ypsilantis with the Berkeley Bevatron in the fall of 1955 (38, 39). Charge, mass, and stability against spontaneous decay of the antiproton were the first properties ascertained.

The central problem was to find particles with charge $-e$ and mass equal to that of the proton. This was accomplished by determining the sign and magnitude of the charge, and the momentum and velocity of the particle. From the relation

$$p = mc\beta\gamma \qquad\qquad 1.$$

the mass was then found. Here p is the momentum, m the rest mass, c the velocity of light, v the velocity of the particle, and $\beta = v/c$, $\gamma = (1-\beta^2)^{-1/2}$.

The apparatus employed is shown in Figure 1. The trajectory of the particles fixes their momentum if the charge and the magnetic fields are known. The latter are measured directly and the trajectory is checked by the wire-orbit method: a flexible wire with an electric current i and subject
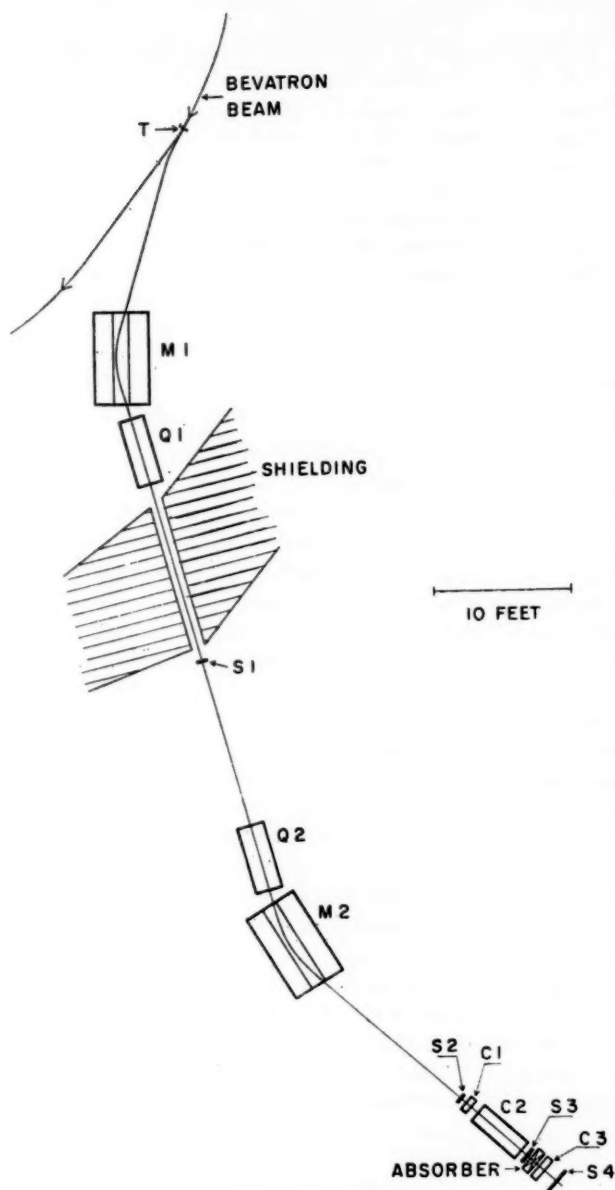
FIG. 1. Original mass spectrograph of Chamberlain, Segrè, Wiegand, & Ypsilantis (39)
For characteristics of components see Table II.

TABLE II

CHARACTERISTICS OF COMPONENTS OF THE APPARATUS

S1, S2	Plastic scintillator counters 2.25 in. diameter by 0.62 in. thick
C1	Cerenkov counter of fluorochemical O–75, ($C_8F_{16}O$); $\mu_D = 1.276$; $\rho = 1.76$ gm. cm.$^{-3}$ Diameter 3 in.; thickness 2 in.
C2	Cerenkov counter of fused quartz: $\mu_D = 1.458$; $\rho = 2.2$ gm. cm.$^{-3}$ Diameter 2.38 in.; length 2.5 in.
Q1, Q2	Quadrupole focusing magnets: Focal length 119 in.; aperture 4 in.
M1, M2	Deflecting magnets 60 in. long. Aperture 12 in. by 4 in. $B \cong 13,700$ gauss

to a mechanical tension T in the magnetic field takes exactly the form of the orbit of a particle of charge e and momentum p if

$$T/i = p/e. \qquad 2.$$

The particles in passing through the scintillation counters $S_1S_2S_3$ give rise to pulses having the same pulse height as those caused by protons of the same momentum, thus indicating that the magnitude of the charge is e and not $2e$ or greater. The trajectory determines the momentum p and also that the sign of the charge is negative. The measurement of the velocity is the most difficult part of the experiment, especially because antiprotons are accompanied by a very heavy background flux of pions mixed with some electrons and muons in a ratio of the order of 50,000 pions to one antiproton. It is accomplished by measuring the time of flight between scintillators S_1, S_2, and corroborated by the response of the special (40, 106) Cerenkov Counter C_2 which responds only to particles with $0.75 < \beta < 0.78$. Cerenkov Counter C_1 is in anticoincidence and responds to particles with $\beta > 0.79$, helping to eliminate pions and lighter particles. Scintillator S_3 has the purpose of ensuring that the antiproton traverses the whole apparatus.

The momentum of a particle passing through the instrument was 1.19 Bev/c. The velocity of an antiproton of this momentum is $0.78c$, whereas a meson of the same momentum has $v = 0.99c$. Their times of flight between S_1 and S_2 were 51 and 40 millimicroseconds, respectively. The time of flight and the response of C_2 represent independent velocity measurements, and combined with the other counters as described allow the identification of the particle as an antiproton and a measurement of its mass to within 5 per cent accuracy. This apparatus delivers at S_3 certified antiprotons, i.e., it ensures that when the expected electronic signals appear, an antiproton has passed through it and emerged at S_3.

A more luminous version of the apparatus which gives about 80 times as many antiprotons as the one described above has also been described (2). At 6.2 Bev this last apparatus gives, as an order of magnitude for practical purposes, one transmitted antiproton of momentum 1.19 Bev/c for every 2×10^{10} protons impinging on a carbon target 6 in. thick.

A spectrograph using repeated time-of-flight measurements, without Cerenkov counters, has been built by Cork and his co-workers (42); its performance is similar to that of the spectrograph in (2), but it is better suited for lower momenta where Cerenkov counters are inconvenient.

The following sections contain discussions of the extent to which the properties mentioned in Table I have been verified.

Charge.—The sign of the charge is determined by the curvature of the trajectory, and its magnitude by the pulse size in the counter experiments and by the grain density in photographic emulsions. Ruling out the possibility of fractional charges, it is $-e$, identical with the charge of the electron (39).

Mass (14, 33, 39).—The first antiproton experiment gave the mass to an accuracy of 5 per cent. The most precise value of the ratio of the antiproton mass to that of the proton is obtained by the combined use of a measurement of momentum by the wire method and range in a photographic emulsion: a value of 1.010 ± 0.006 has been obtained for the ratio; however, the error reported does not take into account possible systematic errors in the determination of the momentum which, estimated very conservatively, might cause an error in the mass of about 3 per cent.

It is interesting to measure the mass of the antiproton by the use of photographic emulsions only, without a separate measurement of the momentum: this has been accomplished by (*a*) the combination of ionization and residual range and (*b*) by the combination of ionization and multiple scattering. Ionization was measured by grain density or by measuring the average fraction of a track occupied by silver grains. The emulsions were calibrated directly, using protons or deuterons. This work has given a ratio for Method (*a*) of 1.009 ± 0.027, and for Method (*b*) of 0.999 ± 0.043. Again the errors are only statistical. Possible systematic errors might be as high as 3 per cent (14).

The conclusion is that the identity of the mass of the proton and of the antiproton has been verified experimentally to an accuracy of about 2 per cent.

Spin and magnetic moment.—There are no direct observations of these quantities for the antiproton. A possible method of measurement would be the following: antiprotons generated with a momentum vector at an angle with the momentum of the particle incident on the target are likely to be polarized. If so, the polarization is in a direction perpendicular to the plane defined by the two momenta mentioned above. If the antiprotons are not polarized at creation, they may be polarized by scattering but this would increase very appreciably the intensity requirements for an experiment. Assume they are polarized and pass them through a magnetic field H parallel to the momentum. The polarization vector rotates by an angle

$$2\frac{\mu H d}{\hbar c \beta} = \alpha \qquad\qquad 3.$$

where μ is the magnetic moment, d the length of the field, and $\hbar$ Planck's constant divided by 2π. The angle α is directly measurable by scattering the antiprotons on a target and observing the asymmetry of scattering at different azimuths. All other quantities except μ are easily measurable. The experiment seems feasible with present techniques (67, 97). The spin of the antiproton could also be considered as directly verified experimentally if the magnetic moment were to be found, as expected, equal in magnitude to that of the proton; in fact, the factor 2 of Equation 3 is based on a spin $\frac{1}{2}$ for the antiproton; however, strictly speaking, this experiment would measure only the gyromagnetic ratio of the antiproton.

Annihilation.—The prediction from Table I is that a nucleon-antinucleon pair at rest will annihilate, releasing the energy $2\ mc^2$. No information is given on the form of the energy release; thus, for an electron-positron pair, γ-rays are emitted, whereas for a nucleon-antinucleon pair, pion production is the dominant mode of annihilation. Starting from a nucleon-antinucleon pair, positive, negative, or neutral pions may be obtained, the latter decaying within 10^{-16} sec. into γ-rays. The charged pions also decay into μ mesons and neutrinos, but the μ mesons decay further into electrons, positrons, and neutrinos; and in matter the positrons left over annihilate with electrons. Thus, within microseconds the whole rest mass of the system has degraded to forms of energy of rest mass zero with the exception of the case of the antiproton-neutron annihilation, in which an electron is left over. Without entering, at present, into any details concerning the annihilation process, it is clear that in a photographic emulsion where only charged particles leave a track it will not be possible to follow all the annihilation products, but only the charged ones. If, however, at the stopping point of an antiproton an energy release greater than mc^2 is observed, the conclusion must be drawn that the antiproton has annihilated another nucleon, because the visible energy liberated is already greater than the rest energy of the antiproton. The first observation of this phenomenon is reported in (32).

Other methods of observing the annihilation of an antiproton are based on the light emitted either as Cerenkov light or as scintillation light by the charged particles produced directly or indirectly in the annihilation process.

Two typical instruments using Cerenkov light and scintillation light, respectively, are shown in Figures 2 and 3. In Figure 2 the radiator is a large block of glass of refractive index 1.649 for the D lines and radiation length of 2.77 cm. It is observed by a bank of photomultipliers. The light observed is Cerenkov radiation due to the showers produced by neutral pions or produced directly by charged pions (23). In Figure 3 (30) the radiator is a composite sandwich of lead and plastic with an average density of 3.84 gm. cm.$^{-3}$, an average radiation length of 1.7 cm., and a thickness corresponding to three annihilation mean free paths. The total dimensions of the "sandwich" are about $60 \times 60 \times 60$ cm. Both instruments have low resolving power, and the annihilation of an antinucleon produces pulses which vary greatly in magnitude. Nevertheless, an apparatus similar to that of Figure

2 was used in order to see large annihilation pulses when antiprotons selected by the spectrograph of (39) were sent into a piece of glass. The results obtained "were not inconsistent with the expected behavior of antiprotons," but the largest energy release observed as Cerenkov light corresponded only to 0.9 Bev (21, 22).

Production in pairs.—The evidence on this subject comes from the excitation function. The data are still very scanty, but the fact that no anti-

¼" THICK X 4" DIAMETER LEAD CONVERTER

12" DIAMETER X 7" THICK GLASS DISKS

5" PHOTOMULTIPLYERS

IRON MAGNETIC SHIELDS

4" DIAMETER X I" THICK COINCIDENCE
PLASTIC SCINTILLATOR

6" DIAMETER X I" THICK ANTI-COINCIDENCE
PLASTIC SCINTILLATOR

12"
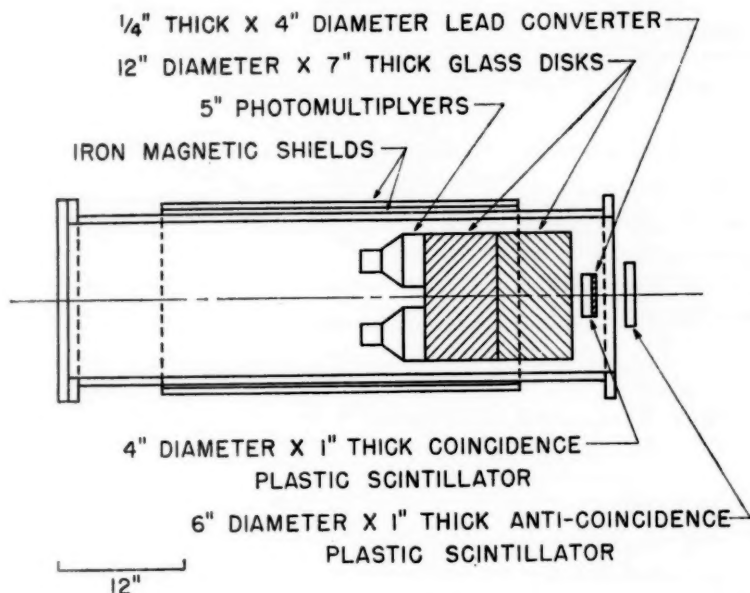
FIG. 2. Schematic arrangement of the pulse height spectrometer showing the glass phototubes, and magnetic shield, as well as the anticoincidence counter, lead, and coincidence counters. These two scintillation counters insure that the electron showers, which are pulse height analyzed, start in the 0.25-inch lead converter and thus are centered in the glass, and start at its front surface. From (23).

protons have been observed at an energy lower than 4.0 Bev for the Bevatron beam is an indication of the production in pairs (39).

Thresholds for production in pairs are given in the following Table III for different processes. Very little is known of the production cross sections and their energy-dependence (see section on Production), but if the production were not in pairs, process (1) with protons at rest would have, for instance, a threshold of only 2.35 Bev and the other correspondingly lower. The observed facts do not seem reconcilable with such an hypothesis:

Decay constant.—Antiprotons in a vacuum must be stable. Antineutrons must decay with a mean life of 1040 sec. In the different experiments per-
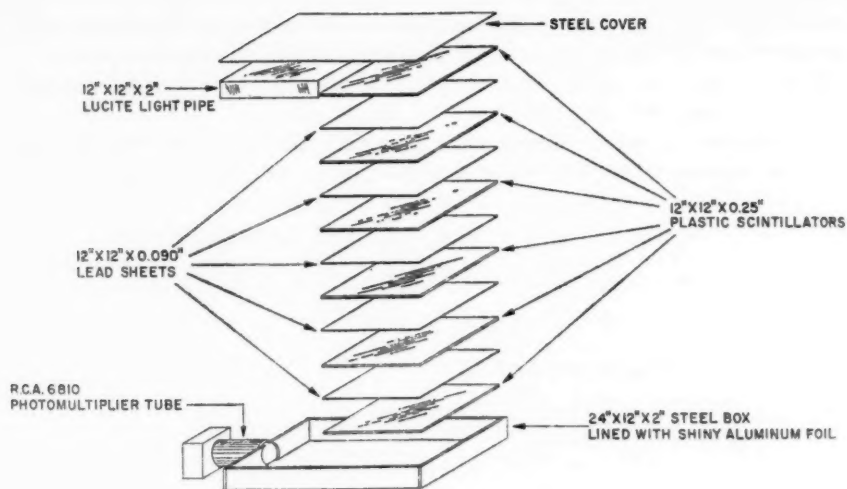
FIG. 3a. Element of the annihilation detector. From (30).
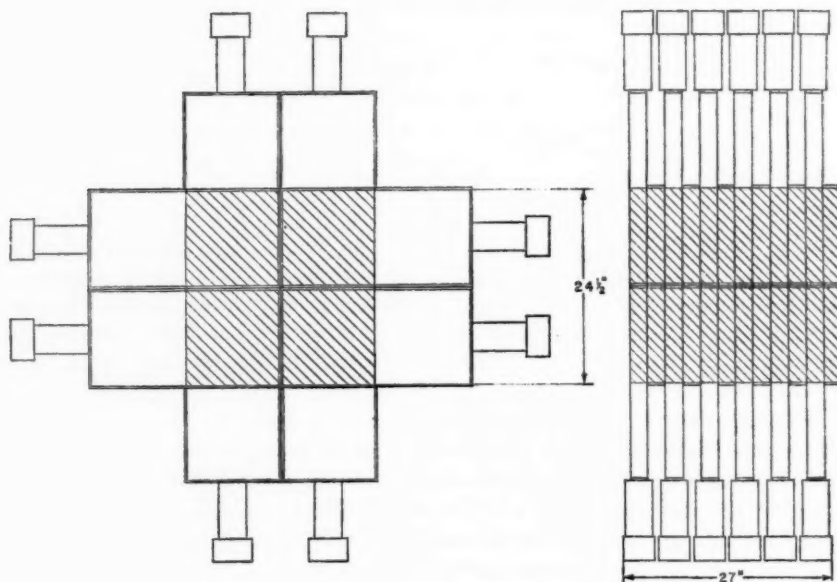
FIG. 3b. Assembly of the annihilation detector. From (30).

TABLE III

Thresholds for Nucleon Antinucleon Pair-Production
(Bev kinetic energy in the laboratory)

Process	Target at rest	Target with Fermi Energy of 25 Mev
1) $p+p \to 3p+\bar{p}$	5.63	4.30
2) $\pi+p \to 2p+\bar{p}$	3.60	2.85
3)* $p+p \to p+p+\pi$	$(T_\pi=3.60)$ 4.06	$(T_\pi=2.85)$ 3.08

p stands for proton or neutron. Naturally electric charge must balance in the reaction.

* Line 3 indicates the proton minimum energy required in order to obtain pions of energy T_π in a p-p collision.

formed heretofore, the times of flight involved are up to 10^{-7} sec. The decay constant cannot be much less than the time of flight, otherwise no antiprotons would be observed. Thus the lower limit for the mean life is 10^{-7} sec.

In conclusion it can be said that the properties of Table I are essentially verified.

Nucleonic Properties of the Antiproton

The total isotopic spin T of an antinucleon is clearly 1/2 and the formula for the charge

$$\frac{q}{e} = T_3 + \frac{N}{2} \qquad\qquad 4.$$

where N is the number of nucleons, suggests the assignment of $T_3 = -\frac{1}{2}$ to the antiproton and $T_3 = \frac{1}{2}$ to the antineutron. Thus a proton-antiproton pair has $T_3 = 0$, but $T = 1$ or 0, whereas the proton-antineutron pair or the antiproton-neutron pair have $T = 1$.

The intrinsic parity of the antiproton and the antineutron is -1 if that of the proton and neutron is assumed to be $+1$. A justification of this assignment of intrinsic parity is that Dirac's theory predicts for the electron-positron pair in the $^1S_0$ state a 2-quanta annihilation with the polarization of the 2 quanta perpendicular to each other corresponding to a pseudoscalar matrix element $(e_1 \cdot e_2 \times p)f(p)$ (e_1, e_2 unit vectors indicating the polarization of the quanta; p relative momentum). This prediction has been verified experimentally and forces the electron and positron to have opposite parities [see (44)]. The same is assumed to hold for the proton-antiproton pair and for the neutron-antineutron pair. A summary of these properties is presented in Table IV (83, 90, 105).

The next discussion will be on those properties which are not predictable on the basis of charge conjugation. They are the most novel ones and their study has barely begun. They will be divided into collision cross sections, modes of annihilation, and production.

TABLE IV

SPIN, PARITY, I-SPIN OF NUCELONS AND ANTINUCLEONS

	Proton	Neutron	Antiproton	Antineutron
Spin S	1/2	1/2	1/2	1/2
I-spin T	1/2	1/2	1/2	1/2
3rd comp. of I-spin T_3	1/2	−1/2	−1/2	1/2
Parity	+	+	−	−

Collision cross sections.—Collisions of antiprotons on nuclei may lead to elastic scattering, inelastic scattering, annihilation, or charge exchange. The corresponding cross sections will be called σ_e, σ_i, σ_a, σ_c. Also considered is the reaction cross section $\sigma_r = \sigma_i + \sigma_a + \sigma_c$ and the total cross section $\sigma_t = \sigma_r + \sigma_e$. The experimental data obtained thus far are rather sketchy. The case of antiproton-nucleon scattering and the case of scattering from complex nuclei will be treated separately.

A typical apparatus used experimentally (36) is shown in Figure 4. A certified antiproton falls on the target which is placed in the slots of Y and, if it is annihilated, it gives Cerenkov light detectable by the photomultipliers. If it crosses the target without annihilation and falls into a cone of semi-aperture 14° or 20° it is detected by the circular scintillators. If it is scattered by an angle $\theta \geq 20°$ it is not detected by the scintillators or by the target box.
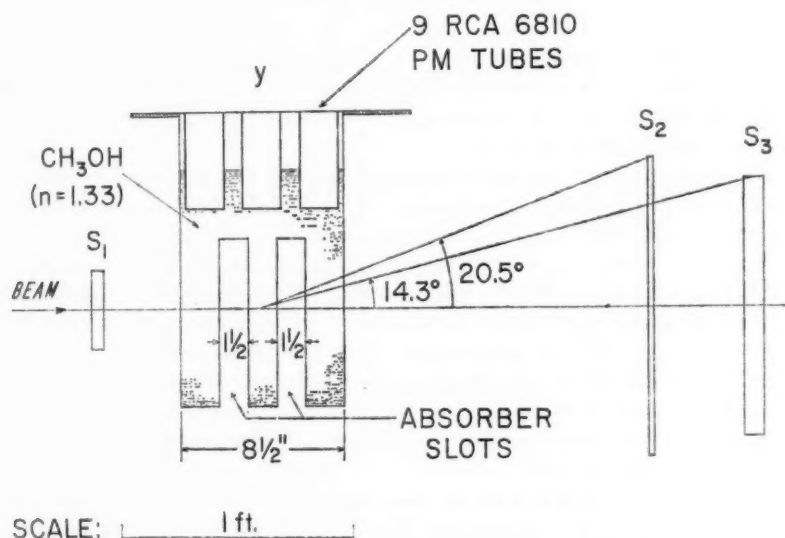
FIG. 4. Arrangement for measuring annihilation cross section and $\sigma_i(\theta)$. From (36).

With this apparatus one measures separately σ_a and σ_e (20°); the latter symbol means that the elastic scattering has occurred with an angle larger than 20°. A "good geometry" arrangement which measures σ_t is shown in Figure 5 (43). The data accumulated with these or other methods are shown in Tables V and VI. The errors quoted are only statistical. The whole subject is in a very early stage of development and the picture we have thus far is a sketchy one. Moreover, there are some features of the experimental results obtained thus far which look suspicious; in particular, the ratio between the scattering and total cross section in hydrogen should be reinvestigated.

It must be noted that most of the diffraction scattering is included in the data for beryllium and carbon. Namely, if one computes $\sigma_e(\theta)$ for $\theta = 0$, in-
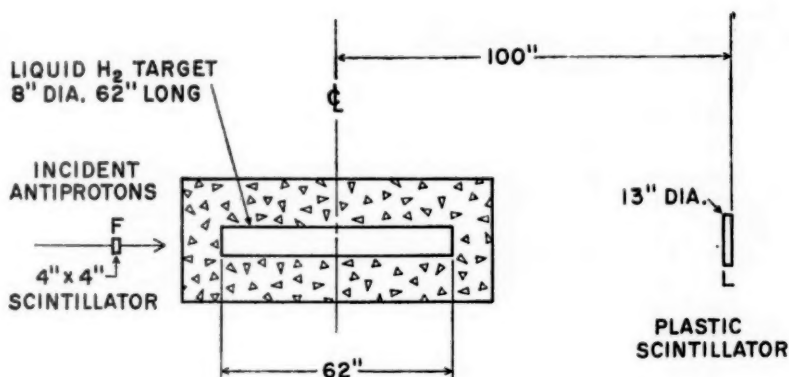
FIG. 5. Good geometry arrangement for measuring total $\bar{p} - p$ cross sections. From (43).

cluding all diffraction, the cross sections are increased by about 10 per cent. In the data for oxygen, copper, silver, and lead, diffraction scattering is practically excluded because $\theta \geq 14°$.

In Table V the data at 450 Mev have been obtained by investigation of H_2O, D_2O, and liquid oxygen and by suitable subtraction procedures. The reason for this is that liquid hydrogen has a refractive index too small to be used in a Cerenkov counter to detect annihilation. The data "n" are a simple subtraction of D_2O and H_2O observations. However, a large "Glauber correction" (58) is necessary in order to take into account the shielding of the neutron by the proton in the deuteron. The extent of this correction is somewhat uncertain (20, 58). The data n are corrected values.

The data on hydrogen give the puzzling result that if the data in good geometry are compared with the data at 450 Mev which are in poor geometry, there is no difference in cross section to account for any diffraction scattering. This point needs further experimental investigation.

The salient fact emerging from all these observations is that the cross sections which are obtained for all processes involving antiprotons are large

(37). There have been many theoretical papers on the interpretation of the $\bar{p}$ cross sections. At present the most promising line of approach to the interpretation of the experimental results seems to be a theory of Ball & Chew [12; see also 69, 73, 108] which accounts for the large $p\bar{p}$ and $n\bar{p}$ cross sections. Combination of their nucleon-antinucleon results with the optical

TABLE V

ANTIPROTON NUCLEON CROSS SECTIONS (IN MILLIBARNS)

T Mev	θ degrees	$\sigma_s(\theta)$	σ_a	σ_c	$\sigma_t(\theta)$ ‡	σ_t proton*†	σ_t neutron*†	Reference
H 20–230	5	71 ± 25	$\leq 86 \pm 45$					60
150	0	58 ± 11						3
133	0	72 ± 10		10 ± 3	166 ± 8	28	54	41
190	0				135 ± 16	25	45	41
197	0	64 ± 8		11 ± 3	152 ± 7	25	44	41
265	0	50 ± 7		8_{-3}^{+6}	124 ± 7	24	37	41
300	0				104 ± 14	23	35	43
333	0	49 ± 5		7 ± 2	114 ± 4	23	34	41
450	14	15 ± 12	89 ± 7	10 ± 6	104 ± 8	(25)	33	36
450	20	17 ± 12			102 ± 8	(24)	33	36
500	0				97 ± 4	30	35	43
700	0				94 ± 4	45	35	43
D 450	14		135 ± 7		174 ± 8	(54 ± 2)	—	36
450	20				172 ± 8	(45 ± 2)	—	36
"n" 450	14		46 ± 8		70 ± 8	(29 ± 1)		36
450	20				70 ± 8	(21 ± 1)		36
n 450	14		74		113			36
450	20		74		113			36

* From the compilations of Beretta, L., Villi, C., and Ferrari, F., *Nuovo cimento*, **12**, Suppl., 499 (1954); Djelepov, V. P., and Pontecorvo, B., *Atomnaya Energ.*, **3**, 413 (1957).

† Numbers in parenthesis directly measured [see (36)].

‡ $\sigma_t(\theta) = \sigma_a + \sigma_c + \sigma_s(\theta) + \sigma_i$; for $\theta = 14°$ or larger most of the diffraction scattering is not counted in $\sigma_t(\theta)$.

model theory will account for the antiproton cross sections in complex nuclei.

The Ball-Chew model starts from an analogy with nucleon-nucleon scattering. There a model with a repulsive core of $(1/3)(\hbar/m_\pi c)$ radius and a pion cloud surrounding it is assumed and has been shown by Gartenhaus (54) and by Signell & Marshak (99) to give reasonably good agreement with experi-

TABLE VI

$\bar{p}$-Complex Nuclei Cross Sections (in Millibarns)

Target	T (Mev lab)	θ degrees	$\bar{p}$			$\bar{p}^+$	$\sigma_r\bar{p}/\sigma_r\bar{p}^+$	References
			$\sigma_r(\theta)$	σ_a	$\sigma_t(\theta)$	$\sigma_r(\theta)$		
Be	500	2.57			460			43
	500	0			484 ± 60			43
	700	3.65			367			43
	700	1.90			416			43
	700	0			425 ± 50			43
C	700	25.0	436 ± 19					43
	700	2.64			575 ± 59			43
	700	0			657 ± 79			43
	300	3.55	568 ± 102		618 ± 111			43
	300	0			655 ± 130			43
O	457	14	556 ± 10	453 ± 9		292 ± 2		2
	457	20	517 ± 10			246 ± 2		2
	457	0	590 ± 12			340 ± 4	1.74 ± 0.04	2
Cu	411	14	1240 ± 82	1040 ± 61		719 ± 5		2
	411	20	1220 ± 88			640 ± 4		2
	411	0	1260 ± 91			880 ± 10	1.44 ± 0.11	2
Ag	431	14	1630 ± 170	1500 ± 157		1052 ± 6		2
	431	20	1640 ± 183			924 ± 6		2
	431	0	1635 ± 188			1170 ± 12	1.39 ± 0.16	2
Pb	436	14	2850 ± 225	2010 ± 182		1662 ± 36		2
	436	20	2680 ± 254			1461 ± 10		2
	436	0	3005 ± 275			1845 ± 40	1.62 ± 0.16	2
	650		2330 ± 285					43

ment. The nature of the hard, repulsive core is unaccounted for from a pion-theoretical point of view and must be considered as a phenomenological hypothesis, whereas the pion cloud can be treated from the point of view of the Yukawa interaction with due refinements. For a nucleon-antinucleon system the hard, repulsive core is replaced by an absorbing core. This is motivated by theory and justified by the large experimental annihilation cross section. Any antiproton which overlaps even slightly with the core seems to undergo annihilation. This core is surrounded by a meson cloud charge conjugate to the meson cloud surrounding a proton, and the interaction between proton and antiproton can be calculated by the same methods as the proton-proton cross section, provided one remembers that the "mesonic charge" of the antiproton and of the proton are opposite. Thus forces derived from the exchange of an even number of pions have the same sign in both cases, but forces derived from the exchange of an odd number of pions have opposite signs in the two cases. This program is carried out by introducing an interaction energy

$$V_c + V_{LS}(L \cdot S) + V_T S_{12} \qquad 5.$$

containing a central, spin-orbit, and tensor part. From this one obtains an "equivalent potential" for the eigenstates of the total angular momentum including centrifugal repulsion:

$$V \begin{Bmatrix} l = J+1 \\ l = J-1 \end{Bmatrix} = V_C - \frac{3}{2} V_{LS} - V_T + \frac{J(J+1)+1}{Mr^2}$$

$$\pm \left[\left(\frac{2J+1}{Mr^2} - \frac{2J+1}{2} V_{LS} - \frac{3V_T}{2J+1} \right)^2 + \frac{36J(J+1)}{(2J+1)^2} V_T^2 \right]^{1/2} \quad 6.$$

$$V(l = J) = V_C - V_{LS} + 2V_T + \frac{J(J+1)}{Mr^2} \cdot \quad 7.$$

With these potentials one constructs the phase shifts and the penetration coefficients for the partial waves.

The V_C, V_{LS}, V_T are chosen following Gartenhaus (54) and Signell & Marshak (99) for the V_{LS} part, but introducing the sign changes required by the change of sign of the interaction energy corresponding to the exchange of one pion. The calculation of Ball and Chew is limited to s, p, and d waves, i.e., to energies <150 Mev, but even so it gives very interesting results as shown in Table VII.

TABLE VII

THEORETICAL CROSS SECTIONS FOR NUCLEON ANTINUCLEON INTERACTION IN
MB AT 140 MEV (LAB) ACCORDING TO (30)

	$p\bar{p}$	$n\bar{p}$	pp	np
Absorption	73	69		
Scattering	74	79	29	60
Charge exchange	21			

The limitation in energy of the present calculations derives first from the nonrelativistic approximations made, as for instance the use of a potential; and second from the fact that in order to extend the theory to higher energies details near the boundaries of the black zone, which are unknown, become important. The reason for this is that the total potential surrounding the core is composed of a centrifugal part and a part originating from the nuclear forces. The sum of the two forms a barrier which is very wide and flat on the top. This barrier can be treated very adequately with the WKB method and for a given s, p, or d partial wave usually gives either perfect transparency or perfect opacity, fairly independently of any reasonable core radius. For higher angular momenta these circumstances no longer obtain.

The Ball-Chew model also can be used to calculate angular distributions for elastic scattering. These have been computed by Fulco (53) and show a peak in the forward direction (Fig. 6), very different from the np angular distribution. Experimental results, although not very abundant yet, seem to confirm this feature of the model, which is mainly due to the diffraction scattering connected with the annihilation (3). It is necessary to check further the prediction of this type of model against experiment, but at this time it seems to offer great promise of accounting for the facts.
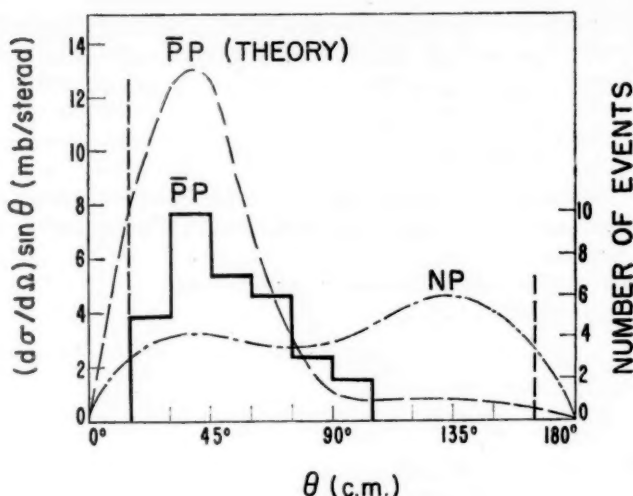
FIG. 6. Angular distribution in $p\bar{p}$-scattering. Theoretical curve from (53) at 140 Mev. Experimental results from (3).

In the same trend of ideas Koba & Takeda (73) conclude that at very large energies ($\lambda \ll a$), $\sigma_a = \sigma_e = \pi a^2$ where a is the radius of the black core, but at lower energies $\sigma_a = \pi(a + \lambda)^2$. Even considering waves of high angular momentum l, the ratio between annihilation and scattering cross sections is limited by the inequality:

$$\sigma_t^{(l)} \leq \frac{4\pi}{k^2}(2l + 1)\frac{\sigma_e^{(l)}}{\sigma_t^{(l)}} \qquad\qquad 8.$$

where $\sigma^{(l)}$ is the cross section for the lth partial wave. Thus, for a given total cross section, a small ratio of elastic to total cross section can be obtained only for large values of l.

Other calculations on the same subject have been performed by Lévy (80). In some respects these resemble Ball and Chew's work, but they try to take into account terms in which many pions, not only one or two, are involved [see also (102)]. They have been further developed by Gourdin et al. (64).

Inelastic collisions in which pions are generated, without annihilation of the antinucleon, have been considered by Barshay (15). He has established selection rules and angular distributions to be expected in such collisions.

In addition to the detailed considerations discussed above there are several relations between elastic cross sections which are independent of detailed models and require only charge independence of nuclear forces; such are found in (9, 31, 74, 83, 94). As examples we mention:

$$\frac{d\sigma}{d\omega}(0^0)_{p\bar{p}\to n\bar{n}} \geq \left(\frac{k}{4\pi}\right)^2\{\sigma_t(\bar{p}n) - \sigma_t(p\bar{p})\}^2 \qquad\qquad 9.$$

where $\sigma_{p\bar{p}\to p\bar{n}}$ means the charge exchange scattering cross section and:

$$\sigma_e(p\bar{p} \to p\bar{p}) + \sigma_c(p\bar{p} \to n\bar{n}) \geq \tfrac{1}{2}\sigma_e(\bar{p}n \to \bar{p}n) \qquad 10.$$

$$\sigma_e(p\bar{p} \to p\bar{p}) = \tfrac{1}{4}\left| a_{if}^{(0)} + a_{if}^{(1)} \right|^2 = \sigma_e(n\bar{n} \to n\bar{n}) \qquad 11.$$

$$\sigma_c(p\bar{p} \to n\bar{n}) = \tfrac{1}{4}\left| a_{if}^{(0)} - a_{if}^{(1)} \right|^2$$

$$\sigma_e(\bar{p}n \to \bar{p}n) = \left| a_{if}^{(1)} \right|^2 = \sigma_e(\bar{n}p - \bar{n}p)$$

where $a_{if}^{(1)}$ is the scattering amplitude for $T=1$ (triplet) between initial and final states and $a_{if}^{(0)}$ is the scattering amplitude for $T=0$ (singlet) between initial and final state.

Relations 11 give rise to triangular inequalities:

$$\left| (\sigma(p\bar{p} \to \bar{n}n))^{1/2} - (\sigma(\bar{p}n \to \bar{p}n))^{1/2} \right|$$
$$\leq (\sigma(p\bar{p} \to p\bar{p}))^{1/2} \leq (\sigma(p\bar{p} \to n\bar{n}))^{1/2} + (\sigma(\bar{p}n \to \bar{p}n))^{1/2} \quad 12.$$

$$\left| (\sigma(p\bar{p} \to n\bar{n}))^{1/2} - (\sigma(p\bar{n} \to p\bar{n}))^{1/2} \right|$$
$$\leq (\sigma(\bar{p}n \to \bar{p}n))^{1/2} \leq (\sigma(p\bar{n} \to n\bar{p}))^{1/2} + (\sigma(p\bar{p} \to p\bar{p}))^{1/2} \quad 13.$$

$$\left| (\sigma(\bar{p}n \to \bar{p}n))^{1/2} \to (\sigma(p\bar{p} \to p\bar{p}))^{1/2} \right|$$
$$\leq (\sigma(p\bar{p} \to n\bar{n}))^{1/2} \leq (\sigma(p\bar{n} \to p\bar{n}))^{1/2} + (\sigma(p\bar{p} \to p\bar{p}))^{1/2}. \quad 14.$$

These relations are valid for the differential cross sections as well as for the total cross sections.

At present there are not enough data to evaluate the scattering amplitudes. Pomeranchuk (94) has pointed out that at high energies we might expect:

$$\left| a_{if}^{(1)} - a_{if}^{(0)} \right| \ll \left| a_{if}^{(1)} \right| \qquad 15.$$

$$\left| a_{if}^{(1)} - a_{if}^{(0)} \right| \ll \left| a_{if}^{(0)} \right|. \qquad 16.$$

These interesting inequalities are justified as follows: for each initial state i of definite angular momentum and isotopic spin the scattering matrix to a given final state f is subject to the sum rule

$$\sum_f \left| S_{fi} \right|^2 = 1. \qquad 17.$$

The amplitudes for elastic scattering in $T=0$ or $T=1$ states are $a_{if}^{(0)} = (S_{ii}^{(0)} - 1)$ or $a_{if}^{(1)} = (S_{ii}^{(1)} - 1)$, whereas all other amplitudes are S_{fi} for $f \neq i$. At high energies the S_{fi} become small because there are many channels and the sum rule forces each individual S_{fi} to be small; however the elastic scattering amplitudes stay comparable to unity because they are equal to $S_{ii} - 1$. As a consequence the amplitudes for elastic scattering $a_{if}^{(1)}$ and $a_{if}^{(0)}$ each tend separately to -1, whereas their difference tends to zero.

Proceeding from the nucleon-nucleon to the nucleon-nucleus processes, an early paper by K. A. Johnson (70) using lowest order perturbation theory predicted elastic cross sections of the order of 0.1 geometric. Duerr, M. H. Johnson & Teller (47, 71), on the basis of a special nonlinear theory of nuclear forces, predicted a total cross section of the order of or larger than the geometrical one. This theory now seems untenable (46), but it foresaw the experimental results.

The most successful treatments of the nucleon-nucleus interactions have been obtained with the optical model (2, 57, 84, 91, 93). In its simplest form one gives to nuclear matter a density distribution using, for example, data from electron scattering. Moreover, nuclear matter has absorption and scattering coefficients which can be connected with the nucleon-antinucleon scattering and annihilation. With such a nuclear model, using geometrical optics, the scattering and absorption by a nucleus are calculated. For a uniform spherical density distribution of radius R the reaction cross section of the nucleus is given by a literal application of geometrical (110) optics as

$$\sigma_r = 2\pi \int_0^R (1 - e^{-2Ks})b db = 2\pi \int_0^R (1 - e^{-2Ks})s ds \qquad 18.$$

where $s^2 = R^2 - b^2$, b is the impact parameter with respect to the center of the nucleus, and the absorption coefficient K is given by

$$K = 3A\bar{\sigma}/4\pi R^3 \qquad 19.$$

with A the mass number and $\bar{\sigma}$ the average total nucleon-antinucleon cross section. A slight refinement of this approach takes into account the finite range of the interaction and the nuclear density distribution. The density distribution used is generally of the form

$$\rho(r) = \frac{\rho_0}{1 + \exp\left[(r - R)/a\right]} \cdot \qquad 20.$$

The parameters have been chosen in (2) with the following values

$$R = r_0 A^{1/3} = 1.08 A^{1/3} \times 10^{-13} \text{ cm.}; \, a = 0.57 \times 10^{-13} \text{ cm.} \qquad 21.$$

The results show good agreement with experiment.

In a similar fashion one may assume a complex potential (57)

$$V(r) = \frac{V + iW}{1 + \exp\left[(r - R)/a\right]} \qquad 22.$$

and calculate the cross sections. Glassgold has obtained good agreement with the present experimental data taking a potential of this form and $a = 0.65 \times 10^{-13}$ cm., $R = 1.30 \, A^{1/3} 10^{-13}$ cm. He has calculated explicitly three cases corresponding to protons and antiprotons as shown in Table VIII.

TABLE VIII

OPTICAL MODEL POTENTIALS

(57) (For all three cases the radius parameter is $r_0 = 1.30$ and the diffuseness $a = 0.65$ 10^{-13} cm.)

Projectile	V (Mev)	W (Mev)
p	− 15	−12.5
$\bar{p}$	− 15	−50
$\bar{p}'$	−528	−50

Calculations with a deep potential well ($\bar{p}'$) as required by the hypothesis of Duerr and Teller seem hardly compatible with the experimental results.

Elastic collisions with small deflections give rise to interesting interference phenomena between coulomb and nuclear scattering. These have been observed in photographic emulsions by G. Goldhaber & Sandweiss (61). They considered scattering down to a projected angle 1.5° and compared the result with that calculated from a black sphere of radius R and a coulomb field. The radius R was assumed to be 1.64 $A^{1/3}10^{-13}$ cm. and corresponds to the annihilation cross section. The agreement with experiment is good. Similar calculations performed with the potentials used by Glassgold also agree with experiment and give further support for his choice $\bar{p}$ of parameters as distinct from the choice $\bar{p}'$.

A more fundamental approach to the determination for the constants of the optical model potential is to connect them to the nucleon-nucleon potential as indicated by Riesenfeld & Watson (111). In the specific case of the antiprotons, the Ball-Chew nucleon antinucleon potential may be used. Some successful steps in that direction have been initiated (3).

The annihilation process.—Information concerning the annihilation process is derived mostly from annihilations in photographic emulsions and bubble chambers (3, 6, 14, 33, 34, 35, 52, 68). From the technical side the most important development for observing the annihilation in photographic emulsions has been the preparation of beams in which the ratio of antiprotons to undesired particles is increased from the value obtained by a simple selection of momentum and direction from the Bevatron target. Such improved beams will be called "purified." In an unpurified beam the ratio of pions to antiprotons is in the range between 5×10^5 to 5×10^4, depending on the momentum selected. In order to have the $\bar{p}$ tracks easily distinguishable from minimum tracks at the entrance of the stack, it is necessary to keep the momentum below about 700 Mev/c. At this momentum the $\pi/\bar{p}$ ratio is about 5×10^5. Increase of the momentum at the entrance is undesirable, not only for the reason given above, but also to keep the stack length manageable.

Efforts to purify the beam were made at an early date by Stork *et al.* (100) but had meager success because the large absorption cross section for antiprotons, unknown at the time, spoiled the performance of the apparatus.

Later a method was devised by which a beam of selected momentum is passed through beryllium absorbers, out of which the different particles emerge with different momenta. A second momentum selector refocuses the different masses in different spots. The antiprotons are accompanied by a background of about 5×10^4 spurious particles per antiproton, which is a gain of a factor 10 in the ratio of antiprotons to background for the momentum considered. Moreover, the background particles are almost entirely electrons and mu mesons coming from the pion decay, with only a few per cent pions left. They interact only weakly in the plates and are much less disturbing than the original pion background (35).

The problem of purification of the beam is encountered also in the use

of bubble chambers. An arrangement (3) has been used in which a purification similar to the one described in (35) is combined with an electronic command of the flashing of the lights of the bubble chamber, limiting it to the cases when an antiproton detector signals the entrance of an antiproton in the bubble chamber.

The purification problem has also been attacked by a combination of electric and magnetic fields in a Wien-type velocity filter. This velocity selector is used in conjunction with momentum analyzers to separate particles of different mass. There are at present two versions of these separators (41, 89) which show great promise.

The annihilations in which the antiproton reaches the end of its range and is at rest will be discussed first. Actually, with the present photographic technique this means that the kinetic energy of the antiproton is <10 Mev.

Up to now it has not been possible to recognize effectively the partner in the annihilation in photographic emulsions. A few stars have been observed with no nucleons and an even number of mesic prongs, which could be attributed to $p\bar{p}$ annihilation, but no certain assignment is yet possible. At this time approximately 220 annihilation stars have been observed and analyzed in photographic emulsions. There are also about 500 stars in propane (3) and 50 in hydrogen (68) but their analysis is incomplete as yet. One hundred and twenty-seven of the photographic emulsion annihilations occurred at rest and 93 annihilations occurred in flight. A typical star is shown in Figure 7.
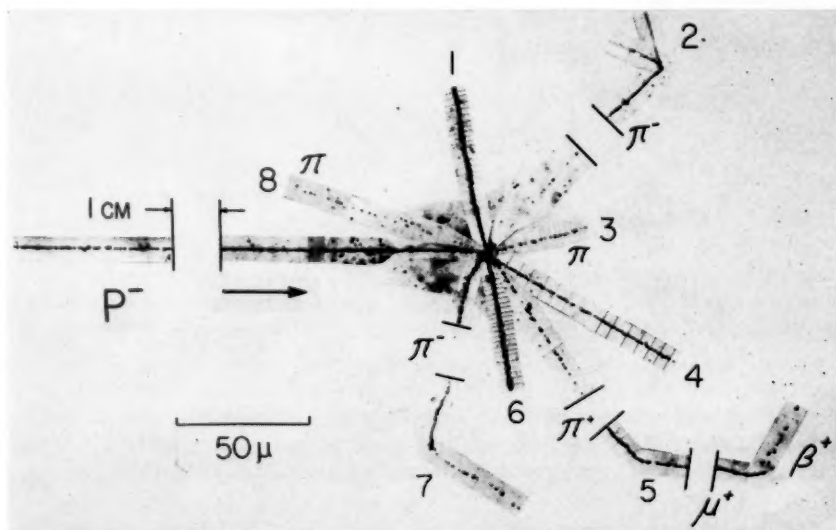
FIG. 7. An annihilation star (36) showing the particles as numbered.

No.	1	2	3	4	5	6	7	8
Identity	p?	π^-	π?	p	π^+	H^3(?)	π^-	π
T (Mev)	10	43	175	70	30	82	34	125

Total visible energy 1300 Mev. Total energy release >1400 Mev.

The fragments observed are π mesons, protons, light nuclei such as deuterons and α-particles, and sometimes, though rarely, K mesons. The maximum number of charged pions in a star thus far observed is six. The maximum number of charged nuclear particles thus far observed is 16. A distribution of the multiplicity of the charged pions is shown in Figure 8.
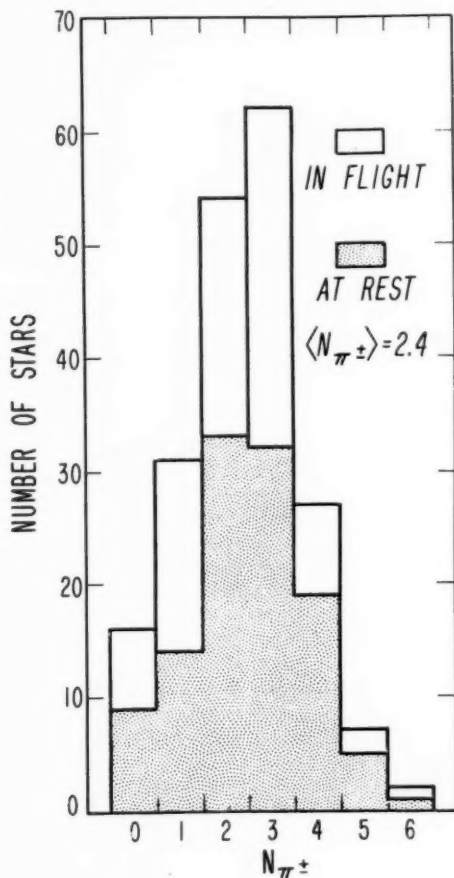
FIG. 8. Number of charged pions per annihilation star in photographic emulsions. Stars in flight give $\langle N_{\pi\pm}\rangle = 2.29 \pm 0.28$. Stars at rest give $\langle N_{\pi\pm}\rangle = 2.50 \pm 0.26$. These numbers are not corrected for scanning inefficiency (see text). From (35).

The following discussion is concerned with the experimental information on the visible energy release. The energy available is: $2\ mc^2 + T - B = W$, where T is the kinetic energy in the center of mass system and B the small (8 Mev) binding energy of the annihilating nucleon. In order to orient the reader on the apportioning of W, reference is made to Figures 10 and 11,

where the fraction of the visible energy going into pions, nucleons, or light nuclei is indicated. The few cases in which K mesons have been positively recognized are excluded from this figure.

Looking more in detail one finds a spectrum of pion energy as in Figure 9 with an average $T_\pi = 199 \pm 18$ Mev for charged pions. For the pions coming to rest in the stack ($T_\pi < 100$ Mev) it is also possible to determine the sign, and one finds a ratio of π^+ to π^- of 0.45 ± 0.1 (35). This number is smaller
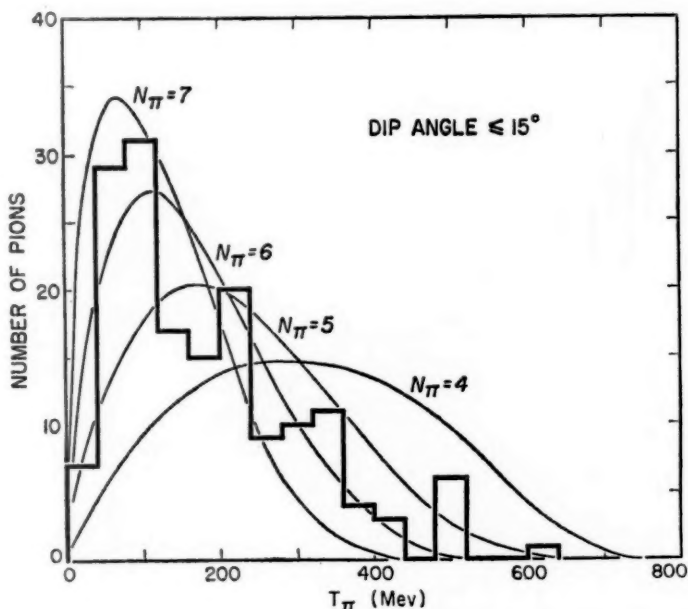
FIG. 9. Distribution of the observed kinetic energy of charged pions emitted in annihilation stars in nuclear emulsions. The curves marked $N_\pi = 4$, etc. are energy distributions obtained by the statistical method on the hypothesis that the average number of pions emitted is 4, 5, etc. Note that the experimental results agree with an average number of pions emitted lying between 6 and 7. From (35).

than one would expect on a naive view of the annihilation process which takes into account the n/p ratio in the nuclei and the conservation of isotopic spin (14, 92). It is, however, to be expected that this ratio is affected by the fact that the observations are limited to a low-energy region.

At this point one might try to estimate the ratio of the energy carried away by charged pions to that carried away by neutral pions. Figures 10 and 11 give a ratio of one to one for the energy carried away by all charged particles to that carried away by neutral particles. Neutrons in secondary processes are known to carry away about twice as much energy as charged nuclear fragments; moreover the efficiency for detecting charged pions is

estimated to about 0.9. Correcting for these factors the best estimate of the
ratio of the energy carried away by charged pions to that carried away by
neutral pions is 1.8.

It is now possible to calculate the average number of pions emitted per
annihilation. The observed average charged pion multiplicity is 2.7 ± 0.2
pions per star. This figure contains a 10 per cent correction for scanning in-
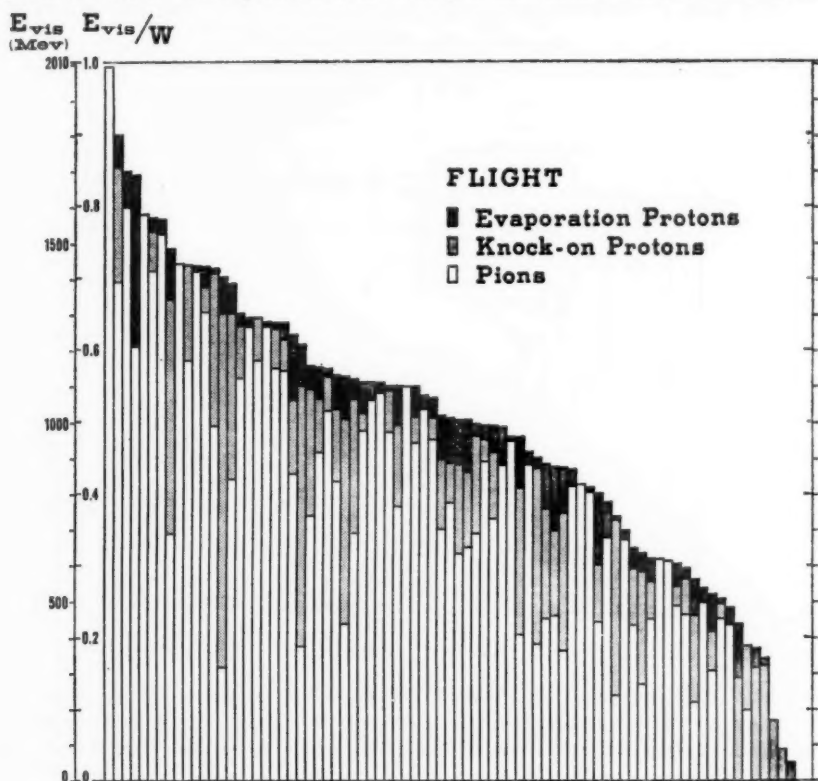
FIG. 10
(See Fig. 11 for caption.)

efficiency. Assuming that equal numbers of pions of each charge are produced
in average in the annihilation process (see later), the number of pions
emitted should be $3/2 \times (2.7 \pm 0.2)$ or 4.0 ± 0.3. To this number must be
added the pions reabsorbed by the nucleus in which the annihilation oc-
curred. Their energy is manifested by the nuclear fragments; they will be
called "converted pions." The number of converted pions is approximately
1.3, as can be inferred from the fact that the nuclear fragments carry away
an energy corresponding to 1.3 times the average total energy of a pion. In
this estimate the energy carried away by the visible nuclear fragments is

multiplied by a factor 2.6 in order to take into account the energy carried by neutrons. By this method one thus arrives at an estimate of the average total number of pions released on annihilation, $\overline{N}_\pi$, of 5.3 ± 0.4.

A similar result also is reached if it is assumed that in annihilation the neutral pions have the same energy spectrum as the charged ones. Dividing the total energy available on annihilation by the average energy per pion (observed 338 Mev) one obtains 5.8 ± 0.3 for the number of pions. This is to
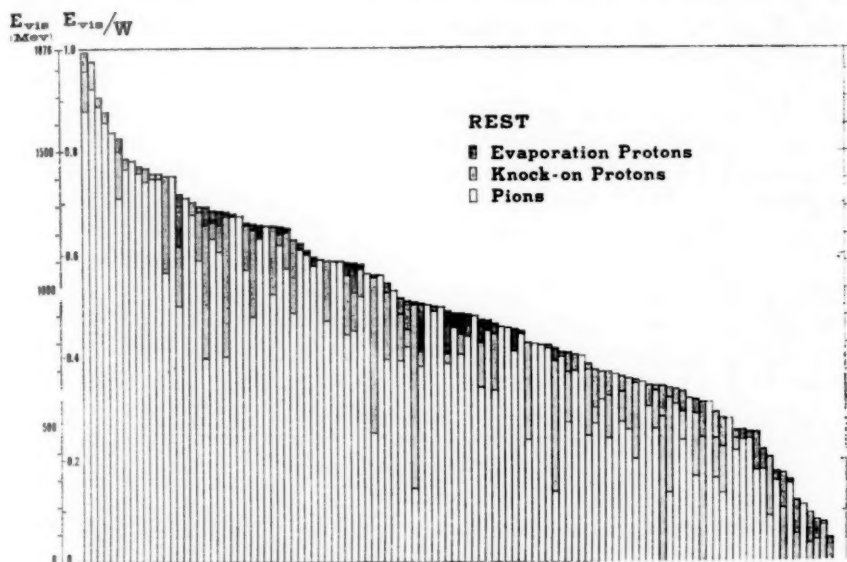
FIG. 11

FIG. 10 and 11. Visible energy in annihilation stars in photographic emulsions. Evaporation protons have $T < 30$ Mev by definition. Knock on protons have $T > 30$ Mev by definition. W is the total energy of the antiproton at annihilation. Note that stars in flight compared with stars at rest have a larger fraction of the energy in nucleons. From (35) and private communication.

be considered as an upper limit because the pions lose some energy before emerging from the nucleus and a better estimate is obtained by considering for each pion an average energy at formation of 360 Mev, and also the average energy going into K-mesons. With these corrections $\overline{N}_\pi = 5.3 \pm 0.5$.

The great majority of the annihilations in photographic emulsions occur in complex nuclei, and if the annihilation occurred deep inside the nucleus, the escaping pions would traverse the nucleus. The mean free path of pions of an energy of 180 Mev in nuclear matter is estimated to be about 10^{-13} cm. [see (81)], i.e., small compared with the nuclear radius, and the escaping pions would be "converted" into nucleons. The fact that only about one in

six of the pions is converted suggests that the annihilation occurs in the very peripheral parts of the nuclei and that most of the resulting pions escape without hitting the nucleus. The large nuclear cross sections are also evidence for this interpretation. Additional support for it comes from the observation that the number of pions "converted" in annihilations of antiprotons in flight is larger by about one than in the annihilations at rest as shown in Figures 10 and 11. This effect is interpreted as due to the deeper penetration of the antiproton in flight into the nucleus, compared to the antiproton at rest. An estimate of the order of magnitude of the mean life of the antiproton in nuclear matter, based on these considerations, is $\sim 2 \times 10^{-24}$ sec.

No angular correlations of the annihilation pions have been observed thus far, although one could perhaps expect that the nucleus should project a shadow and thus the pions might have a tendency to stay in a hemisphere. However, a pion-pion interaction might counterbalance this effect and a clarification of these questions will possibly come from the study of $\bar{p}$ annihilation in hydrogen where the shadow effect is obviously absent.

At the present time there are no separated examples of annihilations in different materials except for unanalyzed hydrogen stars. In propane some of the other stars are certainly due to carbon because they exhibit nucleons among their fragments, or have a balance of charge different from zero. Some might be due to $p\bar{p}$ annihilation but there is no proof that this is the case. For the stars produced by antiprotons coming to rest, there is a selective capture on the part of nuclei different from hydrogen similar to what occurs in the pion capture. The slowing down and capture of antiprotons are discussed theoretically by Bethe & Hamilton (19).

It is interesting to consider the possibility of "no prong" stars (95). They can be produced by charge exchange, in which the antiproton hits a proton and transforms into a neutron-antineutron pair, or by annihilation into neutral pions only. Both processes are rare and in photographic emulsions represent less than 1 per cent of the terminal events.

K-mesons have been found among the annihilation products in 3.5 ± 1.5 per cent of the photographic stars, and it is estimated that they carry away an average 50 ± 25 Mev per star. Λ-particles have also been found among the annihilation products.

On the theoretical side electromagnetic annihilation will be discussed briefly: it is similar to the electron positron (44) annihilation, but has not yet been observed. This is not surprising because it competes very unfavorably against the mesic annihilation. For instance, Brown & Peshkin (26) calculate for the annihilation in flight in the nonrelativistic limit a cross section

$$\sigma = \pi \left(\frac{e^2}{mc^2} \right)^2 \frac{c}{v} F(\lambda) \simeq 3.10^{-30} c/v \text{ cm.}^2 \qquad 23.$$

The factor $F(\lambda)$ takes into account the anomalous magnetic moment of the proton λ and has the numerical value 38.5. On the other hand, the mesic

annihilation cross section is of the order of 10^{-25} cm.[2] The mixed annihilation, into γ-rays and mesons, is also very improbable. It has been considered by Michel (86).

For the purely mesic annihilation, the most important practically, many authors (1, 7, 8, 19, 56, 59, 69, 78) have established selection rules based on the conservation of angular momentum, parity, charge conjugation, and isotopic spin. It is possible to analyze the phenomenon with various degrees of detail. As an example, Table IX compiled by Lee and Yang and containing the main results is reproduced. In general, a given state can produce different numbers of pions; these numbers, however, are either all even or all odd. Thus, states of spin one produce only even numbers of pions. An interesting and exact consequence of charge independence concerns the average number of pions produced in annihilation of an antiproton on a proton and on a neutron, such as would be observed in annihilation against a nucleus containing the same number of neutrons and protons (55). We have then

$$\langle N(\pi^+) \rangle + \langle N(\pi^-) \rangle = 2 \langle N(\pi^0) \rangle. \qquad 24.$$

Selection rules for the emission of K-particles on annihilation have also been considered by Goebel (59) and Gatto (56), and selection rules for the formation of pions in nonannihilating collisions of antiprotons and nuclei have been given by Barshay (15) as previously mentioned.

Apart from selection rules, repeated attempts have been made to apply Fermi's statistical theory (14, 17, 49, 101) to the nucleon-antinucleon annihilation. Using the theory in its simplest form, disregarding conservation of angular momentum and K-meson production, one obtains the results on the multiplicity of the mesons given in Table X.

The only arbitrary parameter entering in the calculation is the interaction volume Ω which is expressed in units of $(4/3\pi)(\hbar/m_\pi c)^3$. One would expect that the volume Ω should be near one, because the interaction range between nucleon and antinucleon is expected to be close to the pion Compton wavelength. The fact that agreement with experiment is obtained instead for Ω close to 10 needs some explanation. One of the most interesting and convincing ideas put forward is due to Koba & Takeda (73). They consider the nucleon and antinucleon surrounded by the pion cloud: on annihilation the bare nucleons destroy each other very swiftly, in a time of the order of $\hbar/2mc^2$, giving rise to a meson multiplicity corresponding to a value of Ω near one; but the mesons of the cloud at the moment of annihilation are also released, because the annihilation is a nonadiabatic process, with respect to the periods of the motions of the pions in the cloud which are of the order of $\hbar/E_\pi$ where E_π is the total energy of the pion in the cloud. E_π is estimated to be approximately 350 Mev from the energy of the annihilation pions. The number of pions in the cloud is estimated to be 1.3 per nucleon or antinucleon. In the annihilation 2.6 pions in average are interpreted as coming from the cloud, the remainder are interpreted as coming from the core annihilations. The core annihilation is treated by the statistical method,

TABLE IX

SELECTION RULES FOR $\bar{p}+p\to N\pi$ OR $\bar{q}+n\to N\pi$

State	Spin parity	C	T	G	$2\pi^0$	$\pi^+ + \pi^-$	$3\pi^0$	$\pi^+ + \pi^- + \pi^0$	$4\pi^0$	$\pi^+ + \pi^- + 2\pi^0$	$2\pi^+ + 2\pi^-$	$5\pi^0$	$\pi^+ + \pi^- + 3\pi^0$	$2\pi^+ + 2\pi^- + \pi^0$
$^1S_0$	$0-$	$+$	0	$+$	×	×	−	−				−	−	−
			1	−	×	×				−	−			
$^3S_1$	$1-$	−	0	−	×	−	×		×	−	−	×		
			−	$+$	×		×	−	×			×	−	−
$^1P_1$	$1+$	−	0	−	×	×	×		×	−	−	×		
			1	$+$	×	×	×	−	×			×		
$^3P_0$	$0+$	$+$	0	$+$			×	×				−	−	−
			1	−	−	−	×	×	−	−	−			
$^3P_1$	$1+$	$+$	0	$+$	×	×	−	−				−	−	−
			1	−	×	×				−	−			
$^3P_2$	$2+$	$+$	0	$+$			−	−				−	−	−
			1	−	−	−			−	−	−			

× means strictly forbidden; − means forbidden so far as the isotopic spin is a good quantum number.

T = isotopic spin, C = charge conjugation operator, G is a quantum number of special interest in the case of systems of zero nucleons. It corresponds to the operator $C\,e^{i\pi T_2}$ and for zero nucleons has the eigenvalues ± 1 as indicated in the table.

TABLE IX—(Continued)

SELECTION RULES FOR $\bar{p}+n\to N\pi$

State	Spin parity	T	G	$\pi^- + \pi^0$	$2\pi^- + \pi^+$	$\pi^- + 2\pi^0$	$2\pi^- + \pi^+ + \pi^0$	$\pi^- + 3\pi^0$	$3\pi^- + 2\pi^+$	$2\pi^- + \pi^+ + 2\pi^0$	$\pi^- + 4\pi^0$
$^1S_0$	$0-$	1	−	×			−	−			
$^3S_1$	$1-$	1	$+$		−	−			−	−	−
$^1P_1$	$1+$	1	$+$	×	−	−			−	−	−
$^3P_0$	$0+$	1	−	−	×	×	−	−			
$^3P_1$	$1+$	1	−	×			−	−			
$^3P_2$	$2+$	1	−	−			−	−			

× means strictly forbidden, and − means forbidden so far as the isotopic spin is a good quantum number.

TABLE Xa

DISTRIBUTION OF PION MULTIPLICITIES, ACCORDING TO FERMI MODEL, FOR
DIFFERENT INTERACTION VOLUMES (PRODUCTION OF K MESONS NEGLECTED).

N_π	Probability for annihilation into N_π pions (%)		
	$\Omega = 1$	$\Omega = 10$	$\Omega = 15$
2	6.4	0.1	0.0
3	63.7	5.6	2.3
4	24.6	21.7	13.4
5	5.0	44.0	40.6
6	0.3	23.7	33.1
7	0.0	5.1	10.6
Average No. of pions N_π	3.3	5.0	5.4

TABLE Xb

DISTRIBUTION OF PION AND K-MESON MULTIPLICITIES ACCORDING TO FERMI
MODEL, FOR DIFFERENT INTERACTION VOLUMES

N_K	N_π	Probability for annihilation into N_π pions and N_K K mesons (%)		
		$\Omega = 1$	$\Omega = 10$	$\Omega = 15$
0	2	3.8	0.0	0.0
	3	37.4	4.6	2.0
	4	14.5	17.9	11.8
	5	2.9	36.1	35.7
	6	0.2	19.5	28.9
	7	0.0	4.2	9.2
2	0	5.9	0.0	0.0
	1	26.7	3.3	1.4
	2	8.3	10.2	6.8
	3	0.3	4.1	4.1
	4	0.0	0.0	0.0
Average No. of pions N_π		2.4	4.5	5.0
Probability of producing a K-meson pair		41.2%	17.6%	12.3%

154   SEGRÈ

and using for the volume Ω the value $8/27$, corresponding to a radius $(2/3)(\hbar/m_\pi c)$ consistent with other values used in the calculation of cross sections, one obtains 2.2 pions on the average from the core annihilation. Thus, the total average multiplicity would be 4.8, to be compared with the experimental value 5.3 ± 0.5. The hypothesis is developed further in order to obtain not only the average number of pions, but also the distribution among different multiplicities. Moreover, the number of K-mesons present in annihilation, which seems smaller than what is predicted by a straightforward application of the statistical theory, agrees better with the Koba-Takeda mechanism. Even if the quantitative agreement with experiment is not perfect, the reviewer thinks that this theory has considerable merit.

Other authors have stressed the many factors that could affect the annihilation process and are neglected in the statistical theory: such factors are the pion-pion interaction (63), the conservation of angular momentum, the relativistic conservation of the center of gravity (79), and other selection rules which might tend to suppress certain multiplicities. Indeed, it is apparent by considering the sensitivity of the results to some details of the calculation (17, 18) that the statistical method cannot reasonably be expected to give quantitative results, as was emphasized by Fermi himself. Adjustment of the parameter Ω might compensate for the crudeness of the approximation. Intermediate theories such as that of Heisenberg and Landau, or modifications of the original Fermi theory introducing a temperature parameter (75, 107), have also been tried with improved agreement with experiment. Conservation of the I-spin combined with the statistical theory also gives predictions for the $\pi^-:\pi^+:\pi^0$ ratio (92).

For the case of low multiplicities Bethe & Hamilton (19) have made a detailed analysis for capture in light elements, establishing in which states the capture must occur in order to give certain results. They consider also the "nuclear Auger effect." An antiproton is captured in a light nucleus from an atomic orbit and goes into a nuclear orbit releasing energy which is taken up by a nuclear proton that is ejected in a way similar to that of the Auger electrons in x-ray phenomena. It is doubtful that this effect takes place to any appreciable extent, since annihilation is probably much faster and takes place before the Auger jump.

An ingenious application of the K multiplicity to measure the spin of the K-meson has been made by Sandweiss (96). In the formulae for the K average multiplicity the statistical weight $(2I_K+1)$ of the K-meson appears and it should be possible to distinguish $I_K=0$ from $I_K=1$ or more. The average number of K-mesons per annihilation is very imperfectly known: the limits are from 1 to 4 per cent. In any case they point to spin 0 for the K-meson.

Production.—The collisions in which antiprotons are produced are most probably either of the type : $p+p\to3p+\bar{p}$ or $\pi^-+p\to p+n+\bar{p}$, with all the variations compatible with charge conservation. In the observations up to now it is not known which of the two types of processes is most effective. Experimentally there are only very uncertain data: some measurements have

given 38×10^{-30} cm.^{2} ster.$^{-1}$ (Bev/c)$^{-1}$ per copper nucleus for the production in the forward direction at $\bar{p}$ momentum of 1.2 Bev/c when the target is bombarded with 6.1 Bev. protons (2).

A few comparisons between different targets show that for the same conditions protons are about as effective as carbon nuclei in producing antiprotons. Considering that the Fermi momentum should also enhance appreciably the production in carbon, the conclusion must be drawn that the nucleons in the carbon nucleus are very ineffective in giving antiprotons. The most natural explanation is the great absorption probability for antiprotons formed inside of the nucleus.

Some calculations which take into account mainly phase-space factors in the p-nucleus collision giving rise to antinucleons are reported in (49) and give $\sigma = 0.6 \times 10^{-26}(\epsilon/mc^2)^{7/2}$ cm.^{2} Near threshold the yield of antiprotons should grow as $\epsilon^{7/2}$, where ϵ is the center-of-mass energy above threshold, if they are formed by pn collisions, or as $\epsilon^{9/2}$ if they are formed by pp collision. The extra factor ϵ in this case comes from the necessity of putting one of the outgoing protons in a p state.

Attempts have been made to derive production cross sections near threshold from pion theory: Thorn (104) has for the reactions: (a) $p + p \to \bar{p} + 3p$ a cross section $1.4 \times 10^{-29}(f^2/4\pi)^4(\epsilon/mc^2)^{9/2}$ cm.^{2}, and for (b) $p + n \to n + 2p + \bar{p}$ a cross section $5.4 \times 10^{-29}(f^2/4\pi)^4(\epsilon/mc^2)^{7/2}$ cm.^{2} with $f^2/4\pi = 15$. Similar calculations by Fox (50) and McConnell (85) are based on an unlikely coupling. Calculations of some features of the production such as energy and angular distribution based on phase space considerations only are to be found in (33).

More recently Barasenkov et al. (13) have treated the antinucleon production problem by the statistical method following the idea of Belenky which considers a virtual particle corresponding to a pion and nucleon in the $J = 3/2$ $T = 3/2$ state. They also introduce two Fermi volumes corresponding to the Compton wavelength of the pion or of the K-meson, and they assume that the volumes to be considered in production differ for various particles. With these hypotheses they compute probabilities of formation of groups of particles and antiparticles at 7 and 10 Bev.

At extremely high energies ($>10^{13}$ev) the statistical method predicts the formation of $0.38(W'/mc^2)^{1/4}$ antiprotons in a nucleon-nucleon collision (W' laboratory energy of incident nucleon) (49).

Antineutrons.—The most convenient and up to now the only practical way of observing antineutrons is to obtain them from antiprotons by charge exchange and detect them by annihilation. This method of production was indicated immediately after the discovery of the antiproton (38) and first demonstrated experimentally by Cork, Lambertson, Piccioni & Wenzel (42) by a counter method in which an antiproton selected from a beam entered an absorber. No charged particle was seen to emerge from it, but an annihilation counter of the type described above showed an annihilation pulse. Similar experiments are reported in (30). The phenomenon is shown graph-

ically in Figure 12, which was taken with a propane bubble chamber (3). The antiproton, recognizable by the curvature and grain density of its track, comes to a sudden end because it loses its charge to a proton giving

FIG. 12. An antiproton enters a propane bubble chamber, and at the point marked with the upper arrow undergoes charge exchange. The antineutron originates the annihilation star (lower arrow). Density of propane 0.42 gm. cm.$^{-3}$. Real distance between charge exchange and origin of star 9.5 cm. $T_{\bar{p}}$ at charge exchange ~50 Mev. From (3).

rise to a neutron antineutron pair. The antineutron annihilates at the spot so marked, giving a typical annihilation star.

It would be highly desirable to be able to detect the antineutrons formed

at the target of the Bevatron without having to form first antiprotons and then charge exchange them. The primary difficulty is the problem of recognizing the antineutrons in the neutral beam emerging from the Bevatron. An ingenious attempt in that direction has been made by Moyer and his co-workers (109) in trying to use antineutrons formed in a reaction:

$$p + n = p + \bar{n} + p + n \qquad\qquad 25.$$

in which the three nucleons on the right escape combined as a He^3 nucleus. The reaction is thus a two-body reaction with kinematics such that detection of the He^3 at a certain angle from the incoming beam assures the presence of the $\bar{n}$ at another angle. Thus a coincidence system, possibly refined by time of flight measurements, should locate the antineutron uniquely. Unfortunately, here also the probability of the three nucleons forming a He^3 nucleus is low. There are not yet definite experimental results.

The charge exchange cross sections have been crudely measured and are indicated in Table V. Actually what has been measured is the integral of $(d\sigma/d\omega)_c$ in the forward directions for which $\theta \leq 17°$ (laboratory); for $p\bar{p}$ 10.9 ± 5.8 mb/ster. was obtained by (30). Most of the charge exchange will deliver antineutrons in a narrow cone in the forward direction in the laboratory, as in the np charge exchange. Explicit theoretical calculations based on the Ball-Chew model are given in (53).

The charge exchange for heavier nuclei has been also observed and there are indications (30) that at 500 Mev the charge exchange per nucleus does not vary greatly with A. This means, of course, that heavy nuclei are very inefficient as charge exchangers. Much of this result may be attributed to the large nucleon-antinucleon annihilation cross section which prevents the antiprotons from penetrating the nucleus, and gives rise to a shadow effect from the target. The antineutrons thus are only formed in grazing collisions with the rim of the target. If neutrons are concentrated on the surface of the nucleus, as is sometimes assumed, there is another reason for depressing charge exchange in heavy nuclei, because a $\bar{p}n$ collision may form antineutrons only if negative pions are emitted at the same time, a condition which certainly lowers the cross section.

Antihyperons.—There also must be antihyperons and the threshold for their formation by pion-nucleon collisions and nucleon-nucleon collisions in Bev (16) is indicated in Table XI.

Baldo-Ceolin & Prowse (11) have reported an event which might be interpreted as a $\bar{\Lambda}_0$ formed by a 4.5 Bev negative pion on a nucleus.

Antiprotons in cosmic rays.—A few possible antiprotons have been found in cosmic rays as mentioned above (6, 24, 25, 98, 103). A Bevatron event very similar in appearance to connected stars found in cosmic rays is reported in (65, 66).

Amaldi has commented on the frequency of observation of antiprotons in emulsions exposed to cosmic rays. His conclusion is that there are more antiprotons, perhaps by a factor 1000, in cosmic rays than one would expect

TABLE XI

Collision	$\bar{\Lambda}^0$	$\bar{\Sigma}$	$\bar{\Xi}$
nn	7.10	7.43	8.9
πn	4.73	5.24	6.12
Most favorable*	4.0	4.2	5.1

* Most favorable means a two stage reaction in which a pion is first formed (48) by a proton on a nucleus and Fermi energies are also considered.

from an estimate based on extrapolations of the Bevatron data (4). However, since the few examples known are doubtful the explanation of the difficulty might be simply found in the interpretation of the events.

Fradkin (51) has considered the possibility of the presence of antiprotons in the primary cosmic radiation and its effect on the east west asymmetry. He concludes that there are less than 0.17 per cent antiprotons in the primary radiation. McConnell (85) has also estimated the possible abundance of antiprotons in cosmic rays on the basis of meson theory. Nucleon anti-nucleon annihilation also has been invoked to explain the high-energy Schein events (85).

COSMOLOGICAL SPECULATIONS

From the cosmological and astronomical point of view no direct tele-scopic observations can reveal antimatter. There are some unrealistic schemes, based on the helicity of neutrinos, which could in principle do it, but they are completely unfeasible at present.

Burbridge & Hoyle (27, 28) have calculated a maximum ratio of antimatter to matter for our galaxy of $\sim 10^{-7}$. They assume an average density of matter of 1 atom cm.$^{-3}$, and they show that the presence of antimatter in concentration larger than 10^{-7} atoms cm.$^{-3}$ would give rise to larger kinetic and magnetic energy of the interstellar gas clouds, and to cosmic radiation of greater intensity, than observed. They calculate also an upper limit for the possible rate of addition of antinucleons to our galaxy q, and find an upper limit of $q = 3 \times 10^{-22}$ antinucleons cm.$^{-3}$ sec.$^{-1}$. These would annihilate with a mean life of 3×10^{14} sec., and about 0.1 of the annihilation energy would go into electrons. The upper limit of q would obtain if the energy of the turbulent motions of the clouds could be ascribed entirely to these electrons.

The maximum value of q could be attained either by capture from an intergalactic medium or by a steady state production in an expanding universe. If the upper limit of the concentration of antimatter (10^{-7} nucleons cm.$^{-3}$) is reached, the radio noise of the Crab Nebula in our galaxy could be accounted for by the annihilation.

Outside of our galaxy the strong radio emission of Cygnus A and Messier 87 could also be due to annihilation processes. Burbridge & Hoyle (29) have pointed out some quantitative coincidences between the energy emitted and what could be expected on annihilation. One would then have a single ex-

planation for the energy of agitation of interstellar clouds in our galaxy, for the radio emission of the Crab Nebula, and for the two extragalactic sources Cygnus A and M 87.

In most cosmological speculations, both steady state and evolutionary, the conservation of nucleons and of leptons would require the simultaneous creation of matter and antimatter in equal amounts. This gives rise to the serious difficulty of a mechanism of separation of matter and antimatter, such as would be given by "antigravity." As an example of a cosmogonic speculation in which antimatter plays a prominent role the reviewer mentions the "universon" of M. Goldhaber (62).

The question of the gravitational behavior of antimatter can ultimately be resolved only by experiment. If the equivalence principle of general relativity is strictly valid, then the antiparticles are subject to the same gravitational actions as a particle of the same inertial mass. The inertial mass of the antiparticles is equal, also in sign, to that of the corresponding particles as shown by the method used for isolating them, which measures directly e/m, by the conservation of charge which establishes the sign of e, and by the laws of electromagnetism.

Even if we are willing to give up the equivalence principle and wish to speculate on "antigravity," namely, on the hypothesis that an antiparticle in a gravitational field be subject to the force opposite to that experienced by a particle, we meet a possible difficulty in the explanation of the behavior of a self-conjugate particle such as a photon, which is known to be subject to gravity.

The equivalence principle could be attributed to the fact that all masses in our universe (earth, sun, our galaxy) are composed of ordinary matter and that the equivalence principle is violated only to an extent connected to the concentration of antimatter in our universe (88). It is clear that all these arguments are extremely speculative and that the existence of antigravity would inflict severe damage on the present structure of physics. Also there is no really strong reason in its favor: on the other hand, only direct experiment can decide the question. For instance, it seems likely that an Eötvös-type experiment of slightly greater accuracy would show whether or not the virtual positrons that arise from vacuum polarization in the Coulomb field of the nucleus possess "antigravity" (96a).

LITERATURE CITED

1. Afrikian, L. M., *Soviet Phys. JETP*, **4**, 135 (1957)
2. Agnew, L. E., Chamberlain, O., Keller, D., Mermod, R., Rogers, E., Steiner, H., and Wiegand, C., *Phys. Rev.*, **108**, 1545 (1957)
3. Agnew, L. E., Elioff, T., Fowler, W. B., Gilly, L., Lander, R., Oswald, L., Powell, W., Segrè, E., Steiner, H., White, H., Wiegand, C., Ypsilantis, T., *Phys. Rev.*, **110**, 994 (1958); *Phys. Rev. Lett.* **1**, 27 (1958); (Private communication)
4. Amaldi, E., *CERN Symposium High-Energy Accelerators and Pion Phys. Geneva, Proc.*, **2**, 111 (1956)

5. Amaldi, E., Castagnoli, C., Cortini, G., Franzinetti, C., and Manfredini, A., *Nuovo cimento*, **1**, 492 (1955)
6. Amaldi, E., Castagnoli, C., Ferro-Luzzi, M., Franzinetti, C., and Manfredini, A., *Nuovo cimento*, **5** (10), 1797 (1957)
7. Amati, D., and Vitale, B., *Nuovo cimento*, **2**, 719 (1955)
8. Amati, D., and Vitale, B., *Nuovo cimento*, **3**, 1411 (1956)
9. Amati, D., and Vitale, B., *Nuovo cimento*, **4**, 145 (1956)
10. Anderson, C. D., *Phys. Rev.*, **43**, 491 (1933)
11. Baldo-Ceolin, M., and Prowse, D. J., *Bull. Am. Phys. Soc.*, **3**, 163 (1958)
12. Ball, J. S., and Chew, G. F., *Phys. Rev.*, **109**, 1385 (1958)
13. Barasenkov, V. S., Barasev, B. M., and Bubelev, E. G., *Nuovo cimento*, **7**, Suppl., 117 (1958)
14. Barkas, W. H., Birge, R. W., Chupp, W. W., Ekspong, A. G., Goldhaber, G., Goldhaber, S., Heckman, H. H., Perkins, D. H., Sandweiss, J., Segrè, E., Smith, F. M., Stork, D. H., Van Rossum, L., and Amaldi, E., Baroni, G., Castagnoli, C., Franzinetti, G., and Manfredini, A., *Phys. Rev.*, **105**, 1037 (1957)
15. Barshay, S., *Phys. Rev.*, **109**, 554 (1958)
16. Beasley, C. O., and Holladay, W., *Nuovo cimento*, **7**, Suppl., 77 (1958)
17. Belen'kii, S. Z., Maksimenko, V. M., Nikishov, A. I., and Rozental, I. L., *Uspekhi Fiz. Nauk*, **62**, 1 (1957)
18. Belen'kii, S. Z., and Rozental, I. L., *Soviet Phys. JETP*, **3**, 786 (1956)
19. Bethe, H., and Hamilton, J., *Nuovo cimento*, **4**, 1 (1956)
20. Blair, J. S., *Nuclear Phys.*, **6**, 348 (1958)
21. Brabant, J. M., Cork, B., Horwitz, N., Moyer, B. J., Murray, J. J., Wallace, R., and Wenzel, W. A., *Phys. Rev.*, **101**, 498 (1956)
22. Brabant, J. M., Cork, B., Horwitz, N., Moyer, B. J., Murray, J. J., Wallace, R., and Wenzel, W. A., *Phys. Rev.*, **102**, 1622 (1956)
23. Brabant, J. M., Moyer, B. J., and Wallace, R., *Rev. Sci. Instr.*, **28**, 421 (1957)
24. Bridge, H. S., Caldwell, D. O., Pal, Y., and Rossi, B., *Phys. Rev.*, **102**, 920 (1956)
25. Bridge, H. S., Courant, H., De Staebler, Jr., H., and Rossi, B., *Phys. Rev.*, **95**, 1101 (1954)
26. Brown, L. M., and Peshkin, M., *Phys. Rev.*, **103**, 751 (1956)
27. Burbridge, G. R., and Hoyle, F., *Astron. J.*, **62**, 9 (1957)
28. Burbridge, G. R., and Hoyle, F., *Nuovo cimento*, **4**, 558 (1956)
29. Burbridge, G. R., and Hoyle, F., *Sci. American*, **198**, 34 (1958)
30. Button, J., Elioff, T., Segrè, E., Steiner, H., Weingart, R., Wiegand, C., and Ypsilantis, T., *Phys. Rev.*, **108**, 1557 (1957)
31. Chamberlain, O., *Padova Venezia Conference, September, 1957* (In press)
32. Chamberlain, O., Chupp, W. W., Ekspong, A. G., Goldhaber, G., Goldhaber, S., Lofgren, E. J., Segrè, E., Wiegand, C., and Amaldi, E., Baroni, G., Castagnoli, C., Franzinetti, C., and Manfredini, A., *Phys. Rev.*, **102**, 921 (1956)
33. Chamberlain, O., Chupp, W. W., Goldhaber, G., Segrè, E., Wiegand, C., and Amaldi, E., Baroni, G., Castagnoli, C., Franzinetti, C., and Manfredini, A., *Nuovo cimento*, **3**, 447 (1956)
34. Chamberlain, O., Chupp, W. W., Goldhaber, G., Segrè, E., Wiegand, C., and Amaldi, E., Baroni, G., Castagnoli, C., Franzinetti, C., and Manfredini, A., *Phys. Rev.*, **101**, 909 (1956)
35. Chamberlain, O., Goldhaber, G., Jauneau, L., Kalogeropoulos, T., Segrè, E., and Silberberg, R., *Padova Venezia Conference* (Study of the annihilation process in a separated antiproton beam, in press)

36. Chamberlain, O., Keller, D. V., Mermod, R., Segrè, E., Steiner, H. M., and Ypsilantis, T., *Phys. Rev.*, **108**, 1553 (1957)
37. Chamberlain, O., Keller, D. V., Segrè, E., Steiner, H. M., Wiegand, C., and Ypsilantis, T., *Phys. Rev.*, **102**, 1637 (1956)
38. Chamberlain, O., Segrè, E., Wiegand, C., and Ypsilantis, T., *Nature*, **177**, 11 (1956)
39. Chamberlain, O., Segrè, E., Wiegand, C., Ypsilantis, T., *Phys. Rev.*, **100**, 947 (1955)
40. Chamberlain, O., Wiegand, C., *CERN Symposium High Energy Accelerators and Pion Phys., Geneva, Proc.*, **2**, 82 (1956)
41. Coombs, C., Cork, B., Galbraith, W., Lambertson, G. R., and Wenzel, W. A., *Bull. Am. Phys. Soc.*, **3**, 271 (1958); *Phys. Rev.* (In press)
42. Cork, B., Lambertson, G. R., Piccioni, O., and Wenzel, W. A., *Phys. Rev.*, **104**, 1193 (1956)
43. Cork, B., Lambertson, G. R., Piccioni, O., and Wenzel, W. A., *Phys. Rev.*, **107**, 248 (1957)
44. DeBenedetti, S., and Corben, H. C., *Ann. Rev. Nuclear Sci.*, **4**, 191 (1954)
45. Dirac, P. A. M., *The Principles of Quantum Mechanics* (Oxford University Press, London, Engl., 1st ed., 1930; 3rd ed., 1947)
46. Duerr, H. P., *Phys. Rev.*, **109**, 1347 (1958)
47. Duerr, H. P., and Teller, E., *Phys. Rev.*, **101**, 494 (1956)
48. Feldman, G., *Phys. Rev.*, **95**, 1697 (1954)
49. Fermi, E., *Progr. Theoret. Phys. (Kyoto)*, **5**, 570 (1950)
50. Fox, D., *Phys. Rev.*, **94**, 499 (1954)
51. Fradkin, M. I., *Soviet Phys. JETP*, **2**, 87 (1956)
52. Frye, G. M., and Armstrong, A. H., *Bull. Am. Phys. Soc.*, **3**, 163 (1958)
53. Fulco, J. R., *Phys. Rev.* **110**, 789 (1958)
54. Gartenhaus, S., *Phys. Rev.*, **107**, 291 (1957)
55. Gatto, R., *Nuovo cimento*, **3**, 468 (1956)
56. Gatto, R., *Nuovo cimento*, **4**, 526 (1956)
57. Glassgold, A. E., *Phys. Rev.*, **110**, 220 (1958)
58. Glauber, R. J., *Phys. Rev.*, **100**, 242 (1955)
59. Goebel, C., *Phys. Rev.*, **103**, 258 (1956)
60. Goldhaber, G., Kalogeropoulos, T., and Silberberg, R., *Phys. Rev.* **110**, 1474 (1958)
61. Goldhaber, G., and Sandweiss, J., *Phys. Rev.*, **110**, 1476 (1958)
62. Goldhaber, M., *Science*, **124**, 218 (1956)
63. Goto, T., *Soryushiron Kenkyu (Japan)*, **15**, 176 (1957); *Nuovo cimento*, **8**, 625 (1958)
64. Gourdin, M., Jancovici, B., and Verlet, L., *Nuovo cimento*, **8**, 485 (1958)
65. Hill, R. D., Johansson, S. D., and Gardner, F. T., *Phys. Rev.*, **101**, 907 (1956)
66. Hill, R. D., Johansson, S. D., and Gardner, F. T., *Phys. Rev.*, **103**, 250 (1956)
67. Hillman, P., Stafford, G. H., and Whitehead, C., *Nuovo cimento*, **4**, 67 (1956)
68. Horwitz, N., Miller, D., Murray, J. J., and Tripp, R., *Am. Phys. Soc.* (Washington meeting, 1958, post deadline paper)
69. Iwadare, J., and Hatano, S., *Prog. Theoret. Phys. (Kyoto)*, **15**, 185 (1956)
70. Johnson, K. A., *Phys. Rev.*, **96**, 1659 (1954)
71. Johnson, M. H., and Teller, E., *Phys. Rev.*, **98**, 783 (1955)
72. Koba, Z., *Progr. Theoret. Phys. (Kyoto)*, **19**, 594 (1958)
73. Koba, Z., and Takeda, G., *Progr. Theoret. Phys. (Kyoto)*, **19**, 269 (1958)

74. Kobsarev, I., and Schmuschkevic, I., *Doklady Akad. Nauk S.S.S.R.*, **102**, 929 (1955)

75. Kretzschmar, M., *Z. Physik*, **150**, 247 (1958)

76. Lee, T. D., Oehme, R., and Yang, C. N., *Phys. Rev.*, **106**, 340 (1957)

77. Lee, T. D., and Yang, C. N., *Elementary Particles and Weak Interactions* (Washington, D. C., 1957)

78. Lee, T. D., and Yang, C. N., *Nuovo cimento*, **3**, 749 (1956)

79. Lepore, J. V., and Neuman, M., *Phys. Rev.*, **98**, 1484 (1955)

80. Lévy, M., *Nuovo cimento*, **8**, 92 (1958)

81. Lindenbaum, S., *Ann. Rev. Nuclear Sci.*, **7**, 315 (1957)

82. Lüders, G., *Naturwissenschaften*, **43**, 121 (1956)

83. Malenka, B. J., and Primakoff, H., *Phys. Rev.*, **105**, 338 (1957)

84. McCarthy, I. E., *Nuclear Phys.*, **4**, 463 (1957)

85. McConnell, J., *Nuclear Phys.*, **1**, 202 (1956)

86. Michel, L., *Nuovo cimento*, **10**, 319 (1953)

87. Mitra, A. N., *Nuclear Phys.*, **1**, 571 (1956)

88. Morrison, P., *Am. J. Phys.* (In press)

89. Murray, J. J., *Bull. Am. Phys. Soc.*, **3**, 175 (1958)

90. Nakai, S., *Progr. Theoret. Phys.* (*Kyoto*), **17**, 139 (1957)

91. Nemirovskii, P. E., *Doklady Akad. Nauk U.S.S.R.*, **112**, 411 (1957)

92. Nikishov, A. I., *Soviet Phys. JETP*, **3**, 976 (1957)

93. Nozawa, M., Goto, T., Yajima, N., and Nakashima, R., *Progr. Theoret. Phys.* (*Kyoto*), **17**, 504 (1957)

94. Pomeranchuk, I. Ya., *Soviet Phys. JETP.*, **3**, 306 (1956); *Zhur. Eksptl. i Teoret. Fiz.*, **30**, 423 (1956)

95. Pontecorvo, B., *Soviet Phys. JEPT*, **3**, 966–(1957)

96. Sandweiss, J., *On the Spin of K-Mesons from the Analysis of Antiproton Annihilations in Nuclear Emulsions* (Doctoral thesis, AEC, Rad. Lab., W-7405-eng-48, 1956)

96a. Schiff, L. I. (Personal communication)

97. Segrè, E., *Padova, Venezia Conference* (In press)

98. Shrikantia, G. S., *Nuovo cimento*, **12**, 807 (1954)

99. Signell, P. S., and Marshak, R. E., *Phys. Rev.*, **109**, 1229 (1958)

100. Stork, D. H., Birge, R. W., Haddock, P. R., Kerth, L. T., Sandweiss, J., and Whitehead, M. N., *Phys. Rev.*, **105**, 729 (1957)

101. Sudarshan, G., *Phys. Rev.*, **103**, 777 (1956) (This paper contains numerical errors)

102. Tarasov, A., *Soviet Phys. JETP*, **3**, 636 (1956)

103. Teucher, M., Winzeler, H., and Lohrmann, E., *Nuovo cimento*, **3**, 228 (1956)

104. Thorn, R. N., *Phys. Rev.*, **94**, 501 (1954)

105. Wick, G. C., *Ann. Rev. Nuclear Sci.*, **8**, 1 (1958)

106. Wiegand, C., *Proc. I.R.E.*, (*Inst. Radio Engrs.*), **6th Scintillation Counter Symposium** (Washington, D. C., 1958)

107. Yajima, N., Kobayakawa, K., *Progr. Theoret. Phys.* (*Kyoto*), **19**, 192 (1958)

108. Yamaguchi, Y., *Progr. Theoret. Phys.* (*Kyoto*), **17**, 612 (1957)

109. Youtz, B., *Am. J. Phys.*, **26**, 202 (1958)

110. Fernbach, S., Serber, R., Taylor, T. B., *Phys. Rev.*, **75**, 1352 (1949)

111. Riesenfeld, W. B., and Watson, K. M., *Phys. Rev.*, **102**, 1157 (1956)

GAMMA-RAY SPECTROSCOPY BY DIRECT CRYSTAL DIFFRACTION[1,2]

By Jesse W. M. DuMond

California Institute of Technology, Pasadena, California

BENT CRYSTAL SPECTROMETER

Ideal Transmission Type Spectrometer

With the exception of certain early work with flat crystals by Rutherford & Andrade (1) and by Frilley (2), to date, crystal diffraction γ-ray spectroscopy has been accomplished almost entirely by means of transmission-type spectrometers using bent quartz crystal focusing. In this type of instrument, whose first conception was published in 1930 by DuMond & Kirkpatrick (3), a thin cylindrical lamina of quartz of uniform thickness is bent so that its neutral plane, initially a right circular cylinder of radius $2R$, assumes the form of a right circular cylinder of radius R.[3] (By the "neutral plane" is meant that plane through the center of the thickness of the crystalline lamina which undergoes neither compression nor elongation when bending occurs.) The lamina is cut from the original unstressed crystal lattice so that the planes to be used in the selective reflection are made to converge after bending in such fashion that, if prolonged, they would all intersect in a common line distant $2R$ from the center of the lamina. Figure 1 illustrates the lamina, seen on edge, before and after bending, with lines indicating the direction of the atomic planes. These planes, after bending, converge in a line represented in projection by the point β. Confining ourselves to two dimensions, the normal projection of the neutral plane and the point β define the "focal circle," which is the locus of focal points R_λ for radiations of different wavelength selectively reflected by the planes of the crystal in accord with Bragg's law, $n\lambda = 2d \sin \theta$. In Figure 1 the thickness and the aperture angle, α, are greatly exaggerated. Cauchois has pointed out that the compression and dilation of the lattice constant, incident to bending, result in front-to-back focusing as well as side-to-side focusing, within the confines of Hooke's law, so that the crystal behaves as though all selective reflection occurred on the neutral plane. It can also be easily shown that for selective reflection in transmission by planes normal to the lamina, the correction to

---

[3] As pointed out in the original DuMond and Kirkpatrick article (3) there are, in fact, two possible types of bent crystal focusing spectrometers, the "transmission" and "reflection" types. This review will be concerned only with the transmission type, since it is the one which adapts itself to the short wavelengths and small Bragg angles encountered in γ-ray spectroscopy.

Bragg's law for crystalline refractive index differing from unity vanishes exactly. This is explained in more detail in Reference 6, p. 241.
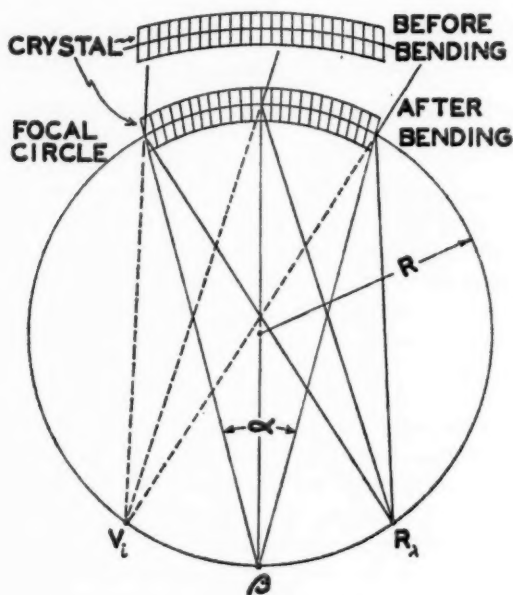
FIG. 1. Transmission-type bent crystal spectrometer, ideal perfectly focusing solution.

SIMPLIFIED TRANSMISSION TYPE SPECTROMETER

Cauchois arrangement.—Cauchois, in 1932 was the first to realize such a transmission spectrometer (for the study of x-ray spectra) in a simplified approximate form (4), by starting with a flat lamina (mica) and bending it cylindrically to radius $2R$ (see Fig. 2). The focal circle is then of radius, R, tangent to the neutral axis of the bent crystal at its center. As a consequence a slight aberration of focus for rays reflected in regions of the crystal remote from its center occurs. This aberration can readily be kept negligible in γ-ray studies. In the Cauchois focusing x-ray spectrometer the source of radiation is outside the focal circle. The radiation propagates through the crystal from the convex to the concave side and by selective reflection, therein, forms a spectrum of focused lines on a cylindrically bent photographic emulsion conforming to the focal circle. The converging beams of radiation used by the crystal have a virtual image point, V_λ, symmetrically situated on the focal circle relative to the real image point R_λ, the arcs βR_λ and βV_λ being equal.

DuMond arrangement.—If, in contrast to the foregoing, the source is

placed, in very concentrated form on the focal circle after the manner first introduced by DuMond (5, 6) for purposes of very short wavelength γ-ray spectroscopy, each atom or nucleus in the source can emit its characteristic radiation into the solid aperture angle, α, of the crystal, and selective reflection will occur throughout this entire solid angle if the source is situated at the correct position on the focal circle for the γ-ray line in question. How-
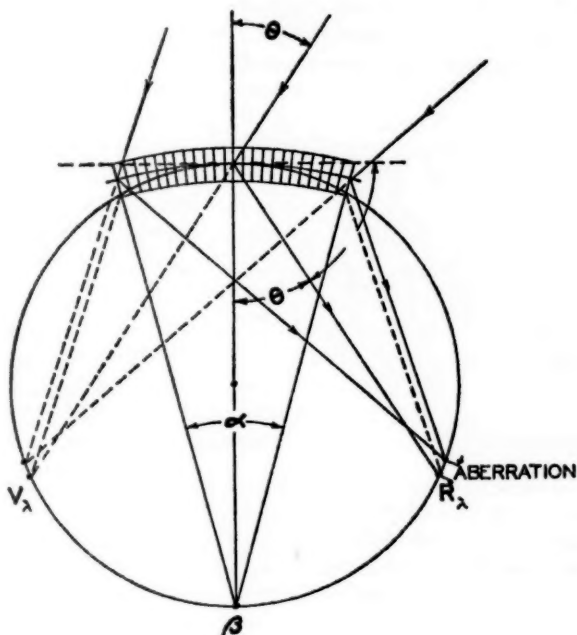
Fig. 2. Transmission-type bent crystal spectrometer, approximate solution of Cauchois. The aperture angle, α, of the crystal is greatly exaggerated to illustrate the geometry of the slight aberration of focus.

ever in the Cauchois arrangement, with the source on the convex side of the crystal, selective reflection of a given wavelength can occur only within an extremely limited angular domain in the horizontal plane. The horizontal acceptance angle is of the order of the diffraction pattern width given by the Darwin dynamical theory or a few seconds of arc for the "perfect" crystals desirable in γ-ray spectroscopy. Figure 3 shows these two ways of using the transmission type instrument. In the second way, with source on the focal circle, the instrument clearly becomes in reality a variable monochrometer. The source must be caused to explore the spectrum by scanning along the focal circle in small steps. This permits plotting a curve of reflected intensity as function of the sine of the Bragg angle; the profiles of the γ-ray lines are

revealed as peaks of varying height.[4] In contrast to this the Cauchois arrangement has the admitted advantage that the lines are all formed simultaneously; but it has the much graver difficulty, for the short wavelengths studied in γ-ray spectroscopy, of shielding the photographic emulsion from the intense direct beam transmitted straight through the crystal lamina, a beam frequently thousands of times as intense as the selectively reflected spectrum under study. In the inverse arrangement, the direct beam can be suppressed and the selectively reflected beam accepted by means of a system of absorbing baffle plates disposed in a fan-shaped geometry which shall be called

ARRANGEMENT I   ARRANGEMENT II
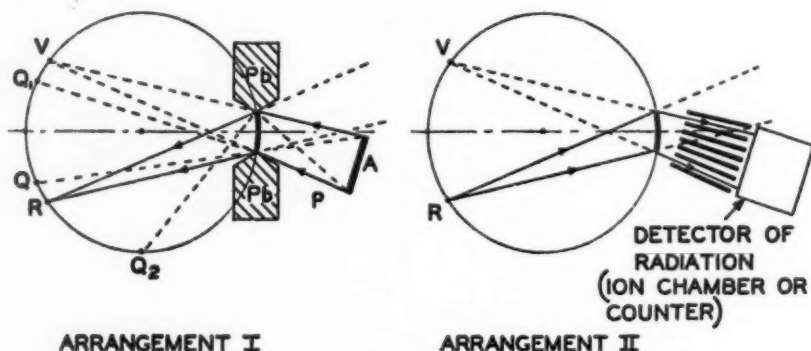
FIG. 3. Two ways of using the transmission-type bent crystal focusing spectrometer. Arrangement I is that of Cauchois with the source on the convex side of the crystal. Arrangement II is that of DuMond in which the source is placed in very concentrated form on the focal circle and the instrument becomes a variable γ-ray monochromator. II is the arrangement permitting study of the shortest wavelengths.

"the collimator" (see Fig. 3), although it has nothing to do with the line width and spectral resolving power of the instrument. The angular resolving power of the collimator, usually 30 to 50 times coarser than that of a good quartz crystal in first order selective reflection, merely determines the shortest wavelength that can be studied before leakage through its partitions and scattering of the direct beam on their surfaces "swamps" the selectively reflected spectral lines with intolerable background intensity. In the Mark I γ-ray spectrometer at the California Institute of Technology, spectral lines of quantum energy up to 1.3 Mev (a wavelength of about 9 milliangstroms) have been successfully recorded and measured this way. Collimators asserted

[4] It should be noted that DuMond's arrangement, in which the *entire* crystal is used simultaneously for reflecting every line, places much more stringent requirements for focusing on the bent crystal than does the Cauchois arrangement in which, depending on how extended the source may be, only a limited region of crystal is used in forming each spectral line. For the technical methods followed to insure and to test for requisite focusing, the reader is referred to the literature (5, 6).

to have still higher geometrical resolving power are reported by a group at Chalk River (7, 8).

DESIGN AND PERFORMANCE OF CALIFORNIA INSTITUTE OF TECHNOLOGY SPECTROMETER

Several mechanical designs of crystal diffraction γ-ray spectrometers are now in successful use, each adapted to different conditions of operation. In the Mark I, a mechanism is provided so that the source explores the spectrum by moving along the focal circle in steps of adjustable size (as small as 0.02 mm. if desired, which corresponds to a wavelength shift of about 0.02 milliangstrom). Simultaneously the focal circle and crystal rotate in small angular steps about a pivot at the center of the crystal in such a way as to maintain the outgoing reflected monochromatic beam of γ-rays always in alignment with the fan-shaped array of collimator partitions. The mechanism designed to realize these kinematic relationships is schematically explained in Figure 4, while Figure 5 is a line drawing of the instrument itself.

The intensity of the monochromatic radiation emerging from the collimator is measured with a large NaI(Tl) crystal and photomultiplier tube. An adjustable differential discriminator selects the γ-ray pulses and rejects the accidentals from cosmic rays and from tube "noise." This discriminator, whose spectral resolving power is, of course, far coarser than that of the crystal diffraction spectrometer, must nevertheless be "tracked" so as to maintain its setting sensibly peaked at the quantum energy of the monochromatic radiation under study in order not to falsify relative line intensities at different wavelengths. A secondary but valuable use for this discriminator permits the determination of the order of the reflection of a given γ-ray peak since peaks reflected in second or third order will have double or triple the quantum energy of first order peaks.

The Mark I spectrometer permits reflection to be observed on the focal circle on both sides of the β-point, and absolute determinations of wavelength are made by measuring the displacement between the two images. This eliminates errors from slight variations in positioning the source in its holder and also permits discrimination between asymmetries in line profile from (a) instrumental causes and (b) true spectral asymmetries from multiplet structure. The Mark I is provided with a "sine screw" drive on which, because of Bragg's law, the wavelength of each setting automatically appears on a linear scale.

In the Mark I with a 2-mm. thick crystal using the (310) planes of quartz in first order, the γ-ray line can be made somewhat less than 0.25 milliangstrom wide at half-maximum. This wavelength width is roughly independent of wavelength and corresponds to a change in Bragg angle of about 21 sec. of arc. With the Mark I instrument the W K α_1 x-ray line with a "natural" spectral breadth of 0.15 milliangstrom can be clearly recognized as broader than most nuclear γ-ray lines. The many x-ray lines which are copiously emitted by the neutron-activated sources used in studies of γ-ray spectra
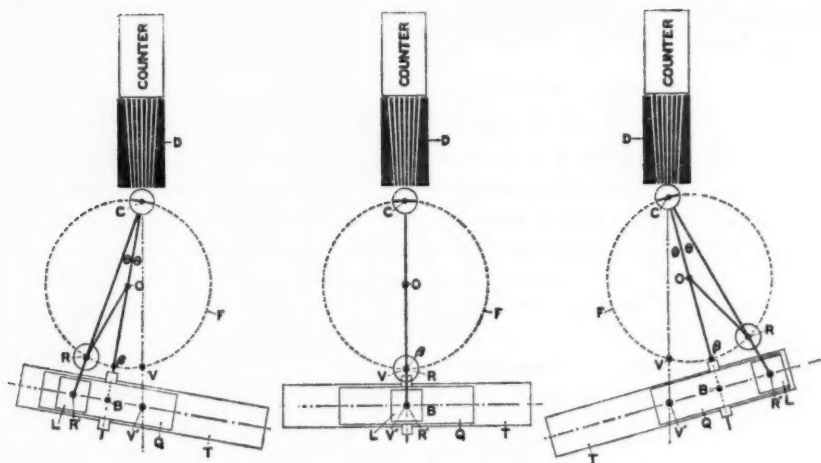
FIG. 4. Illustrating in schematic plan view the kinematics of the Mark I spectrometer. Upper and lower lever arms CR' and $C\beta$, somewhat over two meters long, swing about a common vertical axis at C. The source, R, in a shielded housing is free to travel on rails through a short displacement along the upper arm and is maintained on the focal circle by radius bar, OR, pivoted at O on the lower arm. The bent crystal at C and the lower arm are rigidly coupled together through a shaft passing through the bearing of the upper arm. As the spectrum is explored the upper arm swings in small angular steps twice as large as those of the lower arm so that the divergent beam of monochromatic γ-rays selectively diffracted by the crystal always passes through the collimator channels in an invariable direction. This motion is imparted to the arms by a sine screw drive consisting of two precision lapped longitudinal screws geared together to turn at equal rates in the long carriage, Q,—the lower screw driving the long carriage relative to the pivoted track, T, and the upper screw driving the small carriage, L, through equal displacements relative to the long carriage, Q. The lower arm, $C\beta$, is provided on its outer end with a cylindrical steel shaft sliding in ball bearing guides running transversely to the axis of the long carriage, since the length of the altitude, CB, of the isosceles triangle, $R'CV'$, must vary. In this way the displacement of the pivot, R', on the small carriage, L, away from the center point, B, of the long carriage, Q, as measured by the rotation of the upper precision screw gives a scale proportional to the sine of the Bragg angle and, therefore, proportional to the wavelength. One turn of the screw approximates quite closely 1 milliangstrom when the (310) planes of quartz are used. Settings can be made for selective reflection of the radiation from either side of the crystal planes.

serve as extremely valuable means for calibrating the proportionality factor of that instrument's linear wavelength scale with high precision.

If ΔE is the full energy width of a γ-ray line at half maximum and E its energy, then the resolution, $\Delta E/E$, of the Mark I spectrometer is given by $\Delta E/E \cong 0.3E \cdot 10^{-4}$. Experience has shown that an uncertainty of energy determination corresponding to 1/20 of this resolution or ± 10 ev, whichever
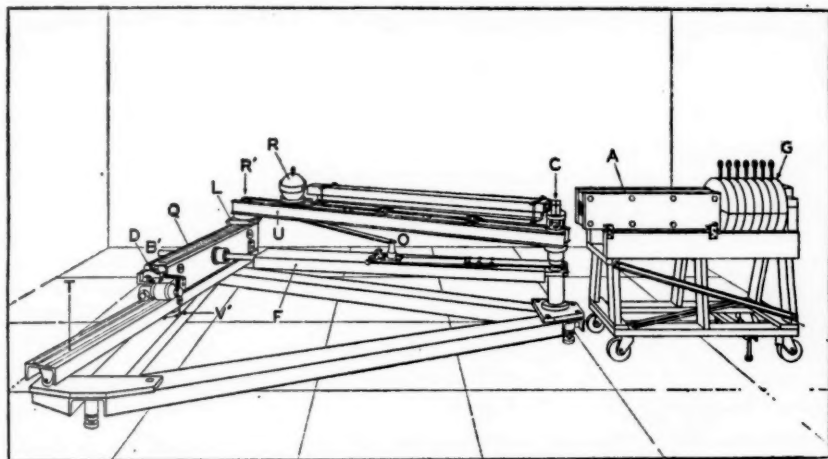
FIG. 5. A perspective line drawing of the Mark I spectrometer. Most of the components are designated with the same letters as are used in Figure 4 and they can be identified in this way.

is the larger, can usually be safely assigned. The energy uncertainty from statistics of counting alone frequently can be made easily half of this or less. At 100 kev the foregoing rule gives for the resolution, $\Delta E/E = 0.3$ per cent and for the uncertainty of energy determination $\pm\sigma_E = \pm 15$ ev or 0.015 per cent.

Very intense sources, usually from tens of millicuries to curie levels of strength, are required in γ-ray spectroscopy by crystal diffraction, and if the source is to be placed on the focal circle following DuMond's arrangement the specific activity must also be high (of order 10 mc. per mg. or better) in order to have the requisite concentration on the focal circle. Lind (9, 10) has shown that the reflection coefficient of the quartz (310) planes varies in proportion to λ^2. Sources of the requisite specific and total intensity are easily obtainable by neutron irradiation in reactors affording neutron flux densities of order 10^{14} n cm.$^{-2}$ sec.$^{-1}$ or higher.

APPLICATIONS OF CRYSTAL DIFFRACTION γ-RAY SPECTROMETERS

Crystal diffraction γ-ray spectroscopy has shown itself to have the following merits: (a) It affords a method of high absolute precision for the determination of γ-ray wavelengths and quantum energies[5] (11) which has

[5] Recent least-squares evaluations (11) of the fundamental constants permit very accurate evaluation of the voltage wavelength conversion constant as follows:

$$E\lambda_g = (12397.67 \pm 0.22) \times 10^{-8} \text{ ev cm.}$$
$$E\lambda_s = 12372.44 \pm 0.16 \text{ kev x-units}$$

been widely used for calibration of magnetic instruments. (*b*) Whenever suitably intense sources are available it is an excellent exploratory instrument yielding well resolved spectra, simple to intepret because of the absence of a multiplicity of peaks for each γ-transition, such as are encountered in internal conversion electron spectra. (*c*) The combination of the crystal diffraction and magnetic spectrometers yields a most powerful tool for determining conversion coefficients. For this it suffices to establish a single normalization factor between the intensity scales of the two instruments because the diffraction instrument measures the γ-rays which have not been converted, while the magnetic instrument measures those that have. The two instruments also complement each other's virtues and defects as regards sensitivity and resolving power in different ranges of energy. Largely for these reasons the Mark I instrument, since its inception and with the help of two companion magnetic instruments (12, 13), has served to determine the decay schemes of some 21 nuclear species [see (14 to 35)] and, in particular, has played an important role in verifying with considerable precision the theoretical predictions of the "collective model" of the nucleus as worked out by the Copenhagen school of physicists under Aage Bohr.

With the Mark I instrument the first spectrum of the annihilation radiation (from the recombination of positrons from Cu^{64} with structure electrons) was observed and shown to consist of a quite sharp line of wavelength, $h/(m_0c)$, slightly broadened by Doppler effect with a breadth and structure consistent with the momentum distribution of the structure electrons in the copper (15, 18).

Neutron capture and other prompt γ-rays in the range below 5 Mev have been studied with a crystal diffraction γ-ray spectrometer at the Argonne National Laboratory (36). The source material is placed inside the CP-5 liquid reactor in one of the horizontal straight-through holes in a region of high neutron flux density. This requires the source to be stationary and hence since the instrument is of the DuMond rather than the Cauchois type, the focusing bent crystal rotates to explore the spectrum while the entire collimator and heavily shielded detector system weighing over 12 tons also rotates to maintain its alignment with the selectively reflected γ-ray beam at twice crystal speed, controlled very accurately by a mirror-and-light-beam servomechanism. The radius of curvature of the bent crystal and the source-to-crystal distance are each 7.7 m. The larger of the two crystal lamina used is 30×30 cm. square and 4 mm. thick. The detector is a square array of 16 NaI(Tl) crystals each with its individual photomultiplier tube providing a sensitive volume 27×27 cm.^{2} in area and 5 cm. deep. Source strengths of order 1000 c. are easily attainable under continuous activation. Instrumental full-line widths of 13.2 sec. of arc at half maximum for the 411.8 Kev line following decay of Au^{198} have been obtained and 50 or more lines from a gold source have been observed. In the case of some neutron-capture γ-ray lines, full widths as narrow as 9 to 11 sec. of arc have been obtained.

Very recently, at the Livermore Radiation Laboratory of the University of California, spectra of so-called "Coulomb exited" γ-rays from stable isotopes have been successfully recorded with a photographic bent crystal diffraction spectrometer of the Cauchois type (37). Figure 6 is a photograph of the very simple spectrometer used in this work. (Its focussing crystal was prepared at the California Institute of Technology.) The A-48 proton linear accelerator was used, employing 25 to 30 ma of protons at 3.7 Mev on a continuously water-cooled target usually of copper upon which the target

FIG. 6. Photographic quartz γ-ray spectrometer of the Cauchois transmission variety with bent quartz crystal prepared at the California Institute of Technology for the use of the Livermore Radiation Laboratory group in the study of Coulomb-excited nuclear γ-rays using the A-48 linear accelerator. The bent crystal in its stainless steel clamping blocks (2 m. radius of curvature) is seen at the extreme right end. The curved plate holder is seen on the radius arm at left.

material had been deposited by vaporization. Exposures of tens of hours were required. For the photographic emulsion in the spectrometer, a special technique with 600-μ-thick nuclear emulsions mounted on 0.030 in.-thick glass was perfected. This is the first time that Coulomb-excited γ-ray spectra have ever been resolved by crystalline diffraction and recorded. Intense x-ray lines also appear in these spectra which serve to calibrate the wavelengths of the γ-ray lines with high precision. To date the wavelengths of some 42 Coulomb-excited γ-lines from 12 different elements have been recorded and measured. In addition 12 lines from 6 isotopes excited by $(p, n\gamma)$ and $(p, p'\gamma)$ reactions and six lines from three isotopes excited by deuteron beam activation have been recorded. Tables I A and B list some of

DuMOND

TABLE IA

GAMMA-RAY WAVELENGTHS WITH BENT CRYSTAL SPECTROMETER ELECTROMAGNETICALLY EXCITED BY PROTON BOMBARDMENT WITH LIVERMORE A-48 ACCELERATOR

Isotope	Natural Isotopic Abundance in Per Cent	Wave Length in Siegbahn x-units	Energy in Kev	Best Previous Value of Energy	Reference
Sm^{152}	26.8	101.54±0.03	121.85±0.03	121.79 ±0.03	47 (cryst.)
Sm^{154}	22.7	150.90±0.02	81.99±0.02	82	39 (scint.)
Gd^{155}	14.7	206.09±0.02	60.03±0.01	60.1	40 (conv.)
Gd^{156}	20.5	139.06±0.03	88.97±0.03	88.97 ±0.01	32 (cryst.)
Gd^{157}	15.7	226.84±0.02	54.54±0.01	55	41 (conv.)
Gd^{158}	24.9	155.61±0.02	79.51±0.02	79	39 (scint.)
Gd^{160}	21.9	164.40±0.02	75.26±0.01	76	39 (scint.)
Tb^{159}	100	213.36±0.02	57.99±0.01	58.0	40 (conv.)
		155.62±0.02	79.51±0.02*	79	39 (scint.)
Dy^{161}	18.9	282.30±0.02	43.83±0.01	44	42 (scint.)
Dy^{162}	25.5	153.41±0.02	80.65±0.02	80.8	40 (conv.)
Dy^{163} (?)	25.0	168.58±0.02	73.39±0.01	—	—
Dy^{164}	28.2	168.58±0.02	73.39±0.01	73.0	40 (conv.)
Ho^{165}	100	150.65±0.03	94.70±0.02	94.793±0.007	43 (cryst.)
		112.55±0.03	109.93±0.03*	116	44 (conv.)
Er^{166}	33.4	153.55±0.02	80.57±0.02	80.7	40 (conv.)
Er^{167} (?)	22.9	157.43±0.02	78.59±0.02	—	—
Er^{168}	27.1	155.04±0.02	79.80±0.02	79.9	40 (conv.)
Er^{170} (?)	14.9	155.99±0.02	79.31±0.02	—	—
Tm^{169}	100	112.71±0.03	109.77±0.03*	109.78 ±0.02	26 (cryst.)
		104.71±0.04	118.16±0.04	118.20 ±0.03	26 (cryst.)
Yb^{171}	14.3	185.43±0.02	66.72±0.01	66.7	40 (conv.)
		163.05±0.02	75.88±0.01	76	45 (p, p)
Yb^{172}	21.8	157.21±0.02	78.70±0.01	78.7	40 (conv.)
Yb^{173}	16.2	157.21±0.02	78.70±0.01	78.8	40 (conv.)
Yb^{174}	31.8	161.81±0.02	76.46±0.01	76.6	40 (conv.)
Yb^{176} (?)	12.7	150.65±0.02	82.13±0.02	—	—
Lu^{175}	100	108.73±0.04	113.79±0.04	113.81 ±0.02	26 (cryst.)

* These γ-rays are cascade transitions.

TABLE IA (*Continued*)

Isotope	Natural Isotopic Abundance in Per Cent	Wave Length in Siegbahn x-units	Energy in Kev	Best Previous Value of Energy	Reference
Hf[176]	5.2	140.04 ± 0.03	88.35 ± 0.02	88.6	40 (conv.)
Hf[177]	18.4	109.57 ± 0.04	112.91 ± 0.04	112	39 (scint.)
Hf[178]	27.1	132.84 ± 0.03	93.14 ± 0.02	93.3	40 (conv.)
Hf[179]	13.8	100.87 ± 0.04	122.66 ± 0.05	123	44 (conv.)
Hf[180]	35.3	132.62 ± 0.03	93.29 ± 0.02	93.3	46 (conv.)
Ta[181]	100	90.89 ± 0.04	136.12 ± 0.06	136.25 ± 0.02	25 (cryst.)
		74.92 ± 0.05	165.15 ± 0.11*	165	44 (conv.)
Re[185]	37.1	98.74 ± 0.04	125.30 ± 0.05	125	44 (conv.)
Re[187]	62.9	92.19 ± 0.04	134.20 ± 0.06	135	44 (conv.)

the wavelengths measured in this way. It is a great pity that the decision to dismantle the A-48 accelerator necessitates the interruption of this very productive work before the program can be completed because it is very unlikely that comparable data will or even can be obtained anywhere else for a long time to come.

Crystal diffraction spectroscopy of short wavelengths by similar methods is being studied also at Chalk River Canada (7, 8, 38) and in the Soviet Union. To date no details of the Soviet workers' results have become available to the author. A 2-m. bent quartz crystal spectrometer similar to the Mark I at the California Institute of Technology has been in operation at Chalk River for about two years. It has been used with marked success in conjunction with a double lens β-ray spectrometer to determine the internal conversion coefficients of γ-rays in Pu[239] (38) in order to study the interesting perturbations which these coefficients exhibit from the effect of finite nuclear size.

TWO-(FLAT) CRYSTAL SPECTROMETER

The Chalk River workers, however, anxious to develop a crystal diffraction instrument suited to higher energies for neutron capture γ-spectra, have built a two-crystal spectrometer (utilizing thick flat crystals rather than the elastically bent quartz lamina heretofore described) which gives promise of great utility. In the bent crystal spectrometer the limitation on the thickness of the bent crystal slab is set by the breaking strength of the crystal. Even for the 7.7-m. radius of curvature in the Argonne Laboratory instrument, this requires a thickness much thinner than the optimum value

DuMOND

TABLE IB

GAMMA-RAY WAVELENGTHS WITH BENT CRYSTAL SPECTROMETER RESULTING FROM NUCLEAR REACTIONS UNDER PROTON BOMBARDMENT WITH LIVERMORE A-48 ACCELERATOR

Bombarded Element	Reaction	Wave Length in Siegbahn x-units	Energy in Kev	Best Previous Value of Energy	Reference
Fluorine	F^{19} $(p, p'\gamma)$	112.61 ± 0.04	109.87 ± 0.04	109	48 (scint.)
Titanium†	Ti^{49} $(p, n\gamma)V^{49}$	136.48 ± 0.03	90.65 ± 0.02	89 ± 1	49 (scint.)
		198.63 ± 0.02	$62.29 \pm 0.01*$	63 ± 1	49 (scint.)
	Unknown	131.50 ± 0.03	94.09 ± 0.02	—	—
Titanium‡	Ti^{49} $(p, n\gamma)V^{49}$	136.50 ± 0.08	90.64 ± 0.05	89 ± 1	49 (scint.)
		198.64 ± 0.02	$62.28 \pm 0.01*$	63 ± 1	49 (scint.)
	Unknown	131.53 ± 0.08	94.07 ± 0.05	—	—
		349.72 ± 0.18	35.38 ± 0.02	—	—
Manganese	Mn^{55} $(p, p'\gamma)$	98.30 ± 0.04	125.87 ± 0.05	125	44 (conv.)
Nickel	Ni^{61} $(p. p'\gamma)$	183.57 ± 0.02	67.40 ± 0.01	70	50 (scint.)
Copper	Cu^{65} $(p, n\gamma)Zn^{65}$	229.44 ± 0.02	53.93 ± 0.01	54	51 (conv.)
		202.17 ± 0.02	$61.20 \pm 0.01*$	65	51 (conv.)
		107.50 ± 0.04	115.09 ± 0.04	119	51 (conv.)
Germanium	Ge^{73} $(p, p'\gamma)$	184.59 ± 0.02	67.03 ± 0.01	67.8	52 (scint.)
Selenium	Se^{80} $(p, n\gamma)Br^{80}$	333.95 ± 0.06	37.05 ± 0.01	37	53 (scint.)

* Cascade γ-ray.
† Plate No. 1.
‡ Plate No. 2.

to give the greatest reflected intensity, even for 1 Mev radiation. Furthermore, a large bending radius implies a large scale for the instrument which in turn requires a huge and very expensive crystal slab, if one does not wish to sacrifice the useful solid angle into which the instrument accepts γ-rays from the source. On the simple assumption that, at the very short wavelengths of interest, the crystal always behaves like a mosaic crystal (an assumption which may, however, be somewhat oversimplified) Knowles (38) arrived at the conclusion that the optimum thickness of a calcite crystal for 1 Mev radiation (the thickness beyond which the attenuation by absorption outweighs the benefit of increased reflecting power) is about 5 cm. if the

(211) planes of calcite are used for the reflection. Knowles, in fact, obtained a curve relating optimum thickness to energy [e.g., Fig. 12 (38)] which is the envelope of a family of curves, each giving the reflecting power of a crystal of fixed thickness as a function of the energy. Thus, he reasoned that in spite of the excessively small solid angles within which the two-crystal spectrometer will accept radiation from a source of γ-rays, the possibility of using extremely thick flat crystals in such an instrument makes it an interesting and promising tool at higher quantum energies.

In the study of neutron capture γ-ray spectra, the source under study must, of course, be continuously activated. Since the Chalk River workers have access with their reactors to some of the highest neutron flux densities in the world, which are capable of maintaining source materials continuously activated to levels of order 10^3 c., the low solid-angular luminosity of the two-crystal instrument has been no obstacle to its use by them. The source material is placed outside the reactor shield in an intense beam of emerging neutrons and the gamma-rays resulting from neutron capture in this sample pass through a collimator to the spectrometer in such a direction that no direct radiation from the interior of the reactor can contribute harmful background. The two calcite crystals are furnished with three Sollar slit baffles, one between the source and the first crystal, the second between the first and second crystals, and the third between the second crystal and the detector (see Fig. 7). The entire system is mechanically mounted with two crystal pivots, one at a fixed point, the other on an arm so as to swing about the first, while the detector system swings on another arm about the second crystal pivot. Thus, the two crystals, the Soller baffles, and the heavily shielded detector are caused to rotate, as the spectrum is being explored, at the appropriate rates to maintain correct alignment with the singly reflected γ-ray beam between the two crystals and the doubly reflected beam from the second crystal to the detector. This is accomplished by means of mirrors mounted above the crystals, employing a double optical lever servo-system similar in principle to the single one used in the Argonne spectrometer. The Chalk River physicists have been remarkably successful in constructing parallel lead partition Soller baffles of very high angular resolving power, 45 sec. of arc only. This spectrometer has been used with two small 2 in. $\times$ 1.5 in. (face) $\times$ 7/8 in.-thick calcite crystals to measure slow neutron capture γ-rays from a Ti radiator up to nearly 2 Mev with a resolution of 0.4 per cent at 1 Mev (see Fig. 8). The resolution is determined by the crystal mosaic spread of roughly 3 sec. and the grating constant, $d = 3.03$ A, of the (211) planes. If the (310) planes of a thick quartz crystal were used (for which $d = 1.18$ A), Knowles asserts that a resolution of order 0.04 per cent at 1 Mev would be achievable. Figure 11 (38) gives an interesting comparison of relative counting rates and sensitivities of flat two-crystal and bent crystal spectrometers.

For the reader who may not be familiar with the principle of the two-crystal spectrometer, it may be helpful to explain that with crystals of high
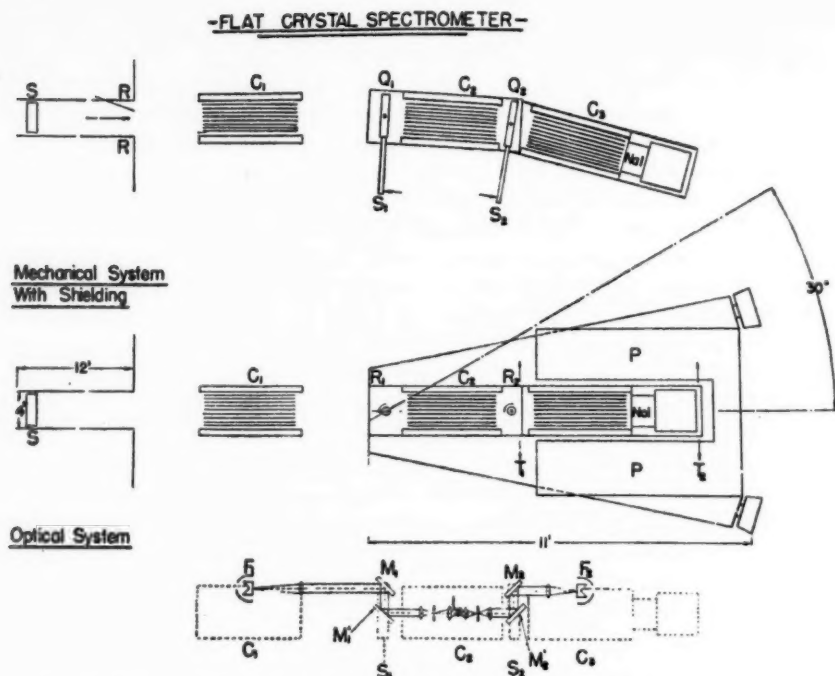
FIG. 7. Schematic plan view of the Chalk River two-crystal γ-ray spectrometer in anti-parallel setting. S is the source of radiation, C_1, C_2 and C_3 are the Soller collimators. Q_1 and Q_2 are the first and second calcite crystals respectively. At bottom the optical servo-mechanism which maintains the appropriate angular relationships between crystals and collimators is shown schematically. This drawing is taken from Reference (38).

perfection it affords enormous angular and spectral resolving power, and that this has nothing whatever to do with the angular resolving power of the collimator baffles. The latter, as in the bent crystal spectrometer, serve only to shield the detector from receiving radiation which has not been selectively reflected by the crystals. Considering the simplest case, if the reflecting planes of the two crystals have the same interplanar spacing and the baffle geometry is such that, for the wavelengths under study, the angles of incidence on the two crystals require reflection in the same order on both of them, then clearly only those beams which leave the first crystal at very close to the same glancing angle as the glancing angle with which they fall on the second crystal can be successively reflected at both crystals. This condition, independent of baffle geometry, automatically selects a very sharply defined glancing angle of reflection at each crystal and simultaneously a wavelength also very sharply defined, related to that angle by Bragg's law. For beams which lie in any plane normal to the acute dihedral angle, ϕ, formed by the two sets of reflecting atomic crystal planes, the glancing
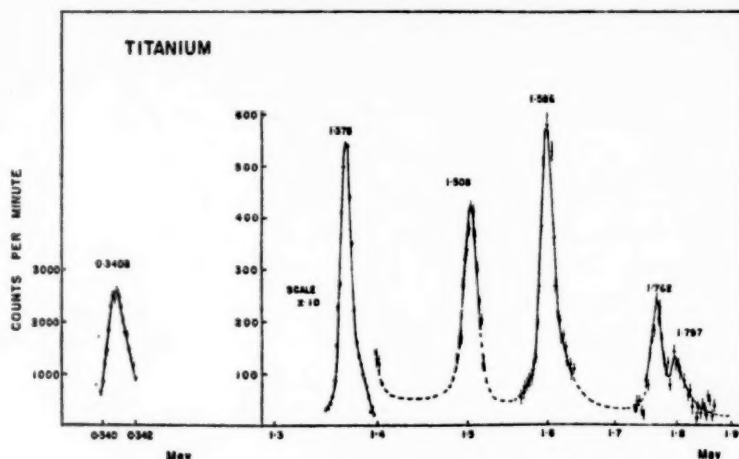
FIG. 8. Slow neutron capture γ-ray spectrum from titanium obtained
with the two-crystal instrument at Chalk River.

angle, θ, selected by the two successive reflections is $\theta=\phi/2$. (For beams
slightly oblique to this reference plane the glancing angle will be slightly
smaller than $\phi/2$ so that a small correction for "cross fire" is required.) The
arrangement affords a monochromator of extremely high resolution. The
spectrum is explored by varying the dihedral angle, ϕ, between the crystals
in very small steps and plotting the intensity of the doubly reflected beam
as a function of the sine of $\theta=\phi/2$. The only angle which critically deter-
mines the selected wavelength is the dihedral angle between the two sets of
crystal planes. In the Chalk River spectrometer (Fig. 7) the radiation passes
completely through the two crystal slabs and this has permitted a design
of the instrument in a very simple way which permits deflecting the beam
at each crystal reflection either in the clockwise or counter-clockwise
sense. To obtain a monochromator the beam must be deflected in the same
sense at both crystals (the so-called "antiparallel case").

Although the Chalk River report makes no explicit mention of this,
there is an obvious advantage also in working with the so-called "parallel
case" in which the beam is deflected in opposite senses at the two successive
crystal reflections. In this case the reflection only takes place when the two
sets of crystal planes are strictly parallel to each other, and when this is
true all wavelengths and directions of propagation in the beam within the
angular limits permitted by the baffles are transmitted. The instrument in
this arrangement no longer serves as a monochromator, but a study of the
"rocking curve" obtained when the second crystal is deflected slightly from
exact parallelism with the first gives exceedingly important information re-
garding the angular and spectral resolution afforded by the two-crystal
combination. This rocking curve, frequently only a few seconds of arc wide
at half maximum height, is, in fact, the fold of the diffraction pattern of the

first crystal into the diffraction pattern of the second crystal. The parallel position rocking curve also serves as a valuable and very sharp datum from which to measure the rotation of the second crystal requisite to bring the latter into the antiparallel position for selective reflection. The second crystal must, in fact, be rotated through twice the Bragg angle, θ, to accomplish this.

In summary it seems safe to conclude that where extremely intense γ-ray sources are available (on the level of hundreds of curies) the two-crystal spectrometer promises to be a very useful tool.

SUPPLEMENTARY INFORMATION

After this manuscript was submitted to the editors the author learned of the existence in Sweden of three other crystal diffraction γ-ray spectrometers. The first of these, a 2-m. focal length instrument with source on the focal circle, constructed by Ryde & Andersson at the Chalmers Institute, Gothenburg (54), seems to have had, at least initially, certain mechanical defects or difficulties which rendered some of the earlier wavelength measurements made with it erroneous.

The second instrument, the work of Beckman at Upsala (55), is a photographic one of the Cauchois type, and, apart from the crystal and plateholders, is the same as the one built by Ingelstam for his thesis on the x-ray spectra of the heavy elements (56). Ilford G-5 emulsions, 100 μ thick, are used. Good agreement as to wavelengths with those obtained in Pasadena with the Mark I is reported by Beckman.

The third Swedish instrument has been built at Upsala by Bergvall and Axelsson under the supervision of Beckman and is of the DuMond type with source on the focal circle. It employs a sodium iodide scintillation crystal detector, and the angular rotation of the bent crystal between corresponding orders of reflection from the two sides of the crystal planes is measured with a high precision divided circle, the same circle as that used earlier by Larsson (57) in Siegbahn's "Tube-spectrometer" for precision x-ray measurements of the Bragg angle. Excellent agreement with the wavelength determinations made with the Mark I instrument at Pasadena is reported as the result of Bergvall's measurements with this instrument. The superiority of the "method of imprisonment" over that of the "freely sprung" crystal lamina, if the highest resolution is desired, seems to have been verified by these workers who have tried both methods. A paper describing this instrument has been prepared but is not yet published. The author is indebted to Pär Bergvall and Olof Beckman for privately communicating the above information.

LITERATURE CITED

1. Rutherford, E., and Andrade, E. N. da C., *Phil. Mag.*, **27**, 854 (1914); **28**, 262 (1914)
2. Frilley, M., *Ann. phys.*, **11**, 483 (1929)

3. DuMond, J. W. M., and Kirkpatrick, H. A., *Rev. Sci. Instr.*, **1**, 90 (1930)
4. Cauchois, Y., *Compt. rend.*, **195**, 1479 (1932)
5. DuMond, J. W. M., *Rev. Sci. Instr.*, **18**, 626 (1947)
6. DuMond, J. W. M., *Ergeb. exakt. Naturw.*, **XXVIII**, 232 (1955)
7. Knowles, J. W., *Bull. Am. Phys. Soc.*, [II]**2**, 16, 218, 231 (1957)
8. Bromley, D. A., *Proc. of the Rehovoth Conf. on Nuclear Structure*, 536 (Lipkin, H. A., Ed., North Holland Pub. Co., Amsterdam, Holland, 614 pp., 1958)
9. Lind, D. A., *Precision Spectroscopy of X- and γ-radiation Using the Focusing Crystal Principle* (Doctoral thesis, California Institute of Technology, Pasadena, Calif., 1948)
10. Lind, D. A., West, W. J., and DuMond, J. W. M., *Phys. Rev.*, **77**, 475 (1950)
11. Cohen, E. R., and DuMond, J. W. M., *Handb. Phys.*, **XXXV** (Springer-Verlag, Berlin, Germany, 454 pp., 1957, in English); Cohen, E. R., Crowe, K. H., and DuMond, J. W. M., *Fundamental Constants of Physics* (Interscience Publishers, New York, N. Y., 287 pp., 1957)
12. Henrikson, H. E., *U. S. Atomic Energy Commission, Rept. S.T.R. 24 Contract A.T. (04-3)-63* (California Institute of Technology, Pasadena, Calif., October, 1956)
13. DuMond, J. W. M., *Ann. Phys. (N. Y.)*, **2**, 283 (1957)
14. DuMond, J. W. M., Lind, D. A., and Watson, B. B., *Phys. Rev.*, **73**, 1392 (1948)
15. DuMond, J. W. M., Lind, D. A., and Watson, B. B., *Phys. Rev.*, **75**, 1226 (1949)
16. Lind, D. A., Brown, J. R., Klein, D. J., Muller, D. E., and DuMond, J. W. M., *Phys. Rev.*, **75**, 1544 (1949)
17. Lind, D. A., Brown, J. R., and DuMond, J. W. M., *Phys. Rev.*, **76**, 1838 (1949)
18. Muller, D. E., Hoyt, H. C., Klein, D. J., and DuMond, J. W. M., *Phys. Rev.*, **88**, 775 (1952)
19. Hoyt, H. C., and DuMond, J. W. M., *Phys. Rev.*, **91**, 1027 (1953)
20. DuMond, J. W. M., Hoyt, H. C., Marmier, P., and Murray, J. J., *Phys. Rev.*, **92**, 202 (1953)
21. Boehm, F., Marmier, P., and DuMond, J. W. M., *Phys. Rev.*, **95**, 864 (1954)
22. Murray, J. J., Boehm, F., Marmier, P., and DuMond, J. W. M., *Phys. Rev.*, **97**, 1007 (1955)
23. Marmier, P., and Boehm, F., *Phys. Rev.*, **97**, 103 (1955)
24. Baggerly, L. L., Marmier, P., Boehm, F., and DuMond, J. W. M., *Phys. Rev.*, **100**, 1364 (1955)
25. Boehm, F., and Marmier, P., *Phys. Rev.*, **103**, 342 (1956)
26. Hatch, E. N., Boehm, F., Marmier, P., and DuMond, J. W. M., *Phys. Rev.*, **104**, 745 (1956)
27. Boehm, F., and Marmier, P., *Phys. Rev.*, **105**, 974 (1957)
28. Hatch, E. N., and Boehm, F., *Phys. Rev.*, **108**, 113 (1957)
29. Boehm, F., Hatch, E. N., and Marmier, P., *Bull. Am. Phys. Soc.*, [II]**1**, 170 (1956)
30. Hatch, E. N., Marmier, P., Boehm, F., and DuMond, J. W. M., *Bull. Am. Phys. Soc.*, [II]**1**, 170 (1956)
31. Boehm, F., *Bull. Am. Phys. Soc.*, [II]**1**, 245 (1956)
32. Hatch, E. N., and Boehm, F., *Bull. Am. Phys. Soc.*, [II]**1**, 390 (1956)
33. Boehm, F., and Hatch, E. N., *Bull. Am. Phys. Soc.*, [II]**1**, 390 (1956)
34. Boehm, F., and Hatch, E. N., *Bull. Am. Phys. Soc.*, [II]**2**, 231 (1957)
35. Hatch, E. N., and Boehm, F., *Bull. Am. Phys. Soc.*, [II]**2**, 212 (1957)
36. Rose, D., Ostrander, H., and Hammermesh, B., *Rev. Sci. Instr.*, **28**, 233 (1957)
37. Chupp, E. L., Clark, A. F., DuMond, J. W. M., Gordon, F. J., and Mark, H., *Phys. Rev.*, **107**, 745 (1957); *Univ. Calif. Rad. Lab. Rept. UCRL 4871* (Liver-

180 DuMOND

more, Calif.); *Bull. Am. Phys. Soc.*, [II]**2**, 396 (1957); *Bull. Am. Phys. Soc.*, [II]**3**, 55 (1958)

38. Knowles, J. W., *Atomic Energy Can. Ltd., Chalk River Project, Rept. No. 6PI-42* (1957)
39. Temmer, G. M., and Heydenburg, N. P., *Phys. Rev.*, **100**, 150 (1955)
40. Mihelich, J. W., Harmatz, B., and Handley, T. H., *Phys. Rev.*, **108**, 989 (1957)
41. Bjerregard, J. H., and Meyer-Berkhout, U., *Z. Naturforsch.*, **11a**, 273 (1956)
42. Heydenburg, N. P., and Pieper, G. F., *Phys. Rev.*, **107**, 1297 (1957)
43. Andersson, B., *Proc. Roy. Soc. (London)*, **69A**, 415 (1956)
44. Huus, T., Bjerregaard, J. H., and Elbek, B., *Kgl. Danske Videnskab. Selskab, Mat.-fys. Medd.*, **30**[17], 1 (1956)
45. Elbek, E., Nielsen, K. O., and Olesen, M. C., *Phys. Rev.*, **108**, 406 (1958)
46. Mihelich, J. W., Scharff-Goldhaber, G., and McKeown, M. L., *Phys. Rev.*, **94**(A), 794 (1954)
47. Boehm, F., Marmier, P., and DuMond, J. W. M. (Unpublished data)
48. Sherr, R., and Christy, R. F., *Phys. Rev.*, **94**, 1076 (1954); **96**, 1288 (1955)
49. Nussbaum, R. H., Wapstra, A. H., Nijgh, G. J., Ornstein, L. T. M., and Verster, N. F., *Physica*, **20**, 165 (1954)
50. Fagg, L. W., Geer, E. H., and Wolicki, E. A., *Phys. Rev.* **104**, 1074 (1956)
51. Bernstein, E. M., and Lewis, H. W., *Phys. Rev.*, **107**, 740 (1957)
52. Temmer, G. M., and Heydenburg, N. P., *Phys. Rev.*, **96**, 430 (1954)
53. Breitenberger, E., *Proc. Roy. Soc. (London)*, **69A**, 453 (1956)
54. Ryde, N., and Andersson, B., *Proc. Phys. Soc. (London)*, **68**, 12, 1117 (1955)
55. Beckman, O., *Nuclear Instr.*, **2**, 1 (1958)
56. Ingelstam, E., *Die K-Spektren der Schweren Elemente* (Inaugural Dissertation presented at Upsala, Sweden, 1937)
57. Larsson, A., *Phil. Mag.*, **3**, 1136 (1927)

CONCEPTUAL ADVANCES IN ACCELERATORS[1]

By David L. Judd

Radiation Laboratory, University of California, Berkeley, California

INTRODUCTION

The most recent review of progress in accelerators (1) to appear in these volumes pertained to developments up to March, 1954. The level of activity in accelerator research and development between that time and the present has been very high, a fact illustrated by the recent bibliography by Behman (2), which covers the period from July, 1954 to June, 1957. This document has 153 pages and contains 716 references to the technical literature which represent the work of nearly a thousand authors. It also contains a useful tabulation of accelerator installations throughout the world, listing information on a total of 500 machines in use or under construction. This mass of information covers a great variety of topics which could scarcely be listed in these pages. The diversity of interests of the readers of these volumes is such that not even a restricted portion of this material can be reviewed in a way which will be both intelligible and useful to all.

Present activity in accelerators consists of a tightly woven combination of invention, science, and technology. The rewards of past accelerator developments have been so great as to stimulate inventiveness in many eager minds. The contributions of science and technology may be said to produce constraints on this inventiveness; science shows which new ideas are consistent with basic principles and indicates what goals are worth seeking, while the state of technology determines what it is practical to do and how much it will cost. As the size, complexity, and sophistication of these machines increases, it becomes less likely that any one individual will be able to conceive a new development, show it to be theoretically sound and likely to open a new scientific door, assess its technical feasibility, and estimate its cost, particularly in the domain of high-energy machines. Progress toward realizing such advances, therefore, requires the coordinated efforts of specialists in many diverse fields, which cannot be reviewed compactly. Nevertheless, the flow of new ideas constitutes the heart of our advance and forms a unifying thread which leads through the entire field of effort. It will, therefore, be the aim of the writer to present not a scholarly review but a discursive account of the key ideas which are making possible the developments of today and tomorrow. This will require some mention of earlier work which precedes the period under review. The choice of material will be guided by the writer's personal interests, and no attempt will be made at a complete coverage of the field. It is hoped that this account will serve to give to the

[1] The survey of the literature pertaining to this review was completed in June, 1958.

physicist who has not been concerned with accelerator design and development an awareness of some of the conceptual problems to which attention has recently been devoted by physicists who are trying to extend the capabilities of these machines. The corresponding range of technical and engineering problems is so wide that a similar treatment of them within the pages of this article is not feasible.

The problem of supplying helpful bibliographical information is difficult for several reasons. Space does not permit any attempt at completeness. Much of the work of greatest current interest is to be found in the several long series of unpublished technical reports issued by the rather large number of laboratories at which accelerators exist or are under construction or study. Unfortunately, the greater portion of these reports is not included in available bibliographies. Perhaps the best single recent source of both general and bibliographical information on high energy accelerators is the first volume of the *Proceedings of the CERN Symposium on High-Energy Accelerators and Pion Physics* (3) held at Geneva in 1956, which should certainly be carefully studied by anyone with a serious interest in this field. A number of recent review articles, books, and bibliographies pertaining to various accelerator topics are also listed in the bibliography (4 to 11); several works of a general nature are listed in (2). In addition, a considerable number of references have been given which pertain to material in the text to follow. A thorough account of the development of present accelerators has been prepared by McMillan for the third volume of *Experimental Nuclear Physics* (12). An encyclopedic coverage of current knowledge in the field of particle accelerators will soon be available in Volume 44 of the *Handbuch der Physik* (12a) which is now in press. This volume will contain comprehensive articles on all of the present types of accelerators; it will no doubt be a standard reference work on this subject for many years to come. However, the writer is convinced that it will continue to be a difficult task for anyone who does not have access to the unpublished report literature to keep abreast of current activity in this field. For this reason the service performed by the staff of the CERN Laboratory in conducting the 1956 conference and in so promptly issuing its proceedings was of the greatest importance; it is to be hoped that another conference of the same type will be held in the near future.

CONCEPTUAL ADVANCES IN HIGH-ENERGY ACCELERATORS

CONCEPTS DEVELOPED BEFORE 1950

Resonance accleration.—The first of these important ideas was of course the concept that a charged particle could be given a high final energy in many successive small increments. This principle of resonance acceleration, applied by Wideröe to linear and by Lawrence to both linear and circular (cyclotron) geometries about 30 years ago, opened the door to the domain of energies beyond those of the single-push electrostatic machines. However, it is worth remarking that just over half of all the accelera-

tors listed by Behman (2) are of this latter type; their many virtues and the extraordinary richness of the nuclear phenomena made available for study by their use have led to a steady increase in their numbers and to many improvements which continue to enlarge their capabilities in the low-energy domain. It will not be possible for us to consider these in the present review.

The linear accelerator work of Wideröe and of Lawrence was ahead of its time, but everyone knows how successful the cyclotron turned out to be. There are now about 50 cyclotrons of conventional type, of varying energies and other capabilities, distributed among about 15 countries around the world. The number of constant-frequency cyclotrons is likely to increase still further as a result of the conceptual advances to be described below.

Cyclotron focusing and energy limitations.—The next advance, with respect to cyclotrons, was the theoretical study of their energy limitations, which are intimately connected with the problem of focusing or controlling the motions of the particles during their acceleration. The work of Bethe & Rose (13), Rose (14), and Wilson (15) in 1937–38 led to a clear picture of the conflicting requirements of orbit stability and higher energy. Stability against displacements out of the orbital plane (henceforth called the z direction) requires the magnetic field to decrease with increasing orbit radius, to secure the proper direction of curvature of the magnetic field lines, while high energies can only be attained if the particles continue to stay in step (i.e., in phase) with the constant frequency, ω, of the accelerating voltage. This requires the magnetic field of induction B to increase with increasing radius so as to match the relativistic increase of the mass, m, so as to satisfy the equation $\omega = eB/(mc) = $ constant (gaussian units). In terms of cylindrical polar coordinates, one may say that the requirements of focusing the particles in z and maintaining the proper rate of change of azimuthal angle, θ, were found to be incompatible, in the simple cyclotron geometry, for acceleration to even modestly relativistic energies.

Phase compensation and Thomas focusing.—The inventiveness required to reach a partial solution of this dilemma appeared almost at once, in the work of Thomas (16) in 1938. He recognized that the simple symmetrical cyclotron geometry was only a very special case, so special as to put a much stronger constraint on controlling the particles than was necessary in more general configurations. By considering magnetic fields having only fourfold symmetry in azimuth, rather than complete rotational symmetry, he found that the functions of focusing in z and phase control in θ could be made independent, at least for slightly relativistic particles. This objective is gained by the additional focusing in z caused by the successive passage of the particles through the wedge-shaped fields formed by alternating hills and valleys of the magnet poles. It was therefore possible to allow the azimuthally averaged field to rise with increasing radius so as to provide phase compensation for the relativistic mass increase, the defocusing tendency being overbalanced by the wedge focusing. This work of Thomas had considerable generality in principle. He wrote down terms cor-

responding to what is now called alternating gradient focusing but discarded them as being small with respect to the averaged effect which is known as Thomas focusing. This concept was applicable to particles whose velocities, v, ranged well up toward that of light, but he calculated in terms of a power series in v/c, and retained only the lowest nontrivial powers, so that the energy limitation of this scheme could not be evaluated. He also considered multiple gap accelerating systems.

Inductive acceleration.—This conceptual advance was so far ahead of the accelerator technology of its time that it did not receive experimental verification until 12 years later. In the intervening time two other new ways of accelerating particles into the relativistic range of speeds became available. The practical application of inductive acceleration to electrons in the betatron was accomplished by Kerst (17) in 1941, with the aid of the careful study of magnetic focusing in radial distance, r, and in z made by Kerst & Serber (18). Their work portrayed the nature of this action so clearly that the resulting motions are now universally known as betatron oscillations, no matter in what magnetic accelerator they may occur. These motions, when small, were shown to be governed in azimuthally symmetric circular accelerators by the two linearized equations

$$\frac{d^2(r-R)}{d\theta^2} + (1-n)(r-R) = 0, \qquad \frac{d^2z}{d\theta^2} + nz = 0,$$

where $n = -(r/B)(dB/dr)$ and is called the magnetic field index. R is the desired orbit radius and B is the magnetic field strength in the orbital plane; z is the displacement normal to the orbital plane and θ the azimuthal angle in this plane. Both displacements, $r-R$ and z, are seen to be sinusoidal if $0 < n < 1$ and to have frequencies $\nu_r = (1-n)^{1/2}$ and $\nu_z = n^{1/2}$, relative to the frequency of circulation, which are somewhat less than unity. By including in these equations those parameters, such as particle mass and velocity, which change slowly during acceleration, Kerst and Serber treated the slow changes in amplitude and energy of these oscillations called adiabatic damping effects. These may produce a contracted beam of very small cross-sectional area at the final energy. Adiabatic damping is important in many accelerator processes and will be referred to again later on. Betatron accelerators have proved to be useful not only in research but also in industrial and medical applications, and their number continues to increase, 70 being listed in Behman's tabulation referred to above.

Phase stability.—The most far-reaching and important new concept following the original idea of repetitive or resonance acceleration was that of phase stability, discovered independently by Veksler (19) in 1944 and by McMillan (20) in 1945. This principle completely divorces the problems of magnetic focusing in r and z from those of control in θ, that is, in phase relative to the alternating accelerating voltage. This principle is so well known that no description of it will be undertaken here. By making possible the frequency-modulated cyclotron, or synchrocyclotron (fixed field, variable frequency),

the electron synchrotron (fixed frequency, variable field), the proton synchrotron (variable field and frequency), and the microtron (fixed field and frequency), it enlarged the domain of what was practical to build by larger amounts and in more directions than any other single idea about accelerator possibilities up to that time. Its importance was quickly realized and exploited by the construction of a number of these accelerators. There now exist about 25 frequency-modulated cyclotrons, 30 electron synchrotrons, and eight proton synchrotrons, including those under construction, operating on this principle and using conventional magnetic focusing. An interesting review of contemporary microtrons, together with proposals for their application to the acceleration of large currents of both protons and electrons to energies in the billion electron volt range, has recently been presented by Roberts (21).

Modern linear accelerators.—At about this time the application of resonance acceleration to linear accelerators, which had lain dormant since Lawrence's early work, was revived because of wartime advances in technology which made possible the production of large amounts of power at very high frequencies. The standing-wave type, applicable to protons and heavier ions, was first developed by Alvarez *et al.* (22). Utilizing a single long cylindrical resonant cavity with an axial electric field through which the particles pass, being shielded by drift tubes from opposing fields during half of each cycle, it contrasts with Lawrence's early version consisting of more nearly lumped circuit elements driven through lines. Linear accelerators were shown by McMillan (23) to be subject to a limitation like that of cyclotrons, in that radial focusing and longitudinal or phase control are incompatible if each is due entirely to the resonant electromagnetic fields and no physical obstructions such as grids or foils are presented to the beam. The lifting of this limitation, which has also been accomplished by considering more general geometries of electric and magnetic fields, will be mentioned later. The number of heavy particle linear accelerators has been increasing rapidly and now stands at approximately 15, including machines under construction.

The same wartime technology which provided power supplies for these machines gave an impetus to the development of high-power klystron tubes operating at even higher frequencies which made possible the development of the electron linear accelerator, initiated by Hansen and carried on so successfully by the Stanford University group (24). In these machines microwave power is fed down a hollow waveguide which is loaded so that the phase velocity of waves is the same as that of the electrons passing through the guide. The particles may be thought of as being accelerated like surfboards on ocean waves. Although McMillan's theorem applies here, the problem of radial focusing is almost nonexistent as a result of the shortening of the waveguide by Lorentz contraction as seen from an electron's rest frame; this makes the relative aperture of the machine seem much larger, since the transverse dimensions are unchanged. To be specific, the radial spread of

particles increases only logarithmically along the guide. The variety of applications of energetic electron beams is illustrated by the listing by Behman of no less than 45 linear electron accelerators.

LIMITATIONS ON ACCELERATORS AROUND 1950

Let us now pause briefly to survey the limitations applying a few years ago to the various types of accelerators described thus far, before considering the more recent concepts which are removing some of these limitations and stimulating the various advances of today.

The ordinary cyclotron was primarily limited as to particle energy, which can only be increased by using very large dee voltages so as to reduce the time of acceleration of a particle and, therefore, the time during which it can fall behind in phase. The dee voltage required varies roughly as the square of the desired energy. Because of the availability of the frequency modulation technique, it seemed uneconomical to push cyclotron proton energies much beyond 20 Mev. However, very high currents, up to milliamperes, can be produced. The extraction of external beams has been a relatively inefficient process, with a large fraction of the circulating particles being lost.

The frequency-modulated cyclotron is limited in energy chiefly by magnet weight and cost, which vary roughly as the third power of the final momentum. It is not likely that the highest present proton energies of about 700 Mev will be exceeded by machines of this type,[2] since proton synchrotrons are more economical for higher energies. There would also be some difficulty in extending the range of frequency modulation much further. The currents of these machines are in the microampere range because the beam is pulsed; one group of particles is accelerated during each cycle of the frequency modulation. The number of particles per pulse depends on a variety of factors which do not allow an indefinite increase. Beam extraction for external experiments was also very inefficient until a few years ago.

The energy of a betatron is limited to a few hundred Mev by radiation losses caused by the centripetal acceleration of the electrons. Its current has been restricted to the microampere range because it also produces a pulsed beam; the time between pulses is limited by the inductance of a large magnet. The number of particles per pulse is limited by space charge effects at injection and by the size of the accelerating chamber, which has a large influence on the cost. Since the electron beams were not usually extracted, only the gamma radiation was available for external experiments. Because injection in electron synchrotrons is similar to that in betatrons, and a pulsed magnet is also used, their currents are subject to similar limitations. External beams were also not available. However, the use of a ring

[2] See Reference (3), *Proceedings of the CERN Symposium on High-Energy Accelerators and Pion Physics*, **1** (1956). Thornton, R. L., 413–18; Mints, A. L. *et al.*, 419–24. In following footnotes, this reference will be mentioned only as Ref. (3).

magnet and radiofrequency acceleration voltages changes the limiting energy appreciably. Much larger radiation losses can be compensated, and a given magnet weight can be distributed differently to contain electrons of much higher momentum. The economically reasonable upper energy is therefore much higher and is determined by the size of the accelerating chamber and the cost of radiofrequency power. The highest energy reached by a conventional electron synchrotron thus far is 1.2 Bev.

The linear accelerators, both ion and electron, are limited in energy only by cost and complexity. Their currents are sharply pulsed, with average currents in the microampere range. The beams are, of course, automatically and completely extracted and may possess very small spreads in energy and angle. Proton linear accelerators suffered beam loss from foils or grids required to produce radial focusing for particles whose axial motion was stable. The highest proton energy attained so far is 68 Mev. Plans for a proton machine of this type at several hundred Mev were cancelled by the British group at Harwell because of the successful development of the regenerative deflector for frequency modulated cyclotrons, to be described below. An electron linear accelerator has reached 650 Mev, and plans for much higher energies will also be mentioned later.

The energy limit of a standard proton synchrotron is primarily an economic question. The dominant factor is the relative aperture of the accelerating chamber required for satisfactory operation, since this fixes the size and weight of the magnet. A reasonable limit probably lies between 10 and 15 Bev, the former for a conservative and the latter for a minimum aperture. Average currents are in the millimicroampere range and are limited by the magnet pulsing rate, the current available from the injector, and the efficiency of injection and capture. The extraction of a primary beam for external experiments is a matter of considerable difficulty, particularly for some magnet geometries, and there are some interesting experiments for which much larger currents would be necessary or desirable.

Of the various limitations mentioned above, the following either have already been made less stringent or removed, or can now in principle be eased: (a) energy limit and beam extraction efficiency of constant frequency cyclotrons; (b) beam extraction efficiency of frequency-modulated cyclotrons; (c) beam current of betatrons and electron synchrotrons; (d) practical energy limit of electron synchrotrons; (e) beam extraction from betatrons and electron synchrotrons; (f) necessity of beam loss from foils or grids in ion linear accelerators; (g) energy limit of proton synchrotrons; (h) beam current of proton synchrotrons; and (i) beam extraction from proton synchrotrons. These improvements over what could be done around 1950 are the result of a group of new concepts which have been developed and applied since that time.

Recent Conceptual Advances

Alternating gradient focusing.—A very important new concept which has had a powerful influence on accelerator developments is that of alternating

gradient focusing, first discovered by Christofilos (25) in 1949 and independently rediscovered and developed by Courant, Livingston & Snyder (26) in 1952. A brief review of this principle has been given in an earlier volume of this series by Blewett (1). Its simplest and most direct effect is to make possible the containment of particles having a given range of transverse momenta in a beam of much smaller transverse dimensions than is possible with conventional focusing forces whose strength is more or less uniform along the beam. However, the ramifications which follow from this effect have led to other possibilities for improving accelerators, to which this concept did not at first appear to be directly applicable.

It is obvious that if a smaller aperture can be used in a ring magnet the same investment in magnet steel will provide a ring of larger radius to accommodate particles of higher momentum, so that the practical energy limits of electron and proton synchrotrons can clearly be raised as a result of this discovery. The exploitation of these possibilities has accounted for the largest part of the efforts of high-energy accelerator design and construction groups for the past several years. An account of the progress of these efforts will be deferred to a later section of this review. It is also clear that this same technique of stronger focusing may be used on linear accelerators (27) to remove the limitation mentioned above so that beam loss due to grids or foils may be eliminated. This procedure, first carried out on the proton linear accelerator at the University of California Radiation Laboratory in Berkeley (22) using electrostatic focusing, has now become a standard part of the design of such machines, with magnetic focusing by quadrupoles inside the drift tubes being most commonly used.

Momentum compaction.—One of the interesting effects associated with alternating gradient focusing in circular accelerators is a phenomenon which has come to be called momentum compaction. To understand it, consider first an ordinary accelerator magnet having rotational symmetry about its axis. If two particles having momenta p and $p+dp$ are moving in circular orbits, their radii will be r and $r+dr$; dr and dp are related by $Br/p=(B+dB)$ $(r+dr)/(p+dp)$, or $(1-n)$ $(dr/r)=dp/p$, where n is the field index defined above, corresponding to the radial field variation $B \propto r^{-n}$. The factor $(1-n)$ may be called the momentum compaction factor, α, being large if a small radial aperture Δr is required to accommodate closed orbits having a given range of momentum Δp, and vice versa. The use of this term is motivated by the observation that if this factor increases, the various orbits of different momenta become compressed together and lie more compactly in an annular region of smaller radial extent.

Next let us consider the same problem in the magnet of a synchrotron with alternating gradients. The field strength along a particular circle of radius r_0 is uniform in space but its radial gradient alternates regularly along the azimuth between very large negative and positive values $(|n|\gg1)$. A particle with the proper momentum p_0 may move in a circle of radius r_0, but a particle with a slightly higher momentum p_0+dp can no longer have

a circular closed orbit. Because of the strong gradients, its closed orbit will consist of symmetrical short curved segments with alternating larger and smaller radii than r_0. Its greatest displacements from r_0 will occur in regions of positive radial field gradient, and vice versa, so that it passes on the average through regions of much greater field strength than at r_0. Thus, the field which it sees corresponds to one of large positive gradient, or negative n, and the momentum compaction factor α will be very large as compared with the simple magnet, in which $0 < n < 1$ to ensure stability of betatron oscillations in both r and z. One effect of this large momentum compaction in alternating gradient synchrotrons is to create a transition energy at which the phase stability vanishes. This phenomenon has been thoroughly investigated; it appears to create no serious problems, and a way of avoiding it altogether has been found by Vladimirski & Tarasov.[3]

Fixed field alternating gradient accelerators.—It is of greater interest to trace another line of development connected with momentum compaction. It was observed in 1954 by Symon (28), working with the accelerator study group sponsored by the Midwest Universities Research Association (MURA), that the momentum compaction, which was large enough to contain momentum spreads $\Delta p/p$ equal to many times the radial aperture $\Delta r/r$, might be used to contain all momenta between the initial value at injection and the final value after full acceleration, within a ring for which Δr was still much less than r. It would then no longer be necessary to pulse the magnet current in synchronism with the increasing energy of a batch of particles being accelerated, so as to keep the batch always near to the radius corresponding to a circular orbit; rather, the magnetic field could be fixed in time while particles could be accelerated at a rate depending only on how rapidly energy could be supplied to them.[4] This conception of a fixed field alternating gradient accelerator (FFAG) has been exploited extensively by the MURA group (29). In addition to developing the basic idea outlined above, they have originated several other new concepts, conducted extensive theoretical and numerical studies of a variety of new types of accelerators, and constructed working models to test several features of these systems. It is interesting that one aspect of their thinking led them through a full circle back to the original work of Thomas mentioned above, which had meanwhile been given an experimental test at the University of California Radiation Laboratory in Berkeley (30) on two models of constant-frequency cyclotrons which accelerated electrons to semirelativistic energies.

The removal of one limitation, that imposed on betatron currents by a very small duty cycle, with the FFAG technique has already been experimentally demonstrated by the MURA group. By providing more change of

[3] For a discussion of transition energy problems, see the several papers on this subject in Ref. (3), pp. 103–25.

[4] Related suggestions have been made independently by Miyamoto, by Ohkaha, and by Snyder. See Ref. (3), pp. 32–33; Ref. (29), Footnote 2.

flux through the guiding magnet ring than is required to reach full energy, particles may reach a target steadily for a large fraction of the time, for example, one-fourth the time if twice the flux change needed for a single particle is available. The extra flux change can be provided since it is independent of the d.c. guide field. This duty cycle is so large compared to that of a conventional betatron as to indicate that currents might be increased a thousandfold or more.

The principal endeavor of the MURA group has been to apply the FFAG concept to high-energy proton synchrotrons. This terminology may be confusing, though, since such a machine would perhaps be better described as a large frequency modulated cyclotron with a very large hole in the middle. Because the center or very low-energy part of the magnet is missing, particles must be accelerated by some other means to at least several Mev before being injected tangentially into the ring from the inside. Some of them would then be trapped into regions of phase stability and accelerated by frequency modulated voltages in the d.c. magnet as in a conventional frequency modulated cyclotron. However, the large momentum compaction, which makes possible the use of a relatively thin annular guiding magnet, will also (in most designs) produce a transition energy as in alternating gradient synchrotrons. The hope of accelerating very high currents is based on the idea that the repetition rate of the accelerating process may be made high, since it is governed by radiofrequency voltages and modulation rates rather than by feasible magnet pulsing rates as in proton synchrotrons. In this way one might hope to handle microamperes rather than millimicroamperes of relativistic protons, and perhaps also much higher electron currents than in conventional electron synchrotrons. These possibilities will be studied on a 50 Mev electron FFAG machine now under construction at the MURA laboratory, and it is in the expectation of its success that one may say that synchrotron beam current limitations have been eased.

Spiral ridge geometries.—One can next raise the question whether an FFAG ring magnet guide field could be extended inward radially to the center, so that particles could be started from rest, as in the cyclotron, rather than injected at a finite initial energy. Conceptually, one would then have again a frequency modulated cyclotron, but with azimuthal variations in the magnet to produce the alternating gradients. The next logical step is to examine the possibility of adjusting the parameters so that the condition of isochronism of all the orbits is restored, removing the need for frequency modulation. In this way the MURA group made contact with the theory of Thomas, which applied only to slightly relativistic particles, and its extension to higher energies by McMillan and by Judd (31) which had led to the Berkeley "clover-leaf" model cyclotrons, as they were called. A large number of workers in many laboratories have also considered these concepts during the last three or four years; some of the ideas and techniques of calculation involved have been independently suggested or worked out at several laboratories. No ade-

quately definitive review of all the problems of constant-frequency relativistic cyclotrons and their treatment has yet been undertaken.[5] It has been shown that the highest kinetic energy obtainable is probably limited by an unavoidable resonance effect at $\nu_r = 2$ (to be described later) to a value approximately equal to the rest energy of the particle. In order to reach energies in this range, it is necessary to spiral the ridges of the Thomas configuration described earlier, which has the effect of further enhancing the focusing in z. Spiral ridge geometries were first proposed and have been studied extensively by the MURA group (29, 32) as a possible form of FFAG ring magnet geometry allowing a reduction of the ring's circumference. A detailed design study for a constant frequency spiral ridge proton cyclotron of energy between 800 and 900 Mev has been made, and a model electron accelerator constructed, by a group headed by Livingston (33) at the Oak Ridge National Laboratory, based on the theoretical work of Welton.[6] The application of spiral or radial ridge pole geometries to improve or extend the performance of more modest constant frequency cyclotrons has been studied extensively by a large number of accelerator groups both in this country and abroad,[7] and has also been successfully applied to the Los Alamos cyclotron by Boyer.[8]

The regenerative deflector.—Thus far the newer concepts associated with easing all of the limitations mentioned above have been discussed, except those associated with the extraction of beams. Some of the most interesting of the presently available techniques are closely related historically to early attempts to understand and facilitate the inverse problem of injection into betatrons and synchrotrons. In 1949 Davis & Langmuir (34) pointed out that azimuthal variations in the magnetic field gradients of these machines could be arranged so as to damp quickly radial betatron oscillations of some of the injected particles, which would help them avoid hitting the injector structure. They noticed that in some cases the oscillations which were damped would grow again. In a general study of these effects, it was found by Judd (35) that this growth was a universal feature

[5] The interested reader may gain some impression of this work by referring to bibliography items 368, 379, 392, and 412 of Ref. (2); to Ref. (3), pp. 9–25, 59, 547–51; and to Ref. (29, 30, 33).

[6] See Ref. (33), pp. 63–117, 187–210c.

[7] Among these laboratories are the University of California at Los Angeles, the University of California Radiation Laboratory, the Universities of Colorado, Florida, Illinois and Michigan, Michigan State University, and the Oak Ridge National Laboratory, in the United States; in Europe, the writer has heard of interest in these possibilities at Harwell in England, at Saclay in France, in Holland, and at Zurich. In some cases the use of frequency modulation is also contemplated. Several groups are planning to accelerate a variety of heavier ions, and to provide for a continuous variation of particle energy by changing the magnetic field strength and the frequency of the accelerating voltage, as has already been done on the conventional cyclotron at the University of California Radiation Laboratory at Livermore.

[8] Boyer, K., Los Alamos Scientific Laboratory, New Mexico (Unpublished work).

of such perturbations, associated with conservation of particle density in phase space; it could only be eliminated by rapidly removing the perturbations after they had done their work. The inverse effect, applying to beam extraction, was proposed by Tuck & Teng (36, 37), who considered its application to frequency modulated cyclotrons and christened it the regenerative deflector. The theory has been developed by LeCouteur (38) and has been successfully applied to several large accelerators of this type. The time variation in these machines is supplied by the accelerating voltage which moves the beam outward in radius into the desired region. The action of the magnetic perturbations can be simply described as pulling the frequency of a betatron oscillation (usually the radial one) toward the nearest field-error resonance value and at the same time supplying the necessary "error" to cause the resonant growth of amplitude which one normally attempts to avoid during acceleration. The principle can also be applied to synchrotrons, both conventional and alternating gradient,[9] but the field variations must then be pulsed at the proper time. By this means electron beams have been extracted from several accelerators. A study of the application of this principle to constant frequency cyclotrons has been made by Rogers (39), and the several groups now designing Thomas or spiral ridge machines will attempt to apply it. Experience with model electron cyclotrons of this type (30) suggests that the beam may be somewhat easier to bring out than in the older symmetrical machines. The application of the concept to the problem of transferring a beam from one accelerator to another or into a "storage" magnet has also received attention (40, 41).

An entirely different method for generating an external beam from a proton synchrotron, based on a sudden change of energy due to traversal of a special target, has been proposed by Wright (42) and by Piccioni et al. (43); it has been successfully installed on the Brookhaven National Laboratory Cosmotron.[10] Its application to the CERN alternating gradient synchrotron has been carefully considered and is felt to be feasible.[11]

PHASE SPACE CONCEPTS APPLIED TO ACCELERATOR PROBLEMS

Having now touched on those new concepts which are making it possible to ease or remove the limitations on the earlier types of accelerators, the writer feels that it is important to point out the increasing application of a very old concept to many types of problems that arise in dealing with groups of particles. This is the concept of the "density of particles in phase space," to which the theorem of Liouville applies, provided that the forces acting on the particles are derived from a Hamiltonian function. It is not necessary to advertise the utility of the general and elegant methods of classical mechanics

[9] See Ref. (3). Vladimirski, V. V., et al., pp. 133–36.
[10] See Ref. (3). Collins, G. B., pp. 129–32.
[11] See Ref. (3). Citron, A., pp. 137–38.

for dealing with systems of large numbers of particles; this constitutes the subject matter of statistical mechanics. It is interesting, however, to point out that new insights and valuable calculational techniques are being gained by their application to relatively simple acceleration and beam-handling situations. It is not necessary to be well versed in the general theory in order to gain a clear appreciation of how the concepts of phase space can be brought to bear on these problems.

BASIC THEORY

For the benefit of the reader who needs a brief review of Hamiltonian mechanics, the essential concepts will next be summarized. Consider a group of identical noninteracting particles, moving under the influence of external forces. Let the coordinates of a particle be denoted by $q_1, q_2, \cdots, q_n$. The system consisting of this particle and the external forces is said to be Hamiltonian if there exists a Hamiltonian function $H(q_1, q_2, \cdots, q_n; p_1, p_2, \cdots, p_n; t)$ depending on the coordinates q_i, the canonically conjugate momenta p_i, and (possibly) the time t, such that the equations of motion of the particle (Hamilton's equations) are:

$$\dot{q}_i \equiv dq_i/dt = \partial H/\partial p_i, \quad i = 1, 2, \cdots, n,$$
$$\dot{p}_i \equiv dp_i/dt = -\partial H/\partial q_i, \quad i = 1, 2, \cdots, n,$$
$$\dot{H} \equiv dH/dt = \partial H/\partial t.$$

(If H does not contain the time explicitly it is a constant of the motion, equal to the total energy of the particle. One may regard the canonical momentum p_i conjugate to the coordinate q_i as being defined implicitly in terms of dq_i/dt, the other q's and p's, and t, by the first of these equations.) Next let us consider the particle to be represented by a point in the $2n$-dimensional phase space whose coordinates are the q's and p's. The point will in general move about in this space. Now suppose each of the many particles to be simultaneously represented in this way. This swarm of points is to be thought of as a group of elements of a fluid, such as molecules of a gas in ordinary space. Liouville's Theorem then states that these points can not move like a gas but are constrained to behave as an incompressible fluid; the number of points per unit volume in the neighborhood of a given point may not change with time, although the neighborhood and the points in it may move about in phase space and vary in shape. The proof is extremely simple. The $\dot{q}_i$ and $\dot{p}_i$ are the $2n$ components of the velocity v_P of a point P in the phase space: the divergence of the flow is

$$\nabla_P \cdot v_P = \sum_{i=1}^{n} \left(\frac{\partial \dot{q}_i}{\partial q_i} + \frac{\partial \dot{p}_i}{\partial p_i} \right) = \sum_{i=1}^{n} \left(\frac{\partial^2 H}{\partial q_i \partial p_i} - \frac{\partial^2 H}{\partial p_i \partial q_i} \right) \equiv 0,$$

and hence there can be no sources or sinks of fluid density. Stated differently, the co-moving derivative of particle density in phase space must vanish.

When stated and proved in this simple way, the theorem may seem at first sight to be so obvious and general as to be devoid of physical content.

It is true its utility rests on finding a Hamilton function for the system (if one exists), or, that is, a set of coordinates and momenta for which the theorem is true. However, in a great many situations of practical interest, this task is simple, while in others it is easy to show that none exists, so that there are no q's and p's for which the density in phase space is conserved. Two simple examples may be helpful here. First, the small betatron oscillations of a particle in a circular accelerator are approximately simple harmonic; considering only one coordinate $q_i = z$, the Hamiltonian of a simple harmonic oscillator is $H = p_z^2/(2m) + kz^2/2$; the equations of motion are $\dot{z} = p_z/m$, $\dot{p}_z = -kz$ (corresponding to $m\ddot{z} + kz = 0$). From the first of these we see that $p_z = m\dot{z}$, as one would expect for a momentum. If the mass m and the "spring constant" k are constant, H is also constant, and each particle moves on an ellipse in the two-dimensional phase space. Because all particles have the same period, those particles which are initially neighbors (either on adjacent ellipses or spaced along a single ellipse) will forever remain neighbors, their density in phase space being constant. However, the theorem also tells us that even if m or k is made to vary explicitly in any manner with the time, so that the paths are no longer ellipses and the Hamiltonian is no longer constant, the conservation of density in phase space will still be maintained. For example, a slow steady increase in k will decrease the q-axis of any ellipse (adiabatic damping of amplitude) but will also necessarily increase its p-axis ("heating" by compression), since if this were not so the number of points inside this ellipse would remain constant while the (two-dimensional) volume available to them would decrease, thus increasing the density at least somewhere inside and violating the theorem. (Note that the result is independent of whether or not there are any points which actually populate this space.)

Next let us consider the effects on this oscillating particle of radiative damping due to the acceleration of charge. The radiation reaction force will also cause a slow decrease of the q-axis of a particle's ellipse, corresponding to amplitude damping. However, in this circumstance the p-axis will also decrease, because the maximum kinetic energy of the particle is also decreased by the amount of energy given up to radiation. Particles with more energy, moving on larger ellipses, will radiate more rapidly, even relatively, than those on smaller ellipses, so that the ellipses will converge, increasing the density of representative points everywhere. It is impossible to construct a Hamiltonian representing this state of affairs because of the way in which the radiation reaction force depends on p and its derivatives.

Before applying phase space arguments to accelerator problems, it is useful to remember that some general classes of systems are known to be Hamiltonian, no matter how complicated they may be, while others are known to be non-Hamiltonian, no matter how simple. Any system of external macroscopic electric and magnetic fields acting on charged particles is Hamiltonian, if radiation effects are neglected, while no system involving scattering and ionization loss from fixed targets or electromagnetic radiation from

accelerated charges can be Hamiltonian.[12] It may also be noted that one need not always use three spatial coordinates for a particle. If the Hamiltonian separates into a sum of terms each involving only one or two p,q pairs, the motions in the restricted two- or four-dimensional phase spaces are independent and may be treated separately. In fact, the coordinates need not even refer to spatial position and the independent variable need not be the time; any Hamiltonian function of pairs of variables provides a theorem of conservation of density in its phase space.[13]

APPLICATIONS TO ELECTRON AND ION OPTICS

It is frequently possible to get useful information by making approximations such as neglecting physical effects which make a system non-Hamiltonian, or neglecting small coupling effects (which, if included, would destroy the separability of the Hamiltonian) in order to deal with a phase space of lower dimensionality. In our first example we will consider this latter case, applying it to the motion in local x and y coordinates of a beam of nearly monoenergetic charged particles whose motion is predominantly in a direction perpendicular to these coordinates. The beam is to be considered as analogous to a pencil of light rays, since it can be bent, focused, and dispersed by any combinations of electric and magnetic fields (which replace the lenses and prisms of optics) on its way from some source to another piece of apparatus into which it is to be directed. This beam is characterized, at any value of distance along the "optic axis," which we call z (although it may not be rectilinear), by the "volume" it occupies in the four-dimensional phase space having coordinates x, y, p_x and p_y. (Motion in the z direction of these locally orthogonal curvilinear coordinates may be neglected if we assume that the particles have a nearly uniform drift velocity component in this direction which is unaffected by small transverse displacements and velocities. This approximation is equivalent to that of treating paraxial rays in geometrical optics.) The limits of the beam in x and y are its geometrical cross-sectional dimensions, while the limits in p_x and p_y are determined by the largest angles α_x and α_y between any of the trajectories and the z axis; $p_x^{max}=\alpha_x^{max}p_z$, $p_y^{max}=\alpha_y^{max}p_z$, and p_z is nearly a constant for the beam. The density of representative points in this space depends on the distribution of density in x, y, α_x, and α_y which occur at the value of z in question. For example,

[12] We neglect the theoretical possibility of including in the Hamiltonian the coordinates and momenta of all the particles in the target or the infinite number of "coordinates" and "momenta" of the electromagnetic field, since this is usually not practical in accelerator problems. We also neglect forces between the particles in our description here. Systems with nonnegligible interparticle forces, such as those involving self-consistent fields and orbits, are also Hamiltonian but have a more complicated interpretation.

[13] For example, see (4), Appendix B (Courant, E. D., and Snyder, H. S., *Annals of Physics*). In following footnotes, this reference will be referred to only as Ref. (4).

if the particles are diverging in a field-free region from a point source at $z = 0$, their paths are straight lines, and there is a perfect correlation between x and p_z, for example; $x = \alpha_x z$, $p_z = \alpha_z p_z$, and α_x is a constant for each particle. Such a beam lies entirely on a two-dimensional surface, where the density is singular. Considering only x and p_z, the points lie along a straight line in this phase plane. Liouville's Theorem then tells us that in principle no system of forces downstream can spread the points out to lie on a finite area of the plane. The line may be bent, rotated, distorted, made to lie along the p-axis (point image of the point source) or along the x-axis (parallel beam) but it will always remain a line, with the same number of points per unit length. (The rather obvious departure from this ideal behavior in practice is due entirely to aberrations whose consideration invalidates the assumption that the behavior in z and p_z may be regarded as independent of and uncoupled from the transverse degrees of freedom.) As another example, particles emanating from a diffuse source, such as a hot filament or ionized gas, will have a continuous distribution in x, p_z, etc., and will fill the occupied part of phase space with a finite density. Then, by Liouville's Theorem, no conceivable system of external forces downstream can bring them to a point focus, a parallel beam, or to any other configuration occupying a lesser volume of the phase space. However, it may in principle displace and distort the shape of this volume in any way. These simple examples are closely related to a well-known intensity theorem in optics, the connection being through the analogy between optics and mechanics which guided Hamilton in his famous work.

Suppose that an injector emits a beam of large angular spread through a small hole. It may be desired to insert the beam into an accelerator with a large aperture in which only small angular spreads can be accepted because of weak focusing. The phase space occupied by the emitted beam has come to be called the "emittance," while the phase space accepted by the accelerator is called the "acceptance" or "admittance." (The units of these quantities are sometimes altered by dividing by the constant momentum p_z, leaving centimeter-radians, for each transverse degree of freedom.) If the emittance is greater than the acceptance, some beam will inevitably be lost in the transfer. If it is less, some empty phase space will be left inside the accelerator aperture. By examining the shapes of the occupied regions at emission and acceptance one may see what type of volume-conserving distortions by focusing elements must occur between them, and determine the field configurations that will be required to achieve these changes in practice. Problems involving energy spreads involve all three spatial dimensions, but useful guidance can be gained from a similar approach. Many workers have used these concepts in designing injection systems for a variety of accelerators.[14] They are also useful in considering the problems of trans-

[14] For example, see Ref. (3), Hereward, H. G., *et al.*, pp. 179–91; Bruck, H., *et al.*, pp. 200–4.

ferring beams of particles from one accelerator to another (40, 41, 44, 45), in determining aperture requirements in alternating gradient focusing devices,[15] and in studying the action of deflecting and extracting systems depending on resonant excitation effects.[16] Many of these calculations employ a simple technique of matrix multiplications in which conservation of phase space density is implied by the use of matrices of determinant unity.[17]

A phase-space calculation can place an upper limit on the number of particles which may be accommodated in an accelerator by multi-turn injection from an injector with given current, energy spread, and transverse distribution, or on the number of particles which it may retain, after acceleration, in a space of given dimensions (46). Of course, the practical problem always remains of how closely such upper limits may be approached; this is determined by aberrations, imperfections in programming the course of events, scattering, and other neglected processes, which in general will dilute the population in phase space or will "stir" into it regions which are empty or more thinly populated with representative points than was the phase space of the original source of particles. In some applications it is useful to consider the flux, or flow, of transverse phase space through the system. Because the points which populate this space behave as elements of an incompressible fluid, this flow is like that of such a fluid; the volume of phase space passing a given point per unit time must be the same at all points during any kind of steady state operation on beams of particles.

Applications to Radiofrequency Acceleration

One of the most interesting applications of these phase space concepts refers to radiofrequency acceleration of particles and has been extensively developed by members of the MURA group.[18] The principle of phase stability, referred to earlier, states that if a particle repetitively traverses an accelerating gap across which an alternating voltage is impressed, whose frequency ω_{rf} is nearly that of the traversals (or an integral multiple of it), then there is some interval between the phase of crossing and a reference phase of the alternating voltage for which the particle motion is stable, in the sense that particles having other phases near to the stable one will undergo oscillations in phase and energy about the stable value. It is pedagogically unfortunate that the same word "phase" is used in this con-

[15] For example, see Ref. (4), p. 11–12, Section 3(b).

[16] For example, Ref. (3). Cohen, S., and Crew, A. V., pp. 140–47.

[17] Considerably more is implied for systems with two or more coordinates. For a general treatment see Ref. (4), p. 30.

[18] See Ref. (3). Symon, K. M., and Sessler, A. M., pp. 44–58. This paper contains several phase space drawings of the type to be discussed below which illustrate some of the many situations of interest that may arise. The reader who is unfamiliar with phase space diagrams of phase stability will find it helpful to refer to these drawings in connection with the discussion to follow, which is necessarily concise because of space limitations.

nection but has nothing to do with the "phase space" of classical mechanics discussed above; here it refers to a phase angle ϕ, defined in terms of the radiofrequency gap voltage $V_0 \sin (\int \omega_{rf} dt + \phi)$ at the time a particle having the phase ϕ crosses the gap. Simplified equations governing acceleration and phase stability may be written by neglecting transverse motions of the particles, as follows:

$$dE/dt = (2\pi)^{-1}\omega(E)eV_0 \sin \left(\int \omega_{rf} dt + \phi \right),$$

$$d\phi/dt = \omega(E) - \omega_{rf}.$$

Here $(2\pi)^{-1}\omega$ is the actual frequency of traversals, and this factor converts energy gain per traversal into energy gain per unit time. It is assumed that ω is a known function of the particle's total relativistic energy E, since the period of circulation, without transverse motions relative to a closed orbit, depends only on the particle energy in a given magnetic field. All of the familiar properties of accelerators based on the principle of phase stability may be qualitatively understood from these two simplified equations. For example, in a frequency-modulated cyclotron ω_{rf} is a given function of time, while $\omega(E) = ecB(r)/E$, the dependence of B on r being replaced by a dependence on E by solving $erB(r) = mvc = [E^2 - (m_0c^2)^2]^{1/2}$. On the other hand, in a relativistic electron synchrotron ω_{rf} is a constant while ω depends both on E and on the time because the magnetic field varies during acceleration. One may construct a plot of E vs. ϕ and trace lines on it corresponding to solutions of these equations. (One should think of this E, ϕ space as being wrapped on the surface of a cylinder, the variable ϕ being periodic and ranging from 0 to 2π.) Such plots are more useful if the difference between E and the time-dependent synchronous value of E is used as the ordinate, since a point representing a particle without oscillations in phase will then be stationary, while particles in stable oscillation circulate around it. Other particles which are not "locked in synchronism" with the accelerating voltage will appear to drift downward, on the average, corresponding to their failure to be accelerated. A sharp line of division, called a separatrix, may be drawn between the domains in which these two classes or particles move; it will completely enclose the stable ones in a region shaped like a tear-drop or fish. It is of interest in conventional phase-stable accelerators to determine the dimensions of this phase-stable area in terms of the parameters of the system, to examine their variations as these parameters change with time, and to determine the manner in which the representative points may crowd in toward the center, representing adiabatic damping of phase oscillations, as the acceleration proceeds.

It is very important to note that the variables E and ϕ are not canonically conjugate, and that the divergence of the flow of points in the E,ϕ plane does not vanish, unless ω is independent of E as in a constant frequency cyclotron. It was noted by Symon & Sessler[18] that this defect could be easily remedied,

for fixed-field accelerators, by using instead of E the appropriate variable W which is canonically conjugate to ϕ, defined by

$$W(E) = \int_{E_0}^{E} dE/\omega(E).$$

The equations then become

$$dW/dt = (2\pi)^{-1}eV_0 \sin\left(\int \omega_{rf}dt + \phi\right),$$

$$d\phi/dt = \omega(W) - \omega_{rf}(t),$$

which may be derived from the Hamiltonian function

$$H = E(W) - W\omega_{rf}(t) + (2\pi)^{-1}eV_0 \cos\left(\int \omega_{rf}dt + \phi\right),$$

in which q and p are replaced by ϕ and W, respectively. Liouville's Theorem may now be applied in this space to study very general properties of radio-frequency acceleration systems in these accelerators. This program has been carried out by the MURA group so thoroughly that it constitutes a new theory of these processes, and has produced several new concepts of acceleration. For an elaboration of these the reader is referred to the paper mentioned above; two of the possibilities will be briefly discussed here as illustrations of these methods.

Phase displacement acceleration.—If the frequency $\omega(E)$ increases with increasing energy, and if ω_{rf} is made to increase with time, then the phase-stable area in the W,ϕ space (called a bucket in MURA terminology) will move upward in W and in energy, accelerating the particles which are "trapped" in it. By Liouville's Theorem the upward motion of this bucket must displace phase space lying outside it to lower values, in the same way that water is displaced downward in a container when a submerged object is raised from its bottom. If this outer phase space were to contain particles they would be decelerated, while those inside the bucket are being accelerated. This observation suggested that particles which are not trapped in buckets could be accelerated by the inverse process of passing "empty" buckets downward through the regions of energy where the particles are located. To carry out this procedure one would simply modulate the applied frequency in the wrong direction. This phase displacement acceleration mechanism appears to be less efficient, when loss rates are considered, than conventional acceleration in buckets but has a special interest for fixed field accelerators having a transition energy at which $d\omega/dE = 0$. Above this energy the applied frequency decreases with increasing energy, so that for every filled bucket coming up to this energy there is automatically present an empty bucket coming down toward it from above. It may be possible to exploit this effect to accelerate particles above the transition energy by phase displacement, so as to enhance the overall acceleration efficiency.

Beam stacking.—When considered in the W,ϕ plane, the dependence of bucket size on $d\omega/dE$ and on the voltage V_0 is easily determined and suggests a number of possibilities for more efficient acceleration techniques. For the region below the transition energy in fixed field accelerators, $d\omega/dE$ decreases with increasing energy; this has the effect of making the bucket area increase, if the voltage is held constant. Therefore, if the area of a bucket is fully occupied at injection, only a small fraction of the final stable area at full energy will be used in holding the occupied part of the phase area, which is conserved. This suggests that a gain in efficiency can be made by beam stacking at an intermediate energy, which consists of turning off the accelerating voltage when a bucket has reached the stacking energy, and going back for another injected pulse. It in turn is also stacked, the first bunch being slightly perturbed in energy by the arrival of the second bucket. The procedure can be repeated until a sizable circulating current has accumulated at the stacking energy; these particles can then all be picked up in a large bucket, which is brought into being by turning on another accelerating voltage, and carried up to a still higher energy. This method has an additional advantage, since the allowable rate of frequency modulation is less, for the same accelerating voltage, at high energies so that a lower repetition rate for the second stage is very appropriate. The stirring or mixing in of empty phase space in such processes can be minimized by appropriately varying the voltage amplitude and the frequency modulation rate so that just before stacking every bucket is nearly full. Quantitative calculations of these possibilities have been made, and it is hoped that by these means very large circulating currents of high-energy particles can be produced. Experimental work at the MURA laboratories with a model accelerator using electrons (47) has already produced some success at accumulating a stacked beam, although the number of buckets stacked is not as yet very large; there remain a number of experimental and theoretical problems to be investigated, including space charge effects and radiofrequency excitation of betatron oscillations.

NONLINEAR OSCILLATIONS

An exceedingly important topic on which considerable progress, both theoretical and experimental, has been made during the period under review is the study of the properties of nonlinear betatron oscillations in periodic focusing structures. This will be briefly discussed at this point because the theoretical discussion of such oscillations is most conveniently made in terms of plots in a two-dimensional phase space. However, the subject is a complex one which has become highly developed, and it will be impossible in this review to give the general reader more than a qualitative understanding of what the problems are and of the nature of the progress that has been made.

The transverse coordinates of a particle's position relative to its desired path, in the presence of magnetic focusing forces, are governed by equations which may be expanded in forms such as

$$d^2x/d\theta^2 + F(\theta)x = \sum_{m+n>1} f_{mn}(\theta)x^m(dx/d\theta)^n.$$

We are neglecting many complications here, such as the existence of additional terms if the particle has a slightly different momentum, the elimination of the first derivative term, and the need for considering two coupled equations. The coefficients $F(\theta)$ and $f_{mn}(\theta)$ will display the azimuthal periodicity of the magnet structure and will depend on the shape of the magnetic field; they will also contain terms connected with centrifugal effects arising from the use of a noncartesian coordinate system.

The simplest, or linearized, approximation is obtained by considering only very small displacements for which the right side may be set equal to zero. The resulting linear differential equation with periodic coefficients is of the Mathieu-Hill type, for which an elegant general theory and useful calculational methods exist. Floquet's Theorem states that the general solution consists of two terms, which may be written in the form

$$x = Ae^{i\nu\theta}P(\theta) + Be^{-i\nu\theta}Q(\theta)$$

where A and B are constants of integration, P and Q have the periodicity of F, and ν may be either real or complex. If it is real, the motion due to each term is that of a sine-wave modulation, at a frequency ν relative to the circulation frequency of the particle around the magnet, of a stationary periodic pattern, which is "fastened" to the magnet. Great importance attaches to the values of ν (also denoted in some of the literature by Q) for the two transverse motions of a particle. If ν is equal to or very near to an integer, and the magnetic field contains an unwanted azimuthal harmonic, or Fourier component, labeled by the same integer, then the particle's transverse motion is driven in resonance by the magnetic perturbation and will grow, causing a spreading and ultimate loss of the beam. Similar difficulties arise if 2ν is near to an integral value where unwanted Fourier components of the field gradient may cause exponential growth of the oscillation amplitudes by generating an imaginary component of ν. This effect is called a subharmonic resonance of order one-half, and can be studied with the linear equation referred to above.

There next arises a question as to the effects of the nonlinear terms on the right which cannot be neglected. One can readily see, in a variety of approximate ways, that these terms may have two kinds of effects. First, they may introduce a dependence of the frequency ν on the amplitude, as in any anharmonic oscillator. Second, they may generate undesirable resonant effects at other rational values of ν, the quadratic terms giving potential trouble when 3ν is near an integer, the third order ones when 4ν is near an integer, and so forth. These are called subharmonic resonances of orders one-third, one-fourth, etc., and are intrinsically nonlinear phenomena. A study of the pair of equations for both transverse motions, which are coupled by nonlinear terms, shows that if ν_z and ν_y are in the ratio of small integers, similar effects may occur. In fact, if three positive or negative integers N_z,

N_y and N_θ exist for which the relation $N_x \nu_x + N_y \nu_y = N_\theta$ is nearly satisfied, one might in general anticipate that an instability of the motion could exist. This is clearly a very serious matter, since one could not hope to avoid all rational values of the ν's.

The practical matter of designing a reliable machine in the presence of such effects is difficult for several reasons. First, no general theory of non-linear differential equations with periodic coefficients is known to exist. Second, many of the existing approximate mathematical techniques apply to systems with dissipative forces, but even rather slowly developing resonant effects may be important if they are not opposed by any damping mechanism. Third, the number of cycles of motion made by a particle in a high-energy accelerator may be very large, so that no digital computing machine could follow it all the way without accumulating serious round-off errors, and no ordinary analogue computer could function with adequate accuracy to study the small terms involved.

Some encouragement can be gained from several sources. First, existing machines function quite well in spite of the myriad high-order small random perturbations which must exist in all of them. Second, one can see by approximate calculations that the higher-order effects are important only for larger amplitudes and over smaller ranges of ν, and that the nonlinear frequency-shifting terms, some of which will be of relatively low order, may move the ν value out of a dangerous range as soon as a very small resonant growth has taken place. Third, the coupling resonances (N_x and N_y of opposite sign) can only exchange energy between the two transverse normal modes and will not lead to unbounded growth of either.

These mathematical questions have been very extensively studied by many workers during the last few years. The various forms of interactions between resonance effects and frequency-shifting effects are best discussed by drawing phase-space plots of the motions. The first extensive study of these questions, as they affect the operation of accelerators, was made by Judd (35) in 1950. He pointed out the effects mentioned above, discussed the implications of the Hamiltonian character of the equations on the phase-space behavior, and showed how the frequency-shifting terms could combat the growth of amplitudes due to nonlinear resonances. In more recent work by Moser (48), Sturrock (8), Hagedorn, Schoch, Kolomenski, and several others[19] these results have also been obtained, by a variety of mathematical techniques, and extended to include systems with a large oscillating component of $F(\theta)$ appropriate to alternating gradient focusing systems. Calculations of a great many specific nonlinear effects have been made, and general

[19] A reasonably complete bibliography of work in this field up to 1956 can be assembled from the literature cited by the several authors whose papers appear in Ref. (3), pp. 237–99; these papers should be consulted in connection with all of the topics discussed in the remainder of this section. The important influence of linear resonance effects on magnetic and mechanical tolerances for the construction of alternating gradient synchrotrons was first pointed out by Adams, Hine & Lawson (65).

techniques have been presented for estimating tolerances to which various unwanted effects must be held for a variety of accelerators. One of the general conclusions with respect to instability (N_x and N_y of the same sign or one of them zero) is that if $|N_x+N_y| = 3$ there can be an instability which may or may not grow to large amplitudes, depending on the numerical values of particular parameters; for $|N_x+N_y| = 4$ there can be stability or instability, depending on the parameters; but for $|N_x+N_y| \geq 5$ stability will prevail in all but very exceptional situations. "Stability" here is to be understood as implying lack of disastrous growth even for the large numbers of cycles of oscillation occurring in accelerators; the mathematical problem of asymptotic behavior, for infinitely long times, related to the "difficulty of small divisors" in celestial mechanics first discussed long ago by Poincaré, remains unsolved.

This sizable body of work refers largely to the perturbations caused by small accidental imperfections. A more difficult task has confronted the MURA group, since the FFAG designs with spiral ridges contain intrinsically large nonlinear effects. For this reason they have carried out many numerical calculations on high-speed digital computers which supplement and greatly extend the large body of numerical work of this sort done by the other groups. Considerable insight into the great variety of possible motions of such systems has been gained by a careful study of the phase plots by which the results of these computations are represented. Digital computer results have proved to be very valuable in studying the instabilities which may exist and, therefore, have played an important role in guiding the theoretical work as well as by increasing confidence in its results.

The inadequate accuracy ascribed above to analog computers does not apply to those used for survey work, or to what surely must be classed as two of the most remarkable analogue computers in the world, the Brookhaven National Laboratory electron analogue (49) and the first MURA model electron FFAG accelerator (50). The first of these machines accelerated electrons from one to ten Mev through an alternating gradient structure using electric rather than magnetic fields throughout. Constructed on the premise that particles could solve their own differential equations of motion much more accurately than humans could, its flexibility allowed for the detailed study and testing of the stability problems discussed above and also those of passage through the transition energy when accelerated. In addition, dynamic effects caused by varying parameters so as to sweep particles through resonances[20] were studied. The MURA machine accelerated electrons from 25 kev to 400 kev in a radial sector geometry. A similar survey of resonance effects was carried out. In all cases the results were consistent with the theoretical expectations.

While there are a number of questions in nonlinear theory yet to be answered, the existing body of theoretical and computational techniques,

[20] See Ref. (3). A simple theory of these dynamic effects has been given by Dunn, P. D., et al., pp. 23–25.

taken together, seems adequate to cope with most problems of single-particle orbits in periodic focusing structures.

CONCEPTS AND PROPOSALS NOT YET REDUCED TO PRACTICE

The accelerator concepts discussed in the section on Conceptual Advances in High Energy Accelerators have all been put into practice, in actual accelerators, in construction in progress, or at least in a preliminary and tentative way in model studies. There have also been put forward in the last few years a number of proposals which for one reason or another are still in the stage of design, calculation, or contemplation. Some of these involve different ways of doing relatively familiar things, in order to reduce costs, gain in current, increase particle energy, or provide increased flexibility of operation. Others involve qualitatively new objectives and raise problems which are unfamiliar and unexplored, or call attention to theoretical possibilities for novel accelerating principles, the practical feasibility of which is as yet completely unknown. This review of conceptual advances would not be complete without including some information on such proposals. It is not intended to present a complete survey here; the examples given below have been selected as illustrative or are included because they have been given much serious study or aroused widespread interest.

VARIATIONS OF EXISTING CONCEPTS

One category of proposals consists of existing ideas or elements in some new combination or permutation. The interest of a number of laboratories in constant frequency radial or spiral ridged cyclotrons of higher energy than can be reached by the standard cyclotron has already been mentioned. By adding some frequency modulation a higher energy can be reached, or the same energy might be attained with a magnet having less drastic ridges. This matter has received careful study at the British Atomic Energy Research Establishment at Harwell,[21] where other types of "hybrid" machines have also been considered. As another example, Kitagaki (51) has proposed a "scanning field" alternating gradient accelerator whose ring magnet consists of alternating elements of two types. Elements of the first type are d.c. bending magnets; those of the secon type provide quadrupole focusing in regions of small radial extent which are made to move radially outward, as a group of particles is accelerated, by programmed currents in pole face windings. He estimates that high repetition rates should be possible because of the small stored energy in the scanning focusing magnets. An additional example of a hybrid machine is the curved linear accelerator proposed by Sinelnikov, Fainberg, and Zeidlits,[22] in which transverse stability is produced by conventional or alternating gradient magnetic fields while the accelerating system is like that in a linear

[21] See Ref. (3). Dunn, P. D., *et al.*, pp. 9–25.
[22] See Ref. (3), pp. 215–17.

accelerator with the usual phase stability. The path is not closed and the particles traverse the structure only once.

Air cored magnets have not found many applications as accelerator guide fields in the past, but a bold effort has been put into the design and construction of an 80,000 gauss air core proton synchrotron at the Australian National University at Canberra.[23] The technical difficulties encountered appear to be formidable. As another example of a possible air core design, a preliminary study has been made at the University of California Radiation Laboratory in Berkeley of a type of conventional alternating gradient proton synchrotron using air core magnets of a compact design originated by Christofilos.

To determine the merits of such proposals requires the application of detailed technical and engineering skills as well as intuition and knowledge of the accelerator art which can only be acquired by long experience. It is possible, but not likely, that a good idea of this sort might languish unnoticed for some time for lack of such attention.

INTERSECTING BEAM PROPOSALS

As particles of increasingly relativistic energies are used to bombard stationary targets, the fraction of the incident energy associated with motion of the center of mass increases, so that a smaller fraction is available in the center of mass system of the colliding particles to produce reactions of interest; in the relativistic range of energies the available energy increases only as the square root of the energy of the moving particle. This difficulty can be overcome in principle if two beams of high-energy particles are directed against each other; for identical particles with equal and opposite energies, the total kinetic energy of the two particles is available in the center of mass system. This fact has been known for a long time but has until recently seemed to be useless because of the high current required in each beam to produce an observable number of interactions. However, the potential capability of an FFAG accelerator to produce large circulating currents by storing successive accelerated groups of particles in its d.c. magnet has led the MURA physicists to consider the problem seriously and to propose two different methods of achieving an intersecting beam system. The first of these[24] consisted of a pair of FFAG proton accelerators whose magnets were tangent to each other and had a straight section, or target region, in common (46). The second, first proposed by Petukhov (52) and independently by Ohkawa (53), is a single FFAG accelerator so arranged as to allow for the simultaneous acceleration and storage of two beams of particles traversing the ring in opposite directions. Two such beams, each containing protons having kinetic energies of 15 Bev, for example, would produce interactions having an available center of

[23] See Ref. (3). Blamey, J. W., pp. 344–58.
[24] See Ref. (3). Kerst, D. W., pp. 36–39.

mass energy of 30 Bev, equivalent to the energy available in the bombardment of stationary protons by an accelerated beam of 540 Bev particles. The cost and complexity of a single accelerator of the latter energy of any type now known are beyond serious consideration; therefore the MURA group has spent much effort in working out a plan to produce two such beams. This bold scheme and the unfamiliar problems it creates have aroused considerable interest among some of the physicists who are concerned about the future of high-energy physics research. The MURA accelerator experts, and others (54), have tried to anticipate and consider the various difficulties which might arise in storing two circulating proton currents of several hundred amperes each and making them intersect; experimentalists have attempted to foresee the problems of geometries, background, particle identification, and rates of data handling involved in obtaining useful information from such collisions. In addition, many others have been led by the estimated size and cost of such a project to contemplate soberly the proper role of particle physics in a scientific program for the future.

It seems clear that a large FFAG machine could accelerate and stack a circulating current of high-energy protons orders of magnitude larger than could other accelerators. However, the rate of beam-beam interactions increases as the square of the current (assuming identical beams), while the rate of interactions of either beam with the residual gas varies with the first power. Therefore, the system would be useless for experiments unless a threshold current, enabling the desired events to be detected in the presence of unwanted background events, could be attained. To indicate the orders of magnitude involved, some recent MURA estimates will be quoted. Two beams of 15 Bev protons are contemplated, with current densities up to 50 amp. per cm.^{2} and total currents of 800 amp. each. These would produce interactions in a region 4 cm.$\times$4 cm.$\times$20 cm. at a rate of 10^8 per sec., assuming a cross-section of 5×10^{-26} cm.^{2} The production of these beams would require the acceleration of about 10^4 buckets of particles over a period of about three minutes. The lifetime of such a beam against multiple scattering would be about half a minute at a conventional accelerator pressure of 10^{-6} mm. Hg, so it is proposed to provide a vacuum of 10^{-9} mm. to extend this lifetime to about eight hours. Such a vacuum is also required to reduce the background from encounters with residual gas nuclei in the interaction region to a tenth of the intersecting beam rate; under these conditions the general background particle density in the experimental area is estimated to be in the range of 10^3 per cm.^{3} per sec. Experimental detection equipment with resolving times of a microsecond or less, such as may result from current developmental efforts on scintillation chambers, seems to be needed for many intersecting beam experiments. Even a single beam from such an accelerator would create unusual possibilities and difficulties. Dual beam operation as outlined above would imply a single beam current capability of many microamperes, corresponding to a single beam average power of a hundred kilowatts or more.

To avoid unwanted resonant instabilities of the beams and unknown plasma effects it has seemed necessary to contemplate applying a clearing field of 20 kv. per cm. to both stacked beams. This would remove neutralizing electrons from the beam which would otherwise be trapped in a potential well of 25 kev depth. The various effects which may disturb the beams when they cross are also interesting and deserve further study. A clearer impression of some of these difficulties may be gained from the behavior of an electron accelerator now under construction at the MURA laboratory; it is of the two-beam type and is designed to produce intersecting beams of 50 amp. each at 40 Mev each.

The general interest in the potentialities of intersecting beam experiments has led to at least three independent proposals (55, 56)[25] for arrangements by which the functions of acceleration and beam storage are carried out in separate structures. One clear advantage is that d.c. ring magnets for storage can be of simple shape and can operate at high field strengths, so as to be smaller and cheaper than the accelerator. However, the problems of transferring a beam of protons efficiently from a circular accelerator to a storage ring do not appear to be particularly simple. One difficulty is that the requirements on optical quality of ejected beams to be used for experiments are much less stringent than on those to be injected into a storage ring; another is that the trapping of many pulses of protons into a d.c. magnet, with or without radiofrequency gaps to maintain phase stability, is not as simple as had first been hoped.[26] Both of these problems are eased if one uses a linear accelerator and works with electrons, whose radiation is quite effective in damping oscillations set up at injection. A detailed design for such a system had been worked out by O'Neill, Barber, Richter & Panofsky (57) to use the 500 Mev Stanford electron accelerator to fill each of two storage magnets with up to an ampere of circulating current at a radius of a meter. Radiation losses would be made up by r.f. voltages providing phase stability. A vacuum of 10^{-9} mm. Hg would be sought for the reasons discussed earlier. The basic experiment would be the measurement of electron-electron scattering; a total counting rate of a few counts per second is anticipated. An additional virtue of the arrangement is that the stored beam could be ejected steadily to provide a single beam at a much more favorable duty cycle than that provided by the accelerator itself. Electron-electron scattering at 1 Bev in the center of mass would require a 1000 Bev accelerator if a stationary target were employed. This experiment is of fundamental importance in probing the limits of validity of present quantum electrodynamics, and it is greatly to be hoped that it can be successfully performed with the relatively small and inexpensive equipment proposed by the Princeton-Stanford team.

[25] See also Ref. (3). Brobeck, W. M., pp. 60–63.

[26] Current developmental work on pulsed delay line ejectors and inflectors at Princeton University (where a novel concentric-ring storage geometry has recently been proposed), together with the use of beam-stacking techniques, may produce a solution of these difficulties (66).

Plasma and Coherent Acceleration Concepts

A number of interesting papers of a speculative nature were presented at the CERN Conference in 1956 by physicists from the Soviet Union. One of the papers, by Fainberg,[27] dealt with the use of a wave guide filled with totally ionized gas, or plasma, as an accelerating structure for a linear accelerator. Such systems were stated to offer several theoretical advantages over more conventional approaches, including the variation of phase velocity over a wider range, better confinement of electromagnetic fields to the useful accelerating regions, location of metallic boundaries in regions of lower field strengths, and the possibility of simultaneous radial and phase stability. Additional theoretical calculations of the propagation of waves in these structures have been made by Mullett (58); it seems that the potentialities of such systems may be worth further study but that it is not yet clear whether all the desired properties can be realized in a practical accelerator.

A concept of another sort, which has created some theoretical interest at a number of accelerator centers, was presented by Budker.[28] He pointed out some interesting properties of a very high current stream of relativistic electrons neutralized by ions at rest and circulating in a d.c. external guide field shaped like that of an ordinary betatron. If such a stream could be induced to contract to a very small cross-sectional area, its individual electrons would move on paths determined largely by the high magnetic field of the stream itself, and would radiate vigorously when undergoing betatron oscillations. Strong radiation damping of these oscillations might then produce an equilibrium by counteracting their growth through multiple scattering on the neutralizing ions. Energy loss by radiation could be regained in an externally applied solenoidal electric field acting along the beam. Budker discussed these proposed equilibria and the stability of the whole beam against some of the perturbing effects that might exist, and raised the possibility that the magnetic field of this stabilized configuration might be used as a guide field for a compact proton accelerator, for example, a 100 Bev accelerator with a radius of about three meters. Early efforts at creating large electron currents were described in a succeeding paper by Budker and Naumov.[29]

Some of the problems associated with attaining this "radiation-cooled" equilibrium of Budker have been considered by individuals or groups of people at Harwell, CERN, Brookhaven, MURA, Berkeley, the University of Washington, the U. S. Naval Research Laboratory, and probably others. Many of these workers have concluded that there does not seem to be any foreseeable way to achieve such a relativistic stabilized electron beam in this equilibrium state with apparatus of reasonable size and power requirements. A basic difficulty seems to be the slowness with which a beam pro-

[27] See Ref. (3). Fainberg, I. A., pp. 84–90.
[28] See Ref. (3). Budker, G. J., pp. 68–75.
[29] See Ref. (3). Budker, G. J., and Naumov, A. A., pp. 76–79.

duced by ordinary means can be made to contract to a very thin thread. During this sizable fraction of a second there are a number of mechanisms which would act to alter the assumed conditions in the beam. Also, supplying an adequate electric field by means of a betatron core for so long a time is impractical, while a radiofrequency field would bunch the beam azimuthally, creating additional problems. The phase space available in the guide field produced by such a ring current becomes very small for accelerated protons of high energy, and the electron beam would radiate megawatts of power of infrared or visible frequencies. For all these reasons the concept does not now appear to be attractive. Nevertheless, the insights gained through these studies stimulated by Budker's proposal may find other applications in the future; several groups are planning experiments of various kinds with strong currents of relativistic electrons.

A new principle for the coherent acceleration of charged particles was set forth by Veksler[30] in an interesting theoretical paper. The method is characterized by the coherent interaction of a physically small bunch of particles (to be accelerated) with another group of charges, a plasma, or an electromagnetic wave; the interaction itself generates the accelerating fields, whose strength would, because of coherence, be proportional to the number of charges in the bunch. Examples discussed included acceleration of a bunch of ions immersed in a high-velocity dense electron beam, involving a "reversal" of Cerenkov losses; coherent "impact" acceleration by collisions between small bunches of particles; and the acceleration of an electrically neutral bunch of plasma by the radiation pressure of an electromagnetic wave. None of these proposals appears to be more than a theoretical possibility as yet, since practical ways of realizing them have not been proposed.

In summary, it may be said that accelerator physicists are only beginning to enter the general field of plasma physics; it is much too early to estimate its possible influence on the accelerators of the future, but it seems likely that some benefits will eventually accrue from combining the skills of particle-orbit and plasma experts.

RECENT PROGRESS IN ACCELERATOR CONSTRUCTION

Although it is not the primary purpose of this review to deal with the construction of accelerators, a tabular summary of recent completions and present construction on the higher-energy machines will be included. This work, though only mentioned here in outline, represents the real progress achieved during the period under review in enlarging our capability to learn about the basic structure of matter. The largest part of the efforts of accelerator physicists and engineers has been devoted to these achievements, and it is to these men that all of those interested in high-energy physics should look with gratitude for making possible the expansion of opportunities to gain new information during the next several years.

[30] See Ref. (3). Veksler, V. I., pp. 80–83.

Information on proton accelerators producing energies above 500 Mev is summarized in Table I, which includes all machines of this category, either existing or under construction, of which the writer is aware. Projects under design or study are not included in the table. The dates refer to the commencement of operation at or near the listed energy or to estimates for future completion of construction. The references listed are the most complete accounts known to the writer that are generally accessible. Much greater detail is usually available in voluminous unpublished project reports. It

TABLE 1

HIGH-ENERGY PROTON ACCELERATORS

Location	Type	Energy (Bev)	Status		References
CERN, Geneva, Switzerland	FM Cylotron	0.6	Operating	1957	
Joint Institute for Nuclear Research, Dubna, U.S.S.R.	FM Cyclotron	0.68	Operating	1954	(3), pp. 148–52, 504–10
University of California Radiation Laboratory, Berkeley	FM Cyclotron	0.72	Operating	1956	(3), pp. 413–18
University of Birmingham, Great Britain	Synchrotron	1	Operating	1953	(6) and references there
Delft Institute of Technology, Netherlands	Synchrotron	1	Construction	1958	
Brookhaven National Laboratory, New York	Synchrotron	3	Operating	1952	(59)
Centre d'Études Nucléaires, Saclay, France	Synchrotron	3	Construction	1959	(3), pp. 200–4, (67)
Princeton University, New Jersey	Synchrotron	3	Construction	1960	(3), pp. 525–29
University of California Radiation Laboratory, Berkeley	Synchrotron	6.2	Operating	1954	(6), (3), pp. 496–503
Atomic Energy Research Establishment, Harwell, Great Britain	Synchrotron	7	Construction	1961	(60)
U.S.S.R.	A.G. Synchrotron	7	Construction	1959	(3), pp. 118–21, 133–36
Joint Institute for Nuclear Research, Dubna, U.S.S.R.	Synchrotron	10	Operating	1957	(3), pp. 339–43, 378–86, 429–34
Australian National University, Canberra	Air core Synchrotron	10.6	Construction	1960(?)	(3), pp. 344–58
Argonne National Laboratory, Illinois	Synchrotron	12.5	Authorized	1962	(3), pp. 42–43
CERN, Geneva, Switzerland	A.G. Synchrotron	25	Construction	1960	(3), pp. 137–38, 307–29
Brookhaven National Laboratory, New York	A.G. Synchrotron	25–30	Construction	1960	(6)

frequently occurs that the press of research prevents publication of the description of an accelerator for several years after its completion. The importance of the *Proceedings of the CERN Symposium* in this connection is obvious from an inspection of the table.

Some remarks about a few of the many features of unusual interest incorporated in this array of machines will next be made. The Geneva and Berkeley frequency modulated cyclotrons obtain their frequency modulation from vibrating blades rather than from the rotating capacitors used in lower energy machines of this type. The experimental area of the Soviet

cyclotron has been very highly developed, provisions having been made for a large number of beams and for simultaneous experiments at several stations. The Delft and Argonne synchrotrons have magnetic guiding fields of zero gradient, focusing being obtained by slanting the pole face boundaries away from the radial direction at the ends of each magnet sector. Injection at Delft will be from a Thomas cyclotron of 10 Mev energy. The machine at Princeton is being built in collaboration with the University of Pennsylvania and is designed to produce a high average current of a tenth of a microampere or more. This is to be achieved by resonating the magnet at 20 cycles per sec. with a capacitor bank handling 6×10^4 kva. and by optimization of the injection conditions. The Soviet 7 Bev alternating gradient machine is designed both for research and to serve as a model for a proposed 50 to 60 Bev accelerator of the same type; the method of Vladimirski and Tarasov, mentioned earlier, for removing the transition energy from the operating range to infinity is to be used in both these machines. An interesting area of development which has been investigated on the Brookhaven and Berkeley synchrotrons is that of beam-controlled acceleration, in which information derived from pickup electrodes is used to control or influence the frequency of the accelerating voltage.[31] A direct feed-back system which damps the phase oscillations has been tested on the Cosmotron (62). Beam-controlled acceleration will be used on both the CERN and Brookhaven alternating gradient synchrotrons.

Electron accelerators for energies above 500 Mev are listed in Table II, to which the description of Table I also applies. An important historical role was played by the Cornell accelerator which gave the first experimental

TABLE II

HIGH-ENERGY ELECTRON ACCELERATORS

Location	Type	Energy (Bev)	Status		References
University of Bonn, Germany	A.G. Synchrotron	0.5	Construction	1958	(3), pp. 482–83
Stanford University, California	Linear	0.65	Operating	1954	(24)
Cornell University, New York	A.G. Synchrotron	1	Operating	1955	(61)
Istituto Nazionale di Fisica Nucleare, Rome, Italy	Synchrotron	1	Construction	1959	(3), pp. 458–62, 475–81
Royal Institute of Technology, Stockholm, Sweden	A.G. Synchrotron	1.2	Construction	1959	
California Institute of Technology, Pasadena	Synchrotron	1.2	Operating	1956	
Laboratoires de Physique Nucléare, Orsay, France	Linear	2	Construction	1959	
Kharkov, U.S.S.R.	Linear	2	Construction	1959	
Harvard University-Massachusetts Institute of Technology, Cambridge, Massachusetts	A.G. Synchrotron	7	Construction	1960	(3), pp. 439–46

[31] See Ref. (3) for a review of these techniques. Johnsen, K., and Schmelzer, C., pp. 395–403.

proof, early in 1954, of the success of alternating gradient focusing in multiple turn accelerators. The use of this focusing in electron accelerators creates special problems at very high energies. The particle orbits are markedly noncircular because of their betatron oscillations in the alternating gradient magnetic field. The large radiation reaction forces therefore have sizable transverse components which can act in the direction of destroying betatron oscillation stability. Careful studies of these and other radiation effects have been made by the Cambridge accelerator group, whose machine design is dominated by radiation considerations. Each electron will radiate several Mev per turn at full energy in this accelerator; the total radiated power will exceed the beam power by more than a factor of two, and the beam load will represent about half of the total radiofrequency power. The effort being expended on these difficult problems seems well worth while in view of the interesting experiments that can be done with multi-Bev electrons, as is clear from the many insights already gained from experiments using the three existing electron accelerators listed in the table.

So many organizations have accelerator projects under study or preliminary design at the present time that an attempt at completeness in listing them would be ill-advised. The large, high-energy, and expensive machines under study in the Soviet Union and by the MURA group have already been mentioned; another proposal in this class is for the construction of a linear electron accelerator for the energy range 15 to 45 Bev at Stanford University.[32] Such a machine would have a length of the order of two miles. Its design and construction seem to involve many engineering problems but to present no new fundamental difficulties; it is not likely that electrons of energies above that of the Cambridge accelerator listed in Table II can be produced by any other method.

The choice of 500 Mev as a lower limit for inclusion of accelerators in the tables does not imply any lack of ingenuity or activity in developing improved methods or extensions of technique for producing particles of lower energies. In addition to the increasing use of cyclotrons for accelerating heavy ions, including carbon, nitrogen, and oxygen in various states of ionization, the cooperative design and parallel construction of two heavy-ion linear accelerators by the University of California Radiation Laboratory and Yale University is noteworthy.[33] These machines can produce useful currents of a considerable variety of ions with energies of 10 Mev per nucleon in each nucleus; particles having a charge to mass ratio more than three-tenths that of a proton are accepted by the main accelerator, which follows a prestripping section that operates at lower ionizations. Another area of progress is in linear accelerators for generating very high currents. A machine of this type has been constructed and operated at the Livermore site of the University of California Radiation Laboratory. It produced an

[32] See Ref. (3). Neal, R. B., and Panofsky, W. K. H., pp. 530–44.

[33] Smith, L., "Linear Accelerators," in *Handbuch der Physik*, **XLIV** (Springer-Verlag OHG, Heidelberg, Germany, in press, 1958) (12a).

average proton current in the range of 10 to 100 ma at 3.75 Mev and could also accelerate deuterons to twice this energy (63). Theoretical and design studies for high current linear accelerators have also been made in the Soviet Union.[34] The popularity of proton linear accelerators as injectors for large machines has led to many advances in their design.[35] A full account of the properties of the proton linear accelerator at the University of Minnesota has recently appeared (64). Beams of protons at 10 Mev, 40 Mev, and 68 Mev are available from this machine, which consists of three separate resonant cavities. A great many other advances in lower-energy machines have been made; to get some impression of the extent of such work the reader may refer to Behman's bibliography (2).

The almost explosive growth of accelerator construction in the energy range above 500 Mev in the past four years is evident from the tables. Of the 25 machines listed, only two were operating before 1954, while eight others have since come into operation; the remaining 15 will probably all be in operation within the next four years. This remarkable construction effort represents the largest expenditure of manpower, materials, and money ever made in the pursuit of basic knowledge for its own sake.

[34] See Ref. (3). Semenov, N. N., *et al.*, pp. 207–12.
[35] See, for example, the four papers on this subject in Ref. (3), pp. 159–78.

LITERATURE CITED

1. Blewett, J. P., *Ann. Rev. of Nuclear Sci.*, **4**, 1–12 (1954)
2. Behman, G. A., "Particle Accelerators, I. Bibliography, II. List of Accelerator Installations," *U. S. Atomic Energy Commission Document, UCRL-8050*, 153 pp. (1958)
3. *Proceedings of the CERN Symposium on High-Energy Accelerators and Pion Physics*, Vol. **1** (Regenstreif, E., Ed., European Organization for Nuclear Research, Geneva, Switzerland, 567 pp., 1956)
4. Courant, E. D., and Snyder, H. S., *Ann. Phys. (N.Y.)*, **3**, 1–48 (1958)
5. Laslett, L. J., *Science*, **124**, 781–87 (1956)
6. Blewett, J. P., *Repts. Progress Phys.*, **19**, 37–79 (1956)
7. Livingston, M. S., *High-Energy Accelerators* (Interscience Publishers, Inc., New York, N. Y., 157 pp., 1954)
8. Sturrock, P. A., *Static and Dynamic Electron Optics; an Account of Focusing in Lens, Deflector, and Accelerator* (Cambridge University Press, Cambridge, Engl., 240 pp., 1955)
9. Frost, F. E., and Putnam, J. M., "Particle Accelerators, I. Bibliography II. List of High-Energy Installations," *U. S. Atomic Energy Commission Document, UCRL-2672* (1954)
10. Livingston, R. S., Howard, F. T., and Rudolph, G., "Bibliography of Cyclotron Literature," *U. S. Atomic Energy Commission Document, ORNL-2023* (1956)
11. Linear Accelerator Issue, *Rev. Sci. Instruments*, **26**, 111–228 (1955)
12. McMillan, E. M., in *Experimental Nuclear Physics*, **3** (John Wiley and Sons, New York, N. Y., in press, 1958)
12a. *Handbuch der Physik*, **XLIV** (Springer-Verlag OHG, Heidelberg, Germany, in press, 1958)
13. Bethe, H. A., and Rose, M. E., *Phys. Rev.*, **52**, 1254–55 (1937)
14. Rose, M. E., *Phys. Rev.*, **53**, 392–408 (1938)
15. Wilson, R. R., *Phys. Rev.*, **53**, 408–20 (1938)
16. Thomas, L. H., *Phys. Rev.*, **54**, 580–98 (1938)
17. Kerst, D. W., *Phys. Rev.*, **60**, 47–53 (1941)
18. Kerst, D. W., and Serber, R., *Phys. Rev.*, **60**, 53–58 (1941)
19. Veksler, V. I., *J. Phys. U.S.S.R.*, **9**, 153–58 (1945)
20. McMillan, E. M., *Phys. Rev.*, **68**, 143–44 (1945)
21. Roberts, A., *Ann. Phys. (N.Y.)*, **4**, 115–65 (1958)
22. Alvarez, L. W., Bradner, H., Franck, J. V., Gordon, H., Gow, J. D., Marshall, L. C., Oppenheimer, F., Panofsky, W. K. H., Richman, C., and Woodyard, J. R., *Rev. Sci. Instruments*, **26**, 111–33 (1955)
23. McMillan, E. M., *Phys. Rev.*, **80**, 493 (1950)
24. Chodorow, M., Ginzton, E. L., Hansen, W. W., Kyhl, R. L., Neal, R. B., Panofsky, W. K. H., and Staff, *Rev. Sci. Instruments*, **26**, 134–204 (1955)
25. Courant, E. D., Livingston, M. S., Snyder, H. S., and Blewett, J. P., *Phys. Rev.*, **91**, 202–3 (1953)
26. Courant, E. D., Livingston, M. S., and Snyder, H. S., *Phys. Rev.*, **88**, 1190–96 (1952)
27. Blewett, J. P., *Phys. Rev.*, **88**, 1197–99 (1952)
28. Symon, K. R., *Phys. Rev.*, **98**, 1152–53 (1955)
29. Symon, K. R., Kerst, D. W., Jones, L. W., Laslett, L. J., and Terwilliger, K. M., *Phys. Rev.*, **103**, 1837–59 (1956)
30. Kelly, E. L., Pyle, R. V., Thornton, R. L., Richardson, J. R., and Wright, B. T., *Rev. Sci. Instruments*, **27**, 493–503 (1956)

31. Judd, D. L., *Phys. Rev.*, **100**, 1804 (1955)
32. Kerst, D. W., Terwilliger, K. M., Symon, K. R., and Jones, L. W., *Phys. Rev.*, **98**, 1153 (1955)
33. "Proposal for a Southern Regional Accelerator," *Oak Ridge National Laboratory Document ORNL 57-4-30 (abridged)*, 245 pp. (1957)
34. Davis, L., Jr., and Langmuir, R. V., *Phys. Rev.*, **75**, 1457 (1949)
35. Judd, D. L., *A Study of the Injection Process in Betatrons and Synchrotrons* (Doctoral Thesis, California Institute of Technology, Pasadena, Calif., 1950)
36. Tuck, J. L., and Teng, L. C., *Phys. Rev.*, **81**, 305 (1951)
37. *Synchrocyclotron Progress Report III, Chap.* **8** (Institute of Nuclear Studies, University of Chicago, Ill., 154 pp., 1950)
38. LeCouteur, K. J., *Proc. Phys. Soc. (London)*, **B64**, 1073–84 (1951)
39. Rogers, E., *Application of Regenerative Deflectors to Constant Frequency Cyclotrons* (Los Alamos Scientific Laboratory, N. M., unpublished report, 1957)
40. Teng, L. C., *Rev. Sci. Instruments*, **27**, 106–7 (1956)
41. Welton, T. A., *Bull. Am. Phys. Soc.*, [II] **3**, 57–58 (1958)
42. Wright, B. T., *Rev. Sci. Instr.*, **25**, 429–31 (1954)
43. Piccioni, O., Clark, D., Cool, R., Friedlander, G., and Kassner, D., *Rev. Sci. Instr.*, **26**, 232–33 (1955)
44. Gordon, M. M., and Welton, T. A., *Bull. Am. Phys. Soc.*, [II] **3**, 57 (1958)
45. Symon, K. R., Stehle, P., and Lichtenberg, D. B., *Bull. Am. Phys. Soc.*, [II] **1**, 344–45 (1956)
46. Kerst, D. W., Cole, F. T., Crane, H. R., Jones, L. W., Laslett, L. J., Ohkawa, T., Sessler, A. M., Symon, K. R., Terwilliger, K. M., and Nilsen, N. V., *Phys. Rev.*, **102**, 590–91 (1956)
47. Terwilliger, K. M., Jones, L. W., and Pruett, C. H., *Rev. Sci. Instr.*, **28**, 987–97 (1957)
48. Moser, J., *Nachr. Akad. Wiss. Göttingen Math.-physik.-Kl.*, *IIa*, **6**, 87–120 (1955)
49. The Brookhaven Electron Analog (six abstracts), *Phys. Rev.*, **100**, 1268–69 (1955)
50. Cole, F. T., Haxby, R. O., Jones, L. W., Pruett, C. H., and Terwilliger, K. M., *Rev. Sci. Instr.*, **28**, 403–20 (1957)
51. Kitagaki, T., *Bull. Am. Phys. Soc.*, [II] **3**, 57 (1958)
52. Petukhov, V. A., *J. Exptl. Theoret. Phys. (U.S.S.R.)*, **32**, 379–80 (1957); *JETP (Translations)*, **5**, 317–19 (1957)
53. Ohkawa, T., *Rev. Sci. Instr.*, **29**, 108–17 (1958)
54. Burren, J. W., Morgan, D., and Walkinshaw, W., *Atomic Energy Research Establishment, Harwell, England, Report A.E.R.E. T/R 2519* (1958)
55. Lichtenberg, D. B., Newton, R. G., and Ross, M. H., *Midwestern Universities Research Association, Madison, Wisconsin, Rept. MURA-110* (1956)
56. O'Neill, G. K., *Phys. Rev.*, **102**, 1418–19 (1956)
57. O'Neill, G. K., Barber, W. C., Richter, B., and Panofsky, W. K. H., *A Proposed Experiment on the Limits of Quantum Electrodynamics* (High-Energy Physics Laboratory, Stanford University, Stanford, Calif., unpublished report, 1958)
58. Mullett, L. B., *Atomic Energy Research Establishment, Harwell, Engl., Rept. A.E.R.E. GP/R 2186* (1957)
59. Cosmotron Issue, *Rev. Sci. Instr.*, **24**, 723–870 (1953)

60. Wilkins, J. J., and Egginton, A. J., *Atomic Energy Research Establishment, Harwell, Engl., Rept. A.E.R.E. GP/R 2181* (1957)
61. Wilson, R. R., *The Cornell Bev Synchrotron* [Cornell University, Ithaca, N. Y., unpublished report, 81 pp., 1956]
62. Rogers, E. J., *Rev. Sci. Instr.*, **29**, 215–17 (1958)
63. Lawrence, E. O., *Science*, **122**, 1127–32 (1955)
64. Day, E. A., Featherstone, R. P., Johnston, L. H., Lampi, E. E., Tucker, E. B., and Williams, J. H., *Rev. Sci. Instr.*, **29**, 457–76 (1958)
65. Adams, J. B., Hine, M. G. N., and Lawson, J. D., *Nature*, **171**, 926–27 (1953)
66. Woods, E. J., and O'Neill, G. K., *Bull. Am. Phys. Soc.*, **3**, 169 (1958)
67. Bruck, H., and Lévy-Mandel, R., *Nuovo cimento*, **2**, Suppl., 423–41 (1955)

THE PRIMARY COSMIC RADIATION[1]

By H. V. Neher

*Norman Bridge Laboratory of Physics, California Institute of Technology,
Pasadena, California*

Introduction

That the true nature of the primary cosmic radiation so long escaped those working in the field now seems quite understandable in view of the many new and unexpected phenomena involved. The search, with the many false leads and interpretations, forms one of the most interesting stories in the annals of science. While we still do not know all the details of the primary radiation, we do know many of the major features; and the once baffling process of the diffusion of the primary radiation through our atmosphere has now largely yielded to the combined attack of many research centers around the world.

By 1941, after the balloon flights of Schein *et al.* (1) showed that most of the particles present at very high altitudes did not multiply in going through lead as electrons were then known to do, it became evident that a major part of the primaries was probably protons. This had been suggested by others prior to 1941, principally by Johnson (2) to account for the east-west effect. But the chief stumbling block in having protons as primaries was in reconciling them with the then known way in which cosmic rays were absorbed in matter. The missing links were gradually supplied. Following the realization that nuclear processes played an important role came the discovery of new particles—the charged pi-meson by Powell's group (3) in 1947, and the neutral pi-meson by the Berkeley group (4) in 1949.

With these particles, together with the older μ-meson and the knowledge of the π-μ decay, it then became possible to understand the process of generation and absorption of secondary particles in the atmosphere. In principle it should have been possible to account for all the energy loss of the primaries as they diffuse down through the atmosphere. Rossi (5) appears to have been the first to make a serious attempt to do this. Later attempts were made by Puppi (6) and Komori (7).

That protons were not the only constituents of the primaries was discovered by Freier *et al.* (8) in 1948 by observing heavy tracks in photographic emulsions exposed to the primary radiation near the top of the atmosphere. These tracks were shown to arise from high-energy nuclei with nuclear charge larger than for nuclei of the air and which therefore must have entered the atmosphere from surrounding space.

The identification of these heavier cosmic-ray particles, their relative as well as their absolute numbers and their distribution of energy, is still a very active part of the research on the primary radiation. A review of the field

[1] The survey of literature pertaining to this review was completed in March, 1958.

was made by Peters (9) in 1951, and some particular aspect of the properties of the primary radiation, its origin and propagation through space, was reviewed by Biermann (10) in 1953.

In this review of the primary cosmic radiation the first concern will be with the species of nuclei represented, i.e., their chemical composition both as to kind and numbers. Next, their energy distribution will be considered. This will be followed by a discussion of the various kinds of fluctuations that occur in the primaries. A brief account also will be given of some of the present ideas about the origin of cosmic rays and of some of the astrophysical implications.

CHEMICAL COMPOSITION OF THE PRIMARIES

The relative abundance of the various nuclei represented in the primaries has an important bearing on the origin of the cosmic rays. Since their energies are much larger than their binding energies, the fact that heavy nuclei, like iron, occur at all is very good evidence that they could not have traveled through many gm. cm.$^{-2}$ of matter or none of them would remain. The question of whether the so-called light elements, Li, Be, and B are present in the primaries was in doubt for some time, but has now been resolved in that there seems to be general agreement that these three elements are about half as abundant as the C, N, and O group.

The technique commonly used is to fly photographic emulsions to as high altitudes as possible. Such flights have been made primarily in the middle latitudes of around 40°, partly because of available facilities, but also because here the lighter nuclei are relativistic; and, hence, their ionization in the emulsion depends on only their charge rather than on both their charge and their velocity.

Recently, McDonald (11) has reported a method which combines the use of both a scintillation and a Čerenkov detector. This combination should, in principle, permit a determination of the velocity spectrum of the various nuclei, as well as separate out the different nuclear charge components. Since the energies of the particles may be determined directly, the results at different latitudes will be independent of geomagnetic theory. The chief difficulty with experiments like McDonald's is that, although each is elegant in itself, the equipment is quite complicated. Hence it would be difficult to make many flights and to determine how the cosmic-ray intensity and composition vary with time. Table I reproduces a list of values for the α-particle flux, collected by McDonald (11). To make the original table somewhat more meaningful the dates when the data were taken have been included. In each case the original author has extrapolated his value to the top of the atmosphere by correcting for the losses as well as for the gains due to fragmentation of heavier nuclei.

The next group of elements, Li, Be, and B are given in terms of their ratio to the C, N, and O group. Again the attempt has been made to extrapolate the measured value in the emulsion back to the top of the atmos-

TABLE I

SUMMARY OF α-PARTICLE FLUX MEASUREMENTS AT $\lambda_m = 55°$ N AND $41°$ N

Method	Author	Year of Flight	Flux of Particles m.$^{-2}$sec.$^{-1}$ster.$^{-1}$
	$\lambda_m = 41°$ N		
Proportional counter	Perlow	1950	110 ± 20
Čerenkov counter and cloud chamber	Linsley	1954	88 ± 8
Čerenkov counter	Horowitz	1954	99 ± 16
Čerenkov counter	Webber-McDonald	1954	82 ± 9
Scintillation counter and Čerenkov counter	McDonald	1955	96 ± 9
	$\lambda_m = 55°$ N		
Scintillation counter	Ney and Thon	1950	340
Proportional counter	Davis *et al.*	1952	320 ± 40
Čerenkov counter and scintillation counter	McDonald	1955	305 ± 25

phere. This extrapolation was the source of the disagreement between various groups for some time, which seems now to have essentially disappeared. Some of the more recent values are given in Table II.

TABLE II

SUMMARY OF RATIO OF LIGHT ELEMENTS Li, Be, AND B TO THOSE OF THE MEDIUM GROUP

N_L/N_M	Author	λ_m
0.37 ± 0.07	Waddington (12)	$46°$ N (Italy)
0.70 ± 0.15	Noon *et al.* (13)	$41°$ N (Texas)
0.32 ± 0.07	Koshiba *et al.* (14)	$41°$ N (Texas)
0.35 ± 0.09	Webber (15)	$41°$ N (Texas)

Table III presents the more recent work of Noon, Herz & O'Brien (13) on the composition of the primaries as determined with emulsions flown by a balloon at geomagnetic latitude $41°$ N.

In a paper to be published soon by Koshiba, Schultz & Schein (14) an attempt is made to identify as many of the constituents of the primaries as possible. The extrapolation to the top of the atmosphere was made by using "the fragmentation probabilities in air which were obtained from the analysis of a total of 209 interactions in the same stack." They also estimate the fragmentation probabilities in hydrogen and make an attempt to extrapolate the constituents back to the source.

TABLE III

THE COMPOSITION OF THE PRIMARIES AT 41° N AS DETERMINED BY NOON,
HERZ & O'BREIN (13)

He	100 ± 20 particles m.$^{-2}$sec.$^{-1}$ster.$^{-1}$
Li, Be, B	3.8 ± 0.5
C, N, O	5.5 ± 0.6
$Z \geq 10$	2.6 ± 0.4

In comparing the abundances of the nuclei found in cosmic rays with the natural abundances of the chemical elements as derived by Suess & Urey (16), it is found that certain discrepancies stand out. One of the chief differences is the relatively large amount of Li, Be, and B in cosmic rays in comparison to their very small abundances in nature. It is assumed by Koshiba, Schultz, and Schein that these nuclei are the result of spallations of the heavier nuclei with the protons of interstellar matter. Assuming no Li, Be, and B at the source and 1 proton per cm.^{3} of interstellar matter on the average, they arrive at the conclusion that the nuclei reaching the earth have been traveling for 5.3×10^6 years. This figure will be discussed later in the section on Origin of Cosmic Rays.

Figure 1 reproduces the curves given by Koshiba *et al.* (14). Curve A is that obtained for the top of the atmosphere; B represents the extension of curve A back to the source; and C gives the relative abundances of the elements as found by Suess & Urey (16). These latter are derived from spectro-
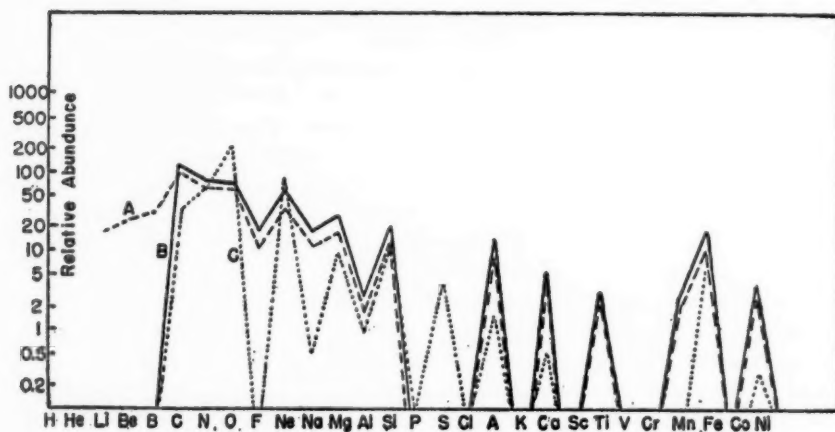
FIG. 1. A comparison of the natural abundances of the elements as given by Suess & Urey (16), with cosmic-ray abundances as given by Koshiba, Schultz & Schein (14). Curve A shows the results of the extrapolation to the top of the atmosphere of the cosmic ray particles. Curve B gives the charge spectrum at the source region. Curve C shows the natural abundances as given by Suess and Urey.

scopic analysis and measurements made on meteorites. In the figure, the width of the bases of the triangles for larger Z (Z = atomic number) represents the uncertainty in the determination of Z.

Some conclusions arrived at from the comparison of the cosmic-ray and the natural abundances are as follows: (a) If a fit of the two sets of data is made at the C, N, and O group then there are about twice as many nuclei with $Z \geq 10$ in cosmic rays as in the natural abundance. (b) The abundance ratio of Mg:Si:Fe is about the same for both sets of data. (c) The larger abundance of elements of even Z, such as Ne, Mg, and Si show up in both sets of data. Elements of odd Z in cosmic rays such as F, Na, and Al may be more abundant because of break-up of the heavier elements. (d) The relative abundances of C, N, and O as determined by Koshiba *et al.* are in the ratio 1.6:1.1:1.0, while the data of Suess and Urey give the ratio 0.16: 0.31:1.00. It is pointed out by these authors that this higher abundance of carbon and nitrogen in cosmic rays compared with oxygen may have an important bearing on the nature of the stars that were the original source of the nuclei.

ENERGY DISTRIBUTION OF THE PRIMARY RADIATION

There are a number of radiations incident on the earth that come either from the sun or from the galaxy. Some of the corpuscular radiations from the sun have energies of 100 kev and in certain cases may reach into the Mev range. Thus, the protons found by Meinel (17) have energies of the order of 100 kev and probably as much as 10 times more at the top of the atmosphere. Similarly, the electrons found by Meredith *et al.* (18) and by Anderson (19) in the auroral zone appear to have energies of the same order of magnitude. It is still uncertain whether these are accelerated locally or whether they come from the sun itself. There are times when the sun does give rise to high-energy particles whose energies overlap the lower part of the cosmic-ray distribution. These outbursts are associated with intense visual flares and have occurred some five times in the last 20 years. These will be discussed later in connection with the fluctuations in cosmic rays.

None of the radiations discussed above are cosmic rays by definition; they are solar corpuscular rays. To qualify as cosmic rays they must come from beyond the solar system. While at one time it seemed to be difficult to account for the large amount of energy in cosmic rays, this difficulty has largely been overcome and very few workers in the field now hold to the solar origin of any appreciable fraction of the cosmic-ray particles. The ideas for and against a solar component will be discussed in the section on the Origin of Cosmic Rays.

The lower limit to cosmic-ray particle energy is usually set at about 1 Bev for protons (10). However, during a very quiescent period of the sun, such as existed in 1954 and 1955, Neher (20, 21) found that, near the geomagnetic north pole, particles were entering the atmosphere which had the characteristics of protons with energies down to 100 Mev. This value would

undoubtedly have gone still lower had the balloon carrying the instruments gone higher, but for the present 0.1 Bev may be taken for the lower limit of cosmic-ray particles. These particles were probably not of solar or local origin because: (a) they were present during a very quiet period of solar activity; (b) they were not present in the auroral zone where Meredith (18) and later Anderson (19) found low-energy radiations; (c) their intensity was very steady in 1954 over a period of at least three weeks.

The evidence then is that cosmic-ray energies extend down to at least 0.1 Bev for protons, and that these are present when the activity of the sun is near the minimum of its 11-year cycle. Solar particles, on the other hand, appear to exist in larger numbers and to have higher energies near a maximum of solar activity than they have near a minimum. There thus appears to be a gap between about 1 Mev and 100 Mev where no experimental evidence for particles exists. Undoubtedly, during a solar flare there are large numbers in this range; but to detect these, as well as those which may exist during a solar minimum, one probably will have to depend on a satellite.

The most direct method of studying the low-energy part of the cosmic-ray spectrum is by the use of photographic emulsions. This technique has been used by a number of groups working in the field, including that at the University of Minnesota. In 1954, during the summer when the sun was very inactive, this group made a balloon flight, with photographic emulsions, at 60° geomagnetic north [see Fowler *et al*. (22)]. These authors found that the differential spectrum of α-particles passed through a maximum at 300 Mev per nucleon, and that at 130 Mev per nucleon the number of α-particles per unit energy range was down to less than one-third of its value at the maximum. In analyzing data from previous emulsions flown in October, 1950 at 55° N by Dainton *et al*. (23) low-energy α-particles were also found. In fact, it appeared that within the statistical errors there was no difference between these two flights in spite of the 6° difference in latitude and the difference in time. Three conclusions that may be drawn from these data are: (a) The maximum in the differential spectrum of α-particles in 1954 was due neither to atmospheric absorption nor to a geomagnetic effect but existed in the primaries. (b) There appeared to be no change in α-particle flux between 1950 and 1954. (c) Any increase in ionization north of Minneapolis at pressures of, say, 15 gm. cm.$^{-2}$ which occurred in 1954 must have been due to protons since there was no increase in α-particles, and heavier nuclei could not penetrate the air down to the instrument.

In contrast to the situation with α-particles during 1954, there was an increase in ionization north of 55° N as shown by Neher (20). This is seen in Figure 2 where the ionization as measured by ionization chambers is plotted against the mass of air overhead. These data were taken on a trip by ship to Thule, Greenland. Simultaneous flights with identical equipment, carefully compared, were made from Bismarck, North Dakota ($\lambda_m = 56°$ N), and corrections for fluctuations in the primaries could then be made. Actually the fluctuations during the summer of 1954 were extremely small from day to day and week to week.
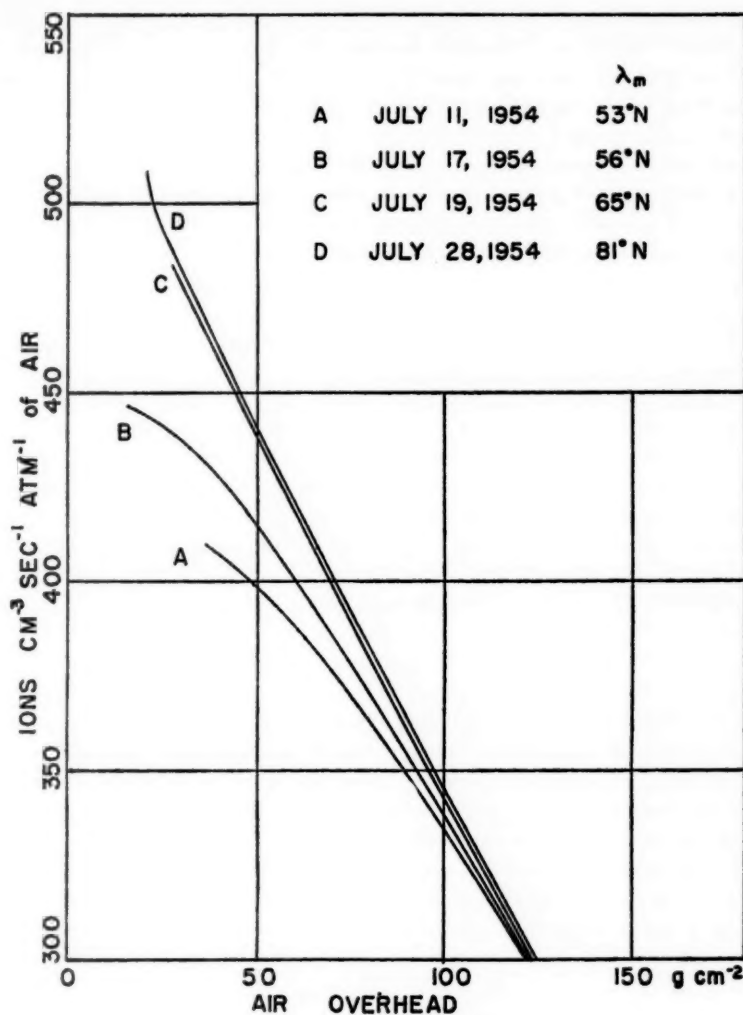
FIG. 2. Ionization vs. air overhead for different latitudes after being corrected for changes at the base station.

Assuming that the increase from Bismarck to Thule in 1954 was in protons only, as the data of Fowler *et al.* (22) indicate, the numbers of protons that cause the increase in areas in Figure 2 could be calculated. These calculations are based on rigidity requirements as well as on the absorption of the low-energy particles in the atmosphere as one proceeds north. Thus the difference in area between curves B and D of Figure 2 is accounted for by a flux of 0.10 protons cm.$^{-2}$ sec.$^{-1}$ ster.$^{-1}$ at the top of the atmosphere of 0.4 Bev average energy.

In the summer of 1955, the situation near the north geomagnetic pole was similar to that in 1954 (21). In fact, the average ionization from five flights at high altitudes was only 2 per cent less, but the fluctuations from day to day were more pronounced than in 1954. The inference, therefore, is that there were about the same numbers of low-energy particles coming in near the north geomagnetic pole in 1955 as in 1954. These findings are confirmed by Winckler & Anderson (24) who made a series of balloon flights going north from Minneapolis in September and October of 1955. These experimenters used Geiger counter telescopes. They also found an increase in counting rate with increase in geomagnetic latitude which they ascribed to protons.

The presence of low-energy particles in the summers of 1954 and 1955 is in contrast to the situation in 1951 found by Neher *et al.* (25). A plot of cosmic-ray intensity at 15 gm. cm.$^{-2}$ residual air pressure versus latitude showed a "knee" at about 56 to 58° geomagnetic north and a plateau for more northerly latitudes. Combining these results with those of Fowler *et al.* on the behavior of α-particles during the nearly similar period, one arrives at the conclusions that the "knee" in the latitude curve at balloon altitudes is probably due to the absence of protons below a certain energy; that the disappearance of the "knee" is due to the reappearance of low-energy protons; and that α-particles and heavier nuclei are either not involved or play a minor role.

In 1956 the ionization due to cosmic rays had dropped to 70 per cent of its value in 1954 at high altitudes near the geomagnetic pole (21), and by August, 1957, Neher & Anderson (26) found that the ionization was less than one-half of its value at 15 gm. cm.$^{-2}$ as compared with 1954. These changes will be further discussed in the section on fluctuations. It is apparent from the above that the energy distribution of the proton component at low energies is very much a function of time.

The α-particle component may be somewhat more constant, or at least, the results of the Minnesota group would so indicate. Fowler & Waddington (27) have made a study of the energy distribution of α-particles in the low-energy range. They give the empirical integral number distribution as

$$N(\geq E) = C/(m_0c^2 + E)^n, \qquad 1.$$

where $C = 370 \pm 100$ for α-particles, $n = 1.50 \pm 0.18$ for energies between 1.8 and 3.0 Bev per nucleon, $(m_0c^2 + E)$ is the total energy per nucleon of the particle in Bev, and the units of N are particles m.$^{-2}$ sec.$^{-1}$ ster.$^{-1}$. Since $m_0c^2 = 0.93$ Bev per nucleon, the above expression is very close to that usually written, where the first term is set equal to unity. By studying jets in emulsions due to α-particles, Fowler and Waddington have made a determination of the exponent n in the above empirical equation and find a value of 1.49 ($+0.23$, -0.20), which holds for energies up to 800 Bev per nucleon. In fact, within the statistical errors, the authors claim that Equation 1 holds for all energies of α-particles from 0.33 to 800 Bev per nucleon.

Waddington (28) has made a study of the heavier nuclei in an effort to determine their energy distribution. He finds that the same form of expression as Equation 1 holds, where again $(m_0c^2 + E)$ is the total energy per nucleon. The value of the exponent obtained was $n = 1.2 \pm 0.3$ for the range 1.8 to 3.0 Bev per nucleon. If one takes the value of $n = 1.5$ as the exponent for all nuclei and the data of Noon, Herz & O'Brien (13) for the numbers of nuclei at 41° geomagnetic north, he may calculate the values given in Table IV for the constant C in Equation 1.

TABLE IV

VALUES OF CONSTANT C IN $N(\geq E) = C/(m_0c^2 + E)^{1.5}$ FOR DIFFERENT PRIMARY NUCLEI. N IN PARTICLES M.$^{-2}$ SEC.$^{-1}$ STER.$^{-1}$

Nucleus	C
He	370
Li, Be, B	14
C, N, O	21
$Z \geq 10$	10

Above values of C and of the exponent of $(m_0c^2 + E)$ probably not valid for energies below 1 Bev per nucleon or above 5 Bev per nucleon, except for He as noted in the text.

Much more information is needed to complete our knowledge of the multi-charged primary nuclei. Some of the questions are: (a) Is there a cut-off at low energies which is not geomagnetic or atmospheric, such as appears to exist in the case of the α-particles? (b) Is the energy distribution at the higher energies the same for all nuclei, except for a constant? (c) What changes occur during a solar cycle or for shorter periods of time? The difficulties connected with getting good statistics are rather formidable so it may be some time before definite answers to the above are forthcoming.

There have been attempts to measure the total number of primary particles by means of Geiger counters carried to high altitudes by balloons. An attempt is then made to extrapolate the counting rate to zero pressure. The experiments usually cited in this connection are those of Winckler (29). Also, attempts have been made to measure the primary flux by means of Geiger counters carried in rockets. In this case, Van Allen's group at the State University of Iowa has probably been the most active. Both kinds of measurements, however, suffer from the serious trouble of also measuring the particles in the albedo, i.e., those particles ejected upward from the atmosphere which may get caught in the earth's magnetic field and returned to the atmosphere. Meredith, Van Allen & Gottlieb (30) have made an attempt to correct their rocket data for this albedo effect. These data are given in Table V. It is quite evident, in view of the large uncertain corrections

(as much as a factor of 3), that rocket data do not give an accurate measure of the primary radiation. Indeed, it is doubtful if cosmic-ray equipment in satellites will be completely free from this albedo effect unless their orbits extend out more than an earth radius from the earth's surface.[2] No attempt seems to have been made to correct Winckler's data, but it is quite evident that albedo also plays a prominent role here and that Winckler's values are too high.

TABLE V

COMPARISON OF NUMBERS OF PRIMARY PARTICLES MEASURED WITH ROCKETS (1955)
WITH VALUES CALCULATED FROM IONIZATION DATA

λ_m	E_{min} (protons) (Bev)	a	b	c		
				1937	1954	1957
0°	14	0.052	0.018	0.012	—	—
41°	3.8	0.126	0.048	0.042	—	—
54°	1.0	0.31	0.11	0.10	0.14	—
87°	0.0	0.48	0.27	0.11	0.24	0.056

Units are particles cm.$^{-2}$ sec.$^{-1}$ ster.$^{-1}$
Column a, before correction for albedo.
Column b, after correction for albedo.
Column c, values calculated from ionization data.

Table V also gives values calculated by Neher *et al.* (20, 25, 26) from data collected at various latitudes and different times with ionization chambers. Since the calculations on the number of primaries is dependent on the areas under ionization-depth curves, the values calculated by this means are much freer from albedo effects. In view of the evidence presented earlier, it appears that most of the changes in the numbers of primaries are in the protons; and that in the latitude-sensitive part, an energy distribution has very little meaning, except at a given time.

Table VI has been prepared from ionization chamber data. The data for the two years 1954 and 1957 may not be representative, although the present thinking is that at the next solar minimum the intensity will probably return to its high value of 1954. A 25 per cent addition has been made to the measured value of the energy flux at the top of the atmosphere to account for neutrino loss. This is in line with the calculations of Puppi (31). The numbers of particles have been calculated using data at various latitudes, with due account taken for the multicharged particles present.

---

[2] *Note added in proof:* The "halo" of charged particles around the earth, recently discovered by Van Allen and his group at the University of Iowa, are probably cosmic-ray albedo particles trapped in the earth's magnetic field.

TABLE VI

DATA ON COSMIC RAYS

(Values given are calculated from ionization chamber data)

Time	Location	Energy cm.$^{-2}$ sec.$^{-1}$ at top of atm.*		Particles cm.$^{-2}$ sec.$^{-1}$ ster.$^{-1}$ at top of atm.†	Energy in outer space cm.$^{-3}$		Ionization in outer space	
		(10^3 ergs)	Bev		(10^{12} ergs)	ev	Ions cm.$^{-3}$ sec.$^{-1}$ atm.$^{-1}$ of air	Milli-roentgens per day
Solar Max.	Equator	2.28 (1937)	1.44 (1937)	0.012 (1937)	0.57	0.36	140‡	5.8
	Near Geomag. Pole	4.25	2.66	0.056				
Solar Min.	Equator	—	—	—	0.76	0.48	>1100	>46
	Near Geomag. Pole	5.70	3.57	0.24				

Data for solar maximum are for 1957 except where noted. Data for solar minimum are for 1954.

* These values have been increased 25 per cent over measured values to account for neutrino loss.

† Best estimate taking account of known composition of primaries.

‡ Calculated from a mean specific ionization of 200 ion pairs cm.$^{-1}$ in air under standard conditions of temperature and pressure.

At the higher energies, i.e., above about 10 Bev per nucleon, energy distributions cannot be deduced from geomagnetic effects. Haber-Schaim (32) has calculated the exponent in a power law E^{-n} from the absorption of μ-mesons in matter. He finds for n in the integral spectrum a value of 1.3 ± 0.22 for the region of 100 Bev.

To study the energy distribution of primaries in the range 10^{15} ev and up, extensive air showers are used. The quantity actually measured is the number of particles in the shower, and the energy of the primary is deduced from theoretical considerations. These are quite well-founded, however, so there seems to be no difficulty in inferring the primary energy distribution. In some remarkable experiments using large scintillation counters spread out over large areas, the group under Rossi at the Massachusetts Institute of Technology has collected data on the directions of arrival as well as on the size of showers. The largest shower so far reported [see Clark *et al.* (33)] contained 1.4×10^9 particles, and this requires an initial energy at the top of the atmosphere of about 10^{19} ev, or more than 1 joule of energy! These authors arrive at an integral energy spectrum, for the region 4×10^{15} ev $< E < 10^{18}$ ev, given by the following (E in ev):

$$N(\geq E) = 2.2 \times 10^{-10}(10^{15}/E)^{2.13} \text{ cm.}^{-2} \text{ sec.}^{-1} \text{ ster.}^{-1}.$$

How particles of such energies can be produced has important astrophysical implications and will be discussed later in the section on the Origin of Cosmic Rays.

FLUCTUATIONS IN THE PRIMARY RADIATION

One of the chief characteristics of cosmic rays is their isotropy. As the earth spins on its axis the particles that initiate events in a counter telescope, say, located at the equator, come from different regions of space. As far as the counting rate of such a telescope is concerned, it makes little difference whether these particles have come from regions in the direction of the sun or from directions opposite to that of the sun. When it is considered that large changes in the radiation striking the earth take place over a period of a solar cycle, indicating some modulating influence in the planetary system under solar control, it is surprising that this mechanism is so well distributed that as the earth rotates on its axis there is little difference in this modulating effect in different directions. This means that the modulating medium does not lie just close to the plane of the ecliptic but must have considerable extension perpendicular to this plane.

The diurnal effect of cosmic rays has been studied a great deal. Due to the smallness of the effect, which is of the order of 1 per cent or less, experiments have been primarily limited to ground level stations. Balloon flights have been made at various times of the day in the attempt to measure a diurnal effect. In particular, one may mention the work of Koshiba & Schein (34) who were interested in the intensity change of heavy nuclei during the day. They found that, on the particular day when their flight was made, a 34 ± 7 per cent change in intensity of the nuclei with $Z \geq 10$ occurred, with a maximum at 9 A.M. local time. They used an interesting technique of moving one set of emulsions with respect to the other, so that the time of passage of a particle could be determined.

Such experiments are of vital importance in determining the nature of the primaries. The limited time that a balloon can be made to keep essentially a constant altitude mitigates against obtaining, by this means, a definite answer to the problem. A satellite carrying a proportional counter or pulse ionization chamber would be an excellent means of obtaining the desired information.

The problem of time variations and particularly the diurnal effect has been reviewed by Sarabhai & Nerurkar (35) up to March of 1956. More recent work has been reported by Elliot & Rothwell (36). The whole problem is in a state of flux. The average diurnal effect is quite small, being only 0.1 to 0.2 per cent over long periods of time for the meson component. The amplitude in the neutron component is more nearly 1 per cent. There is some evidence that the diurnal change is somewhat larger for the lower energy part of the cosmic-ray particles than for those of higher energy, but the effect is not pronounced.

A well established variation in the primaries is the so-called 27-day effect which may be correlated with the rotation of the sun. Forbush was the first to call attention to this and called it quasi-periodic since it persists for several rotations of the sun and then disappears. The same kind of behavior

is familiar in variations in the magnetic field of the earth. Simpson *et al.* (37) have shown that at least for one period, when a pronounced unipolar magnetic region persisted on the sun for a number of revolutions, there was a very definite influence of this region on cosmic rays at the time the region was oriented toward the earth. Whether the 27-day change in cosmic rays is an increase or a decrease is often a difficult matter to decide and the question still seems to be open. As to magnitude, these 27-day changes in neutron intensity at ground level may amount to 5 to 30 per cent, while the changes in meson intensity are about one-third as much. At balloon altitudes at high latitudes the changes may be 7 to 10 times as large on a percentage basis (38) compared with the meson changes at sea level.

It was noticed many years ago that usually, during a magnetic storm, the intensity of cosmic rays decreased from the pre-storm value. These fluctuations have now come to be known as the Forbush-type of decrease. They do not always occur when magnetic storms occur, and there have been definite decreases in cosmic-ray intensity when no magnetic storms were detected. Further, the ratio of the percentage change in cosmic-ray intensity to the percentage change in the earth's magnetic field is not the same from one storm to another. On one occasion, when an ionization chamber was at balloon altitudes and a magnetic storm occurred following the solar flare of July 25, 1946, there was four times the percentage decrease in intensity at the peak of the ionization curve at 41° geomagnetic north as in a ground level ionization chamber at the same latitude (38). It is concluded that the energy-dependence of the Forbush-type of decrease is similar to that of the 27-day quasi-periodic type. These magnetic storm decreases in the meson component may amount to as much as 6 per cent at ground level.

There are other variations such as the day-to-day changes in cosmic rays, but there seems to be no definite correlation between these and any specific events occurring on the sun. There is, however, a definite relationship between solar activity in general and cosmic-ray fluctuations from hour-to-hour and day-to-day. As might be expected, the relationship is a direct one; namely, when the sun is active, as measured by Zurich sun spot numbers, the intensity of the 5303 A corona line, or any other means, the percentage fluctuation in cosmic rays also increases.

The most pronounced changes in cosmic-ray intensity take place during a solar cycle. That a correlation exists between solar activity in general and the intensity of cosmic rays was first pointed out by Forbush (39) in 1954. He found an inverse relationship which showed a total change at ground level from the solar minimum of 1944 to the solar maximum of 1947 of about 4 per cent. The data at high altitudes are much more meager than those at ground level. However, there have been sufficient balloon flights made by now, primarily by Neher *et al.* (20, 21, 25, 26), to establish firmly this relationship at high latitudes. Figure 3 illustrates the situation near the north geomagnetic pole in 1937, 1951, and 1954. As shown in Figure 4, in the year 1937 the sun was near the peak of its activity during that cycle as measured
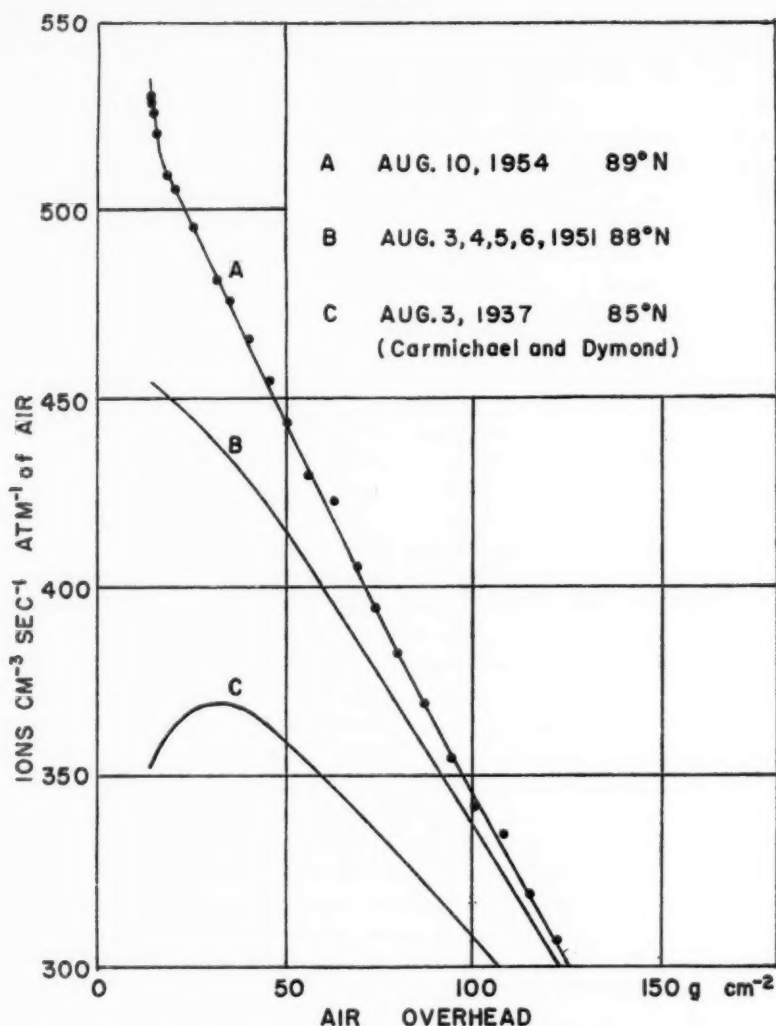
FIG. 3. Curve A was taken when the sun was at a minimum of activity, while B was taken during the waning part of the peak which reached a maximum in 1957. Curve C was taken during the solar maximum of 1937.

by the Zurich sunspot numbers. In 1951 the sun was on the waning part of another cycle, while in 1954 during July and August the sun was extremely inactive.

Continuing on from 1954 it will be noticed (see Fig. 5) that in the summer of 1955 the intensity had decreased slightly, but on the average only 2 per cent at high altitudes from its high value in the summer of 1954. In 1956

(see Fig. 6) the intensity at the lowest pressure had dropped to 75 per cent of its value in 1954, while in the summer of 1957 the intensity near the north geomagnetic pole was only 50 per cent of its value in 1954 at 15 gm. cm.$^{-2}$. It will be noticed that in 1957 the ionization throughout the atmosphere near the pole was only slightly higher than it was at San Antonio, Texas, in 1936. In fact, the total energy per unit time, represented by the areas under the curves, differed by only 4 per cent. As mentioned in the section on Energy Distribution, Neher & Anderson (26) have made an estimate of the number
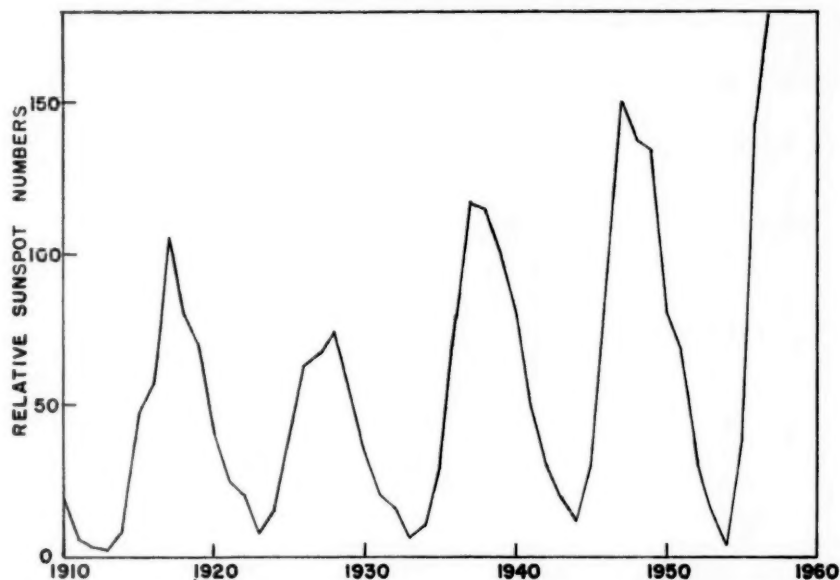
FIG. 4. The Zurich sun spot numbers have climbed rapidly since 1954, reaching a higher value at the end of 1957 than at any time for a large number of cycles.

of primary particles coming in at Thule in 1957 and found that only about one-fourth as many particles were striking the top of the atmosphere in that region as compared with 1954. Now, the earth's magnetic field near the geomagnetic poles allows particles of all energies to come in. Hence, it was concluded that the numbers of primary particles in space near the earth also changed by a factor of four between the solar minimum of 1954 and 1957, when the sun was near a maximum of activity.

This large change in primary particles may be larger than usually occurs during a solar cycle. In Figure 4 the Zurich sunspot numbers are plotted for the past several cycles. The maxima have been getting more pronounced, and the present maximum has reached a higher value than has occurred for a hundred years or more. In Figure 7 the ionization at 15 gm. cm.$^{-2}$ near the geomagnetic pole for the different years has been compared with data of
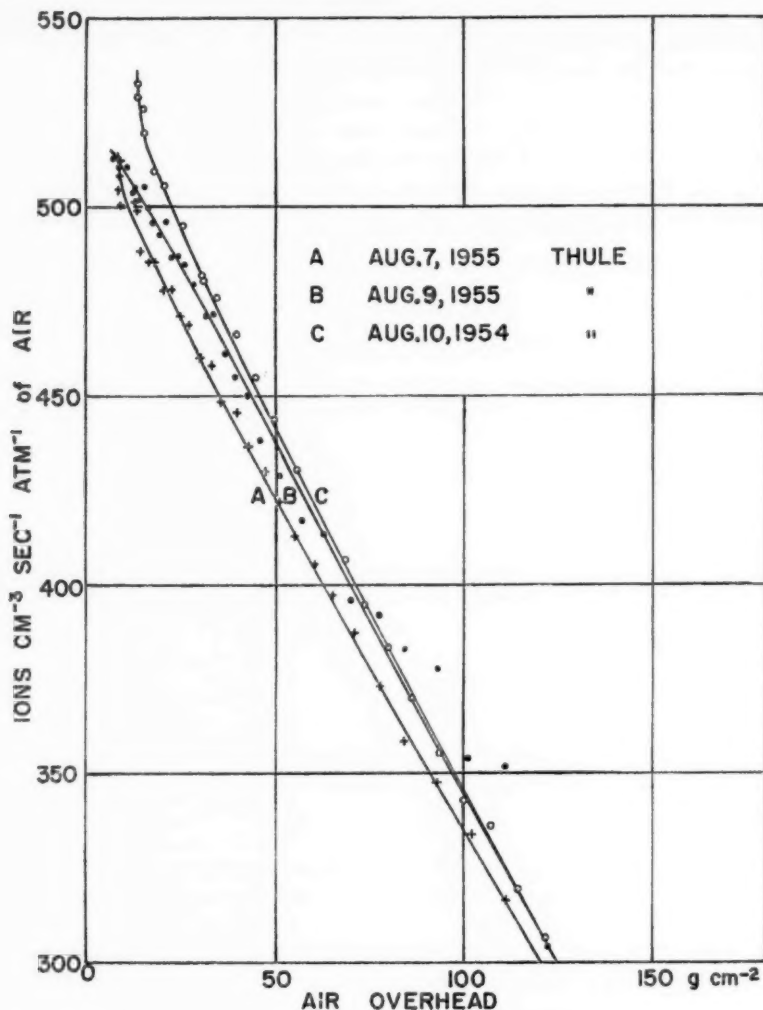
FIG. 5. The average intensity near the north geomagnetic pole in 1955 was only slightly less than in 1954. The difference in curves A and B indicates more higher-energy particles on August 9 than on August 7, since B lies above A at the higher pressures, while at the lowest pressures, the particles that caused A to turn up on August 7 are missing on August 9.

Forbush[3] obtained at Huancayo. The inverse relationship between solar activity, as measured by sunspot numbers, and cosmic-ray intensity is brought out very strikingly.

[3] The author is very grateful to Dr. Forbush for permission to use these data prior to publication.

In spite of these large changes, the average intensity of cosmic rays seems to have remained fairly constant when averaged over long periods of time. Thus, there appears to be a good correlation between the ages of archeological objects dated by C^{14} methods and those determined from historical
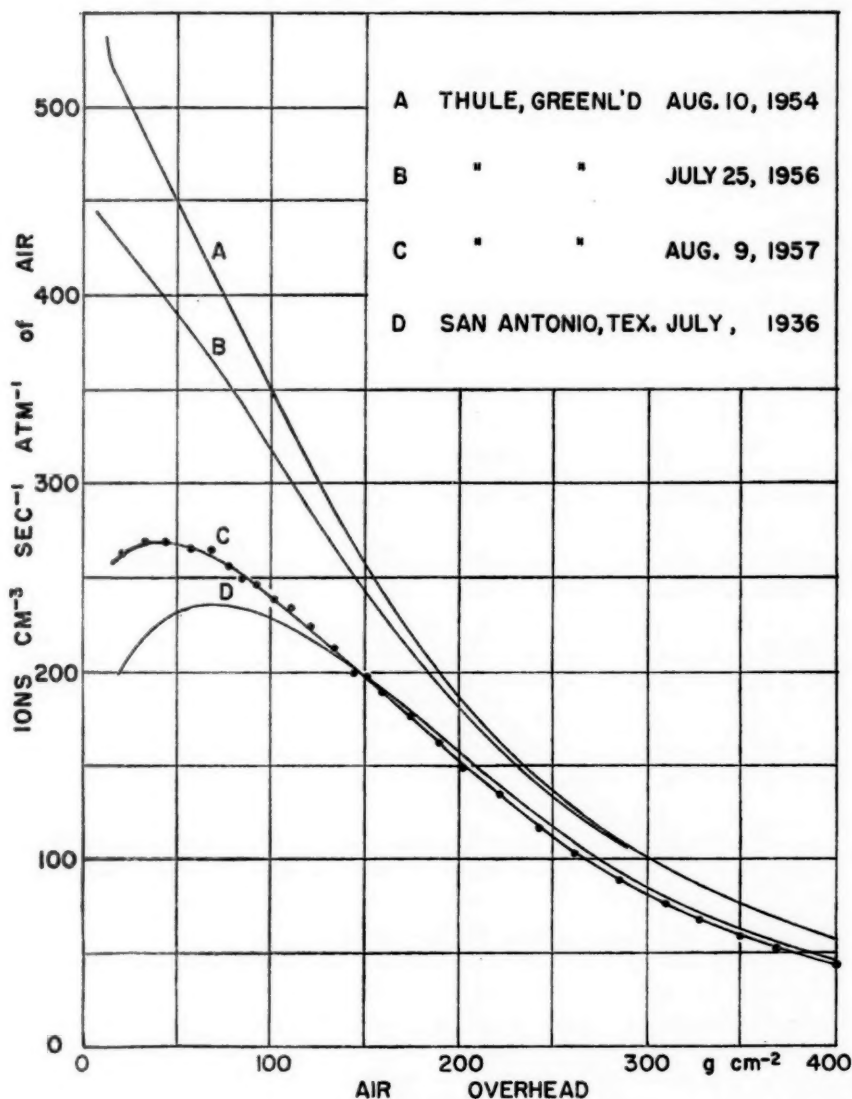
FIG. 6. The ionization at high altitudes near the north geomagnetic pole in 1957 was less than half its value in 1954, the area under the ionization-depth curve was down 34 per cent, and the numbers of primary particles were down by a factor of 4.
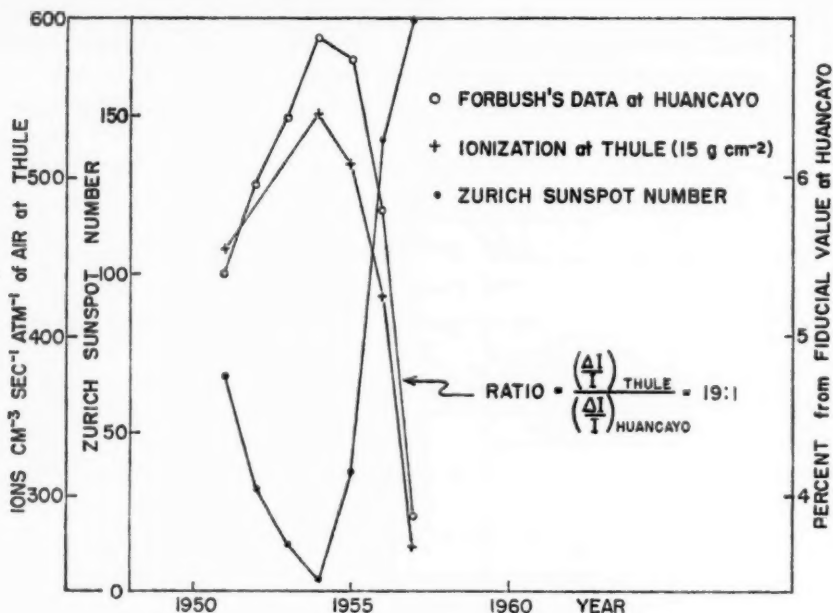
FIG. 7. A comparison of (1) the average yearly values of ionization at Huancayo, Peru, (2) the average ionization at 15 gm. cm.$^{-2}$ of all balloon flights made at Thule, Greenland, in the summer of the corresponding year, and (3) the Zurich sunspot numbers.

records. It should be borne in mind, however, that the sun may have been more or less active in the earlier stages of its life, and the intensity of cosmic rays at the earth may have been different from that in the present epoch.

The search for a satisfactory explanation for the various kinds of fluctuations that occur in cosmic rays constitutes the principal line of research in the field at the present time. That the explanation is to be found in something local, i.e., concerned with our own sun instead of having to do with something happening several light years away seems quite obvious. We suppose, therefore, that beyond about 100 or 1000 A.U. (A.U. = Astromical Unit = average distance between earth and sun) from the sun cosmic rays are constant, at least during the periods of time of interest here.

The solar flare of February 23, 1956 furnished one of the best means yet given to us by nature for studying the region between the sun and the earth. During this most interesting event, the neutron intensity at sea level reached approximately 25 times its normal value due to cosmic rays, while the numbers of particles in space near the earth, but outside its magnetic field, must have increased by at least 250 times. During the initial stages, the particles came in quite anisotropically over the earth. Later, after the maximum had been reached, the radiation came in isotropically, i.e., from no

preferred direction in space. During this latter stage, particles came in at stations like Godhavn, Greenland, where for the energies of particles involved, there should have been none at all had they come directly from the sun.

It is evident, therefore, that at least at the time this flare occurred, there existed diffusing-reflecting regions in the planetary system that affected drastically the paths of particles up to about 10 or 20 Bev of energy (since there was also an increase at the equator). These regions, thought to be turbulent clouds of matter that have come from the sun and which carry, frozen into them, magnetic fields, must have been there before the flare occurred, since the times involved would not allow this matter to travel the necessary distances. If these clouds are present during a time when a solar flare occurs, they must then also be present at other times and presumably are the modulating influences on cosmic-ray particles. While the analysis of this flare constituted a beautiful demonstration that such a modulating mechanism is present in our solar system, it was already evident from previous cosmic-ray work, showing the inverse relationship between solar activity and cosmic-ray intensity, that such clouds must be present.

Morrison (41) has given what seems to be the best general picture of the effect of these turbulent clouds. His thoughts may be briefly stated as follows: We imagine a region of the sun where matter is ejected into surrounding space. That such occurs is amply supported by observations of the sun's corona. There are local magnetic fields on the sun, which will be carried along with the highly ionized and, hence, conducting matter as it is ejected and moves away. Because of low losses, these magnetic fields will continue to exist and will be tied to the ionized matter. The turbulent clouds will expand as they move out from the sun. Their speed will be 1000 to 2000 km. per sec. They will tend to sweep away low-energy cosmic-ray particles since it would require too much time for them to diffuse into these clouds. The higher-energy particles will be less affected. This immediately gives a qualitative dependence on energy that agrees with experiment. These clouds are presumably quite extended. By the time they arrive at the earth their lateral extent will be of the order of 1 A.U. and the density of ions about 1000 cm.$^{-3}$ Such clouds would not, in general, be distinct entities but would overlap one another and would be continually going out of the sun and expanding out into the planetary system. They would be highly turbulent, resulting in a thorough mixing up of the paths of cosmic-ray particles. During an active period of the sun, these clouds might extend out perhaps 100 A.U. so that low-energy cosmic-ray particles would have a very difficult time in reaching the earth. Thus, there would be a reasonable explanation for the "knee" of the latitude curve at high altitudes, i.e., the apparent absence of low-energy particles during an active period of the sun. When the sun is inactive these clouds would presumably disappear, and the earth would receive the full intensity of cosmic rays as they exist in our region of the galaxy. The time lag cannot be large, however, for experiment shows that there is no

more than several months' difference in time between a solar maximum or minimum and the corresponding minimum or maximum, respectively, in cosmic rays.

In such turbulent clouds, it might take hours or days for low-energy particles to find their way into the center. Further, it seems there is no reason why the energy distribution of the low-energy particles should remain the same as the diffusion takes place from one region to another. Thus, it may not be unreasonable that the low-energy particles might decrease in number from one day to the next and those of somewhat higher energy show the opposite effect. This is apparently what happened at high altitudes at Thule, Greenland during the two days, August 7 and 9, 1955. In Figure 5 it will be observed that an August 7 low-energy particles were present that caused the curve at the highest altitudes to turn up. On August 9, these low-energy particles were largely missing but those of higher energy were causing curve B to lie above A deeper in the atmosphere.

The correlation of cosmic rays with solar activity immediately relates the study of their fluctuations to other geophysical phenomena under control of the sun. Some of these other fields, study of which is likely to shed some light on the problem, are the aurora, the ionosphere, the light of the night sky, "whistlers," the magnetic field of the earth both at high and low altitudes, and perhaps also the study of comet tails, for their behavior seems to have some bearing on the matter streaming through them. The important correlations to look for initially would be changes during the solar cycle.

Many problems are posed by the variability of cosmic rays. Depending on the assuracy of the experiment, the results obtained at one time may not be comparable with those at another; an agreement may be quite fortuitous. In general, the composition of the primaries is known, but there is very little information on how it changes during a solar cycle or how the distribution of energy changes for the various nuclei represented. The availability of satellites which should be able to transmit cosmic-ray data over long periods of time may help solve some of the problems.

ORIGIN OF COSMIC RAYS—A FEW REMARKS

It is not intended here to go into the whole subject of the origin of cosmic rays, which would be much too broad for the present purpose. We shall consider first the arguments for and against the sun being an important source. Following this, a few comments on the present ideas about the origin of cosmic rays will be made. The reader who wishes to go into the subject in more detail is referred to: (a) the original article by Fermi (42) on a possible accelerating mechanism of charged particles in interstellar space; (b) an extension by Fermi (43) of the original version of his mechanism; (c) a review article by Rossi (44) which carries the ideas of the origin of cosmic rays up to 1953; (d) a review by Ginzburg (45) of the thinking of the Russian workers up to 1956; (e) a similar review by Morrison (46) which carries the subject through 1956 and includes many interesting ideas.

The original concept of Millikan and others that cosmic rays are really

cosmic was based largely upon the absence of a diurnal effect as it was then determined. When measurements with ionization chambers, carried to high altitudes by balloons, showed that the energy brought to the earth by cosmic rays was about equal to that of all radiant energy from the stars, people began to realize that whatever the mechanism was which gave rise to so much energy it must play an important part in the universe and must be a necessary part of any satisfactory cosmology. The large amount of energy in cosmic rays led some to look very seriously to the sun as a source, since in this case there is no lack of local energy available. The difficulty came in finding an accelerating mechanism that would satisfy the requirements.

One of the obvious conditions that any theory of the sun as the principal source must satisfy is the experimental fact that the diurnal effect is very small. What is usually done is to invoke some kind of storage mechanism to average out the fluctuations which would normally exist if the sun were a source. This storage region might, for example, take the form of the cosmic-ray "hohlraum" proposed by Davis (47) in which he assumes that the conducting matter ejected from the sun pushes back the uniform galactic magnetic field in our neighborhood until the pressures are equalized. Except for necks in the directions of the galactic field, the walls of the region would act as reflectors of charged particles inside, provided their momenta did not exceed certain values. If this storage is for any length of time, as it must be if the sun is to be a more potent source during an active period than when it is quiescent, then it is difficult to account for the inverse relationship between solar activity and cosmic-ray intensity as it is found experimentally and discussed in the section on Fluctuations in the Primary Radiation.

Alfvén (48) has explored the possible accelerating mechanisms in the neighborhood of the sun probably more than anyone else. He envisions streams of conducting matter being ejected from the sun, which, in streaming across an assumed general solar magnetic field, become polarized. This electric field, $v \times B$, would integrate to a very large potential difference across a stream of the order of an astronomical unit in width. High-energy charged particles, going in cycloidal paths around the sun, would presumably be accelerated in passing through such a streaming mass of conducting material. The reader is referred to the article cited in the bibliography for further details.

There are several objections that may be raised about the solar origin of cosmic rays (more accurately they would not be cosmic rays in that case), and, in particular, about the suggestions put forth by Alfvén. (a) Measurements of Babcock et al. (49) have shown that the general magnetic field of the sun is only about 1 gauss at the poles. It is essential for Alfvén's theory that the general field be something like 10 times this. (b) Further, no one has suggested an accelerating mechanism that would be more effective, either in the chromosphere or the corona of the sun, during a period of minimum activity of the sun as compared with the times when the sun is most active. (c) No one has proposed that the particles of energies 10^{14} ev and above are of solar origin (and it would be very difficult to have particles of even 10^{13} ev

generated). It would seem rather fortuitous that an energy distribution of a local source would fit on smoothly to that of a galactic source. (d) It now appears that the elements Li, Be, and B in the primary particles have nearly the same abundance as the C, N, and O group. Since the solar abundances of these light elements are very much smaller than are those of the medium group, their presence must be accounted for by the spallation of the heavier nuclei. But, it is likely that the source of these high-energy particles is not close to the photosphere of the sun, because one might reasonably expect the accelerating mechanism to be accompanied by some kind of visual disturbance. On this basis one would, therefore, look to the corona as a possible source where magnetohydrodynamic effects could be operative. The mass of gas between the earth and the source, in this case, is probably no more than 10^{-7} gm. cm.$^{-2}$, so that the heavier nuclei would need to go many astronomical units to pass through the few grams per cm.^{2} of matter that would be necessary to account for the observed abundance of Li, Be, and B in the primaries. (e) Lastly, if such acceleration of particles were taking place in the corona of the sun, and particularly if this were a more potent source during a solar minimum than during a solar maximum, more radio noise would be expected from the corona during a quiet period of the sun than when it is active. Just the opposite is observed.

Going on the assumption that cosmic rays come from beyond our solar system, there are, at least, the following experimental facts to fit into any theory of origin and acceleration: (a) An inverse power-law energy distribution with an exponent which varies slowly with energy (viz., E^{-n}) holds above about 10^{10} ev. (b) This energy distribution breaks down at the lower energies and, while protons of about 10^8 ev are present, their numbers are much less than what might be expected. There also appears to be a difference in the spectrum of α-particles and protons at the lower energies which can not be accounted for in terms of rigidity requirements or in terms of absorption in the atmosphere. (c) Energies of the primaries extend beyond 10^{18} ev and the highest single event so far measured is about 10^{19} ev or over 1 joule of energy. (d) There seems to be very little, if any, anisotropy of the primaries from the lowest up to the highest energies which can not be explained in terms of solar influences. (e) The energy density of cosmic rays in space is about equal to the radiant energy from the stars, namely, about 0.5 ev cm.$^{-3}$. (f) There appear to be no high-energy electrons or γ-rays in the primaries, certainly no more than 1.0 per cent of the positive particles. (g) The chemical composition corresponds roughly to the natural abundances of the elements, but there are two outstanding exceptions: (i) The nuclei of Li, Be, and B are roughly equal in numbers in cosmic rays to C, N, and O, but are less by a factor of 10^7 in the natural abundances (16). (ii) The heavier nuclei, i.e., $Z \geq 10$, are several times more abundant compared with the C, N, and O group in cosmic rays than in the natural abundances (14). (h) In the C, N, and O group of elements, carbon seems to be relatively several times more numerous in cosmic rays than in the natural abundances (14).

There will undoubtedly be other experimental facts emerging as more in-

formation is gathered about the primaries. The energy distributions of the various nuclei at both the low- and high-energy ends of the spectrum are very inadequately known at the present time. It is also not clear whether the full intensity of cosmic rays which exists in interstellar space really reaches the earth during very low solar activity. It appears, however, that the major characteristics of the primary cosmic rays are included in the above statements.

The relatively large amount of Li, Be, and B in the primaries argues strongly for a break-up of heavier nuclei in colliding with interstellar matter, mostly hydrogen. Assuming a zero abundance of these elements at the source, Koshiba, Schultz & Schein (14) estimate that the heavier nuclei have been traveling for 5.3×10^6 years through the interstellar gas (1 hydrogen atom cm.$^{-3}$ on the average). This time makes understandable the total energy in cosmic rays, because it now appears that interstellar matter is tied together with more or less chaotic magnetic fields, and that the original particles may spend 10^4 times as much time in their wanderings as they would take if their paths were straight, gaining or losing energy by the Fermi process. Thus, the energy density may be much higher than if the particles traveled in straight lines. This diffusion process completely mixes up the directions so that the isotropy also becomes understandable.

The relatively large numbers of heavy nuclei in the primaries, including the high proportion of carbon, argue for certain kinds of stars being the primordial source of the nuclei. [For a very complete discussion of the synthesis of elements in the stars the reader is referred to Burbridge *et al.* (50).] It was suggested in 1934 by Zwicky (51) that supernovae might be the source, and he discussed certain mechanisms. The study of the remnants of a supernova called the Crab nebula, by Oort & Walraven (52), has shown that it possesses some remarkable properties. The high degree of polarization of the continuous light from this object argues strongly for a fairly uniform magnetic field extending over a distance of a fraction of a light year. The polarized light presumably comes from synchrotron radiation resulting from electrons accelerated in orbits about the magnetic field. Since these electrons would soon lose their energy they must be replenished. This might well be the result of nuclear collisions of protons going in similar orbits. These collisions would form π-mesons, which, in turn, would give rise to electrons. The Crab nebula is also the third strongest source of radio noise in the sky, and it is thought that this noise has the same source as the continuum in the visible spectrum, namely, it is the long wavelength end of the synchrotron radiation. It thus seems likely that objects like the Crab nebula are not only sources of high-energy particles, which presumably leak out of the system as time goes on, but that they are also sources of magnetic fields in the galaxy as they continue to expand into space.

Since the whole energy of the universe is ultimately derived from nuclear energy, there seems to be no lack of energy available in supplying what is needed for the turbulent gas clouds in interstellar space, the magnetic fields associated with them, the energy going into radio noise, cosmic rays, and,

of course, the energy of the stars themselves. The problem at the present time is to describe in detail the various processes that are known to occur, in such a way as to make a self-consistent picture.

It is possible that individual stars are the original sources of the nuclei. If so, they must be much more potent than our sun since its total energy output in the form of high-energy particles is many times less than its light output. Furthermore, if a mechanism akin to that suggested by Fermi is to take over the accelerating process, the original source must inject the particles with a certain minimum energy; otherwise the losses by ionization will be greater than the gains. In Fermi's original suggestion (42) this minimum energy for iron nuclei was estimated at 3000 Bev. Modifications to Fermi's mechanism have been proposed which are more rapid than his original model and hence require less injection energy. But one must not lose sight of this requirement and how it can be reconciled with the relatively large abundances of heavy nuclei in the primaries. Babcock (53) has suggested that stars with varying magnetic fields, of which there are large numbers, may be sources of high-energy particles. While the possibilities are certainly present, the details of how particles are accelerated to the necessary energies are still obscure.

The link between radio noise and polarized light from the Crab nebula by means of synchrotron radiation and the strong evidence for high-energy particles, even though the exact mechanism may not be known, has suggested that the nonthermal radio noise comes from synchrotron radiation. The noise coming from the halo of the Andromeda nebula is of this type and presumably our galaxy also has a halo. This brings up the question of storage of particles in the turbulent magnetic fields and gases that make up the halo— an idea that is discussed by Morrison (46). Many radio sources cannot be identified with specific visual objects, and the question arises as to whether these regions may not be important sources of cosmic rays. Some very strong radio noise sources can be identified visually, and photographs taken with the large telescopes usually show something violent taking place. The reader is referred to the review article by Morrison (46) for a discussion of one of the more striking objects in the photographs taken by Baade (54).

Burbridge (55) has called attention to the conditions existing in the Coma cluster of galaxies and has found that the acceleration of particles near the center of the system to energies of 10^{18} to 10^{20} ev should be possible by means of the Fermi mechanism. It is quite likely that the Fermi mechanism is too slow to be effective in interstellar space, and one must look to a Fermi acceleration process operative in supernovae and other objects of a peculiar nature that are emitting large amounts of synchrotron radiation.

CONCLUSION

The present problems in the field of cosmic rays divide themselves into two categories: (a) those having to do with solar influences and (b) those having to do with their origin.

On their way to the earth, cosmic-ray and solar-flare particles act as probes, giving us information on the regions through which they have passed. This information has to do both with the earth's magnetic field and with the regions of the solar system beyond. A matter of some urgency at the present time is to fix as accurately as possible the effective geomagnetic coordinates of the earth's field, in order that a better analysis of the primary radiation itself may be made. It may be that the earth's field is modified at some distance away by the magnetic fields associated with the turbulent clouds that come from the sun. If so, it may require several solar cycles to separate out the two effects.

While these high-energy charged particles are the only known probes of the magnetic fields of the solar system, there are many geophysical and other phenomena that depend on solar activity and, hence, the state of and the amount of matter in the vicinity of the earth. Thus, the sun's corona may be regarded as extending to and beyond the earth's orbit. The problem is to fit all of the known phenomena into a consistent whole.

The change with time of the composition of the primaries, as well as their energy distribution, are not well known at the present time. It is sometimes stated that the various nuclei show the same rigidity cut-off at the low energy end of their spectrum, thus indicating that magnetic fields are responsible. Such a statement needs to be viewed with some caution. The evidence is that it was not true at the last solar minimum.

As to the origin of cosmic rays, it now appears that they are intimately tied up with the dynamics within our galaxy as well as other galaxies. While Millikan's ideas that cosmic rays are the birth or death cries of the atoms are no longer tenable, there exists, instead, the possibility of the much grander concept that cosmic rays are the evidence of the birth cries, life struggles, and death cries of the stars and galaxies.

LITERATURE CITED

1. Schein, M., Jesse, M. P., and Wollan, E. O., *Phys. Rev.*, **59**, 615 (1941)
2. Johnson, T. H., *Phys. Rev.*, **54**, 385 (1938)
3. Lattes, G. M. G., Muirhead, H., Occhialini, G. P. S., and Powell, C. F., *Nature*, 159, 694 (1947)
4. Bjorkland, R., Crandall, W. E., Moyer, B. J., and York, H. F., *Phys. Rev.* **77**, 213 (1950)
5. Rossi, B., *Revs. Modern Phys.*, **20**, 537 (1948)
6. Puppi, G., *Progress in Cosmic Ray Physics*, **III**, 341–87 (North-Holland Publishing Co., Amsterdam, 420 pp., 1956)
7. Komori, H., *Progr. Theoret. Phys.* (*Kyoto*), **13**, 212 (1955)
8. Freier, P., Lofgren, E. J., Ney, E. P., Oppenheimer, F., Bradt, H. L., and Peters, B., *Phys. Rev.*, **74**, 213 (1948)
9. Peters, B., *Progress in Cosmic Ray Physics*, **I**, 193–241 (North-Holland Publishing Co., Amsterdam, 557 pp., 1952)
10. Biermann, L., *Ann. Rev. Nuclear Sci.*, **2**, 335–64 (1952)
11. McDonald, F. B., *Phys. Rev.*, **104**, 1723 (1956)

12. Waddington, C. J., *Phil. Mag.*, **2**, 1059 (1957)
13. Noon, J. H., Herz, A. J., and O'Brien, B. J., *Nature*, **179**, 91 (1957)
14. Koshiba, M., Schultz, G., and Schein, M., *Nuovo cimento* (To be published)
15. Webber, W. R., *Nuovo cimento*, **4**, 1285 (1956)
16. Suess, H. E., and Urey, H. C., *Revs. Modern Phys.*, **28**, 53 (1956)
17. Meinel, A. B., *Astrophys. J.*, **113**, 50 (1951)
18. Meredith, L. H., Gottlieb, M. B., and Van Allen, J. A., *Phys. Rev.*, **97**, 201 (1955)
19. Anderson, K. A., *J. Geophys. Research*, **62**, 641 (1957)
20. Neher, H. V., *Phys. Rev.*, **103**, 228 (1956)
21. Neher, H. V., *Phys. Rev.*, **107**, 558 (1957)
22. Fowler, P. H., Waddington, C. J., Freier, P. S., Naugle, J., and Ney, E. P., *Phil. Mag.*, **2**, 157 (1957)
23. Dainton, A. D., Fowler, P. H., and Kent, D. W., *Phil. Mag.*, **43**, 729 (1952)
24. Winckler, J. R., and Anderson, K. A., *Phys. Rev.*, **108**, 152 (1957)
25. Neher, H. V., Peterson, V. Z., and Stern, E. A., *Phys. Rev.*, **90**, 655 (1953)
26. Neher, H. V., and Anderson, H., *Phys. Rev.*, **109**, 608 (1958)
27. Fowler, P. H., and Waddington, C. J., *Phil. Mag.* **1**, 637 (1956)
28. Waddington, C. J., *Nuovo cimento*, **5**, 737 (1957)
29. Winckler, J. R., Stix, T., Dwight, K., and Sabin, R., *Phys. Rev.*, **79**, 656 (1950)
30. Meredith, L. H., Van Allen, J. A., and Gottlieb, M. B., *Phys. Rev.*, **99**, 198 (1955)
31. Puppi, G., *Progress in Cosmic Ray Physics*, III, 341–383 (North-Holland Publishing Co., Amsterdam, 420 pp., 1956)
32. Haber-Schaim, U., *Nuovo cimento*, **2**, 336 (1955)
33. Clark, G., Earl, J., Kraushaar, W., Linsley, J., Rossi, B., and Schab, F., *Nature*, **180**, 353, 406 (1957)
34. Koshiba, M., and Schein, M., *Phys. Rev.*, **103**, 1820 (1956)
35. Sarabhai, V., and Nerurkar, N. W., *Ann. Rev. Nuclear Sci.*, **6**, 1–42 (1956)
36. Elliot, H., and Rothwell, P., *Phil. Mag.* **1**, 669 (1956)
37. Simpson, J. A., Babcock, H. W., and Babcock, H. D., *Phys. Rev.*, **98**, 1402 (1955)
38. Neher, H. V., and Forbush, S. E., *Phys. Rev.*, **87**, 889 (1952)
39. Forbush, S. E., *J. Geophys. Research*, **59**, 525 (1954)
40. Carmichael, H., and Dymond, E. G., *Proc. Roy. Soc.* (*London*), **A171**, 521 (1939)
41. Morrison, P., *Phys. Rev.*, **101**, 1397 (1956)
42. Fermi, E., *Phys. Rev.*, **75**, 1169 (1949)
43. Fermi, E., *Astrophys. J.*, **119**, 1 (1954)
44. Rossi, B., *Nuovo cimento*, **2**, Suppl., 275 (1955)
45. Ginzburg, V. L., *Nuovo cimento*, **3**, Suppl., 38 (1956)
46. Morrison, P., *Revs. Modern Phys.*, **29**, 235 (1957)
47. Davis, L., Jr., *Phys. Rev.*, **100**, 1440 (1955)
48. Alfvén, H., *Tellus*, **6**, 232 (1954)
49. Babcock, H. W., and Babcock, H. D., *Astrophys. J.*, **121**, 349 (1955)
50. Burbridge, M. E., Burbridge, G. R., Fowler, W. A., and Hoyle, F., *Revs. Modern Phys.*, **29**, 547 (1957)
51. Zwicky, F., *Proc. Natl. Acad. Sci. U.S.*, **20**, 259 (1934)
52. Oort, J. H., and Walraven, T., *Bull. Astron. Inst. Netherlands*, **12**, 285 (1956)
53. Babcock, H. W., *Phys. Rev.*, **109**, 2210 (1958)
54. Baade, W., *Astrophys. J.*, **123**, 550 (1956)
55. Burbridge, G. R., *Phys. Rev.* **107**, 269 (1957)

THE RADIOACTIVITY OF THE ATMOSPHERE AND HYDROSPHERE[1,2]

By Hans E. Suess[3]

Scripps Institution of Oceanography, La Jolla, California

Introduction

Radioactive nuclear species that occur on the surface of the earth can be grouped into three classes: (*a*) Extremely long-lived species that have survived from the time when the elements formed (primary radionuclides) and their daughter products (secondary radionuclides). (*b*) Radioactive nuclei that are currently formed in nature, primarily by cosmic-ray induced processes. (*c*) Man-made radioactive substances, such as those produced through the testing of atomic devices or in nuclear reactors.

Radioactive isotopes follow the geochemical behavior of their respective elements. They can be used as tracers in the study of geochemical processes. If their rates of radioactive decay are comparable with the rates of these processes, then the possibility exists of determining the rate of the geochemical processes through the measurement of radioactivities. The long-lived radioactive species of class (*a*) have proved extremely useful for geologic age measurements and the study of geologic processes of a time scale of millions of years. Phenomena occurring in the atmosphere and hydrosphere, such as mixing and chemical transfer, will occur with time scales rarely exceeding a few thousand years. For their study activities of relatively short half lives will be useful.

It appears now that both the hydrosphere and the atmosphere have to be treated as consisting of at least two parts, between which transfer and exchange of material is relatively slow. One may consider two atmospheric reservoirs: the stratosphere, containing about one-sixth of the atmosphere by weight, and the troposphere. The two marine reservoirs are: the so-called

mixed layer, i.e., water above the thermocline which represents about one-fortieth of the total ocean water, and deep ocean water.

For the study of mixing phenomena between these reservoirs, the discovery of cosmic-ray produced radioactivities has opened a wide field of new possibilities. The most important of these activities is undoubtedly carbon 14 found to occur in nature by Libby (1) in 1948. A few years later natural tritium was discovered by Libby (2) and co-workers and independently by Faltings & Harteck (3). The relatively large amounts of artificially produced tritium released during the past years into the atmosphere have now obscured the original natural tritum distribution. Fortunately, earlier measurements by Libby and co-workers (4, 5) answer most of the questions relative to natural tritum. Following the work of Libby, several investigators have now found a number of additional radioactive nuclear species currently produced by cosmic rays in nature. With respect to the cosmic-ray produced as well as to the artificially formed radioactive nuclei, two types of quantities are primarily of interest: (a) concentrations and (b) production and fallout rates. Concentrations of radioactivities are usually given as disintegrations per unit of time per amount or volume, or curies per amount or volume.

In general, it is necessary to use refined experimental techniques for measurements of low-level activities present in nature. A previous article by Anderson & Hayes (6) summarizes recent advances in these techniques. Libby's method of subtracting the μ-meson background by anticoincidence counting is generally applied for β-counting. Comparable sensitivities can be achieved for the measurement of γ-activities by use of scintillation counting techniques, preferably with multi-channel instruments.

The review article by Kohman & Saito (7) on radioactivity in geology and cosmology contains more general information on properties and occurrence of radionuclei in nature. The following paper can only give a brief account of the nature of geochemical, meteorological, and oceanographic problems involved in the interpretation of the distribution of radioactivity in the atmosphere and hydrosphere of our planet. It attempts to facilitate the selection of the original literature for further study.

PRIMARY RADIONUCLIDES AND THEIR DAUGHTERS

Table I lists the concentrations of the extremely long-lived nuclides in ordinary standard sea water (salinity, 3.5 per cent) according to the most recent measurements. This table does not include the radionuclides Sm^{147}, Lu^{176}, La^{138}, and Re^{187}. The concentrations of these elements are not well known. The relatively high solubility of uranium in sea water is due to carbonate complexing. The solubility of thorium appears to be much smaller.

The upper limit of the thorium concentration listed in Table I is based on two determinations of Pacific Ocean water by Sackett, Potratz & Goldberg (8). Radioactive tracer techniques using Th^{234} were employed. The uranium values given in Table I are those of Rona, Gilpatrick & Jeffrey (9) who employed a mass-spectroscopic isotope dilution technique, with U^{235}

TABLE I

AVERAGE CONCENTRATIONS OF RADIOACTIVE ELEMENTS IN SEA WATER

Ele-ment	Concentration		Isotope	$T_{\frac{1}{2}}$ 10^9y.	d/m liter	Refer-ence
	g/g*	mol./liter				
Th	$<5\times10^{-11}$	$<2\times10^{-10}$	Th[232]	13.9	$<0.01\alpha$	(8)
U	3.3×10^{-9}	1.5×10^{-8}	U[235]	0.71	0.23α	
			U[238]	4.51	5α	(9)
K	3.8×10^{-4}	1×10^{-2}	K[40]	1.3	$470\beta+\gamma$	(7)
Rb	1.21×10^{-7}	1.35×10^{-6}	Rb[87]	59	5.3β	(10)

* Grams of element per gram of sea water.

as spike. These authors obtained, for five samples from the Atlantic and the Gulf of Mexico and for one from the Pacific Ocean, values ranging from 3.19 to 3.45 μg./liter of sea water, with an average as given in Table I. The new rubidium value of Smales & Webster (10) was also determined by means of stable isotope dilution.

Table I does not contain the daughter products of uranium and thorium which behave in a rather complex way. The low solubility of thorium causes Th[230] (ionium, half life 80,000 years) to precipitate with thorium in a time which is short compared to this half life. Urry (11) was the first to attempt to use the ionium concentration in deep-sea sediments for estimates of the rate of sedimentation. However, the ionium concentrations were derived by measuring its daughter radium and by assuming radiogenic equilibrium between ionium and radium. It was shown by Arrhenius & Goldberg (12) that, after deposition, radium migrates into certain minerals and, therefore, may not always remain in the layer of deposition. Radium also redissolves in part with the calcium and goes back into the deep ocean water. This fact was shown by Koczy (13) who found deep ocean water richer in radium than the ocean water in higher layers. Ionium dates of ocean sediments based on radium measurements will, therefore, frequently not be reliable. Such dates can only be accepted after a detailed study of various factors.

Direct measurements of the ionium concentration in sediments by assays of thorium and of its isotopic composition were first attempted by Picciotto & Wilgain (14). More recently, more extensive measurements have been made by Goldberg & Koide (15) leading to reliable values for deposition rates of sediments.

Blifford et al. (16) have recently carried out new measurements of atmospheric radon and thoron concentrations in different parts of the world. The radon concentration is about one order of magnitude higher over con-

tinental areas than over the oceans. It varies with the nature and condition of the soil. The concentration of thoron ($T\frac{1}{2} = 59$ sec) is about a factor of ten smaller than the concentration of radon. The results of Blifford et al., agree with early measurements of Benndorf & Hess (17), but are lower than those reported by Israel (18). A few of Blifford's measurements are listed as examples in Table II. The values represent daily averages at approximately 1600 local time. A diurnal cycle in the radon concentration was found to exist at all locations. This observation agrees with previous findings of

TABLE II

AVERAGE CONCENTRATION OF RADON AND THORON IN AIR FROM MEASUREMENTS
BY BLIFFORD et al. (16) IN 1950 AND 1951

Place	d/m per meter³	
	Radon	Thoron
U.S.A.		
Washington, D. C.	100	4
Chicago, Ill.	50	5
West Coast	10	0.6
Puerto Rico	0.2	0.07
Pacific Islands	1.5	low
North Africa	17	5
Alaska	7	0.1

Wilkening (19). The causes of these effects have not yet been investigated in detail. Pronounced seasonal variations were observed also. Decay products from radon and thoron in rains have been studied by Damon & Kuroda (20). The concentration of radionuclides produced by spontaneous fission of U^{238} in the atmosphere and hydrosphere is today many orders of magnitude below the limits of detection because of the presence of much larger quantities of artificial fission products.

COSMIC-RAY PRODUCED RADIOACTIVITIES

The amount of radioactive particles produced by cosmic-ray events is proportional to the incoming cosmic-ray flux and shows the same dependence on geomagnetic latitude as does the cosmic-ray intensity. The difference in the production rate per $cm._e^2$ between geomagnetic equator and poles is approximately a factor of four (21). The average number of primary cosmic-ray particles that hit the earth is of the order of one per $cm.^2$ and per second. The possibility of secular variations in the cosmic-ray intensity resulting from changes in the magnetic field of the earth and the possible effects of such variations on the radiocarbon inventory have been discussed by Elsasser, Ney & Winckler (22). The number of nuclei of a certain nuclear species

formed by cosmic rays can sometimes be estimated from star production rates in nuclear emulsions or from yields in high-energy experiments (23).

Carbon 14.—An account of the production and distribution of natural radiocarbon has been given in a previous article by Anderson (24) in 1953. The atomic C^{14} produced by (n, p) reaction on N^{14} is oxidized in the atmosphere to molecular CO_2. The possibility has been discussed by Harteck (25) that this oxidation is slow and that the C^{14} remains in the form of carbon monoxide for many years before the oxidation is completed. Experimental proof of such delay in the oxidation will be difficult to obtain because of the presence of man-made carbon monoxide in the atmosphere.

Since 1954 noticeable amounts of artificially produced C^{14} have been added to the atmosphere. The following applies to the situation before artificial C^{14} became significant:

TABLE III

AMOUNT OF CARBON IN THE VARIOUS EXCHANGEABLE RESERVOIRS (1) AS
REVISED IN (28)

Reservoir	Carbon content gm. per cm.$_e^2$
Atmospheric CO_2	0.126
Terrestrial biosphere (living)	0.06
Humus	0.215
Marine biosphere	0.002
Dissolved organic matter in sea	0.533
Total inorganic carbon in sea	6.94
Total exchangeable carbon	7.88

Table III lists the so-called reservoirs into which C^{14} is distributed and the amounts of carbon present in each reservoir (1, 26, 27, 28). As a first approximation, one may assume that the distribution of C^{14} into these reservoirs will occur within a time which is short compared with the average life of C^{14}, i.e., 8000 years. If this assumption is made and if isotope fractionation effects are neglected, a constant C^{14}/C^{12} ratio is to be expected for all the different reservoirs. Actually, minor deviations (of the order of a few per cent) from a completely uniform C^{14}/C^{12} ratio occur for two reasons: (*a*) The equilibrium distribution is not quite uniform because of mass dependent terms in the thermodynamic constants for isotope exchange. (*b*) The exchange and transfer rate of CO_2 between the reservoirs is not infinitely fast compared with the average life of C^{14}.

For the carbonates of surface ocean water these two effects just happen to cancel each other almost completely. Marine beach shells show the same C^{14}/C^{12} ratio within one per cent as organic terrestrial plant material, if one

corrects for effects from industrial fuel combustion (see below), although the C^{13}/C^{12} ratio is about 2.5 per cent higher in carbonate than in wood (29). This difference of 2.5 per cent in the C^{13}/C^{12} ratio corresponds to a difference of 5 per cent in the C^{14}/C^{12} ratio and shells should therefore show a specific C^{14} activity about five per cent higher than that of wood of the same age. Actually, no significant difference in the C^{14} activity of shells and wood is found, and therefore one may say that marine surface material has an apparent age of about 300 or 400 years. This fact can be used for estimating the residence time of CO_2 in the atmosphere before it becomes dissolved into the sea.

If one assumes that mixing within the ocean is fast compared with 400 years, or, in other words, that the average carbon in the ocean shows an apparent age of 300 to 400 years, then the residence time (τ_s) for the carbon in the ocean would be about 300 to 400 years and for the atmosphere (τ_a) about five to seven years. Slower mixing would make these residence times correspondingly larger. The residence time (τ) is defined as the amount of carbon in a reservoir divided by the amount transferred into other reservoirs or exchanged with the carbon of other reservoirs per year.

Values for τ_a can be obtained in an entirely different way by considering the effect of industrial fuel combustion on the specific C^{14} activity of carbon. Between the end of the nineteenth century and 1950, approximately 12 per cent of the CO_2 present in the atmosphere was added to the atmosphere. This was CO_2 derived from the combustion of fossil fuel, and was, therefore, free of C^{14}. If none of this CO_2 had been absorbed by the oceans, or had equilibrated its isotopic composition with other reservoirs, then the specific C^{14} activity of wood grown in 1950 should be about 12 per cent lower than that of wood grown before the beginning of the industrial revolution. Exchange with the carbon of the terrestrial biosphere could lower this effect by not more than a factor of two. The actual decrease in the specific activity of wood since the nineteenth century has been measured by Suess (30), Hayes, Anderson & Arnold (31), Williams (32), and Fergusson (33). A decrease has been observed by all authors and values have been obtained ranging up to four per cent. The high values, however, undoubtedly arise from local contamination of air masses near industrial centers. It seems now fairly well-established that the world-wide C^{14} depletion of atmospheric carbon dioxide in 1950 was about 1.75 per cent. Fergusson gives for this quantity 2.03 ± 0.15 per cent for 1954. The effect is the same within 0.5 per cent in both hemispheres. Fergusson (33) , therefore, concludes that atmospheric mixing across the equator occurs within less than two years.

From these data the rate of uptake of CO_2 in the oceans can be calculated and a value of about seven years is obtained for the residence time τ_a of CO_2 in the atmosphere if fast mixing is assumed in both reservoirs. This value, however, is to be taken here as an upper limit, because slow mixing of the top layer of the oceans above the thermocline into deeper water masses would lead to a shorter residence time of CO_2 in the atmosphere. Revelle &

Suess (26) conclude from the empirical data available that the residence time of CO_2 in the atmosphere before it is dissolved in the sea, τ_a , must be of the order of ten years. It is at present hardly possible to give a more exact figure for τ_a, because the processes which have to be considered for a more accurate calculation seem to have rate constants of comparable orders of magnitude. In particular, the overturn time of the terrestrial biosphere and the mixing rate through the marine thermocline are presumably also of the order of magnitude of ten years and are not well-known.

Attempts to obtain a more accurate figure for τ_a from detailed calculations that include estimates on the rate of internal ocean mixing were made by Craig (28) and by Fergusson (33). Craig gives $\tau_a = 7 \pm 3$ years on the basis of a specific ocean model and independently by comparing the observed C^{14} activities with the estimated cosmic-ray production rate of C^{14}. Fergusson obtains $\tau_a = 2$ years, a result inconsistent with the lower limit derived from the apparent age of surface sea carbonate.

Over the past 50 years a decrease of the order of one per cent in the C^{14} activity of marine carbonates has been observed by Williams (32) and by Rafter (34). This small effect from industrial fuel burning on marine surface carbonate is of the expected magnitude.

Measurements at the Lamont Geological Observatory (35) show the existence in the Atlantic of deep water masses with an apparent C^{14} age of more than 1000 years relative to surface water. Fergusson & Rafter (36) obtained similar results for the South Pacific. More experimental results will be needed for a conclusive interpretation of the picture.

Tritium.—The concentration of the hydrogen isotope, tritium, in rains and surface waters is commonly given in tritium units; one tritium unit is the concentration corresponding to a T/H ratio of 10^{-18}. Surface ocean water and oceanic rain contain in general about one TU of natural tritium, whereas the tritium concentration in rain over continents, in rivers and lakes is of the order of several TU. Since about 1954 these amounts have been radically changed by the addition of artificial tritium into the atmosphere. Fortu-

TABLE IV

AVERAGE NATURAL TRITIUM CONCENTRATIONS (PRE-1954) ACCORDING TO
LIBBY *et al.* (4, 5, 38)

Material	$T/H \times 10^{18}$
Ocean surface water	~ 1
Marine rains	~ 1
Chicago rains	7.8
Mississippi River (St. Louis)	6.0
Lake Michigan	1.6
French and Italian wines (corrected for T decay)	4
Antarctic snow	16

nately, a sufficiently large number of tritium measurements exist on samples collected prior to 1954 which give a fairly complete picture of the occurrence of natural tritium. Measurements of natural tritium are still possible by the application of Libby's idea of using vintage wines as a source of water of a known age from the time before artificial tritium contamination became important. Also Arctic and Antarctic ice contains a record of tritium concentrations from previous times.

As an air mass moves over a continent, its tritium content increases because of an addition of newly formed tritium to the atmosphere and lack of drainage into the ocean. In the evaluation of this effect, the steady-state conditions of the tritium in the water vapor of the air, in the ground water, in lakes, and in rivers have to be considered with respect to incoming and outgoing amounts across the continental boundaries.

A material-balance study of tritium in the water vapor over a continent gives the cosmic-ray production rate of tritium in the atmosphere. Earlier estimates (4, 5) seem to indicate a production rate $\overline{Q} = 0.14$ T/cm.^{2} sec. in agreement with estimates from nuclear production cross sections and cosmic-ray intensities. However, Craig (37) has drawn attention to the fact that the results of Kaufman & Libby (4) and von Buttlar & Libby (5) can only be interpreted in a consistent way by assuming a considerably larger value of $\overline{Q}$. This conclusion follows from a more detailed discussion of meteorological data, as well as from the interpretation of tritium measurements of surface ocean water, with the assumption that mixing times are in agreement with the observed C^{14} distribution.

According to Begemann & Libby (38) a higher $\overline{Q}$ value is also in agreement with more recent observations of the behavior of artificial tritium on the North American continent. Their data on artificial tritium give residence times for tritium in various continental water bodies that can be used for calculating $\overline{Q}$ from the data on the distribution of natural tritium. Begemann and Libby conclude that about one tritium atom/cm.$_e^2$ sec. must reach the surface of the earth. The discrepancy of such a $\overline{Q}$ value with the value $\overline{Q} < 0.4$ derived from tritium production cross sections was taken by Feld (64) and by Craig (37) as an indication that tritium from the sun's surface might be accreted by the earth. If most of the tritium came from extraterrestrial sources, then an influx of about 1.7 T atoms/cm.$_e^2$ sec. would have to be assumed, with about 1.2 atoms/cm.^{2} sec. reaching the earth's surface (37).

The earth's atmosphere contains about 0.5 p.p.m. (by volume) of molecular hydrogen. A very remarkable observation was made by Faltings & Harteck (3) who found that this free hydrogen contains over a thousand times more tritium than the water vapor in air. Harteck & Suess (39) found that the deuterium content of this hydrogen does not correspond to the equilibrium concentration but is approximately the same as in ordinary water. They concluded that the hydrogen must be produced photochemically in the upper atmosphere. Harteck (40) attempted to explain the high tritium concentration in the free H$_2$ by considering the individual steps in the oxidation

mechanism of the cosmic-ray produced tritium atoms to water. However, if slow mixing of stratospheric and tropospheric air is assumed, with a residence time of stratospheric air comparable to the half life of tritium (see below), then it is possible to account for the high tritium concentration of the free atmospheric hydrogen by the simple assumption that it reflects conditions prevailing in the upper atmosphere, where the water vapor concentration is low and the HTO/H_2O ratio should, therefore, be very high.

Beryllium 7 and beryllium 10.—The natural occurrence of these isotopes was discovered by Arnold & Al-Sali (41) and Arnold (42), respectively, and their existence was confirmed by Peters and his collaborators (43, 44). Be^7 is present in measurable amounts in rains. It can, after chemical separation, be identified by its 0.479 Mev γ-radiation that occurs in 11 per cent of the disintegrations. Be^{10} was identified in pelagic sediments of extremely low rate of deposition, so that the extraction from one single sample contained the Be^{10} deposited during some 100,000 years.

A careful theoretical study of cross sections for the production of Be^7 by cosmic rays was made by Benioff (45). From a comparison of $\overline{Q}$ values thus obtained with the empirical ones given by Arnold, Benioff concludes that the Be^7 formed in the stratosphere does not contribute appreciably to the activity found in rains, and that the hold-up time in the stratosphere must be long compared with the Be^7 half life of 54 days. This agrees with observations on artificial fallout (see below). The washout time of Be^7 from the troposphere was found to be of the order of a few weeks, again in agreement with other evidence.

Other cosmic-ray produced radionuclides.—The data on other cosmic-ray produced activities discovered in rains are most incomplete. The values listed in Table V are based on a few measurements of a more or less preliminary nature. In most cases more work seems essential to establish conclusive evidence.

ARTIFICIALLY PRODUCED RADIOACTIVITIES

The man-made radionuclides introduced into the atmosphere and the oceans consist primarily of fission products of U^{235} and Pu^{239}. Hydrogen bombs produce tritium in amounts comparable to or larger than the total inventory of natural tritium on the surface of the earth. The radiocarbon concentration in the atmosphere has been increased noticeably over the past years. Other neutron-induced activities generated by nuclear bombs are relatively small but measurable (52). Finally, the presence of transuranium elements in H-bomb debris has been reported (53).

Fission products.—Our knowledge of the distribution of artificially produced fission products on the surface of the earth is to a large extent based on the work of Libby and co-workers. In particular, Sr^{90} determinations have been carried out at the University of Chicago under the name "Sunshine project" since 1950 (54).

Libby (55) distinguishes three types of fall-out from atomic weapons: (*a*)

TABLE V

Approximate Average Concentrations and Production Rates of Cosmic-Ray Produced Radioactivities

Isotope	$T_{\frac{1}{2}}$	d/m per liter rain	Atoms per cc. rain	$\bar{Q}$: atoms per minute per cm.^{2}		Reference
				Total	Troposphere	
T	12.3y	5 to 100	50,000 to 10^6	100	60	(38)
Be^7	53d	10 to 60	2,000 to 6,000	6.3	1.3	(41, 43)
Be^{10}	2.7×10^6y	in deep sea sediments		3 to 6		(42, 44)
C^{14}	5570y	Spec. mod. carbon activity 14.7 ± 0.5 d/m		150		(46)
Na^{22}	2.6y	$\sim$0.02	$\sim$40			(47)
P^{32}	14.5d	$\sim$1	$\sim$40			(48, 49)
P^{33}	25d	$\sim$0.5	$\sim$30			(49)
S^{35}	87d	$\sim$2	$\sim$400			(50)
Cl^{39}	55 min.	50	2.5			(51)

local fall-out, (b) tropospheric fall-out, and (c) stratospheric fall-out. The local fall-out is mainly caused by settling of large-sized particles and covers considerable areas near test sites. The second type is due to relatively small-sized particles that are not carried into the stratosphere but remain in the atmosphere until they settle out or are brought down by rains. This type of fall-out tends to remain in the same general latitude as the test site, but may circle the earth several times before it is precipitated. Practically all the tropospheric and stratospheric fall-out is brought down by rain (58).

The stratospheric fall-out amounts to about half or more of the total activity produced, depending on firing conditions. Libby finds that the average time this material stays in the stratosphere is of the order of 10 years. Only about 10 per cent of the stratospheric radioactivities descend per year into the tropopause, where they are washed out within a few weeks by rain. A theory of the mechanism of the precipitation of fall-out material by rain has been developed by Greenfield (56). The stratospheric fall-out is the part that produces world-wide effects. It is not well-known yet whether this fall-out is roughly uniform, or whether the downward mixing from the strato-

sphere is much more rapid at high latitudes or along the jet stream belt, as might be expected from meteorologic considerations discussed by Machta (57).

A general consequence of the slow mixing of the atmosphere through the tropopause is a piling up of certain activities produced or introduced in the stratosphere. According to Libby (58) the average concentration of Sr^{90} in stratospheric air per unit of mass is about two orders of magnitude higher than that in tropospheric air. Evidence from T and C^{14} data, and considerations by Benioff (45) regarding Be^7, also indicate such a situation. The slow mixing, however, is unexpected from the point of view of other meteorologic evidence and presents a new and serious meteorologic problem.

In general, no effects of chemical separation of solid fission products can be observed, so that their relative concentrations can be calculated fairly accurately from the respective fission yields and half lives, if the time of origin is known. In turn, observed ratios of amounts of fission products with different half lives allow the calculation of the age of the fall-out sample and the distinction between stratospheric and tropospheric fall-out. For such determinations the measured ratio of Sr^{89} (51d) to Sr^{90} (28y) or that of Ba^{140} (12.8d) to Sr^{90} is frequently used. Libby expects that further measurements of this type will answer the question of whether the relatively high fall-out along a belt between 35° and 55° north latitude is mainly due to tropospheric fall-out from tests conducted in this range of latitude, or to the increased rate of downward mixing from the stratosphere in higher latitude or along the path of the jet stream and the relatively high precipitation in this range of latitude (58). Libby estimates for December 1957 a total world-wide stratospheric fall-out of Sr^{90} of the order of 0.25 d/m per cm.$_6$². For certain latitudes the addition of tropospheric fall-out increases this number. The Sr^{90} fall-out reached maximum values around 45° north of the order of 2.5 d/m per cm.².

The amount of fission products in surface ocean water depends on the amount of fall-out that the particular location has received per unit of surface and on the rate of mixing of the surface ocean water into deeper layers. It is generally assumed that the ocean mixes fast down to the inversion layer, the so-called thermocline, which is at an average depth of about 75 meters. Additional information on the rates of mixing can be expected from further analyses. Sr^{90} determinations have so far given values ranging between 0.01 and 0.3 d/m per liter of sea water (54, 59). The situation in the oceans, however, is complicated by the uptake and enrichment of many elements by marine organisms (52).

Kr^{85} (10.4y) represents a special case among the fission products. As inert gas it remains in the atmosphere. The only data on Kr^{85} in air in the literature are those of de Vries (60) who found that a sample of krypton, collected in March 1955, showed an activity of 25,000 d/m per mole of krypton. This corresponds to about 1.1 d/m per cm.³ of krypton, or 1 d/m per one cubic meter of air. In 1957 the Kr^{85} activity in the atmosphere increased to at least three times this value (61). Nuclear weapons are not the only source of Kr^{85}

released into the atmosphere. It can be assumed that most of the Kr^{85} generated in nuclear reactors finds its way into the atmosphere.

Artificial tritium.—A few days after the Castle tests in Spring, 1954, the amount of tritium in rains in the United States reached levels close to 1000 tritium units. At that time it was possible to measure the tritium concentration in ordinary tap water without electrolytic enrichment. The measurements of Begemann & Libby (38) show that over the following weeks the tritium concentration leveled off corresponding to a decay curve with a period of about 40 days, somewhat longer than the period that would correspond to the residence time of water vapor in the troposphere. Rains in the southern hemisphere and Antarctic snow did not show any marked increase in the tritium concentration. Begemann & Libby (38) assume that most of the tritium produced by an H-bomb remains in the troposphere or is brought back from the stratosphere in the form of relatively large water droplets or more probably ice crystals that settle out much faster than the fine particles containing fission products.

Begemann and Libby estimate that an average of 10^9 tritium atoms (corresponding to 100 d/m of tritium) per cm.^{2} have been deposited on the northern hemisphere as a consequence of the Castle test. No noticeable amount has crossed the equator. At least three more peaks in the tritium concentration of rains have been observed during the past years following the detonation of hydrogen bombs.

This artificial "tagging" of water is being used in the study of ground water inventories, continental water balance, mixing rates, and water circulation patterns (38).

Artificial radiocarbon. In 1956 Libby (55) anticipated an increase in atmospheric C^{14} from neutrons produced in atomic bomb testing. Such increase has now been observed by a number of investigators. Rafter & Fergusson (62) have measured the specific C^{14} activity of CO_2 in surface air of New Zealand, as well as of wood and ocean carbonates. They found an average increase from 1954 until 1957 of about 2.1 per cent per year. A slight indication for an increase before 1954 was present in some results obtained in the Washington Radiocarbon Laboratory (46) from tree ring measurements. Similar results on different materials have been found by de Vries in Holland (63), Munnich in Heidelberg, and Williams in Houston (64). The combined results show that the artificially produced C^{14} has by 1957 increased the C^{14} content of atmospheric CO_2 by about 10 per cent, and hence greatly overcompensated for the effect of the combustion of fossil fuels that since the end of the nineteenth century has led to a steady decrease in the specific C^{14} activity.

LITERATURE CITED

1. Libby, W. F., *Radiocarbon Dating* (University of Chicago Press, Chicago, Ill., 124 pp., 1952)
2. Grosse, A. V., Johnston, W. H., Wolfgang, R. L., and Libby, W. F., *Science*, **113**, 1 (1951)

3. Faltings, V., and Harteck, P., *Z. Naturforsch.*, **5a**, 438 (1950)
4. Kaufman, S., and Libby, W. F., *Phys. Rev.*, **93**, 1337 (1954)
5. Buttlar, H. von, and Libby, W. F., *J. Inorg. & Nuclear Chem.*, **1**, 75 (1955)
6. Anderson, E. C., and Hayes, F. N., *Ann. Rev. Nuclear Sci.*, **6**, 303 (1956)
7. Kohman, T. P., and Saito, N., *Ann. Rev. Nuclear Sci.*, **4**, 401 (1954)
8. Sackett, W. M., Potratz, H., and Goldberg, E., *Science* (In press)
9. Rona, E., Gilpatrick, L. O., and Jeffrey, L. M., *Trans. Am. Geophys. Union*, **37**, 697 (1956)
10. Smales, A. A., and Webster, R. K., *Geochim. et Cosmochim. Acta*, **11**, 139 (1957)
11. Urry, W. D., *Am. J. Sci.*, **240**, 426 (1942); *J. Marine Research (Sears Foundation)*, **7**, 618 (1948)
12. Arrhenius, G., and Goldberg, G., *Tellus*, **7**, 226 (1955); Arrhenius, G., Bramlette, M. N., and Picciotto, E., *Nature*, **180**, 85 (1957)
13. Koczy, F. F., *Rept. Swed. Deep-Sea Expedition*, **10** (2) (In press, 1956)
14. Picciotto, E., and Wilgain, S., *Nature*, **173**, 632 (1954)
15. Goldberg, E., and Koide, M. (Unpublished data)
16. Blifford, I. H., Friedman, H., Lockhart, L. B., and Baus, R. A., *J. Atmospheric and Terrest. Phys.*, **9**, 1 (1956)
17. Von Benndorf, H., and Hess, V., in Müller-Pouillett, *Lehrb. d. Physik*, **5**, 519–662 (F. Vieweg, Braunschweig, Germany, 1928)
18. Israel, H., in *Compendium of Meteorology*, 155 (Malone, T. M., Ed., American Meteorological Society, Boston, Mass., 1334 pp., 1951)
19. Wilkening, M. H., *Nucleonics*, **10**, 6, 36 (1952)
20. Damon, P. E., and Kuroda, P. K., *Trans. Am. Geophys. Union*, **35**, 208 (1954)
21. Simpson, J. A., *Phys. Rev.*, **81**, 639, 895 (1951)
22. Elsasser, W., New, E. P., and Winckler, J. R., *Nature*, **178**, 1226 (1956)
23. Currie, L. A., Libby, W. F., and Wolfgang, R. L., *Phys. Rev.*, **101**, 1557 (1956); Fireman, E. L., *Phys. Rev.*, **97**, 1303 (1955); Soberman, R. K., *Phys. Rev.*, **102**, 1309 (1956)
24. Anderson, E. C., *Ann. Rev. Nuclear Sci.*, **2**, 63 (1953)
25. Harteck, P., *Proc. Nuclear Sci.*, *Meeting* (Houston, Texas, in press, November, 1957)
26. Revelle, R., and Suess, H. E., *Tellus*, **9**, 18 (1957)
27. Arnold, J. R., and Anderson, E. C., *Tellus*, **9**, 28 (1957)
28. Craig, H., *Tellus*, **9**, 1 (1957)
29. Craig, H., *Geochim. et Cosmochim. Acta*, **3**, 53 (1953)
30. Suess, H. E., *Nuclear Processes in Geologic Setting*, 52 (Natl. Research Council, Washington, D. C., 1953); *Science*, **122**, 415 (1955)
31. Hayes, F. N., Anderson, E. C., and Arnold, J. R., *Proc. Intern. Conf. Peaceful Uses Atomic Energy, Geneva*, **14**, 188 (1955)
32. Williams, M. (Private communication)
33. Fergusson, G. J., *Proc. Roy. Soc. (London)*, [A] **243**, 561 (1958)
34. Rafter, T. A., *New Zealand J. Sci. Technol.*, [B] **37**, 20 (1955); **18**, 871 (1957)
35. Broecker, W. S., Ewing, M., Gerard, R., Heezen, B. C., and Kulp, J. L., *J. Deep-Sea Research* (In press)
36. Fergusson, G. J., and Rafter, T. A. (Unpublished data)
37. Craig, H., *Phys. Rev.*, **105**, 1125 (1957); *Natl. Acad. Sci. Natl. Research Council Publ.*, **551**, Chap. 11 (1957)
38. Begemann, F., and Libby, W. F., *Geochim. et Cosmochim. Acta*, **12**, 277 (1957)

39. Harteck, P., and Suess, H. E., *Naturwissenschaften*, **36,** 218 (1949); Suess, H. E.,
    Trans. Am. Geophys. Union, **34,** 343 (1953)
40. Harteck, P., *J. Chem. Phys.*, **22,** 1746 (1954)
41. Arnold, J. R., and Ali Al-Sali, H., *Science*, **121,** 451 (1955)
42. Arnold, J. R., *Science*, **124,** 584 (1956)
43. Thor, R., and Zutshi, P. K., *Tellus*, **10,** 99 (1958)
44. Goel, P. S., Kharkar, D. P., Lal, D., Narsappaya, N., Peters, B., and Yatirajam,
    V., *Deep-Sea Research*, **4,** 202 (1957)
45. Benioff, P. A., *Phys. Rev.*, **104,** 1122 (1956)
46. Suess, H. E., *Science*, **122,** 415 (1955)
47. Marquez, L., Costa, N. L., and Almeida, I. G., *Nuovo cimento*, **6,** 1292 (1957)
48. Marquez, L., and Costa, N. L., *Nuovo cimento*, **2,** 1038 (1955)
49. Lal, D., Narasappaya, N., and Zutshi, P. K., *Nuclear Phys.*, **3,** 69 (1957)
50. Goel, P. S., *Nature*, **178,** 1458 (1956)
51. Winsberg, L., *Geochim. et Cosmochim. Acta*, **9,** 183 (1956)
52. See for example: *Natl. Acad. Sci., Natl. Research Council, Publ.*, **551,** Chap. 11
    (1957)
53. Fields, P. R., *et al.*, *Phys. Rev.*, **102,** 180 (1956)
54. Martell, E. A., "The Chicago Sunshine Method," *Atomic Energy Commission
    Unclassified Report, AECU*-3262 (1956)
55. Libby, W. F., *Science*, **123,** 657 (1956); *Proc. Natl. Acad. Sci. U. S.*, **42,** 365 (1956)
56. Greenfield, S. M., *J. Meteorol.*, **14,** 115 (1957)
57. Machta, L. (Unpublished data); Machta, L., List, R. J., and Hubert, L. F.,
    Science, **124,** 474 (1956)
58. Libby, W. F., *U. S. Atomic Energy Commission Document* (Lausanne address be-
    fore the Swiss Academy of Medical Sciences, March 27, 1958)
59. Sugihara, T. T. (Unpublished data)
60. Vries, H. de, *Appl. Sci. Research* [B], **5,** 387 (1956)
61. Oeschger, H., and Houtermans, F. G. (Personal communications)
62. Rafter, T. A., and Fergusson, G. J., *Science*, **126,** 557 (1957)
63. Vries, H. de, *Science*, **128,** 250 (1958)
64. Personal communications

GEOCHRONOLOGY BY RADIOACTIVE DECAY[1]

By L. T. ALDRICH AND G. W. WETHERILL

Department of Terrestrial Magnetism, Carnegie Institution
of Washington, Washington, D.C.

INTRODUCTION

In 1907 Boltwood (1) published a list of geological ages based on the ratio of lead to uranium in minerals containing uranium and thorium. Although it was not known at the time that thorium also decays into lead, these ages correctly showed that the order of magnitude of geological time was hundreds or thousands of million years. The early work of Boltwood and others had to be constantly re-evaluated in light of subsequent discoveries in nuclear physics, e.g., the discovery of the isotopes of lead and uranium. While the order of magnitude of the time scale remained unchanged it was many years before the problem was sufficiently clarified and the analytical techniques were sufficiently refined so that further contributions to our understanding of earth history could be made. This early historical phase of the work has been reviewed by Knopf *et al.* (2). The measurement of isotopic uranium-lead ages by Aston (3) and Nier (4, 5) was the most significant prewar advance, while the postwar period has seen the extension of the uranium-lead method to common rock-forming minerals and the development of the very important new methods, potassium-argon and rubidium-strontium. Recent reviews of these advances have been given by Kohman & Saito (6), Ahrens (7), Kulp (8), and Wilson, Russell & Farquhar (9), and in the book *Nuclear Geology* (10).

This review will be concerned primarily with developments which have occurred in the few years since these other reviews were written. These developments have been most striking in the fields of potassium-argon and rubidium-strontium dating. Whereas a few years ago these methods were "promising," they have now become the most important methods of mineral age determination. Three years ago, the decay constants of neither K^{40} nor Rb^{87} were known with sufficient accuracy, nor was it known if the common potassium and rubidium minerals would prove to be reliable age indicators. The question of the decay constants is now essentially resolved; and it has been shown that mica, and to a lesser extent feldspar, both common minerals, are usable for the accurate measurement of geological age.

Another important discovery, implicit in older work but clearly brought out by the measurements of Wasserburg & Hayden (11, 12), was that pegmatitic uraninite almost always has concordant U-Pb ages. This fact has greatly simplified the problem of establishing the validity of the K-A and Rb-Sr methods since the uraninite ages have furnished standards for comparison of ages measured by the newer methods.

[1] The survey of literature pertaining to this review was completed in March, 1958.

A discussion is given of discordant uranium-lead ages, a field in which there has been considerable recent work. In contrast to the case of K-A and Rb-Sr, the major problems have not yet been solved, but important measurements bearing on their solution have been made during the last few years. The important and extensive field of the variation in isotopic abundance of lead in lead minerals is not reviewed for reasons of space. Recent literature in this field includes the summary of data compiled by Faul (10) and measurements reported by Geiss (13), Farquhar & Russell (14, 15), and by Vinogradov & Zykov (16). For similar reasons, no discussion of the measurements of the ages of meteorites is included. Readers are referred to the review of Geiss (17) and the publications of Patterson (18), Wasserburg & Hayden (12, 19), Schumacher (20), and Webster, Morgan & Smales (21).

One of the most interesting aspects of this work has been the application of geochronological results to geological problems. This is barely sketched here and will be discussed more fully in a review by Tilton & Davis (2).

DECAY CONSTANTS

For all the decay systems of interest in geochronology except potassium-argon, the age, i.e. the time since the last parent-daughter separation in nature, is given by the relationship

$$t = \frac{1}{\lambda} \ln \left(1 + \frac{D}{P}\right), \qquad\qquad 1.$$

where

$$\lambda = \frac{\ln 2}{\text{half life}} \text{ is the decay constant}$$

and

$$D/P \text{ is the mole ratio of the daughter to the parent nuclide.}$$

From the relationship (Eq. 1) it is seen that an error in the decay constant, or, equivalently, in the half life will cause a proportionate error in the absolute age, while the relative age of two minerals measured by the same decay system will be unaffected by such an error. The establishment of the validity of the various mineral age methods in use has depended upon comparisons of the absolute ages measured by different decay chains, and therefore it has been important to have accurate values for these decay constants. The experimental determination of decay constants will now be discussed.

URANIUM 238

The half life of U^{238} has usually been determined by measurement of the specific alpha activity of natural uranium. Except for a small contribution due to U^{235}, this will be equal to twice the specific activity of U^{238}, because the daughter isotope U^{234} contributes an equal activity. If the source is sufficiently thin so that self-absorption of the α-particles is negligible, the

measurement involves no major difficulties. The sources of errors in absolute α-counting are discussed by Fleming, Ghiorso & Cunningham (23). The results of measurements of the U^{238} half life are listed in Table I. These measurements are in good agreement. Ages in this article are calculated with a U^{238} half life of 4.51×10^9 yr., corresponding to a decay constant of 1.54×10^{-10} yr.$^{-1}$.

TABLE I

MEASUREMENTS OF THE HALF LIFE OF U^{238}

	Specific Activity Natural Uranium (d/min./mg.)*	Specific Activity U^{238} (d/min./mg.)*	Half Life U^{238} (10^9 yr.)
Kovarik & Adams (24)	1501 ± 3		4.50†
Curtis, Stockman & Brown (25)	1501 ± 3		4.50
Kienberger (26)	1502 ± 2		4.50
Kienberger (26)		742.7 ± 1.6	4.49
Kovarik & Adams (27)	1503 ± 3		4.51

* d/min. stands for disintegrations per minute.

URANIUM 235

The measurements of the U^{235} half life are shown in Table II. The measurement of this half life is considerably more difficult than that of U^{238} because of interference from α-particles of U^{238} and U^{234}. This difficulty is reduced by Knight (29) and Fleming, Ghiorso & Cunningham (23) by use

TABLE II

MEASUREMENTS OF THE HALF LIFE OF U^{235}

	Specific Activity Pure U^{235} (d/min./mg.)	Half Life (10^8 yr.)
Clark, Spencer-Palmer & Woodward (28)		7.64*
Knight (29)	4480 ± 140	7.53 ± 0.25
Knight (29)		7.10*
Fleming, Ghiorso & Cunningham (23)	4740 ± 100	7.13 ± 0.16
Sayag (30)		6.82 ± 0.29†
Würger, Meyer & Huber (31)		6.84 ± 0.15

* As recalculated in Fleming et al. (23).
† As recalculated in Würger et al. (31).

of highly enriched sources of U^{235}. Even in these cases, about one-third of the total activity is caused by U^{234}; the U^{235} alpha counts were selected by pulse analysis. In both of these measurements, portions of the same sample

of enriched U^{235} were used, and good agreement was obtained in the measure-
ment of the total specific activity. The difference between these two meas-
urements lies in the pulse height analysis. The data of Knight have been
recalculated by Fleming *et al.*, using the results of their pulse analysis; and
this result is listed separately in Table II.

The other measurements listed in Table II used natural uranium. Clark,
Spencer-Palmer & Woodward (28) reported a half life of 8.91×10^8 yr.
Fleming *et al.* note that these workers were unable to resolve two minor α-
particle groups reported by Ghiorso (32). This error causes their half life to
be too high by about 15 per cent and the half-life value listed in Table II is
the one recalculated by Fleming *et al.* to correct this error.

Sayag (30) and Würger, Meyer & Huber (31) measured the ratios of the
specific activity of U^{235} to that of U^{234}. Then by using previously measured
values of the U^{238} half life, the equilibrium of U^{238} and U^{234}, and the known
abundance of U^{235} in natural uranium, the half life of U^{235} is calculated. A
detailed discussion of this method is given by Würger *et al.* Like Clark,
Spencer-Palmer & Woodward, these workers were unable to resolve the
two minor alpha groups of U^{235}. Würger, Meyer & Huber redetermined the
alpha spectrum and obtained results in agreement with those of Ghiorso.
These data were then used to correct their result for the effect of the neglect
of these alpha groups in the specific activity measurements. They also re-
calculated the data of Sayag, who neglected the minor alpha groups. The
experiment of Fleming, Ghiorso & Cunningham appears to be the most ac-
curate, and their value of the half life $(7.13 \times 10^8$ yr.) is used for the calcula-
tion of ages in this article. This corresponds to a decay constant of 9.71×10^{-10} yr.$^{-1}$. However, the uncertainty in this value is considered to be at
least as great as their quoted error of 2 per cent.

THORIUM 232

Measurements of the Th half life are listed in Table III.

TABLE III
MEASUREMENTS OF THE HALF LIFE OF TH^{232}

	Half Life (10^{10} yr.)
Kovarik & Adams (33)	1.39 ± 0.03
Senftle, Farley & Lazar (34)	1.42 ± 0.07
Picciotto & Wilgain (35)	1.39 ± 0.03

The half life of Th^{232} was determined by direct determination of the spe-
cific alpha activity of natural thorium by Kovarik & Adams (33). In order to
have equilibrium between Th^{232} and Th^{228} (radiothorium), one must use a
source of thorium at least about 50 years old. These workers used the mineral
thorite and assumed that this equilibrium had been established.

Measurements of the ages of minerals have indicated that Pb^{208}/Th^{232} ages are often smaller than uranium-lead ages, even when the two uranium-lead ages are themselves concordant. This fact prompted Senftle, Farley & Lazar (34) and Picciotto & Wilgain (35) to reinvestigate the question of the Th^{232} half life by new methods. By use of a NaI(Tl) scintillation spectrometer, the former authors made an absolute count of the 2.62-Mev gammas from Tl^{208} (ThC'') in equilibrium with parent Th^{232}. Since the thorium series branches at Bi^{212}(ThC), these workers also redetermined the value of this branching ratio and found a value about 7 per cent higher than that reported by Kovarik and Adams. Their Th half-life result can be considered to be in agreement with that of Kovarik and Adams, especially in view of the great difficulty of performing an accurate absolute count of the 2.62-Mev γ-ray; in the presence of the many other gammas. It is also difficult to measure the efficiency of a NaI crystal in this energy region, where the shape of the photopeak is distorted by the effects of pair production.

Picciotto and Wilgain measured the activity of Th^{228} in equilibrium with Th^{232} by counting five-pronged α-stars produced in nuclear emulsions. Their result is in excellent agreement with the other two measurements. Th ages are calculated on the basis of a half life of 1.39×10^{10} yr., which is equivalent to a decay constant of 4.99×10^{-11} yr.$^{-1}$.

POTASSIUM 40

In the case of potassium-argon, there are two decay constants, λ_β giving the rate of β^- decay of K^{40} to Ca^{40} and λ_e giving the rate of electron capture to A^{40}. The age is related to these decay constants by the equation:

$$ t = \frac{1}{\lambda_e + \lambda_\beta} \ln \left(1 + \frac{\lambda_e + \lambda_\beta}{\lambda_e} \frac{A^{40}}{K^{40}} \right). \qquad 2. $$

The error in the age caused by an error in the decay constants is shown in Figure 1. For young minerals, the K-A age is nearly independent of λ_β and varies almost directly with the value of λ_e. For older minerals the sensitivity of the calculated age to errors in λ_β increases while the sensitivity to λ_e decreases. At $t = 3000$ million yr. a 10 per cent error in either λ_e or λ_β will cause about a 5 per cent error in the calculated age.

The decay scheme of K^{40} is shown in Figure 2. The validity of this decay scheme has been reviewed by Morrison (36). The decay scheme is well-established and the only serious uncertainty is the importance of electron capture directly to the ground state of A^{40}. Although this mode of decay has not been observed, the upper limits given for its abundance are not as low as might be desired. Since the possibility of this mode of decay is of considerable importance to K-A dating, the evidence against it will be considered in some detail.

If the upper limit for the ratio of β^+ to β^- activity given by Bell & Cassidy (37) ($< 2 \times 10^{-5}$) is combined with theoretical values for the positron-
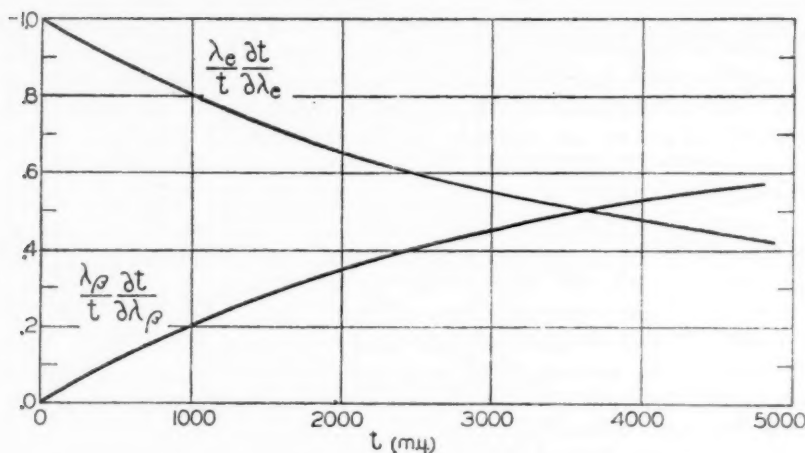
FIG. 1. Curves showing the relative sensitivity of the measured age t (in millions of years) to changes in the decay constants λ_e and λ_β.
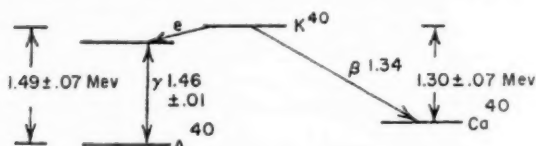
FIG. 2. Potassium 40 decay scheme.

to-electron capture ratio given by Fireman (38), it can be calculated that less than 10 per cent of the electron capture is directly to the ground state. However, as pointed out by Morrison, it is not possible to see how Bell and Cassidy's limit was obtained from their published data. If this measurement is disregarded, the next best limit for this quantity is $<6\times10^{-4}$ set by Colgate (39). This limit is too high to be useful, since it is known from x-ray counting [Sawyer & Wiedenbeck (40)] and from geochronological measurements that not more than about 30 per cent of the electron-capture transitions could go directly to the ground state.

Another estimate of the importance of this direct transition can be made theoretically. The comparative half life for allowed K-capture transitions is given by

$$f(Z, W)t = \tfrac{1}{2}\pi(n_K\psi_K{}^2 W_K{}^2 + n_{L_I}\psi_{L_I}{}^2 W_{L_I}{}^2 + \cdots)t, \qquad 3.$$

where n is the number of electrons in the shell, ψ_K and ψ_{L_I} are the large components of the Dirac wavefunctions in the K and L_I shells, and W_K and W_{L_I} are the respective transition energies.

For

$$4 \leq Z \lesssim 60, \qquad n_K = n_{L_I} = 2, \quad \text{and} \quad W_K \approx W_{L_I};$$

so

$$f(Z, W)t = \frac{1}{2}\pi\psi_K{}^2 \left(1 + \frac{\psi L_1{}^2}{\psi_K{}^2}\right) W_K{}^2 t. \qquad 4.$$

ψ_K can be calculated from the expression given by Major & Biedenharn (41)

$$\log \psi_K{}^2 = (7.9776 - 10) + 0.03256Z - 10^{(0.45775-0.0380236Z)} \qquad 5.$$

and the ratio $\psi_{L_1}{}^2/\psi_K{}^2$ can be estimated from the data of Rose & Jackson (42). By substitution into Equation 4, it is found that

$$\log t = \log (ft) + 0.59.$$

The quantity $\log (ft)$ depends on nuclear matrix elements and on numerical and universal constants. As discussed by Morrison (36), it is reasonable to suppose that the matrix element for the β^- transition from A^{40} to the ground state of Ca^{40} will be nearly the same as that for the transition from K^{40} to the ground state of A^{40}. Then from the value $\log (ft) = 18.46$ for the β^- transition given by Davidson (43), the partial half life for electron capture directly to the ground state of A^{40} is found to be about 3×10^{11} yr. This implies that about 3 per cent of the electron-capture decays go directly to the ground state.

The principal difficulty with this calculation is that for both β^- decay and electron capture the expressions for (ft) appropriate to allowed transitions have been used. It is known that the proper f factor for forbidden transitions is frequently very different; in particular, for $K^{40}\beta^-$ decay, Davidson calculates $\log (f_3 t) = 15.60$ as compared with the allowed value of 18.46. In this connection, Hoff & Rasmussen (44) have shown that, for unique ($\Delta I = 2$, yes) first-forbidden electron capture transitions, ft values calculated using allowed f functions can be compared directly with ft values for similar transitions involving β-particle emission. The error introduced by making this comparison for third-forbidden transitions, as has been done here, has not yet been evaluated. As is evident from the foregoing discussion, there is still considerable uncertainty with regard to the importance of electron capture directly to the ground state. Ages will be calculated with the assumption that there are no such transitions, but definitive evidence justifying the assumption is lacking. Laboratory measurements of the specific beta, gamma, and electron-capture rates are shown in Table IV.

According to the decay scheme (Fig. 2) and if electron capture to the ground state is neglected, the specific gamma activity is equal to the rate of electron capture. Since it can be measured more accurately than the latter quantity, the specific gamma activity is usually used to determine λ_e in Equation 2. In order to measure the specific gamma activity, it is necessary to determine the absolute rate of emission of 1.46-Mev γ-rays from a known quantity of potassium. The principal difficulty in this experiment has been in determining the efficiency of the counting apparatus for γ-rays of this energy, as has been discussed in an earlier publication (62). Briefly, the difficulty is that there are no suitable γ-ray standards in this energy range

TABLE IV

DETERMINATIONS OF THE SPECIFIC GAMMA AND BETA
ACTIVITY OF NATURAL POTASSIUM

Investigators	Activity	
	γ/gm. sec.	β/gm. sec.
Gleditsch & Graf (45)	3.6 ±0.8	
Graf (46)		26.8±1.2
Ahrens & Evans (47)	3.42±0.07*	
Hess & Roll (48)	2.6	
Stout (49)		30.6±2.0
Sawyer & Wiedenbeck (50)	2.88±0.3†	
Spiers (51)	2.97	30.5
Faust (52)	3.6 ±0.4	31.2±3.0
Graf (53)	3.4 ±0.5	
Houtermans, Haxel & Heintze (54)	3.1 ±0.3	27.1±1.5
Smaller, May & Freedman (55)		22.5±0.7
Sawyer & Wiedenbeck (40)		28.3±1.0
Good (56)		27.1±0.6
Delaney (57)		32.0±3
Burch (58)	3.37±0.09	
Suttle & Libby (59)	2.96±0.3	29.6±0.7
Backenstoss & Goebel (60)	3.50±0.14	
McNair, Glover & Wilson (61)‡	3.33±0.15	
Wetherill (62)	3.39±0.12	

* Recalculated using $E_\gamma = 1.46$ Mev.

† Recalculated using $\lambda_\gamma/\lambda_\beta = 0.20$ for K^{42}.

‡ Recalculated using their $\lambda_e/\lambda_\beta = 0.121$ and their specific beta activity of 27.5/gm. sec.

which have a simple decay scheme consisting of a relatively energetic beta followed by a single gamma.

This makes it very hard to determine the efficiency of a Geiger counter or ionization chamber because these detectors do not distinguish between the several γ-rays of different energies emitted in a complex decay scheme. The last two measurements of the gamma activity in Table IV circumvented this difficulty by the use of NaI(Tl) scintillation spectrometers. Although these results are in good agreement, this agreement may not be very significant because the experiment of McNair, Glover & Wilson (61) was designed to measure the branching ratio λ_e/λ_β and their value of the gamma activity is dependent on the accuracy of their measurement of λ_β.

Potassium-argon ages in this article will be calculated on the basis of a specific gamma activity of 3.4 γ/gm. sec. which is believed to be within 5 per cent of the true value of this quantity. This corresponds to a value of the partial electron capture decay constant of 5.85×10^{-11} yr.$^{-1}$.

Determinations of the absolute beta activity are also tabulated in Table IV. Problems of self-absorption may be expected to be somewhat alleviated because of the relatively high maximum energy (1.34 Mev) and because the shape of the spectrum is roughly the usual one (63). However, the low specific activity necessitates the use of a thick source in order to obtain an appreciable counting rate. Thin sources, together with high counting rates, have been obtained with sources enriched in K^{40} (40). Unfortunately, the exact isotopic abundance of the potassium was not measured and, therefore, these results are not more accurate than those obtained by the use of natural potassium. By combining 4π counting with enriched thin sources of known isotopic composition, it should be possible to make a definitive measurement of the specific beta activity.

Ages in this article are computed on the basis of a specific beta activity of 27.6 β/gm. sec. corresponding to a partial β^- decay constant of 4.72×10^{-10} yr.$^{-1}$. As shown in Figure 1, the accuracy of the age of a mineral is not very dependent on the accuracy of this constant.

RUBIDIUM 87

Measured values of the Rb^{87} half life are shown in Table V. Measurement of the absolute specific activity of Rb^{87} is very difficult because of the unusually large number of very-low-energy β-particles in the spectrum of this isotope (66, 67, 68). Although the maximum energy is 275 kev, the average energy is only about 45 kev. Because of the very high absorption of these

TABLE V

MEASUREMENTS OF THE HALF LIFE OF Rb^{87}

	Specific Activity d/min./mg.	Half Life* 10^{10} yr.
Haxel, Houtermans, & Kemmerich (64)	43.5	5.95
Kemmerich† (65)	63.1	4.10 ± .4
Curran, Dixon & Wilson (66)	40.4	6.41 ± .3
MacGregor & Wiedenbeck (67)	40.6	6.37 ± .3
Lewis (68)	43.7	5.93 ± .3
Geese-Bähnisch & Huster (69)	60.1	4.30 ± .3
Flinta & Eklund (70)	42.2	6.1 ± .1
Huster & Rausch‡		4.95
Libby (71)	52.9 ± .2	4.88 ± .2
Flynn & Glendenin (1958)§		4.85 ± .2

* The half lives have been calculated from the observed counting rates. In some cases these differ slightly from the values calculated by the authors.

† Half life recalculated on basis of correct decay scheme.

‡ Private communication, 1956.

§ Private communication, 1958.

soft β-particles in the source, the exact shape of the spectrum in this low-energy region is unknown. Many of the earlier determinations did not deal properly with the problem of counting all of the low-energy electrons.

Progress in the determination of the Rb[87] specific activity has depended on minimizing self-absorption and on the use of 4π counters so as to eliminate the necessity of complex corrections for back-scattering. Considerable progress in this direction has been made by Huster, Geese-Bähnisch & Rausch [(69); private communication, 1956]. The most recent result of these workers is 4.95×10^{10} yr. obtained with the use of conducting sources of only 10 μgm. cm.$^{-2}$ thickness. However, by using absorbers and plotting to zero absorber thickness, Huster (private communication, 1957) finds a half life of 4.6×10^{10} yr., in disagreement with the value obtained with very thin sources. For this reason, he feels there may still be an unknown source of error in his earlier measurement.

More recently, Flynn & Glendenin (private communication, 1958) have counted the specific activity of natural rubidium by dissolving an organic salt in a liquid scintillator, and have obtained a preliminary half life of 4.85 $\times 10^{10}$ yr. Their extrapolation to zero pulse height amounts to 5 to 10 per cent of their total counting rate, which compares favorably with the best results of Huster, Geese-Bähnisch, and Rausch. Flynn and Glendenin are presently studying closely the rseponse of their liquid scintillator to electrons of a few kilovolts energy, in order to permit a more accurate measurement of the half life.

The recent measurement of Libby (71) makes use of a thick-source technique designed for routine measurements. The relationship between the absolute activity of the sample and the observed counting rate has not been thoroughly investigated for the case of such an unusual beta-spectrum as that of Rb[87].

The ages reported in this paper are calculated on the basis of a decay constant of 1.39×10^{-11} yr.$^{-1}$ corresponding to a half life of 50×10^9 yr. This value is near to that of Huster and Rausch was found by a comparison of Rb-Sr ages with concordant U-Pb ages of uraninites (72).

ANALYTICAL TECHNIQUES

The methods by which microgram quantities of the elements used in measurements of radioactive ages are determined have all been discussed (73 to 76, 144, 145). It is sufficient here to say that the elements U, Th, Pb, Rb, Sr, K, and A can be determined with a precision of 5 per cent or less in all the minerals which have been found to be interesting for these studies. Interlaboratory comparisons of determinations of K, A, Rb, and Sr from the same mineral (77, 21, 123) are encouraging in their degree of conformity, despite the different approaches used in the determinations. The differences which have been found (78) are difficult to interpret since the analyses have not been done on splits of the same mineral. With sufficient attention to details, the errors could readily be reduced to the point where errors attribut-

able to analytical techniques could be resolved with much greater certainty from variations in the ages caused by geological factors.

THE NATURE OF THE AGREEMENT OF MINERAL AGES

This section contains primarily the measurements of ages obtained on minerals which, by their occurrence in the same rocks, are assumed to be cogenetic or which contain two long-lived parent isotopes, thus permitting the measurement of two independent ages of the mineral. This approach is taken because of the variations which have been found in the ages of minerals for which two independent ages have been obtained. It seems, as a result of such measurements, that it is not too conservative to consider the agreement of at least two independent ages necessary for the establishment of the absolute age of a rock. In talking about the agreement of such ages, one must present all of the data available and, therefore, the disagreements form an equally important part of the discussions.

It is actually possible to determine the age of a rock by a number of independent methods. For example, all uranium minerals may, in principle, be measured by two independent decay chains. Because of the chemical similarity of Rb and K, K minerals usually contain Rb; therefore, the ages of these minerals may also, in principle, be measured by two independent methods. Many rocks contain uranium, thorium, and potassium minerals so that, for these, five independent ages may be measured. This section will discuss comparisons of mineral ages in the following order: (*a*) U-Pb and Th-Pb ages of uraninites; (*b*) comparison of ages from cogenetic uraninites and mica; (*c*) K-A and Rb-Sr ages of micas; (*d*) K-A ages of feldspars; (*e*) U-Pb and Th-Pb ages of minerals other than uraninite; (*f*) comparison of uranium-lead and uranium-helium ages; (*g*) comparison of rubidium-strontium and uranium-radiation-damage ages; and (*h*) dating of sedimentary rocks.

U-Pb AND Th-Pb AGES OF URANINITES

Figure 3 is a histogram showing the distribution of the ratio of the U^{238}-Pb^{206} age to the U^{235}-Pb^{207} age for all measurements on uranium minerals reported by Faul (10) or which have been published since then. For localities from which different minerals have been analyzed, each mineral is plotted independently to establish the reliability of ages from different uranium minerals. For those localities where many measurements of the same mineral (such as Lake Athabaska and the Witwatersrand) have been made, the one with the most concordant U-Pb ages has been chosen arbitrarily to represent that location so that the histogram would not be improperly weighted by a single geologic location. The U^{238}-Pb^{206} and U^{235}-Pb^{207} ages have been picked because they are directly calculated from the mole ratio of daughter to parent isotope as is true in the case of K-A and Rb-Sr ages. It must be pointed out (and it will be discussed more fully in the section on Discordant Uranium-Lead Ages) that the differences in these two ages must
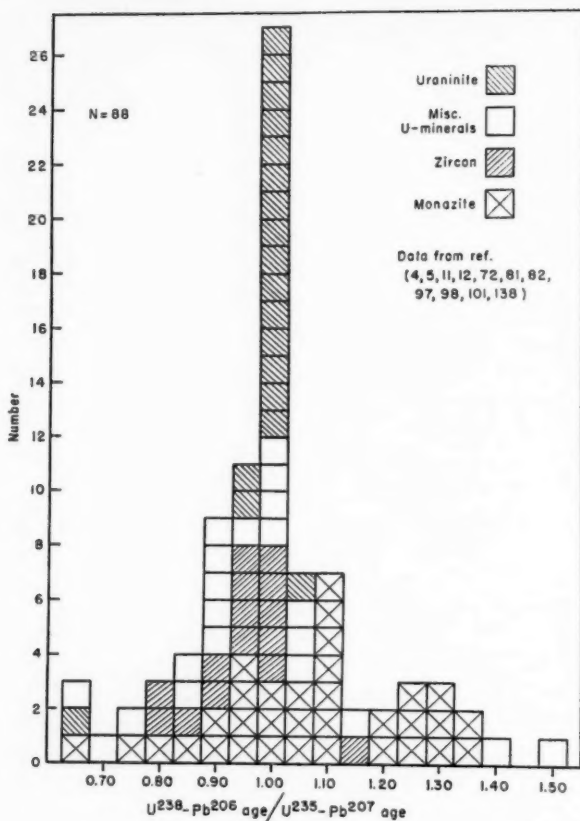
FIG. 3. Histogram of the ratio of U^{238}-Pb^{206} age to the U^{235}-Pb^{207} age for a number of uranium minerals.

be less than 3 per cent if either is necessarily to be considered close to the true age of the mineral. If the Pb-Pb age[2] of the mineral had been used instead of the U^{235}-Pb^{207} age in the ratio given as the abscissa, the variation in Figure 3 would have been greatly increased.

From Figure 3, it is apparent that the spread in the U-Pb ages is so large that for any mineral but uraninite it is optimistic to use a single

[2] The Pb-Pb age, derived from the equations for two U-Pb ages, is the solution for t of the equation

$$\frac{Pb^{207}}{Pb^{206}} = \frac{U^{235}}{U^{238}} \frac{(e^{\lambda_{235}t} - 1)}{(e^{\lambda_{238}t} - 1)}.$$

It has been shown by Nier (4) that this age is affected less than the other two U-Pb ages by losses of parent or daughter element in the mineral.

U-Pb age as a measure of the absolute age of the mineral. Carefully selected samples of pegmatitic uraninite seem to give uniformly concordant U-Pb ages (11, 12, 72). Table VI gives the U-Pb and Th-Pb ages of uraninites. It is seen that only two measurements lie outside 1.00 ± 0.05 for the ratio of the U^{238}-Pb^{206} age to the U^{235}-Pb^{207} age. No other uranium mineral provides such uniformly concordant ages. Without the uraninite data, the distribution of U-Pb ages would discourage anyone attempting to find the absolute age of a uranium mineral. Since uraninite is not a common rock-forming

TABLE VI

U-Pb and Th-Pb Ages of Uraninites

Location	Ages in Millions of Years			Ref.
	U^{238}-Pb^{206}	U^{235}-Pb^{207}	Th^{232}-Pb^{208}	
Cooke City, Montana	2600	2640		(79)
Huron Claim, Manitoba	1860	2170	1360	(80)
Viking Lake, Saskatchewan (Sample 1)	1850	1880	1670	(11)
Viking Lake, Saskatchewan (Sample 2)	1790	1830	1640	(72)
Ingersoll Mine, S. Dakota	1580	1600	1440	(74)
Wilberforce, Ontario	1040	1050	1010	(72)
Cardiff Mine, Ontario	1020	1020		(72)
Cardiff Township, Ontario	1000	1020	870	(11)
Gordonia, S. Africa	1010	1015	1215	(81)
Parry Sound, Ontario	994	993	897	(11)
Gaya District, India	885	910	1005	(82)
Romteland, Norway	890	892	900	(80)
Lac la Ronge, Manitoba	565	868		(80)
Biundni, India	735	735	935	(82)
Morogoro, Tanganyika Terr.	608	607		(81)
Bemasoandro, Madagascar	390	410	465	(81)
Chestnut Flat, N. Carolina	375	380		(72)
Branchville, Conn.	367	365	318	(12)
Portland, Conn.	268	266	239	(11)

mineral, the chief value of its concordant ages is in testing other methods of determining radioactive ages. The Th-Pb age of uraninite is often less than either of the U-Pb ages, so that there exist, even for this mineral, unexplained discrepancies in the ages obtained. It should be noted, however, that the determination of Pb^{208} usually involves a correction for nonradiogenic Pb^{208} which amounts to about 10 per cent of the total. Further, this correction is based on the presence of an ion current attributed to Pb^{204} which is of the order of one part in 20,000 of the neighboring Pb^{206} ion current. The problem of properly evaluating the correction to the Pb^{208} is therefore

not inconsiderable and may account at least in part for the Th-Pb discrepancies in uraninites.

COMPARISON OF AGES FROM COGENETIC URANINITES AND MICA

The uniform concordance of the U-Pb ages of uraninites gives confidence of the reliable nature of such ages. Here uraninite ages will be used as standards by which K-A and Rb-Sr ages can be tested. Table VII gives the data on the comparisons which have been made. The excellence of the agreement of all ages gives one confidence that agreement of the K-A and Rb-Sr ages is another reliable criterion of the age of the pegmatite from which the mica is collected.

TABLE VII

COMPARISONS OF U-PB AGES OF URANINITES WITH K-A AND RB-SR AGES OF COGENETIC MICA. DECAY CONSTANTS USED: $\lambda_\beta(RB^{87}) = 1.39 \times 10^{-11}$ yr.$^{-1}$, $\lambda_\beta(K^{40}) = 4.72 \times 10^{-10}$ yr.$^{-1}$ AND $\lambda_e = 0.585 \times 10^{-10}$ yr.$^{-1}$

Location	Ages in Millions of Years			Ref.
	U-Pb	Rb-Sr	K-A	
Cooke City, Montana	2620	2750	2500	(79)
Viking Lake, Saskatchewan	1870	1970	1780	(72, 83)
Keystone, S. Dakota	1600	1650	1380	(74)
Wilberforce, Ontario	1050	1000	920	(72, 83)
Cardiff Mine, Ontario	1020	1030	960	(72, 83)
Parry Sound, Ontario	994		940	(11)
Spruce Pine, N. Carolina	375	375	335	(72, 83)
Branchville, Connecticut	366		369	(12)
Portland, Connecticut	267	258	269	(11, 84)

COMPARISON OF RB-SR AND K-A AGES OF MICAS

That the agreement of Rb-Sr and K-A ages of micas is not unusual and is frequent in the fine-grained granites, as well as the coarse-grained pegmatites, is shown in Figure 4. If the metamorphic rocks are excluded, the two ages agree with each other within 10 per cent for over 80 per cent of the micas. Since the daughter elements are quite different for these two methods, agreement of the ages is considered a strong indication that these rocks satisfy the assumption that the mica has formed a closed system since it was formed. The shape of the distribution can be most simply understood by assuming the Rb-Sr ages to be more nearly correct and the K-A ages to be affected occasionally by varying amounts of argon leakage. With so many variables available, this is but one of many possible explanations. That this assumption is not completely without empirical foundation is shown in Table VIII, which gives the comparison of the Rb-Sr ages of feldspar and
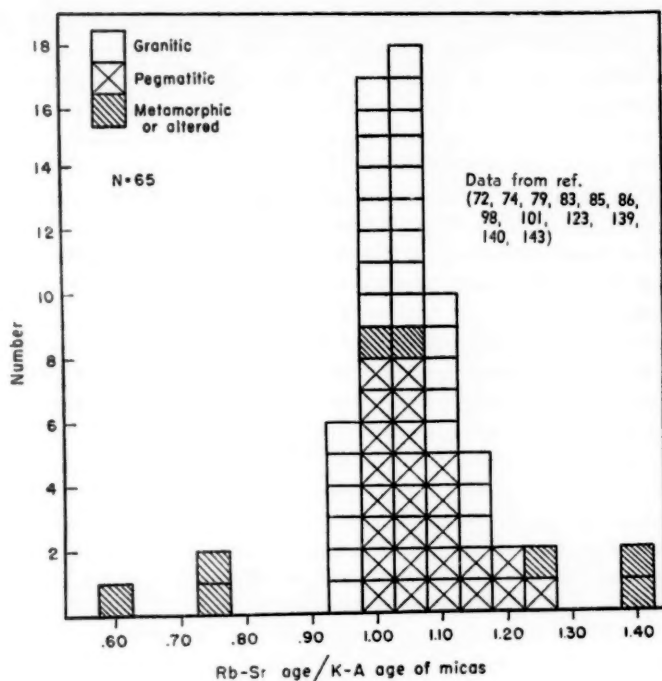
FIG. 4. Histogram of the ratio of the Rb-Sr age to the K-A age for micas from a number of rocks.

TABLE VIII

RB-SR AGES OF FELDSPAR AND MICA FROM THE SAME ROCK

Location	Ages in Millions of Years		Ref.
	Feldspar	Mica	
Christmas Lake, Wyoming	2770	2800	(79)
Quad Creek, Wyoming	2730	2530	(79)
Catlin Creek, W. Australia	2740	2810	(85)
Londonderry, W. Australia	3080	2780	(85)
Grosmont, W. Australia	2890	2840	(85)
Wodgina, W. Australia	2860	2970	(85)
Keystone, S. Dakota	1600	1650	(74)
Brown Derby Mine, Colorado	1290	1390	(75)
Quartz Creek Granite, Colorado	1490	1320	(75)
Cutler Batholith (Peg.), Ontario	1760	1750	(86)
Copper Cliff "Rhyolite," Ontario	2360	1730	(86)

mica from 11 rocks. The agreement is within 10 per cent for all but the Copper Cliff rhyolite, which is definitely a metamorphic rock. The Rb-Sr age of this feldspar may be a remnant of the early history of this rock. The general agreement of the Rb-Sr ages of the two minerals is empirical evidence for the conclusion that this age is independent of mineral type. Also, a study (75) was made of several micas from the same pegmatite whose Rb concentration showed a range of a factor of three. For these micas, the ratio Sr^{87}/Rb^{87} had an extreme displacement of less than 10 per cent from the mean, and a mean deviation of 5 per cent. This indicates that the ratios Sr^{87}/Rb^{87} might be expected to be characteristic of the rock unless otherwise demonstrated.

In measurements of the Rb-Sr age of minerals low in Rb, the correction for the common Sr becomes very important. It is customary to use the Sr^{88} as a measure of the normal Sr^{87} present. The validity of this assumption was demonstrated by Gast (87) and confirmed by Gerling & Suhokoliukov (88). They show that the variation in the Sr^{87}/Sr^{88} ratio has been at most 2 per cent in the life of the oldest terrestrial rocks. This variation is to be compared with a change of 20 to 30 per cent in the Pb^{206} and Pb^{208} isotopic abundances in lead minerals, which is attributable to additions of lead from the uranium and thorium decay in the same time. Thus correction for common strontium is relatively straightforward.

Included in the data of the histogram of Figure 4 are the data of Table IX which shows ages obtained on several rocks in the Lake Huron district of Ontario (86). This small group of metamorphic rocks was collected from an area included in a circle of radius less than 50 miles, centered just west of Sudbury. The complexity of the relationships of the ages in Table IX and the spread between the K-A and Rb-Sr ages shown in the histogram demon-

TABLE IX

RB-SR AND K-A AGES OF ROCKS FROM THE REGION OF
SUDBURY, ONTARIO

Rock	Mineral	Ages in Millions of Years	
		Rb-Sr Age	K-A Age
Wavy Lake Granite	Biotite	1075	1025
Cutler Batholith			
Granite	Biotite	1325	1330
Pegmatite 1	Muscovite	1750	1390
Pegmatite 2	Muscovite	1700	1370
Copper Cliff Rhyolite	Muscovite	1730	1350
	Biotite	1220	2070
Sudbury Gabbro	Biotite	1325	1770
Sudbury Breccia (Matrix)	Biotite	1440	1770

strate the need for measuring both ages. Work in progress indicates that this complexity will not be unusual in metamorphic rocks. Some of the age values probably reflect the history of the rocks prior to their most recent crystallization.

K-A AGES OF FELDSPARS

In addition to the data above, other measurements bearing on the K-A ages have been made. The early work on this method was an attempt to find the electron capture decay constant of K^{40} from the ratio A^{40}/K^{40} of the feldspar and the U-Pb age of the cogenetic uraninite as shown above for mica. The data obtained largely by Wasserburg, Hayden & Jensen (11, 12) are given in Table X, where the K-A age of the feldspar is calculated with the use of the decay constant obtained in the laboratory measurements discussed in the section on Decay Constants (K^{40}). Tabulated with the age is

TABLE X

URANINITE-FELDSPAR COMPARISONS

Location	Ages in Millions of Years		Per Cent A^{40} Retentivity	Ref.
	U-Pb Age	K-A Age		
Portland, Connecticut	267	210	77	(12)
Branchville, Connecticut	367	273	75	(12)
Parry Sound, Ontario, Microcline I	994	815	78	(11)
Parry Sound, Ontario, Microcline II	994	760	72	(11)
Parry Sound, Ontario, Albite	994	658	60	(11)
Cardiff Township, Ontario I	1010	860	81	(11)
Cardiff Township, Ontario II	1010	810	76	(11)
Wilberforce, Ontario	1030	840	77	(90)
Keystone, S. Dakota	1600	1100	59	(90)
Viking Lake, Saskatchewan	1890	1630	79	(11)

the per cent of argon retained in the feldspar, calculated from the K present and from the U-Pb age. The average retentivity is 0.73 with a mean deviation of 0.06. The feldspar data could also be explained without the assumption of argon loss if the value of λ_e for K^{40} were lowered by about 25 per cent. The histogram in Figure 5 shows the ratio of the ratio, A^{40}/K^{40}, for mica, to that for feldspar from the same rock, for all samples reported in the literature. From comparisons of K-A ages of mica with U-Pb ages of uraninite and Rb-Sr ages of the mica itself, it is believed that the K-A age of the mica approximates the true age of the rock. The wide variability in the ratio of A^{40}/K^{40} of the mica to A^{40}/K^{40} of the feldspar indicates the uncertainty in the feldspar K-A ages. A plot of the ratio A^{40}/K^{40} as a function of the age
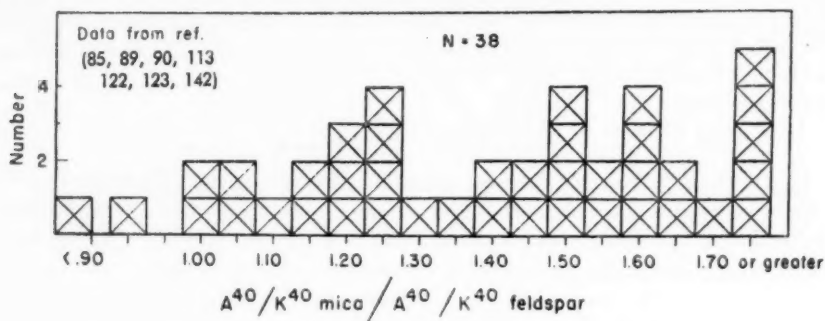
FIG. 5. Histogram of the ratio of the ratio A^{40}/K^{40}, of mica to that of feldspar from the same rock.

of the rock shows that the variability found does not depend in a pronounced way on the age.

Reynolds (89) has studied the retentivity of argon by mica and feldspar when these minerals are heated and finds that his experiments would predict the mica-feldspar discrepancy observed if heating were the cause. Gerling & Morozova (91) have measured the activation energy of micas for argon retention and conclude from their data that micas should be suitable for age measurements. Gentner *et al.* (92, 93, 94) and Curtis & Reynolds (95) have considered diffusion as the possible source of the apparent argon loss from sylvite. Gentner bases his argument in part on the diffusion of helium in sylvite, and Reynolds differs as to the relevance of this experiment to the explanation of argon loss because of the greatly differing size of the helium and argon atoms. Reynolds also concludes that diffusion of A^{40} in KCl should be much slower than that of K in KCl.

The assumption that no primary argon is included in mica has been tested in one instance by Damon & Kulp (96) who find 10^{-6} cc. NTP or less of argon per gram in a calcium mica, margarite. This is to be compared with $\sim 10^{-5}$ cc./gm. of radiogenic A^{40} in a 100-million-year old potassium mica. From the mica-feldspar differences and the relationship of the Rb-Sr and K-A ages of micas, it seems evident that variable argon leakage is the most probable explanation of all the empirical data available.

U-Pb and Th-Pb Ages of Minerals Other Than Uraninite

In addition to uraninite, the only minerals containing U and Th which have been studied in sufficient number to permit tentative conclusions regarding the reliability of their ages are monazite and zircon. The results of measurements on monazite have been discussed by Tilton & Nicolaysen (97) and Vinogradov (98). Those given by Tilton are typical and are shown along with the available K-A and Rb-Sr ages of presumably cogenetic micas in Table XI. From this table it is seen that even for monazite the Th-Pb age is often unreliable. If one were to pick a single one of the monazite age de-

termination methods as being most reliable, it would be the Pb-Pb age, but even this is an unsatisfactory generalization. Acid leaching studies by Tilton & Nicolaysen (97, 99) on the three monazites studied gave some evidence which suggested that leaching could account for some of the discrepancies observed. There seems to be no correlation of the age pattern found with microscopic appearance or x-ray pattern of the mineral. When the monazite ages are concordant, it is seen that the Rb-Sr age and, to a lesser extent, the K-A age agree with the concordant U-Pb and Th-Pb ages.

TABLE XI

COMPARISON OF U-PB AND TH-PB AGES OF MONAZITE AND RB-SR
AND K-A AGES OF COGENETIC MICA

Monazite	Ages in Millions of Years					
	U^{238}-Pb^{206}	U^{235}-Pb^{207}	Pb^{207}-Pb^{206}	Th^{232}-Pb^{208}	Rb-Sr	K-A
Ebonite Claims, Southern Rhodesia, (146)	2620	2620	2620	2640	2650	2310
Jack Tin Claims, Southern Rhodesia, (146)	2210	2460	2660	1940		
Irumi Hills, Northern Rhodesia, (146)	1990	2330	2640	1380		
Antsirabe, Madagascar, (81)	1370	1850	2450	610		
Yadiur, India, (82)	1410	1820	2330	1800		
Soniana, India, (82)	635	697	913	611		
Huron Claim, Manitoba, (5)	3180	2840	2600	1830	2650	2160
Las Vegas, New Mexico, (5)	1730	1560	1340	770	1490	1280
Goodhouse, S. Africa, (92)	930	915	880 ±60	900	960	920
Houtenbeck, S. Africa, (92)	1400	1230	930 ±50	940		
Steenkamps Kraal, S. Africa, (97)	1080			990		
Brown Derby, Colorado, (97)	1590	1420	1170	995	1410	1300

Another mineral which has been studied in considerable detail is zircon. The suggestion by Larsen, Keevil & Harrison (100) that the amount of uranium in these minerals should make them suitable for age determination, the fact of their occurrence in common rocks, and the subsequent efforts of Larsen and his colleagues to provide a simple method for this determination, have all served as an impetus for this work. Tilton *et al.* (101) present complete data on all zircons for which U, Th, and Pb concentrations, and the isotopic composition of the lead, have been published. Table XII gives the U-Pb and Th-Pb ages of these zircons for which K-A and Rb-Sr ages are available. As in the case of the uraninites, it is seen that when the U-Pb ages agree, they also agree with the K-A and Rb-Sr ages of the associated mica. When the U-Pb ages are discordant, the Pb^{207}–Pb^{206} age most nearly agrees with the mica age. Again, the Th^{232}-Pb^{208} age is so often discordant that it is the least reliable method of measuring ages by radioactive decay. No criterion has been found, such as natural grain size, common lead contamina-

TABLE XII

U-Pb and Th-Pb Ages of Zircons Compared with Rb-Sr and K-A Ages of Cogenetic Mica (101)

Sample	Ages in Millions of Years					
	U^{238}-Pb^{206}	U^{235}-Pb^{207}	Pb^{207}-Pb^{206}	Th^{232}-Pb^{208}	Rb^{87}-Sr^{87}	K^{40}-A^{40}
Redstone, N. H. Granite	187 ± 5	184 ± 5	140 ± 60	190 ± 5	185	168
Wichita Mts., Okla. Sample "A" pegmatite	520 ± 12	527 ± 10	550 ± 30	506 ± 12	510	460
Capetown, S. Africa Granite	330 ± 10	356 ± 15	530 ± 50	238 ± 20	600	505
Tory Hill, Ontario Syenite	940 ± 25	960 ± 15	1015 ± 25		990	890
Cardiff Uranium Mine Ontario, Pegmatite	900 ± 25	930 ± 15	1000 ± 25	990 ± 50	1030	960
Pike's Peak, Colo. Granite	624 ± 25	707 ± 20	980 ± 40	313 ± 12	1020	980
Llano, Texas Granite	950 ± 25	990 ± 15	1070 ± 25	890 ± 40	1100	1060
Bagdad, Arizona Granite	630 ± 20	770 ± 30	1210 ± 80	271 ± 16	1390	1360
Quartz Creek, Colo. Granite "A"	925 ± 25	1130 ± 25	1540 ± 140	530 ± 110		
Quartz Creek, Colo. Granite "B"			1700 ± 60		1310	1280

tion, or mineral processing, which correlates completely with the age pattern observed.

The Pb-α method of determining ages of zircons was first discussed by Larsen *et al.* (100, 102) and consists of an attempt to measure the Pb/(U+Th) ratio by α-counting of U+Th and spectrochemical methods for the determination of Pb. It is apparent that the Pb-α method, which measures essentially the U^{238}-Pb^{206} age, even if done accurately, would provide the least reliable U-Pb age.

RELIABILITY OF U-HE⁴ METHOD

Since the review by Hurley (10), the only published data are those of Damon & Kulp (103). This study of the He⁴ content of minerals by the method of isotope dilution indicated larger amounts of He than had been measured by volumetric techniques. It would appear that these new techniques should be applied to a number of samples of known age before complete distrust of the U-He⁴ age method becomes too general.

COMPARISON OF AGES DETERMINED BY RB-SR AND U-RADIATION DAMAGE

Most of the radiation damage measurements have been compared to the Pb-α measurements on the same zircon (104). Recently, Fairbairn & Hurley (105) showed that there was almost no relationship between Rb-Sr age of a mica and the age determined from the radiation damage and alpha activity of zircon from the same rock. It is possible that even though this method does not provide other than minimum age, it may be related to the subsequent history of the rock in some as yet undetermined way.

DATING OF SEDIMENTARY ROCKS

This section ends with the discussion of the interesting data on authigenic minerals in sedimentary rocks. Wasserburg, Hayden & Jensen (12) demonstrated the existence of radiogenic A^{40} in these minerals and, in the relatively small suite studied, showed that the K-A ages obtained had the correct order when related to the stratigraphic sequence. This work was extended to many more samples and stratigraphic positions by Lipson (106), and the conclusions of the two groups are in agreement. Cormier *et al.* (107) studied a suite of glauconites, using the Rb-Sr age, and have demonstrated the existence of small amounts of radiogenic Sr^{87} in these minerals. Without minimizing the contribution of the work which has been done, it must be pointed out that the two ages have not been measured on the same minerals, so that there is no check as yet on the argon retentivity of glauconite. Also, with the large amounts of common Sr present, more sophisticated methods are required than those used by Cormier *et al.* to make the radiogenic Sr^{87} determinations of glauconite sufficiently precise to make the Rb-Sr ages meaningful. Thus, both methods require considerable effort before the ages of authigenic minerals can be stated with great certainty. Studies of K-A ages of sylvites by Gentner *et al.* (92, 93, 94, 108), and by Reynolds and co-workers (95, 109) have shown the difficulty of interpreting the effect of argon loss on the ages of these minerals.

The importance of determining the ages of sedimentary rocks directly may be emphasized by the fact that the Holmes time scale (110) is based on U-Pb ages of three minerals, only one of which has direct fossil control. This one sample has a ratio of its U-Pb ages of 0.89 and, therefore, is so discordant that it is difficult to know the true age. The measurement of the age of sedimentary minerals offers the possibility of establishing directly an absolute fossil time scale.

OTHER MEASURES OF GEOLOGIC TIME

Included in this section are methods based on the natural radioactivity of Re^{187}, Lu^{176}, and Th^{230} and on those radioactive nuclides which occur in nature but which, because of their short half lives, depend on the cosmic-ray neutron flux for their production. Any discussion of C^{14} will be excluded, since the literature in this field is now so comprehensive that books are written about it. Long-lived nuclides other than the three mentioned are omitted because no direct evidence of the daughter products has as yet been observed in natural sources.

The Re^{187} β-decay half life has long been eluding measurement. Positive evidence of its decay was first reported by Naldrett & Libby (111) and Suttle & Libby (141), who used a low-level Geiger counter, and has since been confirmed by Herr, Hintenberger, Merz, and Voshage (112, 147) by the detection of the Os daughter in a number of molybdenites containing rhenium. Using a proportional counter, Dixon & McNair (114) failed to detect any Re activity and set the maximum energy of the β-decay at less than one kev. They deduce a half life $>10^{15}$ yr., so that there remains contradictory counting evidence for the half life; from the geological method it is estimated to be of the order of 6×10^{10} yr. The fact that Re is but a minor constituent of molybdenum minerals, which are themselves rare, will probably limit the usefulness of its decay for geologic time measurements. This decay will also provide a means of studying the geochemistry of Re and Os.

The presence of radiogenic Hf in Lu minerals has also now been established (115). The half life of Lu^{176} has been found to be 2.1×10^{10} yr. in laboratory counting experiments by Glover & Watt (116). The geologic occurrence of minerals containing Lu is rare, and it would seem most likely that measurements on geological materials would have their chief value to geology as a means for studying the geochemistry of the elements involved rather than for determining ages.

Gerling, Levskii & Afansjeva (117) have observed the occurrence of A^{38} in K minerals, and concluded from the relationship of A^{38} to chlorine content that the A^{38} present could not be due to (α, n) or (α, p) reactions on Cl^{35}. A^{38}/K ratios were also found to be independent of the proximity of uranium minerals, from which it was concluded that the $K^{41}(n, \alpha)Cl^{38}$ reaction was not the source of the A^{38} found. Further, these authors found that the ratio A^{38}/K has a definite relation to the age of the mineral. It is their opinion that the A^{38} must, therefore, be due to the decay of a long-lived isomer of K^{38} which has an abundance of about 10^{-10} gm./gm. K and a decay constant of about 10^{-9} yr.$^{-1}$. Recently, Wasserburg & Bieri (private communication), using an instrument at the University of Minnesota which had never been used for analyzing argon with excess A^{38} in it, looked for A^{38} in a mica of known age. These workers found at most one-tenth the A^{38} predicted from the decay constant and abundance suggested by Gerling *et al*. It will, therefore, be necessary to resolve the contradiction of these two similar experi-

ments before the consequences of the existence of a long-lived K^{38} can be seriously discussed.

The continuous production in the oceans and short half life $(8.3 \times 10^4$ yr.) of Th^{230} have held promise of a convenient method for studying sedimentation rates. A recent study of Volchok & Kulp (118) confirms the earlier work of Piggot & Urry (119) and demonstrates the need for ideal sedimentation conditions in order that the measurements may be consistent.

Another long-lived nucleus whose existence in natural sources has been demonstrated is Cl^{36}, produced by neutron capture in chlorine. Schaeffer & Davis (120) have shown significant amounts of Cl^{36} to be present in two samples of surface rocks only. The utility of Cl^{36} dating for special types of recent $(10^4$ yr.) geologic processes affecting surface rocks at high altitudes is suggested by them.

A third short-lived $(2.5 \times 10^6$ yr.) nucleus, Be^{10}, has been found to be present in ocean cores by Arnold (121). This nuclide is thought to result from high-energy neutrons in the cosmic-ray flux reacting with oxygen and nitrogen in the atmosphere. Sedimentation rates determined from the specific activity of the core material in counts/sec. cm.^{3} agree with those estimated from other measurements, and this agreement indicates both the constancy of the cosmic-ray flux and a production rate of Be^{10} of about 0.03 nuclei/cm.^{2} sec.

Potential methods now exist for measuring the time of formation of rocks of all ages. The largest period of uncertainty still lies in the region between 3×10^4 and 10^7 yr., but improved understanding and technology will almost certainly eliminate this gap.

DISCORDANT URANIUM-LEAD AGES

The fact that uranium has two long-lived isotopes, U^{238} and U^{235}, makes possible the determination of two ages, one calculated from the ratio Pb^{206}/U^{238} and the other from the ratio Pb^{207}/U^{235}. These two ages will be concordant, that is, they will be equal to one another and to the true age of the mineral if the following assumptions are fulfilled: (a) There have been no gains or losses of parent or daughter elements since the formation of a mineral; (b) There have been no gains or losses of intermediate members of the radioactivity decay system, for example, radon or ionium; (c) Proper corrections have been made for the initial concentration of radiogenic daughter product; (d) The chemical analyses have been properly performed, and the correct decay constants have been used. With present techniques and knowledge, assumption (d) can be fulfilled and will not be discussed further.

As a result of the pioneer work of Nier (4, 5), it was immediately clear that the two ages commonly did not agree, presumably because of the failure of one or more of these assumptions. In this case, the ages are said to be discordant. In principle, discordant ages may convey more information than
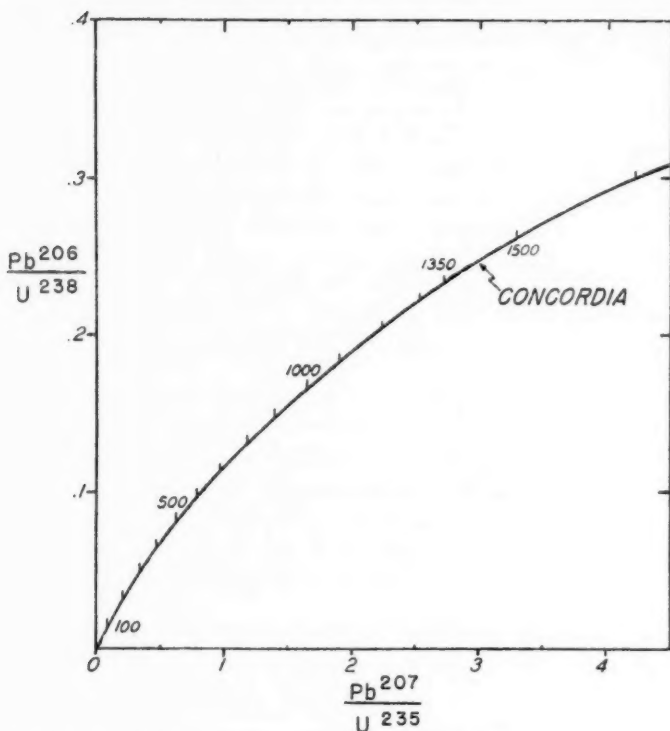
FIG. 6. Plot of Pb^{206}/U^{238} vs. Pb^{207}/U^{235} which is useful for the interpretation of discordant U-Pb ages. The curve is the locus for concordant ages, and the corresponding ages are given.

do concordant ages, since they have been affected by the pre- or post-mineralization history of the mineral. In this section, the effects of the various possible causes of discordance will be discussed; and, to the extent that present knowledge allows, the relative importance of these causes will be evaluated. The geochemical problems involved are very complex, and a complete understanding of all cases of discordance may well be impossible. However, progress is being made, and it is beginning to be possible to make use of some of the information potentially available from discordant ages.

While it is possible to generalize Equation 1 to include the case of the failure of the assumptions, the algebraic expressions involved are frequently so complex that it is difficult to visualize the physical processes (124, 125). For this reason, the understanding of discordant uranium-lead ages is facilitated by use of a diagram (Fig. 6), in which the mole ratio Pb^{206}/U^{238} is plotted as ordinate and the mole ratio Pb^{207}/U^{235} as abscissa. In the particular case of uranium-lead ages, Equation 1 takes the form:

$$\frac{\text{Pb}^{206}}{\text{U}^{238}} = e^{\lambda_{238}\tau_0} - 1$$

$$\frac{\text{Pb}^{207}}{\text{U}^{235}} = e^{\lambda_{235}\tau_0} - 1.$$

6.

If assumptions (a), (b), and (c) are valid, the ages τ_0 calculated from these two equations will be concordant, and τ_0 will be the true age of the mineral. In this case, to every age τ_0 there will correspond unique values of the ratios $\text{Pb}^{206}/\text{U}^{238}$ and $\text{Pb}^{207}/\text{U}^{235}$ defined by Equation 6. The locus of these values for $0 < \tau_0 < \infty$ is the curve marked "concordia" on Figure 6. Discordant ages will be represented by points lying off this curve, while "accidentally" concordant ages are those which happen to lie on the curve in spite of the fact that one or more of the assumptions is not valid.

GAIN OR LOSS OF LEAD OR URANIUM

The generalized equations given by Wickman (124) and Wetherill (125) may be used to calculate the locus of various hypothetical histories of lead-uranium fractionation. One particularly interesting case, that of loss of lead or gain of uranium during a short episode, will be discussed here.

Figure 7 shows the locus of points representing discordant ages resulting from varying amounts of uranium-lead fractionation in minerals having a true age $= \tau_0$ of 1500×10^6 yr. and a time of fractionation $\tau_1 = 300 \times 10^6$ yr. ago. It is seen that this locus is a straight line intersecting the curve "concordia" at $\tau_0 = 1500 \times 10^6$ yr. and $\tau_1 = 300 \times 10^6$ yr. It has been shown analytically that this curve is actually a straight line (125). This leads to a simple graphical procedure for calculating discordant uranium lead ages resulting from episodic fractionation of lead and uranium, which will now be described.

For the case of a mineral having an age τ_0 which has lost lead or uranium during a geologically short episode τ_1 years ago, the position of the point (Q_1) characteristic of this mineral may be found by the following procedure: (a) Draw a straight line passing through the point on the curve "concordia" corresponding to a true age τ_0 and that corresponding to a true age τ_1 (see Fig. 8). (b) Defining the length of the straight segment $\overline{\tau_0 \tau_1} = L_1$, measure off a distance along this segment of length $l_1 = R_1 L_1$ from τ_1; R_1 is the ratio by which $\text{Pb}^{206}/\text{U}^{238}$ and $\text{Pb}^{207}/\text{U}^{235}$ changed at time τ_1. That is, R_1 is the ratio of $\text{Pb}^{206}/\text{U}^{238}$ immediately after loss to $\text{Pb}^{206}/\text{U}^{238}$ immediately before loss. For example, if half the lead were lost with no loss of uranium, then $R_1 = 1/2$ and $l_1 = 1/2\ L_1$, and the resulting point will be at the mid-point of the line $\overline{\tau_0 \tau_1}$. If, on the other hand, one-third of the uranium were lost, $R_1 = 3/2$ and $l_1 = 3/2\ L_1$.

The case of multiple episodic fractionation of uranium or lead can be calculated in the same way by now using Q_1 as the starting point and repeating the procedure to find Q_2, etc., as has been described more fully elsewhere (125).

$\dfrac{Pb^{206}}{U^{238}}$

$\dfrac{Pb^{207}}{U^{235}}$
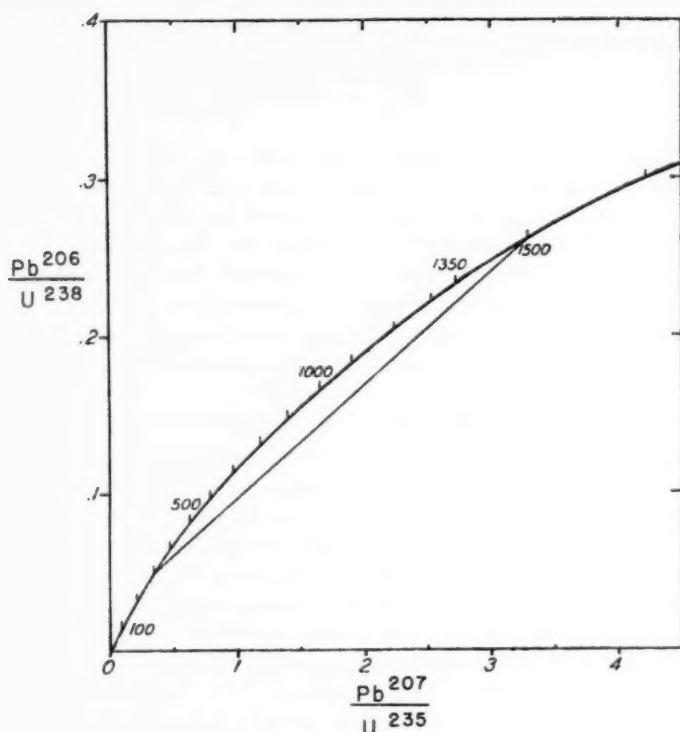
Fig. 7. Diagram showing the locus of points representing minerals 1500 million years old which have lost lead 300 million years ago.

In the case of a group of minerals having a true age τ_0 and losing various amounts of lead at a time τ_1 in the past, the isotopic ratio $(Pb^{207}/Pb^{206})_{\tau_1}$ of the lead which is lost will be the same for all the minerals and can be determined from the slope (m) of the straight line $\overline{\tau_0\tau_1}$ by use of Equation 7,

$$\left(\frac{Pb^{207}}{Pb^{206}}\right)_{\tau_1} = m\left(\frac{U^{235}}{U^{238}}\right)_{present} \qquad 7.$$

where, in the calculation of m, proper consideration must be given to the fact that the scales on the ordinate and abscissa of these diagrams are generally different. If the lead which has been lost at τ_1 can be found, possibly in minerals such as galena or pyrite, its isotopic composition would be given by Equation 7 after the Pb^{204} has been used for the proper corrections for any nonradiogenic lead in these lead minerals.

This graphical procedure leads to another interesting conclusion. Even in the case of multiple fractionations, if every fractionation results in the
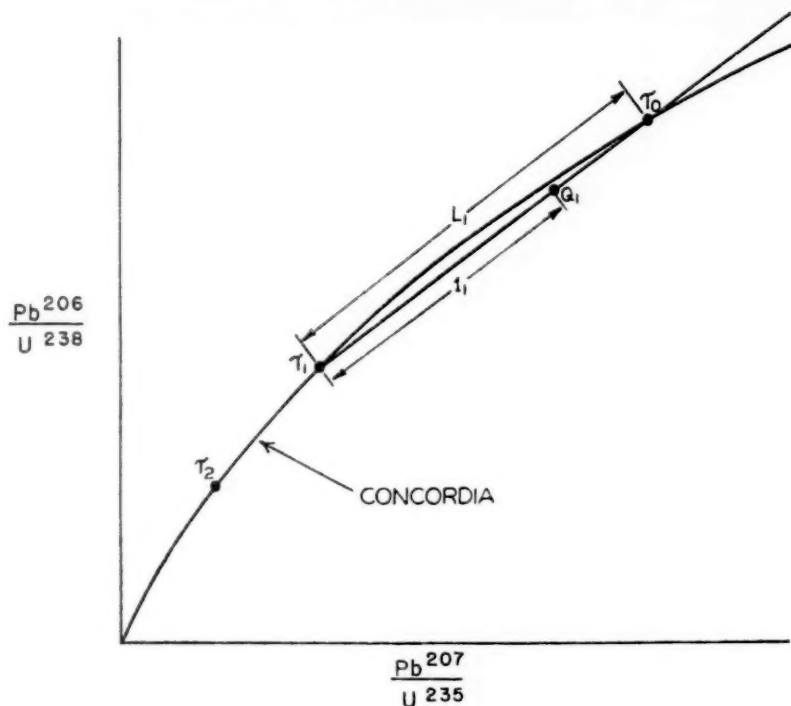
FIG. 8. Diagram illustrating the graphical procedure described in text.

net loss of lead or the net gain of uranium, the resulting point from which the discordant "apparent" ages can be calculated will be in the sector A of Figure 9. On the other hand, if every fractionation consists of a net loss of uranium, the resulting point will be found in the sector B. Only by such combinations as loss of lead at one time and loss of uranium at some greatly different time can the point fall outside of sectors A and B. Figure 9 is drawn for $\tau_0 = 1350 \times 10^6$ yr.

In the physically reasonable case where the magnitude of the fractionations is sufficient to cause grossly discordant ages but still does not involve almost total loss of lead or uranium, the regions accessible to points are still more limited. For example, Figure 10 shows the area of the diagram accessible to points representing minerals having a true age of 1350 million yr. which have lost up to 50 per cent of their lead and up to 25 per cent of their uranium during geological time. The fact that the shaded area of the diagram forms a rather long thin band pinching in toward the point on concordia representing the true age of the mineral forms the basis of a suggested method for determining the true age of a group of cogenetic minerals even when no regularities are apparent (126).
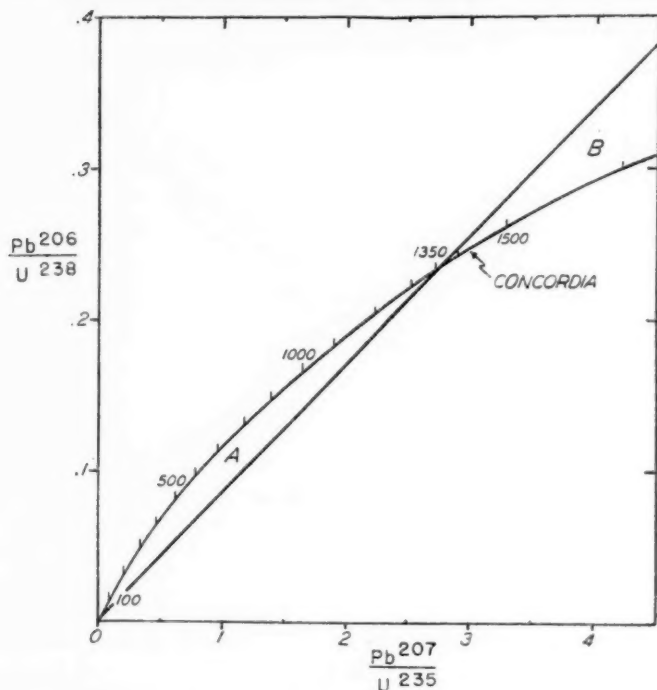
FIG. 9. Diagram showing the areas representing minerals that
have lost lead (A) or lost uranium (B).

LOSS OR ADDITION OF INTERMEDIATE DAUGHTER PRODUCTS

Since the intermediate daughter products have different chemical proper-
ties and the time spent as a particular intermediate element is greatly dif-
ferent for the two decay chains, the possible patterns of discordant ages
resulting from gain or loss of intermediates are very complex. On the other
hand, for loss of an intermediate product to be important, a significant
fraction of the intermediate product must continually be lost over the entire
history of the mineral. Even complete loss of all intermediate products in
one of the decay systems over a time short compared to the age of the mineral
will have a negligible effect on the measured age. This contrasts with the
foregoing case of lead-uranium fractionation where a relatively small frac-
tionation during a short episode will cause grossly discordant ages.

Most of the discussion regarding the loss of intermediate product has
concerned loss of radon, Em^{222}, an intermediate product of the U^{238} series,
which has been expected to be lost more easily than its counterpart actinon,
Em^{219}, in the U^{235} series, since radon has a half life of three days, while actinon
has a half life of only 4 sec. Actinon would not be expected to diffuse very
far before it decayed, and its loss would have to depend on some higher-
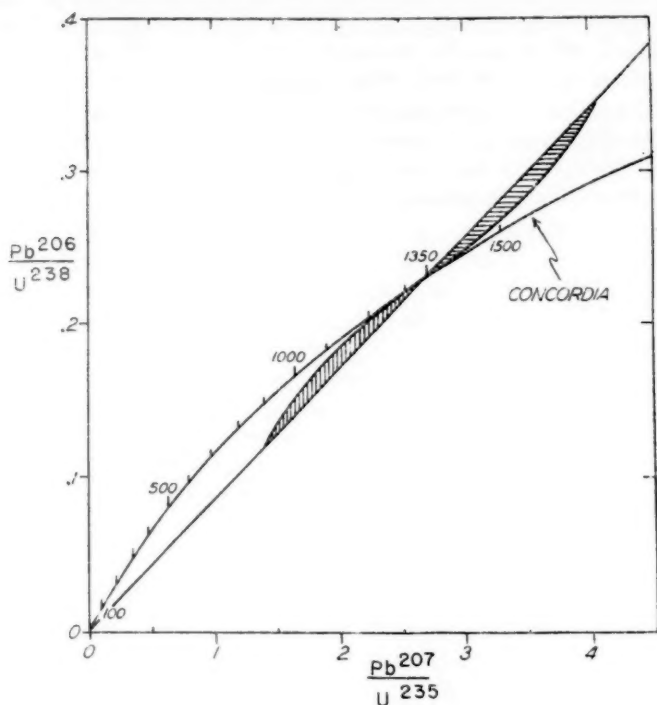
F<small>IG</small>. 10. Diagram showing the area representing minerals that have lost up to
50 per cent of their lead or up to 25 per cent of their uranium.

energy processes, such as nuclear recoil following alpha emission. The locus
of discordant ages produced by radon loss will be a vertical straight line on
a Pb^{206}/U^{238} vs. Pb^{207}/U^{235} plot.

P<small>RESENCE OF</small> R<small>ADIOGENIC</small> L<small>EAD AT THE</small> T<small>IME OF</small> M<small>INERALIZATION</small>

In most cases, it is possible to correct properly for the initial concentra-
tion of Pb^{206} and Pb^{207} by use of the nonradiogenic isotope Pb^{204}. However, in
some cases it may be that the original lead in the mineral was not of normal
composition, and the correction will then be in error, and the resulting
"apparent" ages will be discordant and neither of them will equal the true
age τ_0.

Figure 11 shows the case of $\tau_0 = 1200 \times 10^6$ yr. with an initial radiogenic
lead isotopic composition $Pb^{207}/Pb^{206} = 0.12$. Points representing various
cogenetic minerals with different amounts of this radiogenic lead will be
spread out along a straight line starting at τ_0 on concordia and intersecting
concordia again at 1900 million yr. Thus the effect of the initial radiogenic
lead is exactly the same as loss of lead at 1200×10^6 yr. by a mineral 1900×10^6

yr. old. Furthermore, the ratio Pb^{207}/Pb^{206} of the lead which was lost, given by Equation 7, will be exactly the same as the Pb^{207}/Pb^{206} ratio $=0.12$ of the assumed initial radiogenic lead. Thus, this result is actually what would be expected if a mineral of true age 1900×10^6 yr. had lost lead 1200×10^6 yr. ago; from a slightly different point of view, the true age could be regarded as 1200×10^6 yr., with the remaining radiogenic lead regarded as initial radiogenic lead. Thus, the distinction between episodic loss and initial radio-
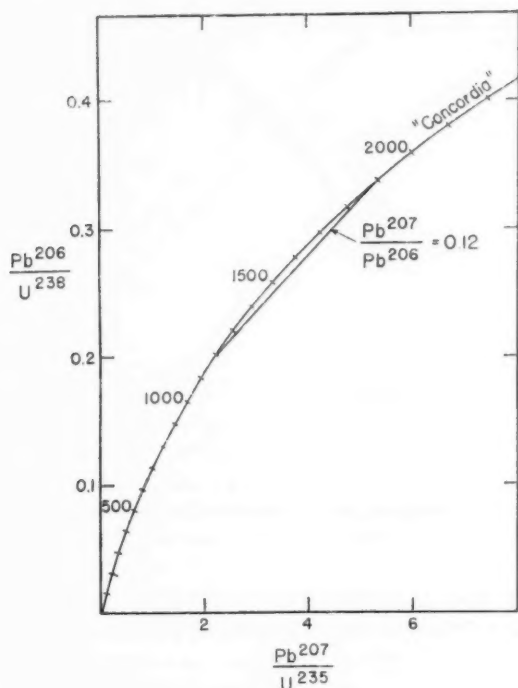
FIG. 11. Diagram showing the locus of points representing minerals 1200 million yr. old which contained primary radiogenic lead of isotopic composition $Pb^{207}/Pb^{206} = 0.12$.

genic lead cannot generally be made from either the pattern of discordant ages or from a study of isotopic composition of the radiogenic lead of neighboring lead minerals. In order to distinguish between these two interpretations in those cases where this distinction is more than a matter of point of view, additional evidence is necessary. For example, if the uranium minerals seem to have a high concentration of this original radiogenic lead, whereas other minerals such as feldspars have but little, it would not seem plausible to suppose that this radiogenic lead was attracted in some way to the uranium mineral. Therefore, in this case it is more probable that the

radiogenic lead was in the uranium mineral because it never left, and the situation should more properly be regarded as a case of lead loss.

ACCIDENTAL CONCORDANCE

By use of the graphical scheme for calculating the effects of episodic lead-uranium fractionation described in the section on Gain or Loss of Lead or Uranium, it can be seen that, if the time of fractionation (τ_1) is near the true age τ_0, the chord connecting these two points will not lie very far from the curve concordia, and the ages represented by points along this chord will appear to be concordant within experimental error, even though they are unequal to τ_0. This situation becomes more serious for young minerals, as in this region the curvature of concordia becomes very small. Thus, minerals less than about 250 million yr. old will usually appear concordant even though they are not, and concordance will no longer be a valid criterion for acceptance of the age as the correct one.

However, it may prove significant that loss of intermediate daughter product will cause discordance even in young minerals, and if accurate age measurements are made on young minerals, it may be possible to evaluate the importance of loss of these intermediate products. This may be difficult because of the small amount of radiogenic Pb^{207} relative to normal Pb^{207} usually found in these young minerals.

LABORATORY EXPERIMENTS BEARING ON THE ACTUAL CAUSES OF DISCORDANCE

In general, laboratory investigations suffer from the almost insurmountable difficulty of reproducing in the short time span available for the experiment the effects which occurred over millions of years in nature. However, measurements have been made which shed some light on the possible causes of discordance.

Lead-uranium fractionation.—Leaching experiments on various uranium and thorium minerals have been carried out by Tilton (99) and by Starik (127). These workers find that there is a relationship between the relative ease of removal of lead, uranium, and thorium from a mineral and the type of fractionation needed in order to explain the observed discordant ages. Some of the results of Tilton are shown in Figure 12 and in Table XIII.

Figure 12a shows the isotopic composition of the lead removed from the Goodhouse monazite by acid washing. The material removed has nearly the same isotopic composition as the original mineral except for an excess of common lead. Only small quantities of uranium, thorium, and lead were removed from the mineral, and there was not much fractionation of these elements. The ages (shown in Table XI) are concordant. For the Houtenbek monazite (Fig. 12b), on the other hand, the uranium-lead ages are discordant in a direction corresponding to loss of uranium. In the washing experiment, uranium was removed more readily than lead and thorium, and the lead removed was highly enriched in uranium lead, a result which indicates that
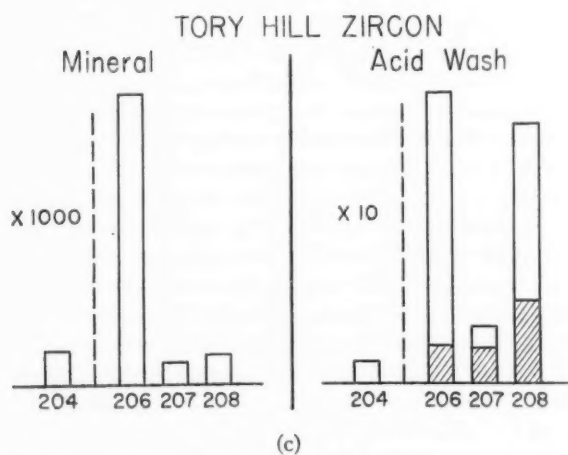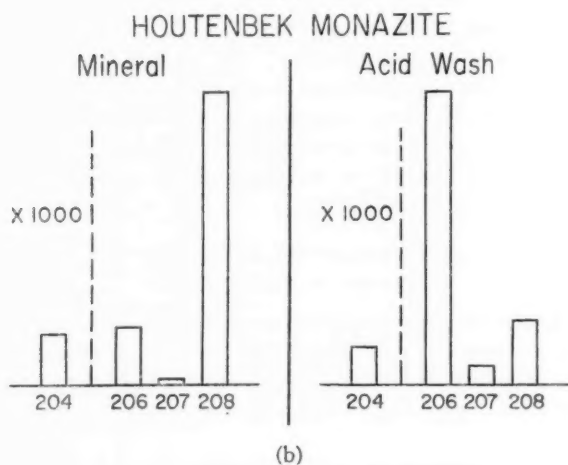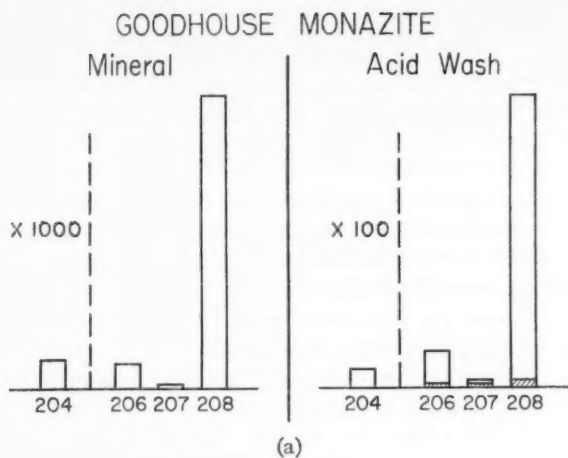
FIG. 12a,b,&c. The isotopic composition of lead removed by acid washing. The shaded areas illustrate the portion of the Pb^{206}, Pb^{207}, and Pb^{208} in the acid wash which is nonradiogenic.

TABLE XIII

PERCENTAGES OF U, TH, PB WHICH ENTERED ACID WASHES

Sample	Per Cent Entering Acid Wash		
	U	Th	Pb
Monazite, Goodhouse, S. Africa	2.0	1.7	1.4
Monazite, Houtenbek, S. Africa	7.3	1.8	4.8
Zircon, Tory Hill, Ontario			15

uranium and its daughters had been in positions where they could easily be removed chemically. The Tory Hill zircon (Fig. 12c) has concordant uranium-lead ages, but the thorium age is much too low. By acid washing, thorium lead (Pb^{208}) is readily removed, while little uranium lead, uranium, and thorium are lost.

All these results support the hypothesis that the observed discordant ages are produced by parent-daughter fractionation. Similar results are found by Starik; however, he does not report isotopic analyses of the leached lead.

Loss of intermediate daughter products. Starik (127) and Giletti & Kulp (128) have published data on the loss of emanation from uranium and thorium minerals. Starik finds, at low temperatures, that radon is lost to a greater extent than the other isotopes of emanation, but the effect is not as great as might be expected from the great difference in half lives. This observation suggests that some energetic process, probably nuclear recoil, causes some of the emanation isotopes to be in cracks and pores in the rock where the subsequent daughter products might be readily leached. Quantitatively, the effect of loss of emanation was not found to be serious for uranium minerals which are generally used for age determination (zircon, uraninite, monazite) but can be serious for altered and secondary uranium minerals.

Kuroda (129) has studied the ratio of the activity of the radium isotopes from the U^{235} and U^{238} series which should be in equilibrium with their long-lived parent isotopes. He finds that in many uraninites and pitchblendes the Ra^{223} occurring in the U^{235} series is excessive by as much as 12 per cent. If this observation is generally true and the effect has existed over the entire lifetime of the mineral, appreciable discordance should result. Confirmation of this surprising effect and further investigation along these lines would be valuable. However, it must be remembered that experiments of this sort are dependent on the recent history of the mineral, and the presence of ground water and other superficial causes of alteration may have disturbed the equilibrium of parent and intermediate daughter products in recent times.

INTERPRETATION OF DISCORDANT URANIUM-LEAD AGES

Because of the great variety of possible causes of discordance, in most cases not much can be said concerning the actual cause. However, when

measurements have been made on a number of specimens which have had a similar geological history, it seems to appear that inferences may be made concerning the cause of discordance and the geological history.

There are two cases in the literature where a number of discordant ages from a given locality have been published. The first is the Goldfields region around Lake Athabaska, Saskatchewan [Collins, Farquhar & Russell (130); Eckelmann & Kulp (131)], and the other is the Witwatersrand of South Africa [Louw (132); Davidson (133); Ahrens (134, 135); Wetherill (136); Russell & Ahrens (137)].

The experimental data of Collins, Farquhar & Russell (130) and of Eckelmann & Kulp (131) are plotted in Figure 13. Table XIV shows the results of measurements of Wasserburg & Hayden (11) and Wetherill *et al.* (83) on minerals from a pegmatite at Viking Lake in this region. These measurements indicate a period of rock formation in this region about 1900 million yr. ago. In line with the discussion of episodic fractionation of lead and uranium, the group of points spread along the line between 1900 million yr. and 200 million yr. on concordia can be interpreted as having been
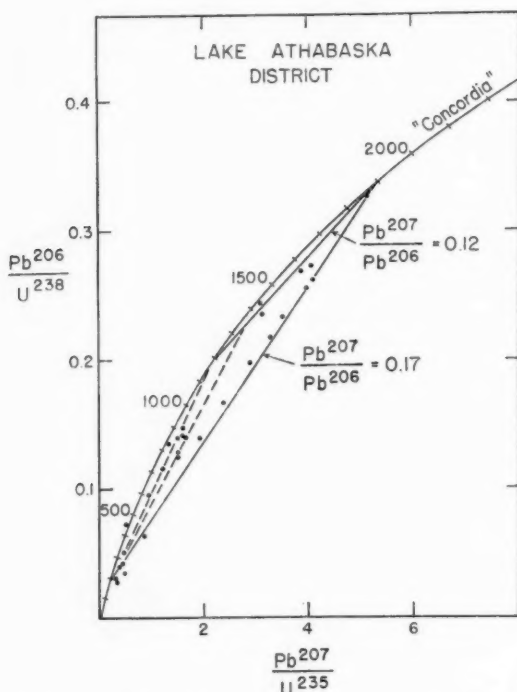
FIG. 13. Discordant U-Pb ages, from Lake Athabaska, Saskatchewan (130, 131). The lines marked $Pb^{207}/Pb^{206} = 0.17$ and 0.12 represent radiogenic lead found in lead minerals which can be interpreted as some of the lead lost by the minerals.

TABLE XIV

AGE DETERMINATIONS ON PEGMATITE, VIKING LAKE, SASKATCHEWAN

Mineral	Ages in Millions of Years					
	$U^{238}\text{-}Pb^{206}$	$U^{235}\text{-}Pb^{207}$	$Pb^{207}\text{-}Pb^{206}$	K-A	Rb-Sr	Ref.
Uraninite	1850	1880	1910			(11)
Uraninite	1790	1830	1870			(83)
Mica				1800	1970	(72, 83)
Feldspar				1630		(11)

formed 1900 million yr. ago and having suffered lead removal 200 million yr. ago. A second group of minerals appears to be 1900 million yr. old and to have lost lead 1200 million yr., ago, while a third group was severely altered 1200 million yr. ago and again underwent uranium-lead fractionation 200 million yr. ago. This is the possible interpretation obtained by Eckelmann & Kulp (131) by numerical calculation, and it is more readily recognized by this graphical presentation. In addition, these two groups of workers have analyzed six samples of anomalous (radiogenic) lead from lead minerals in this area and found two types. In one case, the ratio radiogenic Pb^{207}/Pb^{206} is equal to 0.12 ± 0.01, and in the other case 0.17 ± 0.01. Straight lines having these slopes are plotted in Figure 13; and, in line with the previous discussion, this lead may be interpreted as some of the lead which was lost during the episodes of uranium-lead fractionation.

Appealing as this intepretation may be, it is unfortunately not unique. First, there is the undeniable scatter in the points, which is what would be expected from two episodes of fractionation; nevertheless, it makes interpretation more difficult. The same data could be interpreted as representing minerals about 200×10^6 yr. old which contain primary radiogenic lead, as discussed earlier. However, in view of the evidence for 1900×10^6 yr. old rocks in the area, this is probably one of those cases where the difference is a matter of point of view. Russell & Ahrens (137) have offered an alternative explanation of such regularities. They suggest that by the process of nuclear recoil, about 9 per cent more intermediate daughter product is lost from the U^{235} system than from the U^{238} system. This will also result in similar linear patterns. However, it is difficult to envisage a mechanism which will result in the constant 9 per cent difference regardless of whether a little or almost all of the intermediate product is lost. Furthermore, this explanation requires that the Athabaska minerals be fundamentally of two different ages, about 1200×10^6 yr. and 1900×10^6 yr., and offers no explanation for the group along the line between 1900×10^6 yr. and 1200×10^6 yr., nor for the radiogenic lead with $Pb^{207}/Pb^{206} = 0.12$ found in the lead minerals. Therefore, the first explanation, that given by Eckelmann and Kulp, seems to fit the data in the simplest and most satisfactory way.

In order to explore further the causes of discordant ages, it will be necessary to have more such collections of data, preferably from granites and pegmatites, perhaps in such areas as the Appalachians where there is good evidence that many of the rocks were formed about 1000×10^6 yr. ago and were metamorphosed about 300×10^6 yr. ago. A more extensive collection of published discordant ages is given by Eckelmann & Kulp (138).

CONCLUDING REMARKS

This review has been primarily concerned with showing the extent to which the methods for the determination of mineral age have been established. It now seems clear that the tools are at hand with which the age provided by any method can be tested. It would then seem appropriate to present here one example of the use of mineral ages to establish the existence of a large geologic province whose form could have hardly been imagined using classical geologic methods. The data are given in Table XV and consist of Rb-Sr and K-A ages of granitic rocks collected in the western United States solely on the basis that they were Precambrian (139). This table does not include all the Precambrian rocks in these states but does include all that have been measured. Their geographic distribution is shown in the map of Figure 14. The lettered positions locate rocks with ages markedly different from 1350×10^6 yr. Other rocks of this approximatie age (1350×10^6 yr.) have been found in eastern Oklahoma, central Missouri, the upper Michigan

TABLE XV

K-A and Rb-Sr Ages of Rocks From Western United States

		Ages in Millions of Years	
Sample Location		K-A	Rb-Sr
1.	Gneiss, Zoroaster, Grand Canyon, Arizona	1350	1370
2a.	Lawler Peak Granite, Bagdad, Arizona	1360	1390
2b.	Pegmatite in Lawler Peak Granite	1380	1500
3.	Pegmatite, Wickenberg, Arizona	1120	1300
4.	Pidlite Mine, Mora Co., New Mexico	1280	1490
5.	Granite, Sandia Mountains, Albuquerque, New Mexico	1300	1340
6.	Harding Mine, Dixon, New Mexico	1260	1300
7.	Uncompahgre Granite, Mesa Co., Colorado	1300	1320
8.	Granite, Doyleville, Colorado	1280	1310
9.	Brown Derby Pegmatite, Ohio City, Colorado	1300	1390
10.	Silver Plume, Colorado	1230	1360
11.	Granite, Sherman, Wyoming	1380	1410
A.	Thermopolis, Wyoming	2250	2420
B.	Keystone, S. Dakota	1380	1650
Ca.	Pikes Peak, Colorado	1060	1090
Cb.	Llano, Texas	1060	1100
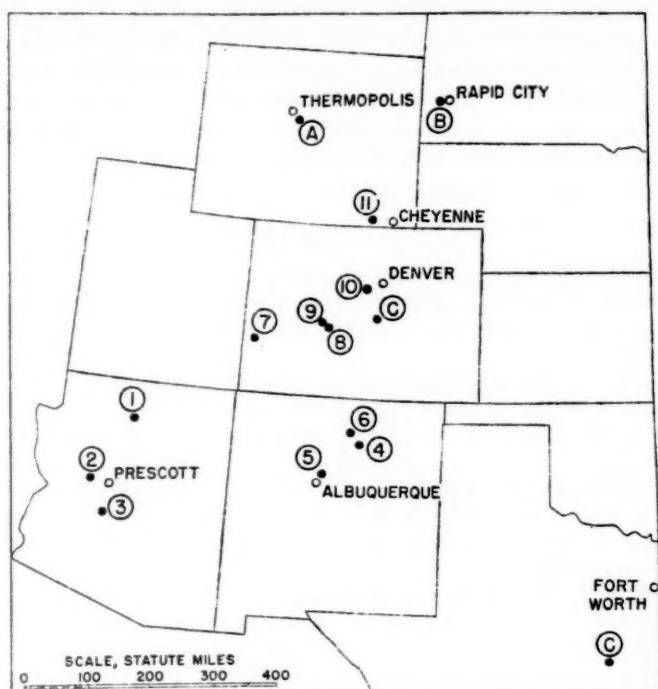
Fig. 14. Geographic distribution of measurements of Table XIII showing the wide distribution (1 to 11) of rocks 1350 million yr. old and the occurrence of rocks of different age (A, B, C).

peninsula, and eastern Ontario. It would appear that a widespread geologic event by which micas were formed occurred 1350×10^6 yr. ago and that no subsequent geologic event, including that which produced the present mountain structure in southwest United States, removed or seriously distorted the evidence for the geologic activity which produced the minerals studied. Other examples of this type of data exist, and the patterns are beginning to emerge as additional data are obtained. There remains to be learned the extent of the simultaneity of geologic events on a world-wide scale.

In summary, the assumptions required for a valid mineral age—that the minerals form a closed system for the elements involved and that none of the daughter element is included when the mineral is formed—are tested, at least in part, by the determination of both the Rb-Sr and K-A age of the mineral. The agreement of these two ages is believed to be an indication of the absolute age of the mineral. Further, it has been found that micas often show evidence of satisfying the assumptions even when the U and Th

minerals do not. It is concluded that the most reliable method for determining the age of common rocks is from the K-A and Rb-Sr ages of mica. Data exist which indicate that discordant U-Pb ages of several minerals from the same geologic unit may, in some cases, provide both the age of rock formation and the time the rocks were altered. Similar information may be included in the discordance of K-A and Rb-Sr ages, but insufficient data are available to know how to derive this information at present.

LITERATURE CITED

1. Boltwood, B. B., *Am. J. Sci.*, **23**, 77 (1907)
2. Knopf, A., Schuchert, C., Kovarik, A. F., Holmes, A., and Brown, E. W., "The Age of the Earth," *Natl. Acad. Sci. (U.S.)-Natl. Research Council*, 487 pp. (1931)
3. Aston, F. W., *Proc. Roy. Soc. (London)*, **A140**, 535 (1933)
4. Nier, A. O., *Phys. Rev.*, **55**, 150–63 (1939)
5. Nier, A. O., Thompson, R. W., and Murphy, B. F., *Phys. Rev.*, **60**, 112–16 (1941)
6. Kohman, T. P., and Saito, N., *Ann. Rev. Nuclear Sci.*, **4**, 401 (1954)
7. Ahrens, L. H., *Phys. and Chem. Earth*, **1**, 44 (1956)
8. Kulp, J. L., *Advances in Geophysics*, **2**, 179 (Academic Press, New York, N.Y., 286 pp., 1955)
9. Wilson, J. T., Russell, R. D., and Farquhar, R. M., *Handbuch der Physik*, **47**, 288–363 (Springer-Verlag, Berlin, Germany, 659 pp., 1956)
10. Faul, H., Ed., *Nuclear Geol.* (John Wiley & Sons, New York, N. Y., 414 pp., 1954)
11. Wasserburg, G. J., and Hayden, R. J., *Geochim. et Cosmochim. Acta*, **7**, 51–60 (1955)
12. Wasserburg, G. J., Hayden, R. J., and Jensen, K. J., *Geochim. et Cosmochim. Acta*, **10**, 153–65 (1956)
13. Geiss, J., *Z. Naturforsch.*, **9A**, 218 (1954)
14. Farquhar, R. M., and Russell, R. D., *Trans. Am. Geophys. Union*, **38**, 552 (1957)
15. Russell, R. D., Farquhar, R. M., and Hawley, J. E., *Trans. Am. Geophys. Union*, **38**, 557 (1957)
16. Vinogradov, A. P., and Zykov, S. I., *Doklady Akad. Nauk S.S.S.R.*, **105**, 126 (1955)
17. Geiss, J., *Chimia (Switz.)*, **11**, 349 (1957)
18. Patterson, C. C., *Geochim. et Cosmochim. Acta*, **7**, 151 (1955)
19. Wasserburg, G. J., and Hayden, R. J., *Phys. Rev.*, **97**, 86 (1955)
20. Schumacher, E., *Z. Naturforsch.*, **11A**, 206 (1956)
21. Webster, R. K., Morgan, J. W., and Smales, A. A., *Trans. Am. Geophys. Union*, **38**, 543 (1957)
22. Tilton, G. R., and Davis, G. L., *Frontiers in Geochemistry* (Abelson, P. H., Ed., John Wiley & Sons, Inc., New York, N. Y., to be published, 1958)
23. Fleming, E. H., Jr., Ghiorso, A., and Cunningham, B. B., *Phys. Rev.*, **88**, 642–52 (1952)
24. Kovarik, A. F., and Adams, N. I., Jr., *J. Appl. Phys.*, **12**, 296 (1941)
25. Curtis, L. F., Stockman, L., and Brown, B. W., *Natl. Bur. Standards (U.S.)*, *Rept. A-80* (Unpublished data, 1941); Discussed in Reference (23)

26. Kienberger, C. A., *Phys. Rev.*, **76**, 1561 (1949)
27. Kovarik, A. F., and Adams, N. I., Jr., *Phys. Rev.*, **98**, 46 (1955)
28. Clark, F. L., Spencer-Palmer, H. J., and Woodward, R. N., *Bull. Jealott's Hill Research Sta., Imp. Chem. Ind., Ltd.; Declassified Rept. BR-522* (Unpublished data, 1944)
29. Knight, G. B., *U. S. Atomic Energy Commission Report, ORNL K-663* (Unpublished data, 1950)
30. Sayag, G. J., *Compt. rend.*, **232**, 2091 (1951)
31. Würger, E., Meyer, K. P., and Huber, P., *Helv. Phys. Acta*, **30**, 157 (1957)
32. Ghiorso, A., *Phys. Rev.*, **82**, 979 (1951)
33. Kovarik, A. F., and Adams, N. I., Jr., *Phys. Rev.*, **54**, 413–21 (1938)
34. Senftle, F. E., Farley, T. A., and Lazar, N., *Phys. Rev.*, **104**, 1629 (1956)
35. Picciotto, E., and Wilgain, S., *Nuovo cimento*, **4**, 1525 (1956)
36. Morrison, P., *Phys. Rev.*, **82**, 209 (1951)
37. Bell, P. R., and Cassidy, J. M., *Phys. Rev.*, **79**, 173 (1950)
38. Fireman, E. L., *Phys. Rev.*, **75**, 1447 (1949)
39. Colgate, S. A., *Phys. Rev.*, **81**, 1063 (1951)
40. Sawyer, G. A., and Wiedenbeck, M. L., *Phys. Rev.*, **79**, 490 (1950)
41. Major, J. K., and Biedenharn, L. C., *Revs. Modern Phys.*, **26**, 321 (1954)
42. Rose, M. E., and Jackson, J. L., *Phys. Rev.*, **76**, 1540 (1949)
43. Davidson, J. P., Jr., *Phys. Rev.*, **82**, 48 (1951)
44. Hoff, R. W., and Rasmussen, J. O., *Phys. Rev.*, **101**, 280 (1956)
45. Gleditsch, E., and Graf, T., *Phys. Rev.*, **72**, 640 (1947)
46. Graf, T., *Phys. Rev.*, **74**, 831 (1948)
47. Ahrens, L. H., and Evans, R. D., *Phys. Rev.*, **74**, 279 (1948)
48. Hess, V. F., and Roll, J. D., *Phys. Rev.*, **73**, 916 (1948)
49. Stout, R. W., *Phys. Rev.*, **75**, 1107 (1949)
50. Sawyer, G. A., and Wiedenbeck, M. L., *Phys. Rev.*, **76**, 1535 (1949)
51. Spiers, F. W., *Nature*, **165**, 356 (1950)
52. Faust, W. R., *Phys. Rev.*, **78**, 624 (1950)
53. Graf, T., *Rev. Sci. Instr.*, **21**, 285 (1950)
54. Houtermans, F. G., Haxel, O., and Heintze, J., *Z. Physik*, **128**, 657 (1950)
55. Smaller, B., May, J., and Freedman, M., *Phys. Rev.*, **79**, 940 (1950)
56. Good, M. L., *Phys. Rev.*, **83**, 1054 (1951)
57. Delaney, C. F. G., *Phys. Rev.*, **82**, 158 (1951)
58. Burch, P. R. J., *Nature*, **172**, 361 (1953)
59. Suttle, A. D., Jr., and Libby, W. F., *Anal. Chem.*, **27**, 921–27 (1955)
60. Backenstoss, G., and Goebel, K., *Z. Naturforsch.*, **10A**, 920 (1955)
61. McNair, A., Glover, R. N., and Wilson, H. W., *Phil. Mag.*, **1**, 199 (1956)
62. Wetherill, G. W., *Science*, **126**, 545–49 (1957)
63. Feldman, L., and Wu, C. S., *Phys. Rev.*, **87**, 109 (1952)
64. Haxel, O., Houtermans, F. G., and Kemmerich, M., *Phys. Rev.*, **74**, 1886–87 (1948)
65. Kemmerich, M., *Z. Physik*, **126**, 399–409 (1949)
66. Curran, S. C., Dixon, D., and Wilson, H. W., *Phys. Rev.*, **84**, 151 (1951)
67. MacGregor, M. H., and Wiedenbeck, M. L., *Phys. Rev.*, **86**, 420–21 (1952)
68. Lewis, G. M., *Phil. Mag.*, **43**, 1070 (1952)
69. Geese-Bähnisch, I., and Huster, E., *Naturwissenschaften*, **41**, 495–96 (1954)
70. Flinta, J., and Eklund, S., *Arkiv Fysik.*, **7**, 401 (1954)

71. Libby, W. F., *Anal. Chem.*, **29**, 1566 (1957)
72. Aldrich, L. T., Wetherill, G. W., Tilton, G. R., and Davis, G. L., *Phys. Rev.*, **103**, 1045–47 (1956)
73. Inghram, M. G., *Ann. Rev. Nuclear Sci.*, **4**, 81 (1954)
74. Wetherill, G. W., Tilton, G. R., Davis, G. L., and Aldrich, L. T., *Geochim. et Cosmochim. Acta*, **9**, 292–97 (1956)
75. Aldrich, L. T., Davis, G. L., Tilton, G. R., and Wetherill, G. W., *J. Geophys. Research*, **61**, 215–32 (1956)
76. Aldrich, L. T., *Science*, **123**, 871 (1956)
77. Aldrich, L. T., Wetherill, G. W., and Davis, G. L., *Geochim. et Cosmochim. Acta*, **10**, 238–40 (1956)
78. Jamieson, R. T., and Schreiner, G. L. D., *Proc. Roy. Soc. (London)*, **B146**, 257–69 (1957)
79. Gast, P. W., Kulp, J. L., and Long, L., *Trans. Am. Geophys. Union*, **39**, 322–34 (1958)
80. Kulp, J. L., and Eckelmann, W. R., *Am. Mineralogist*, **42**, 154–64 (1957)
81. Holmes, A., and Cahen, L., *Colonial Geol. and Mineral Resources*, **5**, 3–38 (1955)
82. Holmes, A., *Proc. Geol. Assoc. Can.*, **7**, 81–105 (1955)
83. Wetherill, G. W., Wasserburg, G. J., Aldrich, L. T., Tiltion, G. R., and Hayden, R. J., *Phys. Rev.*, **103**, 987–89 (1956)
84. Powell, R. M., Pinson, W. H., Jr., Fairbairn, H. W., and Cormier, R. F., *Bull. Geol. Soc. Am.*, **68**, 1782 (1957)
85. Jeffery, P. M., *Geochim. et Cosmochim. Acta*, **10**, 191–95 (1956)
86. Wetherill, G. W., Davis, G. L., and Aldrich, L. T., *Trans. Am. Geophys. Union*, **38**, 412 (1957)
87. Gast, P. W., *Bull. Geol. Soc. Am.*, **68**, 1449–54 (1955)
88. Gerling, E. K., and Suhukoliukov, U. A., *Geokhimiya*, No. 3, 187 (1957)
89. Reynolds, J. H., *Geochim. et Cosmochim. Acta*, **12**, 177 (1957)
90. Wetherill, G. W., Aldrich, L. T., and Davis, G. L., *Geochim. et Cosmochim. Acta*, **8**, 171–72 (1955)
91. Gerling, E. K., and Morozova, I. M., *Geokhimiya*, No. 4, 304–11 (1957)
92. Gentner, W., Prag, R., and Smits, F., *Geochim. et Cosmochim. Acta*, **4**, 11 (1953)
93. Gentner, W., Goebel, K., and Prag, R., *Geochim. et Cosmochim. Acta*, **5**, 124 (1954)
94. Gentner, W., and Trendelenberg, E., *Geochim. et Cosmochim. Acta*, **6**, 261–67 (1954)
95. Curtis, G. H., and Reynolds, J. H., *Bull. Geol. Soc. Am.*, **69**, 151–60 (1958)
96. Damon, P. E., and Kulp, J. L., *Am. J. Sci.*, **255**, 697–704 (1957)
97. Tilton, G. R., and Nicolaysen, L. D., *Geochim. et Cosmochim. Acta*, **11**, 28–40 (1957)
98. Vinogradov, A. P., *Geokhimiya*, No. 5, 3–17 (1956)
99. Tilton, G. R., *Trans. Am. Geophys. Union*, **37**, 224–30 (1956)
100. Larsen, E. S., Jr., Keevil, N. B., and Harrison, H. C., *Bull. Geol. Soc. Am.*, **63**, 1045–52 (1952)
101. Tilton, G. R., Davis, G. L., Wetherill, G. W., and Aldrich, L. T., *Trans. Am. Geophys. Union*, **38**, 360–71 (1957)
102. Larsen, E. S., Jr., Waring, C. L., and Berman, J., *Am. Mineralogist*, **38**, 1118–25 (1952)
103. Damon, P. E., and Kulp, J. L., *Trans. Am. Geophys. Union*, **38**, 945–53 (1957)

104. Holland, H. D., *Nuclear Processes in Geologic Settings*, 85 (Natl. Acad. Sci., Natl. Research Council Publ. 400, Washington, D. C., 204 pp., 1955)
105. Fairbairn, H. W., and Hurley, P. M., *Trans. Am. Geophys. Union*, **38,** 99–107 (1957)
106. Lipson, J., *Bull. Geol. Soc. Am.*, **69,** 137–50 (1958)
107. Cormier, R. F., Herzog, L. F., Pinson, W. H., and Hurley, P. M., *Bull. Geol. Soc. Am.*, **67,** 1681 (1956)
108. Smits, F., and Gentner, W., *Geochim. et Cosmochim. Acta*, **1,** 22 (1950)
109. Folinsbee, R. E., Lipson, J., Reynolds, J. H., *Geochim. et Cosmochim. Acta*, **10,** 60 (1956)
110. Holmes, A., *Trans. Geol. Soc. Glasgow*, **21,** 145 (1947)
111. Naldrett, S. N., and Libby, W. F., *Phys. Rev.*, **73,** 487, 987 (1948)
112. Herr, W., Hintenberger, H., and Voshage, H., *Phys. Rev.*, **95,** 1691 (1954)
113. Gentner, W., and Kley, W., *Geochim. et Cosmochim Acta*, **12,** 323 (1957)
114. Dixon, D., and McNair, A., *Phil. Mag.*, **45,** 1099 (1954)
115. Herr, W., Merz, E., Eberhardt, P., and Signer, P., *Z. Naturforsch.*, **13A,** 268 (1958)
116. Glover, R. N., and Watt, D. E., *Phil. Mag.*, **2,** 699 (1957)
117. Gerling, E. K., Levski, L. K., and Afansjeva, L. I., *Doklady Akad. Nauk S.S.S.R.*, **109,** 813–15 (1956)
118. Volchok, H. L., and Kulp, J. L., *Geochim. et Cosmochim. Acta*, **11,** 219–46 (1957)
119. Piggot, C. S., and Urry, W. D., *Bull. Geol. Soc. Am.*, **53,** 1187 (1942)
120. Schaeffer, O. A., and Davis, R. *Ann. N. Y. Acad. Sci.*, **62,** 105 (1955)
121. Arnold, J. R., *Science*, **124,** 584 (1956)
122. Goldich, S. S., Baadsgaard, H., and Nier, A. O., *Trans. Am. Geophys. Union*, **38,** 547–51 (1957)
123. Baadsgaard, H., Goldich, S. S., Nier, A. O., and Hoffman, J. H., *Trans. Am. Geophys. Union*, **38,** 539–42 (1957)
124. Wickman, F. E., "Nuclear Processes in Geologic Settings," 62 *Natl. Acad. Sci.-Natl. Research Council Publ. 400*, 204 pp. (1955)
125. Wetherill, G. W., *Trans. Am. Geophys. Union*, **37,** 320–26 (1956)
126. Tilton, G. R., Wetherill, G. W., *et al.*, *Carnegie Inst. Wash. Yearbook*, **55,** 95 (1955–56)
127. Starik, I. E., *Geokhimiya*, No. 5, 18 (1956)
128. Giletti, B. J., and Kulp, J. L., *Am. Mineralogist*, **40,** 481 (1955)
129. Kuroda, P. K., *Ann. N. Y. Acad. Sci.*, **62,** 177 (1955)
130. Collins, C. B., Farquhar, R. M., and Russell, R. D., *Bull. Geol. Soc. Am.*, **65,** 1 (1954)
131. Eckelmann, W. R., and Kulp, J. L., *Bull. Geol. Soc. Am.*, **67,** 35 (1956)
132. Louw, J. D., *Trans. Geol. Soc. S. Africa*, **57,** 209 (1954)
133. Davidson, C. F., *Mining Mag.*, **92,** 152 (1955)
134. Ahrens, L. H., *Geochim. et Cosmochim. Acta*, **7,** 294 (1955)
135. Ahrens, L. H., *Geochim. et Cosmochim. Acta*, **8,** 1 (1955)
136. Wetherill, G. W., *Geochim. et Cosmochim. Acta*, **9,** 290 (1956)
137. Russell, R. D., and Ahrens, L. H., *Geochim. et Cosmochim. Acta*, **11,** 213 (1957)
138. Eckelmann, W. R., and Kulp, J. L., *Bull. Geol. Soc. Am.*, **68,** 1117–40 (1957)
139. Aldrich, L. T., Wetherill, G. W., and Davis, G. L., *Bull. Geol. Soc. Am.*, **68,** 655–56 (1957)

298 ALDRICH AND WETHERILL

140. Hurley, P. M., Pinson, W. H., Fairbairn, H. W., and Cormier, R. F., *Trans. Am. Geophys. Union*, **38**, 396 (1957)
141. Suttle, A. D., Jr., and Libby, W. F., *Phys. Rev.*, **95**, 866 (1954)
142. Carr, D. R., and Kulp, J. L., *Bull. Geol. Soc. Am.*, **68**, 763–84 (1957)
143. Fritze, V. K., and Strassman, F., *Z. Naturforsch.*, **11A**, 277–80 (1956)
144. Tilton, G. R., Patterson, C., Brown, H., Inghram, M., Hayden R., Hess, D., and Larsen, E. S., Jr., *Bull. Geol. Soc. Am.*, **66**, 1131–48 (1955)
145. Tilton, G. R., Aldrich, L. T., and Inghram, M. G., *Anal. Chem.*, **26**, 894–98 (1954)
146. Holmes, A., *Nature*, **173**, 612 (1954)
147. Herr, W., and Merz, E., *Z. Naturforsch.*, **13A**, 231 (1958)

NUCLEAR ASTROPHYSICS[1]

By A. G. W. CAMERON

Atomic Energy of Canada Ltd., Chalk River, Ontario, Canada

INTRODUCTION

Like many interdisciplinary subjects, that of nuclear astrophysics has had a very slow beginning, followed by a rapid spurt of activity during the last five years, when simultaneous progress in each of its parent fields reached the stage where experiments and calculations in nuclear physics could throw meaningful light on astrophysical observations. At the turn of the century Kelvin and Helmholtz had shown that release of gravitational potential energy would suffice to maintain the luminosity of the sun for some tens of millions of years, but it was soon realized that this was an insufficient source of solar energy, since the geologists found that many of the earth's rocks had ages nearly two orders of magnitude greater than the above figure. It was then proposed that the sun derived its energy from the disintegration of heavy elements such as uranium and thorium, but this theory also became inadequate when it was found that the sun was composed mostly of hydrogen and contained only very small traces of the heaviest elements. Eddington and Jeans thought that the source of solar energy must lie in the conversion of mass into energy, either in some total conversion process or through the transformation of hydrogen into heavier elements. Nuclear physics was then too young a science to allow these hypotheses to be investigated.

A vital step forward was taken when Atkinson & Houtermans (1) showed that charged particles had a small but finite probability of penetrating Coulomb potential barriers, and that there could thus be a slow but significant rate for the amalgamation of charged particles in stellar interiors at the temperature of several million degrees which had been calculated to exist there. It became apparent that solar-energy generation must result from energy release by exothermic nuclear reactions. The specific reactions responsible for the energy generation were established in papers by Bethe (2), Weizsacker(3) , and Bethe & Critchfield (4). More recent work has done much to improve our knowledge of the reaction rates involved (5, 6).

Meanwhile, it was becoming apparent to the astrophysicists that several classes of stars existed with abundances of certain elements which were strikingly different from those in normal stars. Many stars were found to have unusually large amounts of carbon; some of these also contained large excess abundances of heavy elements; and a few showed, in their spectra, strong lines of the unstable element technetium. A variety of other abundance anomalies was also present. It was thus evident that additional nuclear reactions must take place in stellar interiors. Salpeter (7) showed that helium could be converted into carbon and heavier elements. Cameron

---

[1] The survey of literature pertaining to this review was completed in March, 1958.

(8) and Greenstein (9) found a mechanism by which neutrons could be produced and captured by the heavy elements.

More detailed investigations of stellar abundances now showed that there were systematic differences in the abundances of the elements in stars formed recently as compared to those formed a long time ago. While there appeared to be little difference in the relative abundances of most of the elements, it was found that the fraction of the mass of a star composed of elements heavier than hydrogen was correlated with the age of the star, with very old stars commonly having only 10 per cent of the heavy-element content of the sun and recently formed stars usually having a larger fraction of heavy elements than the sun. It was also found that in addition to the obvious explosive ejection of matter from stars which occurs in novas and supernovas, a large number of stars were continuously emitting clouds of gas into space, presumably as a result of magnetic activity on their surfaces.

The resulting picture of a gradual enrichment of the interstellar medium in the ordinary heavier elements, as a result of nuclear processing in stellar interiors, acted as a spur to nuclear physicists to investigate other nuclear reactions which might be expected to occur under various conditions in stellar interiors. They were greatly assisted in this endeavour by the new semiempirical cosmic abundance distribution of Suess & Urey (10). These investigations were very successful and have resulted in a quantitative theory of the origin of the elements (11 to 17). The remainder of this article is largely a review of this theory and of the evidence supporting it.

The Stellar Populations

In the spring of 1957 a conference on the problem of stellar populations was held at the Vatican. The conclusions reached there have been summarized by Hoyle (18). It now appears necessary to recognize at least five distinct populations of stars in our galaxy. The oldest stars, with ages of about 6 to 7×10^9 years, include two populations, the Halo (or Extreme) Population II and the Intermediate Population II. The Halo group is nearly spherical, extends very far out into space, and consists of stars whose content of elements heavier than helium is very variable but averages about 0.3 per cent by weight. The Intermediate Population II stars occupy a somewhat more flattened region, and their heavy-element contents are of the order of 1 per cent, or a little less. These two populations contain about 15 to 20 per cent of the mass of the galaxy.

Most of the mass of the galaxy is contained in the Disk Population, a very flattened group of stars with ages 4 to 6×10^9 years. The heavy-element content varies from 1 to 2 per cent. The group includes our sun which has a heavy-element content of 1.5 per cent.

The younger stars belong to the Older (or Intermediate) Population I and the Extreme Population I. The latter is most closely associated with the gas and dust in the galaxy. Perhaps about 10 per cent or a little less of the mass of the galaxy consists of these populations of stars. The heavy-

element content ranges up to about 4 per cent. These stars are closely associated with the gas and dust in the spiral arms of the galaxy.

Only about 2 per cent of the mass of the galaxy is in the form of gas and dust. Most of this material is concentrated in the spiral arms, although low-density, high-velocity gas clouds also form a spherical halo around the galaxy. The rate of star formation in the spiral arms appears sufficient to exhaust the gas there in less than 10^9 years, but this gas seems to be replenished by ejection from the large number of stars in the central regions of the galaxy.

STELLAR EVOLUTION

The physical quantities of interest in stellar interiors include temperature, density, gas pressure, radiation pressure, radiative opacity, chemical composition, rate of energy generation, and rate of energy transport. These quantities are functions of position in the star. They are related by four differential equations and by several physical laws (19). With these equations it is possible to construct a complete model of a star and then follow the changes which take place in the structure of the star as nuclear reactions change the chemical composition of the interior. However, this is a problem of considerable mathematical difficulty which requires numerical integration of the differential equations. The history of the subject has been one of using successively better approximations in the numerical treatment. Future progress requires the use of high-speed computers; it is limited at the present time by the great cost of computing time. For example, Hoyle estimates that it requires about 100 hr. of computing time to follow the evolution of one star of specific mass and initial chemical composition on an I.B.M. 704 computer. It would be desirable to follow the evolution of at least 100 such stars of different characteristics. However, 704 computing time usually rents for several hundred dollars per hour.

Astrophysicists find it very useful to plot diagrams correlating the surface temperatures and luminosities of stars. These diagrams are sometimes called "Hertzsprung-Russell diagrams." The points representing most of the stars in such diagrams fall within a narrow band called the "main sequence." Most of the rare and unusual types of stars, such as red giants, white dwarfs, many types of variables, and pre- and postnovas are plotted in separate regions of the Hertzsprung-Russell diagram away from the main sequence. One of the major problems in the study of stellar evolution is to determine how the points representing various kinds of stars move within the Hertzsprung-Russell diagram as the stars evolve.

When a mass of gas condenses from the interstellar medium, the gravitational potential energy which is released is partly stored as internal heat, raising the internal temperature, and partly radiated from the surface into space. When the central temperature reaches the vicinity of 10^6 °K. the deuterium is destroyed by thermonuclear reactions (20). In a star like the sun the energy so released may halt the contraction process for several million years. At somewhat higher temperatures the small amounts of

lithium, beryllium, and boron present are destroyed in reactions with hydrogen, forming as products He^3 and He^4. Then the contraction is halted, the star settles onto the "main sequence," and the energy generation now results from the conversion of hydrogen to helium by reactions to be discussed in the following section. For a star like the sun the contraction process probably took between 50 and 100 million years.

It takes a long time for the conversion of hydrogen to helium to take place in the central regions of most stars. The age of the sun is probably about 4.5×10^9 years, or perhaps slightly more. In this time about half of the original hydrogen at the center has been converted to helium (21). The central temperature and density have risen slightly to maintain the energy generation rate. The total luminosity of the sun has risen about 60 per cent over its original value since it first settled on the main sequence. Since the mean surface temperature of the earth can be expected to vary approximately as the fourth root of the solar luminosity, it appears likely that the mean surface temperature was lower than the freezing point of water until about 2×10^9 years ago, and, therefore, conditions were probably less favourable for the propagation of life in the remote past.

For a star of about 1.25 times the mass of the sun, a typical value for older stars evolving away from the main sequence, the hydrogen will be exhausted in the central regions in about 5×10^9 years (22). A slight further contraction must then set in until the central temperature is raised and the burden of energy generation is taken up by the hydrogen gas surrounding the helium core. For about another 10^9 years this "shell source" of energy continues to convert hydrogen into helium in regions of the star progressively farther from the center. At the same time a major structural change takes place in the star. Numerical integrations of the differential equations of the stellar interior show that the helium core contracts by a large factor; eventually densities in the vicinity of 10^5 gm./cm.^{3} are reached at the center. The outer envelope of the star expands by a large factor. The star has now become a "red giant." Its luminosity has increased by a factor of several hundred over that which it had on the main sequence, but the surface area is so large that the surface temperature is quite low. Some stars start ejecting clouds of gas at this stage in their evolution (23).

Thermonuclear reactions normally are very sensitive to temperature, but stars usually have a built-in regulatory mechanism which prevents thermonuclear reactions from "running away" and causing an explosion. If we consider a local rise of temperature, the thermonuclear reaction rates will be increased, but the gas will expand until the temperature falls and the thermonuclear reactions are quenched. However, at densities in the vicinity of 10^5 gm./cm.^{3} the Pauli exclusion principle causes the electrons to form a degenerate gas with a very high thermal conductivity. The regulatory mechanism no longer works. Most of the energy resides in the electrons and only a small amount in the ions, so that the properties of the gas are very insensitive to the temperature. Eventually the temperature of the central

stellar regions reaches about 10^8 °K. At this point helium thermonuclear reactions commence. When the energy generation from these reactions exceeds the outward flux of energy, the gas heats and expands rapidly until it becomes nondegenerate and the normal regulatory mechanism quenches the helium reactions. The large amount of energy generated during the core expansion may cause internal mixing between the hydrogen and helium regions in the star.

The further evolution of the star has not yet been followed by quantitative calculations based on evolutionary model sequences. Stars in later stages of evolution appear to lose mass. Some of them may attain very high values of central temperature and density. It is possible to calculate in a general way the chemical evolution of these stars simply by assuming higher temperatures and seeing what nuclear reactions then become possible. In this way many anomalous abundances of the elements which appear to exist in some stars in advanced stages of evolution can be explained.

Eventually all the stars appear to end their existence as white dwarf stars. These are very compact structures in which the electrons form a degenerate gas. Their average mass is about 0.6 times that of the sun (24). The degeneracy pressure of the electrons prevents these stars from contracting, and hence they contain no nuclear energy sources, but are gradually radiating away their internal heat. This is a process that requires many billions of years.

HYDROGEN THERMONUCLEAR REACTIONS

Until recently the study of stellar structure and evolution has not required very exact knowledge of thermonuclear reaction rates. The reason for this is that stellar models were not very well determined, and an error in the energy generation rate could be compensated by a small change in temperature. The situation has now changed, however, since stellar models, particularly of the sun, have been greatly improved. Interest has also arisen in the chemical evolution of a star. Since the relative rates of two thermonuclear reactions which give different product nuclides are very much less sensitive to temperature than the reaction rates themselves, it has become important to determine these rates as accurately as possible.

In a hot gas the number of nuclear reactions of one kind per cm.^{3} per second is $r = n_1 n_2 \langle \sigma v \rangle$ where n_1 and n_2 are the number densities of the reacting particles, v is the velocity of the particles in the center-of-mass system, and σ is the cross section for the reaction at the velocity v. At any temperature the probability distribution of velocities is the Maxwell distribution; at higher velocities the most important factor in the distribution function is e^{-cv^2}, where c is a constant. The charged particles must penetrate their mutual Coulomb barrier with energies small compared to the barrier height. Under such circumstances the dominant factor in the barrier penetration probability is $e^{-c'/v}$ where c' is a constant. The product of these two exponential functions is strongly peaked at about 5 or 10 times kT under normal

conditions of interest. The major contribution to the thermonuclear reaction rate comes from bombarding energies in this optimum range unless there is a nearby resonance, in which case the resonance energy is preferred. Such resonances can increase thermonuclear reaction rates by as much as five or six orders of magnitude. Furthermore, at the fairly high densities present in stellar interiors, electron shielding can lower the effective Coulomb barrier height, but this effect usually increases the reaction rates by less than a factor two.

For a nonresonant thermonuclear reaction the number of reactions per second per nucleus of type 2 is (5):

$$p = 4.34 \times 10^5 \frac{\rho x_1 (A_1 + A_2) S}{A_1^2 A_2 Z_1 Z_2} \tau^2 e^{-\tau} \text{ sec.}^{-1}$$

where

$$\tau = 42.48 \left[\frac{Z_1^2 Z_2^2 A_1 A_2}{A_1 + A_2} \right]^{1/3} T^{-1/3}$$

and

$$S = \sigma(E) E \exp \left[31.28 Z_1 Z_2 \left(\frac{A_1 A_2}{A_1 + A_2} \right)^{1/2} E^{-1/2} \right] \text{kev barn,}$$

and Z_1, Z_2, A_1, A_2 are the charge and mass numbers of the reacting particles, ρ is the density of the gas in gm./cm.^{3}, x_1 is the fractional concentration by weight of the particles of type 1, T is the temperature in units of 10^6 °K., and E is the bombarding energy in kev in the center-of-mass system. The nuclear reaction function S is approximately constant when there are no resonances near the optimum thermonuclear bombarding energy.

The nuclear cross sections at optimum thermonuclear bombarding energies are much too small to be measured in the laboratory. Progress in nuclear astrophysics has thus depended on calculations of these cross sections from nuclear theories and on the measurement of the cross sections at relatively low laboratory energies and extrapolation to the thermonuclear region, sometimes with the help of nuclear dispersion theory. In the case of resonant thermonuclear reactions, it is necessary to determine the appropriate properties of the nuclear state involved.

The main source of energy generation in the sun and in other stars of lesser luminosity is the proton-proton chain, or, more correctly, one of several proton-proton chains. These chains are shown in Figure 1. The basic reaction in all of them is $H^1(p, \beta^+\nu)D^2$. The probability that a beta decay will take place during the small interval that two protons are in collision is extremely small, but nevertheless it can be calculated from the known properties of the nuclear two-body system and from beta-decay theory (5, 16, 17). The cross-section factor is $S = 28.5(1+0.008\ E) \times 10^{-23}$ kev barn ± 10 per cent. The error in this reaction rate is compounded about equally between the uncertainty in the Gamow-Teller coupling constant in beta decay and in the calculation of the matrix element for the transition (5). L. Heller (private

PROTON-PROTON CHAINS

$$H^1(p,\beta^+\nu)\,D^2(p,\gamma)\,He^3(He^3,2p)\,He^4$$
$$\searrow(\alpha,\gamma)\,Be^7(e^-,\nu)\,Li^7(p,\alpha)\,He^4$$
$$\searrow(p,\gamma)\,B^8(\beta^+\nu)\,Be^8(\alpha)\,He^4$$
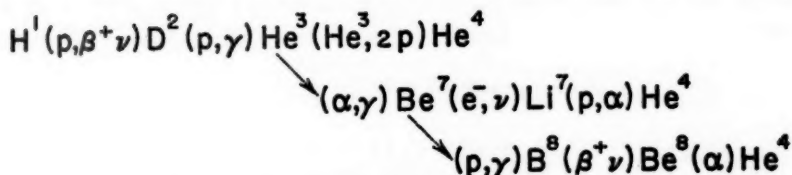
Fig. 1. The proton-proton chains of reactions.

communication) has investigated the effects of vacuum polarization on the reaction rate; he finds the factor S to be decreased by approximately 1.5 per cent because of this effect. He also finds the transition matrix element to be more uncertain than supposed by Saltpeter.

The second reaction in the chains, $D^2(p, \gamma)He^3$, has the rather small cross-section factor $S = 7.8 \times 10^{-5}$ kev barn (25), but since it follows a reaction so very much slower, the deuterium is very rapidly destroyed in stellar interiors.

There are two possible reactions by which the He^3 can be destroyed. At smaller temperatures He^3 builds up to a fairly large equilibrium abundance and the principal destructive reaction is $He^3(He^3, 2p)He^4$, with $S = 1.2 \times 10^3$ kev barn (17). This reaction forms one He^4 nucleus for each two proton-proton reactions.

At higher temperatures the He^3 concentration in equilibrium becomes much smaller, and the principal destructive reaction becomes $He^3(\alpha, \gamma)Be^7$. The cross-section factor for this reaction has recently been found to be 0.7 kev barn [(26) and private communication from Holmgren]. This reaction rate is very much larger than had previously been estimated (5), and the reaction is very likely an example of a direct capture reaction. In such reactions, if there are states in the compound nucleus with only small binding energy and a large reduced width for the bombarding particle, there is a relatively large cross section for the bombarding particle (with appropriate angular momentum) to be captured by an electric dipole transition. The cross section for this process must be calculated directly rather than from nuclear dispersion theory because almost all of the contributions to the transition matrix element can come from outside the usual nuclear radius (27).

It appears that the $He^3(\alpha, \gamma)Be^7$ reaction was of little importance in the sun when it was first formed, but now with a slightly higher central temperature and a larger He^4 concentration, it appears that the $He^3(\alpha, \gamma)Be^7$ reaction predominates in the central regions of the sun (27).

The next branch in the proton-proton chains occurs when we consider mechanisms for the destruction of Be^7. In stellar interiors this nucleus is completely ionized almost all the time, but it can decay by capturing one

of the free electrons present. The rate for this process has been estimated for
a system of high temperature and low density by replacement of the wave-
function for a K electron at the nucleus by that for a free electron (27); the
result is

$$p_{\text{electron capture}} = 1.9 \times 10^{-9} \frac{(1 + x_{\text{H}})}{T^{1/2}} \text{ sec.}^{-1} ,$$

where the symbols are as before and x_{H} is the fractional concentration by
weight of hydrogen. At higher densities this capture rate is probably some-
what reduced.

Be^7 can also be destroyed by the Be$^7(p, \gamma)$B^8 reaction. Since the last
proton in B^8 is bound by only 136 kev, it is likely that the rate for this
reaction is fairly large owing to the direct capture process; one factor that
limits it is the reduction in the reduced proton width of the ground state
caused by the coupling between equivalent particles. Cameron (27) estimates
the reaction rate constant to be about 0.8 kev barn. Christy & Duck [quoted
in (28)] estimate this quantity to be 0.2 kev barn. According to these esti-
mates the rate of formation of B^8 is somewhat less than that of the electron
capture of Be^7 at the center of the sun.

If B^8 is formed, it rapidly beta-decays to Be^8 in the 3-Mev excited state,
which in turn rapidly becomes two α-particles. The rate of formation of He^4
is twice that in the case of the He^3(He^3, $2p$)He^4 reaction, since one He^4
nucleus is formed for each proton-proton reaction, regardless of whether
Be^7 captures protons or electrons. However, if B^8 is formed, the effective
rate of energy generation per proton-proton reaction is not doubled, since
about 27 per cent of the energy of He^4 formation is lost from a stellar in-
terior in the form of the high-energy neutrinos emitted in the decay of B^8.
These neutrinos have an average energy of about 7 Mev.

Cameron (27) has estimated that the flux of B^8 neutrinos at the earth is
about 2×10^9 cm.$^{-2}$ sec.$^{-1}$. According to R. Davis, Jr. (private communica-
tion) this flux should be detectable by the Cl$^{37}(\nu, e^-)$A^{37} reaction if more
than 10,000 gallons of CCl$_4$ are placed in a deep mine. It is expected that
neutrinos from the sun will drive this reaction, whereas neutrinos from a
reactor will not, if the two-component neutrino hypothesis (51) is correct.
If a 10,000-gallon CCl$_4$ experiment should give a positive result, then Reines
(private communication) estimates that a meaningful negative result in the
D$^2(\bar{\nu}, \beta^+)2n$ reaction can be obtained with a slightly enlarged Cowan-Reines
apparatus (29) placed in a deep mine. This reaction is expected to be induced
by reactor but not solar neutrinos. These experiments may eventually help
to establish a fundamental point in beta-decay theory.

Red giant stars have deep outer convective envelopes. If the convection
extends down to depths at which Be^7 is formed, then a small but greater than
natural equilibrium abundance of the decay product Li^7 may be maintained
at the surface (8, 27). Many red giant stars do show unusually strong lines
of lithium (52 to 55).

Massive stars and stars with shell-energy sources obtain most of their energy generation by the carbon-nitrogen-oxygen cycles. The CNO cycles are shown in Figure 2. The most accurate measurements of the cross-section factors for these reactions have been made with a high-current ion source at Livermore (30, 31). For $C^{12}(p, \gamma)N^{13}$, $S = 1.2$ kev barn, and for $N^{14}(p,\gamma)O^{15}$, $S = 2.8$ kev barn. It is possible that the $N^{14}(p, \gamma)O^{15}$ reaction may have a thermal resonance, since there is one more level in the appropriate region of excitation energy in the mirror nucleus N^{15} than has been found in O^{15}; but since typical level shifts between mirror nuclei are of the order of 1 Mev, the chances are small that this resonance occurs in the region of the thermo-nuclear bombarding energies, which is only a few kev wide.

CARBON-NITROGEN-OXYGEN CYCLES
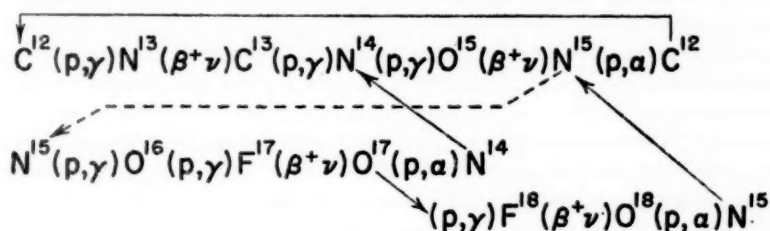
Fig. 2. The carbon-nitrogen-oxygen cycles of reactions.

For the $C^{13}(p, \gamma)N^{14}$ reaction, older measurements give $S = 6 \pm 2$ kev barn (6). Preliminary measurements at Livermore (W.A.S. Lamb and R. E. Hester, private communication) give a value twice as large, but these cannot yet be considered reliable. The ratio of abundances of the C^{12} and C^{13} isotopes at equilibrium in the carbon-nitrogen cycle is of particular astrophysical interest. From analyses of molecular bands caused by the C_2 molecule in red giant stars, it has been found (56) that the ratio of C^{12} to C^{13} abundances commonly lies in the range of 3 to 4; in other stars and on earth it is very large. With the older values of S quoted above, the carbon-nitrogen cycle equilibrium abundance ratio is 4.3 ± 1.6, in agreement with the idea that carbon has been processed into CN equilibrium abundance ratios in many of the red giant stars.

The first branching point in the CNO cycles occurs when we consider proton reactions with N^{15}. For $N^{15}(p, \alpha)C^{12}$, $S = (1.1 \pm 0.3) \times 10^5$ kev barn. This is much the fastest of the CN cycle reactions, and the equilibrium abundance of N^{15} is correspondingly very low. The other possible reaction is $N^{15}(p, \gamma)O^{16}$. Old estimates of the cross-section factor (16) gave $S = 11$ kev barn. However, it now appears that the rate of this reaction is enhanced by interference between nearby levels, and it may be as much as an order of magnitude larger than previously thought. Hence the branching ratio for proton capture lies in the range 10^{-3} to 10^{-4}. This represents an appreciable

possible leakage of C and N isotopes to O^{16}, since the CN part of the CNO cycles may be traversed of the order of 10^3 times before hydrogen has been completely converted into helium in a star.

Cross sections for the reaction $O^{16}(p, \gamma)F^{17}$ have recently been measured by Tanner and Pixley at the California Institute of Technology, by Lamb, Hester, and Pixley at Livermore, and by Griffiths and Robertson at the University of British Columbia (private communications). Their results give $S = 6 \pm 2$ kev barn. This is another direct capture reaction. Under typical temperature conditions in hot stars, this indicates that the destruction of O^{16} is two orders of magnitude slower than the $N^{14}(p, \gamma)O^{15}$ reaction, which is the slowest of the CN cycle. This rate is sufficient to deplete O^{16} by a large factor before hydrogen is exhausted in a star.

The subsequent reactions are faster than the destruction of O^{16}, owing to the larger reaction widths associated with exothermic charged-particle emission. Most of the O^{16} nuclei are fed into the CN cycle via the $O^{17}(p, \alpha)N^{14}$ reaction. The smaller number that branch via the $O^{17}(p, \gamma)F^{18}$ reaction will be almost completely fed into the CN cycle by the $O^{18}(p, \alpha)N^{15}$ reaction. The cross-section factors for these reactions have not yet been measured. Because O^{16} is destroyed faster than it is replenished by leakage from the CN cycle, in full equilibrium in the CNO cycles the ratios of C to N to O nuclei will be about 1 to 100 to x, where $1 < x < 10$. These numbers are slightly sensitive to temperature. They are essentially in agreement with the abundances determined to be in the ratios 0.25 to 100 to 8 for the highly-evolved star HZ44 (32). In this case it would appear that the CN part of the cycle had been frozen with an equilibrium abundance characteristic of 10×10^6 °K.

Hydrogen thermonuclear reactions with heavier nuclei are also of interest. The small amount of fluorine in a star is fed into the CNO cycles by the $F^{19}(p, \alpha)O^{16}$ reaction. The cross-section factor for the $Ne^{20}(p, \gamma)Na^{21}$ reaction has been measured at Livermore (33); the results imply $S = 60$ kev barn for energies of astrophysical interest. At the higher hydrogen consumption temperatures of shell source giant stars, the Ne^{20} will thus be largely converted to Ne^{21}. There is considerable interest in the fate of the Ne^{21} so formed which can be destroyed by the $Ne^{21}(p, \gamma)Na^{22}$ reaction. Marion & Fowler (34) estimate that little Ne^{21} destruction will occur, whereas Cameron (16) believes that most of the Ne^{21} will be destroyed. In view of the possible importance of Ne^{21} for neutron production, an experimental clarification of the situation is most desirable. It is likely that significant modifications of the Ne^{22} and Na^{23} abundances will also occur via the reactions $Ne^{22}(p, \gamma)Na^{23}$ and $Na^{23}(p, \alpha)Ne^{20}$.

HELIUM THERMONUCLEAR REACTIONS

He^4 is stable in stellar interiors until very high temperatures are reached because Li^5 is unstable to proton emission and Be^8 is unstable to α-particle emission. However, the Be^8 decay energy is 94 kev, which is only about 10

kT for temperatures $T \sim 10^8$ °K. Hence the rate of formation of Be^8 in the hot, dense helium core of a red giant star can become appreciable. A statistical mechanical calculation shows that one part in 10^9 of the helium will be in equilibrium in the form of Be^8 at 10^8 °K and 10^5 gm./cm.^{3}. This amount is very small, but the $Be^8(\alpha, \gamma)C^{12}$ is a resonant thermonuclear reaction, and the formation of C^{12} can start by this process when the temperature and density reach the indicated values. The resonance level concerned is the second excited state of C^{12} at 7.65 Mev.

It has been shown (35) that this state decays into three α-particles, and that the reverse process is therefore possible. On the likely but not completely proved assumption that this state is $0+$, Ferrell [quoted in (35)] has calculated a width of 1.4×10^{-3} ev for the electric quadrupole transition to the first excited state at 4.43 Mev, with a possible error of a factor two, although he now believes that the possible error may be larger than this (private communication). Radiation to the ground state would not be expected since 0-to-0 transitions are forbidden, but it is disturbing that the actual radiative mode of decay of the 7.65 Mev level has not yet been established experimentally. The ratio of the α-particle width to that for a 3.22 Mev radiation is at least 1000 (W. A. Fowler, private communication).

Because the α-particle width is so much larger than the radiation width of the 7.65 Mev state, the rate of formation of C^{12} can be calculated from statistical mechanical considerations. To a good approximation, a small abundance of the 7.65 Mev state exists in equilibrium with helium; C^{12} is formed by radiative leakage from this state (35, 36). A determination of the radiation width of this state, either for 3.22 Mev radiation or perhaps for a transition to some other possible level in the range 4.43 to 7.65 Mev, is very desirable.

Once C^{12} has been formed, further helium capture reactions are possible. The $C^{12}(\alpha, \gamma)O^{16}$ reaction is nonresonant. Most of the reaction cross section probably is contributed by the Breit-Wigner tail of the 7.12 Mev level in O^{16} (27, 36). However, the next reaction, $O^{16}(\alpha, \gamma)Ne^{20}$, may be resonant, since the 4.97 Mev level in Ne^{20} lies very near the optimum thermonuclear bombarding energy. Only states which have spin and parity either both even or both odd can be formed by combining α-particles with O^{16}. It has been found experimentally (37) that the 4.97 Mev level is $1\pm$, $2\pm$, or $3+$, with $1\pm$ considered unlikely. Thus if the 4.97 Mev state can be formed by the $O^{16}(\alpha, \gamma)Ne^{20}$ reaction, it would have to be $2+$ or perhaps $1-$.

Cameron (16) among others (13, 38, 39) has solved the differential equations for the formation and destruction of C^{12}, O^{16}, and Ne^{20} in helium thermonuclear reactions. He finds that at very high rates of energy generation most of the reactions form only C^{12}, with little processing of C^{12} to heavier nuclei. However, if the $O^{16}(\alpha, \gamma)Ne^{20}$ reaction is resonant and the 4.97 Mev level has not too small a reduced α-particle width, then at low rates of energy generation there is an efficient processing of material into the form of Ne^{20}. Practically no processing of material beyond Ne^{20} is to be expected.

Among highly evolved stars are "helium stars" and Wolf-Rayet stars which appear to show effects caused by helium thermonuclear reactions (57). Many of these stars show no lines of hydrogen; these often have very strong lines of carbon. Those with weak lines of hydrogen usually show very weak carbon lines and very strong nitrogen lines, suggesting the formation of carbon followed by processing in the CN cycle. There does not appear to be any case in which oxygen is much enhanced, although several cases exist with unusually strong neon lines. These latter stars suggest that the $O^{16}(\alpha, \gamma)Ne^{20}$ reaction is indeed resonant. It is also probable that the giant carbon stars have large carbon abundances because of carbon formation by helium burning.

Neutron Capture on a Slow Time Scale

In addition to the principal helium thermonuclear reactions described in the preceding section, additional reactions with less abundant isotopes are of interest because of the neutron production which results from them. The reactions which may be of greatest importance in this connection are $C^{13}(\alpha, n)O^{16}$ and $Ne^{21}(\alpha, n)Mg^{24}$. These reactions can provide prolific sources of neutrons only if certain assumptions are correct.

We have seen that the equilibrium abundance of C^{13} in the carbon cycle is very small. Therefore, very few neutrons result from reactions with the C^{13} remaining after hydrogen exhaustion in a star. However, it has been postulated that when the main helium reactions start in a red giant star, enough C^{12} can be formed in the core expansion process to allow the formation of much C^{13} when the hydrogen and helium regions of the star mix. The optimum condition for producing neutrons and having them available for capture in heavy elements is the mixing ratio of about 1 proton per 10 C^{12} nuclei. This allows substantial amounts of C^{12} to be converted to C^{13}, but only a small amount of the C^{13} is further processed to N^{14} (16). Because of the rather large cross section for the $N^{14}(n, p)C^{14}$ reaction, N^{14} is a poison which competes strongly with heavy elements for the neutrons.

The abundance of Ne^{21} originally present in a star is also very small and would give few neutrons. The $Ne^{21}(\alpha, n)Mg^{24}$ reaction can be an important neutron source only if appreciable quantities of Ne^{21} are formed in hot shell sources by the $Ne^{20}(p,\gamma)Na^{21}$ reaction and are not destroyed by the $Ne^{21}(p, \gamma)Na^{22}$ reaction. This is a question which must be settled by nuclear-physics experiments, in contrast to the $C^{13}(\alpha, n)O^{16}$ problem which must be settled by astrophysical calculations. If the $Ne^{21}(\alpha, n)Mg^{24}$ reaction is important, it will take place in the later stages of helium consumption in a stellar core when the temperature is 1.6×10^8 °K. or more. At this time N^{14} may have been destroyed by the $N^{14}(\alpha, \gamma)F^{18}$ reaction and N^{14} may, therefore, not act as a poison for heavy-element synthesis. It is desirable to obtain more information about the F^{18} compound nucleus in order to see whether this will happen.

When the neutrons are produced they interact mostly with the overwhelmingly abundant He^4, which cannot capture them but moderates them

until they are in thermal equilibrium with their surroundings. The expected temperatures of formation range from 1.0 to 1.6×10^8 °K., and the neutrons in thermal equilibrium have Maxwell distributions peaked near 10 to 15 kev. These neutrons are then captured by the nuclides present in proportion to the abundances and capture cross sections of those nuclides.

The changes in the abundances of nuclei produced by neutron capture have been calculated by Cameron (16). He assumed the initial composition of the heavy nuclei to be that given by Suess & Urey (10), which is illustrated in Figure 3. These abundances have been deduced from astrophysical, geochemical, and meteoritic analyses and have been smoothed using empirical rules of nuclear regularities. The actual values of Suess and Urey have been modified in Figure 3 to achieve a compromise with solar abundance determinations made at the University of Michigan (L. H. Aller, private communication). It may be noted that the gross features of the abundance distribution consist of a general decrease with increasing mass number up to about $A = 100$, followed by roughly constant abundances, with a superposed giant peak centered about Fe^{56}. There are many finer details. All these features must be explained as resulting from various nuclear reactions in
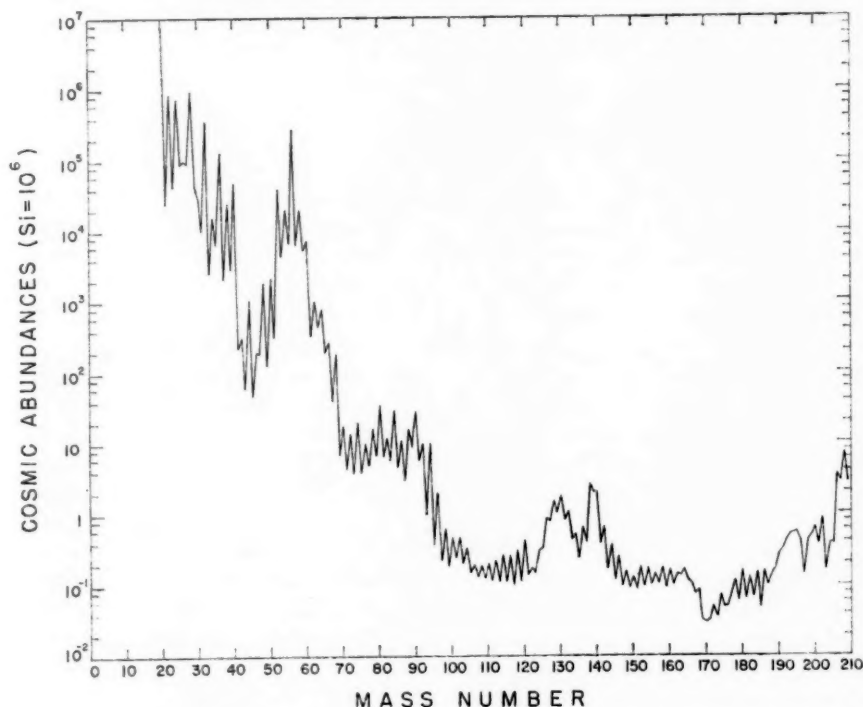
FIG. 3. The cosmic abundances of the mass numbers according to Suess and Urey, slightly modified by Cameron to achieve a compromise with University of Michigan determinations of solar abundances.

stars before one can justify the general theory of nucleogenesis indicated in the introductory section.

Neutron capture cross sections averaged over resonances depend on neutron strength functions, level spacings, and radiation widths. Cameron (16) computed average cross sections at 11 kev using the best experimental and theoretical knowledge of these quantities available in 1956. Better cross sections could now be calculated, but the general features of the earlier calculation are unlikely to be changed. The neutron capture cross sections are greatly reduced at the positions of closed neutron shells. Hence, in the neutron capture process, nuclei with closed neutron shells will be much more abundant than neighbouring nuclei.

When neutrons are first introduced into the natural abundance mixture of the elements, most of them are captured by the nuclei of the iron abundance peak. The average time between neutron captures in a given nucleus probably lies in the range 1 to 10^5 years, so that most radioactive nuclei formed have a chance to decay before another neutron is captured. As the capture proceeds, the original iron-peak nuclei become spread out over the entire range of higher mass numbers, increasing the abundances of heavy elements by large "overabundance" factors. Neutron capture beyond bismuth leads to a region of short-lived α-particle emitters which decay to lead isotopes, so nuclei accumulate at the upper end of the capture chains as lead and bismuth isotopes. The solution of the abundance equations following the injection of 20 neutrons per initial silicon atom is shown in Figure 4. It may be seen that abundances in the heavy-element region have been increased by factors of several thousand. Only certain isotopes are synthesized in this way, since there is almost always only one stable nuclide formed per mass number by neutron capture on a slow time scale. The abundances of the heavy nuclei formed in this way depend on the iron peak abundances initially present in the star and not on the original abundances of heavier nuclei themselves. Thus this process uses the products of high-temperature processes (see next section) in other stars which have previously exploded.

The most striking evidence for the existence of neutron capture on a slow time scale is provided by the presence of technetium lines in the spectra of giant stars of classes S and N (the latter are carbon stars). The longest-lived isotope of this element is Tc^{99}, with a half life of 2×10^6 years. This isotope is one of the "stable" members of the capture path for neutron capture on a slow time scale. S stars generally have increased abundances of heavier elements, although very few quantitative analyses have yet been made. Carbon stars appear to show evidence for increased abundances of heavy elements, but the excess abundances are smaller, indicative of a greater dilution of the neutron capture products at the surface. Barium stars also show increased abundances of heavy elements, but no lines of technetium, which may have decayed in these objects. Burbridge & Burbridge (40) have analyzed the abundances in one barium star and find them to be consistent with synthesis by neutron capture on a slow time scale.
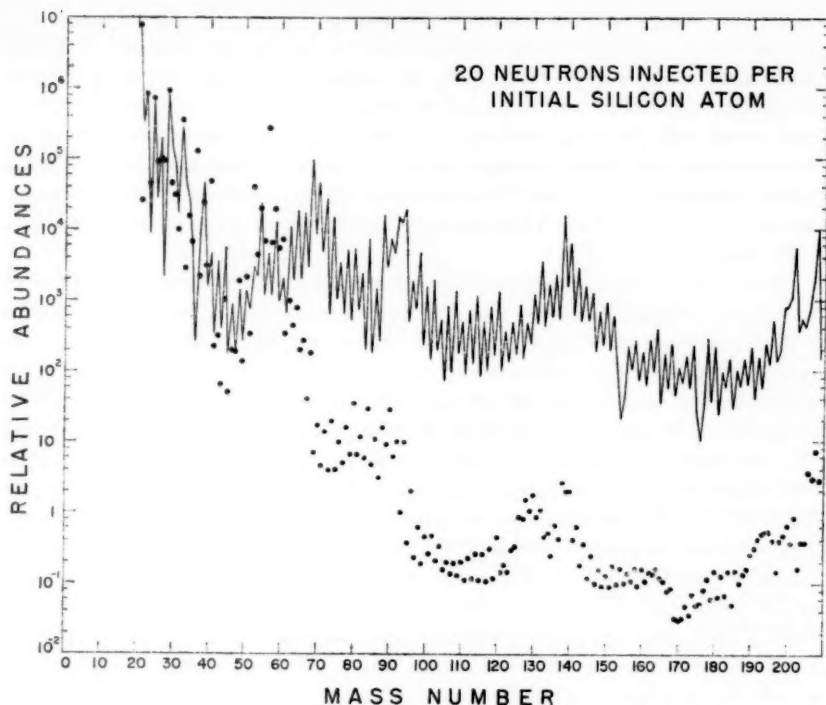
FIG. 4. Changes in the cosmic abundances of the mass numbers produced by the capture of 20 neutrons injected per original silicon atom. The dots show the initial abundance distribution.

REACTIONS AT VERY HIGH TEMPERATURES

After the exhaustion of helium in a stellar core, the material is inert in a thermonuclear sense until the temperature rises to the vicinity of 10^9 °K. At this and higher temperatures many different nuclear reactions can take place and it becomes increasingly difficult to follow the course of the chemical evolution of the star. The discussions of these reactions that have appeared (13, 16, 17) have been only qualitative. Quantitative calculations are very desirable.

Following helium exhaustion, with allowance for possible mixing of the products with hydrogen, the principal constituents of the gas may be C^{12}, N^{14}, O^{16}, and Ne^{20}. In the vicinity of 10^9 °K., reactions between these products can take place. Usually the emission of neutrons, protons, and α-particles in these reactions is exothermic, and these particles will quickly be captured by other nuclei present. In this way many different nuclei in the mass range 20 to 30 can be formed. The reactions mentioned may be called heavy-ion thermonuclear reactions.

At the same time certain photonuclear reactions take place. The $Ne^{20}(\gamma, \alpha)O^{16}$ reaction is one of the first to set in. At somewhat higher temperatures, (γ, n), (γ, p), and (γ, α) reactions can take place in various nuclei. These particles are expected to initiate a series of synthesizing reactions which will form elements out to the region of calcium and titanium. Photoneutron reactions interspersed with positron emission and electron capture will destroy the heavy elements which were formed by neutron capture on a slow time scale. This process may be called photodisintegration on a slow time scale.

If the central temperature of a star becomes 3×10^9 °K. or more, then all nuclei are subject to very fast photodisintegration. The particles thus ejected are very quickly captured by other nuclei. It is hopeless at the present time to try to follow these reactions in detail, but from statistical mechanics the equilibrium abundances of the various nuclear species can be calculated. The only uncertainties in this calculation are those associated with the energies and angular momenta of the low-lying levels of the nuclei with which we are concerned. It turns out that in the temperature range 3 to 5×10^9 °K. the nuclei with the greatest binding energies per nucleon are those with the largest equilibrium abundances. This gives a sharp abundance peak centered about Fe^{56}. Burbridge *et al.* (17) have performed these calculations for a variety of temperatures, densities, and ratios of neutrons to protons, and they have also estimated the changes which will occur in these distributions when the gas containing them is suddenly cooled. Their results are shown in Figure 5, where they are compared with solar abundances measured at the University of Michigan. It may be seen that the equilibrium-frozen abundances agree very well with those in the sun over most of the iron peak, differing only at the base of the peak at a level where nuclei can be produced by other mechanisms.

In the equilibrium process some nuclei with fairly high abundances are unstable to positive and negative beta decay. The neutrinos and antineutrinos emitted in such decays escape from the star with negligible interactions. The loss of energy in this form helps to promote the slow collapse of the stellar core, raising the central temperature and density. This may be called the Urca process, following Gamow & Schoenberg (41), although the details of the process are considerably different from the ones they envisaged.

When the temperature exceeds about 5×10^9 °K. the nature of the equilibrium abundance distribution changes radically. There is still a local peak centered about Fe^{56}, but the most abundant nucleus becomes He^4. The change from favouring Fe^{56} to favouring He^4 by a large factor occurs over a narrow range of temperatures and density. The combinations of temperature and density corresponding to the transition region are plotted in Figure 6.

If the representative point of the center of a star crosses the transition line in Figure 6, then the iron peak nuclei there must be converted to He^4. This is a very endothermic process. The energy for the conversion can only be obtained at the expense of the gravitational potential energy of the core. Therefore, the core must undergo a major collapse with a time scale of only
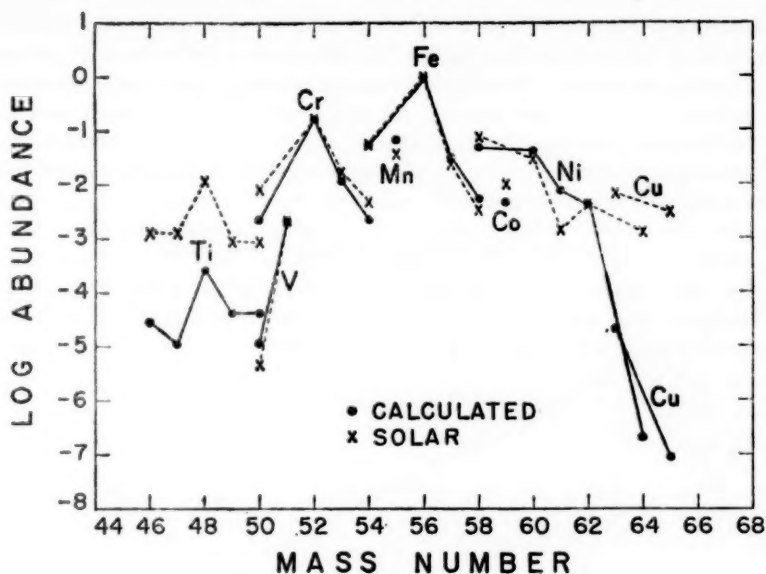
FIG. 5. The equilibrium-frozen abundances of the iron peak nuclei computed by Burbidge, Burbidge, Fowler, and Hoyle and compared with the solar abundance determinations made at the University of Michigan.
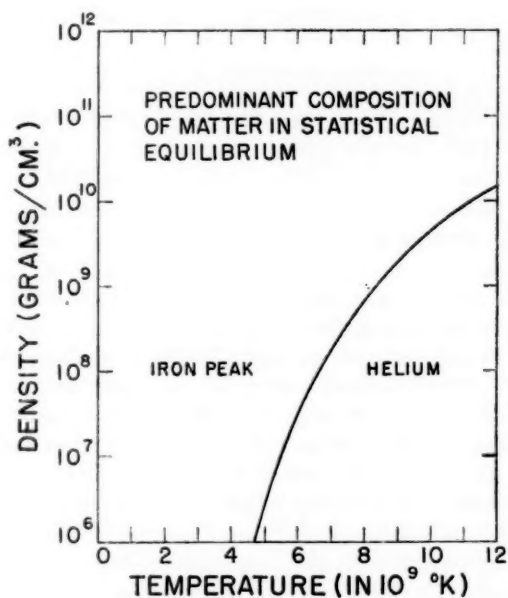
FIG. 6. A temperature-density diagram showing the regions in which the iron peak and helium abundances are predominant.

a few seconds. The outer layers of the star, collapsing in their turn, are suddenly heated to temperatures of 10^8 °K. or more by the release of gravitational potential energy. These outer layers are likely to contain hydrogen and helium, and the rapidity of the nuclear reactions at such high temperatures will cause a thermonuclear explosion in which much of the outer mass of the star is blown off into space with a high velocity. This gives a convincing picture of a supernova explosion.

NEUTRON CAPTURE ON A FAST TIME SCALE

The light curves of supernovas fall into two classes, called Types I and II. The best measured light curve for a supernova of Type I, that for the supernova in IC 4182 measured by Baade (42, 43), is shown in Figure 7.
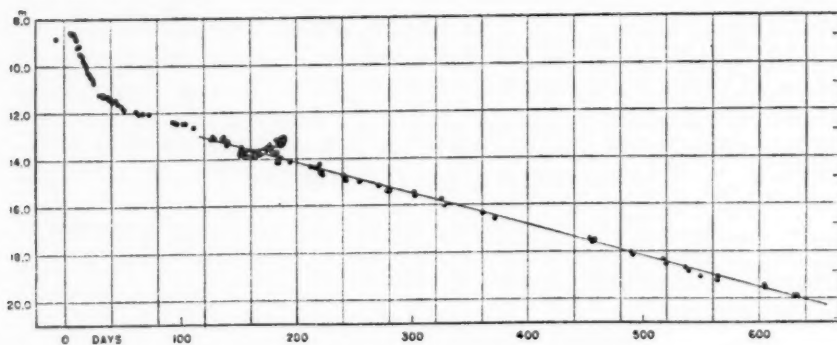
FIG. 7. Light curve of the Type I supernova in IC 4182, measured by Baade.

The characteristic feature here is the long straight exponential tail, although it must be emphasized that the straightness of the exponential decay in the last half of the curve is very uncertain because of possible errors in the normalization and calibration of the photographic magnitude scale for faint magnitudes. Type II supernovas do not exhibit this exponential tail in their light curves.

It has been suggested that the exponential tails of Type I supernovas are produced by some radioactivity decaying with their half life of 55 ± 1 days (14, 44). The most promising activity for this purpose appears to be Cf^{254}. This isotope decays predominantly by spontaneous fission. Other nuclei decaying predominantly by spontaneous fission have half lives much shorter than 55 days. Hence Cf^{254} releases very much more energy than any other nuclides with comparable half lives which may be formed, and thus the single decay period of this one nuclide can dominate the light curve. Nevertheless, other activities present may produce a light curve with a slightly different apparent half life from that of its principal contributor. There are at present two conflicting but accurate measurements of the Cf^{254} half life: 56.2 ± 0.7 days (45) and 61 ± 1 days (S. G. Thompson, private communication).

Cf^{254} can be synthesized in a supernova explosion only as the result of a

neutron capture process which proceeds on a fast time scale. Let us defer for the moment the question of a suitable source of neutrons and consider what happens when heavier elements are exposed to a very high neutron flux at a temperature of about 5×10^8 °K.

The capture path for the fast time scale is illustrated in Figure 8. Starting with Fe[56] as an example, neutrons are captured in rapid succession until the neutron binding energy falls so low that photoneutron emission takes place at the same rate as neutron capture. At the stated temperature this will occur in the vicinity of a neutron binding energy of 2 Mev. When a nucleus has
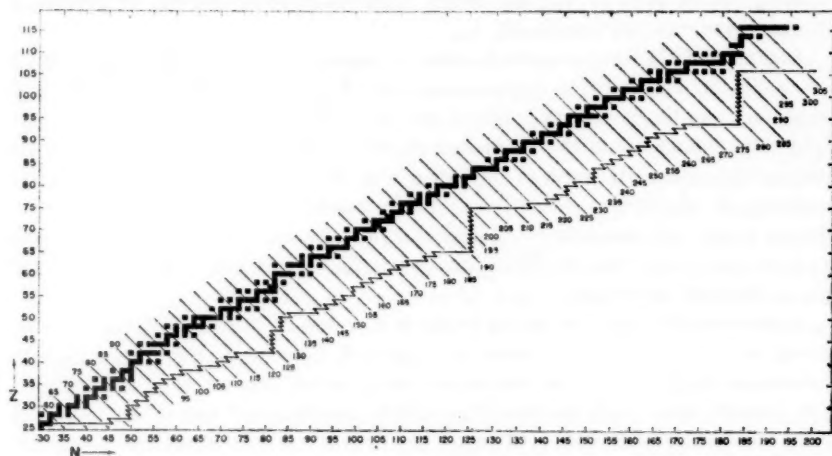
FIG. 8. Illustrative capture path for neutron capture on a fast time scale. In the diagram the number of protons in the nucleus is plotted against the number of neutrons, the positions of beta-stable nuclei are plotted as black squares, and the neutron capture path is shown as the jagged line starting with Fe[56]. Diagonal lines denote mass numbers.

reached this point on the diagram it must wait until a beta decay takes place (with a half life usually < <1 sec.). Further neutron capture then follows until the next beta-decay waiting point is reached. Figure 8 was constructed from a shell-corrected table of neutron binding energies (46) with the illustrative assumption that all waiting points occur just before the first isotope with a neutron binding energy of less than 2 Mev. It may be noted that at the closed neutron shells the capture path approaches the valley of beta stability more closely than usual. In equilibrium the abundances of the nuclides on the capture path are proportional to the beta-decay half lives at the waiting points. Since these half lives are considerably longer near the valley of beta stability, the nuclides with closed neutron shells may be expected to be formed with greater abundances in neutron capture on a fast time scale.

When a nucleus reaches a very large mass number, further neutron capture will lead to fission. The point at which this occurs is very uncertain. With differing views about the systematics of the fission process, Burbridge

et al. (17) believe fission occurs at about $A = 260$, whereas Cameron (16) believes that it does not occur until about $A = 287$, when the nucleus has reached the next hypothetical closed shell of 184 neutrons. Following fission the two fragments will capture further neutrons.

Burbridge *et al.* (14, 17) have postulated that neutrons are produced in a layer of the supernova in which the abundances of hydrogen and of elements in the vicinity of neon are comparable. In the explosion the hydrogen is rapidly exhausted, forming proton-rich nuclides of mass numbers beyond 20. Some of these, such as Na^{21} and Al^{25}, quickly decay by positron emission, forming nuclei, such as Ne^{21} and Mg^{25}, from which neutrons can be produced by exothermic (α, n) reactions.

Cameron (27) has computed neutron capture cross sections (at 55 kev) for nuclei on the neutron capture path of Figure 8. He finds that typical cross sections lie in the vicinity of one millibarn. On the other hand, the lighter nuclides formed by the proton capture reactions, which can decay by positron emission, all undergo exothermic (n, p) reactions with cross sections probably of the order of one barn. These nuclei would, therefore, quickly absorb nearly all the neutrons, and the protons released would regenerate positron emitters. Hence this is an unsatisfactory reaction mechanism for heavy-element synthesis.

Cameron (27) has attempted to make a virtue of this difficulty by postulating the reaction cycles shown in Figure 9. Here it is assumed that the amount of hydrogen before the explosion is much smaller than that of C^{12}. It is rapidly consumed by the $C^{12}(p, \gamma)N^{13}$ reaction. N^{13} has a half life of 10 min., but one per cent of it will decay to C^{13} in 10 sec. Neutrons are produced by the $C^{13}(\alpha, n)O^{16}$ reaction; the $N^{13}(n, p)C^{13}$ reaction replaces the C^{13}, and the $C^{12}(p, \gamma)N^{13}$ reaction replaces the N^{13}. In order to produce much Cf^{254},

NEUTRON PRODUCTION IN SUPERNOVAS
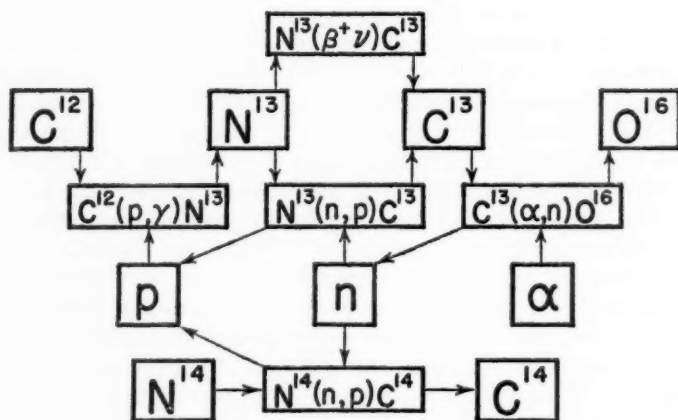
FIG. 9. A suggested cycle of reactions which may be responsible for neutron production and capture on a fast time scale.

about 100 or more neutrons should be captured on the average per initial Fe^{56} nucleus. The $N^{13}(n, p)C^{13}$ reaction has a cross section of 1.1 barn at 55 kev (47). It follows that there should be about 10^5 C^{12} nuclei per Fe^{56} nucleus in the exploding layer. However, according to the tables of Suess & Urey (10), only about 10^4 C^{12} nuclei will be available if all the hydrogen and most of the helium are converted to C^{12}. Hence this postulate fails by one order of magnitude.

Because of this, Cameron (27) has postulated that the hydrogen is exhausted by the C^{12} $(p, \gamma)N^{13}(\beta^+\nu)C^{13}$ reactions before the explosion begins. It is inevitable that some of the C^{13} produced will be further processed to N^{14}, but with the small amount of hydrogen postulated the C^{13}/N^{14} ratio may easily be 10 or more. The $N^{14}(n, p)C^{14}$ cross section is only 1.4 millibarn (Macklin and Gibbons, private communication), so that this reaction does not take place until the heavy nuclei have reached the first waiting points. The protons released then induce the remaining cycles of Figure 9, but a C^{12}/Fe^{56} ratio of 10^4 is now sufficient to allow the synthesis of large amounts of Cf^{254}. Even so, there is not much freedom in the initial composition required to obtain this result. In Population II stars with a much smaller iron abundance, there is much more freedom in the initial composition needed for Cf^{254} synthesis, and this may be why Type I supernovas seem to occur mainly among Population II stars. The mechanism shown in Figure 9 may be the principal source of O^{16} formation in nature.

There is another possible neutron source which has not yet been investigated in detail [(17) and Hoyle, private communication]. When Fe^{56} is converted to helium in a supernova explosion, 13 He^4 nuclei and 4 neutrons are produced. If the dynamics of the explosion process cause some of this material to be ejected into cooler regions, some of the He^4 may recombine to form light elements, and neutron capture on a fast time scale may start with them.

OTHER REACTIONS ON A FAST TIME SCALE

In the previous considerations it was necessary to assume small mixtures of hydrogen with other elements. Presumably some explosions occur (particularly Type II supernovas lacking exponential light curve tails) in which there is much hydrogen in the exploding layers. In these cases hydrogen will not be exhausted in reactions with light elements. Just as in the case of neutron capture, proton capture on a fast time scale will add protons to nuclei until waiting points are reached at which (p, γ) and (γ, p) reaction rates are equal; following positron emission further proton addition can occur. But proton addition rates are very much slower than neutron addition rates and become increasingly slower as the nuclear charge increases. Nevertheless, some proton addition may occur to even very heavy nuclei which are present before the explosion starts.

If such exploding layers are raised to temperatures in the vicinity of 2.5×10^9 °K., rapid photoneutron emission from heavy elements will occur until the neutron binding energy becomes about 4 Mev larger than the proton binding energy. Then proton emission will be followed by further

neutron emission (16). These are photodisintegration reactions on a fast time scale.

Both of these sets of reactions can form some beta-stable heavy nuclei which do not lie on any neutron capture paths.

ANALYSIS OF NUCLIDE ABUNDANCES

We have seen that the nuclei with $12 \leq A < 70$ can be synthesized in a variety of reactions, and it is difficult in many cases to decide which mechanism has been more important in any given case. For heavier nuclei fewer mechanisms have been operative and analysis is easier.

In Figure 10 are shown the Suess-Urey abundances of nuclei with odd mass numbers. The distinctive features of this curve have been interpreted as follows (12, 15, 16, 17, 48): The sharp peaks at mass numbers 90, 140, and 208 correspond to nuclei with closed shells of 50, 82, and 126 neutrons. They are attributed to formation by neutron capture on a slow time scale. The broad peaks at mass numbers 80, 130, and 195 have a reduced odd-even mass number variation, as may be seen in Figure 3. They are attributed to formation by neutron capture on a fast time scale on the parts of the capture path which approach the valley of beta stability at closed neutron shells (see Fig. 8). The reduced odd-even effect is expected because there should be essentially no odd-even effect in the beta-decay half lives at these waiting points.

The secondary peak at $A = 164$ is more controversial. It may be seen from Figure 3 that the odd-even effect is reduced here also, and hence the peak must be attributed to neutron capture on a fast time scale. Burbridge *et al.* (17) attribute it to a "stabilization" effect which results in approximate constancy of neutron binding energies for deformed nuclei. They expect that
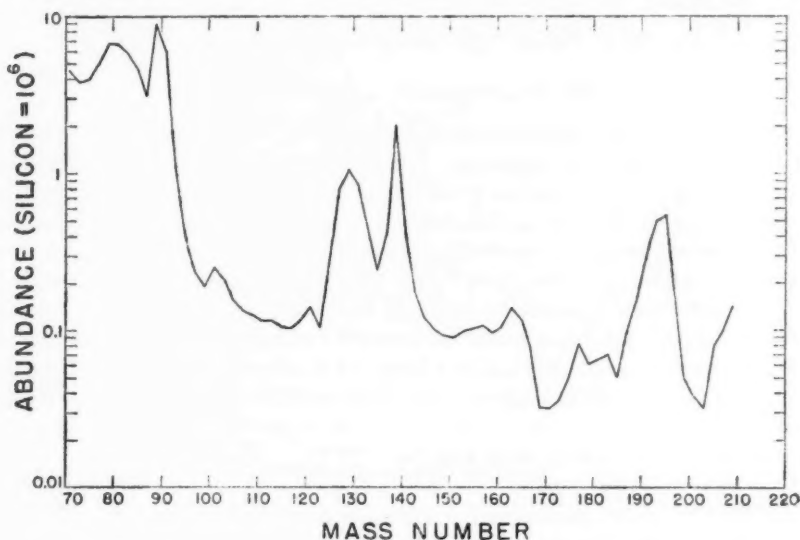
FIG. 10. The abundances of odd mass numbers according to Suess and Urey.

the capture path will approach the valley of beta stability to some extent, thus leading to larger equilibrium abundances. However, this suggested effect does not occur in Figure 8, although the "stabilization" effect is present in the masses from which the figure was constructed. Cameron (16) explains the peak as a fission fragment peak formed when the hypothetical abundance peak at $A = 287$ fissions following the termination of neutron production. The other fission peak would lie at $A = 123$ where it is hidden in the shoulder of the broad peak there. The resolution of this question is important for geophysical considerations. Burbridge *et al.* (17) expect another "stabilization" peak around $A = 250$ which would increase the natural abundance of uranium and thorium. Cameron does not expect an effect of this kind.

The abundances of different kinds of isobars give additional information. We may define a shielded isobar as one which lies on the neutron capture path for the slow time scale and to which synthesis on a fast time scale cannot contribute. The latter contributions go instead to an unshielded isobar of the same mass number which lies on the neutron-rich side of the slow-time-scale capture path. Some isobars cannot be formed by neutron capture at all; these will be called excluded isobars. They may be formed by proton capture and by photodisintegration on a fast time scale; a few of them are also formed by photodisintegration on a slow time scale.

The Suess-Urey abundances of these three classes of isobars are plotted in Figure 11. The unshielded isobars, shown by circles, exhibit all the characteristics which were noted in the odd-A abundances and attributed to neutron capture on a fast time scale. The shielded isobars, attributed to the slow time scale and shown by triangles, exhibit different trends. Lack of isobars near closed neutron shells has eliminated most of the evidence for
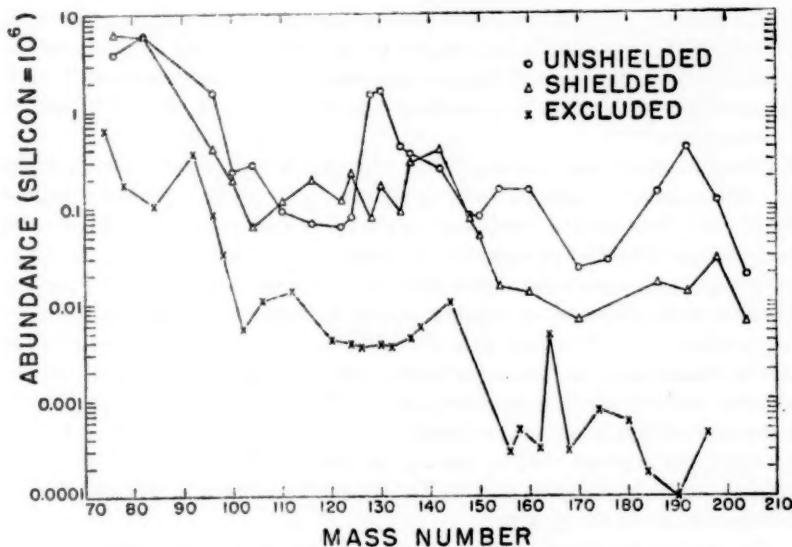
Fig. 11. The abundances of three classes of isobars according to Suess and Urey.

the abundance spikes there, but it may be noted that the general level of abundances below $A = 140$ is about a factor of five higher than the level above $A = 140$. This satisfactorily reproduces a trend, shown in Figure 4, which is very insensitive to the number of neutrons captured on the slow time scale. The excluded isobars, shown by crosses, are expected to be formed from the products of neutron capture on a slow time scale, and it is satisfactory to find that the triangles and crosses have the same general trends. Above $A = 150$ there are four high abundances among the excluded isobars and six low abundances. The four high cases represent nuclei which can be formed by photodisintegration on both fast and slow time scales. The six low cases can be formed on the fast time scale only. Below $A = 150$ no such effects are visible, and it is probable that proton capture on a fast time scale has been the dominant mode of production there.

Nuclear Reactions on Stellar Surfaces

The previous discussion seems to give a satisfactory account of the formation in stellar interiors of He^4, Li^7, and nuclides with $A \geq 12$. D^2, Li^6, Be^9, B^{10}, and B^{11} are not synthesized in significant amounts in stellar interiors, and their natural abundances are very low. However, it appears possible that they may be made in stellar surface reactions.

Many stars of spectral types A and F seem to be just evolving away from the main sequence, so that only hydrogen thermonuclear reactions have been operative. They have intense surface magnetic fields, often amounting to several thousand gauss averaged over a hemisphere. These fields are often variable with a period of a few days; quite often the sign of the surface field changes during the period. The spectra of these stars usually show unusually strong and variable lines of certain elements, many of which appear to be greatly increased in abundance in certain patches on the stellar surface. The elements Si, Cr, and Mn often appear to be overabundant by moderate factors of 2 to 10; Sr, Y, and Zr can be overabundant by factors of 20 to 30; and the rare earths can be overabundant by factors of several hundred or thousand.

These increases are not consistent with any interior nuclear activity, but they have been interpreted as resulting from stellar surface reactions (16, 17, 49). Two sets of conditions appear to be necessary to explain all the observations. The first of these is the acceleration of a portion of the charged particles of the surface gas, probably by the Fermi mechanism in twisted magnetic fields (58) near star spots, to energy distributions given by a power law, probably $\sim E^{-3}$, where E is the particle energy. Heavier particles can also be accelerated to the same energy per proton if they are stripped of electrons early in the acceleration process. The important nuclear reactions produced by these reactions are spallation reactions and probably some particle addition reactions such as (α, n), $(\alpha, 2n)$, $(\alpha, 3n)$, as well as heavy-ion collisions such as $O^{16}(O^{16}, \alpha)Si^{28}$. The neutrons produced are captured by hydrogen to form deuterium.

The second mechanism appears to be the formation of limited regions of hot plasma with kinetic temperatures ~ 1 Mev. In such regions the ions have

a Maxwellian distribution of energies, and only the collisions of singly charged particles are effective in inducing nuclear reactions. But combinations of (p, γ), (d, p), and (d, n) reactions can drive heavier nuclei up the valley of beta stability. It is proposed that the large rare-earth overabundances are synthesized in this way.

These magnetic variable stars are very rare in space, and they cannot have synthesized the natural abundances of the light elements. However, it is not unlikely that most stars pass through a period of intense surface magnetic activity when they are forming from the interstellar medium and getting rid of most of the entrapped magnetic field. There is some preliminary evidence for such activity in contracting stars (50). Most of the lightest elements may have been produced under such circumstances.

Much fuller accounts of these various processes in nuclear astrophysics appear in the two main summaries of the field which have been prepared (16, 17).

Pycnonuclear Reactions and Stellar Explosions[2]

It was shown in this article that the conversion of significant quantities of Fe^{56} into Cf^{254} was a marginal process under the supernova explosion conditions which were postulated. It appeared that very small quantities of hydrogen must be mixed throughout a major fraction of the star in a region consisting mostly of C^{12} and He^4. While this appeared to be a possible mechanism, it was not an appealing one, and was adopted only because no better mechanism appeared possible.

Since the article was written the writer has been investigating the problem of nuclear reactions at high densities. This investigation was prompted by the consideration that only very massive stars may be able to evolve and contract quickly enough to drive the central temperature over the threshold for the iron-to-helium conversion process. Stars of smaller mass may start cooling after reaching some stage of nuclear evolution at their centers, particularly after having formed the statistical iron peak. The tendency for cooling will be offset by the tendency of the star to contract and release gravitational potential energy. The maximum amount of matter (not containing hydrogen) which can form a stable white dwarf configuration is 1.21 solar masses (59), and the oldest stars now evolving off the main sequence have masses in excess of this. Therefore, unless the mass of the star can be greatly reduced by continuous emission of gas, the contraction of the star must continue until something catastrophic takes place or nuclear densities are attained.

At very high densities, electron shielding neutralizes the nuclear charge at a relatively small distance from the nucleus, and the ions of low energy have very much smaller classical turning points than at low densities. In fact, it turns out that the classical turning points depend only slightly on the bombarding energies of the ions. The barrier penetrabilities are much greater for these ions than at low densities because of the decreased thickness

[2] Note added June, 1958.

of the barrier. When the density becomes high enough the barrier penetrability becomes nearly independent of the bombarding energy, and the entire Maxwellian distribution of ion energies participates with about equal probability in producing nuclear reactions. Reaction rates are then much more sensitive to density than to temperature, and it appears more logical to describe nuclear reactions taking place under these circumstances as "pycnonuclear" reactions (Gr. *pyknos;* compact, dense).

When stellar contraction reaches a point where a region containing helium and carbon attains a density of about 4×10^6 gm./cm.^{3}, the pycnonuclear reaction rate becomes large enough so that the rate of energy generation will exceed the rate at which energy can be transmitted by conduction (the degenerate gas has a very high thermal conductivity) to the surface and there radiated. The gas must then heat until a sufficient amount of it has become nondegenerate and has expanded so that what have become thermonuclear reactions are quenched. Since density conditions are more extreme than those encountered at the center of red giant stars, the process of heating and expansion is likely to be more violent. Hence, this appears to be the mechanism of the ordinary nova explosion. Other reactions may trigger nova explosions: for example, the combination of two C^{12} ions in the reactions $C^{12}(C^{12}, p)Na^{23}$ and $C^{12}(C^{12}, \alpha)Ne^{20}$ sets in at a density of 2×10^9 gm./cm.^{3} After the first such explosion it is quite likely that both C^{12} and He^4 will be mixed to the center of the star.

After expelling a small amount of mass in a nova explosion, the star will evidently radiate the remaining energy released in the explosion and will then contract again. If the central temperature is near 2×10^7 °K., then more exact calculations show that the $C^{12}(\alpha, \gamma)O^{16}$ pycnonuclear reactions will trigger another explosion when the central density becomes about 2.5×10^6 gm./cm.^{3} Evidently the star must undergo a series of explosions until sufficient mass has been lost to allow a stable configuration to be reached with a central density less than 2.5×10^6 gm./cm.^{3} or until helium has been exhausted at the center of the star (and presumably throughout most of the volume). Since the average white dwarf star has a central density of 2×10^6 gm./cm.^{3} (24), it appears that the former alternative is the one usually occurring.

If the material at the center of the star has been converted into iron peak nuclei, and if the central density can reach 2×10^{11} gm./cm.^{3} without a pycnonuclear explosion occurring in the outer layers, then the central regions of the star must collapse. The reason for this is that the Fermi level of the electrons becomes so high (about 25 Mev) that the iron peak nuclei will capture enough electrons to become nuclei which are unstable to neutron emission. Schatzman (60) has shown that stars of this kind, which have a mean molecular weight per electron which increases toward the center, are dynamically unstable. A series of rapid electron captures and neutron emissions takes place until the nuclei have been reduced to the vicinity of Mg^{33}. The nuclei then fuse to form new nuclei with mass numbers in the vicinity of 60. The outer layers of the star will also collapse, heat, and explode as in the previously suggested supernova mechanism.

If the linear dimensions at the center of the star decrease by a factor three, and the density by a corresponding factor of about 30, then the bulk of the material will have been converted to neutrons, with only enough nuclei left to maintain the Fermi level of the electrons at about 25 to 30 Mev. The average mass number of these nuclei will be about 40, and for every such nucleus there will be about 1000 neutrons present. After the outer layers of the star have exploded some of this inner core will also expand, and it will be exploded away from the star when the Fermi level of the electrons drops and the neutrons are captured on a fast time scale. In this way quite adequate amounts of Cf^{254} can be produced to account for the light curves of Type I supernovas.

According to this picture the more massive stars of Population I may undergo supernova explosions by the iron-to-helium conversion mechanism, but it is unlikely that much production of Cf^{254} will take place in them. The less massive stars of Population II are likely to undergo nova explosions and settle down as white dwarf stars with an average mass of about 0.6 solar masses, or to undergo supernova explosions by the iron-to-neutron conversion process with the production of large quantities of Cf^{254}. This picture appears to be in accord with the observed facts concerning nova and supernova explosions (61).

LITERATURE CITED

1. Atkinson, R., and Houtermans, F., *Z. Physik.*, **54,** 656 (1928)
2. Bethe, H. A., *Phys. Rev.*, **55,** 434 (1939)
3. Weizsacker, C., *Physik, Z.*, **39,** 633 (1938)
4. Bethe, H. A., and Critchfield, C. L., *Phys. Rev.*, **54,** 248 (1938)
5. Salpeter, E. E., *Phys. Rev.*, **88,** 547 (1952)
6. Fowler, W. A., *Mém. soc. roy. sci. Liège*, **14,** 88 (1954)
7. Salpeter, E. E., *Astrophys. J.*, **115,** 326 (1952)
8. Cameron, A. G. W., *Phys. Rev.*, **93,** 932 (1954); *Astrophys. J.*, **121,** 144 (1955)
9. Greenstein, J. L., in *Modern Physics for the Engineer* (Ridenour, L., Ed., McGraw-Hill Book Co., Inc., New York, N. Y., 267 pp., 1954)
10. Suess, H. E., and Urey, H. C., *Revs. Modern Phys.*, **28,** 53 (1956)
11. Fowler, W. A., Burbridge, G. R., and Burbridge, E. M., *Astrophys. J.*, **122,** 271 (1955)
12. Cameron, A. G. W., *Atomic Energy of Canada Ltd., CRP-652* (1956)
13. Hoyle, F., *Astrophys. J.*, Suppl. 1, 121 (1954)
14. Burbridge, G. R., Hoyle, F., Burbridge, E. M., Christy, R. F., and Fowler, W. A., *Phys. Rev.*, **103,** 1145 (1956)
15. Cameron, A. G. W., *Publs. Astron. Soc. Pacific*, **69,** 201 (1957)
16. Cameron, A. G. W., *Atomic Energy of Canada Ltd., CRL-41* (1957)
17. Burbridge, E. M., Burbridge, G. R., Fowler, W. A., and Hoyle, F., *Revs. Modern Phys.*, **29,** 547 (1957)
18. Hoyle, F., in *Proc. Conf. on the Problem of Stellar Populations* (In press, 1958)
19. Chandrasekhar, S., *An Introduction to the Study of Stellar Structure* (Dover Publishers, New York, N. Y., 509 pp., 1957)
20. Salpeter, E. E., *Phys. Rev.*, **97,** 1237 (1955)
21. Schwarzschild, M., Howard, R., and Harm, R., *Astrophys. J.*, **125,** 233 (1957)
22. Hoyle, F., and Schwarzschild, M., *Astrophys. J.*, Suppl. 2, ¹ ′1955)
23. Deutsch, A. J., *Astrophys. J.*, **123,** 211 (1956)

24. Greenstein, J. L., *Handbuch der Phys.*, **50**, 161 (1958)
25. Heller, L., *Astrophys. J.*, **126**, 341 (1957)
26. Holmgren, H. D., and Johnston, R. L., *Bull. Am. Phys. Soc.*, **3**, 26 (1958)
27. Cameron, A. G. W., *Atomic Energy of Canada, Ltd.*, *CRL-41*, 2nd ed. (1958)
28. Fowler, W. A. (To be published, 1958)
29. Cowan, C. L., and Reines, F., *Phys. Rev.*, **107**, 1609 (1957)
30. Lamb, W. A. S., and Hester, R. E., *Phys. Rev.*, **107**, 550 (1957)
31. Lamb, W. A. S., and Hester, R. E., *Phys. Rev.*, **108**, 1304 (1957)
32. Munch, G., *Astrophys. J.* (To be published, 1958)
33. Pixley, R. E., Hester, R. E., and Lamb, W. A. S., *Bull. Am. Phys. Soc.*, **2**, 377 (1957)
34. Marion, J. B., and Fowler, W. A., *Astrophys. J.*, **125**, 221 (1957)
35. Cook, C. W., Fowler, W. A., Lauritsen, C. C., and Lauritsen, T., *Phys. Rev.*, **107**, 508 (1957)
36. Salpeter, E. E., *Phys. Rev.*, **107**, 516 (1957)
37. Gove, H. E., Litherland, A. E., and Ferguson, A. J., *Bull. Am. Phys. Soc.*, **3**, 36 (1958)
38. Nakagawa, K., Ohmura, T., Takebe, H., and Obi, S., *Progr. Theoret. Phys.* (*Kyoto*), **16**, 507 (1956)
39. Hayakawa, S., Hayashi, C., Imoto, M., and Kikuchi, K., *Progr. Theoret. Phys.* (*Kyoto*), **16**, 507 (1956)
40. Burbridge, E. M., and Burbridge, G. R., *Astrophys. J.*, **126**, 357 (1957)
41. Gamow, G., and Schoenberg, M., *Phys. Rev.*, **59**, 539 (1941)
42. Mayall, N. U., *Sci. Monthly*, **66**, 17 (1948)
43. Baade, W., Burbridge, G. R., Hoyle, F., Burbridge, E. M., Christy, R. F., and Fowler, W. A., *Publs. Astron. Soc. Pacific*, **68**, 296 (1956)
44. Borst, L. B., *Phys. Rev.*, **78**, 807 (1950)
45. Huizenga, J. R., and Diamond, H., *Phys. Rev.*, **107**, 1087 (1957)
46. Cameron, A. G. W., *Atomic Energy of Canada Ltd.*, *CRP-690* (1957)
47. Macklin, R. L., and Gibbons, J. H., *Bull. Am. Phys. Soc.*, **3**, 26 (1958)
48. Coryell, C. D., *Mass. Inst. Technol. Lab. Nuclear Sci. Ann. Progr. Rept.* (1956)
49. Fowler, W. A., Burbidge, G. R., and Burbidge, E. M., *Astrophys. J.*, Suppl. **2**, 167 (1955)
50. Hunger, K., and Kron, G. E., *Publs. Astron. Soc. Pacific*, **69**, 347 (1957)
51. Lee, T. D., and Yang, C. N., *Phys. Rev.*, **105**, 1671 (1957)
52. McKellar, A., and Stillwell, W. H., *J. Roy. Astron. Soc. Can.*, **38**, 237 (1944)
53. Sanford, R. F., *Astrophys. J.*, **99**, 145 (1944)
54. Fujuta, Y., *Astrophys. J.*, **124**, 155 (1956)
55. Kennan, P. C., and Teske, R. G., *Astrophys. J.*, **124**, 499 (1956)
56. McKellar, A., *Publs. Dominion Astrophys. Observatory, Victoria, B.C.*, **7**, 395 (1948)
57. Greenstein, J. L., *Mém. soc. roy. sci. Liège*, **14**, 307 (1954)
58. Parker, E. N., *Phys. Rev.*, **109**, 1328 (1958)
59. Rudkjobing, M., *Publ. Kobenhavns Observatory*, **160**, (1952)
60. Schatzman, E., *White Dwarfs* (North-Holland Publishing Co., Amsterdam, 180 pp., 1958)
61. Payne-Gaposchkin, C., *The Galactic Novae* (North-Holland Publishing Co., Amsterdam, 336 pp., 1957)

PRACTICAL CONTROL OF RADIATION HAZARDS IN PHYSICS RESEARCH[1]

By Burton J. Moyer

Department of Physics, University of California, Berkeley, California

Introduction

The recent growth of nuclear technology and the increasing industrial applications of radioactivity and ionizing radiations have been accompanied by assiduous attention to the control of radiation hazards. Probably no previous basic technologic development has received such thorough consideration in regard to its essential hazards.

In research activities, however, as distinguished from an industrial situation, routines of procedure are not prevalent, and unprecedented operations are characteristic of the work. Moreover, the regular attention of an industrial safety officer is not typically at hand, and it is frequently incumbent upon the experimenter to evaluate the hazards to himself and to others of his present or contemplated activities. Even in the larger research laboratories where radiation safety departments or committees function, it is essential that the experimenter be always alert to the radiation exposure possibilities inherent in his work, particularly with regard to the unanticipated acts and arrangements carried out in the heat of trouble-shooting or in the drive to get a job done.

It is proposed in the following brief discussion to represent contemporary thinking concerning radiation hazards and their evaluation, which should be of practical assistance to the laboratory worker and to those responsible for the design and operation of physical apparatus and experiments which involve nuclear radiation or x-rays.

Control of radiation hazards involves (*a*) their anticipation and prior estimation; (*b*) their measurement or field evaluation; and (*c*) the devising of shielding and procedures which insure adequate safeguards, yet allow experimental freedom. In the present limited discussion, the author principally treats items *a* and *b*. He will not emphasize the problems or techniques of precise dosimetry from the standpoint of the radiologist, but will rather indicate the means of applying instrumentation and techniques, familiar to the practicing physicist, to the evaluation of radiation component intensities in his laboratory and its environs. The concerns of item *c* are treated in contemporary journals devoted to nuclear technology and in such surveys as that by Blizard (1).

Contemporary Definitions of Permissible Radiation Levels

The continuing consideration of the biologic effects of radiation has led to a redefinition, as of January, 1957, of recommended permissible levels. Such

[1] The survey of literature pertaining to this review was completed in April, 1958.

recommendations are issued by the National Committee on Radiation Protection and may be found in contemporary form for external radiation in (2) and (3) of the bibliography. The possibility of incorporating radioactive materials into the body by inhalation or ingestion requires limitations also upon concentrations permissible in air and on laboratory surfaces. The N.C.R.P. recommendations in this regard are given in (4) and (5), but they are subject to revision to make them consistent with the recent redefinitions of permissible exposure as given in (2).

A brief summary of the recommendations pertaining to "whole-body exposure" is as follows:

RECOMMENDED PERMISSIBLE OCCUPATIONAL EXPOSURE

Average rate for long-continuing exposure	5 rem/yr.*
Maximum exposure per $\frac{1}{4}$ yr. (if above rate is exceeded)	3 rem
Maximum exposure per week (if above rate is exceeded)	0.3 rem

TOTAL PERMISSIBLE ACCUMULATED DOSE (OCCUPATIONAL)

$$D(\text{acc.}) = 5(N-18); \text{ where } N \text{ is age in years.}$$

(It is intended that persons under 18 years of age shall not be occupationally exposed to radiation beyond the nonoccupational limit stated below.)

RECOMMENDED LIMIT FOR NONOCCUPATIONAL EXPOSURE

Yearly dose is to be less than 0.5 rem.

---

* For definition of the rem, see section below on Practical Measurement of Radiation Levels.

For further detail on permissible external exposure the reader should consult (2, 3). Relaxation by a factor of two has been allowed when only the skin absorbs dosage, and relaxation by a factor of five has been permitted only if hands and feet are exposed. Other details relating to the nature of the radiation and age of the person exposed are also stated.

The lowering of average yearly permissible exposure to 5 rem for persons occupationally involved with radiation, and to 0.5 rem for those in the environment but not occupationally involved, was caused by concern over possible elevation of genetic effects and possible shortening of average life-span as the exposed fraction of the total population increases. Damage to blood-forming organs remains as the prime consideration with respect to the specific individuals receiving occupational exposure.

In relation to the value of 0.5 rem/yr. which is recommended for the noninvolved persons in the environment, it is significant to note that the natural background of exposure for cosmic rays and natural radioactivity is typically 0.10 to 0.15 rem/yr. The shielding required for an accelerator, sufficient to insure a cumulative radiation increment of about four times natural background for all regions outside the controlled area, becomes a significant cost item and one whose planning must be considered from the beginning.

For purposes of calculation of expected external radiation intensities, and also for the interpretation of some types of survey counter data, it is necessary to express the permissible field intensity in terms of flux density of photons or of neutrons. In Table I are given various flux densities which "singly" will deliver 5 rem in 50 working weeks of 40 hr. each. Values three times these are permissible if not continuously sustained and if the year's accumulation does not exceed 5 rem. Values for the nonoccupational environment would be one-tenth these values if the radiation field is present

TABLE I

NEUTRON AND PHOTON FLUX DENSITIES AT VARIOUS ENERGIES WHICH WILL
SINGLY DELIVER 5 REM IN FIFTY 40-HOUR WEEKS OF EXPOSURE

[For neutron data see (6) and for photons (7)]

Neutron Energy (Mev)	Neutron Flux Density (cm.$^{-2}$ sec.$^{-1}$)	Photon Energy (Mev)	Photon Flux Density (cm.$^{-2}$ sec.$^{-1}$)
Thermal	670	0.02	2.5×10^3
0.0001	520	0.04	14.7×10^3
0.005	570	0.06	21.0×10^3
0.02	97	0.10	16.0×10^3
0.1	83	0.20	6.7×10^3
0.5	30	0.40	3.0×10^3
1.0	18	0.60	2.0×10^3
2.5	20	1.0	1.3×10^3
5.0	18	2.0	0.8×10^3
7.5	17	4.0	0.5×10^3
10	17	6.0	0.35×10^3
30	10	10.0	0.23×10^3

only 40 hr./wk., and they will be proportionately smaller if the radiation duty factor is greater.

The recommended permissible limits of airborne radioactivity, and of laboratory surface contamination, are intended in some cases to insure against harmful exposure of critical organs where possible inhalation or ingestion could incorporate into the body active elements with specific metabolic destinations (such as bone in the case of Ra); and in other cases, where general body exposure results, to limit tissue dosage to levels as defined above. The contamination levels as listed in (4, 5) apply to continuous exposure; consequently, a relaxation in inverse proportion to the "duty factor" of laboratory work is available. However, the new requirements (2) call for a factor-of-three reduction of the listed contamination levels for those elements which irradiate the whole body or gonads; and when persons not occupationally involved are concerned, an additional reduction by a factor of ten is recommended.

Research activities may occasionally require a radiation exposure of considerable momentary intensity, not to be often repeated. In such cases, the recommendations permit the acceptance of a week's exposure limit, 0.3 rem, providing no further exposure is allowed during the week. The policy to be encouraged, however, is one of minimizing exposure by the anticipation, planning, and provision of all safeguards which are economically and operationally feasible.

EXAMPLES OF PHYSICS LABORATORY RADIATION HAZARDS

The following selection of situations is suggestive of hazards or undesirable exposures which can readily occur incidental to the progress of experimental work. It is by no means a thorough presentation of radiation protection problems, but is rather a description of typical practical circumstances encountered.

Because the eyes are particularly subject to exposure in some of the following cases, it is desirable to state the presently regarded threshold dosages to the human eyes for the inducing of vision-disturbing cataract. In the case of x- or γ-ray exposure, an accumulated dosage of at least 500 roentgens is considered to be the practical threshold. In the case of neutrons the value is about 30 rep (8, 9). For fast neutrons this means an integrated flux of about 10^{10} neutrons per cm.^{2}, and for thermal neutrons, about 10^{11}/cm.^{2}. (An earlier figure for fast neutrons was smaller by about a factor of 10.) The cataract formation is typically delayed for several years after the accumulated exposure.

Irregular operations with radioactive sources.—Routine manipulations of pile irradiation samples or accelerator targets, and the chemical processing of intensely active materials, are engineered with handling equipment, lead enclosures, and lead glass or indirect viewing ports so that persons regularly engaged in these activities will not be exposed beyond permissible levels. Occasionally, however, it becomes necessary to perform a repair operation or adjustment upon a target or sample in the progress of a "run," and the experimenter is strongly tempted to contrive a local wall of lead bricks and perform his operation by reaching around the wall with hand tools, while peering over the top to see his work. (A reactor physicist would hardly be so tempted in view of his typical probe activities, but this is a familiar situation to accelerator experimenters.)

Such operations should be attempted only when a reliable probe ionization chamber is at hand with which to determine the exposure level to be encountered. It is not unusual, for example, that a cyclotron target should possess an initial activity which delivers a few rem per hour at a distance of one meter and very much more at a short distance where the beta emission is effective. A person dealing with this on a makeshift basis as described could receive a very considerable dose to his hands and to the long bones of the legs (important in blood formation) even though his trunk were shielded by a lead wall; and while the eyes would not, in one such operation, be

likely to receive a cataractogenic exposure, the increment of radiation to them could be considerable in these terms.

Target facilities should include an adequately shielded work bench for such necessary tasks, with reliable probe ionization chambers and a wall clock so that intensities and times can be easily observed. A measure of accumulated exposure for the individuals concerned, to be entered into their radiation history should be required.

Neutron exposure situations.—Shielding of reactors and accelerators is presumably designed so as to maintain neutron flux densities within the permissible bounds stated above. In some of the earlier accelerator installations insufficient regard was given to the importance of roof shielding over the machine, and this type of shielding weakness is probably the most frequent defect which needs attention in reducing environmental levels to the new standards.

Neutron exposures have accounted for some cases of cataract among nuclear physicists which are usually traceable to some acute dosage or to a prolonged exposure under more moderate, but yet above-tolerance situation.

One type of experimental arrangement which can result in considerably elevated neutron exposure in a limited area is the use of an intense beam for cross section experiments outside the reactor or accelerator shielding enclosure. Direct access to the beam is of course prevented, but the number of neutrons scattered out of the beam by a substantial column of attenuating material can be shown by simple calculation with typical data to create local areas, often accessible to people and frequently occupied by the experimenters, where the fast neutron flux densities may be as much as 10 or 20 times that nominally permissible. With a possible cataract threshold of 10^{10} per cm.^{2} of fast neutrons, the experimenter who expects to spend several years working in the typical background flux associated with an accelerator cannot afford to ignore the exposure increment imparted by such special experimental conditions.

Such operations as aligning counters by hand in intense neutron beams, or directly viewing the primary target where the neutrons are created, are to be eschewed and must never be undertaken without adequate evaluation of the possible exposure to the eyes which may be encountered.

Exposure to beams of charged particles.—For proton- and alpha-particle beams of sufficient energy to penetrate a few millimeters or more into body tissue, the possible hazards can be extreme. Sound precautions with respect to electrical and mechanical interlocks to prevent inadvertent passage of persons into direct beams or strong scattered fluxes of such particles are absolutely essential.

As an illustration one may consider a beam of protons of high enough energy to penetrate deeply into the body. Each proton will deliver about 30 Mev to the tissue in the last centimeter of its range. If the beam is presumed to be 10^{-8} amp., and if its cross-section area, together with scattering and range straggling, allows the various beam particles to deliver their last

30 Mev increments within a tissue volume of 10 cm.^{3}, the dosage rate to this volume of tissue would be about 3×10^3 rep/sec.! Clearly, a very brief exposure in which a vital organ was the region of beam termination could be extremely damaging.

Again suppose that an experimenter exposes his eyes to protons scattered from a target in the beam with an energy in the region of 20 Mev. The accumulation in his eye of a flux of only about 10^7 such protons would impart to the sensitive region the 30 rep which could be cataractogenic. This number of scattered protons could quite conceivably enter the eye in a time of a few minutes, assuming reasonable beam intensities and target nature.

An interesting special case of particle beam hazard is afforded by the beams of π^- mesons which are available in several laboratories in the world. Such mesons, upon coming to rest in the tissue, would be captured by carbon and oxygen nuclei and induce nuclear disruptions, or "stars," in each of which the fragments will carry a total kinetic energy of about 100 Mev, approximately half of which will be dissipated in tissue within a centimeter of the capture site. It must be granted, however, that this type of hazard is more in the nature of an interesting exception than a prevalent concern.

Laboratory and atmospheric contamination.—A radiologically clean laboratory is essential both from the standpoint of health and of good research. The freedom from background of interfering activities, which is required for many problems, is consistent with the concern for protection of people and may frequently require more rigorous suppression of contamination than is dictated by health considerations alone.

From the standpoint of health hazard, an important aspect of contamination is airborne radioactivity, which is now regarded as the most important avenue by which active materials may find their way into the human body and is generally felt to be a greater potential laboratory hazard than surface contamination of benches and floors (10). This is particularly true for the heavy alpha-emitters.

Careful planning and maintenance of airflow and ventilation systems are thus required whenever operations are involved which can create significant concentrations of dust, mist, or vapor of active isotopes; and a valid and reliable means of monitoring the air is essential. Concentrations which have been stated as permissible are given in (4) and are subject to slight revision and interpretation as previously mentioned in the section on permissible radiation levels. The permissible air concentrations for a few prominent materials are given as examples in Table II on the basis of continuous (168 hr./week) exposure.

The values given may be multiplied by a factor of four in case the exposure exists on a 40 hr./week schedule rather than continuously, but it is immediately apparent that some of these stated levels are almost immeasurably low, particularly in the "Environmental" column.

Presumably, the research laboratory which only occasionally engages in operations which might contribute airborne activity need not expend the

TABLE II

PERMISSIBLE AIR CONCENTRATIONS OF SELECTED ISOTOPES ON BASIS OF CONTINUOUS EXPOSURE [Revised (4)]

Isotope	Critical Organ	Permissible concentrations in $\mu c./ml.$ of air	
		Occupational	Environmental
H^3 (as HOH^3 or H^3_2O)	Total body	7×10^{-6}	7×10^{-7}
C^{14} (as $C^{14}O_2$	Bone (and fat)	5×10^{-7}	5×10^{-8}
Na^{24}	Total Body	7×10^{-7}	7×10^{-8}
P^{32}	Bone	1×10^{-7}	1×10^{-8}
S^{35}	Skin	1×10^{-6}	1×10^{-7}
Fe^{55}	Blood	6×10^{-7}	6×10^{-8}
Fe^{59}	Blood	1.5×10^{-8}	1.5×10^{-9}
$Sr^{90}+Y^{90}$	Bone	2×10^{-10}	2×10^{-11}
I^{131}	Thyroid	3×10^{-9}	3×10^{-10}
Po^{210} (insol.)	Lungs	7×10^{-11}	7×10^{-12}
U^{238} (insol.)	Lungs	1.6×10^{-11}	1.6×10^{-12}
Pu^{239} (insol.)	Lungs	2×10^{-12}	2×10^{-13}

resources necessary to provide for air monitoring at these levels which apply to daily routine operations; but it is clear that an adequate means of evaluating the activity in the air must be provided, which is appropriate to the extent of such operations. This evaluation is discussed in the subsequent section on measurements.

The contamination of surfaces with beta and gamma emitters is to be maintained low enough, as prescribed in (5), so that the radiation dosage rate immediately above the surface does not exceed 1 mrep/hr. For certain isotopes specified in (5), such as Sr^{90} for example, the dosage rate permissible is one-tenth this value. The principal hazard is not so much the general bodily irradiation, but the possibility that such activity might be removable and thus become airborne or be ingested by way of contact with the hands. Particular care is required to prevent direct entrance of activity into the blood stream through cuts or open wounds.

All evidences of surface contamination should be followed by efforts to remove the activity. That which is fixed may be regarded with reference to the permissible level stated in the previous paragraph for beta-gamma activity. Fixed alpha-activity may be covered by paint or a similar covering which absorbs the α-particles, with a suitable indication made of the existence of embedded activity if its lifetime and nature warrant future concern.

Decontamination and disposal techniques are specified in (5, 11) and in numerous recent articles in related technical literature, including detailed instructions of procedures to be followed in emergencies created by spills and

accidents. Anticipation of possible mishaps and prior planning of facilities and procedures to be utilized in the event of accident is an essential ingredient of work with radioactive materials.

Practical Measurement of Radiation Levels

A precise measurement of the biologically significant radiation dosage potentially available from a given radiation field is typically a very difficult accomplishment. Moreover, it is usually not necessary, except in research problems dealing with the biologic effects of radiation, to strive for great precision, since sufficient conservatism has been employed in the establishment of the permissible levels to relieve the experimenter of the necessity of making a major research problem out of his radiation field evaluations.

Nevertheless, for those who will spend the years of their professional lifetime working with radiation, it is necessary to be confident that the cumulative exposure is within conservative limits and that no acute exposures occur through misjudgment based upon inadequacy of measurement techniques.

General comments on radiation measurements.—The biologic effect of radiation is related in first approximation to energy absorption from the radiation field by the biologic medium. Since the energy absorption results in excitation and ionization of the constituent molecules and atoms, it seems plausible that an adequate field evaluation could be made by simply employing an ionization chamber whose walls and gas are comparable in average atomic number to that of the biologic medium. Indeed, if only a single instrument were to be selected this would be the choice.

However, biologic damage is dependent not only upon the total energy absorbed per gram of the medium, but also upon the density of energy loss along the paths of the charged particles traversing the medium as a result of the incident radiation. The various types of radiation can deliver widely different densities of energy loss along the charged particle paths they produce, and consequently there are different values of "relative biological effectiveness" (R.B.E.) assigned to them. This effect is summarized in the data of Table III, taken from a publication of the International Commission on Radiological Protection (12; see also 2).

The practical meaning of these R.B.E. values is this: if a means is found for evaluating the energy delivery per gram of body tissue by a known type of radiation, then the biologic dosage delivered, relative to that produced by the same energy absorption from x-rays, is given by the R.B.E. factor.

One roentgen of hard x- or γ-radiation will deliver to 1 cm.^{3} of wet muscle tissue about 93 ergs of absorbed energy. By definition, one "roentgen equivalent physical" (rep) of any type of radiation is that which delivers this same amount of absorbed energy to tissue per cm.^{3} (or approximately, per gram). Then the biologic dosage, measured in roentgens equivalent man (rem) will be the product of specific energy adsorption expressed in rep multiplied by the R.B.E. factor. Thus:

$$rem = rep \times R.B.E.$$

TABLE III

Relative Biological Effectiveness vs Specific Ionization

Ave. Spec. Ioniz., ion pairs/micron in water	R.B.E.
Less than 100	1
100–200	1–2
200–650	2–5
650–1500	5–10
1500–5000	10–20

Relative Biologic Effectiveness vs Radiation Type

Radiation Type	Biologic Effect Involved	R.B.E.
X-rays, γ-rays, and β-rays of all energies	Whole-body irradiation (blood-forming organs critical)	1
Fast neutrons,† and Protons below 10 Mev	Whole-body irradiation (cataract formation critical)	10
Naturally occurring α-particles	Carcinogenesis	10*
Heavy recoil nuclei (from neutron collisions)	Cataract formation	20

* Alpha-particle irradiation of tissue has often been assigned an R.B.E. of 20.
† For slow and thermal neutrons a conservative R.B.E. value is 5.

(Another energy absorption unit, the "rad," is coming into frequent usage. The rad is an absorbed dose of 100 ergs/gm., from any type of radiation, and in any medium of concern. When applied to human tissue, the rad and the rep are thus nearly synonymous, differing only by the factor 100/93).

From the foregoing it is clear that even though a means is found for determining the rep (or rad) dosage from a radiation field, it is still necessary to estimate the intensities of the various components in order to assign an R.B.E. and to determine the biologically significant exposure. Thus, measurements of fast neutron, slow neutron, and gamma flux densities must be separately made when these components are present; and for this reason the permissible levels in terms of flux densities of these radiations were given in Table I. If one knows by some prior means the approximate fractionation of the mixed field among these various components, he may choose to measure the "rep dosage" by means of a properly designed "tissue equivalent" ionization chamber, and then multiply by an R.B.E. factor deduced from the known relative component intensities. The work of Rossi (13) should be consulted in this connection [see also (14), Chap. 15].

A useful summary of monitoring methods and instruments, with their

qualifications and limitations indicated, is to be found in (14), and useful recommendations on measurement methods are given in (15).

Survey of gamma field intensities.—Since the R.B.E. value of x- and γ-radiation is unity, an ionization chamber with walls and gas (air) of low atomic number is generally suitable. If may be calibrated by reference to the field of a radium source of known strength, sealed in a standard capsule with 0.5 mm. platinum wall, for which the field intensity in r/hr. is given by:

$$\text{Intensity (r/hr.)} = 8.4 \times \frac{\text{Milligrams of Ra}}{(\text{distance in cm.})^2}; \quad \text{i.e.,}$$

$$I = 8.4 \, \frac{m}{d^2}.$$

Generally, the chamber wall thickness should be at least equal to the maximum range of secondary electrons generated therein by the γ-radiation; but it should not be many times this thickness or the attenuation of the gammas by the wall will lead to a low reading.

When soft x- or γ-rays, considerably below 100 kev, are the main constituent of the field, it is particularly important that wall thickness be not excessive and that the wall and gas materials do not contain elements whose K-absorption energies lie in the energy region to be evaluated. The general problems of air or tissue equivalence, which will be important if precision of calibration over a wide energy range is necessary, are discussed in numerous places and well presented by Boag [(14), Chap. 4].

The radiation fields of some accelerators and x-ray devices consist of repeated pulses of short duration in which the instantaneous intensity may be very high while the time average is only nominal. In such cases it is essential for a valid measurement to insure that recombination of ions does not occur during a brief period of high ion density during and immediately following the radiation pulse. Boag (14, 16) presents recombination theory and data to enable one to estimate the recombination correction. In any circumstance, the chamber voltage must be sufficiently high to provide saturation in the ion collection current.

Survey of beta-particle radiation.—Here again, the R.B.E. is unity, so an air-filled ionization chamber with walls sufficiently thin to transmit the majority of the β-particles will give ionization currents proportional to dosage if the particle flux is essentially uniform through the chamber. Generally, the failure of some of the soft betas to penetrate the walls results in a deficiency in response; but if a thin window exists in the chamber wall facing the source of particles, the chamber can respond to all that is biologically important since, from the standpoint of external radiation hazard, it is not necessary to record the effects of radiation which would not penetrate the human skin (5 to 10 mg./cm.^{2}).

A practical difficulty is presented, however, if one considers, for example, a survey for beta contamination of a surface. The recommended regulations prescribe that not over 1 mrep/hr. should be obtainable immediately above

a surface. In an air ionization chamber at atmospheric pressure, 10^{-3} rep/hr. produces an ion current of only about 10^{-16} amp. per cm.^{3} of chamber volume. Thus, if a chamber volume of 1 liter is employed, all of which is uniformly irradiated at the rate equivalent to 10^{-3} rep/hr., the total current would be only 10^{-13} amp. For certain isotopes (5) the recommended contamination level is only 10^{-4} rep/hr., and the current is 10^{-14} amp. for 1 liter volume.

Such currents are readily measurable by electrometer circuits and techniques, but they are not measured readily by simple hand-portable equipment. As a result, beta contamination survey is commonly done with a thin-window, portable geiger counter device possessing a count-rate output meter and possibly also an audible counting rate indication. A typical β-emitting material will give about 200 counts/min. per cm.^{2} of exposed counter window when the radiation level is equivalent to 10^{-3} rep/hr. Scintillation counters and proportional counters are, of course, also adaptable to survey use. The monitoring of airborne beta material will be discussed below in the paragraph on Air Monitoring of this section.

Measurements of alpha-emitting surface contamination.—The hazards from alpha-emitting materials are essentially zero from the standpoint of external radiation, since clothing and skin prevent irradiation of important bodily tissues because of the short ranges of natural alpha-particles in matter. The hazard associated with alpha contamination lies in the possibility of it being ingested via contact with hands, or inhaled through its becoming airborne as vapor or dust.

In view of the very small tolerable body burdens, and consequently small permissible air concentrations for many of the alpha-emitters (see Table II), it is good practice to clean away all removable alpha-contamination which can be detected. That which is not removable is then covered with paint so as to fix it permanently.

Surveys for alpha-emitting surface contamination usually utilize either a very thin-windowed, flat proportional counter, or a scintillation counter with large phosphor area. Each has its advantages and shortcomings; but each is capable of operation with discrimination against β- and γ-radiation on the basis of pulse-height selection.

The proportional counter type is frequently preferred because of easy portability, large counter area, light counter weight, and a flat shape which is easily inserted in shelves and similar structures. Most simply, it is an air proportional counter; but if greater complication is admissible, a gas-flow counter into which a selected counter gas (e.g., Argon plus 5 per cent CO_2) is constantly admitted at known pressure may be employed. The latter option eliminates problems caused by humidity variations but requires the provision of a portable supply of counter gas.

The discrimination between the majority of the α-particle pulses and those arising from beta and conversion electrons is unambiguous in a properly functioning proportional counter, particularly if the depth of the counting volume is only one or two centimeters.

The scintillation type of alpha counter most advantageously employs a large area, thin layer of an inorganic phosphor such as zinc sulphide (silver-activated). The short range and high rate of energy loss of the α-particle permits the thin inorganic scintillators, with their freedom from saturation effects in light output, to discriminate effectively between the alpha-induced scintillations and those induced by beta-particles and electron events from gamma conversion. The energy loss and light output for an electron traversing the thin phosphor is small compared to that from an α-particle if the thickness is matched to a typical α-particle range in the phosphor material.

Photomultiplier tubes possessing large, end-window, photocathode areas capable of viewing several square inches of phosphor are applicable to this purpose. A representative instrument of this type is described by Ryder & Hardison (17), in which a photomultiplier tube of 5 in. photocathode diameter views a 24-in.^{2} area of ZnS.

While the scintillation instrument is free of some problems, such as insulator noise, which may beset proportional counters, it has certain serious drawbacks: (a) it is bulky, and will not easily probe into confined spaces, (b) it is very sensitive to magnetic fields because of the electron trajectories in the photomultiplier, and in some laboratory situations the necessary amount of magnetic shielding becomes inconveniently heavy.

A standard reference source of alpha-particle emission must be always available to check the functioning of any type of alpha-counting equipment.

Evaluation of neutron fields.—In the shielding of nuclear particle accelerators and reactors, the adequate attenuation of the fast neutrons is usually the ultimate problem. The radiation field which exists outside the shielding of such a device consists largely of fast and slow neutrons and the capture γ-radiation from neutrons captured in the outer layer of the shield and in surrounding materials. The propagation of radiation at large distances from high-energy accelerators is principally due to the multiple scattering of neutrons in air, and is consequently often referred to as "sky-shine," particularly because the original escape of the neutrons is often primarily through an inadequate top shield over the accelerator.

Biologic effects from fast neutrons occur by their collisions with tissue nuclei, and particularly with hydrogen, to create heavily ionizing recoil particles. For slow neutrons the effects come partly from the γ-rays from neutron capture in body hydrogen: $n+H^1 \rightarrow H^2 + \gamma$, (2.2 Mev) and partly from capture in body nitrogen: $n+N^{14} \rightarrow C^{14} + H^1$ (.61 Mev). These explain the large values of R.B.E., namely, 10 for fast neutrons and about 5 for slow neutrons. The potency of fast neutrons for producing cataract is believed to be attributable to the dense ionization along recoil particle paths in the cells of the lens of the eye.

Neutron survey work which seeks to obtain spectral intensity information is very difficult in the very low flux densities near the permissible levels, especially since the directional properties of the flux are neither simple nor well known. It is possible, however, to secure information in the general

categories of slow, fast, and high-energy neutrons; and it is possible to approximate a mean energy value for the neutrons of the field.

Before mentioning specialized counters, we will first discuss the measurements feasible with the best, single, general purpose counter for neutron work, namely, the BF_3 proportional counter (or boron-wall proportional counter, if preferred). Such an instrument should be available in any laboratory involving neutron work.

(a) Measurement of slow neutron flux by observing the counting rate with and without a cadmium jacket, typically .030 in. thick [see, for example (18)]. The calculated counter efficiency proves to be satisfactory as a calibration if the counter is in good condition and properly biased.

(b) Measurement of total neutron flux density, without reference to energy; i.e., an energy-insensitive measurement (up to perhaps 20 Mev). It has been often observed that a particular thickness of $(CH_2)_n$ jacket surrounding a given BF_3 counter will provide a nearly uniform efficiency of counting over a wide range of neutron energies. De Pangher (19) has exploited this characteristic for neutron field flux estimates. In Figure 1 are displayed experimental curves by Hess (20) giving counting response vs neutron energy for various $(CH_2)_n$ jacket thicknesses surrounding a proportional counter $1\frac{1}{4}$ in. in diameter and 7 in. long (active volume). The jackets extended somewhat beyond the active volume at each end. For a counter of this size and shape, a jacket thickness of $2\frac{1}{4}$ in. is seen to provide a rather uniform efficiency between 0.025 and 14 Mev.

(c) Estimation of effective fast neutron energy. If a BF_3 counter is surrounded by a large envelope of cadmium, with sufficient space within for $(CH_2)_n$ jackets of various thicknesses, an instructive curve can be determined by plotting counting rate vs jacket thickness. The presence of the Cd envelope is to absorb the slow neutrons so as to permit the build up of counter response with jacket thickness to be well revealed.

In Figure 2, data from Hess (20) show such curves for neutrons of various energies. This kind of data, while far from giving spectrum information, does at least give one a feeling for the effective energy with which he is dealing.

The previous possibilities with the simple BF_3 counter are given because they are immediately available to most experimenters at nuclear laboratories. Calibration of the foregoing arrangements, for cases b and c, can be achieved by use of a standard Po-Be or Ra-Be neutron source of known strength.

Neutron field measurements of greater analytic information require techniques and instruments which cannot be discussed within this space. Useful sources of information are supplied by [Bemis, Chap. 10 (14); Rossi, Chap. 15 (14); Moyer (21); Hurst (22); and Hornyak (23)].

The application of photographic emulsions to the measurement of integrated flux densities is essentially the only method of personnel monitoring for fast neutrons, and the posting of such emulsions in various locations in areas of concern provides a useful comparison with the results of instrument surveys. Cheka summarizes emulsion technique for fast neutrons (24).
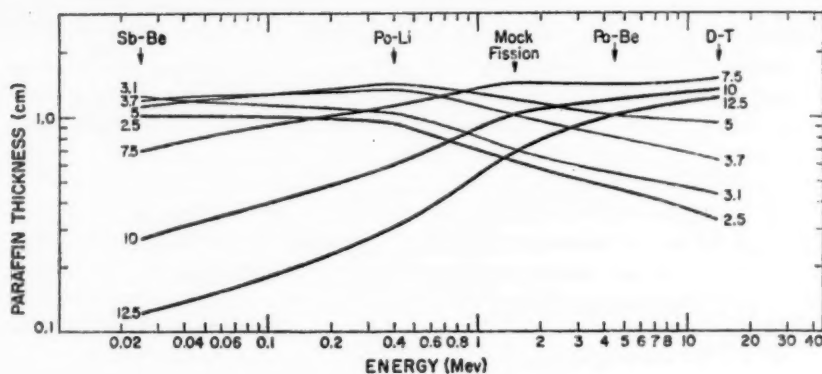
FIG. 1. BF₃ average efficiency as a function of neutron energy for various paraffin thicknesses, corrected to an isotropic flux distribution. The entire assembly was covered by Cd. The averaging over the 4π solid angle has introduced an error of as much as 10 per cent. (Paraffin thickness in cm.)

Air monitoring.—For certain types of laboratory work it is desirable to obtain a continuous air monitor record. This is particularly true for routine work with tritium, and would also be true for laboratories where regular work with the heavy alpha-emitters proceeds. Devices for this purpose typically utilize a filter, through which air is drawn, to collect particulate activity; or
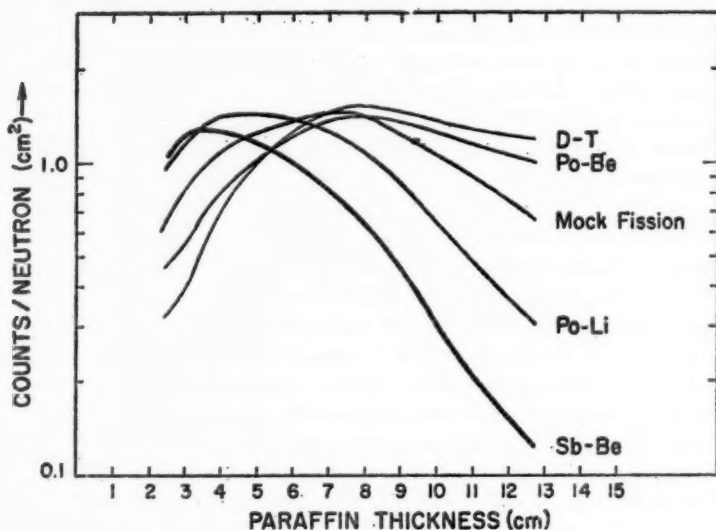
FIG. 2. BF₃ counting rate as a function of paraffin thickness for various neutron sources, corrected to an isotropic flux distribution. The entire assembly was covered by Cd.

alternatively an electrostatic precipitator to drive particles on to a moving tape which is monitored by scintillation counting. Such instruments do not fall into the category of small laboratory equipment. Recent examples are described by Eustler *et al.* (25) for tritium, and by Sawle (26) and Knowles (27) for airborne alpha-emitters.

The laboratory worker who needs only an occasional measure of airborne activity may usefully employ the ionization chamber method with a sensitive electrometer of the Lindemann or vibrating reed type. The evacuated chamber is allowed to fill itself with air in the region of concern. Its internal ionization current is then measured with the electrometer after the enclosed radon and thoron daughter products have decayed away. These radioactive gases are always present in the atmosphere because of earth radioactivity, and they with their daughters give ionization typically greater than the levels to be measured for the laboratory. However, they decay to negligible activity within a few days.

This technique is familiar, highly sensitive, and can be very dependable; and it is applicable to either beta or alpha activities. Its use for tritium evaluations is described by Zeigler & Schwebel (28).

Personal monitoring and records.—The use of film badges and pocket dosimeters for individual exposure data is by now so standardized as to require no discussion as to methods. Bemis (14, Chap. 10) summarizes current practice; and Ehrlich (29) presents a thorough analysis of photographic dosimetry.

It must be remembered, however, that in a mixed radiation field the precise meaning of film badge densities is unknown. Nevertheless, their use as a monitor of departures from normal is justified. But film badge data must always be supplemented by survey work adapted to the type of radiation field of concern. The regular use of badges posted in chosen locations to keep a long-term record of levels and their changes is highly desirable.

There is as yet no useful history known to the author of court cases involving alleged radiation injury which will give indication as to what kinds of evidence and instrument records provide the most valuable data in legal actions. But, unquestionably, the increasing public recognition of radiation as a factor in well-being requires the maintenance of good records of personal exposures and of the radiation history of the work areas involved. Reasonable agreement among various methods which purport to measure the same field components or exposures provides an important check on the validity of the evaluations.

LITERATURE CITED

1. Blizard, E. P., *Ann. Rev. Nuclear Sci.*, **5**, 73–98 (1955)
2. *Natl. Bur. Standards* (*U.S.*), *Handbook No. 59*, 79 pp. (1954) (This is supplemented by an accompanying insert, "Maximum Permissible Radiation Exposures to Man," issued January 8, 1957, by the National Committee on Radiation Protection.)
3. *Radiology*, **68**, 260–61 (1957)
4. *Natl. Bur. Standards* (*U.S.*), *Handbook No. 52*, 45 pp. (1953)

5. *Natl. Bur. Standards (U.S.), Handbook No. 48,* 24 pp. (1951)
6. Snyder, W. S., and Neufeld, J., *Brit. J. Radiol.* **28,** 342 (1955)
6a. *Natl. Bur. Standards (U.S.), Handbook No. 63,* 88 pp. (1957)
7. Moteff, J., *Nucleonics,* **13,** 24 (1955)
8. Abelson, P. H., and Kruger, P. G., *Science,* **110,** 655 (1949)
9. Ham, W. T., *Arch. Ophthalmol.,* **50,** 618–43 (1953)
10. Eisenbud, M., Blatz, H., and Barry, E., *Nucleonics,* **12** (8), 12 (1954)
11. *Natl. Bur. Standards (U.S.), Handbook No. 42,* 30 pp. (1949)
12. *Brit. J. Radiol.,* Suppl. 6, 19 (1955)
13. Rossi, H. H., and Failla, G., *Nucleonics,* **14** (2), 32 (1956)
14. *Radiation Dosimetry,* 454–503, 667–91 (Hine, G. J., and Brownell, G. L., Eds., Academic Press, Inc., New York, N. Y., 1956)
15. *Natl. Bur. Standards (U.S.), Handbook No. 51,* 31 pp. (1952)
16. Boag, J. W., *Brit. J. Radiol.,* **23,** 601 (1950); **25,** 649 (1952)
17. Ryder, F. D., and Hardison, H. V., *Nucleonics,* **15,** 82 (1957)
18. Moyer, B. J., *Nucleonics,* **10** (4), 14–17 (1952)
19. De Pangher, J., and Roesch, W. C., *Phys. Rev.,* **100,** 1793a (1955)
20 Hess, W. N., *Univ. Calif. Radiation Lab.* (Personal communication, Feb., 1958)
21. Moyer, B. J., *Nucleonics,* **10** (5), 14–19 (1952)
22. Hurst, G. S., *Brit. J. Radiol.,* **27,** (318), 353 (1954)
23. Hornyak, W. F., *Rev. Sci. Instr.,* **23,** 264 (1952)
24. Cheka, J. S., *Nucleonics,* **12** (6), 40 (1954)
25. Eustler, B. C., Evans, G. L., Hiebert, R. D., Mitchell, R. N., Robbins, M. C., and Watts, R. J., *Nucleonics,* **14,** 114–17 (1956)
26. Sawle, D., *Nucleonics,* **14,** 90–95 (1956)
27. Knowles, D. J., *Nucleonics,* **13,** 98–103 (1955)
28. Zeigler, C. A., and Schwebel, A., *Nucleonics,* **15,** 64 (1957)
29. Ehrlich, M., *Natl. Bur. Standards (U.S.), Handbook No. 57,* 28 pp. (1954)

CELLULAR RADIOBIOLOGY[1,2]

By Thomas H. Wood

Department of Physics, University of Pennsylvania, Philadelphia, Pennsylvania

TABLE OF CONTENTS

I. INTRODUCTION

The larger portion of this article is a review of those papers published during 1957 that deal with the effects of ionizing and ultraviolet radiations

[1] The survey of literature pertaining to this review was completed in February, 1958.

[2] The following abbreviations have been used in this chapter: DRF (dose reduction factor); LET (linear energy transfer); RBE (relative biological effectiveness); DNA (deoxyribonucleic acid); DNAase (deoxyribonuclease); RNA (ribonucleic acid); r (roentgen); kr (kiloroentgen).

on simple biological systems. This review differs somewhat from the preceding ones in this series [Mortimer & Beam (113); Gray (68); Powers (147)] in that a particular aspect of interest to the reviewer is considered in some detail. No attempt has been made to survey the fields of radiation chemistry and mammalian radiobiology even though studies in these areas may be pertinent to cellular radiobiology. Biochemical changes following irradiation are also not intensively considered, as Holmes (77) has recently reviewed this material.

As excellent review by Kimball (92) on the nongenetic effects of radiations on microorganisms has appeared during the year. The proceedings of the Stockholm conference on radiobiology contain a wealth of material and several of these reports [e.g., (2, 45)] are discussed in this review. Reviews by Pauly (136) on physiological changes following irradiation, by Konzak (97) on genetic effects of radiation on higher plants, and by Wichterman (191) on the radiobiology of protozoa contain many topics of interest to the cellular radiobiologist. The reader's attention is called to a challenging monograph by Reid entitled *Excited States in Chemistry and Biology* (154) which is worth careful scrutiny. *Radiation Biology*, edited by Hollaender (75), can still be considered to be the standard reference in this field and can be consulted with profit. A number of more specific reviews are considered in appropriate places in this article.

II. SOME MODELS FOR PRIMARY RADIATION DAMAGE

The inactivation of the simplest systems by ionizing radiations involves many coupled steps. The first step—the spatial and temporal transfer of radiation energy as ionizations and excitations—is known satisfactorily, at least in a qualitative sense. The subsequent events—migration and utilization of this energy to cause primary radiation damage, modification of the primary radiation damage, biological repair or amplification of this damage, and the appearance of detectable endpoints for this damage—are all intriguing problems of cellular radiobiology.

Perhaps the chain in this sequence most amenable to attack is the problem of the migration of radiation energy from its original spatial configuration to the points where primary radiation damage is irreversibly inflicted. There have been several models developed which are concerned with this step of the radiation process. These models, in spite of their over-simplification, have been and will continue to be valuable in that they stimulate research to prove or disprove their validity.

A. DIRECT ACTION MODEL

In this formulation, developed most successfully by Lea (105) and refined by Pollard and his co-workers (143, 144), radiation modification of the biological units of concern is postulated to be brought about by means of ionizations directly within the unit. The efficiency of inactivation should depend on the density of ionization (LET) and on the physical state of the ir-

radiated system (e.g., whether dispersed or condensed). The radiation damage occurs at the point of the original ionizations; there is little if any migration of this energy.

From these assumptions and mathematical interpretations of the consequences of such inactivation events, Lea was able to account for many of the radiobiological phenomena known in the mid-1940's; among these were the inactivation of viruses and simple cells under certain conditions, gene mutations, and chromosome aberrations. Pollard and his collaborators have used these concepts to estimate the size and structure of many biological units, often with amazing success. There can be no question that ionizations within molecules can change their structure and subsequent function; hence, direct action inactivation of biological units must always be present.

B. INDIRECT ACTION MODEL

The direct action model in its original form takes no account of the modification of primary radiation events by various physical and chemical agents. Its adherents have made no claim for its universal applicability to radiobiological phenomena; it would be expected to be appropriate only if there is no transfer of radiation energy between the target molecule and its environment. The development of the radiochemistry of water, the success of these concepts in dealing with the effects of ionizing radiations on *in vitro* enzyme systems, the modification of radiation damage by various chemical and physical agents, and the general failure of the direct action model to describe inactivation efficiencies quantitatively all led to the development of the indirect action model. Here, ionizations within water molecules produce free radicals; these can then diffuse over reasonably long distances within the cell (variously estimated from 30 A to a few microns), bringing about, on successful collision with vital molecules, structural modifications and subsequent modification of function.

The most general formulation of the indirect action hypothesis is that of Zirkle & Tobias (205). They assume that radiation effects on a particular target can not only be brought about by direct action but also by free radicals (or other "poisons") produced by the ionization of water. The farther away from the target these poisons are produced, the less the probability they have of migrating from the point of production to the target. In the migration or indirect action model, account is taken of physical or chemical agents which affect the production of free radicals, their diffusion, their lifetimes, the efficiency of reaction with the target region, etc. For example, the oxygen effect (increased radiosensitivity in the presence of oxygen) is accounted for usually by the production of the HO_2 radical; the phase effect (decreased radiosensitivity in the frozen state compared to the liquid state), by diminishing diffusion in the solid phase; the desiccation effect (decreased radiosensitivity in dried materials compared to wet ones), by a decreased production of free radicals in the absence of water.

The migration model should not be considered as having eliminated in

any sense the direct action model; it simply is a more general formulation that includes as a part of itself the direct action hypothesis, the results of both direct and indirect action inactivation being described in the mathematics of classical target theory.

C. Modifiable Direct Action Model

The migration model was created because of the inability of the direct action formulation, in its original sense, to account for the action of chemical and physical modifying agents and because of the feeling that free radical mechanisms known to be operative in the radiobiology of *in vitro* systems and virus systems should play a role in cellular systems. Recently Alexander and others (2) have demonstrated modification of radiation damage in systems in which indirect action is unlikely (water-free systems). Alper and Howard-Flanders (4, 78) have suggested, as a result both of the demonstration of modification in "direct action systems" and of the inability of the migration model in its simplest form to account for certain observed phenomena, that free radical inactivation in the sense of the migration model is not of primary importance in cellular radiobiology. They propose, instead, that the primary radiation processes that occur within the target volume either inactivate the target completely or leave it in an excited state. This excited state can either recover or it can be irreversibly affected in a detrimental fashion by reaction with oxygen or various chemicals in its environment. This excited state, called a metionic state by Alper, is postulated to have a lifetime of possibly between 10^{-3} and 10^{-6} sec. Again, the inactivation kinetics are those of classical target theory. The essential feature of this and the direct action model is that the radiation energies bringing about the injurious effects are transferred directly from the ionizing particles to the affected sites; there is no intermolecular energy transfer.

D. Recent Pertinent Experiments

The indirect action and the modifiable direct action models contain within themselves the classical direct action model of Lea. Thus, the comparison here should be between these two models. Undoubtedly, neither model is wholly correct; a model is at best an approximate description of the way nature operates. Its value lies in its ability to stimulate new experimentation, which in turn allows a better description of nature. The present evaluation is intended to point out the inadequacies of both models and to suggest features any successful model must have.

The case for direct action has been summarized elsewhere in considerable detail (105, 143); recent papers will be discussed in a later part of this review. It should be mentioned that the usefulness of the direct action model in calculating geometrical sizes or molecular weights has recently been questioned by Alexander (3). He feels that energy transfer processes occur both between and within molecules even in the solid state and that these will introduce serious errors in volume calculations, especially in smaller volumes

(e.g., enzymes); for larger structures (e.g., viruses) values deduced from target theory calculations will be more meaningful. Hutchinson (80) has also found what may be a transfer of radiation energy through a molecular layer of enzymes (see III.B.1).

Hutchinson, Preston & Vogel (83) have studied the inactivation of invertase, alcohol dehydrogenase, and coenzyme A by several ionizing radiations in both wet and dry yeast cells. The radiosensitivity in wet cells compared to dry cells is 2:1 for invertase, 20:1 for alcohol dehydrogenase, and 100:1 for coenzyme A. Extracted enzymes irradiated in the dry state have sensitivities similar to those found in dried cells. Enzymes in thoroughly dried cells are 2 to 4 times as radioresistant as those in cells having only 5 per cent water. Hutchinson (81) analyzes these data in terms of the migration model of Zirkle and Tobias and finds that the mean radical diffusion distance for all three enzyme systems in wet cells is of the order of 30 A; it is interesting to note that if water is uniformly distributed around molecules within the cell, the mean water thickness is also about 30 A. If Hutchinson's interpretations are correct and if these effects are generally applicable for other targets within cells, these short diffusion distances force a re-evaluation of certain aspects of the indirect action hypothesis. At the oxygen concentrations at which the oxygen effect becomes important (about 5 μM/L for most microorganisms), oxygen molecules are about 700 A apart; thus, the probability of a collision between H and O_2 during a 30 A migration to form HO_2 (the mechanism most often considered for the oxygen effect) is very low.

It is very difficult not to interpret these studies from the indirect action hypothesis. For example, the sensitive volume of coenzyme A in dry yeast, as calculated from target theory, is within a factor of two of the geometrical volume as determined by other methods; however, the sensitive volume in wet yeast is approximately 100 times larger.

Alexander (3) has described the conditions which he feels are necessary to connect an oxygen effect to a direct action mechanism. The oxygen effect must be demonstrated in a material in which the action is known to be direct (operationally, this would mean in the complete absence of water), and the oxygen effect should decrease with increasing LET (at higher LET, the radiation effect would be so severe that further insult by oxygen would be redundant). To test this hypothesis, he irradiated crystalline trypsin (4 to 6 per cent water) with 2 Mev electrons, Co^{60} γ-rays and polonium α-particles in air and in the absence of oxygen. Inactivation of enzyme activity was exponential with dose in all cases. The response to Co^{60} and electrons was the same; for these two radiations, the presence of oxygen (air) reduced the inactivation dose by 30 per cent. There was no oxygen effect with α-particles. Alexander suggests two mechanisms that might ⌐ ⌐ount for the oxygen effect: (a) that previously discussed, namely, an excited state induced by radiation which can react with oxygen to produce an irreversible inactivation; and (b) a reaction in which O_2^- radical could inactivate the target molecule. Alexander found that crystalline trypsin (4 to 6 per cent water)

had the same radiosensitivity as that vacuum-dried; it is not clear from his report if vacuum drying removed additional water. It should be remembered that Hutchinson, Preston & Vogel (83) found that removal of 5 per cent of the water from yeast changed their radiosensitivity by a factor of 2 to 4. The possible importance of residual water will be discussed later.

Howard-Flanders & Alper (78) have studied the radiation response of three microorganisms (*Escherichia coli*, *Shigella flexneri*, and haploid *Saccharomyces cerevisiae*) at various oxygen concentrations with both x-rays and fast neutrons. Oxygen concentrations were accurately controlled even at very low concentrations by an ingenious system which allowed continuous equilibrium by gases even during irradiation. The DRF for x-irradiation in the absence of oxygen was about 3 for the bacteria and 2.4 for the yeast; with neutron irradiation, about 1.5 for *Shigella* and 1.6 for yeast. In all cases half of the maximum oxygen effect was obtained at about an oxygen concentration of 5 μM/L (separation between O_2 molecules of about 700 A). These results are interpreted by means of the modifiable direct action mechanism already discussed. They postulate that some of the affected targets will normally recover unless they react with oxygen to produce an organic peroxide which is irreversible. Under anoxic conditions, from these results, about two-thirds of the target molecules ionized by x- or γ-rays would be able to recover, whereas in the presence of oxygen all ionizations would lead to irreversible and detectable change. The lifetime of the oxygen-sensitive excited molecules is estimated to be less than 0.02 sec. (from experiments in which irradiated material is quickly switched from a nitrogen to an oxygen atmosphere) and greater than approximately 1 μsec. (the number of collisions of oxygen with the excited target under these conditions, is approximately 10^6 collisions/second). Howard-Flanders and Alper suggest that if cellular inactivation follows the mechanism of the modifiable direct action model, then classical target theory can be applied to nondried systems in the oxygenated state because, according to their ideas, there is no migration of radiation energy and a single ionization has a probability of one of being effective under aerobic conditions. It must be pointed out that if this concept of target theory is correct, then the large number of investigations which have been concerned with measuring molecular weights and structural configurations are invalidated, since these studies for the most part have been carried out within an oxygen-free environment (i.e., a vacuum).

Wood & Taylor (197) have compared the x-ray sensitivities of two strains of yeast (a fermenting strain and a respiring strain) under both aerobic and anaerobic conditions at $-10°$C. in both liquid (supercooled) and frozen suspensions. The DRFs afforded by anoxia in the liquid phase were 1.4 and 2.3 for the respiring and fermenting strains, respectively; in the frozen phase, 1.7 and 2.1, respectively. The overall DRFs for both anoxia and freezing together were 2.9 and 3.4 for the respiring and fermenting strains, respectively. These authors analyze the data in terms of indirect action, and consider that the overall radiation "cross section" for this system is com-

posed of four parts: (a) a portion eliminated by anoxia only; (b) a portion eliminated by freezing only; (c) a portion eliminated by freezing or anoxia; and (d) a portion affected by neither anoxia nor freezing. The fact that an oxygen effect was found in the solid state made necessary an investigation of the amount of cellular water actually frozen at various temperatures [Wood & Rosenberg (196)]. In yeast, approximately 10 per cent of the cellular water is unfreezable, even at $-72°C$. (one definition of bound-water). If this unfrozen water can serve as an interface on which oxygen can be absorbed, then an additional parameter is available to explain an oxygen effect in the frozen state. Wood and Taylor discuss the possible role of bound-water in radiobiological processes and believe that it may play an important role in incompletely dried systems.

Alexander (2) has expressed a view that the demonstration of a phase effect in radiosensitivity is evidence for the operation of a radical mechanism. However, Alper (5) chooses to explain the phase effect as being due to the elimination, in the frozen state, of reactions between her metionic state and reactive agents other than oxygen that would react to make restoration impossible. Freezing at low enough temperatures would be expected to eliminate all diffusion processes, so it is difficult to see how additional protection could be afforded by anoxia in the frozen state over that afforded by the frozen state alone. Her ideas, of course, can be salvaged by the same means used by Wood and Taylor, namely, by considering the role unfrozen or bound-water might play. Thus, both the indirect action model and the modifiable direct action model are not adequate in their simplest formulations to account for additional protection afforded by anoxia in the frozen state; it is necessary to add one additional parameter in either case for an adequate explanation.

In a very interesting study Ebert & Howard (53) have investigated the effects of high pressures of nitrogen and hydrogen gases on the x-ray response (growth rate of roots) of *Vicia faba*. When irradiation is carried out in the presence of 1 atm. of air plus 50 or 100 atm. of hydrogen, considerable protection is afforded over the condition when only air is present (DRF's of 1.4 and 1.8, respectively). High hydrogen pressure would not be expected to affect oxygen concentration per se; however it might be expected to increase HO_2 production if oxygen is also present; thus, they infer that under these conditions HO_2 inactivation is not of primary importance. They postulate that organic radicals produced in the presence of oxygen, rather than HO_2 radicals, are the damaging entities. Ebert and Howard also find that pressures of nitrogen from 20 to 120 atm. in the presence of 1 atm. of air give full protection against the oxygen effect (DRF of 2.5). This, they believe, might be attributable to nitrogen replacing oxygen that is absorbed on critical sites thereby reducing radiosensitivity.

None of the experiments described above are definitive in that they eliminate either the indirect action model or the modifiable direction action model from further consideration. Alper and Howard-Flanders (5, 78) feel that the

modifiable direct action model offers explanation of existing experimental results, and they find it unnecessary to retain any aspects of indirect action. However, the foundations of cellular radiobiology (radiochemistry and the radiobiology of aqueous suspensions of biological materials) cannot be so easily crumbled. Free radicals are undoubtedly formed within the cell on irradiation and they undoubtedly react with and modify target molecules.

. A considerable amount of evidence is now available that indicates that the HO_2 radical may not play a predominant role in the oxygen effect [see Alper (5) for review of earlier information]. The demonstration of an oxygen effect in dried materials is evidence that HO_2 need not be involved in all oxygen-sensitive systems. Furthermore, if Hutchinson's (81) interpretation of the mean diffusion distance of free radicals (of the order of 10's of A) in *in vivo* system is generally applicable, the probability of HO_2 radical formation is low. The mechanism for oxygen dependence postulated in the modifiable direct action model may be considered an explanation of the oxygen effect in aqueous systems.

On the other hand, it is very difficult to explain by use of the modifiable direct action model cases in which target theory analysis gives a volume for the target region greater than the overall geometrical volume. Such computations indicate that an energy transfer process as postulated by the indirect action model must have occurred. Thus quantitatively, the modifiable direct action model is not completely satisfactory.

It seems at this time that the best operational model to stimulate experiments at a fundamental level is one using the best parts of both models. It should be remembered that both models use the formulations of target theory; they differ only in the absence or presence of mechanisms by which radiation energy can be transferred from the environment to the target being considered.

III. SOME FACTORS INFLUENCING RADIATION RESPONSE

A. RADIATION PARAMETERS

1. *Linear energy transfer* (LET).[3]—The spatial configuration in which radiation energy is laid down is known to influence greatly the relative biological response (RBE) of the test system. Since our ultimate understanding of radiation effects will be at the atomic level, it seems desirable to direct our attention at this level. For this reason it is suggested that the unit of LET be expressed as electron volts per angstrom (ev/A), the angstrom being a convenient unit of atomic separation.

Two recent contributions to the evaluation of LET for various ionizing radiations have been made. Burch (27) has defined a mean LET and has

[3] The numerical values for LET given in this review are for the most parts estimates made by the reviewer and in some cases may be quite inaccurate. It is recommended that individual authors give such estimates themselves.

made calculations for several of the often used radiations. Snyder & Neufeld (174), taking account of energy loss caused by nuclear and electronic collisions, have made similar calculations.

Two important papers dealing with LET have been discussed in some detail in Section II.D [Alexander (3); Howard-Flanders & Alper (78); see also (60, 98, 181)]. Hutchinson, Preston & Vogel (83) have found no significant influence of LET over a range from 0.03 to 10 ev/A on the radiation sensitivity of several enzymes normally found in yeast cells under conditions in which the enzymes were irradiated (*a*) in "wet" cells, (*b*) in "dried" cells, and (*c*) outside the cell in the dry state.

Setlow (165) has studied the activation of dried T2 virus by deuterons and α-particles over the LET range 2 to 12 ev/A. The RBE for this process changes but slightly from 2 to 5 ev/A but increases by about 50 per cent at 12 ev/A. She interprets the data as indicating that two ionizations are required for suppression of ability to lyse bacteria.

Donnellon & Morowitz (50) have irradiated *Bacillus subtilis* spores with protons, deuterons, and alphas such that the LET varies over a range from 0.6 to 33 ev/A. RBE increases by approximately a factor of 7 over the range of LET used. The authors interpret their results in the light of target theory as indicating that two or more potential targets are in the spore and that at least one of the targets requires a large amount of energy for inactivation. They speculate that at low LET a genetic target requiring a single ionization for inactivation may be involved, whereas at high LET cytoplasmic damage may be involved. Soft x-rays (half-value layer, 0.065 mm. Al) are found to be approximately twice as effective as harder x-rays (14.2 mm. Al HVL) in the inactivation of spores of *Bacillus megaterium* [Powers *et al.* (149)].

Cessation of growth of the apical cell mass of the root of *Vicia faba* has been found by Spalding, Langham & Anderson (177) to be the same for equal dose of β-particles from tritium (0.2 ev/A) and 175 kvp x-rays (0.3 ev/A). Co[60] γ-rays (0.04 ev/A) are comparable to x-rays, but radon α-rays (12 ev/A) have a RBE of 5.8 [Spalding (176)].

Radiation damage from x-rays (reduction of seedling height) is increased as much as threefold if irradiated dormant barley seeds are stored for 24 hr. between the radiation treatment and germination; no such delayed effect is found with fast or thermal neutrons [Curtis *et al.* (41)]. In the same system, Caldecott *et al.* (33) have found that dry seeds (4 per cent water content) display more radiation damage from x-rays (0.3 ev/A) if added immediately to oxygenated water after x-ray treatment; there is no appreciable modification after fast (∼2 ev/A) or slow (∼10 ev/A) neutron treatment (see Section III. C.2). Nilan & Phillips (120) have studied the comparative effects of thermal neutrons (∼10 ev/A) and x-rays (0.4 ev/A) on the production of chromosome aberrations in normal and calcium-deficient barley seeds. The calcium-deficient seeds exhibited a higher frequency of chromosome aberrations and were more sensitive to x-irradiation; there was no differential sensitivity with thermal neutrons.

A rather disturbing picture of the comparative effects of 220 kvp x-rays (0.2 ev/A), 0.4 Mev γ-rays (0.04 ev/A), and 30 Mev x-rays (0.03 ev/A) on the frequency of chromosome aberrations in *Tradescantia* has been published by Bora (23). When scoring is done after 72 hr., the 30 Mev radiation seems to be less effective than the others; however, with 137-hr. scoring, the 0.4 Mev γ-rays are more effective in producing aberrations than either of the others. He assumes that different mechanisms are involved in the induction of chromosomal breaks by the roentgen rays (220 kvp and 30 Mevp) and the γ-rays. It is difficult to understand this interpretation, especially on LET considerations.

Three reports have appeared recently on the influence of LET on dominant lethal damage in *Drosophila*. Using egg-hatch as the endpoint determination, Sheppard *et al.* (169) find that the RBE of fast neutrons (~2 ev/A) relative to 250 kvp x-rays (0.2 ev/A) is definitely greater than two. Fast neutron dose-effect curves are exponential; x-ray curves are concave downwards. Thus RBE's vary from 4.5 at low doses to 2.9 at higher doses. Using the same criterion of damage, Alexander (1) finds that the RBE's of 1.2 Mev γ-rays (0.05 ev/A) and 22 Mev x-rays (0.03 ev/A) are both approximately 0.7, compared to 200 kev x-rays (0.3 ev/A). Paterson (135) also reports a similar value.

2. *Wavelength.*—A recent survey of various aspects of ultraviolet action can be consulted with profit [Setlow (166)]. Action spectra for ultraviolet effects on several proteins have been reported by Setlow & Doyle (167).

Quanta of wavelengths less than 2000 A may have enough energy to ionize molecules of biological importance. Thus an investigation of the vacuum ultraviolet may provide the information that might link the effects of ionizing radiations and ultraviolet radiations. Preliminary results by Setlow, Watts & Douglas (168) indicate that the quantum yields for inactivation of the enzymes trypsin and chymotrypsin are constant between 1900 and 1600 A; the yield at 1200 A is five times that at the longer wavelengths.

3. *Dose rate and fractionation.*—Powers *et al.* (148) have developed a technique for the x-irradiation of dry spores of *B. megaterium* that allows the recognition of small differences in radiosensitivities. Thus it has been possible to detect a 12 per cent change in the radiosensitivities of spores treated at 850 and 1600 r/min., the higher intensity being more effective (149). It is unlikely that such small differences in dose rate would be operative at the primary level of radiation damage. The exposure times in their experiments are several hours, an amply long time to allow biochemical factors to become operative. Fractionation studies using the higher dose rate would be of value in determining at which level the modification is operative. See Section IV. A for other studies in which the fractionation times are such as to implicate metabolic recovery (22, 32, 37, 86, 87, 162).

B. ENVIRONMENTAL FACTORS

1. *Phase state, dehydration, and temperature.*—It is worthwhile to consider the similarities and differences between radiation studies done with frozen

and with dried materials. Very often it is assumed that for radiobiological purposes these two conditions are equivalent; certainly in many cases the same degree of protection is afforded by drying and by freezing [see (17, 66)]. However, Wood & Taylor (198) have found that with yeast irradiated at $-72°C.$, it is not the temperature existing during irradiation nor the amount of cellular water frozen that is of primary importance in determining the radiosensitivity, but rather the rate at which these cells are frozen to the irradiation temperature. In the temperature range from $0°$ to $-35°C.$, cells slowly frozen attain a very radioresistant state, being approximately four times as resistant at $-35°$ as at $0°$; the radiosensitivity for slowly frozen cells remains essentially constant from $-35°$ to $-72°C.$ However, cells frozen at a rate typical of the bath temperature (fast-frozen) show an increasing sensitivity from $-35°$ to $-72°C.$, where they attain a sensitivity characteristic of the liquid phase $(0°)$. Slow-frozen cells are progressively dehydrated by salts in their external medium as the irradiation temperature is lowered and freezing progresses; this dehydration would be expected to reduce the radiosensitivity according to the indirect action hypothesis. On the other hand, cells frozen at faster rates have their internal water frozen before they can be dehydrated. Upon irradiation, energy derived from the radiations will be released in the same geometrical pattern as in the liquid phase cell; this energy is postulated to be stored then in the ice phase until thawing when the subsequent state of action will be similar to that in the liquid phase cell. Those conclusions are made more likely by the fact that cells slowly frozen by step-wise methods to $-72°C.$ show a sensitivity characteristic of slow-frozen cells (very resistant) instead of that characteristic of fast-frozen cells (liquid phase sensitivity). In addition, cells frozen at a fast-rate to $-72°C.$ and then irradiated at higher temperature, $-50°$, show a response typical of $-72°$. In another paper (197) these authors point out that with frozen cells a portion of the cellular water (bound-water) is not in the frozen state and may be of importance for radiobiological processes. Thus before drying and freezing are equated as far as radiobiological processes are concerned, the position of the frozen water (within or without the cell) and the role of the bound- or unfrozen water must be considered.

A pigmented *Sarcina* bacterium studied by Bellamy, Kilburn & Terni (17) has been found to be approximately five times as resistant when irradiated in the dried state as when irradiated in suspension. Frozen suspensions of cells have the same sensitivity as dried samples. Similarly, Ginoza & Norman (66) find that frozen or dried samples of either tobacco mosaic virus and its extracted nucleic acid all have the same radiosensitivity. They find that an interesting additional protection of approximately twofold is given to the nucleic acid when 2 per cent glutathione is added before freezing or drying. Okada (125) reports a greatly decreased x-ray inactivation of DNAase when irradiated in the frozen state. The temperature dependence of *B. megaterium* spores to x-rays has been investigated by Webb, Ehret & Powers (187) between 4.5°K. and room temperature; sensitivity is about 30 per cent greater at room temperature than at the lowest temperature investigated. Their

results are such that they rule out the simple application of an Arrhenius temperature relationship over this entire range.

Hutchinson (80) has studied the inactivation of a thin layer of enzyme by low-energy electrons (several hundred volts). Such layers cannot be inactivated below a certain level regardless of the radiation dose. This indicates that there is no appreciable transfer of radiation energy at room temperature from the outer, irradiated molecules to those deeper within the layer. At 100°C. an additional molecular layer is inactivated. This could be due to either a true energy transfer or to some kind of cross-linking induced by the high temperature. Braams (25) has also suggested that radiation energy transfer within molecules is temperature dependent.

Sarič (161) has found that with winter oat seeds the x-ray sensitivity decreases with increasing age of the seed (harvest time). The water content of these seeds decreases from 79 to 20 per cent, the youngest seeds having the highest water content. It would thus appear, if one assumes that it is primarily the water content that is influencing radiosensitivity, that the radiosensitivity decreases with water content. However, water changes in such a system might follow metabolic conditions which may be of primary importance.

Siegel (170) has studied the ultraviolet inactivation of two strains of tobacco mosaic virus under conditions where the virus was irradiated both in the dried and in the wet state. Both strains are equally sensitive when dried; one of the strains, however, is approximately five times as resistant when irradiated in the wet state. In a bacterial virus specific for *B. megaterium*, however, the ultraviolet sensitivity is approximately twice as great in the wet condition as when the virus is irradiated dry [Friedman (63)]. Other papers of possible interest are (2, 3, 31, 32, 33, 41, 83, 118).

2. *Oxygen concentration.*—The oxygen effect and its importance in radiobiology has been discussed in Section II. D; several papers dealing with this subject are reviewed there (3, 53, 78, 197). Bachofer & Pottinger (14) have found that oxygen protects bacteriophage T1 from both x-irradiation and hydrogen peroxide inactivation. They consider that the oxygen protection for T1 is not due to the removal of atomic hydrogen by oxygen as postulated by Alper for S13 phage (4), but suggest it is attributable to a reaction between the phage and oxygen, this complex conferring stability upon the phage. Another case of oxygen protection has been described in an interesting study of cocarbolylase and thiamine by Ebert & Swallow (54). In the presence of high concentrations of alcohol, oxygen may actually protect from radiation damage, presumably because of competition between oxygen molecules and the enzyme for radicals produced by the irradiation of the alcohol.

Okada and his co-workers have studied the inactivation of DNAase by radiations (125 to 129). It is concluded from studies on inactivation by hydrogen peroxide and by hydrogen peroxide plus ferrous sulfate or ultraviolet irradiation that OH radicals are important in this inactivation process.

Less inactivation from x-irradiation is obtained in oxygen-free solutions than in oxygenated ones. They conclude that OH and HO_2 radicals are primarily responsible for irradiation damage in this system. Okada (126) has analyzed this data from a kinetic viewpoint developed on the assumption of a prevailing steady-state. The half lives of the effective free radicals are estimated to be 10^{-7} to 10^{-9} sec. The kinetics suggest that only one of 10 radicals which react with a DNAase molecule is effective in causing a loss of enzymatic activity. The effectiveness of various materials in protecting against indirect effects was determined. DNA was found to have high protective ability and it is suggested that this is due to a complex between DNAase and DNA.

Bruce (26) has found a DRF for the oxygen effect of about 2 in x-irradiated yeast; see also Wood & Taylor (197) and Howard-Flanders & Alper (78) for related work with yeast.

When the appearance of normal anaphases 24-hr. after x-irradiation is used as an index of radiation effect in ascites tumour cells, air-saturated suspensions are found to be 3.7 times as sensitive as air-free suspensions, and oxygen suspensions 4.7 times as sensitive [Conger (39)]. Dittrich (49) reports very similar results. Neary (118) has confirmed earlier observations that the DRF due to anaerobic conditions in *Vicia faba* is about 2.5 for γ-irradiation; the criterion of damage is reduction in rate of root elongation. Kihlman, Merz & Swanson (90) suggest that the oxygen effect, as far as chromosome breaking in *Vicia* is concerned, is attributable to a change in the bound iron of the chromosomes from the reduced to the oxidized form. With the same material and same criterion Wolff & Luippold (195) obtained a DRF in the oxygen effect of about 2. From a study of the modification of chromosome aberrations in onion root tips by x-rays, Riley (156) concludes that factors other than oxygen concentration at time of irradiation may be important in influencing radiosensitivity. The influence of anoxia during x-irradiation on the induction of mutations of linked endosperm factors has recently been studied [Konzak (96)]. Entire endosperm mutants were reduced fourfold by anoxia; mosaic endosperm, 1.9; nonmosaics, 1.8. If observed endosperm phenotypic changes represent breaks, specific chromosomal regions (as marked by genetic loci) may respond differently to anoxia as far as radiosensitivity is concerned.

X-irradiations in nitrogen, air, and oxygen of *Drosophila* spermatids show oxygen has no appreciable effect over air but nitrogen lowers radiation effects (autosomal translocations) considerably [Oster (132)]. On the other hand, in spermatozoa in the male or in the female, nitrogen and oxygen modify dose response below and above the air response about equally. It may be inferred from these results that spermatids may have more oxygen normally present or available. *Habrobracon* eggs show a consistently greater radiation response to anoxia than do spermatozoa, irrespective of sensitivity of their chromosomes to x-rays [Whiting & Murphy (190)]. The DRFs for the oxygen effect vary from 1.6 to 2 for eggs and from 1.2 to 2 for spermatozoa. They suggest that the water content of these cells might be the basic

factor involved in this difference. Their conclusions favor the breakage hypothesis (as contrasted to the recovery hypothesis) as regards the mechanism of the oxygen effect.

Irradiation of dry pollen of *Tradescantia paludosa* with monochromatic ultraviolet light of various wavelengths has shown no significant difference in the number of chromatid and isochromatid aberrations when treatment was in air or in nitrogen [Kirby-Smith & Craig (95)]. Giese, Iverson & Sanders (65) find no oxygen effect on the survival of yeast exposed to ultraviolet radiation [see also (2, 7, 12, 31, 33, 59)].

3. *Chemicals.*—Several mechanisms for chemical modification of radiation damage have been proposed; among these are scavenger action for free radicals (54, 160), oxygen removal (78), repair of primary radiation damage (20), sensitization for radiation damage (16), free radical production (54), shielding of sensitive molecules (106, 146), and metabolic inhibition (12).

Littman, Carr & Clauss (106) have studied the effectiveness of various chemicals (aldehydes, dialdehydes, ketoaldehydes, and keto acids) in protecting cysteine against γ-irradiation (Co^{60}). Their results indicate that the masking of radiosensitive groups by specific chemical reactions may be a more effective way of reducing certain effects of ionizing radiation than the addition of free radical acceptors.

An interesting study has been made by Rosen & Boman (159) and by Rosen, Brohult, & Alexander (160) on the effects of γ-rays on solutions of human serum albumin, using both loss of sedimentation with ultracentrifugation and change in chromatographic response as measures of radiation damage. They believe that the radiation effects are largely caused by indirect action, since the magnitude of the radiation effect depends on the initial protein concentration. Thiourea, cysteamine, and sodium benzoate are all found to be effective protectors at concentrations of around $10^{-3}M$. From the shapes of the dose-effect curves they infer that thiourea and cysteamine protect by reacting with free radicals and after reactions are no longer effective as protectors. The product formed by the interaction of free radicals and sodium benzoate is thought, however, to continue to be effective as a free radical remover with approximately constant efficiency.

Augenstine (10) has found that at certain concentrations the inactivation of protein solutions is larger than is to be expected from freely diffusing radicals alone. This additional effect, classified as an "activated ion" effect, accounts for target volumes 45 and 200 times the molecule volumes for chymotrypsin and trypsin, respectively.

Bachofer and his co-workers have studied extensively the action of various chemicals in modifying the radiations response of T1 bacteriophage. Cyclohexanecarboxylic acid and various benzene derivatives have been used by Bachofer & Hartwig (13) in order to determine what effect the substituent groups and their positions on the ring would have on the protective ability of each compound; x-irradiations were carried out with variations in pH, dose, and concentration of the compounds. Cyclohexanecarboxylic acid

affords high protection; o-, p-, and m-aminobenzoic acids protect in that order, the first being approximately equal to cyclohexanecarboxylic acid. Intermediate concentrations protect better than high or low concentrations; higher survivals are generally produced at higher pH values. Hydroxybenzoic acids are less effective protectors; benzoic acid was a poor protector. Various reducing agents have been found to be extremely effective in protecting against x- or γ-irradiation. In particular, KCN and $NaNO_2$ give DRF's varying from one to approximately three as their molarities are increased from 10^{-7} to 10^{-2} [Bachofer & Pottinger (14)]. From this and other evidence they believe that even though oxygen protects T1 from ionizing radiations, this system is inactivated chiefly by the oxidizing action of ionizing radiations. Pottinger & Bachofer (146) have also compared the protection afforded by various inorganic salts against the effects of x-rays and heat. It is found that $0.1 M$ concentrations of various salts protect against x-rays in the following order: $NaNO_2$, $NaNO_3$, $(NH_4)_2SO_4$, $CaCl_2$, NaCl, $MgSO_4$. On the other hand, the above salts protect T1 against thermal effects in practically the reverse order. They conclude that radiation protection is brought about by these salts effectively isolating phage from radicals produced upon irradiation and thereby protecting virus DNA. It is suggested that these give heat protection by forming complexes with DNA, thereby stabilizing phage against denaturation.

The ability of sodium nitrite to protect various biological systems against x-rays has been attributed to several mechanisms, one of which, enhancement of the ability of catalase to decompose hydrogen peroxide, has been investigated by Bachofer (11) with bacteriophage T1. Irradiations were carried out in the presence of catalase, of sodium nitrite, and of the two combined; both are effective protectors. Sodium nitrite enhances neither the protective ability of catalase nor the ability of catalase to decompose hydrogen peroxide; nitrite probably acts as a reducing agent.

A report of chemical protection against the direct effects of x-irradiation is made by Ginoza & Norman (66). They find that glutathione added before drying or freezing tobacco mosaic virus gives twofold protection. They feel that in this supposedly water-free system there should be little indirect effect. A similar type of protection has been found by Moutschen & Bacq (115) in barley seeds soaked in solutions of glutathione before drying and subsequent x-irradiation; diminution in seedling height was used as the criterion of radiation damage. It would be worthwhile to test the effectiveness of glutathione in the dry state in the absence of oxygen, as the effectiveness of many protective chemicals seems to be greatly diminished under anoxic conditions. For example, Howard-Flanders & Alper (78) find that cystamine (0.004 M) gives no protection to bacteria irradiated under anoxic conditions. Menadione diphosphate (Synkavite; tetrasodium dimethyl 1,4-naphthohydroquine diphosphate) gave no protection under aerobic or anaerobic conditions. Bora (22) also reports that menadione diphosphate at $3 \times 10^{-4} M$ concentration does not affect the frequency of chromosomal aberrations in *Vicia faba*

caused by x-irradiation; menadione diphosphate alone does not produce breaks in this material.

The effectiveness of various chemicals in reducing the frequency of chromosome interchanges, deletions, and anaphase bridges in onion root tips has been studied by Riley (156). The order of effectiveness of the various chemicals depends on the endpoint used; the author believes that factors other than the amount of oxygen present at time of irradiation may be operative in bringing about the differences in protective ability.

Fairbanks (57, 58) has found that *E. coli* protected with aminoethyl thiosouronium bromide hydrobromide (AET) before massive irradiation and subsequent lyophilization has magnetic resonance patterns different from those of cells not so protected. It is postulated that free radicals react with the protective agent.

Reid (155) has suggested that radiation damage may be less severe in anesthetized tissue because of the possibility that molecules of an anesthetic may act as traps for energy absorbed in tissue and may thus compete with the biologically important groups which normally receive this energy.

Steffensen (179) has extended his original studies on the influence of calcium on spontaneous chromosome aberrations by examining the combined action of x-irradiation and cation imbalances on this effect in *Tradescantia* microspores from plants grown under various conditions. Chromosome aberrations induced by irradiation were not increased over control values in cultures with excess manganese, deficient iron, or deficient magnesium concentrations. Those plants grown on suboptimal calcium, however, showed a significant increase in the occurrence of interchanges and interstitial deletions. These observations indicate that calcium is required for the stability of the chromosomes. Steffensen suggests that calcium forms chelate bonds with phosphate end-groups between different DNA species along the chromosome. Nilan & Phillips (120) have obtained similar results with diploid barley seeds. The frequency of chromosome aberrations induced by x-rays is higher in calcium-deficient seeds. However, when irradiation was with thermal neutrons, there was no calcium effect on frequency of chromosome aberrations. These authors support Steffensen's hypothesis of the action of calcium and attribute the difference in the effectiveness of x-rays and thermal neutrons to LET.

Hollaender (76) cites work by himself and Girolami in which they have been able to protect significantly against x-ray induced mutations in *E. coli* by use of cysteamine. Other papers on chemical protection are (17, 21, 42, 65, 89, 90, 101, 127).

C. Postirradiation Physical Factors

1. *Visible light.*—A number of studies have appeared which deal with the photoreactivation of a variety of biological effects modified by ultraviolet radiations. Among these are: RNA and DNA synthesis [Iverson & Giese (85)]; mutation rates [Altenburg & Altenburg (7)]; colony formation

[Deering & Setlow (46), Giese *et al.* (65), Northrop (123), Uecker & Pichl (139, 186)]; chromosome aberrations [Kirby-Smith & Craig (95)].

An interesting study on the ultraviolet inactivation and photoreactivation of a virus M5, specific for *B. megaterium*, has been made by Friedman (63). This virus was irradiated both in the wet and dried states and assayed using three strains of the host bacterium. With hosts H1 and H2, the same survival is obtained with wet, photoreactivated virus and with dry, photoreactivated or nonreactivated virus; the sensitivity of wet, nonphotoreactivated virus is about twice as great. However, with host H3, no reactivation is observed for either the wet or dried virus, the wet virus being about twice as sensitive as the dry virus. Thus, the virus photoreactivation properties depend not only on the water content of the virus but also on its host.

The possession of certain cytochromes in *Azotobacter* is associated both with the ability of these cells to be photoreactivated and the sensitivity of their respiratory system to ultraviolet light [Goucher & Kocholaty (67)].

Zelle *et al.* (202) have studied the photoreactivation of both cellular inactivation and mutation to streptomycin independence in two strains of *E. coli* after irradiation with ultraviolet light of 2250 and 2650 A. The photoreactivation of both strains following irradiation with 2650 A follows a similar pattern, maximum photoreactivation being obtained after about 20 min. under the given experimental conditions. However, after 2250 A irradiation, one of the strains shows little photoreactivation and indeed shows a sensitization to the visible light after a 30-min. exposure. These differences in ultraviolet response and photoreactivation in different strains of the same organism are indicative of the complexity of these processes.

Several factors of importance in photoreactivation have been studied with yeast by Giese *et al.* (65). Irradiated yeast recovers to a considerable extent in the dark if storage is at 28°C., but there is little recovery at 5°C. The ability of a yeast suspension treated with ultraviolet light to be photoreactivated declines much more rapidly if stored at 28° than at 5°C. Photoreactivation occurs equally well under aerobic and anaerobic conditions.

An interesting photoreactivation phenomenon has been observed in ultraviolet-induced recessive, lethal mutations in dechlorinated *Drosophila* eggs [Altenburg & Altenburg (7)]. Photoreactivating light, applied for 3.5 min. immediately following a 3.5-min. dose of ultraviolet light, lowered the mutation rate from about 6 to about 1 per cent. Photoreactivation for 10 min. gives complete recovery. However, if photoreactivation is simultaneously applied during ultraviolet treatment, the induced rate is about 5 per cent, indicating little recovery under this condition. Ten minutes of ultraviolet irradiation give a 3 per cent mutation rate which was increased to 10 per cent by 10-min. posttreatment with "photoreactivating" light.

Kirby-Smith & Craig have observed no photoreactivation of ultraviolet-induced chromosome damage in dry pollen of *Tradescantia* (95).

2. *Oxygen.*—There are several recent reports on the influence of oxygen after irradiation on the overall radiation response. Pronuclear fusion in

Ascaris eggs is susceptible to x-irradiation damage as evidenced by a delay in the fusion process; a partial recovery can be brought about by anaerobic treatment following irradiation [Bachofer (12)]. Such recovery processes may be attributed to a retardation of aerobic events which lead to a manifestation of radiation damage with no concomitant decrease in anaerobic events which may aid in a reversal of radiation damage.

Caldecott and his co-workers (31, 32, 33) have investigated the modification of radiation-induced injury by post-treatment with oxygen. Barley seeds that contained either 4 or 16 per cent water in the embryo were x-irradiated and then hydrated in the presence or absence of oxygen for various times. Seedling height after six days was the effect scored. Seeds with 4 per cent water showed striking sensitivity to hydration in the presence of oxygen; seeds with 16 per cent water showed no difference in sensitivity. Seeds with either water content showed no postirradiation hydration effect after fast- or thermal-neutron irradiation. The lack of an effect following neutron irradiation is postulated as resulting from their high LET which gives dense clusters of energy, thereby irreversibly inactivating a sensitive region. With radiations of lower LET, damage may be reversible; if oxygen is available to react with partially damaged sites before restoration occurs, a biologically detectable event occurs. These authors speculate that in the seeds with 16 per cent water, aerobic metabolic processes are occurring at such a rapid pace that an aerobic condition is created in those sites affected by irradiation (i.e., the nucleus) and hence, no postirradiation oxygen effect can be observed. However, with cells of 4 per cent water content, postirradiation exposure to oxygen results in irreversible, detrimental effects.

3. *Temperature.*—Again, the year's work has brought forth a varied picture as regards the influence of low temperatures following radiation exposure. Freezing dry barley seeds after irradiation inhibits their deterioration while in the frozen state, but on warming to 23°C., deterioration proceeds as in freshly exposed seeds [Konzak *et al.* (99)]. Donnellon & Morowitz (50) find no difference in the survival of irradiated spores of *B. subtilis* when incubated immediately after exposure or when incubated following an 8-hr. detention at 5°C. On the other hand, Ehrenberg & Lundquist (55) found that germination of irradiated barley seeds at lower temperatures increased radiation damage as measured by frequency of chromosomal aberrations and by degree of growth inhibition. With *Chlamydomonas* Jacobson (86, 87) has found, by the use of fractionation techniques with x-rays, that recovery processes between radiation fractions function better at 25° than at 10°C. He thus associates metabolic processes with the recovery phenomenon. Pahl & Bachofer (134) find that *Ascaris* eggs show better survival following 28,000 r of x-rays if incubation is at 30° rather than 20° or 15°C.

Buzzell (28) has studied the thermal reactivation of *E. coli* B inactivated by ultraviolet irradiation. Incubation in liquid broth agar at 46.5°C. (there is apparently no multiplication at this temperature) for times of the order of a few hours is effective in restoring colony-forming ability to approximately

90 per cent of those that are capable of being restored. The kinetics of this restoration process depend on the previously administered ultraviolet dose; from these kinetics, Buzzell estimates that six sensitive sites for ultraviolet irradiation exist per bacterium. The ultraviolet sensitivity of the bacterium decreases as it approaches the resting state, possibly because of a decrease in the number of the sensitive sites. She believes that the primary ultraviolet action is to transform cell metabolites into poisons: a bacterium survives under conditions which inhibit growth and which allow such poisons to diffuse away before acting on a sensitive site. Other temperature studies (12, 21, 51, 65, 99) are discussed elsewhere.

4. *Chemicals.*—Recently Hurwitz, Rosano, & Blattberg (79) have failed to find reactivation by metabolites in *E. coli* inactivated by heat or chemicals as earlier reported by Heinmets, Taylor & Lehman (73). The former authors have shown, using statistical studies and millipore filters, that the "reactivation" reported by Heinmets, Taylor and Lehman is caused by multiplication of the unkilled bacteria during the incubation period. Thus there is considerable reason to question the report by Heinmets *et al.* (72) on the metabolic reactivation of ultraviolet inactivated bacteria, since their techniques in the two studies were similar. Furthermore, the fact that no reactivation was observed by Heinmets *et al.* when metabolites were added to solid plating medium casts doubts on their interpretations.

Kanazir, Kaćanski & Krajinćanić (88) have reported that *Salmonella typhimurium*, in which cell survival is reduced to one-third by ultraviolet irradiation, may be chemically reactivated to approximately 90 per cent survival by the addition of an extract made from unirradiated cells. "Factors" present in the extract restore the synthesis of genetically "good" DNA in irradiated cells. Bećarević (16) finds that in ultraviolet irradiated yeast the synthesis of catalase is partly suppressed; this synthesis can be restored by the addition of yeast extract immediately after irradiation. Restoration of catalase synthesis does not set in before an incubation period of about two hours. During this period, there is a restoration of RNA synthesis in the treated, irradiated cells.

Division delay in *Chilomonas paramecium* is found by Ducoff (51) to be a function of dose (x-rays). Both generation time and recovery time from the radiation-induced division delay are similarly affected by incubation temperature and by organic growth media. No recovery occurred in the absence of a utilizable nitrogen source. Ducoff believes that recovery from radiation-induced division block is an active metabolic process, involving nitrogenous intermediates.

The number of x-ray-induced, recessive, lethal, and deleterious mutations in *Paramecium aurelia* can be reduced by one-quarter by post irradiation exposure to streptomycin for 3 to 4 hr. [Kimball, Gaither & Wilson (93, 94)]. This effect is found only in animals irradiated in the first third of the interdivisional interval and then only when streptomycin is added within one hour of irradiation. It is believed that at least part of the mutational process

is not completed until late interphase, perhaps at the time of chromosome replication; until the process is completed it is subject to spontaneous reversal.

Betz & Booz (20) have observed that the rate of nuclear pycnosis of rat thymus cells irradiated with 300 r of x-rays *in vitro* is decreased approximately 50 per cent by 0.5 per cent cysteamine or cystamine; there is no protection of cells irradiated *in vivo* with 10 gm./100 gm.-rat of the above chemicals. From these experiments it is not clear if the lack of protection in the *in vivo* irradiations is caused by a low concentration of the protective chemicals. It is suggested that the *in vitro* protection of thymic cells may be attributable to the action of the protective chemicals after the irradiation, and not during the radiation treatment.

It has been shown that dry seeds of *Vicia faba* after being exposed to 3000 r of x-rays show a 50 per cent decrease in rate of mitosis when added to nutrient bouillon. However, if the bouillon is fortified with either cysteine or cysteamine, there is no diminution in the rate of mitosis [Krahe, Künkel & Schmermund (101)]. However, additions of glutathione, cysteine, and homocysteine to irradiated DNAase solution fail to reactivate the enzyme [Okada (127)].

Tanada (182) has studied the absorption of rubidium by excised mung bean roots following ultraviolet irradiation; ultraviolet treatment is detrimental to rubidium absorption. Cysteamine, cysteine, and glutathione were found to reduce the loss in absorption in ultraviolet-treated material when added after irradiation; no photoreactivation of rubidium absorption was found.

D. Biological Factors

1. *Ploidy.*—The use of target theory to obtain information on cells of unknown ploidy is discussed in Section V. C. (189, 201). A single *Tradescantis paludosa* flower bud which contained a mixed population of haploid and diploid microspores was irradiated with 500 r of x-rays while the cells were in postmeiotic interphase; examination was at the microscopore mitotic division [Conger & Johnston (40)]. Diploid cells were found to have almost exactly twice as many aberrations as the haploids, i.e., the aberration frequency per chromosome was the same in haploid and diploid cells. They conclude from this observation that the space over which chromosome breaks can interact to produce an exchange is very limited. Swaminathan & Natarajan (181) have questioned this conclusion. Using haploid, tetraploid, and hexaploid species of wheat, they find that although x-rays and P^{32} β-rays give a fixed number of chromosome breaks per unit length of chromosome in the three ploidies, fast neutrons give approximately 10 times as many breaks in the hexaploid species as in the diploid or the tetraploid. They conclude that the frequency of interaction of chromosome breaks depends on both ploidy and LET.

Owen & Mortimer (133) have continued the very interesting work with

yeast concerned with the influence of ploidy on radiosensitivity. By mating x-irradiated haploid or diploid cells with unirradiated haploids of opposite mating types and observing the viability of the zygotes as revealed by cell multiplication, the frequency of dominant lethals induced in the irradiated haploid and diploid cells has been determined. Although diploid cells are less sensitive to x-irradiation than haploids, the frequency of dominant lethals induced in diploids is considerably greater than in haploids. There is a DRF of approximately two between the haploid and diloid dominant lethal curves, suggesting that the amount of dominant lethal damage depends on the product of ploidy and dose.

Clark & Webb (36) have found that cultures made from cells of *Nocardia corallina* which have survived 18 kr of x-rays are more sensitive to subsequent x-irradiation than the parent cells; maximum sensitivity was obtained after four successive irradiations of survivors, after which radiation response became more resistant. The initial sensitization conforms with the unpaired-defect theory of Tobias (184) which is applicable to diploid cells; the subsequent increasing resistance may be due to the selection of normally occurring resistant coccoidal cells initially present in a small per cent of the original population.

Clark (35) has discussed the influence of ploidy on the radiosensitivity of *Habrobracon* at various stages of development. There is no simple correlation between ploidy and radiosensitivity throughout the life cycle. Clark speculates that changes in radiosensitivity may come about as a result of a balance between dominant and recessive lethals that varies with stage development.

2. *Division state.*—By means of a microbeam apparatus, Davis, Simon-Reuss & Smith (45) have irradiated chick fibroblasts with polonium α-particles. The sensitivity of a cell increases by a factor of ten from prophase to metaphase; this sensitivity seems to increase with the state of condensation of the chromosomes.

Spermatogonia counts in irradiated male mice given 5 to 100 r of Co^{60} γ-rays indicate that late type A, intermediate, and early type B spermatogonia are equally sensitive [Oakberg (124)]. Scoring of all type A spermatogonia indicates they are more resistant to higher doses (30 to 100 r).

Two papers should be mentioned that deal with radiosensitivity of *Drosophilia* sperm at various stages of development. Alexander (1) finds more radiation damage (as revealed by the induction of dominant lethals) in young spermatids than in more mature cells. Oster (132) suggests that the high sensitivity of spermatids may be caused by more intra- or intercellular oxygen, or both, being present. Clark (35) finds that in *Habrobracon*, diploids (female) are more sensitive to irradiation than haploids (male) in the cleavage stage; however, during the larva and pupa stages, haploids are more sensitive than diploids. This change in haploid-diploid sensitivity can be explained if one assumes that in the cleavage stage most radiation damage is of a dominant nature, and in the larva and pupa stages, of a recessive nature.

By the study of cultures of *Bacillus cereus* during the course of sporgtula-
tion, Romig & Wyss have found that the increased level of resistance ex-
hibited by the spores to the lethal effects of ultraviolet light develops as
much as two hours before heat resistance is manifested (158). The ultra-
violet resistance of the developing spores was correlated with the appearance
of the forespore, whereas heat resistance is delayed until development of the
mature spore. In the process of spore formation, susceptibility to photo-
reactivation and to the lethal effect of low doses of ultraviolet are lost at
about the same time.

Yeast cells in the logarithmic growth phase are much less sensitive to
ultraviolet radiation (loss of colony-forming ability) than those past this
phase [Giese *et al.* (65)]. Nitrogen starvation increases ultraviolet sensitivity
more than glucose starvation alone. Ultraviolet resistance in carbohydrate-
starved yeast is decreased by supplying glucose; nitrogen-starved yeast be-
comes much more resistant when supplied with yeast extract although in-
organic nitrogen has no effect. Cyanide also has no effect on ultraviolet in-
jury [see also (51, 71, 84, 85, 87, 94, 111, 152)].

3. *Metabolic state.*—It is now generally recognized that there is no abso-
lute measure of radiation damage in a biological system; the damage depends
on many factors not necessarily connected with the primary radiation
processes. Among the most important of those factors is the metabolic state
of the system before, during, and after the radiation process. All recovery
processes could probably be considered as affecting the metabolic state of
the test system.

The cleavage delay that is induced in *Ascaris* eggs by x-rays can be re-
duced by either anaerobic treatment or KCN exposure following radiation
[Bachofer (12); Pahl & Bachofer (134)]. Hydration in oxygen-free suspen-
sions following x-irradiation of dormant barley seeds favors restitution of
chromosome breaks [Caldecott & Curtis (31)]. Thus, in these studies re-
covery is to be associated with an anaerobic metabolic process.

Ducoff (51) has studied the recovery of *Chilomonas paramecium* from
radiation-induced division block; this recovery requires an active metabolic
process which involves nitrogenous intermediates. The same author finds
that the division delay induced by ionizing radiation in *Tetrahymena* is not
dependent on the synthesis of DNA or DNA-like material (52). Fractionated
doses of x-rays are less effective than equal, single doses in the inactivation
of *Chlamydomonas reinhardi* when the cells are stored at 30°C. between
fractions; however when storage is at 0°C., there is no diminution by
fractionation [Jacobson (86, 87)]. The model used by Jacobson in his discus-
sion of these results is interesting in that it assumes a progressive sensitiza-
tion of the irradiated material with increasing dose, i.e., a multihit process.
In order for the recovery process associated with the fractionation to be
operative, the cells must be in an active metabolizing state. Whether this
recovery consists in the repair of chromosome breaks or in the reversal of
some other incomplete radiation-induced process is not clear. (It would be

interesting to compare these results with another similar organism having exponential survival to determine if recovery is only possible in multihit processes.)

Fermenting and respiring strains of related haploid yeasts have been found to differ in their radiation response when irradiated under aerobic and anaerobic conditions, and in frozen and liquid suspensions [Wood & Taylor (197)]. The same general pattern was also obtained for a wild-type and a derived "petite" strain. It seems probable that the difference in radiation response is due to metabolic differences in these strains [see also (29, 60, 158, 177)].

IV. SOME EFFECTS OF RADIATIONS

A. CYTOLOGICAL EFFECTS

A very convincing demonstration of the efficacy of free radicals in producing chromosome aberrations in barley has been given by Phillips (138). Dormant barley seeds were exposed to radicals produced by combining dilute solutions of hydrogen peroxide and ferric sulfate. The frequency of chromosome fragments in seeds treated in this manner is 15 or 20 times the frequency found in those treated with either peroxide or ferric sulfate alone. The ratio of chromosome-chromatid breaks was more typical of that induced by x-irradiation than by radiomimetic chemicals.

Kirby-Smith & Craig (95) have made a significant contribution to the literature with their study on the induction of chromosome aberrations in dry pollen of *Tradescantia* by ultraviolet radiation. The aberrations scored were chromatid and isochromatid breaks, chromatid-chromatid exchanges, and chromosome fragmentation. No time-intensity relationship was found over the intensity range studied. Irradiation in air and nitrogen causes no significant difference in the number of chromatid and isochromatid aberrations; from this it is inferred that ozone plays no role in these experiments. However, the percentage of incompletely fused isochromatid aberrations is greater for material irradiated in nitrogen than in air. There is no photo-recovery of ultraviolet-induced chromosome damage in the dry pollen. The action spectrum for chromosome breakage is in good agreement with nucleic acid absorption curves. The ratios of chromatid to isochromatid breaks to chromatid-chromatid interchanges are approximately 1:0.5:0.05 for ultra-violet of wavelength 2650 A; the comparable ratios for x-ray induced aberrations are 1:3:1. Thus, it seems that the ends of chromosomes broken by ultraviolet do not rejoin to the same extent as those produced by ionizing radiation. This same conclusion regarding decreased reunion in chromosomes broken by ultraviolet radiations compared to x-irradiated ones has been reached by Steinitz-Sears & Sears (180). Wheat pollen was given ultraviolet and x-ray doses equal in their capacities to break chromosomes, and reciprocal translocations and partial and whole chromosome deficiencies were scored.

Kihlman (89) has studied the production of chromosome aberrations in

Vicia faba by several heavy metal complexing agents. KCN produces structural chromosome changes in root tips; this effect increases with oxygen concentration. Pretreatment with 2,4-dinitrophenol does not influence cyanide action. The effectiveness of 8-ethoxycaffeine is almost completely inhibited by cyanide. Sodium fluoride, potassium thiocyanide, carbon monoxide, and sodium azide were found to have no radiomimetic effects under the conditions used. Under anaerobic conditions the effects of cyanide and cupferron were qualitatively and quantitatively equal; however, there is no oxygen effect with cupferron. Cyanide completely inhibits action of catalase and peroxidase. Hydrogen peroxide, alone or with cyanide, is without radiomimetic effect. From these studies it appears as if hydrogen peroxide is not involved in the production of chromosome aberrations by cyanide. Kihlman suggests that cyanide and other heavy metal complexing agents may produce chromosome aberrations by reacting with iron or other heavy metals present in chromosomes. Kihlman, Merz & Swanson (90) have tested many of the above agents for sensitization of *Vicia* to x-rays: only cyanide and cupferron were effective. Cyanide in concentrations as low as 2×10^{-5} M enhances x-ray effects, but only in the absence of oxygen. The distribution of breaks indicates that cyanide sensitizes for x-rays and not vice versa. These authors suggest that the oxygen effect, as far as chromosome breaks are concerned, may be due to a sensitization of the chromosomes caused by their bound iron being in an oxidized state.

Davidson (42) has studied the production of point unions (interstitial and terminal unions) in *Vicia faba* by x-rays and 8-ethoxycaffeine. He concludes that, since point unions are produced by both of these agents, their modes of action are similar. Such interpretations must be made with caution, however, for the same end effects may be brought about by quite different intermediate processes.

X-ray studies on the production of chromosome aberrations in wheat of various ages have led Nilan & Gunthardt (119) to suggest that the increased sensitivity found in older seeds may be caused by the accumulation of metabolic wastes such as putrescine and cadaverine. These are mutagenic and strong chelating agents which could act by forming complexes with calcium and magnesium ions that may be the bonding agents between DNA species (120, 179, 195).

X-ray fractionation studies on seedling roots of *Allium cepa* indicate that there are two classes of broken ends of chromosomes (as judged by their average restitution times) induced by irradiation [Cohn (37)]. The frequency of chromosome exchanges at metaphase was determined for two doses of x-rays each of 800 r given in 30 sec., separated by time intervals of from 0 to 15 hr. Within 15 min. a substantial fraction of the broken ends rejoin; some ends remain open for as long as four hours. Carbon monoxide prevents the restitution of both types of breaks, and the effect of carbon monoxide is light-reversible (38). Cohn interprets these results as evidence against the existence of ionic linkages (calcium and magnesium ions) in chromosomes

whose reunion, presumably, would not be retarded by carbon monoxide. He now feels that iron is somehow involved in the organization of chromosomes (private communication).

Wolff & Luippold (195) had earlier reported experiments on seeds of *Vicia faba* that indicated that chromosome breaks induced by x-rays were of two classes: those having lifetimes of only about a minute and those persisting from one-half to two hours. This information was obtained by varying the dose rate. Experiments with ethylenediamine tetraacetic acid tetrasodium salt (Versene), a chelating agent which would be expected to "tie-up" broken chromosome ends at the location of calcium or magnesium ions, show an increase in aberration yield. This increase is associated by these authors with a decrease in the restitution processes involving those breaks normally having a very short lifetime. Thus, an identification is made between ionic bonds in the case of breaks having a short lifetime and covalent bonds for those having a longer lifetime. This latter type of break requires a source of energy for the biosynthesis of the bonds formed in closing.

With dormant barley seed, Schooler, Nilan & Phillips (162) find no significant fractionation effect (intervals between fractions from 1/2 to 96 hr.). The biological effects scored were injury (seedling height and yield survival), frequency of seedling mutations, and frequency of chromosome aberrations. The dose rate was comparable to those used in other studies (37, 38, 195). If there are two classes of bonds, the first type (ionic, having short lifetimes) would not be detected with the fractionation schedule used and the second (covalent, requiring metabolic energy expenditures for restitution) might not be present in the dormant embryo system used here.

Caldecott & Curtis (31) have dealt with the question of whether aerobic physiological activity is required for restitution or reunion in chromosome breaks in barley seeds. Seeds are inactivated in the dormant state and are added afterwards to oxygenated or oxygen-free water. In oxygenated material there is actually an increase in detectable radiation damage (interchanges and other anomalies). Hydration in the absence of oxygen favors restitution of chromosome breaks. The major portion of the restitution occurs within 30 min. after seeds are subjected to hydration. These results indicate that the energy required for restitution of radiation-induced chromosome breaks does not result from aerobic physiological activity.

Conger & Johnston (40) have observed that x-irradiated haploid and diploid *Tradescantia* microspores have the same number of exchange aberrations per chromosome. From this instance, they infer that if two chromosome breaks are to exchange, they must be closer together than the average chromosome distance in the diploid cell. This observation has been confirmed by Swaminathan & Nataraj (181) in diploid, tetraploid, and hexaploid strains of wheat with x- and β-irradiations. However, with fast neutrons the hexaploid strain shows approximately 10 times the number of breaks per 100 μ of chromosome length as the diploid or tetraploid strain. Thus in this system the aberration frequency is independent of the ploidy when LET is

low but is a function of both ploidy and LET when LET is greater than that for P^{32} β-radiation. Careful studies with a spectrum of LET's and with various ploidies would allow estimates to be made of the interaction distance for exchange aberrations.

There are many reasons for believing that the detrimental effects of ionizing radiations are primarily caused by damage to the genetic apparatus of the cell. Most of the work in cellular radiobiology today is motivated by the operational philosophy that radiation damage is nuclear; however, occasional investigations do not apparently fit into this convenient framework. Bacq *et al.* (15) find that anucleate fragments of the alga *Acetabularia mediterranea* are more sensitive to x-irradiation than are nucleate fragments. In whole cell irradiation, the cytoplasm most distant from the nucleus dies more quickly and in a higher percentage of cases than the region surrounding the nucleus. The comparative sensitivities of nucleate and anucleate cellular fragments to ultraviolet light have also been studied by Skreb & Errera (173) and by Errera & Vanderhaeghe (56). Nucleate fragments of *Amoeba proteus* are less injured by ultraviolet than are anucleate ones; starvation for 10 days increases ultraviolet sensitivity of both nucleate and anucleate fragments (173); ultraviolet damage in both types of fragments can be partially reversed by visible light. The rate of glycogen utilization is also decreased by ultraviolet treatment. With *Acetabularia mediterranea* (56), the same picture exists, i.e., the cytoplasm appears to be more sensitive to ultraviolet light than the nucleus as demonstrated by a decreased survival and regeneration of the anucleate fragments as compared with nuclear ones. Irradiation of only the cytoplasm of a whole cell has the same effect as the irradiation of the whole cell. When only the shizoïd (which contains the nucleus) is irradiated, there is less injury than when the whole cell or only the cytoplasm is irradiated. Irradiation of the shizoïd only can even cause a precocious stimulation of growth and morphogenesis. Cytological examinations have demonstrated an immediate nuclear damage by ultraviolet, even though the nucleus was not within the irradiated area.

On the other hand, Munro (116) has found cytoplasm to be relatively radioresistant. By means of tungsten micro-needles on which polonium is deposited, he has irradiated small regions of chick cells in tissue culture. Irradiation of the chromosomal region at metaphase produces sticky bridges at anaphase. When only parts of the cytoplasm and spindle are irradiated, no abnormalities are seen although the dose at a point 5μ from the chromosomes is up to 30 times that needed to produce sticky bridges when the chromosomes are treated. Other papers concerned with cytological effects are discussed elsewhere (18, 22, 23, 39, 55, 96, 152, 156, 194).

B. Nucleic Acid Synthesis and Growth

The early events of infection with strains U1 and U2 of tobacco mosaic virus and the nucleic acid isolated therefrom have been compared by Siegel, Ginoza & Wildman (172). Infective centers initiated by intact virus and

irradiated with ultraviolet light at different times after initiation of infection display an initial lag period during which no change in resistance to ultraviolet light occurs; this lag is 2.5 hr. for the U1 strain and 5 hr. for the U2 strain. In contrast, infective centers caused by the nucleic acid isolated from these strains behave alike and display no lag before they begin to increase in ultraviolet resistance. The authors conclude that when infection is initiated by the intact virus, the nucleic acid of the virus must be freed from the protein component before infection is established and replication begins.

Five criteria of ultraviolet damage have been used by Deering & Setlow (46) in their study on the effects of low doses of ultraviolet light on *E. coli* B. The ability of a cell to divide within three hours of irradiation (microscopic observations) is the most sensitive; the loss of colony formation ability is approximately 10 times as resistant. On the other hand, at low doses there is no measurable loss in the rates of DNA synthesis, RNA synthesis, and total mass increase (protein synthesis). The action spectrum for division inhibition has a maximum at 2652 A. In these studies filament formation in the irradiated cells was microscopically observed; the DNA and RNA content of the filaments is the same, per unit mass of cells, as for the normally dividing cells. In another study with *E. coli* B, Iverson & Giese (85) find that 2540 A ultraviolet light stops both DNA and RNA synthesis immediately in out-of-log-phase cells, but stops only DNA synthesis immediately in log-phase cells. Thus they propose that there are at least two loci of action for ultraviolet that are effective in affecting RNA synthesis. They find that 2260 A radiation is ineffective in changing RNA or DNA synthesis but does affect cell viability. They postulate that the lethal action of 2260 A radiation is on a part of the cell not involved in nucleic acid synthesis.

The restoration of the synthesis of DNA in ultraviolet-irradiated *Salmonella* by cellular extracts (88), and the restoration of the synthesis of catalase in ultraviolet-treated yeast by yeast extract (16) have been discussed in Section III. C. 4.

Iverson & Giese (84) have been able to double the amount of DNA present in *Tetrahymena pyriformis* by heat treatment before ultraviolet irradiation. They find a greater resistance to ultraviolet in heat-treated cells, and they feel that this is correlated with the greater content of DNA. Thus the ultraviolet sensitivity is inversely proportional to the amount of DNA present.

Continuous x-ray exposure of a steady-state population of diploid yeast (6 kr per generation) results in a 2.5-fold increase in generation time [Welch (188)]. However, as such a treatment also increases the average size of cells, the decrease in total growth rate must be less than 60 per cent. Yeast irradiated in the exponential phase of growth show a decrease in six hours of as much as 40 per cent in carbohydrate per unit of weight [Spoerl & Looney (178)]. Cell wall glucans showed the greatest decrease; cell mannans the least. RNA per unit of weight showed little change, and on a per cell basis increased markedly. *Chilomonas paramecium* exposed to 15 kr or less of x-rays

show no decrease in growth rate (number of cells); exposure to 30 kr decreases the growth rate by almost a factor of two [Ducoff (51)].

Perry (137) has studied changes in the ultraviolet absorption spectrum of new heart cells in tissue culture following irradiation with an ultraviolet microbeam. Small areas (50 μ^2 or less) of chromosomes and interphase nuclei show an appreciable decrease in the absorbance at the site of irradiation around the 260 mμ region when irradiated with ultraviolet radiation. Since in nuclear material, especially chromosomes, the extinction at 260 mμ is to a great extent attributable to the purine and pyrimidine bases of DNA, it is concluded that at the site of irradiation there is a decrease in the number of intact bases. Other papers of interest are (30, 47, 66, 69, 70, 71, 110, 121, 122).

C. MUTAGENIC EFFECTS

Mortimer's (133) very interesting and important work on the relative importance of dominant and recessive lethal inactivation in yeast by x-rays has been extended by considering the dominant lethality induced in diploid yeast (see Section III. D. 1). Mortimer (112) has also studied the x-ray induction of homozygosis in diploid yeast that was heterozygous at a number of different loci concerned with adenine synthesis. This induction (as evidenced by variant colonies) increases linearly with dose and with distance of locus from its centromere. Mitotic crossing-over is responsible for the majority of the variant colonies. At doses which produce only a small degree of inactivation of these cells, it is estimated that a high percentage of the surviving cells experiences alteration of their genotype.

Colonies grown from irradiated cultures of *Chlamydomonas* show a considerable variation in size [Wetherell & Krauss (189)]. This variability depends on the ploidy of the irradiated strain and on the growth media, the variation in colony size being increased for polyploid cultures and for plating on a complete medium. There is also increased survival on a complete medium, compared with a marginal medium, with the difference being quantitatively accounted for by the increased number of small colonies on the complete medium. It is believed that small colonies arise from cells in polyploid strain that have heterozygous radiation damage, the homologous chromosome partially compensating for the loss in its homologue. Subcultures grown from small colonies show that this characteristic is inherited.

Four yeast cultures derived from an irregularly segregating ascus of *Saccharomyces* have been tested for x-ray sensitivity by Pittman & Pedigo (141). All cultures show exponential survival characteristic of haploid strains; however, one strain was approximately twice as resistant as the other three. The exact nature of the decreased sensitivity of the one strain is not known.

When *E. coli* B is incubated for a short period before exposure to ultraviolet light, in a minimal medium supplemented by yeast extract, by a combination of purines and pyrimidines, by riboflavin, or by *p*-aminobenzoic acid, both the frequency of mutation (aberrant color response on eosin-

methylene blue agar) per unit dose and the maximum mutation frequency are found to increase considerably [Haas & Doudney (71)]. The purine-pyrimidine influence has been studied by the use of synchronized cultures; maximum increase in frequency is obtained during periods of maximum nucleic acid synthesis, little or no increase being observed following the first nuclear division. The increased mutation frequency obtained by incubation in the presence of purines and pyrimidines bears no relation to the nucleic acid content of the cell, but more likely is related to the presence of nucleic acid precursors which have been modified by irradiation. This incorporation is dependent on the synthesis of protein immediately following radiation exposure. Haas and Doudney believe it probable that the radiation percursor interaction is at least at the stage of ribosides, and it is possible that ribotides are involved which may have to be associated with the nucleic acid template in the final stage of nucleic acid synthesis for maximum mutagenic effect.

Induced mutation rates in males hatching from dechorionated and ultra-violet-irradiated *Drosophila* eggs have been studied by Altenburg & Altenburg (6). The increase in mutation rate from 1.1 per cent at the lowest dose to 4.7 per cent at twice that dose is sufficiently large to indicate that the rate of mutations may rise as the square of the dose, or at least at a higher than linear rate. Further increase in dose failed to produce a significant increase in the mutation rate.

A comparative study has been made by Konzak & Singleton (98) of the phenotypic changes in maize endosperm tissue produced by irradiation of pollen with thermal neutrons, x-rays, γ-rays and ultraviolet radiation to determine whether the spectra of mutation produced by these various radiations would be similar. Genetic testers on different chromosomes were used. If it is assumed that the phenotypic changes observed were due to chromosome breaks, the quantitative variation in response to the various radiations indicates that different chromosome regions were affected differently by the four radiations. The authors feel, however, that the similarities in breakage patterns are perhaps more significant than the differences. [See also (1, 7, 35, 36, 93, 94, 96, 169).]

D. BIOCHEMICAL EFFECTS

An extensive review of biochemical effects of ionizing radiations has recently been prepared by Holmes (77).

An interesting report on the inheritance of radiation damage in yeast has been given by Galtsova (64). The first generation of survivors of *Saccharomyces ludwigii* to 60 kr of x-rays shows an approximate increase of two in the number of free sulfhydryl groups when compared with unirradiated controls. The progeny of these irradiated cells show this effect, in a degree, to the one hundredth cell generation. A simple "dilution" of the initial radiation damage could hardly account for detectable damage beyond 10 generations; this phenomenon could then only be accounted for by a change in the reproduction processes.

Yost & Robson (200) have concluded from a study of irradiated rat liver mitochondria that oxygen uptake may be a faulty criterion for estimating the health of an irradiated cell; 70 per cent of the phosphorylation mechanism of their system may be lost with no apparent effect on the oxygen uptake. Either the phosphorylation mechanism is much more sensitive to γ-irradiation than is the cytochrome oxidase, or there is a protective mechanism specific for the electron transport system. Rajewsky, Gerber & Pauly (153), from a study of this same system, conclude that the inactivation processes are largely due to indirect action.

Laser & Thornley (102) have found that x-irradiation of *E. coli* B enhances its ability to oxidize maltose under certain conditions; they attribute this to induced enzyme formation.

E. Miscellaneous Effects

1. *Paramagnetic resonance.*—Paramagnetic resonance techniques are now at the point where changes in spectra after large doses of ionizing radiations are suggestive of suspected molecular changes. If the sensitivity of these or similar techniques can be improved by one or two orders of magnitude, real progress will be made in understanding something of the events occurring between radiation absorption in biological materials and the observable end effects.

Zimmer, Ehrenberg & Ehrenberg (203) have detected spectral changes similar to those shown by free organic radicals when glycine and barley embryos are x-irradiated. These effects may be detected at doses as low as 25 kr. Glycine shows no oxygen dependence as measured by paramagnetic resonance studies; however, with barley, irradiation in the presence of air is 1.3 times as effective as irradiation with nitrogen. The half life for the decay of the amplitude of this effect in barley is about 25 hr. Box, Freund & Hoffman (24) have studied radical formation by x-rays in some 80 organic compounds in powdered form. In most cases the paramagnetism persists for periods of months. In some powders the number of such stabilized radicals is of the same order of magnitude as the number of ionizations produced by the radiation. Fairbanks (57, 58) has found qualitative differences in the shape of the resonance curves for x-irradiated *E. coli* when irradiated with and without AET, a protective material. A review of nuclear and electron paramagnetic resonance and their applications to biology has been prepared by Sogo & Tolbert (175).

2. *Viscosity.*—Nucleic acid extracted from x-irradiated tobacco mosaic virus is found to have a lower intrinsic viscosity than that isolated from non-irradiated virus [Lauffer, Trkula & Buzzell (104)]. This change in viscosity is to be associated with a lower average particle length in irradiated nucleic acid and this data indicates that x-rays break nucleic acid rods. To get a change in viscosity corresponding to an average of one break per nucleic acid particle, a dose eight times that required to give an average of one radiation event per particle is required. The authors believe that this dis-

crepancy indicates that the structure of RNA may be a coil of several strands; an average radiation event might cause loss of ability to reproduce but only the exceptional event (one of eight) would cause a breakage of the multi-strand particle. On the other hand, Buzzell, Trkula & Lauffer (30) find that, with ultraviolet, 30 times the inactivating dose is required to give a change in intrinsic viscosity corresponding to one break per nucleic acid particle. McLaren & Takahashi (110) find also that extracted nucleic acid is inacti-vated by ultraviolet without change in viscosity. The extracted nucleic acid has a higher ultraviolet sensitivity than the virus itself, the naked RNA being about six times as sensitive as the incorporated RNA. They speculate that virus protein may prevent excited nucleic acid from undergoing reaction with the solvent, from unfolding, or from irreversible breakage or disassocia-tion of radicals by a caging action. They feel that the inactivation step with ultraviolet must be rather local on the RNA chain and does not involve chain breakage.

3. *Permeability.*—Potassium retentivity of yeast after irradiation with x-rays, 2537 A ultraviolet, and the near ultraviolet has been examined by Bruce (26). With x-rays, under aerobic conditions, both the loss of potassium retentivity and cell survival (as revealed by colony formation) are exponen-tial with respect to the dose, cell survival being about four times as sensitive. Under anaerobic conditions, cell survival is again exponential and about twice as resistant as under aerobic conditions, but potassium retentivity decreases only slightly up to doses of 160 kr at which point the slope ap-proximates that of aerobic conditions. Thus, for cell survival and for ability to retain potassium, two different types of inactivation sites are involved. Furthermore, those sites involved in potassium retentivity are apparently much more sensitive to x-radiation in the presence of oxygen or to free radicals which are produced in the presence of oxygen. With 2537 A ultra-violet a sharp decrease in survival is found, whereas the retention of potas-sium is decreased relatively slowly. At 3400 to 4000 A both processes are affected approximately to the same extent; in this region, the membrane effect may be the determining factor in survival. The release of cellular con-stituents after x-irradiation of *E. coli* B/r has been studied by Billen (21) who finds that nucleic acid fragments primarily constitute the 260 mμ ab-sorbing material released by such cells. Such release, however, is inhibited by various factors (absence of exogenous metabolite, presence of arsenate, low temperature of incubation) which indicate a marked dependence on metabolic activity. Ultraviolet has a similar effect.

4. *Sensitization to and by other agents.*—Additivity studies with radia-tions and high temperatures are often useful in that they suggest whether similar or different inactivation mechanisms are involved in the two proc-esses. A study of the loss of serological activity of ovalbumin irradiated with γ-rays while in the lyophilized state has led Fricke, Leone & Landmann (61, 62) to comment that the irradiated system behaves essentially as a mixture of protein molecules which have either completely retained or

completely lost their original serological activity. They suggest that the underlying mechanism involves structural degradation rather than localized chemical changes in the protein molecule, for small chemical changes would not be expected to lead to a complete loss of serological activity.

Using T1 bacteriophage as a test system, Pottinger & Bachofer (146) have compared the effectiveness of a series of inorganic salts in protecting against x-ray and against thermal denaturation. Protection against heat is afforded by 0.1 M solutions in the following order: $MgSO_4$, $CaCl_2$, $(NH_4)_2SO_4$, NaCl, $NaNO_3$, $NaNO_2$. This order is practically reversed for x-ray protection. They speculate that these salts protect against x-rays by isolating phage from free radicals (perhaps by a type of dehydration); heat protection, by complexes formed between the salts and phage DNA, thereby stabilizing phage.

Tobacco mosaic virus that survive x-ray doses sufficient to lower population survival to the 1 per cent level are no more sensitive to thermal inactivation than nonirradiated virus [Buzzell, Trkula & Lauffer (29)]. Since this virus has no "memory" of its previous x-ray treatment, it is inferred that x-ray inactivation is an all-or-none effect.

Hirschfield *et al.* (74) have determined the sensitivity of ultraviolet-irradiated protozoa (*Blepharisma undulans*) to high pressure lysis following irradiation. After irradiation with either 6000 or 12,000 ergs/mm.[2] of ultraviolet of various wavelengths (230 to 365 mμ), cells were subjected to the minimum pressure that was sufficient to lyse 50 per cent of the cells. The critical lysis pressure of unirradiated cells was 10,000 psi; greater sensitivities were evident at 230, 280, and 265 mμ, the critical lysis pressures being 5000, 6500, and 7000 psi, respectively. These relative sensitivities to pressure are interpreted on the basis of fairly specific ultraviolet effects on proteins (280 mμ) and on nucleic acids (265 mμ), and of more general effects upon the cell cortex at 230 mμ.

The effectiveness of pre- and post-treatment with both infrared (820 to 1300 mμ) and far-red (710 to 820 mμ) on x-ray induced chromatid aberrations has been examined by Withrow & Moh (194) with *Tradescantia* and *Vicia*. At a dose level of 150 r, pre- or post-treatment with infrared does not significantly affect aberrations. However, both pre- and post-treatments with far-red increase chromatid breaks and exchanges; there is no sensitizing effect on isochromatid breaks. Yost & Benneyan (199) have found that infrared radiation delivered for 24 hr. to female *Drosophila* does not modify the effect of ionizing radiations on the induction of crossing-over. From these results, it is concluded that chromosome breakage is an unlikely mechanism to explain induced crossing-over, and it is suggested that the effect is upon the coiling pattern of the chromosomes.

5. *Others.*—An interesting technique has been developed by Korogodin (100) for estimating radiation damage in diploid yeast for low doses. He has found that the magnitude of the variance of colony diameter changes by a factor of nearly five, while survival changes by a factor of less than two. It is probable that this technique is useful only for a diploid organism as

there is considerably less variation in colonial size in haploid yeast than in diploid yeast (personal observations). The above phenomenon fits in nicely with Tobias' model for unpaired defects in diploid organisms (184). A careful study has been carried out by Luzzio & Kereiakes (109), again using diploid yeast, on the uptake of some dozen often-used dyes by these cells after x-irradiation. There is no appreciable uptake of any of these dyes for radiation doses less than those inactivating at least 90 per cent of the population. Thus they caution that care should be taken in evaluating studies in which staining with vital dyes is used as a criterion of viability.

It is well established that cells injured by irradiation to a point where continued cell division (usually scored by colony formation) is impossible may still divide several times. For example, Puck *et al.* (152) find that HeLa cells irradiated with minimum inactivation doses of x-rays divide for from four to five generations, synthesize some proteins, are susceptible to virus destruction, synthesize virus, and take up vital stains. Thus all of these functions are more resistant to x-irradiation than the ability to carry on continued division. Jacobson (87) also has noted that x-irradiated *Chlamydomonas* that were incapable of forming colonies may divide several times.

Respiratory deficient cells ("petites") seldom occur (1/10,000) in tetraploid yeast; however, up to 30 per cent of the survivors in a population exposed to 3100 ergs/mm.^{2} of ultraviolet radiation may be deficient [Pittman (140)]. This increase in the number of deficients is not a result of selection by the radiation, for the deficient cells are more sensitive to ultraviolet than are normals. Deficients do not revert to normals. The irreversible nature of this change and the relative ease of its induction are consistent with the hypothesis of cytoplasmic rather than genic damage.

Astaldi & Verga (8) have found that human leucocytes kept at 37°C. after 1000 r of x-irradiation suffer a loss in their average glycogen content as a function of time. Irradiated neutrophiles suffer about a 50 per cent increase in loss of their glycogen, compared to controls, over an 18-hr. period; irradiated lymphocytes, a 90 per cent increase in loss. The mechanism of this effect is not clear.

Norman & Field (122) find that *in vitro* DNA from *E. coli* can be modified by a few hundred r of x-rays such that a detectable change occurs (electric birefringence measurements). However, there is no detectable change following 10,000 r for *in vivo* irradiation [Norman & Rowen (121)]. Thus for the endpoint being assayed, DNA is much better protected *in vivo* than *in vitro*. These authors point out that in *E. coli* DNA must be virtually in the solid state. Norman and Field conclude from these studies that indirect effects are not important in causing radiobiological damage in cells. It should be mentioned that flow birefringence techniques detect primarily a difference in the length distributions of the irradiated system; this endpoint may have only limited usefulness in detecting radiation damage at a level which has biological significance.

Acetylcholinesterase from electric eel organ is found to be at least eight

times more radiosensitive in dilute suspensions than in tissue [Serlin & Cotzias (164)]. Electric eel organ is a tissue of high water content (92 per cent); lyophilized tissue (6 to 7 per cent water) shows no increased resistance over that of normal tissue. Serlin and Cotzias believe that there is an association of the soluble enzyme with the interfacial surface of the organ pulp, thus resulting in resistance to indirect radiation effects. It is not certain that the degree of lyophilization (6 to 7 per cent water) in these studies is sufficient to guarantee that indirect effects are eliminated (see Section III.B.1).

V. OTHER ASPECTS OF CELLULAR RADIOBIOLOGY

A. INSTRUMENTATION

Several important papers on microbeam apparatus have appeared during the year. Zirkle has summarized the biological results obtained by his group using both proton and ultraviolet microbeams and has discussed some of the design features of both types of instruments (204). Another microbeam apparatus, not described previously in detail, is that of Davis & Smith (43) in which 5.25 Mev polonium alphas are collimated by copper discs pierced with holes of a few microns diameter. These holes are made by evaporating tin on copper discs (44). Munson (117) has described an instrument involving microcollimation and a flow tube which allows single bacteria to be irradiated; no biological results are yet available. Alpha-particle irradiation of parts of single cells in chick tissue cultures has been carried out by Munro (116) by means of tungsten micro-needles on which polonium is deposited.

Pohlit (142) has described a unit in which electrons of energies between 30 and 150 Kev can be electrostatically focussed into a cone. A collimation of approximately $1 \times 1 \mu$ is claimed; no reports are yet available of any biological results obtained with this instrument.

A small interference-filter monochromator system especially designed for the irradiation of biological material covering the range from 365 to 800 $m\mu$ has been described by Withrow (193). This instrument has a resolution of about 10 $m\mu$ throughout the visible spectrum and can produce irradiances as high as 2000 μ watts/cm.[2]

B. MATHEMATICAL RADIOBIOLOGY

Some calculations that will be of interest to those using the techniques of target theory to obtain information on sizes and shapes of biological entities have been given by Ore (131). For spherical and cylindrical geometries, the approximations normally used agree with the more accurate formulations given here to within a few per cent. Chapiro (34) has discussed and given a mathematical formulation of the interaction of free radical clusters; LET, intensity, and scavenger concentration are considered. Hutchinson's (81) mathematical discussion of the indirect action model can be consulted with profit by those seriously interested in the foundations of radiobiology.

C. TARGET THEORY

Excellent reviews on the use of classical target theory for the estimation of molecular weights and geometrical shapes are available [Pollard *et al.* (143, 144)].

There is one aspect of target theory to which the reviewer would like to direct attention, the use or rather misuse of the extrapolation method suggested by Atwood & Norman (9) to obtain "hit" or "target" numbers. For such numbers to have even mathematical significance two conditions must hold: (*a*) the tangent to the survival curve must be taken at a position on the curve at which there is no change in the slope, that is, where the survival of the residual population is exponential with respect to additional dose; and (*b*) the number that emerges from such an operation must be properly interpreted in terms of a model for radiation damage. With respect to the first condition, few experiments are taken to low enough survival levels to meet the above requirement; for example, with diploid yeast this condition is not met for survival levels above 10^{-5}. With respect to the second condition, a model appropriate for the particular organism must be used; for example, with a diploid organism whose haploid analogue has exponential survival, the extrapolate (when properly obtained) is not the ploidy number, two, but two raised to the nth power where n is the number of sensitive sites [see Tobias (184) for some of the proper models]. An operationally more significant approach to obtaining target numbers is that outlined by Kimball (91) [see also (201)].

Alexander (3) has pointed out that the existence of energy transfer processes within and between molecules in the solid state and the sensitization of dry materials (e.g., trypsin) by oxygen [also, protection of tobacco mosaic virus by glutathione (66)] make it impossible to adopt the purely statistical approach inherent in target theory for the calculation of meaningful geometrical volumes. These factors are most serious when the sensitive volume is relatively small as in the case of trypsin; for much larger structures such as viruses the values deduced from target theory should be more informative. Braams (25) also suggests that movement of radiation effect from site of ionization to sites important for inactivation influences target theory calculations considerably.

Fluke (60) has estimated the target mass for xanthine oxidase by using the loss of three different enzymatic functions as a measure of radiation damage; the target mass is approximately one-half of the estimated molecular weight, but it is still much larger than the estimated sizes of the reactive sites of enzyme activity. Guild & DeFilippes (47, 70), using cyclotron particles, have studied dried pneumococcus transforming principle and state that 300,000 is the minimum molecular weight of a section of a DNA molecule that is required for transformation to streptomycin resistance in pneumococcus. Data obtained by Hutchinson, Morowitz & Kempner (82) indicate that the physical structures involved in amino acid incorporation in

E. coli have molecular weights between 1 and 10 million; if such units were spherical, their diameters would be 150 to 300 A.

Dried tobacco mosaic virus has been found to have a sensitive target volume approximately one-twelfth that of the anhydrous virus volume; this target volume is approximately equal in size to the nucleic acid of the virus [Buzzell, Trkula & Lauffer (29)]. Data obtained by Setlow (165) indicate a requirement of two ionizations for the suppression of ability of T2 bacterial virus to kill *E. coli* B; a molecular weight of about 1.5 million is estimated for the involved viral unit. S13 bacteriophage is inactivated by decay of incorporated radioactive atoms (P^{32}) at one-seventh the rate of death of T2 although both viruses have the same x-ray sensitivity [Tessman, Tessman & Stent (183)]. If S13 is similar to T2 and other strains previously studied, only one of ten P^{32} disintegrations kills the phage particle, and S13 would then contain 3×10^{-7} gm. of nucleic acid per particle or have an associated molecular weight of 20 million. However, if S13 is intrinsically more radiosensitive than other phages, a lower limit of 3×10^{-18} gm. of nucleic acid per S13 particle (a molecular weight of 2 million) is estimated, assuming every P^{32} disintegration is lethal.

A very interesting use of target theory has been made by Preiss (150) in studying the position of invertase within yeast cells. Electrons of energies from 400 to 5000 ev were used to bombard dried yeast and the residual invertase activity was determined at each energy. From these experimental results and by assuming that the invertase is located in an ellipsoidal thin shell within the cell, Preiss finds that the experimental results are consistent with a location of the invertase in a shell 500 A within the yeast and 500 A thick.

Zelle & Ogg (201) have used the model proposed by Tobias (184) to estimate the ploidy of a strain of *E. coli* from x-ray survival curves. The best fit of the theoretical curve to the experimental data gives a ploidy number of 2 and a sensitive site number between 12 and 18. These authors emphasize that such an analysis alone cannot supply critical proof of the ploidy of an unknown strain. It is refreshing to find a reluctance on their part to use the extrapolation method so often misused to estimate the so-called "target number." Wetherell & Krauss (189), however, used the extrapolation method of Atwood & Norman (9) to obtain "target numbers" for strains of *Chlamydomonas* of known and uncertain ploidies, with no conclusive results.

Bernstein (19) has found that a phage of *Salmonella typhi* which has been inactivated by ultraviolet can be reactivated by multiple infection of a sensitive host. Analysis of the experimental data suggests that there are about four ultraviolet sensitive units in this phage. By a study of the thermal reactivation of ultraviolet inactivated *E. coli* B, Buzzell (28) has estimated that there are approximately six sensitive sites per bacterium and that damage to a single site results in inactivation. The early events of tobacco mosaic virus infection have been studied by Siegel & Wildman (171) by following the

ultraviolet sensitivity of infection as a function of time after inoculation. The survival of infection as a function of dose is exponential for approximately five hours, after which the appearance of new intracellular infectious particles is indicated by a change to a multitarget type survival curve.

Rogers & Von Borstel (157) have studied loss of hatchability upon α-irradiation of the acentrically located nucleus of *Habrobracon* eggs. The diameter of the radiation-sensitive areas from target theory considerations is about $2.4\,\mu$; the cytological nucleus is about $2.8\,\mu$.

D. RADIOMIMETICS

A survey of the literature on radiomimetic agents has been made by Demmler (48). He concludes that the primary reactions of ionizing radiations and radiomimetic agents are generally different even though the secondary effects may be the same (mutations, nuclear fragmentation, metabolic changes, chromosome aberations, etc.).

The action of atomic hydrogen (produced in an electric arc) on crysteine results in a variety of reactions, the most important being the formation of hydrogen sulfide and cystine; there is no attack on the amino group [Littman, Carr & Brady (107)]. Similar results were obtained with glutathione.

Several recent papers indicate that hydrogen peroxide per se is not nearly so injurious to biological materials as are free radicals that can be produced from hydrogen peroxide either by treatment with catalytic amounts of Cu^+ or Fe^{++} or by ultraviolet radiation. The frequency of chromosome fragments in dormant barley seeds is increased 15- to 20-fold by the simultaneous exposure of this material to hydrogen peroxide and ferric sulfate over controls subjected to either hydrogen peroxide or ferric sulfate alone [Phillips (138)]. The pattern of chromosome aberrations produced in this fashion is much the same as that produced by x-rays. Enhanced effects are found and the same interpretation given by DeFillippes & Guild (47) with transforming principle, by Bachofer & Pottinger (14) with T1 bacteriophage, and by Okada (125) with DNA.

Laskowski & Stein (103) have compared the action of ultraviolet irradiation and hydrogen peroxide exposure on two different yeast strains. One of these strains is more sensitive to ultraviolet radiation but is less sensitive to hydrogen peroxide exposure. This difference in response can be interpreted as indicating a difference in the modes of action of ultraviolet radiation and peroxide exposure.

Luzzati & Chevallier (108) find the inactivation kinetics of *E. coli* B and B/r are different for ultraviolet radiation and peroxide exposure.

By use of a streptomycin-dependent strain of *E. coli*, Fenn *et al.* (59) have found that the number of spontaneous mutants to the streptomycin-independent variety is increased 1.5 to 2.4 times by treatment for 16 hr. with 6 to 10 atm. of oxygen. Pressures of other gases do not give this effect.

Both ultraviolet irradiation and lipide peroxides have been found by

Wilbur *et al.* (192) to be effective in inhibiting cleavage, reducing spindle size, and causing abnormal shape changes in fertilized eggs (*Chaetopterus* and sea urchin). Lipide peroxides are also found in irradiated eggs. They thus suggest that some of the effects of ultraviolet light could be brought about by organic peroxides formed by ultraviolet irradiation.

E. Dose Anomalies

In general, one associates increased radiation doses with greater damage to the irradiated system. However, there have been many reports of stimulated growth, increased survival, and other processes normally associated with a nonpathological condition following radiation exposure; it is difficult to explain most of these reports and the listing of the following papers indicates the rather frequent occurrence of events which do not fit into our over-simplified picture of the pattern of events following radiation.

Pyknotic counts in thymic cells from rats x-irradiated *in vivo* decrease as doses are increased from a few hundred roentgens to 20 kr [Trowell, Corp & Lush (185)]. Schrek has observed a similar effect in rabbit thymus cells (163); he finds that these cells can be killed with x-rays in two different ways. Up to 1000 r the dead cells become pyknotic in the ordinary way. After 10,000 r most cells undergo "delayed fixation" and eventually disappear by slow autolysis without going through a pyknotic stage. Internodal cells of *Chara vulgaris L.* show a progressive increase in elongation as they are exposed to x-ray doses from 50 to 600 kr, a fourfold increase being obtained [Moutschen (114)]. As the radiation dose is increased from 200 to 600 kr, the elongation decreases to the level characteristic of 50 kr. These cells never show mitotic activity and are of plasmoidal constitution. This absence of proportionality between dose and biological effect is believed to be attributable to enzyme liberation by x-rays. Moutschen & Bacq (115) have confirmed that seedlings grown from barley seeds exposed to 400 kr are higher than those exposed to but 200 kr. Okada & Peachey (130) find that DNAase II (rat liver) activity increases following Co^{60} exposure (2 to 10×10^5 r). Treatment of mitochondria with sonic vibration also elevates activity. These authors feel that the increased activity is caused by structural damage to the mitochondria. Such radiation damage is capable of explaining many of the stimulating effects reported as arising from irradiation.

F. Radiobiology of Mammalian Cells

The very exciting work by Puck and his group on the radiobiology of populations of mammalian cells gives promise of allowing an explanation of certain aspects of mammalian radiobiology in terms of cellular phenomena. This group has extended its work to both long-established and freshly isolated cultures of various tissues, and they find that in all cases these cells display 2-hit survival curves with LD_{37} values from 75 to 175 r [Puck *et al.* (152)]. A considerable amount of evidence indicates that radiation damage

results from damage to the nucleus, but it is unlikely if such effects are attributable to simple, single gene mutations. The 2-hit property of the survival curves could be a result of inactivation caused by reactions between two damaged ("sticky") chromosomes. The entire work of this group has been reviewed by Puck (151). Radiation studies in HeLa cells are also reported by Pomerat, Kent & Logie (145) and by Montgomery, Bonner & Roberts (111).

Bender (18) has studied the induction of chromosome aberrations by x-rays in normal, diploid human tissue culture; approximately 0.3 total breaks per cell per 100 r are reported. It is interesting to note that if such breaks lead to cellular inactivation, an LD_{37} for such cells would be around 300 r, a figure comparable to that obtained by Puck. Guild (69), from studies on the radiosensitivity of transforming principle, has concluded that biological effects of doses in the range 100 to 1000 r could result from primary damage to the cell's genetic material.

LITERATURE CITED

1. Alexander, M. L., *Genetics*, **42**, 357 (1957)
2. Alexander, P., in *Advances in Radiobiology*, 8–13 (Oliver and Boyd Ltd., London, Engl., 503 pp., 1957)
3. Alexander, P., *Radiation Research*, **6**, 653–60 (1957)
4. Alper, T., *Radiation Research*, **2**, 119–34 (1955)
5. Alper, T., *Radiation Research*, **5**, 573–86 (1956)
6. Altenburg, E., and Altenburg, L. S., *Rec. Genetics Soc. Am.*, **26**, 358 (1957)
7. Altenburg, L. S., and Altenburg, E., *Rec. Genetics Soc. Am.*, **26**, 358 (1957)
8. Astaldi, G., and Verga, L., *Experientia*, **13**, 244–245 (1957)
9. Atwood, K. C., and Norman, A., *Proc. Natl. Acad. Sci. U.S.*, **35**, 696–709 (1949)
10. Augenstine, L., *Radiation Research*, **7**, 301 (1957)
11. Bachofer, C. S., *Exptl. Cell Research*, **10**, 665–74 (1956)
12. Bachofer, C. S., *Science*, **123**, 139–40 (1956)
13. Bachofer, C. S., and Hartwig, Q. L., *Radiation Research*, **5**, 528–41 (1956)
14. Bachofer, C. S., and Pottinger, M. A., *J. Gen. Physiol.*, **40**, 289–310 (1956)
15. Bacq, Z. M., Vanderhaeghe, F., Damblon, J., Errera, M., and Herve, A., *Exptl. Cell Research*, **12**, 639–48 (1957)
16. Bećarević, A., *Biochim. et Biophys. Acta*, **25**, 299–303 (1952)
17. Bellamy, W. D., Kilburne, R. E., and Terni, S. A., *Abstr. Natl. Biophys. Conf.*, 10 (Columbus, Ohio, March 4 to 6, 1957)
18. Bender, M. A., *Science*, **126**, 974–75 (1957)
19. Bernstein, A., *Virology*, **3**, 286–98 (1957)
20. Betz, E. H., and Booz, G., *Compt. rend. soc. biol.*, **151**, 396–99 (1957)
21. Billen, D., *Arch. Biochem. Biophys.*, **67**, 333–40 (1957)
22. Bora, K. C., *Acta Radiol.*, **47**, 397–406 (1957)
23. Bora, K. C., *Acta Radiol.*, **47**, 321–26 (1957)
24. Box, H. C., Freund, H., and Hoffman, J. G., *Radiation Research*, **7**, 305 (1957)
25. Braams, R., *Radiation Research*, **7**, 305 (1957)
26. Bruce, A. K., *Radiation Research*, **7**, 306 (1957)
27. Burch, P. R. J., *Brit. J. Radiol.*, **30**, 524–29 (1957)
28. Buzzell, A., *Arch. Biochem. Biophys.*, **62**, 97–108 (1956)

29. Buzzell, A., Trkula, D., and Lauffer, M. A., *Arch. Biochem. Biophys.*, **63**, 470–76 (1956)

30. Buzzell, A., Trkula, D. T., and Lauffer, M. A., *Abstr. Natl. Biophys. Conf.*, 16 (Columbus, Ohio, March 4 to 6, 1957)

31. Caldecott, R. S., and Curtis, H. J., *Abstr. Natl. Biophys. Conf.*, 17 (Columbus, Ohio, March 4 to 6, 1957)

32. Caldecott, R. S., Konzak, C. F., and Johnson, E. B., *Radiation Research*, **7**, 308 (1957)

33. Caldecott, R. S., Johnson, E. B., North, D. T., and Konzak, C. F., *Proc. Natl. Acad. Sci. U.S.*, **43**, 975–83 (1957)

34. Chapiro, A., *Radiation Research*, **6**, 11–26 (1957)

35. Clark, A. M., *Am. Naturalist*, **91**, 111–19 (1957)

36. Clark, J. B., and Webb, R. B., *J. Bacteriol.*, **74**, 23–30 (1957)

37. Cohn, N. S., *Genetics*, **41**, 639 (1956)

38. Cohn, N. S., *Genetics*, **42**, 366 (1957)

39. Conger, A. D., *Ann. N. Y. Acad. Sci.*, **63**, 929–36 (1956)

40. Conger, A. D., and Johnston, A. H., *Nature*, **178**, 271 (1956)

41. Curtis, H. J., Delihas, N., Caldecott, R. S. and Konzak, C. F., *Radiation Research*, **7**, 311 (1957)

42. Davidson, D., *Chromosoma*, **9**, 39–60 (1957)

43. Davis, M., and Smith, C. L., *Exptl. Cell Research*, **12**, 15–34 (1957)

44. Davis, M. I., and Smith, C. L., *J. Sci. Instr.*, **34**, 32–33 (1957)

45. Davis, M. I., Simon-Reuss, I., and Smith, C. L., *Advances in Radiobiology*, 114–17 (Oliver and Boyd, Ltd., London, Engl., 503 pp., 1957)

46. Deering, R. A., and Setlow, R. B., *Science*, **126**, 397–98 (1957)

47. DeFilippes, F. M., and Guild, W. R., *Radiation Research*, **7**, 312 (1957)

48. Demmler, R., *Strahlentherapie*, **103**, 695–713 (1957)

49. Dittrich, W., *Advances in Radiobiology*, 86–89 (Oliver and Boyd, Ltd., London, Engl., 503 pp., 1957)

50. Donnellon, J. E., Jr., and Morowitz, H. J., *Radiation Research*, **7**, 71–78 (1957)

51. Ducoff, H. S., *Physiol. Zoöl.*, **30**, 268–80 (1957)

52. Ducoff, H. S., *Exptl. Cell Research*, **11**, 218–20 (1956)

53. Ebert, M., and Howard, A., *Radiation Research*, **7**, 331–41 (1957)

54. Ebert, M., and Swallow, A. J., *Radiation Research*, **7**, 229–35 (1957)

55. Ehrenberg, L., and Lundquist, U., *Hereditas*, **43**, 390–402 (1957)

56. Errera, M., and Vanderhaeghe, F., *Exptl. Cell Research*, **13**, 1–10 (1957)

57. Fairbanks, A. J., Jr., *Radiation Research*, **7**, 314 (1957)

58. Fairbanks, A. J., Jr., *Abstr. Natl. Biophys. Conf.*, 28 (Columbus, Ohio, March 4 to 6, 1957)

59. Fenn, W. O., Gerschman, R., Gilbert, D. L., Terwilliger, D. E., and Cothran, F. V., *Proc. Natl. Acad. Sci. U. S.*, **43**, 1027–32 (1957)

60. Fluke, D. J., *Abstr. Natl. Biophys. Conf.*, 29 (Columbus, Ohio, March 4 to 6, 1957)

61. Fricke, H., Leone, C. A., and Landmann, W., *Radiation Research*, **7**, 316 (1957)

62. Fricke, H., Leone, C. A., and Landmann, W., *Nature*, **180**, 1423–25 (1957)

63. Friedman, M., *Radiation Research*, **7**, 386–93 (1957)

64. Galtsova, R. D., *Mikrobiologiya* **24**, 137–40 (1957)

65. Giese, A. C., Iverson, R. M., and Sanders, R. T., *J. Bacteriol.*, **74**, 271–79 (1957)

66. Ginoza, W., and Norman, A., *Nature*, **179**, 520–21 (1957)

67. Goucher, C. R., and Kocholaty, W., *Arch. Biochem. Biophys.*, **68**, 30–38 (1957)
68. Gray, L. H., *Ann. Rev. Nuclear Sci.*, **6**, 353–422 (1956)
69. Guild, W. R., *Radiation Research*, **7**, 320 (1957)
70. Guild, W. R., and DeFilippes, F. M., *Biochim. et Biophys. Acta*, **26**, 241–51 (1957)
71. Haas, F. L., and Doudney, C. O., *Proc. Natl. Acad. Sci. U. S.*, **43**, 871–73 (1957)
72. Heinmets, F., Lehman, J. J., Taylor, W. W., and Kathan, R. H., *J. Bacteriol.*, **67**, 511–22 (1954)
73. Heinmets, F., Taylor, W. W., and Lehman, J. J., *J. Bacteriol.*, **67**, 5–12 (1954)
74. Hirschfield, H. I., Zimmerman, A. M., Landau, J. V., and Marsland, D., *J. Cellular Comp. Physiol.*, **49**, 287–94 (1957)
75. Hollaender, A., Ed., *Radiation Biol.*, **1**, 1–1265 (1954); **2**, 1–593 (1955); **3**, 1–765 (1956)
76. Hollaender, A., *Advances in Radiobiology*, 123–31 (Oliver and Boyd, London, Engl., 503 pp., 1957)
77. Holmes, B. E., *Ann. Rev. Nuclear Sci.*, **7**, 89–134 (1957)
78. Howard-Flanders, P., and Alper, T., *Radiation Research*, **7**, 518–40 (1957)
79. Hurwitz, C., Rosano, C. L., and Blattberg, B., *J. Bacteriol.*, **73**, 743–46 (1957)
80. Hutchinson, F., *Radiation Research*, **7**, 323 (1957)
81. Hutchinson, F., *Radiation Research*, **7**, 473–83 (1957)
82. Hutchinson, F., Morowitz, N., and Kempner, E., *Science*, **126**, 310 (1957)
83. Hutchinson, F., Preston, A., and Vogel, B., *Radiation Research*, **7**, 465–72 (1957)
84. Iverson, R. M., and Giese, A. C., *Exptl. Cell Research*, **13**, 213–23 (1957)
85. Iverson, R. M., and Giese, A. C., *Biochim. et Biophys. Acta*, **25**, 62–68 (1957)
86. Jacobson, B. S., *Radiation Research*, **7**, 324 (1957)
87. Jacobson, B. S., *Radiation Research*, **7**, 394–404 (1957)
88. Kanazir, D., Kačanski, K., and Krajinčanić, B., *Biochim. et Biophys. Acta*, **23**, 224–25 (1957)
89. Kihlman, B. A., *J. Biophys. Biochem. Cytol.*, **3**, 363–80 (1957)
90. Kihlman, B. A., Merz, T., and Swanson, C. P., *J. Biophys. Biochem. Cytol.*, **3**, 381–91 (1957)
91. Kimball, A. W., *Biometrics*, **9**, 201–11 (1953)
92. Kimball, R. F., *Ann. Rev. Microbiol.*, **11**, 199–220 (1957)
93. Kimball, R. F., Gaither, N., and Wilson, S. M., *Radiation Research*, **7**, 325 (1957)
94. Kimball, R. F., Gaither, N., and Wilson, S. M., *Genetics*, **42**, 661–69 (1957)
95. Kirby-Smith, J. S., and Craig, D. L., *Genetics*, **42**, 176–87 (1957)
96. Konzak, C. F., *Radiation Research*, **6**, 1–10 (1957)
97. Konzak, C. F., *Quart. Rev. Biol.*, **32**, 27–45 (1957)
98. Konzak, C. F., and Singleton, W. R., *Proc. Natl. Acad. Sci. U. S.*, **42**, 239–45 (1956)
99. Konzak, C. F., Caldecott, R. S., Delihas, N., and Curtis, H. J., *Radiation Research*, **7**, 326 (1957)
100. Korogodin, V. I., *Biofizika*, **2**, 180–88 (1957)
101. Krahe, M., Künkel, H. A., and Schmermund, H. J., *Strahlentherapie*, **102**, 288–90 (1957)
102. Laser, H., and Thornley, M. J., *Radiation Research*, **7**, 326 (1957)
103. Laskowski, W. and Stein, W., *Naturwissenschaften*, **44**, 236–37 (1957)
104. Lauffer, M. A., Trkula, D., and Buzzell, A., *Nature*, **177**, 890 (1956)

105. Lea, D. E., *Actions of Radiations on Living Cells,* revised ed. (Cambridge University Press, London, Engl., 416 pp., 1955)
106. Littman, F. E., Carr, E. M., and Clauss, J. K., *Science,* **125,** 737–38 (1957)
107. Littman, F. E., Carr, E. M., and Brady, A. P., *Radiation Research,* **7,** 107–19 (1957)
108. Luzzati, D., and Chevallier, M.-R., *Ann. inst. Pasteur,* **93,** 366–75 (1957)
109. Luzzio, A. J., and Kereiakes, J. G., *Exptl. Cell Research,* **13,** 615–17 (1957)
110. McLaren, A. D., and Takahashi, W. N., *Radiation Research,* **6,** 532–42 (1957)
111. Montgomery, P. O'B., Bonner, W. A., and Roberts, F. F., *Proc. Soc. Exptl. Biol. Med.,* **95,** 589–91 (1957)
112. Mortimer, R. K., *Radiation Research,* **7,** 439 (1957)
113. Mortimer, R. K., and Beam, C. A., *Ann. Rev. Nuclear Sci.,* **5,** 327–68 (1955)
114. Moutschen, J., *Experientia,* **13,** 240 (1957)
115. Moutschen, J., and Bacq, Z. M., *Compt. rend. soc. biol.,* **150,** 2046–49 (1956)
116. Munro, R., *Advances in Radiobiology,* 108–13 (Oliver and Boyd, Ltd., London, Engl., 503 pp., 1957)
117. Munson, R. J., *Advances in Radiobiology,* 105–7 (Oliver and Boyd, Ltd., London, Engl., 503 pp., 1957)
118. Neary, G. J., *Nature,* **180,** 248–49 (1957)
119. Nilan, R. A., and Gunthardt, H. M., *Caryologia,* **8,** 316–22 (1956)
120. Nilan, R. A., and Phillips, L. L., *Northwest Sci.,* **31,** 139–44 (1957)
121. Norman, A., and Rowen, J. W., *Biochim. et Biophys. Acta,* **22,** 203–4 (1956)
122. Norman, A., and Field, J. A., Jr., *Arch. Biochem. Biophys.,* **71,** 170–78 (1957)
123. Northrop, J. H., *J. Gen. Physiol.,* **40,** 653–61 (1957)
124. Oakberg, E. F., *J. Exptl. Zool.,* **134,** 343–56 (1957)
125. Okada, S., *Arch. Biochem. Biophys.,* **67,** 95–101 (1957)
126. Okada, S., *Arch. Biochem. Biophys.,* **67,** 102–12 (1957)
127. Okada, S., *Arch. Biochem. Biophys.* **67,** 113–20 (1957)
128. Okada, S., and Gehrmann, G., *Biochim. et Biophys. Acta,* **25,** 179–82 (1957)
129. Okada, S., Gordon, E. R., King, R., and Hempelmann, L. H., *Arch. Biochem., Biophys.,* **70,** 469–76 (1957)
130. Okada, S., and Peachey, L. D., *J. Biophy. Biochem. Cytol.,* **3,** 239–48 (1957)
131. Ore, A., *Radiation Research,* **6,** 27–39 (1957)
132. Oster, I. I., *Genetics,* **42,** 387 (1957)
133. Owen, M. E., and Mortimer, R. K., *Nature,* **177,** 625–26 (1956)
134. Pahl, G., and Bachofer, C. S., *Biol. Bull.,* **112,** 383–89 (1957)
135. Paterson, R., *Brit. J. Radiol.,* **30,** 354–55 (1957)
136. Pauly, H., *Wissenschaftliche Grundlagen des Strahlenschutzes,* 56–83 (G. Braun, Karlsruhe, Germany, 429 pp., 1957)
137. Perry, R. P., *Exptl. Cell Research,* **12,** 546–59 (1956)
138. Phillips, L. L., *Science,* **124,** 889–90 (1956)
139. Pichl, H., and Uecker, W., *Naturwissenschaften,* **44,** 287 (1957)
140. Pittman, D. D., *Exptl. Cell Research,* **11,** 654–56 (1956)
141. Pittman, D. D., and Pedigo, P. R., *Genetica,* **28,** 27–30 (1956)
142. Pohlit, W., *Strahlentherapie,* **103,** 593–97 (1957)
143. Pollard, E. C., *Advances in Biol. and Med. Phys.,* **3,** 153–89 (1953)
144. Pollard, E. C., Guild, W. R., Hutchinson, F., and Setlow, R. B., *Progr. in Biophys. and Biophys. Chem.,* **5,** 72–108 (1955)
145. Pomerat, C. M., Kent, S. P., and Logie, L. C., *Z. Zellforsch. u. mikroskop. Anat.,* **47,** 175–97 (1957)

146. Pottinger, M. A., and Bachofer, C. S., *Arch. Biochem. Biophys.*, **70,** 499–506 (1957)
147. Powers, E. L., *Ann. Rev. Nuclear Sci.*, **7,** 63–88 (1957)
148. Powers, E. L., Ehret, C. F., and Bannon, A., *Appl. Microbiol.*, **5,** 61–64 (1957)
149. Powers, E. L., Ehret, C. F., Bannon, A., and Prock, A., *Radiation Research*, **7,** 443 (1957)
150. Preiss, J. W., *Radiation Research*, **7,** 443 (1957)
151. Puck, T. T., *Advances in Biol. and Med. Phys.*, **5,** 75–101 (1957)
152. Puck, T. T., Morkovin, D., Marcus, P. I., and Cieciura, S. J., *J. Exptl. Med.*, **106,** 485–500 (1957)
153. Rajewsky, B., Gerber, G., and Pauly, H., *Strahlentherapie*, **102,** 517–21 (1957)
154. Reid, C., *Excited States in Chemistry and Biology* (Butterworths Scientific Publications, London, Engl., 215 pp., 1957)
155. Reid, C., *Science*, **125,** 396–97 (1957)
156. Riley, H. P., *Genetics*, **42,** 593–600 (1957)
157. Rogers, R. W., and Von Borstel, R. G., *Radiation Research*, **7,** 484–90 (1957)
158. Romig, W. R., and Wyss, O., *J. Bacteriol.*, **74,** 386–91 (1957)
159. Rosen, D., and Boman, H. G., *Arch. Biochem. Biophys.*, **70,** 277–82 (1957)
160. Rosen, D., Brohult, S., and Alexander, P., *Arch. Biochem. Biophys.*, **70,** 266–76 (1957)
161. Sarić, M. R., *Radiation Research*, **6,** 167–72 (1957)
162. Schooler, A. B., Nilan, R. A., and Phillips, L. L., *Northwest Sci.*, **31,** 80–91 (1957)
163. Schrek, R., *Arch. Pathol.*, **63,** 252–59 (1957)
164. Serlin, I., and Cotzias, G. C., *Radiation Research*, **6,** 55–66 (1957)
165. Setlow, J., *Virology*, **3,** 374–79 (1957)
166. Setlow, R., *Advances in Biol. and Med. Phys.*, **5,** 37–74 (1957)
167. Setlow, R., and Doyle, B., *Biochim. et Biophys. Acta*, **24,** 27–41 (1957)
168. Setlow, R., Watts, G., and Douglas, C., *Abstr. Natl. Biophys. Conf.*, 64 (Columbus, Ohio, March 4 to 6, 1957)
169. Sheppard, C. W., Slater, M., Darden, E. B., Jr., Kimball, A. W., Atta, G. J., Edington, C. W., and Baker, W. K., *Radiation Research*, **6,** 173–87 (1957)
170. Siegel, A., *Nature*, **180,** 1430–31 (1957)
171. Siegel, A., and Wildman, S. G., *Virology*, **2,** 69–82 (1956)
172. Siegel, A., Ginoza, W., and Wildman, S. G., *Virology*, **3,** 554–59 (1957)
173. Skreb, Y., and Errera, M., *Exptl. Cell Research*, **12,** 649–56 (1957)
174. Snyder, W. S., and Neufeld, J., *Radiation Research*, **6,** 67–78 (1957)
175. Sogo, P. B., and Tolbert, B. M., *Advances in Biol. and Med. Phys.*, **5,** 1–35 (1957)
176. Spalding, J. F., *Radiation Research*, **7,** 452 (1957)
177. Spalding, J. F., Langham, W., and Anderson, E. C., *Radiation Research*, **4,** 221–27 (1956)
178. Spoerl, E., and Looney, D., *Abstr. Natl. Biophys. Conf.*, 67 (Columbus, Ohio, March 4 to 6, 1957)
179. Steffensen, D., *Genetics*, **42,** 239–52 (1957)
180. Steinitz-Sears, L. M., and Sears, E. R., *Genetics*, **42,** 621–30 (1957)
181. Swaminathan, M. S., and Natarajan, A. T., *Nature*, **179,** 479–80 (1957)
182. Tanada, T., *Am. J. Botany*, **44,** 723–25 (1957)
183. Tessman, I., Tessman, E. S., and Stent, G. S., *Virology*, **4,** 209–15 (1957)
184. Tobias, C. A., in *Symposium on Radiobiol.*, 357–84 (Nickson, J. J., Ed., John Wiley & Sons, Inc., New York, N. Y., 465 pp., 1952)
185. Trowell, O. A., Corp, M. J., Lush, W. R., *Radiation Research*, **7,** 120–28 (1957)

186. Uecker, W., and Pichl, H., *Naturwissenschaften*, **44,** 311 (1957)
187. Webb, R. B., Ehret, C. F., and Powers, E. L., *Radiation Research*, **7,** 459 (1957)
188. Welch, G., *Radiation Research*, **7,** 460 (1957)
189. Wetherell, D. F., and Krauss, R. W., *Am. J. Botany*, **44,** 609–19 (1957)
190. Whiting, A. R., and Murphy, W. E., *J. Genet.*, **54,** 297–303 (1956)
191. Wichterman, R., *Bios*, **28,** 3–20 (1957)
192. Wilbur, K. M., Wolfson, N., Kenaston, C. B., Ottolenghi, A., Gaulden, M. E., and Bernheim, F., *Exptl. Cell Research*, **13,** 503–9 (1957)
193. Withrow, R. B., *Plant Physiol.*, **32,** 355–60 (1957)
194. Withrow, R. B., and Moh, C. C., *Radiation Research* **6,** 491–500 (1957)
195. Wolff, S., and Luippold, H. E., *Proc. Natl. Acad. Sci. U. S.*, **42,** 510–14 (1956)
196. Wood, T. H., and Rosenberg, A. M., *Biochim. et Biophys. Acta*, **25,** 78–87 (1957)
197. Wood, T. H., and Taylor, A. L., *Radiation Research*, **6,** 611–25 (1957)
198. Wood, T. H., and Taylor, A. L., *Radiation Research*, **7,** 99–106 (1957)
199. Yost, H. T., Jr., and Benneyan, R. N., *Genetics*, **42,** 147–60 (1957)
200. Yost, H. T., Jr., and Robson, H. H., *Biol. Bull.*, **113,** 198–206 (1957)
201. Zelle, M. R., and Ogg, J. E., *J. Bacteriol.*, **74,** 485–93 (1957)
202. Zelle, M. R., Ogg, J. E., and Hollaender, A., *Proc. Soc. Exptl. Biol. Med.*, **96,** 285–87 (1957)
203. Zimmer, K. G., Ehrenberg, L., and Ehrenberg, A., *Strahlentherapie*, **103,** 3–15 (1957)
204. Zirkle, R. E., *Advances in Biolog. and Med. Phys.*, **5,** 103–46 (1957)
205. Zirkle, R. E., and Tobias, C. A., *Arch. Biochem. Biophys.*, **47,** 282–306 (1953)

INFORMATION THEORY IN RADIOBIOLOGY[1,2]

By Henry Quastler

Department of Biology, Brookhaven National Laboratory, Upton, New York

Introduction

Biological effects of radiation are produced by small amounts of energy. This is possible because the early stages of radiation reactions occur in small regions of molecular or macromolecular dimensions (1). The problem is how such local effects are amplified into disturbances of entities which are many orders of magnitude larger. This is a problem of relating malfunction of a system to perturbations of its components.

One aspect of this problem is that of relating the probability of system malfunction to some measure of component perturbation. Relations of this type constitute one of the major concerns of information theory. It is established that the probability of malfunction of a system can be stated in terms of three variables: the functional capabilities of the components in the presence of a given kind and degree of disturbance, the way in which these capabilities are apportioned to external tasks and internal stabilization, and the number of components making up the system (2, 2a, 3, 4). The relation is, in general, of the form:

$$\epsilon = A \cdot 2^{-\eta N}, \text{approximately}, \qquad\qquad 1.$$

where

ϵ = probability of a malfunction per single task;

A = a constant, depending on the nature of the components and the way in which they are utilized;

η = a measure of the fraction of the capabilities used for internal stabilization;

N = the number of components.

Relations of this type characterize many situations some of which are not unfamiliar to the radiobiologist, as will be shown later (Equation 2d).

The concepts of information theory are not, as a rule, stated in such general terms. The customary applications deal with communications between people. The systems considered are messages; malfunction is defined as an error, committed by the receiver of a message, as to the information it was supposed to convey. The probability of error is derived from an analysis of events occurring at the component level. The components of messages are the basic units of representation and conveyance of information, or symbols. Their functional values are called "information content" and defined as the average amount which they can contribute to the representation

---

of information. Perturbations affecting discrete units are necessarily quantal, and consist in the replacement of one symbol by another. The perturbations caused by random disturbances ("noise") are most serious because they are unpredictable in detail. Substitutions of some randomly scattered components lead to equivocation, upon reception of any particular signal, as to the nature of the symbol intended. This results in loss of (average) information per symbol. The information content of a symbol, minus the information lost due to noise, is a measure of the informational performance; the maximum of this function is called channel capacity and measures the informational capability per symbol in the presence of a given level of noise. More generally, it refers to the functional capabilities of components, the first of the factors in the relation between component perturbation and systems failure.

On the component level we deal with equivocation, not necessarily with error. Error relates to the function of the whole message; equivocation may but does not always cause errors. A message can be protected, to a degree, against equivocation by proper organization. In order to recognize alterations of a symbol, there must be somewhere else in the message some indications as to what it ought to be. In other words, a stabilized message must contain a message about itself. This is "redundant" information which must be implicitly contained in the information to be conveyed; yet it competes with the latter for the limited information capabilities of the components. This is the dilemma which forces some apportionment of the functional capacity of symbols between external task (information conveyed) and internal stabilization (protection against error arising from equivocation). Thus arises the second factor in the relation between systems failure and component perturbation.

Information is an expensive commodity, and, therefore, redundant information must be used efficiently. This can be done best if there are many components in the message, a situation which allows the establishment of many and varied interconnections. The third factor in the relation between systems malfunction and component perturbation is thereby explained.

There does not exist, at this time, a general calculus by which one could find optimum uses of redundant information in every situation and compute the resulting error rates. It is established, however, that some very simple procedures will yield results which are not far from optimum, with ensuing error rates approximating Equation 1. In the parlance of communication theory, ϵ is the probability of error per message, A is related to the channel capacity per symbol, η is a function of the difference between channel capacity minus information used for payload, and N is the number of symbols.

Information theory, in its present form, has arisen out of a desire to make optimum use of existing vehicles for communication between people. This background suggests that caution is advisable in extending the use of

information theory to fields far removed. Yet such generalization is by no means impossible (2, 5 to 12). The relation of "information" (in the technical sense) to conscious processes is incidental, not essential. The informational value of a process is completely determined by the degree of selection which it entails, and does not depend on the method used for selection nor on the motivation behind it (13). In this sense, selecting a particular key on the typewriter in making up this message compares quite closely to a microsomal particle selecting a particular amino acid in the course of synthesizing protein. A person may feel that his selection is subject to free choice and based on insight, and he doubts whether the particle feels likewise; however, this difference is in his private domain, and does not affect the information value associated with the public result of the process.

The concern about the normative aspect of much of information theory is less easily disposed of. It is very doubtful whether the more sophisticated coding procedures developed by mathematicians and engineers may ever serve as a model of biologic events. It was mentioned, however, that fairly good coding procedures can be produced with very modest effort; therefore, without asking too much from evolution, one may postulate that living things use redundant information in a reasonably efficient way, which is one form of Dancoff's principle (14). It is all that is needed to extend to radiobiology the relation between component alteration and system failure stated in equation 1.

INFORMATION THEORY OF RADIATION LETHALITY

In terms of total information content.—It is intuitive that living things are highly ordered systems, that some order must be maintained if an organism is to survive, and that orderliness is reduced by normal wear and tear; this is the basis of the "entropic theory of aging" (15 to 18). Given that some of the critical aspects of orderliness are vested in molecular arrangements, and that radiation is very effective in disturbing molecular arrangements, it follows that some radiation effects might be understood in terms of reduction of orderliness. This is the "information theory of radiation damage" which was first proposed by Yockey (19).

In two places (18, 19) Yockey develops his informational analysis of death due to irradiation and normal aging. The total order implicit in the organization of an organism beginning life is equated to the total information content of some message; the gradual loss of orderliness, to increasing equivocation. A certain amount of equivocation is incompatible with survival. Thus, normal life expectancy will depend on the amount of information present at birth and on the rate at which it is lost; irradiation will be lethal if it destroys enough of the information present at that time to raise the equivocation beyond the critical level.

Using the total amount of equivocation as an index of the condition of an organism implies that components are functionally interchangeable, at

least to some degree. This concept, for biologic systems, is plausible only if the components in question are numerous and independently subject to perturbation. Such a situation can be formulated in terms of a function familiar to the radiobiologist, namely, a multi-hit mechanism with a large number of "hits-to-kill" (20). This function approximates a step function. Therefore, a given amount of equivocation, if produced by a large number of independent events, will be reached in nearly constant time. But death occurs at different times, or after different doses of radiation, even in populations which are as homogeneous as one can make them. This means that either the critical level of equivocation or the initial amount of information must be variable. Yockey adopts the latter alternative; he proves that a perfectly homogeneous system is unstable in the presence of perturbations, thus implying variations even in the closest approximations to homogeneous populations which one can obtain. One aspect of these variations will be a distribution of information contents, established in the zygote or at some very early stage of development.

The model implies that the shapes of the age-mortality and the dose-mortality curves are functions of the original distribution of information contents. If this is so, then the analysis of this distribution is of greatest importance. Some common dose-survival curves can be related to a rectangular initial distribution of information contents; but, this is not decisive evidence. Critical tests of the theory became possible if one adds another hypothesis favored by Yockey: that the perturbations due to irradiation, aging, and raised temperature are largely identical. In this case, the survival curves for the three conditions can be derived from one another (18).

In Yockey's model, the probability of failure changes brusquely at a given value of equivocation. Although all-or-none phenomena are not uncommon in biology, one has to consider the possibility of a gradual increase of the probability of failure with rising equivocation. This is an application of Sacher's "stochastic theory of lethality" (21). Sacher's theory is based on the concept of a physiologic space with as many dimensions as there are independent variables, with "lethal bounds" enclosing all constellations of variables compatible with life, with aging represented by a steady approach to some region of the lethal bound, and with a stochastic element introduced by random fluctuations of any or all physiologic variables. To each constellation of physiologic variables and to each point on the lethal bound must correspond a certain value of equivocation, but whether this abstraction preserves enough character to be useful remains to be seen. At least, there exists a positive feedback between degree of disorder (or equivocation) and the amplitude of fluctuations (22).

In terms of components.—The basic analysis of systems failure in terms of component perturbation (Equation 1) is easily extended to radiobiologic applications. Consider a system with components subject to both spontaneous failure and inactivation by irradiation. Let there be N such components, and

the organization such that functioning of at least one component suffices for survival. Consider the period of acute disturbance following irradiation. Let p be the probability, for any component, that it will not fail spontaneously during this period, and P_D the probability that it will escape the acute effects of irradiation with a dose D. Under these conditions, the mortality rate μ_D following dose D will be

$$\mu_D = (1 - pP_D)^N \qquad\qquad 2.$$

which, for small values of pP_D goes over into

$$\mu_D = e^{-pNP_D}, \text{ approximately.} \qquad\qquad 2a.$$

If the inactivation of components by radiation is a first order reaction, then

$$P_D = e^{-D/D_0}$$

(where D_0 is a scale factor) and

$$\mu_D = e^{-pNe^{-D/D_0}}. \qquad\qquad 2b.$$

[For $p = 1$, Equation 2 turns into the well-known multitarget formula (20). For small values of μ, the approximation used in Equation 2a is much better than the customary

$$\text{Survival rate} = 1 - \mu_D \approx Ne^{-D/D_0}.$$

Also, fitting the survival curve by sight involves a notorious danger of erroneous extrapolation, which is less likely to happen with μ_D.]

Suppose now that the first-order system discussed is itself a component of a second-order system organized in the same manner from N' first-order systems. The mortality rate for the second-order system, μ_D', will be found by iteration of Equation 2:

$$\mu_D' = [(1 - pP_D)^N]^{N'} \qquad\qquad 2c.$$

which, for most situations of interest, can be simplified to

$$\mu_D' = e^{-pNN'e^{-D/D_0}}, \text{ approximately.}$$

μ_D can be considered as a mortality rate associated with a system of arbitrarily high order:

$$\mu_D = e^{-pe^{-D/D_0}(NN'N''\cdots)}. \qquad\qquad 2d.$$

This equation is equivalent to the information theory relation,

$$\epsilon = A \cdot 2^{-\eta N}.$$

The factor, A, becomes unity because by extending the observation throughout the whole acute postirradiation phase, almost every error situation will be expressed. The factor $2^{-\eta}$ defines the stability of the components, and compares to $e^{-pe^{-D/D_0}}$. Finally, $(NN'N'' \cdots)$ is the total number of components, counted at the level of radiosensitive units, regardless of any hierarchy of organization. The equivalence of Equation 2d to Equation 1

guarantees that its validity is general and not restricted to the very special situation used in the derivation.

In dealing with a system of unknown order and number of components, the factors in the product

$$pNN'N'' \cdots$$

merge into a single parameter ν:

$$\mu_D = e^{-\nu e^{-D/D_0}} \qquad\qquad 3.$$

where ν is a measure of the organizational stability, or effective redundancy, of the system at the level of components affected by radiation, and D_0 is a scale factor relating the physical dosage unit to the sensitivity of the components with respect to the particular radiation used. Equation 3 is a natural generalization of the multitarget formula, with the parameter ν substituted for the actual property "number of targets." The price of the generalization is that the merger of several physical properties into a single parameter makes it impossible to analyze the properties themselves; the advantage achieved is that the formulation can be expected to hold for very complex organizations.

How well this expectation is fulfilled is seen in Figure 1. By taking negative logarithms twice, Equation 3 is transformed into a straight line:

$$-\log_e(-\log_e \mu_D) = \log_e \nu + D/D_0. \qquad\qquad 3a.$$

SYMBOL	SPECIES	ν	D_0	REFERENCE
+·····+	COLPID. COLP.	3700	?	CROWTHER,J.A., PROC. ROY. SOC. B, 100:390 (1926)
●——●	DROSOPHILA	4.8	180	PACKARD,C., & EXNER,F.M.,RADIOL. 44:357 ('45)
----	GUINEA PIG	360	39	LAMARQUE,P.,& GARY BOBO,J.,PROC.INTERN. CONF. PEACEF. USE AT. EN. VO. II ('56)
■——■	GUINEA PIG	740	50	ELLINGER,F., ET AL.,NAV.MED.RES. INST.13:311 ('55)
△——△	HAMSTER	7900	64	KOHN,H.I.,& KALLMAN,R.F.,RADIAT. RES. 6:37 ('57)
□——□	CHICK	4700	91	STEARNER,S.P., & TYLER,S.A.,RAD.RES.7:253 ('57)
▲——▲	CHICK EMBRYO	37000	90	KOHN,H.I., & KALLMAN,R.F.,RAD. RES. 9:710 ('56)
○——○	CHICK EMBRYO	55000	93	OFTEDAL,P.,PROGR. RADIOBIOL.,OLIVER & BOYD,EDINBURGH '56
X·····X	CHLAMYDOMON.	5.6	2005	JACOBSON,B.S.,RAD.RES.7:394 ('57) (DOSE X I /10)
—·—·—·—	BOMBYX M.	25	318	LAMARQUE,P., & GROS,C., JOUR.RAD.ELECTR. 26:129 ('44)
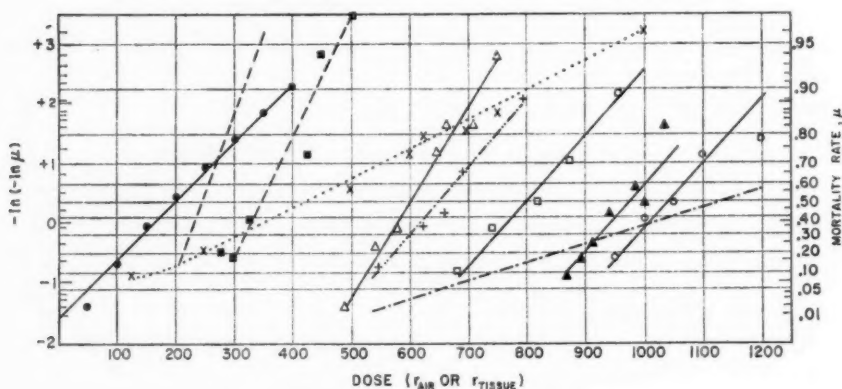
FIG. 1. Dose-mortality curves—various organisms.

SYMBOL	ln ν	D_0	REFERENCE
o——o	(11.5)	(1700)	CRONKITE, E.P., ETAL., SCIENCE 122:148('55) AND RES. REPT. NAV. MED., RES. INST. 13:99 ('55) OPEN CIRCLES:
•——•	(14.2)	52	KILLING TIME AROUND 18 DAYS ; CLOSED CIRCLES : AROUND 13 DAYS
△——△	14.1	45	PATT, H.M., ET AL., J. CELL. COMP. PHYSIOL. 42: 327 ('53)
□——□	(12.3)	(280)	KOCH, R., ET AL., DEUTSCHE MED. WCHSCHR. 82: 1069 (57) OPEN SQUARES: KILLING TIME
■——■	(8.8 ·	30	AROUND 18 DAYS; CLOSED SQUARES: AROUND 10 DAYS
◊——◊	14.2	52	CHAPMAN, W.H., RAD. RES. 2:502('55) (DATA FOR MALE MICE)
▽——▽	13.2	45	DELIHAS, N., & CURTIS, H.J., RAD. RES. 8:166 ('58)
x——x	11.5	45	UPTON, A.C., ET AL., RAD. RES. 4:117 ('56)
+——+	9.0	55	CARTER, R.E., ET AL., RAD. RES. 4: 413 ('56) (DATA FOR MALE MICE)
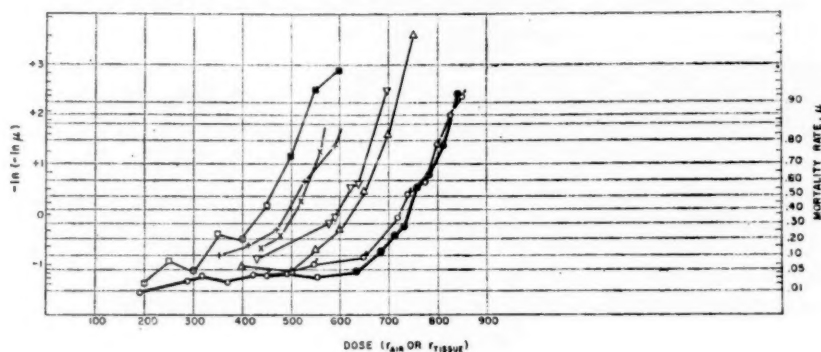
FIG. 2. Dose-mortality curves—mice.

A number of reliable dose-mortality curves was culled from the literature more or less at random, beginning with the historical Colpidium curve. It is seen that, for a great variety of organisms, the expected straight lines appear. All multitarget curves must equally fit into the scheme. The nature of the two parameters suggests that differences (due to place, time, age, etc.) in the general condition of the experimental objects should affect the internal stability or effective redundancy, and therefore the intercept; this is confirmed by the sets of nearly parallel lines for chicks (three sets of data) and guinea pigs (two sets). Differences in radiation quality or dosage unit should affect the slope; only where radiations differ in the number of targets affected in a single event will the intercept vary.

Survival data on mice show the expected slight variations in slope and considerable variations in position, but they also yield strongly bent curves instead of straight lines (Fig. 2). (Most curves show an additional final upturn not shown on the graph, because of mortality reaching 100 per cent earlier than predicted from linear extrapolation from the preceding portion of the curve.) These facts are related to differences in prevalent mode of death associated with various levels of lethality. They are evident in differences in mean killing time, in contrast to guinea pigs and hamsters (Fig. 1) where dominance of a single mode of death is indicated by killing times remaining constant over a wide range of lethality. The most complete data available are those obtained by Cronkite et al. (23) during an atom bomb test. In this material, two killing times dominate; one in the low mortality

range, and one associated with moderate and high mortality; the former corresponds to the "slow component" (24) and the latter to the well-known "marrow death." Each is associated with a straight line (the transition between the two is only one point "off"). These two straight lines constitute part of the apparent curvature seen with less complete data; the final upturn is due to incidence of one of the faster modes of death.[3]

In the analysis of chronic radiation effects or natural aging, no natural time unit is available, and a frequency factor must be introduced to relate the time unit used to durations of "duty cycles" (assumed to remain constant—a not unplausible hypothesis). One may equate the random loss of orderliness due to age to a first-order decay of the effective redundancy, ν. Then, if m_t is the natural mortality rate per unit time:

$$m_t = ke^{-\nu_0 e^{-t/t_0}} \qquad\qquad 4.$$

where k is the number of "duty cycles" per unit time, ν_0 the initial number of components, t the age, and t_0 a scale factor. Forming the Gompertz function,

$$G_t = \log_e m_t,$$

we get[4]

$$G_t = \log_e k - \nu_0 e^{-t/t_0} \qquad\qquad 4a.$$

which for small values of t/t_0 is equivalent to the usual form,

$$G_t = (\log_e k - \nu_0) + \frac{\nu_0}{t_0} t. \qquad\qquad 4b.$$

For large values of t/t_0, Equation 4a seems to fit the data better than 4b.[5]

Irradiation with a single dose may irreversibly reduce ν; then

$$m_{D,t} = ke^{-\nu_0 e^{-D/D^*} e^{-t/t_0}} \qquad\qquad 5.$$

where D^* is a scale factor not necessarily identical with the D_0 of the acute reaction. Setting

$$t' = t + \frac{Dt_0}{D^*}$$

we get an effective change in age:

$$m_{D,t} = ke^{-\nu_0 e^{-t'/t_0}}. \qquad\qquad 5a.$$

This is the "aging" effect as described by Brues & Sacher (25). It is not necessary to assume that the reduction of ν by aging and irradiation involve the same mechanisms, or even levels of organization. Accordingly, the addi-

---

[3] A glance at the ordinate in Figures 1 or 2 shows that the functional scale is distorted in a fashion not too different from a probit scale; hence, approximate fits on one scale can be matched on the other.

[4] Because of the presence of the constant k, taking logarithms a second time will not result in a straight line as with Equation 3.

[5] Alternatively, one could derive the usual form of G_t from Equation 3.

tivity of radiation effect to age does not necessarily imply a simple increase of radiation sensitivity with age (26).

Irreversible reduction of ν by chronic irradiation at a dose rate D' yields an effective change in time scale (25):

$$m_{D',t} = ke^{-\nu_{0}e^{-t/t_0'}}$$ 5b.

with

$$\frac{1}{t_0'} = \frac{1}{t_0} + \frac{D'}{D^*} .$$

Reversible effects of chronic irradiation at a constant dose level should result in shifting ν to a lower level, $\nu_{D'}$, which is equivalent to the irreversible effect of a single dose, Equation 5a. Auerbach's data (27) on the relation between skin cancer incidence and amount of sunlight are compatible with this model.

Thus, the relation defined by Equation 1 is seen to account for a very vast range of dose-mortality relations.

ELEMENTARY RADIATION EFFECTS AND INFORMATION DENSITY

In the preceding section, we have dealt with highly redundant, very complex systems, where the final malfunction of the system is far removed from the elementary component perturbations; in the analysis of these systems, we had to deliberately submerge any reference to number and nature of these elementary components into a general parameter "effective redundancy." The study of small systems with few organizational levels between the whole system and the sites of elementary radiation effects has led to the complementary concept of "information density." The development of this concept is due to Morowitz (28).

Consider a system with N components, each of known information content H and known susceptibility to radiation, $1/D_0$. Let this system be the exact organizational opposite to the system previously considered: that is, perturbation of any single component results in malfunction. This implies that virtually all the information in all components is essential, or in Morowitz's terminology, that the system has the maximum information density obtainable, namely, H per component. Suppose it turns out that it takes about r perturbed components to cause malfunction. This can indicate one of the four extreme situations: (a) only $1/r$ of all components carry essential information, and they are distributed throughout the system; the information density is H/r; (b) the system consists of a coherent segment with information density H—the "target!"—and a $(r-1)$ times larger segment with information density zero; (c) the system is stabilized to the degree that it can tolerate the equivocation due to $(r-1)$ perturbations; the information density is $H[1-(r-1)/N]$, and near maximum if $N \gg r$; (d) the system consists of subsystems of size k, each stabilized against up to r perturbations;

the information density is $H[1-(r-1)/k]$. This is near maximum if $k \gg r$. Many real cases should be intermediate between the four extremes.

The various situations can be distinguished by producing coherent clusters of perturbations of varying size, or, in radiation terms, by using radiations of different linear energy transfer (LET) along the ionization tracks (30). An interesting finding was made in studying the inactivation of spores with a wide variety of irradiations: the cross section kept increasing with increasing LET for as far as it could be studied. This is interpreted as meaning that the spore contains several subsystems of varying information density, all necessary for survival; as the LET is increased, more and more subsystems become vulnerable (28).

In many small biologic objects, it was found that the region of high information density takes up a sizable fraction of the whole mass, and saturation sizes of clusters are very much smaller than the number of atoms in this region. On this basis, Morowitz postulates that the information density of some living structures must be very high, not more than one or two orders of magnitude below the maximum. To determine actual values, one has to identify the elementary units in radiation response, and estimate their information content. Morowitz argues that atoms and small molecules certainly are perturbed in a quantal fashion by irradiation; the amount of information per atom or molecule has been estimated by various means with reasonably good agreement (14, 29). On these grounds, Morowitz computes a very high information density of the essential portions of living structures of the order of one bit per atom.

While atoms and small molecules are units perturbed by ionization, it is not certain that they are the largest unit in living matter to do so. It seems, for instance, that enzymes cease to function as entire units (31, 32, 33), and that enzyme inactivation is caused by single events occurring under irradiation: with high probability by ionizations within (31, 34) or in the neighborhood (32) of the enzyme, with lower probabilities by collision with radiation-produced radicals. This set of indications could be interpreted as evidence of high information density, but it is hard to reconcile with the fact that enzymes will tolerate considerable amounts of chemical changes without ensuing malfunction. Alternatively, one might consider the possibility that a single ionization within an enzyme molecule causes many perturbations (34) or that there are weak links which give way, causing the structure to collapse, if there is any serious perturbation anywhere in the molecule (32). Effectively, such a weak link would constitute a protective mechanism because it would tend to eliminate "damaged" protein molecules. Enzymes may be considered as representative basic components of radiation responses. The functional information content of an enzyme, with roughly 1000 atoms, is approximately 10 bits (35). Applying Morowitz's argument to this unit, we obtain maximum information densities of approximately 1/1000 bits per atom. It is clear that much analysis will be needed to impose narrow brackets on the estimates of information densities in living matter.

Information Theory of Radiosensitivity

Our oft-verified relation,

$$\text{Error rate} = ke^{-\nu e^{-D/D_0}},$$

implies a classification of factors contributing to radiosensitivity: those which operate on k, which has the nature of a frequency factor, or, more generally, is related to the expression of errors; those which operate on ν, the effective redundancy; and those which operate on the cross section and thus affect D_0. The last group of factors has been extensively studied in connection with target theory (20, 30, 36); very little can be said about factors in the first group; concerning factors acting on ν, a few speculations may be permissible at this place.

In simple systems, ν stands for the actual degree of multiplicity; that is the situation dealt with in the "multitarget" analysis (20). In complex systems, ν indicates an "effective" degree of redundancy,

$$\nu = \eta N$$

with contributions from actual multiplicity of components (N) and their internal stability (η). All situations which are characterized by low η or N must be associated with high sensitivity.

Early stages of radiation reactions take place on the molecular and macromolecular level. It is a matter of fact that, on this level, high multiplicity is associated with every-day function, and low multiplicity with the reconstruction of functional elements. Thus, enzymatic action is much better protected by multiplicity than enzyme production; gene action is better protected than gene reproduction and distribution. Radiosensitivity (due to low multiplicity) is associated more with production than with function of biologic entities.

The internal stability, η, depends on the amount of functional capabilities apportioned to checking and correcting of error. The successful use of these capabilities depends on harmonious interplay between components. There is a whole class of situations in which this interplay is compromised: all situations in which a change of behavior pattern occurs. Harmonious interplay is based on signals producing proper effects; with components of limited informational capabilities, like or similar signals must be used for different effects in different situations; accordingly, confusion is most likely to occur when some components have adopted a new behavior pattern and others have not yet done so. This description may sound anthropomorphic: but biologists in many fields will have no difficulty recognizing the pattern indicated in many biologic processes.

Both the production of new elements and changes in behavior pattern are associated with re-organization. The postulate, therefore, is proposed that low ν and high sensitivity are associated with processes of re-organization, where high sensitivity applies to both causation and manifestation of damage (37). This postulate implies the three parts of the law of Bergonnié &

Tribondeau (38): cells which frequently divide are sensitive—and most divisions are associated with re-organization of material of one cell into that of two; cells with many divisions in the future are sensitive—they have many occasions to manifest damage; cells which show little differentiation in form and function are sensitive—as they commence to differentiate, and thereby re-organize, they will have many occasions to manifest damage. The postulate also accounts for some exceptions to the law of Bergonié and Tribondeau: spermatocytes divide rapidly without being particularly sensitive—but meiosis is largely a matter of distribution without much re-organization; in many cell lineages, the most sensitive phase is not that of the earliest, least differentiated cells, but usually the phase just preceding differentiation, or the early steps of differentiation or re-organization; in the developing central nervous system, the most radiosensitive cells are those which do not divide at all any more but are rapidly re-organizing from undifferentiated to differentiated cells (39).

LITERATURE CITED

1. Dessauer, F., *Quantenbiologie* (Springer-Verlag, Berlin, Germany, 178 pp., 1954)
2. Shannon, C. E., and Weaver, W., *The Mathematical Theory of Communication* (University of Illinois Press, Urbana, Ill., 117 pp., 1949)
2a. Khinchin, A. I., *Mathematical Foundation of Information Theory* (Dover Publications, Inc., New York, N. Y., 120 pp., 1957)
3. Goldman, S., *Information Theory* (Prentice-Hall, Inc., New York, N. Y., 385 pp., 1953)
4. Feinstein, A., *Proc. I.R.E. (Inst. Radio Engrs.) Trans. on Inform. Theory, PG-IT*, 2–22 (1954)
5. Brillouin, L., *Science and Information Theory* (Academic Press, Inc., New York, N. Y., 320 pp., 1956)
6. Rothstein, J., in *Proceedings 1st Conference on Biophysics* (Yale University Press, New Haven, Conn., 1958)
7. Quastler, H., Ed., *Essays on the Use of Information Theory in Biology* (University of Illinois Press, Urbana, Ill., 273 pp., 1953)
8. Yockey, H. P., Ed., *Symposium on Information Theory in Biology* (Pergamon Press Inc., New York, N. Y., 1958)
9. Quastler, H., Ed., *Information Theory in Psychology* (The Free Press, Glencoe, Ill., 436 pp., 1955)
10. Wiener, N., *Cybernetics* (John Wiley and Sons, Inc., New York, N. Y., 194 pp., 1948)
11. Ashby, W. R., *An Introduction to Cybernetics* (Chapman and Hall Ltd., London, Engl., 295 pp., 1957)
12. Foerster, H. v., Ed., *Cybernetics* (Trans. 6th to 10th Conf. of The Josiah Macy, Jr., Foundation, New York, N. Y., 1950 to 1954)
13. Quastler, H., *Proc. I.R.E. (Inst. Radio Engrs.), Trans. on Electronic Computers, EC-6*, 192–94 (1957)
14. Dancoff, S. M., and Quastler, H., in *Essays on the Use of Information Theory in Biology* (University of Illinois Press, Urbana, Ill., 273 pp., 1953)
15. Jones, H. B., *Advances in Biol. and Med. Phys.*, **4**, 281–337 (1956)
16. Jones, H. B., in *Symposium on Information Theory in Biology* (Pergamon Press, to be published, 1958)
17. Jones, H. B., in *Mammalian Aspects of Basic Mechanisms in Radiobiology* (Natl. Acad. Sci.-Natl. Research Council, Publ., Washington, D. C., 203 pp., 1957)
18. Yockey, H. P. in *Symposium on Information Theory in Biology* (Pergamon Press, Inc., New York, N. Y., to be published, 1958)
19. Yockey, H. P., *Radiation Research*, **5**, 146–55 (1956)
20. Zirkle, R. E., in *Symposium on Radiobiology* (John Wiley and Sons, Inc., New York, N. Y. 465 pp., 1952)
21. Sacher, G. A., *Radiology* **67**, 250–58 (1956)
22. Sacher, G. A., in *Symposium on Information Theory in Biology* (Pergamon Press, Inc., New York, N. Y., to be published, 1958)
23. Cronkite, E. P., Bond, V. P., Chapman, W. H., and Lee, R. H., *Science* **122**, 148–50 (1955)
24. Koch, R., Catsch, A., and Langendorff, H., *Deut. med. Wochschr.*, **82**, 1069–72 (1957)
25. Brues, A., and Sacher, G., in *Symposium on Radiobiology* (John Wiley and Sons, Inc., New York, N. Y., 465 pp., 1952)

26. Hursh, J. B., and Casarett, G. W., *Brit. J. Radiol.* **29,** 169 (1956)
27. Auerbach, H. (Personal communication)
28. Morowitz, H. J., in *Symposium on Information Theory in Biology* (Pergamon Press, Inc., New York, N. Y., to be published, 1958)
29. Morowitz, H. J., *Bull. Math. Biophys.,* **17,** 81–86 (1955)
30. Pollard, E. C., Guild, W. R., Hutchinson, F., and Setlow, R. B., *Progr. in Biophys. and Biophys. Chem.,* **5,** 72–108 (1955)
31. Pollard, E. C., *Advances in Biol. and Med. Phys.* **3,** 153–89 (1953)
32. Augenstine, L., in *Proc. 1st Conf. Biophysics* (Yale University Press, New Haven, Conn., to be published, 1958)
33. Fluke, D. J., in *Proc. 1st Conf. Biophysics* (Yale University Press, New Haven, Conn., to be published, 1958)
34. Platzman, R. L., and Franck, J., in *Symposium on Information Theory in Biology* (Pergamon Press, Inc., New York, N. Y., to be published 1958)
35. Quastler, H., in *Essays on the Use of Information Theory in Biology* (University of Illinois Press, Urbana, Ill., 273 pp., 1953)
36. Lea, D. E., *Actions of Radiations on Living Cells* (The Macmillan Co., New York, N. Y., 402 pp., 1947)
37. Quastler, H., in *Mammalian Aspects of Basic Mechanisms in Radiobiology* (Natl. Acad. Sci.-Natl. Research Council, Publ., Washington, D. C., 203 pp., 1957)
38. Bergonié, J., and Tribondeau, L., *Compt. rend. acad. sci.* **143,** 983–84 (1906)
39. Hicks, S. P., *Physiol. Revs.* **38,** (1958)

AUTHOR INDEX

AUTHOR INDEX

SUBJECT INDEX

Accelerators, high-energy
  adiabatic damping in, 194
  analogue, 203
  beam deflectors, 192
  beam stacking in, 200
  bibliographies, 182
  conceptual advances, 182-92
  construction, recent
    progress in, 209-13
  fixed field alternating
    gradient (FFAG), 189
  injection into, 191
  instabilities in, 203
  limitations of, 186-87
  microtrons, 185
  nonlinear oscillations in,
    200-4
  phase displacement in, 199
  projects under study or
    design, 212
  radiation damping in, 194
  resonances in, 191
  subharmonic, 201-2
  tabulations of, 181-82,
    210, 211
  transition energy in, 190,
    200
  untested concepts
    air cored accelerator
      magnets, 205
    "hybrid" accelerators,
      204
    plasma and coherent
      acceleration, 208-9
    radiation cooled electron
      beams, 208
    see also Intersecting
      beam proposals
  variable energy, 191
  see also Linear acceler-
    ators
Ages of minerals, see Min-
  eral ages
Air-monitoring, 340
Albedo of cosmic-ray
  particles, 225-26
Alpha contamination, survey
  of
  permissible air concentra-
    tions, 337
  proportional counter, 337
  scintillation counter, 337,
    338
Alpha particle
  energy distribution, 222,
    224
  flux in cosmic radiation,
    218
Alternating gradient focus-
  ing, 184, 187-88

  in linear accelerators
    188
Annihilation radiation, meas-
  urement of, 170
Analogue accelerator, 203
"Antigravity," 159
Antihyperons, threshold
  for formation, 140, 157
Antimatter, upper limit of
  concentration, 158-59
Antineutron
  and antiproton, parity,
    135
  charge exchange cross
    sections, 157
  detection by annihilation,
    155-57
  field describing, 28
Antinucleons
  spin of, 36-39
  see also Antiparticles
Antiparticles, 127-59
  particle-antiparticle re-
    lations, 128
Antiproton
  annihilation process, 144-54
    electromagnetic anni-
      hilation, 150-51
    mesic annihilation, 151-52
    pions, average number
      emitted per annihila-
      tion, 148
    purification of the beam
      144-45
    spectrum of pion energy,
      147
  in cosmic rays, 157-58
  nucleonic properties of,
    135-58
    collision cross sections,
      136-44
    isotopic spin, 135
    parity of antiproton and
      antineutron, 135
  production of, 154
  verification of Dirac's
    attributes of, 128-35
    annihilation, 132-33
    charge, 131
    decay constant, 133, 135
    mass, 131
    production in pairs, 133
    spin and magnetic
      moment, 131-32
"Antiparallel case," 177-78
Antiunitary operator, 18
Argon 38, occurrence of in
  potassium minerals,
    278
Argon 40

  diffusion of in potassium
    chloride, 274
  electron capture, 261
Argonne National Lab-
  oratory 7.7 m. bent
  crystal gamma-ray
  spectrometer, 170
Atmosphere, radioactivity
  of, 243-54
Atmospheric contamination
  airborne radioactivity,
    332
  contamination of surfaces,
    333-34
Atomic Energy of Canada
  bent crystal gamma-
    ray spectrometer, 173
Authigenic minerals, in
  sedimentary rocks, 277

B

Bacteria, radiobiology of,
  348, 351, 353, 355,
  359-61, 364, 370-73
Ball and Chew model, 138-40, 144
Barium stars, 312
Baryon
  "baryon number," 40
  conservation laws, 39-41
Beam deflectors
  energy-loss, 192
  regenerative, 192
Beams of charged particles
  antiproton, 144
  betatron beam extraction,
    187
  cataract-producing expos-
    ure to, 331-32
  stacking in accelerators,
    200
Bent crystal gamma-ray
  spectrometers
  Argonne National Labora-
    tory 7.7 m. spectrom-
    eter, 170
  Atomic Energy of Canada
    spectrometer, 173
  California Institute of
    Technology spectrom-
    eter, 167-70
  energy resolution, 168-69,
    173
  energy wavelength con-
    version constants, 169
  ideal transmission type, 163
  merits and value of, 169-73
  simplified approximate
    transmission type,
    164-67

411